The role of poly (ADP-ribose) polymerase-1 in the regulation of the stress inducible transcription factor, nuclear factor kappa-B

Jill Elizabeth Hunter

Thesis submitted in partial fulfilment of the requirements of the regulations for the degree of Doctor of Philosophy

Newcastle University
Faculty of Medical Sciences
Northern Institute for Cancer Research

i. Declaration

I hereby declare that the work presented in this thesis is original and was carried out at the Northern Institute for Cancer Research, at Newcastle University between October 2007 and April 2011.

No part of this work is being, or has been submitted for a degree, diploma or any other qualification at any other university.

Signed: JILL HUNTER

Date: 19.01.12

ii. Abstract

The stress inducible transcription factor, NF-κB, induces genes involved in proliferation and apoptosis. Aberrant NF-κB activity is common in cancer and contributes to therapeutic-resistance. Moreover, constitutive NF-κB activation has been shown to contribute to malignant progression through the regulation of gene expression. Poly(ADP-ribose) polymerase-1 (PARP-1) is activated during DNA strand break repair and is a known transcriptional co-regulator. The role of PARP-1 function during NF-κB activation using siRNA knockdown of either p65 or PARP-1, or the potent PARP-1 inhibitor, AG-014699, was investigated. Survival and apoptosis assays showed that NF-κB $p65^{-/-}$ mouse embryonic fibroblasts (MEFs) were more sensitive to ionising radiation (IR) than $p65^{+/+}$ MEFs. Co-incubation with p65 siRNA, PARP siRNA or AG-014699 radio-sensitised $p65^{+/+}$, but not $p65^{-/-}$ MEFs, demonstrating that PARP-1 mediates its effects on survival *via* NF-κB. Furthermore, a combination of p65 siRNA and AG-014699 radio-sensitised $p65^{+/+}$ MEFs to the same extent as either agent alone, strongly indicating that PARP-1 and NF-κB are mechanistically linked. PARP-1 is known to be vital for the repair of single strand breaks (SSBs). SSB repair kinetics, and the effect SSB repair inhibition by AG-014699 were similar in $p65^{+/+}$ and $p65^{-/-}$ cells. Since inhibition of SSB repair did not radio-sensitise $p65^{-/-}$ cells, these data show that radio-sensitisation by AG-014699 is due to downstream inhibition of NF-κB activation, and independent of SSB repair inhibition. PARP-1 catalytic activity was essential for IR-induced p65 DNA binding and NF-κB-dependent gene transcription, whereas for TNF-α treated cells, PARP-1 protein alone was sufficient. It can therefore be hypothesised that this stimulus-dependent differential is mediated *via* stimulation of the Poly(ADP-ribose) (PAR) polymer, which was induced following IR, not TNF-α. Poly(ADP-ribose) glycohydrolase (PARG) is the major enzyme responsible for the catabolism of the PAR polymer. In order to inhibit degradation of the PAR polymer a potent and specific PARG inhibitor was used. Increased polymer stability following IR, by virtue of inhibition of polymer degradation, led to the persistence of NF-κB DNA binding, an increase in anti-apoptotic gene expression and a protection against IR-induced cell death. These data confirm a role for the PAR polymer in the activation of NF-κB following DNA damage.

Microarray analysis showed that the TNF-α driven transcription of NF-κB-dependent inflammatory and immune response genes was unaffected by AG-014699,

suggesting that targeting DNA-damage activated NF-κB using AG-014699 may overcome toxicity observed with classical NF-κB inhibitors without compromising other vital inflammatory functions. An investigation into the role of PARP-1 in DNA damage activated NF-κB activation in glioblastoma cells was also undertaken to assess the potential utility of AG-014699 in tumour types known to express constitutively active NF-κB. PARP-1 activity was vital for both radio- and chemo-sensitisation of U251 glioblastoma cells, and in IR- or temozolomide- treated cells, PARP-1 mediated its effects on survival *via* NF-κB. Importantly, these data confirm the findings in the MEFs by demonstrating that radio- or chemo-sensitisation by AG-014699 is due to downstream inhibition of NF-κB activation, and independent of SSB repair inhibition. Hence, these data highlight the potential of PARP-1 inhibitors to overcome NF-κB-mediated therapeutic resistance and widens the spectrum of cancers in which these agents may be utilised.

The therapeutic potential of a potent inhibitor of NF-κB subunit DNA binding, PBS-1086, was also assessed in the NF-κB $p65^{+/+}$ and $p65^{-/-}$ MEFs and the MDA-MB-231, T47D and MCF7 breast cancer cell lines. DNA binding and luciferase reporter assays showed that PBS-1086 inhibited IR-induced p65 and p50 DNA binding and NF-κB-dependent gene transcription in $p65^{+/+}$ cells. Co-incubation with PBS-1086 or p65 siRNA radio-sensitised $p65^{+/+}$, but not $p65^{-/-}$ cells, demonstrating that PBS-1086 mediates radio-sensitisation *via* the p65 NF-κB subunit. Gene expression analysis showed that PBS-1086 inhibited IR-induced transcription of known NF-κB-regulated anti-apoptotic genes. MDA-MB-231 cells were found to have the highest constitutive levels of DNA binding of all NF-κB subunits. PBS-1086 radio-sensitised all three breast cancer cell lines. In survival assays, all breast cancer cell lines tested were also sensitive to PBS-1086, however, MDA-MB-231 cells were the most sensitive to PBS-1086 alone. Thus, high NF-κB DNA binding activity appears to correlate with sensitivity to PBS-1086. Collectively these data highlight the potential of modulating NF-κB activity, either by PARP-1, or directly *via* inhibition of subunit DNA binding, to restore radio- and chemo-sensitivity in cancers with aberrantly active NF-κB, and to overcome NF-κB mediated therapeutic resistance.

iii. Acknowledgements

First of all I'd like to thank my supervisors, Elaine Willmore, Julie Irving, Barbara Durkacz and Stephany Veuger. Barbara – you are truly an inspirational scientist, thank you so much for giving me the opportunity to come to Newcastle and work with you, I've learnt so much. Julie and Elaine – this thesis wouldn't have happened if it wasn't for the two of you. Thank you for all of your time, effort, help, support and guidance. Also thank you for letting me develop my own ideas (and make my own mistakes!) Stephany – thank you for laying the groundwork, which has allowed me to take the project in my own direction.

Mam and Dad – thank you for always being behind me 100 %, and for all of your love and support. I love you both very much.

A special thank you must go to Evan. Normal scheduling can now resume…I promise! I love you xx

I must say a big thank you to the other members of 'Team Babs', past and present ('Team Purple' now)…Sarah Elliott, Clark Crawford, Isabella Swidenbank, Emily Mould and Sue Tudhope. From day one you all made me feel so welcome, it's been a pleasure to work with you, and I hope we will continue to be friends for a long time to come (you can't get rid of me that easily!)

I must acknowledge all of the people I have worked with, and the friends I have made at the POG over the last few years. Thank you for making it such a great place to work. There are too many people to mention everyone individually but Laura Gamble, Sarah, Elaine, Clark, Emma Haagensen, Claire Worrall, Yvette Drew, Joanne Munck and Zoe Davison deserve a special mention, as do the ladies that have accompanied me on many lunchtime trips to the gym – all of the hours spent on those spin bikes and throwing kettlebells around have really kept me sane whilst writing up…cheers ladies!

There are also many people outside of science who have helped me throughout my PhD…even though they glaze over at the sheer mention of transcription factors or DNA repair! Nikki – thank you for making Newcastle such a great place to be. The girlies from home (Steph, Gemma, Katie and Dani) – thank you for always making me laugh! Also, Rach, Holls and Carolyn (Chubb!) thank you for the many hours spent chatting on the phone.

Finally, this work would not have been possible without the funding from Cancer Research UK, and the kind support of the following; Pfizer for providing AG-014699, Profectus BioSciences, in particular Jie Zhang, for providing the NF-κB inhibitors, Professor Neil Perkins (Newcastle University), Professor Ron Hay (Dundee University) and Professor Gilbert de Murcia (Ecole Superieure de Biotechnologie de Strasbourg) for providing cell lines.

Thank you :o)

iv. Contents

v. List of Figures

vi. List of Tables

vii. List of Abbreviations

3-AB: 3-aminobenzamide

AAG: Alkyl-adenine DNA glycosylase

AD: Alzheimer's disease

ADP-HPD: Adenosine 5'-diphosphate (hydroxymethyl) pyrrolidinediol

ADPRS: ADP-ribose synthetase

ADPRT: ADP-ribose transferase

AML: Acute myeloid leukaemia

AP: Apyrimidinic/apurinic

AP-1: Activator protein-1

APE-1: Apurinic endonuclease-1

APH-1: Anterior pharynx-defective 1

APP: Amyloid precursor protein

ApoE: Apolipoprotein

ATM: Ataxia telangiectasia mutated

AURKA: Aurora kinase A

AURKB: Aurora kinase B

BAFF: B-cell activating factor of the TNF family

BCA: Bicinchonic acid

BER: Base excision repair

BIRC6: baculoviral IAP (inhibitor of apoptosis) repeat containing 6

BRCT: BRCA-1 C-terminal domain

BSA: Bovine serum albumin

BZ: Benzamides

CARM1: Coactivator-associated arginine methyltransferase 1

CBP: Creb binding protein

CCL5: Chemokine ligand 5

cFLAR: CASP8 and FADD-like apoptosis regulator

CDC20: Cell division cycle 20

CDKN1A: Cyclin-dependent kinase inhibitor 1A (p21)

cDNA: complementary DNA

CK2: Casein kinase II

COX-2: Cyclooxygenase-2

CLL: Chronic lymphocytic leukaemia

cRNA: copy RNA

CXCL1: chemokine (C-XC motif) ligand 1

CXCL10: chemokine (C-XC motif) ligand 10

DDR: DNA damage response

DLBCL: Diffuse large B-cell lymphoma

DMSO: Dimethylsulphoxide

DNA: Deoxyribose nucleic acid

DNA-PK: DNA-dependent protein kinase

dNTPs: deoxyribonucleoside triphosphates

DOX: Doxorubicin

DPQ: 3,4-dihydro-5-[4-(1-piperidinyl)butoxyl]-1(2H)-isoquinolinone

dRP: Deoxyribose-phosphate

DSB: Double strand break

dsRNA: double-stranded RNA

ECL: Enhanced chemiluminesence

EGF: Epidermal growth factor

ELISA: Enzyme-linked immunosorbent assay

ELKS: Protein rich in glutamate, leucine, lysine and serine

EMSA: Eletrophoretic mobility shift assay

ERKs: Extracellular signal-related kinases

EtBr: Ethidum bromide

FACs: Flow cytometric

FAM: Fluorescein

FAP: Familial adenomatous polyposis

FBS: Foetal bovine serum

FEN-1: Flap endonuclease 1

FRET: Fluorescence resonance energy transfer

GBM: Glioblastoma multiforme

GCLP: Good Clinical and Laboratory Practise

GRR: Glycine rich region

H_2O_2: Hydrogen peroxide

HAM/TSP: HTLV-I–associated myelopathy/tropical spastic paraparesis

HDAC1: Histone deacetylase-1

HIF-1α: Hypoxia-Inducible Factor-1 alpha

HLH: Helix-loop-helix

HRP: Horseradish peroxidase

HRR: Homolgous Recombination Repair

IAPs: Inhibitor of apoptosis proteins

IBD: Inflammatory bowel disease

IFNγ: interferon-gamma

IL-1: Interleukin-1

iNOS: Inducible nitric oxide

IκB: Inhibitor of kappa-B

IKK: Inhibitor of kappa-B kinase

IPA: Ingenuity Pathway Analysis

IR: Ionising radiation

IRF1: Interferon regulatory factor 1

LD_{50}: Dose of γ-irradiation or drug to give 50 % reduction in survival

LMP-1: Latent membrane protein-1 of the Epstein Barr virus

LPS: Lipopolysaccharide

LZ: Leucine zipper

LTβ: Lymphotoxicin beta

MAPK: Mitogen-activated kinase pathway

MEF: Mouse embryonic fibroblast

MHC: Major histocompatibility complex

MGMT: Methyl guanine methyl transferase

MMPs: Matrix metalloproteinases

MNC: Mononuclear cells

mRNA: messenger RNA

NAD^+: Nicotinamide adenine dinucleotide

NCSTN: Nicistrin

NEMO: NF-κB essential modulator

NFAT: Nuclear factor of activated T-cells

NF-κB: Nuclear factor kappa-B

NGF: Nerve growth factor

NER: Nucleotide excision repair

NES: Nuclear export sequence

NHEJ: Non-homologous end-joining

NIK: NF-κB inducing kinase

NLS: Nuclear localisation sequence

NMN: Nicotinamide mononucleotide

NS: Non-specific

OD: Optical density

OS: Overall survival

OTM: Olive Tail Moment

PAR: Poly(ADP-ribose)

PARG: Poly(ADP-ribose) glycohydrolase

PARP: Poly(ADP-ribose) polymerase

PARP-1: Poly(ADP-ribose) polymerase-1

PBS: Phosphate buffered saline

PBS: Profectus BioSciences

PCNA: Proliferating cell nuclear antigen

PCR: Polymerase chain reaction

PEN-2: presenilin enhancer 2

PEST: Domain rich in proline, glutamate, serine and threonine

PI: Propidium iodide

PI3K: Phosphatidyl-inositol 3-kinase

PIASγ: Protein inhibitor of activated stat-gamma

PIKKs: PI3K-like protein kinases

PLK: Polo-like kinase

PRMT1: Protein arginine methyltransferase 1

PS: Phospholipid phosphatidylserine

qRT-PCR: Quantitative real time PCR

RA: Rheumatoid arthritis

RANK: Receptor-activator of NF-κB

RHD: Rel homology domain

RIN: RNA Integrity Number

RISC: RNAi-induced silencing complex

RNAi: RNA interference

RT-PCR: Reverse transcriptase PCR

SAGE: Serial analysis of gene expression

SAR: Structural activity relationship

siRNA: small interfering RNA

SDS-PAGE: Sodium dodecyl sulphate-polyacrylamide gel electrophoresis

SLE: Systemic lupus erythematosus

SNPs: Single nucleotide polymorphisms

SSB: Single strand break

SUMO: Small ubiquitin like modifier

TAD: Transactivation domain

TAK1: TGF-β activated kinase-1

TBL1: Transducin β-like protein 1

TCR: T-cell receptor

TGF-α: Transforming growth factor-alpha

TMZ: Temozolomide

TNBS: 2,4,6-trinitrobenzene sulfonic acid

TNF-α: Tumour necrosis factor-alpha

TNFR: TNF receptor

TNIP1: TNFAIP3 interacting protein 1

TNKS1: Tankyrase 1

TOP2A: Topoisomerase II alpha

TRAF-1: TNF-receptor associated factor-1

TPA: (12-O-tetradecanoyl-phorbol-13-acetate)

TPP: Tristetraprolin

TSG: Tumour suppressor gene

TTFT: Time to first treatment

UA: Unstable angina

UV: Ultraviolet

WRN: Werner syndrome protein

WT: Wild-type

XIAP: X-linked inhibitor of apoptosis

XRCC1: X-ray repair cross complementing 1

XTT: sodium 3'-[1-(phenylaminocarbonyl)- 3,4-tetrazolium]-bis (4-methoxy-6-nitro) benzene sulphonic acid hydrate in RPMI without Phenol red

Chapter 1. Introduction

1.1 Cancer

Cancer is often defined as being the overall name given to a large, heterogeneous class of diseases, in which cells have acquired properties which allow them to undergo uncontrolled growth and proliferation, evade cell death, invade the surrounding tissues, and in some cases metastasise to other locations *via* the lymphatic system or bloodstream. Cell growth and genomic integrity is tightly regulated in normal cells, by several classes of genes, however in tumour cells this regulation is often lost, due to hereditary or acquired abnormalities in regulatory genes, such as tumour suppressors and oncogenes. A small percentage of cancers, approximately 5-10 % are hereditary, whereas spontaneous ones are associated with acquired mutations of key genes, through a number of risk factors including the exposure to genotoxic and mutagenic agents.

Cancers are often classified by both the location of their origin and the type of cell that most resemble. These include the most common type of cancer, which are carcinomas, and tend to be tumours which have arisen from epithelial cells, for example those developing in the lung, breast or colon. Cancers originating in mesenchymal cells give rise to cancers in the connective tissues, called sarcomas. There are two major classes of cancers which arise in the haematopoietic cells and mature in the lymph nodes and blood are referred to as lymphomas and leukaemias, respectively. Finally, tumours derived from immature cells or embryonic tissues are often called blastomas and those which present in the testes or ovaries are sometimes called germ-cell tumours.

In 2007, cancer was attributable for 7.9 million deaths worldwide, which was 13 % of all human deaths (Jemal et al., 2011). Although rates of cancer are rising, it should be noted that this is primarily a disease of old age, and it is highly likely that the increasing incidence is due to an increased ageing population, especially in developed countries. Encouragingly however, statistics from Cancer Research UK show that cancer survival rates have doubled in the last 40 years, that more than 7 out of 10 children with cancer are now successfully treated, breast cancer death rates have fallen by almost a fifth in the past 10 years and more than 95% of men with testicular cancer are now successfully treated (www.cancerresearchuk.org). This is due to new advances in treatment and also surgical techniques, often in used in combination with the existing therapeutic modalities, which are chemotherapy, radiotherapy and surgical resection. The prognosis of cancer is heavily dependent on the type of cancer, also the extent and location of the disease.

In 2000, a landmark review by Hanahan and Weinberg was published, in which the six 'Hallmarks of cancer' were defined. These showed that a tumour cell had six key acquired or hereditary characteristics, which lead to the development, or spread, of cancer. These were; sustaining a proliferative signal, evading growth suppressors, activating invasion and metastasis, enabling replicative immortality, inducing angiogenesis and resisting cell death (Hanahan and Weinberg, 2000). These hallmarks still provide a solid foundation for understanding tumour growth and metastatic dissemination, whilst also illustrating that there can be a large diversity in each type of cancer, and in an individual tumour. However, a large body of data has been generated since this review, and these hallmarks have been updated to include a number of new capabilities shared by tumour cells. Figure 1.1 is taken from this review and shows the now ten hallmarks of cancer, which along with the original six, include; avoiding immune destruction, tumour-promoting inflammation, genome instability and mutation and deregulating cellular energetics (Hanahan and Weinberg, 2011).

Research in oncology over the last few years has also centred on targeted therapies, or personalised medicine, meaning that drugs specific to a mutation or type of cancer have been developed, such as the use of Poly (ADP-ribose) polymerase (PARP) inhibitors for BRCA-defective breast and ovarian cancers (reviewed in section 1.3.4.1). Figure 1.1 also illustrates novel therapies, currently in development or clinical trials, which target each of the ten hallmarks, as a means of overcoming cancer by directly targeting these key characteristics. It is also the hope that by targeting these hallmarks, which are unique to cancer cells, there will be fewer side effects for patients, as the normal tissues do not share these cancerous characteristics, and therefore should remain unaffected by these new treatments.

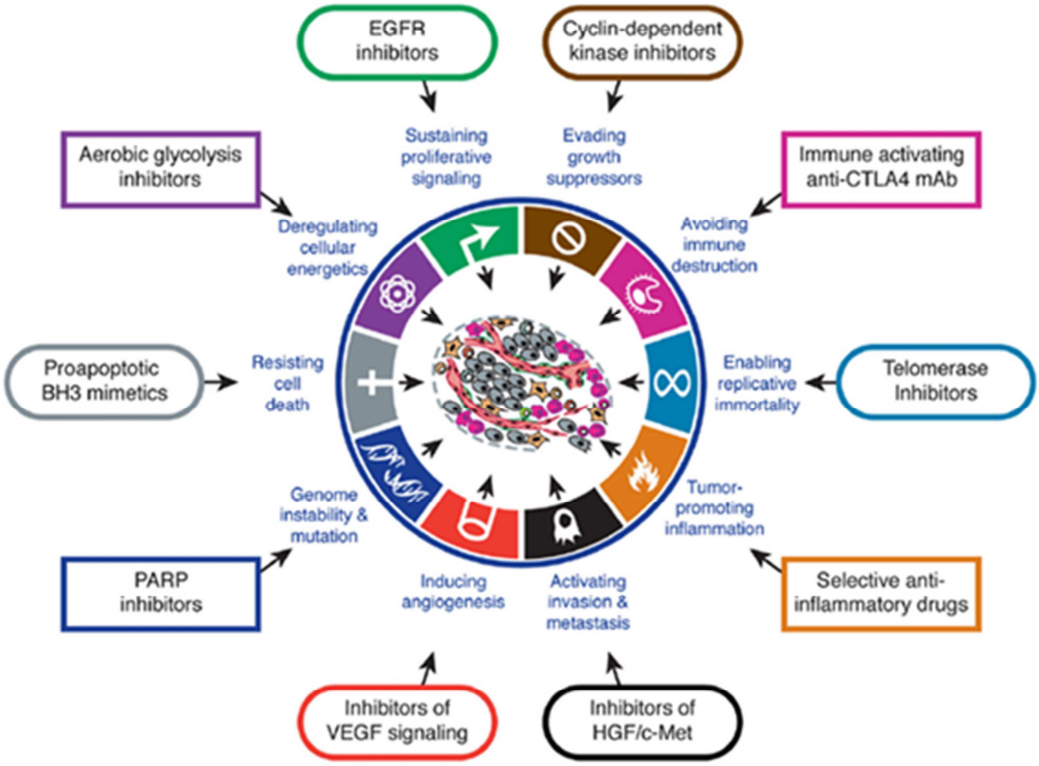

Figure 1.1: The Hallmarks of Cancer This figure shows the 10 'hallmarks' of cancer as assigned by Hanahan and Weinberg (2011). It also shows some of the novel drugs which are designed to specifically target these hallmarks. Some of these drugs have been licenced for use and others are in clinical trials, however these are just a representation and there are many others in development that are associated with these.
Taken from: (Hanahan and Weinberg, 2011)

1.1.1 Cancer therapeutics

As previously mentioned, the three principle approaches to the treatment of cancer are surgery, radiotherapy and chemotherapy. In the case of many solid tumours, such as breast or lung carcinomas, surgery is usually the first modality used. This is dependent on the tumour being accessible and aims to excise as much of the tumour mass as possible. However, it often means that some normal tissue, and in some cases the lymph nodes are also removed, in order to limit the risk of relapse. In many cases, it is not possible to surgically remove all of the cancerous tissue and as a result of this, radiotherapy is used as an adjunct therapy in many cases, with the aim of suppressing the rate of cell division in any tumour cells that remain following surgical resection. In some very advanced tumours, surgery may be used as a means of palliative care, as it can significantly reduce the tumour burden for a patient.

Radiotherapy, like many chemotherapeutic agents, directly damages the DNA of the tumour cells. In this case the DNA damage is by ionising radiation (IR) and can be used either as the principle means of local control, in order to reduce tumour burden prior to surgery, or as an adjunct to surgery (described above). It may be applied externally (beam therapy) or internally (brachy therapy) and the two approaches can be combined. Radio-therapy is a main-stay of treatment for a large range of solid tumours, such as breast, lung, prostate and brain tumours, including glioblastoma, and is one of the cornerstones of cancer treatment today. Interestingly, statistics from the Cancer Research UK, showed that 40% of people whose cancer is cured receive radiotherapy as part of their treatment (www.cancerresearchuk.org), which really highlights the importance of this type of treatment.

Surgery and/or radiotherapy are only effective in locally-confined tumours and are therefore, not suitable in all cases, such as leukaemia and lymphomas. In these, and many other cases, chemotherapy is administered. It should be noted that the majority of patients will receive systemic chemotherapy at some point during their illness, and that this type of treatment can be given an an adjunct to either radio-therapy or surgery. There are many classes of chemotherapeutic drugs, and hence it is not possible to review them all in detail here. Briefly, these DNA-damaging therapies include alkylating agents such as temozolomide (TMZ), topoisomerase I and II posions, such as camptothecin and doxorubicin (DOX) and nucleoside analogues, such as fludarabine. These agents are very effective; however they can also be toxic to normal cells, particularly in cells which by their nature proliferate rapidly, such as those in the gastrointestinal tract, bone marrow, testes or ovaries. This can therefore lead to quite severe side effects, such as loss of fertility and myelosuppression. As a result, anti-cancer drugs tend to have a steep dose response curve for both toxic and therapeutic effects,

New therapeutics which could be used in combination with existing agents are constantly being developed, these include targeted drugs, such as those which inhibit key DNA repair proteins, such as PARP inhibitors (section 1.3.4). These agents may increase the therapeutic-index of the conventional radio- and chemotherapies being administered, thus reducing the side effects associated with these agents. Other forms of treatment include hormone therapy, gene therapy, immunotherapy, bone marrow

transplant and peripheral blood stem cell transplants in conjunction with high dose chemotherapy. More recent developments in cancer treatment include the introduction on monoclonal antibody therapies, which includes Rituximab that targets CD20 found on the surface of B cells, and is used to treat chronic lymphocytic leukaemia (CLL), as well as other forms of leukaemia and lymphoma.

1.1.2 Oncogenes and tumour suppressors

Carcinogenesis is dependent on both oncogenes and tumour suppressor genes. In general, an oncogene is a gene which has the potential to cause cancer, and in many tumour cells these oncogenes are mutated or highly expressed. A proto-oncogene is a 'normal' gene, which has become an oncogene due to a 'gain-of-function' mutations or increased expression. Many proto-oncogenes encode proteins involved in signal transduction, cell proliferation or differentiation. These include *RAS*, *WNT*, *MYC*, and *ERK*. A further example of an oncogene is the Bcr-abl gene formed during a chromosomal translocation between chromosomes 9 and 22, and often referred to as the Philadelphia Chromosome. Bcr-Abl codes for a receptor tyrosine kinase which is constitutively active, leading to uncontrolled cell proliferation, and the development of chronic myeloid leukaemia (Chen et al., 2010).

In contrast, tumour suppressor genes (TSGs) are genes which protect the cell and aid in the maintenance of genomic integrity. Mutations in TSGs tend to be 'loss-of-function' and may reduce or completely abolish activity of such genes which negatively regulate critical cellular functions. This can then lead to enhanced cellular proliferation, blocked differentiation, or the suppression of cell death pathways, and hence the progression of cancer. Unlike oncogenes, TSGs generally follow the Knudson two-hit hypothesis, which was first proposed for the retinoblastoma (Rb) protein, a known TSG (Knudson, 1971). This hypothesis suggests that a mutation or loss of both alleles of a gene must be affected before an effect manifests itself. Knudson analysed a subset of retinoblastoma cases, which can be either familial or occur sporadically, and found that hereditary retinoblastoma occurred at a younger age than the sporadic disease. This lead Knudson to hypothesise that multiple 'hits' to DNA were necessary to cause cancer. In this case, a 'hit' is classified as a mutation in a key gene. In familial retinoblastoma tumours, the initial hit was inherited in the DNA, and any second insult would rapidly lead to cancer.

However, in sporadic retinoblastoma, two ‘hits’ must occur before the onset of tumourigenesis, hence explaining the age difference.

Another important TSG is the p53 protein, encoded by the *TP53* gene. This TSG is often referred to as the ‘guardian of the genome’ and is known to regulate the apoptotic pathway, particularly in response to DNA damage (Lane, 1992). p53 is an important transcription factor (section 1.1.3) and is a common target for genetic alterations in cancer, with around 50 % of tumours possessing mutations in the p53 gene (Ozaki and Nakagawara, 2011). This includes colorectal, breast and lung carcinomas, as well as many haematological malignancies and neurological cancers. Interestingly, p53 is a notable exception to the Knudson hypothesis, as heterozygous loss is enough to result in a loss of functional protein in this case.

1.1.3 Transcription factors and cancer

Transcription factors are vital proteins that bind to specific DNA consensus sequences and therefore control gene transcription and control a number of cellular processes. A number of transcription factors are de-regulated in cancer, and many are known oncogenes and TSGs (section 1.1.2), and some very brief examples will be discussed here. The *MYC* gene, which codes for the myc family of transcription factors, is over expressed in Burkitt's Lymphoma following a chromosomal translocation. This results in uncontrolled growth and is thought to drive the development of this type of lymphoma. Hence, *MYC* is often deemed to be an oncogene (Taub et al., 1982). The TSG, p53, is an important transcription factor, known to regulate genes associated with apoptosis and cell cycle progression. As previously discussed, p53 is frequently de-regulated in many different types of cancer (Ozaki and Nakagawara, 2011). Other transcription factors which have been implicated in the progression and onset of various cancers include c-JUN, β-catenin, NOTCH, the STAT family of transcription factors, and also Nuclear Factor-kappaB (NF-κB) (Darnell, 2002). The role of NF-κB in cancer will be discussed in detail in section 1.2.4.3.

1.2 Nuclear factor kappaB (NF-κB)

Transcription factors, such as Nuclear Factor kappa-B (NF-κB) regulate and respond to changes in the environment, and mediate such responses through alterations in gene

expression (Hayden and Ghosh, 2004). The stress-inducible transcription factor NF-κB, has the ability to both induce and repress gene expression (Perkins, 2007) and plays a crucial role in many biological processes. NF-κB was first identified by its binding to the enhancer region of the immunoglobulin kappa (κ) light chain gene in B cells in order to regulate the human immune response (Suh and Rabson, 2004), and consequently it's activity was initially associated with infection and immunity; however knockout mouse models (Table 1.1) have revealed a role for NF-κB family members in normal development, and their expression has been documented in various cell types. There are a number of genes regulated by NF-κB, including those controlling apoptosis, cell adhesion, inflammation, proliferation, immune responses, cellular stress and tissue remodelling (Bonizzi and Karin, 2004, Gerondakis et al., 1999, Hayden and Ghosh, 2004, Pahl, 1999, Pasparakis et al., 2006).

NF-κB activity has been found to be regulated by both tumour suppressors and oncogenes, hence having profoundly different effects, mediating either enhanced or inhibited cellular proliferation or apoptosis (Perkins and Gilmore, 2006). Consequently inappropriate NF-κB activity has been implicated in the pathology of inflammatory diseases and cancers (discussed in sections 1.2.4.1 and 1.2.4.3) and has made the transcription factor a target of much clinical investigation (Kim et al., 2006). Therefore NF-κB is a topic of investigation by many groups, in order to understand more about the role played by the transcription factor in terms of its activity, selectivity and role in signalling. However, the abundance of processes in which NF-κB is known to be associated means that there is a huge expanse of literature available surrounding the subject. Here, the aim is to review only those key aspects of its activity relevant to the study in question.

1.2.1 The NF-κB superfamily and associated proteins

The term NF-κB can be used to refer to either the entire family of transcription factors or simply a single subunit, but often it is used to denote specific transcriptionally active homo- or hetero-dimers. Members of the NF-κB superfamily are conserved throughout evolution, and present in most species, which the exception of yeast and *C. elegans*. Therefore, the majority of studies on model organism within this field are undertaken in mammalian cells (Gilmore, 2006).

1.2.1.1 NF-κB subunits

All NF-κB proteins are characterised by a conserved N-terminal domain of approximately 300 amino acids named the Rel-homology domain (RHD) which is composed of β-sheets and bears a structural resemblance to the well-known immunoglobulin domain (Figure 1.2). This domain is responsible for DNA binding, dimerisation and interaction with Inhibitor of NF-κB (IκB) proteins. It is known that the Rel subfamily members (RelA, RelB and c-Rel) are found predominantly in the cytoplasm bound to inhibitor IκB proteins. This binding sequesters the NF-κB:IκB complex to the cytoplasm thereby keeping NF-κB in an inactive state (Perkins, 2007).

.

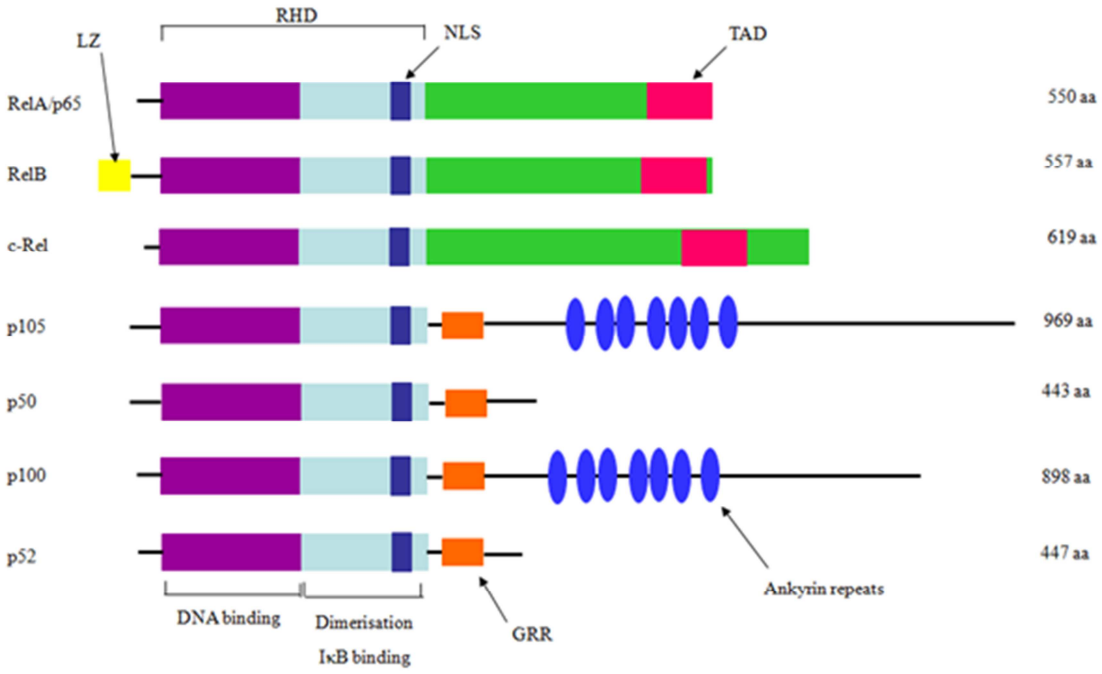

Figure 1.2: The seven NF-κB/Rel family members RHD: Rel homology domain. NLS: Nuclear localisation sequence. TAD: Transactivation domain. LZ: Leucine zipper. GRR: Glycine rich region.
Adapted from: (Chen and Greene, 2004)

There are five NF-κB genes, *NFKB1*, *NFKB2*, *RELA*, *c-REL* and *RELB*, which encode the seven members of the human NF-κB family p105 (p50), p100 (p52), RelA/p65, c-Rel, and RelB (Hayden and Ghosh, 2004). These family members are further subdivided according to their transcriptional properties, for example, c-Rel, RelB and p65 proteins all contain C-terminal, non-homologous, transactivation domains (TAD).

These TAD are responsible for the transcriptional activity of these proteins at target gene promoters *via* interaction with the basal transcriptional machinery and co-regulators (Chen et al., 2005b). The p105 and p100 proteins contain C-terminal ankyrin repeats with inhibitory properties which are removed during processing to reveal the active factors p50 and p52 respectively. The resultant p50 and p52 proteins do not contain TADs and therefore mediate their transcriptional activity *via* hetero-dimerisation or interaction with transcriptional regulators, such as BCL3 (Hayden and Ghosh, 2004).

The diversity afforded to the NF-κB family through the ability to homo- and hetero-dimerise suggests a multifunctional role for these transcription factors and there is new data emerging constantly about novel functions of each of the subunits and associated proteins. Animal knock-out models have, however, provided a host of data purporting to the exact functionality of each subunit and also the associated proteins. This is summarised in Table 1.1. This table not only details the knockout of each of the five subunits, but also the inhibitory protein, BCL3 (discussed is section 1.2.1.2) and the inhibitor of kappa-B kinase (IKK) family members, which are discussed in section 1.2.1.3. It should be noted here that these traditional gene knockouts may not provide the best route to determine the exact role of individual subunits as loss of one NF-κB subunit can result in a rebalancing of the other subunits, thus meaning there is a compensatory effect. Furthermore, p65 can regulate the expression of other subunits, it is important to take this into account.

Knockout	Phenotype	Biological role	Reference
p65/RelA	Embryonic lethal at E15-16 due to massive liver degeneration	Crucial for normal development and for the protection against TNF-α apoptotic signalling	(Beg et al., 1995)
p50	No developmental abnormalities. Multi-focal defects in immune response including decreased immunoglobulin production and defective humoral responses. B cells do not respond to lipopolysaccharide (LPS)	Indicates the importance of dimers containing p50 in inflammatory signalling. Also suggests that p50 is redundant in TNF-α induced apoptotic signalling	(Sha et al., 1995)

	stimulation		
p52	Mice are unable to generate antibodies to T-dependent antigens. B cell follicles and dendrite cell networks are absent	Mice lack both the p100 precursor and the p52 subunit. Suggests that p52 is important in neurological cell development	(Franzoso et al., 1998)
c-Rel	Mice develop normally however they exhibit significantly reduced B-cell proliferation and have irregular germinal centres and reduced numbers of marginal zone B cells	Suggests that c-Rel has a role in haematopoiesis and B cell development	(Kontgen et al., 1995)
RelB	Mixed inflammatory cell infiltration in multiple organs. Myeloid hyperplasia. Loss of dendritic cell function	Indictaes that RelB has a role in maintaining cellular immunity	(Weih et al., 1995)
BCL-3	Similar phenotype to that of p52 knockout. Mice fail to generate appropriate T-dependent antibody response to some viruses and have impaired germinal centre reactions	Role in antigen-specific priming of T and B cells	(Bours et al., 1993)
IKKα	Not embryonic lethal, however at E18.5 mice have rudimentary limbs and tail, craniofacial deformaties and skeletal abnormalities. Mice also have an increased thickness to the epidermis	Crucial role for IKKα in skeletal and dermal development. Some evidence for hyper-proliferation of cells in basal layers of the epidermis due to IKKα knockout	(Li et al., 1999a)
IKKβ	Embryos die at E14.5 due to liver degeneration and apoptosis. Do exhibit some basal NF-κB DNA binding activity in response to TNF-α/IL-1	Similar to p65 knockout. Essential role of IKKβ the protection apoptotic signalling	(Li et al., 1999b, Tanaka et al., 1999a)
NEMO/IKKγ	Embryos die at E12.5-13 due to severe liver damage due to apoptosis. No NF-	Required for the protection against apoptosis and also the	(Rudolph et

	κB DNA binding activity in response to TNF-α/IL-1	activation of NF-κB	al., 2000)

Table 1.1: The biological role of NF-κB associated proteins This details the knockout of each of the five subunits, but also the inhibitory protein, BCL3 and the IKK family members, which are discussed later in this chapter

1.2.1.2 NF-κB inhibitory proteins

The classical definition of an inhibitor of κB (IκB) protein is two fold: to bind to, and prevent activation of, an NF-κB dimer, and to undergo degradation upon stimulation to allow rapid activation of the transcription factor. There are seven well characterised members, which include IκB-α, IκB-β, IκB-ε, BCL-3 and IκB-γ, the structures of which are shown in Figure 1.3. The NF-κB precursor proteins, p100 and p105 are also classified as inhibitory proteins, and the structure of these are shown in Figure 1.2. Importantly, all seven inhibitory proteins contain five to seven ankyrin repeats that have the ability to form elongated cylinders to bind the dimerisation domain of NF-κB dimers (Hatada et al., 1992).

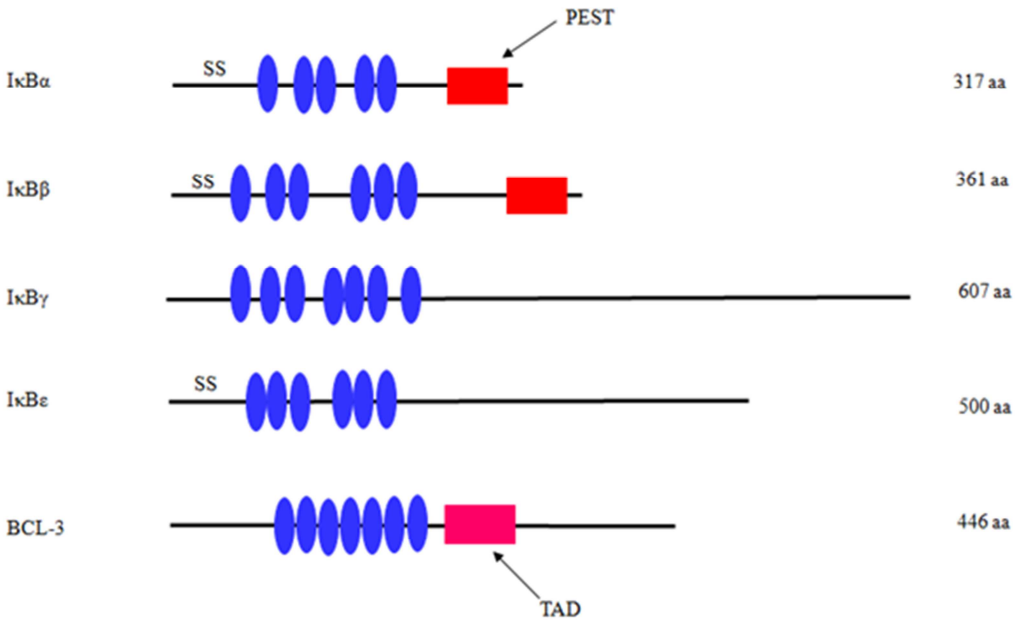

Figure 1.3: The Inhibitor of NF-κB (IκB) proteins SS: Phosphorylation of two serine residues. PEST: Domain rich in proline (P), glutamate (E), serine (S) and threonine (T).
Adapted from: (Chen and Greene, 2004)

The mechanism of NF-κB activation is both cell type and stimulus specific (see section 1.2.2) and the indivdual IκB proteins have been linked to different activation pathways.

IκB-α is involved in the canonical or traditional pathway of NF-κB activation induced by numerous agents including tumour necrosis factor-α (TNF-α) and lipopolysaccharide (LPS). Huxford *et al.*, (1998) solved the crystal structure of IκBα in complex with the NF-κB p50/p65 heterodimer revealing a mechanism for the inhibition of this heterodimer (illustrated in Figure 5). This group reported that the IκB proteins mask a conserved nuclear localisation sequence (NLS) found in the RHD of p65, whilst the NLS of p50 remains accessible (Huxford et al., 1998). This accessible NLS on p50 along with a nuclear export sequences (NES) on IκBα and p65 result in the constant shuttling of IκBα:NF-κB complexes between the nucleus and the cytoplasm, although the steady-state location is in the cytosol (Huang et al., 2000). The equilibrium between the localisations is altered on degradation of IκBα by removal of its NES and unmasking of the p65 NLS, resulting in the nuclear localization of active NF-κB (Hayden and Ghosh, 2004).

Following stimulation, IκBα is phosphorylated by the IκB-kinase (IKK) complex (section 1.2.1.3) at residues Serine 32 and 36, targeting the protein for polyubiquitination. This ubiquitination of Lysine 21 and 22 of the IκBα protein then targets it for degradation by the 26S proteasome (Hayden and Ghosh, 2004). Following degradation of the inhibitory protein, NF-κB dimers translocate to the nucleus where they initiate transcription using the promoters of target genes. The promoter of the *NFKBIA* gene, which encodes the IκBα protein, contains multiple NF-κB consensus sequences, and as a result the level of IκBα is regulated by NF-κB (Hertlein et al., 2005), illustrating a negative feedback mechanism.

The IκBβ and IκBε proteins are associated with dampening oscillations of transcriptional activity during long-term stimulation of NF-κB subunits during processes such as T-cell activation in the immune response (Chen et al., 2004, Saccani et al., 2004). IκBα and IκBβ have some structural and sequence similarity but unlike IκBα, IκBβ does not contain a NES which means that inhibitory complexes it forms with NF-κB dimers do not undergo a cytoplasmic-to-nuclear shuttling process in the resting state (Chen et al., 2004). IκBβ is not fully degraded following stimulation, and although p65 null cells display a marked reduction in IκBα, the IκBβ levels are barely detectable suggesting this protein is not regulated by NF-κB (Hertlein et al., 2005).

The non-canonical pathway of NF-κB activation (section 1.2.2.2) results in the processing and release of p52 NF-κB subunits from its precursor protein, p100. These precursors contain ankyrin repeats which are cleaved within a glycine rich region to produce the active subunits. Therefore it is thought that p105 and p100 display an inherent IκB activity of their own (Hayden and Ghosh, 2004). Interestingly, the study of lymphotoxin β (LTβ) mediated p100 processing has suggested that p100 is an inhibitor of p65 as well as p52. Cell lines deficient in the p100 protein displayed retarded p65 activity in response to LTβ, but not TNF-α, suggesting a stimulus-specific role for this protein in regulating NF-κB activity (Basak et al., 2007).

Other IκB proteins, including BCL-3, are different from those previously discussed as they are constitutively nuclear, not degraded following signalling and appear to facilitate transcriptional activation. As previously mentioned, BCL-3 binding to either of the repressive subunits, p50 or p52 can facilitate DNA binding through complex formation (Perkins, 2007).

1.2.1.3 IKK complex

The activation of NF-κB signalling can be modulated by a diverse range of stimuli; however two of the three major pathways associated with these processes converge on the IKK complex. The IKK complex is a 700-900 kDa structure comprising IKKα, IKKβ and IKKγ (Figure 1.4), the latter of which is often referred to as the NF-κB essential modulator (NEMO). The IKK complex is responsible for the phosphorylation of IκB proteins, which in turn targets them for degradation and allows translocation of the active NF-κB dimer to the nucleus. The IKKα and IKKβ subunits display just over 50 % sequence identity, both containing a N-terminal kinase domain, leucine zipper (LZ) and helix-loop-helix motifs (HLH) within their C-terminal regions. These proteins also share a key lysine 44 residue within the ATP-binding site of the kinase, which is essential for their activity. Mutational studies have revealed an essential role for the HLH and LZ domains within these IKK subunits in the phosphorylation of serine residues of target protein. Although IKKγ/NEMO lacks kinase activity, it has been shown to be essential for NF-κB transcriptional activation (Perkins, 2007). In fact knockout mouse models of individual IKK components (Table 1.1) have shown that both IKKβ and IKKγ/NEMO are essential for the protection against apoptosis and that IKKα is essential for skeletal and dermal development (Li et al., 1999b, Rudolph et al., 2000, Tanaka et al., 1999a).

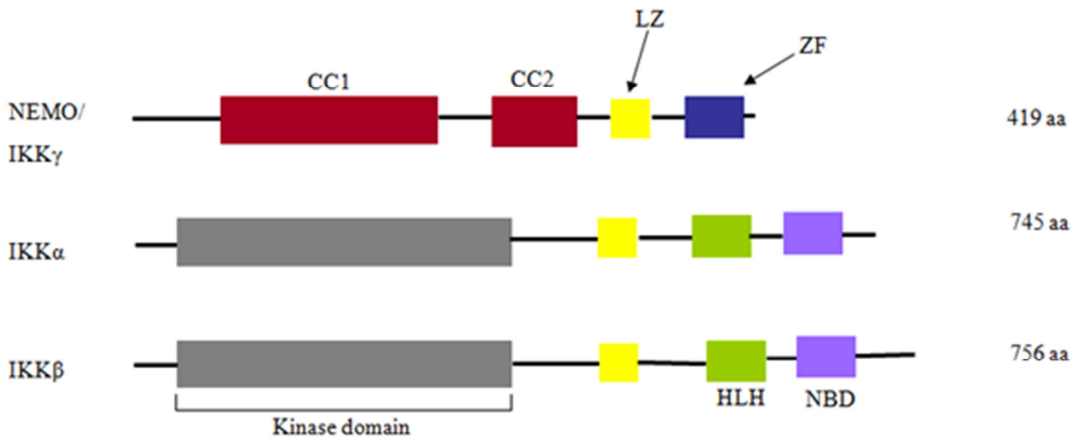

Figure 1.4: Three core subunits of the IKK complex LZ: Leucine zipper. GRR: CC: Coiled-coil. ZF: Zinc finger. HLH: Helix-loop-helix. NBD: NEMO-binding domain. Adapted from: (Chen et al., 2004)

IKKα, IKKβ and IKKγ/NEMO remain the most well characterised members of the IKK complex, however other associated family members, including IKKε have been identified. During signalling, members of both the NF-κB and IκB superfamilies, as well as chaperone proteins, have been shown to associate with the IKK complex. Interestingly, IKKε has recently been shown to have oncogenic properties in breast cancer (Boehm et al., 2007), and the SUMOylation of this IKK protein is also essential for the activation of NF-κB following DNA damage by the topoisomerase II posion, etoposide (Renner et al., 2010).

Importantly, the IKK complex has many known functions that are independent of its role in the activation of NF-κB (Chariot, 2009). Most recently it has been shown that the IKK complex is important in the induction of autophagy (Criollo et al., 2010). In particular, IKKβ can phosphorylate a number of other substrates, including the tumour suppressor, FOXO3a, which in this case results in a protection against apoptosis (Huang and Tindall, 2006). It can also activate 14-3-3β when the protein is complexed to tristetraprolin, resulting in the stabilization of cytokine, chemokine and growth factor mRNAs (Gringhuis et al., 2005), suggesting that like NF-κB, the IKK complex is an important mediator of inflammatory signalling. IKKβ has also been linked to the proliferative Mitogen-activated kinase pathway (MAPK) pathway since the p105 NF-κB subunit is found complexed to the ERK kinase, TPL2, in some unstimulated cells. Hence, IKKβ-mediated proteolysis of the p105 subunit, can result in TPL2 release and

MAPK pathway activation (Waterfield et al., 2004). Tu *et al.*, (2006) described that IKKα regulated oestrogen-induced cell-cycle progression by indirectly inducing the transcription factor, E2F1 in MCF7 cells (Tu et al., 2006). This IKK protein is thought to play a role in cell proliferation through the regulation cyclin D1 expression. IKKα regulates cyclin D1 expression in a number of ways, including, through the activation of the NF-κ p52 subunit (Rocha et al., 2003).

It is often difficult to disentangle the NF-κB subunit specific effects and those which are NF-κB independent IKK effects due to the types of experiment performed. For example many mouse models are IKK knockouts or mutants, or cell culture experiments use the IκB super repressor. It is highly likely the tumour promoting effects (section 1.2.4.2) derive from a combination of both the NF-κB subunits and also independent IKK functions but this is an area which requires much further work.

1.2.2 NF-κB activation pathways

There are several distinct NF-κB activation pathway (Figure 1.5), often referred to as the canonical, non-canonical and atypical pathways (Perkins, 2007).

1.2.2.1 Canonical pathway activation

The canonical, or classical pathway of NF-κB activation is stimulated in response to inflammatory stimuli in the cellular environment, for example the pro-inflammatory cytokines TNF-α and interleukin-1 (IL-1), growth factors, such as epidermal growth factor (EGF) and transforming growth factor-α (TGF-α), engagement of the T-cell receptor (TCR) or exposure to bacterial products, such as lipopolysaccharides (LPS) (Hayden and Ghosh, 2004). This pathway, shown in Figure 1.5, is dependent on the IKK complex in particular IKKβ, which is responsible for the rapid phosphorylation of of IκBα at serine residues 32 and 36, which targets IκBα for ubiquitination and subsequent proteosomal degradation, which in turn results in the active NF-κB hetero-dimer (commonly the p65:p50) dimer, in translocating to the nucleus. This in turn allows NF-κB to bind to specific consensus sequences in the promoter region of target genes, or κB elements, and regulate gene transcription. Subsequently, this rapid induction of the canonical pathway can be terminated by the NF-κB dependent endogenous inhibitors, for example A20, which serve to turn off this transient transcriptional activation (Hayden and Ghosh, 2004, Perkins, 2006). It should also be noted that other IκB proteins, including IκBβ and IκBε can also be phosphorylated in

response to canonical pathway stimuli, however the kinetics of this are much slower (Perkins, 2007).

IKKβ and IKKγ/NEMO cooperate to mediate the classical NF-κB activation pathway, targeting IκBα in preference to the β protein and it has been reported that IKKγ/NEMO is key in the activation of the IKK complex since activation of the canonical pathway leads to complex, lysine 63-linked ubiquitination of signalling molecules, which ultimately results in the ubiquitination of IKKγ/NEMO, which is also lysine 63-linked (Perkins, 2006). This ubiquitination differs from lysine 48-linked ubiquitination, which mediates protein degradation, in that it is implicated in the signalling of proteins containing ubiquitin-binding domains (Burns and Martinon, 2004, Chen, 2005, Krappmann and Scheidereit, 2005). Kinases are then recruited to ubiquitinated IKKγ/NEMO and subsequently the IKK complex, such as TGFβ-actived kinase 1 (TAK1), which has the ability to phosphorylate IKKβ at serine residues 177 and 181, resulting in the activation of this IKK component (Burns and Martinon, 2004, Chen, 2005, Krappmann and Scheidereit, 2005, Perkins and Gilmore, 2006).

The canonical pathway can also be activated by genotoxic stimuli, including IR and other DNA-damaging chemotherapeutic drugs, in a manner which is dependent on IKKγ/NEMO-IKKβ activation (Janssens and Tschopp, 2006). This is discussed in detail in section 1.4. Briefly, NEMO translocates to the nucleus and is SUMOylated and subsequently phosphorylated by the checkpoint kinase, ataxia telangiectasia mutated (ATM), known to signal and respond to double stranded DNA breaks (DSBs). The sumoylation of NEMO is then displaced by mono-ubiquitination, which results in the ATM:NEMO complex relocating back to the cytoplasm to activate IKKβ. Wu *et al*,.(2006) reported this link between ATM and NEMO in 2006, and also suggest that the process requires and IKK-associated protein called ELKS (a protein rich in glutamine (E), leucine (L) lysine, (K) and serine (S)) (Wu et al., 2006). ATM, along with other DNA repair proteins, poly(ADP)-ribose polymerase-1 (PARP-1) and the DNA-dependent protein kinase (DNA-PK) are also implicated in the regulation of NF-κB in response to DNA damage and will be discussed further in sections 1.4 and 1.5.

Most recently, hypoxia has been shown to activate NF-κB in an IKK-dependent manner through phosphorylation of the IKK complex by the upstream kinase TAK1 along with the calcium/calmodulin dependent kinase 2, the E2-ubiquitin ligase, Ubc13 and the E3

ligase XIAP (Culver et al., 2010, Melvin et al., 2011). Furthermore, NF-κB subunits have also demonstrated the ability to both bind and activate the hypoxia inducible factor 1α (HIF-1α) gene (Rius et al., 2008, van Uden et al., 2008)

1.2.2.2 Non-canonical pathway activation

A second pathway for NF-κB activation is the non-canonical pathway (Figure 1.5), and whereas IKKβ is the predominant activator of NF-κB nuclear translocation in the canonical pathway (Bonizzi and Karin, 2004, Pasparakis et al., 2006), it is IKKα that is mainly involved in this pathway (Perkins, 2003). In this instance, IKKα is activated by the NF-κB-inducing kinase (NIK) in response to stimulation of the lymphotoxin-β and CD40 receptors, the latent membrane protein-1 (LMP-1) of the Epstein Barr virus or the B-cell activating factor of the TNF family (BAFF). This results in the formation of p52 from p100 after IKK-α mediated phosphorylation of Lysine 855 (within the p100 protein) results in the recruitment of a ubiquitination complex and targeting of the protein for cleavage (Scheidereit, 2006). This results in the frequent activation of RelB:p52 heterodimers which may result in the activation of a distinct subset of NF-κB-dependent genes (Perkins, 2007).

1.2.2.3 Atypical pathway activation

A third mechanism for NF-κB activation (Figure 1.5) has been described in response to stimuli such as hydrogen-peroxide and nerve growth factor (NGF) and is called the atypical, or IKK-independent pathway (Perkins, 2007). The outcome in this case is the phosphorylation of IκBα at tyrosine 42 which leads to free NF-κB by either degradation or dissociation of the IκB member (Perkins, 2006, Perkins and Gilmore, 2006). Expression of the HER2 oncogene, which is over-expressed in approximately 25% of all breast cancers, and also treatment with ultraviolet (UV) light can also activate NF-κB in an IKK-independent manner by mediating the phosphorylation of IκBα in its C-terminal PEST domain, by casein-kinase-II (CK2) (Perkins, 2006).

1.2.3 NF-κB activation stimuli and the transcriptional response

The NF-κB pathway is activated by a diverse range of agents ranging from endogenous cytokines to DNA-damaging agents and pathogens. Activation of NF-κB signalling pathways, by the well characterised stimuli, such as TNF-α or LPS, are relatively universal and converge at the IKK complex. However, the upstream signalling cascades

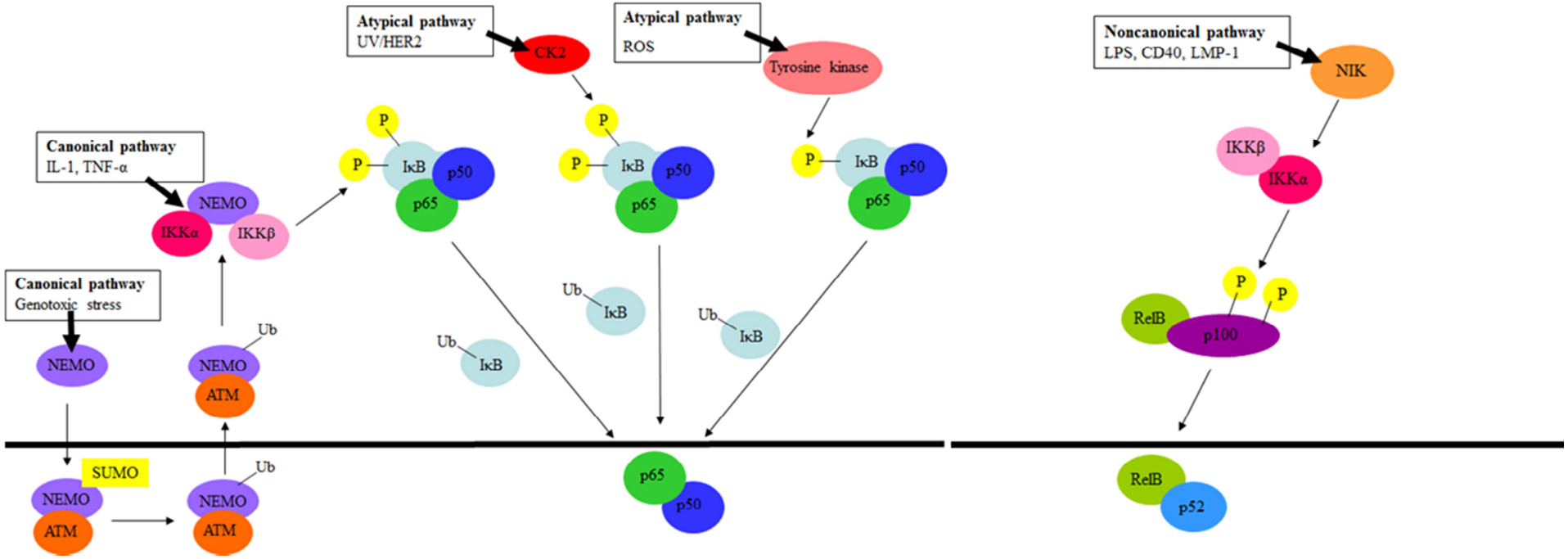

Figure 1.5: NF-κB activation pathways The canonical pathway (left) is activated by various stimuli including TNF-α and IL-1. This results in the phosphorylation of IκB, targeting it for ubiquitination by the IKK complex, which frees the p65-p50 heterodimer, allowing it to translocates to the nucleus. This pathway is also activated in response to genotoxic stress via the SUMOylation of NEMO and the complexing of this IKK component to ATM. The atypical pathway (centre) can be activated in 2 ways – the first by ultraviolet light which results in IκB phosphorylation by casein kinase2 and the second by hypoxia resulting in phosphorylation by a tyrosine kinase. The non-canonical pathway (right) results in activation of IKKα by NIK followed by phosphorylation of the p100 subunit by IKKα. Consequently proteosome-dependent processing of p100 to p52 leads to activation of p52-RelB heterodimers. Adapted from: (Perkins, 2007)

tend to be stimulus specific, and the transcriptional output is also governed by the activation stimulus.

The most well characterised stimulators of NF-κB activation are those associated with the immune and inflammatory responses. Inflammatory cytokines, such as IL-1β and TNF-α, bind to cell surface receptors inducing a downstream signalling cascade which leads to NF-κB activation. Following either of these stimuli, the NF-κB transcriptional response is most often associated with the up-regulation of key inflammatory mediators, including cytokines and chemokines, such as CXCL10 (Hein et al., 1997) and IL-8 (Kunsch and Rosen, 1993). Interestingly, both TNF-α and IL-1β are NF-κB target genes themselves. TNF-α mediates the activation of NF-κB as well as that of the Activator Protein-1 (AP-1) transcription factor. To this end, the two transcription factors work in concert in promoting programmed cell death, and the balance of these factors is key in determining the apoptotic function of a cell (Dutta et al., 2006). For example, TNF-α-mediated NF-κB activation is known to up-regulate the expression of the Fas receptor (Chan et al., 1999) and its ligand (Matsui et al., 1998), which induce apoptosis.

Similarly, bacterial pathogens such as LPS, a component of the gram positive cell bacterial wall, are able to stimulate NF-κB transcriptional activity and mediate the production of immune and inflammatory response genes *via* the Toll-like receptor signalling (Coll and O'Neill, 2010). Whilst TNF-α activates NF-κB in a canonical pathway/IKKβ-dependent manner, it has been shown that CD-40 and LTß bind to members of TNF receptor (TNFR) family and mediate the non-canonical NFKB2 processing. In fact TNFR family ligands stimulate both the classical and non-classical NF-κB activation pathways with additional domains contained within their receptors thought to mediate this dual activation (Hayden and Ghosh, 2004, Hayden et al., 2006).

Induction of NF-κB by genotoxic stress and subsequent DNA damage recognition pathways is a well-documented phenomenon, and in recent years many studies have started to elucidate the mechanisms by which DNA-damage activates NF-κB. (This is discussed is more detail in sections 1.4 and 1.5). The cellular response to DNA damage is somewhat complex. Whereas low doses of TNF-α have been shown to activate NF-κB in many cellular systems, the activation of NF-κB by DNA-damaging agents is appears to be much more cell type specific. For example, Brach *et al.*, (1993) illustrated that doses of IR as low the clinically relevant dose of 2 Gy were sufficient to activate

NF-κB in the human myeloid cell line, KG-1 using electrophoretic mobility shift assays (EMSAs) (Brach et al., 1993), whereas the optimum dose for the U1-Mel melanoma cell line was found to be 3-4.5 Gy (Sahijdak et al., 1994), whilst Ashburner *et al.*, (1999) found that doses as high as 20 Gy failed to activate NF-κB in other human tumour cell lines (Ashburner et al., 1999).

More recently, hyper-lethal doses of IR have been used to activate NF-κB, and study the downstream signalling associated with this (Stilmann et al., 2009, Veuger et al., 2009). Both of these groups have investigated the role of PARP-1 in the activation of NF-κB following DNA-damage, and have found that PARP-1 activity, which is known to be induced following single stranded DNA breaks (SSBs), is vital for the activation of NF-κB after high doses of IR. This discussed in detail in section 1.3.2.1 Furthermore, other DNA repair proteins, such as ATM and DNA-PK are also required for the activation of NF-κB following DNA damage (Basu et al., 1998, Hinz et al., 2010, Ju et al., 2010, Liu et al., 1998, Panta et al., 2004, Veuger and Durkacz, 2011, Wu et al., 2006), and the mechanisms associated with this are discussed in section 1.4.

The activation of NF-κB by DNA damaging agents is reported to confer a cell survival advantage through the induction of anti-apoptotic genes, such as the inhibitor of apoptosis proteins (IAPs) (Stehlik et al., 1998, You et al., 1999). It is not only anti-apoptotic genes which are regulated by NF-κB, but genes associated with cell proliferation, angiogenesis and metastasis are also under the control of NF-κB, and are widely reported to contributes to malignant progression through this gene expression. Activation of NF-κB by DNA damaging chemotherapeutic agents is therefore postulated to be one of the major mediators of both chemo- and radio-resistance (Biswas et al., 2001, Wu and Kral, 2005), and hence the inhibition of NF-κB is an attractive therapeutic strategy (section 1.2.5).

However, it should be noted that a subset of NF-κB activating agents are able to mediate a pro-apoptotic function for this transcription factor. Exogenous agents such and UV-C and daunorubicin, a commonly used chemotherapy drug, activate NF-κB via both IKK-dependent and -independent mechanisms resulting in a repression of anti-apoptotic genes. This repressive function is mediated by the p65 NF-κB subunit which associates with the histone deacetylase -1 (HDAC1) protein repressing transcription at target promoters in response to these stimuli (Campbell et al., 2004).

1.2.4 NF-κB and disease

NF-κB has been associated with numerous pathologies including inflammatory diseases such as arthritis, immune responses, atherosclerosis and the progression of many metastatic cancers (Hayden and Ghosh, 2004). It is the regulation of gene expression by NF-κB, which mediates this link with human disease, and therefore understanding the molecular events which result in the de-regulation of NF-κB activation, and its subsequent gene regulation, is key in the development of therapeutic targets for the treatment of these numerous disease states. Much of the research surrounding NF-κB has been directed towards inflammatory diseases and malignancies, however, alterations in NF-κB activation has also been reported in asthma, HIV and AIDS, and liver disease, to name but a few (DeLuca et al., 1999, Kumar et al., 2004). The function of NF-κB in a selection of key diseases is discussed briefly below.

1.2.4.1 NF-κB in inflammatory disease

The role of NF-κB activation in inflammation (Tak and Firestein, 2001) is well documented and it is the kinase, IKKβ which has been reported as the primary participant in the production of proinflammatory stimuli associated with NF-κB activation (Aupperle et al., 1999). Aupperle *et al.,* (1999) showed that IKKβ is expressed in fibroblast-like synoviocytes and has a crucial role in NF-κB activation following either TNF-α or IL-1 stimulation. This study used synoviocytes isolated from the synovium of patients with rheumatoid arthritis (RA) and osteoarthritis, and illustrates that, in both groups, immunoreactive forms of IKKα and IKKβ were constitutively expressed at the mRNA level. This would suggest that NF-κB is also constitutively active in these cell types, something which is supported by the induction of cytokines found here which are known to be regulated be NF-κB. These include IL-6, IL-8 and ICAM-1 (Aupperle et al., 1999).

Other proinflammatory cytokines induced by NF-κB in concert with another transcription factor, AP-1, have also been implicated in the pathology of RA after NF-κB over-expression was noted in the synovium of such patients. This study showed that when NF-κB and AP-1 are simultaneously activated by either IL-1 or TNF-α in synoviocytes, the expression of matrix metalloproteinases (MMPs) is increased. MMPs are known to contribute to the destruction of bone and cartilage in an RA joint (Han et al., 1998). The authors also found that NF-κB induced transcription of other known inflammatory response molecules including cyclooxygenase-2 (COX-2) and inducible

nitric oxide (iNOS) in these cell types (Han et al., 1998). Therapies targeted at NF-κB blockade are now being developed for use in RA patients and these include NF-κB decoy oligonucleotides which are administered either by injection or viral gene transfer. Results have shown that these can inhibit streptococcal cell wall-induced arthritis in rats, in part by decreasing the production of cytokines, and mediating the induction of apoptosis (Miagkov et al., 1998).

Increased NF-κB nuclear activity in airway epithelial cells of asthmatic patients was found to be common, along with the high expression levels of the proinflammatory cytokines, chemokines, Cox-2 and iNOS (Hart et al., 1998). Another condition, Helicobacter pylori-associated gastritis is also marked by increased NF-κB, and in this case disease severity correlates with the number of NF-κB positive cells (van Den Brink et al., 2000). NF-κB has been implicated in the prolonged inflammation and resultant lack of bowel function in Chrohn's disease and ulcerative colitis. Moreover, corticosteroids, which are known to inhibit NF-κB transcriptional activitation, have long been used to treat inflammatory bowel disease (IBD) (Kumar et al., 2004). Notably, patients that suffer from IBD have been shown to have an increased risk of developing bowel cancer, and it has been postulated that the NF-κB transcriptional axis is involved in this disease progression (Greten et al., 2004).

The gene encoding the NEMO subunit of the IKK complex is located on the long arm of the X chromosome and its mutation is causative of a number of genetic pathologies, including *Incontinentia pigmenti*. This results in severe skin inflammation and cutaneous skin lesions (Berlin et al., 2002) as the associated truncated form of NEMO is able to interact with the α and β-subunits of the IKK complex, but it displays a defect in subsequent NF-κB activation. Similarly, rare inherited mutations in the *IKBA* gene result in severe immunodeficiency associated with a lack of immune memory. Critically these patients display a point mutation at Ser-32 within the IκB-α protein resulting in a deficit in the classical activation pathway of NF-κB (Courtois et al., 2003).

1.2.4.2 NF-κB and Cancer

NF-κB is known to regulate genes involved with apoptosis, cell proliferation and differentiation (Hayden and Ghosh, 2004); therefore it is unsurprising that this transcription factor is implicated in many cancers. Aberrant NF-κB activity has been documented in numerous tumour types including pancreatic, lung, breast and prostate,

as well as some haematological malignancies (Basseres and Baldwin, 2006). NF-κB has been shown to contribute to key events within tumour progression including metastasis, angiogenesis and the avoidance of apoptosis (Figure 1.6). The role of NF-κB in malignant progression is a topic of continuing research for a number of groups around the world, as is the development of compounds which inhibit NF-κB function. Currently, the mounting body of data suggests that NF-κB plays an important role in the progression of many cancers but it is important to mindful that most of these studies have been undertaken in cancer cell line models, and may not reflect the *in vivo* situation. Moreover, some studies are vague and do not elucidate the precise mechanisms by which NF-κB is associated with the progression of cancer. A brief discussion of the literature relevant to this study is undertaken here.

There have been a number of links between chronic inflammation and the development of cancer. NF-κB was implicated in the production of growth factors crucial for the growth of neoplastic cell and cancer progression, when it was observed that loss of IKKβ, the primary participant in the production of pro-inflammatory stimuli associated with NF-κB activation (Aupperle et al., 1999), in myeloid cells led to a decrease in tumour size accompanied by reduced levels of tumour derived inflammatory cytokines (Kim et al., 2006). Another study observed a reduction in tumour number but not size, alongside reduced expression of NF-κB- dependent anti-apoptotic gene expression, in an IKKβ defective model of colitis associated bowel cancer (Karin, 2006). These data indicate a cell-type specific role for NF-κB in tumour progression.

The majority of studies to date have concentrated on the role of p65 transcriptional activation in cancer, and there is a wide body of literature which documents the de-regulation, and most commonly, the aberrant activation of this subunit in many forms of cancer and leukaemia where is correlates with poor prognosis and an increased metastatic potential (Prasad et al., 2010). It remains to be seen whether constitutive activation of p65 is more common than that of other subunits in cancer, or whether this is simply due to more research being undertaken. For example, traditional methods of assessing NF-κB DNA binding such as EMSAs, lent themselves to the assessment of the p65 and p50 subunits rather than the others as antibodies against these particular subunits were readily available and easy to use, however more recently robust antibodies have been developed against the other subunits.

More recently however, it was found that the human *REL* gene, that encodes the c-Rel protein, is the only NF-κB transcription factor for which there is a retroviral counterpart, that is acutely oncogenic. Moreover, retroviral vectors for the overexpression of chicken, mouse or human c-Rel were also found to transform chicken lymphoid cell *in vitro* (Gilmore, 1999, Starczynowski et al., 2003). Amplification of chromosome 2p, on which the *REL* gene is located have been detected at significant frequencies in human B- and T-lymphoma, including Hodgkin's lymphoma and diffuse large B-cell lymphoma (DLBCL), where it has been shown to correlate with poor prognosis (Davis et al., 2001, Fukuhara et al., 2006, Houldsworth et al., 2004, Rosenwald et al., 2002, Rosenwald et al., 2003). These data suggest that the increased copy number of *REL*, in turns leads to over-expression of the c-Rel protein, which can saturate the IκB proteins and lead to aberrant activation of c-Rel and up-regulation of its target genes, however many studies are purely correlative in this case and have not explored the functional aspects of *REL* overexpression.

Other NF-κB family members and associated proteins and genes have been implicated in oncogenesis and tumour progression in lymphomas and other haematological malignancies. A transforming truncation of the p100 gene at 10q24 has been recognised in the t(14:19) translocation involving the BCL3 protein have been demonstrated in DLBCL and CLL (Neri et al., 1991). Recently, Compagno *et al.*, (2009) reported that over 50 % of some subsets of DLBCL carried multiple mutations in negative (A20) and positive (*CARD11, TRAF2, TRAF5, MAP3K7 (TAK1)* and *TNFRSF11A (RANK)*) regulators of NF-κB. They also found that A20, which is a target for NF-κB-dependent gene expression and encodes a ubiquitin-modifying enzyme involved in termination of NF-κB activation, was most commonly affected, with approximately 30% of patients displaying biallelic inactivation resulting from mutations or deletions. Interestingly, this group went on to undertake some functional studies by re-introducing A20 into some DLBCL cell lines carrying biallelic inactivation of the gene, and showed that A20 induced apoptosis and cell growth arrest,. These data suggest a putative tumour suppressor role for A20 (Compagno et al., 2009).

It has been postulated that aberrant NF-κB activation in cancer is responsible for the up-regulation of anti-apoptotic genes, meaning that the tumour cell can evade death. These genes include; those coding for the TNF-receptor associated factor-1 (TRAF-1) and TRAF-2 (Pahl, 1999), *IEX-1L* (Wu et al., 1998) and importantly two members of the

Bcl-2 family, *BFl-1/A-1* and *Bcl-xl* (Lee et al., 1999a, Zong et al., 1999). Some groups have also reported that NF-κB activity enhances that of Bcl-2 in primary hippocampal neurons (Tamatani et al., 1999) and Epstein-Barr virus transformed lymphocytes (Feuillard et al., 2000). However, others have illustrated that it is Bcl-2 over-expression which enhances the activity of NF-κB (Ricca et al., 2000), nevertheless, both demonstrated that NF-κB activity induces anti-apoptotic genes. Using the breast cancer cell line, MCF-7 and the colon cancer cell line, HCT116, Bours *et al.*, (2000) showed that NF-κB inhibition results in decreased Bcl-2 expression, and increased expression of Bax, a pro-apoptotic gene (Bours et al., 2000).

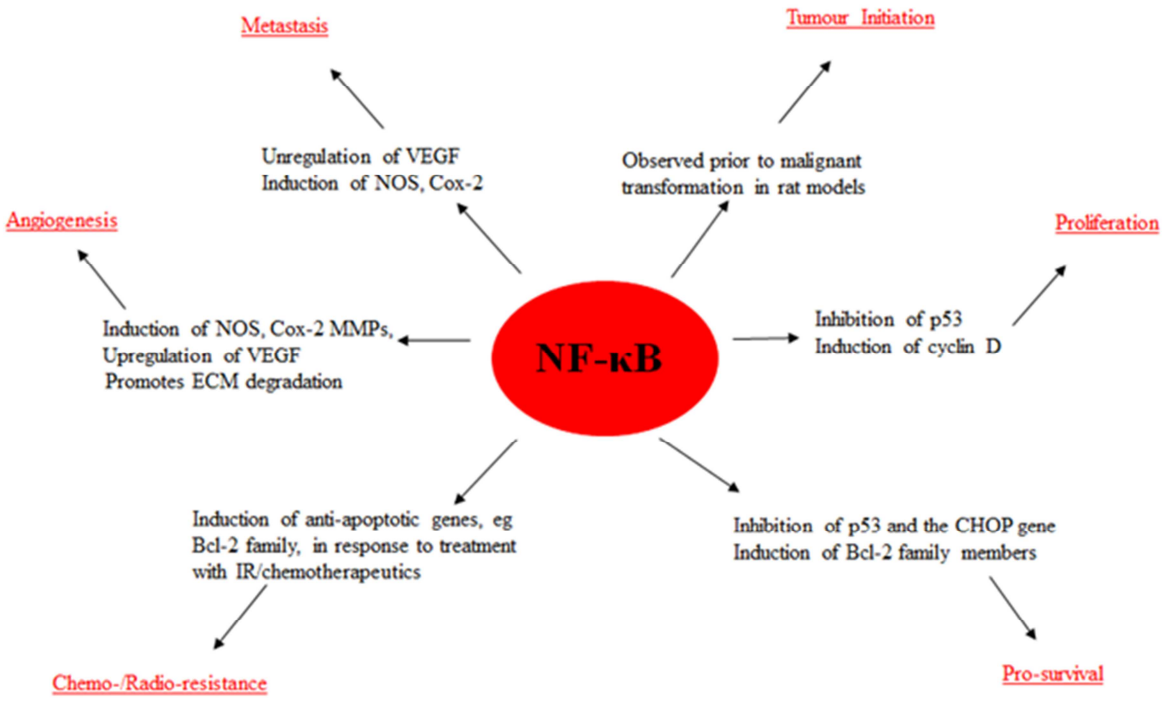

Figure 1.6: NF-κB and the development of cancer NF-κB is involved in the initiation, development and spread of various cancers, including breast cancer in which the transcription factor is constitutively active. NF-κB is known to activate genes involved with cell proliferation, and the inhibition of apoptosis and angiogenesis, which are known to contribute to the development of cancer.
Adapted from: (Wu and Kral, 2005)

NF-κB activation is known to induce genes associated with proliferation, such as cyclin D1 after the IκBα phosphorylation by IKKα. Cyclin D1 is known to aid in cell cycle control via CDK4 and CDK6 (Rocha et al., 2003). Guttridge *et al.*, (1999) noted that, in mammary epithelium, a member of the TNF-family, RANK (receptor-activator of NF-κB) induced the activation of NF-κB via IKKα, therefore inducing high levels of proliferation in these cells (Guttridge et al., 1999). It is noteworthy that there is a positive correlation between the over-expression of cyclins D and E and the

pathogenesis of breast cancer (Wu and Kral, 2005). The cyclin D1 gene is up regulated in 20% of early stage human breast cancers, whilst the cyclin D protein is over-expressed in over 50% (Dickson et al., 1995). It has been suggested that cyclin E is oncogenic as breast cancer develops in approximately 10% of transgenic mice expressing this cell cycle protein (Bortner and Rosenberg, 1997). Poor prognosis of the disease was associated with high levels of both cyclin E and cyclin D1 (Berglund and Landberg, 2006). Unlike cyclin D, it not known if cyclin E is an NF-κB target gene, however one group has reported an association between the two at G1-S phase (Chen and Li, 1998), indicating a further role for NF-κB in cell cycle progression.

NF-κB is also implicated in the regulation of some known tumour suppressor proteins, including p53, BRCA1 and BRCA2, all of which are involved in the cellular response to DNA damage (see section 1.3.2.1). Negative regulation of p53 by NF-κB is thought to contribute to tumourgenesis, through a number of mechanisms (Perkins, 2007). Tergaonkar *et al*., (2002) detailed how levels of the E3 ubiquitin ligase, MDM2 are controlled by NF-κB, hence negatively regulating the stability of p53 (Tergaonkar et al., 2002). The up-regulation of anti-apoptotic genes by NF-κB is also thought to antagonize the pro-apoptotic functions of the tumour suppressor. Ravi *et al.,* (1998) provided evidence which documented how the p65 NF-κB subunit and p53 regulated each other's activity by vying for finite pools of p300 and CBP (CREB binding protein), which are necessary for the transactivation of both factors (Ravi et al., 1998). The work of Huang, *et al.,* (2007) furthered knowledge in this field by finding that CBP, although bound to p53 in unstimulated cells, becomes phosphorylated at serine residues 1382 and 1386, by IKKα, following TNF-α stimulation. This results in CBP becoming detached from p53, allowing it to bind to p65 and activate NF-κB (Huang et al., 2007). It has now been hypothesised that aberrant activation of NF-κB, leading to inhibition of p53 could contribute to tumourgenesis (Tergaonkar and Perkins, 2007), something which the work of Huang *et al*., (2007) indicted by finding that constitutive activation of IKKα and the subsequent phosphorylation of CBP were common in lung cancers (Huang et al., 2007).
BCRA2 is a tumour suppressor gene associated with familial predisposition to breast and ovarian cancers (Wooster et al., 1995). It may also have a role in the regulation of cell growth and proliferation (Gretarsdottir et al., 1998). The over-expression of BRCA2 has been noted in many sporadic breast cancers, even though there are no known somatic mutations in the gene in these cases (Teng DH et al Nat Genet 1996). Wu *et al.,* (2000) found that NF-κB binds to the BRCA2 promoter and induces

expression of the gene using MCF-7 cells. Cells transfected with p50 and p65 constructs had marked increases in the BRCA2 promoter and in BRCA2 mRNA (Wu et al., 2000). These findings illustrate that NF-κB regulates BRCA2 expression, and therefore that alterations in NF-κB expression could contribute to the findings that BRCA2 is also over-expressed in breast tumours (Bieche et al., 1999). BRCA1 is also associated with familial breast cancers, and this tumour suppressor is known to function as a co-activator of NF-κB, increasing the activity of NF-κB target promoters (Benezra et al., 2003). This may contribute to protection against apoptosis in BRCA1 mutated breast cancers.

1.2.5 Development of NF-κB inhibitors

NF-κB has been implicated in a number of pathologies, including inflammatory disease and cancer, therefore making the inhibition of this transcription factor an attractive target for therapy. To date there are over 750 known inhibitors of the NF-κB pathway, and these include both naturally-occurring and chemical compounds. These inhibitors can be divided into broad categories depending on where they act, such as at receptor or adaptor level, directly at the IKK complex or IκB phosphorylation, proteosomal degradation of IκB, nuclear translocation of NF-κB or at the NF-κB DNA binding level (Gilmore and Herscovitch, 2006).

Inhibitors that act at the receptor level aim to block signal before it can activate the IKK complex, such as anti-TNF-α antibodies which have been shown to have the potential for the treatment of RA and inflammatory bowel disease (Filippova et al., 2002). The adaptor proteins, TRAFs are the next step in cytokine signalling for NF-κB activation *via* the canonical pathway (Bradley and Pober, 2001). TRAF-2 is recruited to TNF receptors and required for TNF-α mediated NF-κB activation, and a mutant TRAF2 lacking its N-terminal RING finger domain has been found to inhibit this activation (Hsu et al., 1996). TRAF6, however, interacts with the IL-1 receptor and a dominant negative mutant of this protein inhibits NF-κB activation by IL-1 (Cao et al., 1996).

There are a number of inhibitors that target the IKK complex. These include both natural and synthetic ATP analogues, including SC-839 which inhibits both IKKα and IKKβ, with a 100-fold preference for the latter (Gilmore and Herscovitch, 2006) and compounds such as BMS-345541 which has an allosteric effect on both kinases, again with greater affinity for IKKβ (Burke et al., 2003). Naturally-occurring compounds,

such as Parthenolide, derived from the Feverfew plant, have been shown to inhibit the IKK complex (Yip et al., 2004), and chemical inhibitors, including LC-1, have been developed as analogues of this. LC-1 has been widely studied, especially in the context of haematological malignancies. It has anti-tumour activity in acute myeloid leukaemia (Jenkins et al., 2008) and it also synergies with the nucleoside analogue, fludarabine, which is a standard treatment for CLL. To this end is it now in Phase I clinical trials in the UK for CLL (Hewamana et al., 2008a, Hewamana et al., 2008b, Hewamana et al., 2009). Other IKK inhibitors also use IKKγ/NEMO as a target, for example May *et al*., (2000) described how the introduction of a cell permeable peptide of 10 amino acids that corresponds to the NEMO binding domain of IKKβ could block both the binding of NEMO to the other IKK complex components and thus, the induction of NF-κB *via* the canonical pathway (May et al., 2000). Most recently, a NEMO binding peptide (NBP), has been shown to inhibit constitutive NF-κB activity and as a result, reduces tumour burden in a canine model of relapsed, refractory DLBCL (Gaurnier-Hausser et al., 2011).

However, there have been some concerns over the use of IKK inhibitors, mainly due to toxicity issues. It is well documented that NF-κB activation is vital for the cellular inflammatory and immune responses, and it has been postulated that long-term inhibition of the entire pathway could have some negative impact on the cell. The IKK complex has many known functions within the cell (Chariot, 2009), and therefore it is thought that inhibition may be cytotoxic. Long-term NF-κB inhibition may also increase the likelihood of immunodeficiency, since it plays a pivotal role in the innate and adaptive immune response, and can possibly delay bone marrow recovery as indicated by some reports of chemotherapeutic induced apoptosis of hematopoietic progenitors (Grossmann et al., 1999, Turco et al., 2004). It has therefore been postulated that specifically targeting DNA-damage-activated NF-κB may be a viable therapeutic strategy (Hunter et al., 2011, Veuger and Durkacz, 2011, Veuger et al., 2009), although this would require much further investigation, to ensure that the essential inflammatory response functions of NF-κB were unaffected.

Other groups have suggested that targeting the ATM:NEMO interaction described by Wu *et al.*, (2006), using an ATM kinase inhibitor, could also provide a viable therapeutic strategy for targeting DNA-damaging induced NF-κB activation (Wu et al., 2006). To this end, the recent work of Veuger and Durkacz (2011), used the known

ATM inhibitor, KU55933 (Hickson et al., 2004), to show that the radio-sensitisation of a panel of breast cancer cell lines by the inhibitor was mediated through the effects on NF-κB activation, not through the inhibition of DSB repair, challenging the traditional dogma surrounding these small molecule inhibitors of DNA repair enzymes (section 1.4) (Veuger and Durkacz, 2011).

The stabilisation of the IκB proteins or prevention of their degradation are other points in the NF-κB cascade that are targeted in order to inhibit NF-κB. The β-amyloid peptide which is deposited in the amyloid plaques which are characteristic of Alzheimer's Disease, is known to upregulate IκB expression, thus lowering NF-κB activity (Bales et al., 1998). Zhou *et al.,* (2005) reported that a protein from the bacterial pathogen, *Yersinia* called YopJ acts as a deubiquitinase for IκBα, thus stabilising it. YopJ also prevents the nuclear translocation of NF-κB, another point which is often targeted in the NF-κB activation pathway (Zhou et al., 2005).

Bortezomib, a proteosome inhibitor has demonstrated considerable efficacy against multiple myeloma both i*n vitro a*nd i*n vivo* (Adams, 2004), along with some other tumours, as well as being an inhibitor of NF-κB of myeloma cells *in vitro* (Cusack et al., 2000). Although proteosome inhibitors are targeted in the suppression of NF-κB, it is not clear whether it is the anti-tumour effects exhibited by bortezomib are mediated by inhibition of the transcription factor (Gilmore and Herscovitch, 2006). For example, there have been reports recently which have suggested that bortezomib can act synergistically with other NF-κB pathway inhibitors, such as the IKK inhibitor, LC-1 (Hideshima et al., 2009, Walsby et al., 2010). Many other proteins are targeted for proteosomal degradation, including the tumour suppressor p53 (Asher and Shaul, 2005), so it is possible that the efficacy of bortezomib and other proteasome inhibitors is due to the stabilisation of other key proteins with known roles in cancer, other than NF-κB.

It has been postulated that targeting the NF-κB transcriptional axis at the DNA binding and transcriptional level using a PARP-1 inhibitor, could overcome some of the toxicity problems associated with global NF-κB inhibition by IKK inhibitors, for example, as described above. There is increasing evidence that PARP-1 is required as a nuclear co-activator of NF-κB-dependent transcriptional activation (Chang and Alvarez-Gonzalez, 2001, Hassa et al., 2003, Hassa et al., 2001, Hassa et al., 2005, Hassa and Hottiger, 1999, Hunter et al., 2011, Stilmann et al., 2009, Veuger et al., 2009), and this is

discussed in more detail in section 1.5. The work of Veuger *et al.,* (2009) showed that inhibition of PARP-1, using the small molecule inhibitor, AG-14361, considerably reduces NF-κB activation in response to IR, thus suggesting that the potentiation of IR-induced cytotoxicity by AG14361 is mediated by the inhibition of NF-κB activation (Veuger et al., 2009). However, although these data are very encouraging and suggest a novel therapeutic angle for the use on these compounds, the mechanism of action remains unclear. Moreover, studies thus far have used experimental PARP inhibitors, which may have off-target effects, hence an investigation using a potent and specific PARP inhibitor, used in clinical trials should be undertaken in order to elucidate the mechanism.

Another mechanism of targeting NF-κB at the DNA binding and transcriptional level is to specifically inhibit the Rel domain of the subunits, meaning that these compounds inhibit subunit DNA binding, which results in the inhibition of NF-κB. In this class of inhibitors, PBS-1086 has been reported as a Rel inhibitor, which it is more potent at inhibiting the DNA binding of both RelA and RelB when compared with IKK inhibitors such as, parthenolide (Oh et al., 2011). Oh *et al.,* (2010), reported that PBS-1086 suppressed spontaneous lympho-proliferation and inhibited the production of pro-inflammatory cytokines in PBMCs from HTLV-I–associated myelopathy/tropical spastic paraparesis (HAM/TSP) patients *via* the inhibition of NF-κB DNA binding. To this end, PBS-1086 was shown to be a Rel inhibitor and therefore inhibit the DNA binding of p65, p50 and RelB as well as luciferase expression in a 293/NF-κB-luciferase reporter cell line (Oh et al., 2011).

1.3 Poly(ADP-ribose) polymerase-1 (PARP-1)

The report by Roitt (1956) was the first to suggest that there was a an enzyme capable of comsuming nicotinamide adenine dinucleotide (NAD^+), by showing that intracellular NAD^+ occurred in tumours that had been treated with alkylating agents (Roitt, 1956). This then led to the discovery of the enzyme responsible for this depletion of NAD^+ by Chambon *et al.,* (1963). This group found that the incorporation of radio-activity from [^{14}C]-ATP into an acid insoluble material in a preparation from the nucleus of hen livers was decreased over 1000-fold in the absence of nicotinamide mononucleotide (NMN) (Chambon et al., 1963). They demonstrated that a polymer of ADP-ribose was generated from ATP and NMN, with NAD^+ as an intermediate precursor (Chambon et

al., 1963). Another group then showed that NAD^+ contained an ADP-ribose moiety which was incorporated into the ADP-ribose polymer, by a nuclear enzyme, and that this simultaneously resulted in the release of nicotinamide (Nishizuka et al., 1967, Reeder et al., 1967). The enzyme was initially called ADP-ribose synthetase (ADPRS) or ADP-ribose transferase (ADPRT) but was later renamed poly(ADP-ribose) polymerase-1 (PARP-1), which is the currently-used name.

PARP-1 is an abundant 113kDa nuclear protein found in eukaryotes (Jagtap and Szabo, 2005). It is ubiquitously expressed in all mammalian, and many eukaryotic cells, and it has been estimated that there are approximately 1×10^6 molecules per cell (Chatterjee and Berger, 2000). PARP-1 is considered to have a role in many cellular processes including DNA repair, gene expression and transcriptional regulation, chromatin structure formation, cell differentiation and transformation, and also cell dysfunction and necrosis due to its ability to deplete cellular energy pools (Zingarelli et al., 1998).

PARP-1 is known to act a sensor and signalling molecule for both SSBs and DSBs (Veuger et al., 2004), and there have a been a number of reports which have shown that the catalytic activity of PARP-1 is dependent on its activation by DNA strand breaks (Benjamin and Gill, 1980). The transcription of the PARP-1 enzyme is unchanged in response to DNA damage (Bhatia et al., 1990), and remains at a constant high level. However, it is widely accepted that in the presence of DNA strand breaks, often by virtue of DNA damage, PARP-1 enzymatic activity is greatly increased (de Murcia et al., 1997). PARP-1 is responsible for catalysing the formation of ADP-ribose polymers from NAD^+, by cleaving NAD^+ at the N-glycosidic bond between the nicotinamide and ribose rings thus releasing nicotinamide as a by-product (Ueda and Hayaishi, 1985). This is shown in Figure 1.7.

Alvarez-Gonzalez and Mendosa-Alvarez (1995) described the synthesis of poly(ADP-ribose) (PAR) polymers as a 3-step process; initiation, elongation (which is the addition of successive ADP-ribose residues by ribose-ribose O-glycosidic linkages) and branching (which is the formation of ribose-ribose bonds between ADP-ribose moieties). It should be noted that PAR can be up to 200 residues long, and at this point they can form complex structures which can resemble nucleic acids (Alvarez-Gonzalez and Mendoza-Alvarez, 1995). PAR also have very short half-lives, as they are rapidly degraded by the poly(ADP-ribose) glycohydrolase (PARG) enzyme . PARG is

responsible for the rapid catabolism of PAR (shown in Figure 1.7). PARG is ubiquitously expressed at low levels in all cells and tissues (Bonicalzi et al., 2005).

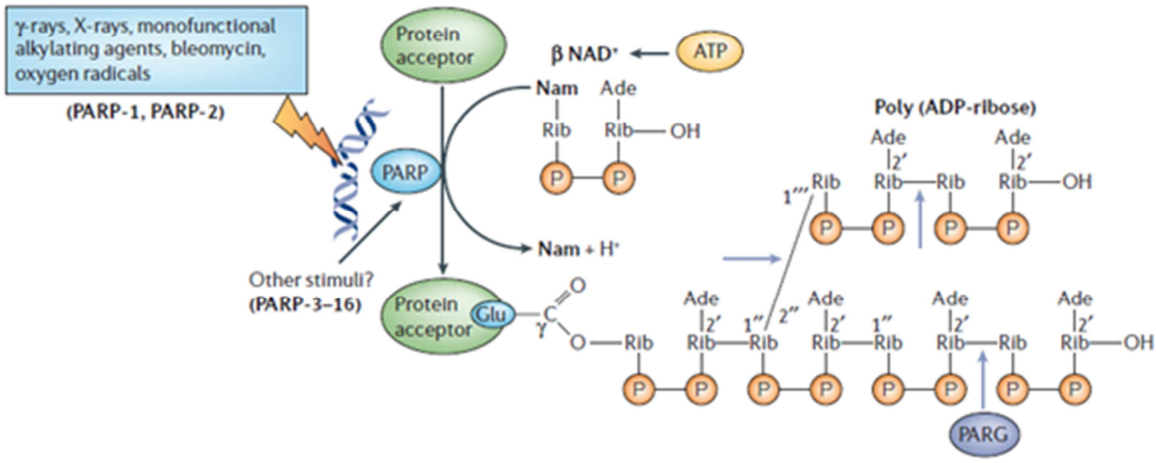

Figure 1.7: Metabolism of poly(ADP-ribose) during DNA damage and repair
Following DNA-damage, PARP-1 and PARP-2 hydrolyse NAD+, releasing nicotinamide (Nam) and H^+, and catalyse the successive transfer of the ADP-ribose moiety to nuclear protein acceptors. The reaction is initiated by the formation of an ester bond between the amino-acid acceptor (Glu, Asp or COOH-Lys) and the first ADP-ribose; polymer elongation involves the catalysis of a 2′–1″ glycosidic bond; polymer branching occurs on average after 20 ADP-ribose units and branching points are located at regular distances (every 40–50 ADP-ribose units). The degradative nuclear enzyme PARG has endo- and exoglycolytic activities that cleave glycosidic bonds between ADP-ribose units. The concurrent actions of DNA-dependent PARPs, PARG and NAD+-recycling enzymes contribute to NAD+ consumption in heavily damaged cells. The stimuli that activate PARP-3–16 are not known. P, phosphate; Rib, ribose
From: (Schreiber et al., 2006b)

Once PARP-1 is activated by DNA strand breaks and synthesises PAR, it then transfers the polymer to acceptor proteins by covalent modification of glycine residues (Figure 1.7). PARP-1 itself is the main acceptor of the polymer chains *in vivo*, and this is often referred to as the automodication. PAR has a large overall negative charge, as do DNA binding regions of DNA, and therefore the automodification of PARP-1 results in the enzyme being dissociated from the DNA due to electrostatic repulsion (Ueda and Hayaishi, 1985). Other PAR acceptors include nuclear proteins such as histones, transcription factors, topoisomerases and DNA and RNA polymerases (D'Amours et al., 1999). This is often referred to as automodification by PARP-1, or ADP-ribosylation, which can alter the function of proteins (Althaus and Richter, 1987).

It is important to note that although PARP-1 is the most well characterised component of the PARP family, at least 18 other family members have been documented. PARP orthologues are broadly characterised by the presence of the β-α-loop-β-α NAD^+ fold. The specifics of the catalytic domain differ between family members, and result in a broad functionality of this protein group (Schreiber et al., 2006b). This includes PARP-2, PARP-3, Tankyrase-1 and vault-PARP. Although this study is not necessarily concerned with the activities of the PARP superfamily proteins other than PARP-1, a very brief discussion of PARP-2, the most closely related family member is included here.

The existence of residual DNA damage activated poly(ADP-ribosyl)ation in PARP-$1^{-/-}$ mouse embryonic fibroblasts (MEFs) allowed researchers to identify PARP-2, a structurally related protein with over 60 % homology (Ame et al., 2004). PARP-2 protein is also activated by DNA strand breaks, and it has been reported that PARP-1 and PARP-2 can heterodimerise to facilitate DNA repair. Despite a reduced ability of PARP-2, in comparison to PARP-1, to catalyse ADP-ribose polymerisation, a combined role for these proteins in genome maintenance is indicated by the fact that PARP-1 or PARP-2 knockout mice are viable, whereas double knock out animals are embryonic lethal (Schreiber et al., 2002, Schreiber et al., 2006b).

1.3.1 Structure of PARP-1

The PARP-1 gene is located on chromosome 1q41-42 (Cherney et al., 1987) and is known to encode a protein which contain 23 exons and 1014 amino acids, and has a molecular weight of 113 kDa (Kurosaki et al., 1987). PARP-1 consists of three functional domains, and its functionality in terms of DNA repair (section 1.3.2.1) can be related back to its structure (Figure 1.8).

The N-terminal portion of the protein contains two zinc fingers, which are responsible for DNA-binding during complex formation (Mazen et al., 1989). It was not surprising that PARP-1 contained the metal ions since a variety of other DNA-dependent reactions require zinc. Mazen *et al*., (1989), found that PARP-1 binds DNA nicks in a zinc-dependent manner (Mazen et al., 1989), and is has also been reported that the three zinc fingers (FI and FII) are differentially required for the recognition of strand breaks (Ikejima et al., 1990). The first zinc finger (FI), recognises both single and DSBs

(Gradwohl et al., 1990), whilst the second zinc finger (FII) detects predominantly SSBs, meaning that both fingers are required for activation by SSBs but only the first finger is required for activation by DSBs. Recently, a third zinc finger was identified, which was shown to co-ordinate DNA-dependent enzyme activation (Langelier et al., 2008). This DNA binding domain also contains a caspase cleavage site (Jagtap and Szabo, 2005), that is often cleaved in the early stages of apoptosis. Adjacent to the DNA binding domain, there is a nuclear localisation signal (NLS), which is vital for the transport of PARP-1 to the nucleus (Schreiber et al., 1992).

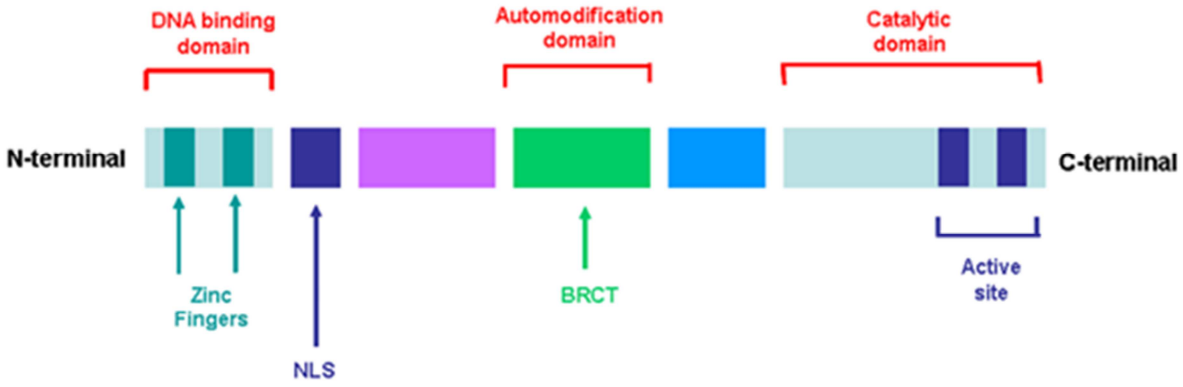

Figure 1.8: Structure of human PARP-1 showing functional elements The three functional domains are visible in the modular organisation. The amino-terminal of PARP-1 is responsible for DNA binding and damage sensing, *via* zinc fingers and the NLS (nuclear localisation sequence) portion. The automodification domain contains a breast cancer susceptibility protein with carboxy-terminus (BRCT) which is common in many DNA repair and cell-cycle proteins, and this portion aids in protein-protein interactions. The carboxy-terminus houses the catalytic centre of PARP-1 and it is this region which has the highest amount of homology with other PARP family members.
Adapted from (Jagtap and Szabo, 2005)

ADP-ribosylation of PARP-1 occurs within the centrally located automodification domain of the protein, along with the heteromodification of histones H1 and H2B, and initiates chromatin- structure relaxation in order to allow DNA repair enzymes to access the break. This domain contains 15 highly conserved amino acid residues thought to be the major autoribosylation sites (Uchida et al., 1993). It also contains a BRCA-1 C-terminal domain (BRCT) motif, which mediates interactions between several DNA repair and cell cycle checkpoint proteins and is found in a number of proteins involved in the response to DNA damage. In this case, it is important for interactions with XRCC1, histones, DNA polymerase-β and transcription factors (Bouchard et al., 2003). In addition, this domain is involved in PARP-1 dimerization and other protein-protein interactions (Burkle et al., 2002).

The highly conserved catalytic domain is located at the C-terminal end of the enzyme (Kameshita et al., 1984, Lindahl et al., 1995), and is responsible for binding NAD^+. This domain also contains what is often referred to as the 'PARP signature', which is a region of 50 amino acids that are 100 % conserved amongst invertebrates and 92 % across all species (de Murcia and Menissier de Murcia, 1994).

1.3.2 The functions of PARP-1

It is very important to note that the function of PARP-1 may be mediated by the synthesis of the PARs that confer a negative charge on modified proteins, although the precise physiological role of polymerisation in response to DNA damage is unclear, and is something which will be addressed as part of this thesis. It has been postulated that the large overall negative charge caused by the attachment of the polymers results in electrostatic repulsion of PARP-1 from the negatively charged DNA (Ueda and Hayaishi, 1985). It is also fair to say that ADP-ribosylation of acceptor proteins, and those in close proximity, may alter their biochemical and physiological properties, altering their affinity for other cellular macromolecules or perhaps DNA.

PARP-1 is known to act a sensor and signalling molecule for both SSBs and DSBs (Veuger et al., 2004). This enzyme not only has a role in DNA repair, but in cell dysfunction and necrosis due to its ability to deplete cellular energy pools (Zingarelli et al., 1998), and it has also been found to stimulate the transcription of pro-inflammatory genes (Jagtap and Szabo, 2005), a function that PARP-1 has in with NF-κB. Importantly, PARP-1 has also been implicated in the co-regulation of numerous transcription factors (Kraus, 2008, Kraus and Lis, 2003). These functions are described in more detail below.

1.3.2.1 The role of PARP-1 in single strand break repair

PARP-1 is a highly abundant enzyme (Chatterjee and Berger, 2000), which rapidly synthesises PAR in response to DNA damage (Ueda and Hayaishi, 1985). The rapid polymer synthesis consumes large amounts of cellular energy due to the depletion of NAD^+ and ATP, and the fact that PARP-1 is highly conserved suggest that PARP-1 plays a fundamental role in the early-DNA damage response network. The work of Durkacz *et al*., (1980) was the first to show that PARP-1 was required for cellular recovery from DNA damage. They reported that the classical PARP-1 inhibitor, 3-aminobenzamide (3-AB) could potentiate the cytotoxicity of alkylating agents and

prevent DNA strand break re-joining (Durkacz et al., 1980). Moreover, intracellular levels of the PARP substrate, NAD^+ have been shown to be acutely lowered by agents that generate DNA damage (Roitt, 1956). PARP-$1^{-/-}$ cell lines exhibit a similar phenotype to that of cells lacking in base excision repair (BER) proteins, and many studies using inhibitors of this ribsoylating enzyme have demonstrated its role in DNA repair (Dantzer et al., 1999).

Studies using a variety of DNA damaging agents have pinpointed a role for PARP-1 in BER pathway. The most potent activators of PARP-1 include monofunctional alkylating agents, such as temozolomide, and IR, which induce legions repaired by the BER pathway. UV irradiation, which predominantly causes lesions that are repaired by nucleotide excision repair (NER), is not a potent PARP-1 activator (de Murcia and Menissier de Murcia, 1994) and furthermore, (Satoh et al., 1994) showed that any stimulation of PARP-1 activity by UV irradiation was due to the repair of minor pyridine hydrate lesions, known to be processed by BER. To this end, the repair of UV damage is not inhibited by PARP-1 inhibitors (Cleaver et al., 1983). Figure 1.9 illustrates the differing types of DNA damage, and the different lesions which result from this damage along with the pathway used to repair the damaged DNA.

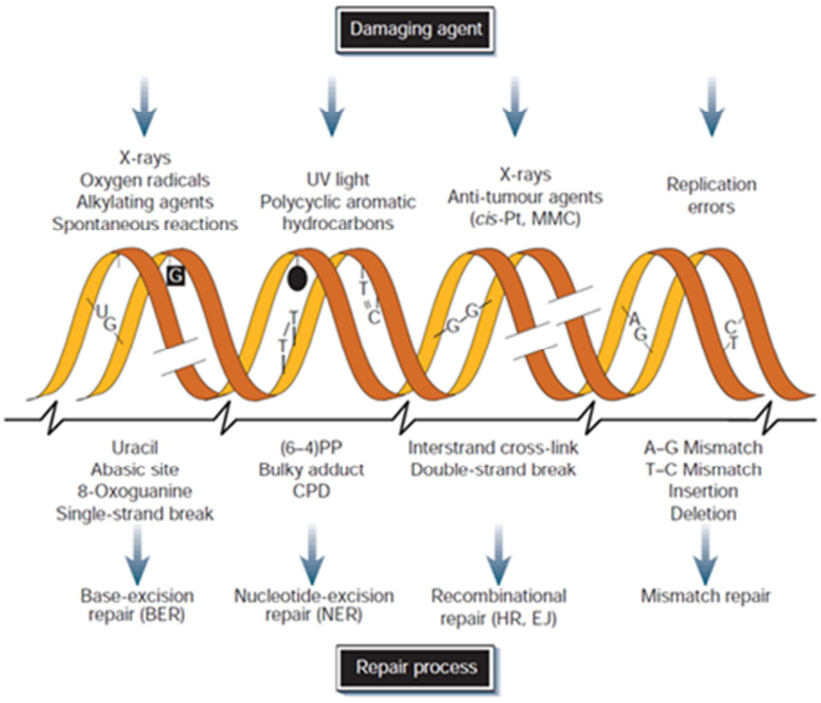

Figure 1.9: DNA damage and repair mechanisms Common DNA damaging agents (top); examples of DNA lesions induced by these agents (middle); and most relevant DNA repair mechanism responsible for the removal of the lesions (bottom). From: (Hoeijmakers, 2001)

The BER pathway (Figure 1.10) has evolved to protect cells against mutations induced by oxidative, alkylating and other DNA-damaging agents (Hoeijmakers, 2001). BER is therefore one of the major pathways to repair base lesions and apyrimidinic/apurinic (AP) sites which cause, or are processed to produce, SSBs but do not result in a distortion of the DNA helix (Ataian and Krebs, 2006). DNA glycosylases, such as alkyl-adenine DNA glycosylase (AAG), initiate BER by recognising and removing modified or improper bases. These glycosylases cleave the N-glycosidic bond between the target base and the deoxyribose-phosphate backbone producing an AP site (Frosina et al., 1996). This site is then processed by either the short-patch or long-patch BER pathway (Figure 1.10). It must be noted that DNA glycosylases are essential in the initiation of both pathways, and their action is followed by a number of sequential steps (Prasad et al., 2001). The distinction between these two pathways may not be as clear cut as early reports suggested since they share some common factors (Le Page et al., 1998).

Lesions undergoing the short-patch mechanism (right hand side of Figure 1.10), which is dominant in mammalian cells, are processed by 5'-acting apurinic (AP) endonucleases, such as APE 1, which cleaves the adjacent phosphodiester bond leaving a 5'-terminal deoxyribose-phosphate (dRP) moiety and a 3'-hydroxyl group. DNA polymerase β (pol β) then fills the single nucleotide gap and removes the dRP group through lyase activity. The strand break is then sealed by a complex of DNA ligase III and XRCC1 (X-ray repair cross complementing 1), a scaffolding protein (Lindahl and Wood, 1999).

Frosina *et al.*, (1996) were the first to conclude that a second pathway for BER, which is proliferating cell nuclear antigen (PCNA)-dependent, is active in mammalian cells (Frosina et al., 1996). This was later termed the long-patch BER (left hand side of Figure 1.10), and is responsible for approximately 20 % of overall repair. This method involves the replacement of a short oligonucleotide sequence containing the AP (apurinic) site and approximately 6-13 nucleotides in the 3' orientation from this site (Matsumoto et al., 1999). It has been found that PARP-1 is involved in triggering long-patch BER, by recognising a single stalled nucleotide. PARP-1 has also been found to be cross-linked with BER intermediates (Lavrik et al., 2001). Once PARP-1 is bound and the PCNA is at the AP site, an AP endonuclease (Robson and Hickson, 1991) can generate a strand break with DNA pol δ/ε being recruited to extend the 3'-hydroxyl

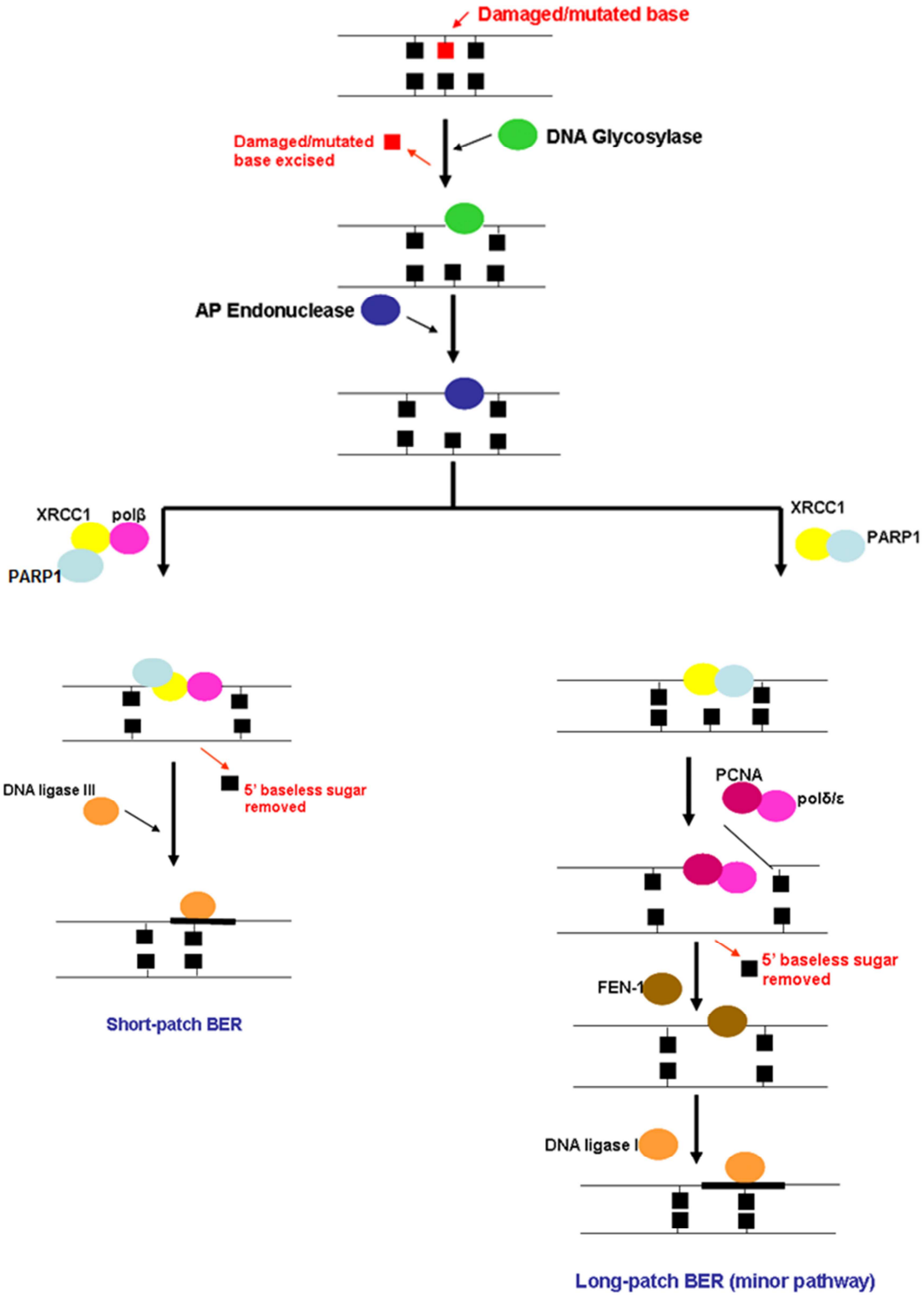

<u>Figure 1.10</u>: The short-patch and long-patch BER pathways. The DNA glycosylase, AAG removes damaged bases and the apurinic (AP) endonuclease produces an abasic site. BER can then proceed in 2 ways. The short-patch pathway uses DNA polβ and XRCC1, a scaffold protein to fill the gap and remove the baseless sugar. The nick is sealed by DNA ligase III. The long-patch pathway recruits PARP-1 and PCNA before polδ/ε can extend the 3'-hydroxyl group. The backbone is displaced and removed by FEN-1, which also works with DNA ligase 1 to reseal the nick.
Adapted from (Hoeijmakers, 2001)

group (by approximately 7 nucleotides) whilst also displacing the strand which contains the terminal deoxyribose phosphate (Klungland and Lindahl, 1997). Frosina *et al.* (1996) also suggested that the displaced strand is removed by formation of a DNA flap structure (a bifurcated structure, composed of double stranded DNA and the displaced strand). This was later called flap endonuclease 1 (FEN1), and it thought to work in conjunction with DNA ligase I, which reseals the nick (Klungland and Lindahl, 1997).

PARP-1 is more widely associated with long-patch BER (Frosina et al., 1996) and evidence from Dantzer *et al.*, (1999) support this with findings that PARP-1-deficient fibroblasts had significantly reduced (>50 %) long-patch repair activity, suggesting that the catalytic activity of this protein may augment this excision repair pathway without being essential (Dantzer et al., 1999). However, another publication from this group also suggests that PARP-1 is involved in the short-patch repair mechanism, to a certain degree, as the PARP-$1^{-/-}$ fibroblasts in their study exhibited some reduced activity in this branch of the BER pathway (Dantzer et al., 2000).

It has also been suggested that PARP-1 may be a member of a multiprotein complex suggesting that PARP-1 may be involved in recruiting components of the BER complex to the damaged site. An association of PARP-1 with DNA pol β has been described by (Dantzer et al., 2000). XRCC1, a protein that acts as a molecular scaffold, interacts with all components of the complex individually. Accordingly, an association of PARP-1 with XRCC1, has been demonstrated (Caldecott et al., 1996, Masson et al., 1998). Most recently, a study used a laser to give cells a micro-site of DNA damage, similar to that from IR, at microscopic sites, and using fluorescence microscopy, they showed how XRCC1 was recruited to ADP-ribosylated PARP-1 (Okano et al., 2003, El-Khamisy et al., 2003). XRCC1 can be ADP-ribosylated *in vitro,* perhaps allowing XRCC1 to act in its role as a structural component of the BER complex (D'Amours et al., 1999). Alternatively, PARP-1 may itself undertake a structural role in order to stabilise the two broken ends thus enabling ligation to take place (Lindahl et al., 1995).

Moreover, a role for PARP-1 in signalling direct SSBs in DNA, as a results of genotoxic agents such as IR and monofunctional alkylating agents, but not lesion modification associated BER has been postulated An emergence of evidence for additional functions for PARP-1 following double stranded DNA breaks indicates a promiscuous nature for this enzyme within the context of DNA repair.

1.3.2.2 The role of PARP in double strand break repair

The majority of the literature focuses on the role of PARP-1 in the BER pathway, however the enzyme has been implicated in other DNA repair pathways (Figure 1.9). As discussed previously, PARP-1 is rapidly activated in response to DNA damage, and therefore has been deemed an essential modulator of genomic stability. Interestingly, disruption of the *PARP1* gene results in gene amplification and sister chromatid exchange in response to DSBs, suggesting a defect in DSB repair. Similarly, the interaction of the Werner syndrome protein (WRN), a Rad51 associated helicase, and PARP-1, described by Susse *et al.,* (2004) suggests a role for this enzyme in the error-free Homolgous Recombination Repair (HRR) pathway (Susse et al., 2004).

PARP-1 has been implicated in the repair of DSBs by a number of groups (Audebert et al., 2004, Loser et al., 2010, Mitchell et al., 2009, Veuger et al., 2004, Wang et al., 2006). Veuger *et al.,* (2004) showed that DSB repair was inhibited in cell lines deficient in DNA-PK when treating with PARP-1 inhibitors in response to IR, suggesting a role for PARP-1 enzyme in DSB repair (Veuger et al., 2004). Following this, Wang *et al.,* (2006) reported that PARP-1 was responsible for DSB repair *via* a slow operating Non-Homologous End Joining (NHEJ) pathway (Wang et al., 2006). NHEJ is responsible for repair of the majority of DSBs mediated by DNA-PK, which is made up of the subunits, DNA-PKcs, Ku70, Ku80, and also XRCC4, DNA Ligase IV and Artemis (Khanna and Jackson, 2001, Sancar et al., 2004). However, Wang *et al.,* (2006) showed that although NHEJ mutant cells exhibited an apparent inhibition of repair, there was some re-joining by an alternative NHEJ pathway. This report went on to show that PARP-1, in combination with DNA Ligase III, could repair DSBs in the absence of the Ku proteins (Wang et al., 2006), hence providing a back-up pathway for early DSBs encountered by the cell.

Furthermore, Wang *et al.,* (2006) demonstrated that PARP-1 could compete with the Ku proteins for DNA ends, but that PARP-1 has a much lower affinity for these, again supporting the theory that PARP-1 mediated DSB repair is an alternative to the classical NHEJ pathway. Mitchell *et al.,* (2009) extended these existing data by investigating the activation of both PARP-1 and DNA-PK by differing DNA ends and their interaction in the response to IR. This group found that inactivation of both enzymes was not additive, suggesting that PARP-1 and DNA-PK cooperate within the same pathway to promote DSB repair. Moreover, they reported that the affinities of the two enzymes for

oligonucleotides with blunt, 3'-GGG or 5'-GGG overhanging termini were similar. However, DNA-PK was significantly more efficient when activated by a 5'-GGG overhang, whereas PARP-1 had a preference for blunt-ended DNA and required a separate factor for efficient stimulation by a 5'-GGG overhang (Mitchell et al., 2009). These data therefore suggested that both PARP-1 and DNA-PK were required for fast phase of resolution of IR-induced DSBs.

1.3.2.3 PARP-1 as a regulator of chromatin structure

Three early reports described how the formation of PAR at the sites of DNA damage could serve to temporarily extract histones from the DNA, hence loosening chromatin structure (Althaus et al., 1993, Althaus et al., 1994, Realini and Althaus, 1992). This phenomenon is often referred to as the histone shuttling model, and occurs due to the association between the positively charged histones and negatively charged PAR. The interaction between the two is either through attraction to automodified PARP-1 or by direct covalent modification of histone H1 by PARP-1. This results in electrostatic repulsion from the negatively charged DNA, and in turn the displacement of histones and the relaxation of chromatin structure. This effect is only transient and reassembly of the chromatin structure occurs following polymer degradation by PARG, which allows histones to re-associate with the DNA.

It has been postulated that local disruption of chromatin structure may be critical for repair as this gives rise to a more open chromatin structure rendering the damaged site more accessible to repair enzymes. This is especially true in areas where chromatin is highly condensed, but also important as it can alter the steric hindrance imposed by the tightly wound chromatin structures. Many essential repair factors and enzymes are part of large complexes, DNA-PK for instance, and the function of such complexes may be impeded in the presence of chromatin. It is important to note that the shuttling of histones may not only be important in facilitating the DNA repair functions of PARP-1, but may also allow other proteins to access the DNA. This could include transcription factors, particularly since PARP-1 is known to function as a transcriptional co-regulator. To this end, Schreiber *et al*., (2006) demonstrated that PARP-mediated poly(ADP-ribosyl)ation of histone proteins, in response to steroids that activate development of *Drosophila melanogaster*, facilitated their removal from the DNA strand, resulting in transcriptional activation (Schreiber et al., 2006a). Importantly, a role for PARP-1 in the regulation of numerous transcription factors has emerged recently, and will be

discussed in more detail in section 1.3.2.4. A role for the catalytic activity of PARP-1 in the embryonic development of the model organism *Drosophila melanogaster*, had also been proposed (Tulin and Spradling, 2003, Tulin et al., 2002). The *D.melanogaster* genome contains a single *PARP* gene homologous to PARP-1. Mutation of this gene, alongside the use of inhibitors of the PARP enzyme, illustrated an essential role for this protein in the organisation of chromatin structure during the developmental process. These studies have not only demonstrated a role for PARP-1 enzymatic activity in non-DNA repair processes, but also challenged the central dogma that PARP-1 is only activated in response to DNA strand breaks, an interesting theory that warrants further investigation.

1.3.2.4 PARP-1 - a transcriptional co-regulator

There is an increasing body of evidence suggesting that PARP-1 is a promoter-specific nuclear co-regulator (either a co-activator or co-repressor) of numerous transcription factors. This includes the sequence-specific DNA –binding transcriptional regulators, NF-κB, B-Myb, Oct-1, AP-1, Sp1, NFAT, Elk1, HIF-1α and HTLV-Tax-1 (Kraus, 2008), however the role of PARP-1 in regulation of these factors can be diverse. PARP-1 may act *via* through local modification of chromatin structure (Althaus et al., 1994) and/or modulation of transcription factor activity *via* direct binding to gene regulating sequences, or physical interactions with proteins including transcription factors (Kraus, 2008, Kraus and Lis, 2003, Martin-Oliva et al., 2006). In some cases, the transcription factor is thought to recruit PARP-1 to the promoters of relevant targets but this is likely to dependent on both the cell type concerned and whether or not PARP-1 enzymatic activity is required for co-activation/-repression. A detailed review of the role of PARP-1 in the activation of NF-κB is undertaken in section 1.5.

1.3.2.4.1 Regulation of transcription factors by PARP-1

One of the earliest reports regarding the role of PARP-1 as a transcriptional regulator was by (Nie et al., 1998). This group demonstrated that the transcription factor Oct-1 could interact with the automodification domain of PARP-1 and that the interaction increased Oct-1 DNA binding to the octomer motif in the DRα promoter. Oct-1 is known to regulate genes involved in both cell cycle progression and differentiation (Pierani et al., 1990).

A report by Cervellera and Sala (2000) investigated the role of PARP-1 in the activator of the B-Myb transcription factor (Cervellera and Sala, 2000), which plays a role in the control of cell growth and differentiation (Nomura et al., 1988). Aberrant expression of B-Myb can contribute to tumourigenesis (Hibi et al., 1998, Raschella et al., 1999). Cervellera and Sala (2000) found that transient transfection of PARP-1 into the haematopoietic cell line, HL-60, increased B-Myb transactivation. Using two PARP-1 catalytic mutants this group also demonstrated that PARP-1 enzymatic activity is not required for PARP-1-dependent co-activation of B-Myb (Cervellera and Sala, 2000).

There have also been reports on the regulation of AP-1 by PARP-1 (Andreone et al., 2003, Chiarugi, 2002). For example, the known inhibitors of PARP, 6(5H)-phenanthridinone and benzamide have been shown to reduce both AP-1 and NF-κB DNA binding activity and hence inhibit the transcription of key target genes including TNF-α, IL-2 and IFNγ (Chiarugi, 2002). Furthermore, AP-1 DNA binding was completely abolished in PARP-1 deficient MEFs when compared with PARP-1 proficient MEFs (Andreone et al., 2003).

Martin-Oliva *et al*., (2006) used the PARP inhibitor 3,4-dihydro-5-[4-(1-piperidinyl)butoxyl]-1(2H)-isoquinolinone (DPQ) to investigate the role of PARP-1 in the activation of the transcription factor, Hypoxia-Inducible Factor-1 (HIF-1α) (Martin-Oliva et al., 2006). Hypoxia is a hallmark of cancer in solid tumours, and has been associated with poor response to chemotherapy and malignant progression. HIF-1α is the major regulator of tumour cell adaptation to hypoxic stress (Vaupel, 2004). Martin-Oliva *et al*., used cDNA microarrays and found that key genes were differentially expressed in mice treated with the carcinogen 12-*0*-tetradecanoylphorbol-13-acetate (TPA) alone *versus* TPA in combination with DPQ. These included genes associated with inflammation and angiogenesis (*Hif-1α, Nfkbiz* and *S1009a*), and were all confirmed by real-time PCR. Further investigations using a luciferase reporter assay showed that HIF-1 activation was completely absent in PARP-1-deficient fibroblasts following treatment with the Iron chelator DFO (a known activator of HIF-1) and this also was attenuated by DPQ in PARP-1 proficient MEFs. Furthermore, PARP inhibition resulted in a down-regulation of HIF-1α protein expression following treatment with DFO. Expression of HIF-1α target genes, *Igfbp3, Bnip3* and *Vegf-A* was upregulated by DFO in PARP-1-proficient MEFs, however the effect was abbroagted by use of the PARP inhibitor, DPQ (Martin-Oliva et al., 2006).

A recent study also details the interplay between PARP-1 and the Extracellular signal-related kinases (ERKs). ERKs are key components of the MAPK signalling pathways, thus regulating a myriad of cellular process including growth, proliferation and differentiation. After phosphorylation by the MAPK kinase, MEK1/2, ERK1 and ERK2 can transolcate to the nucleus where they activate their substrates, including transcription factors, such as Elk1 (Lenormand et al., 1998). Cohen-Armon *et al.*, (2007) showed that PARP-1 could be bound by activated ERK2, and that this binding stimulated PARP-1 enzymatic activity and resulted in increased automodification. PARP-1 that had been activated in this way was then shown to significantly increase ERK2 phosphorylation of its downstream effector, Elk1. This in turn resulted in an increase in histone acetylation and expression of target genes, including *c-fos* (Cohen-Armon et al., 2007).

It has been reported that some transcription factors can be poly ADP-ribosylated through an interaction with PARP-1 (Zaniolo et al., 2007). This includes, Sp1 a transcriptional activator from a zinc-finger family of transcription factors (comprising Sp1 to Sp9) (Lania et al., 1997). Zaniolo *et al.*, reported that PARP-1-deficient cells expressed lower levels of Sp1 protein compared with PARP-1-proficient cells. They showed that PARP-1 and Sp1 physically interact using co-immunoprecipitation assays, and that this interaction allows Sp1 to be poly ADP-ribosylated, resulting in a reduction of Sp1 binding its DNA consensus sequence. To confirm these data, the group went on to use the PARP inhibitor, PJ-34 and showed that addition of this restored DNA binding of Sp1 (Zaniolo et al., 2007).

PARP-1 has also been implicated in the regulation of the transcription factor, Nuclear factor of activated T-cells (NFAT), which is known to be the major regulator of IL-2 (Jain et al., 1992). In 2008, Olabisi *et al.*, showed that the C-terminal catalytic domain of PARP-1 binds to and poly ADP-ribosylates a Glutamate residue in the DNA binding domain of NFAT. They also demonstrated that ADP-ribsylation promoted NFAT DNA binding using the PARP inhibitor PJ-34, and that both PARP-1 and NFAT were recruited to the IL-2 trancription loci following T-cell activation (Olabisi et al., 2008).

1.3.3 PARP-1 and disease

As previously discussed, PARP-1 plays a key role in numerous DNA repair pathways, as well as cell death signalling and transcriptional regulation. De-regulation of PARP-1

has also been implicated in a range of human diseases, in particular malignant conditions, and intriguingly both elevated and decreased expression of the *PARP1* gene has been demonstrated in human cancer cell lines (Masutani et al., 2005). Consistent with reports that PARP-1 is an essential mediator of genomic stability (PARP-1-deficient cells have a much higher rate of sister chromatid exchange than PARP-1-proficient cells (de Murcia et al., 1997), a reduction in *PARP1* expression in breast, colon and leukaemic cell lines has been shown to correlate with heightened genomic instability and tumourigenesis (Masutani et al., 2005).

Nosho *et al.,* (2006) reported that elevated levels of the PARP-1 gene in the early stages of sporadic colorectal tumours were linked to elevated cyclin D1, β-catenin and c-myc expression, and correlated with increased tumour size and advanced histopathology (Nosho et al., 2006). Another group used the PARP inhibitor, PJ-34 in familial adenomatous polyposis (FAP), and reported a reduction in the incidence of tumours, suggesting that the use of PARP inhibitor in FAP represented a novel target for the prevention of this disease (Mabley et al., 2004).

Polymorphisms in the *PARP1* gene have been identified and one in particular, the V726A is associated with an increased risk of some types of cancer, including prostate and lung (Lockett et al., 2004, Zhang et al., 2005a). However, other studies into this polymorphism have shown that it is associated with a decreased risk of non-Hodgkins' lymphoma (Jin et al., 2010). Single nucleotide polymorphisms (SNPs) in both the APE1 and XRCC1 genes have been associated with poor prognosis and survival in colorectal and bladder cancers (Moreno et al., 2006, Sak et al., 2005). It should be noted that another study has shown that PARP-1 activity and expression were not dependent on SNPs (Zaremba et al., 2011).

De-regulated PARP-1 activity has been shown to contribute to autoimmune diseases, something it shares with the transcription factor NF-κB. For example, Systemic lupus erythematosus (SLE) is a chronic autoimmune disease which affects multiple body tissues including the heart, lung and kidneys, and antibodies directed against the PARP-1 protein have been detected in the serum of SLE patients. Polymorphisms in the *PARP1* gene have also been associated with two common autoimmune conditions, rheumatoid arthritis and type 1 diabetes (Criswell et al., 2000, Tsao et al., 1999).

1.3.4 PARP inhibition

The concept of DNA repair inhibition represents a valid clinical target for the treatment of cancer, along with many other diseases. For example, targeting the kinase activity of ATM, DNA-PK and the cell cycle checkpoint proteins CHK1 and 2 using small molecules has been widely studied for the treatment of malignant disease, and found to induce cell death in tumour cells (Lord et al., 2006). There is a huge amount of literature regarding the inhibition of DNA repair proteins and enzymes, and for this reason a brief discussion focussed on the most important aspects of PARP-1 inhibition and the clinical relevance will be undertaken here.

As previously discussed, the ability of PARP-$1^{-/-}$ cell lines to repair genetic lesions induced by alkylating agents *via* the BER pathway is severely reduced (Dantzer et al., 1999). However, whilst deficient cell lines represent a useful tool for the examination of protein functions, small molecule inhibitors have proven critical for the translational aspect of research surrounding PARP-1 function (reviewed in sections 1.3.2). PARP inhibitors are almost always competitive inhibitors of NAD^+ (Bryant and Helleday, 2004), and the design of early inhibitors, including the nicotinamides (Fujimura et al., 1967) and the benzamides (BZ) (Purnell and Whish, 1980, Shall, 1975), designed in order to compete with NAD^+ for the nicotinamide binding domain of PARP-1. There were a number of caveats associated with these rudimentary inhibitors, not least the lack of specificity. For example, the BZ derivative, 3-aminobenzamide (3-AB), which is still used in contemporary studies to assess PARP-1 function, has been shown to affect *de novo* purine synthesis at the concentrations required to inhibit PARP (Moses et al., 1990). Further problems with these classical PARP inhibitors also include low potency and poor aqueous solubility (Griffin et al., 1995).

Influential research undertaken over 30 years ago first demonstrated a defect in the BER pathway in the presence of the PARP inhibitor 3-AB (Durkacz et al., 1980), and this group were the first to suggest that this could be a viable therapeutic strategy for the treatment of leukaemia and cancers. Following this, a whole host of small molecule inhibitors of PARP function have been developed by a number of pharmaceutical companies (Drew and Plummer, 2009) and have been widely used in a range of studies, and have now entered early phase clinical trials. A brief history of PARP inhibitor development is given below.

A series of dihydroquinolinones were reported by Suto *et al.,* (1991) as showing a 50-fold improved potency over the previous bench-mark compound, 3-AB (Suto et al., 1991). Following this, the Drug Development group at Newcastle University developed a series of novel inhibitors for the use as both chemo- and radio-sensitisers, which included the quinazolinone, 8-hydroxy-2-methyl-quinazolin-4-[3H]one (NU1025) (White et al., 2000) and the benzamidazoles, 2-(4-hydroxyphenyl)benzamidazole-4-carboxamide (NU1085) and 2-methylbenzamidazole-4-carboxamide (NU1064) (White et al., 2000) (Figure 1.11). These compounds were rigourously tested in a range of cell culture systems, including human tumour cells, to exploit the potentiation of a range of anticancer agents (Curtin et al., 2004, Smith et al., 2005) however, like earlier inhibitors of PARP-1, these compounds were found to exhibit poor aqueous solubility. More recently, the tricyclic indoles which have enhanced solubility and potency have been developed through a collaboration with Agouron Pharmaceuticals. These include AG14361 (1-(4-dimethylaminoethylphenyl)-8,9-dihydr-7H-2,7,9a-benzo[cd]azulen-6-one) (Calabrese et al., 2004), and the inhibitor used in the studies reported here, AG-014699 (8-fluoro-2-(4-((methylamino)methyl)phenyl)-4,5-dihydro-1H-azepino[5,4,3-cd]indol-6(3H)-one), which is currently in Phase II clinical trials (Thomas et al., 2007). Small molecule inhibitors of PARP-1 are shown in Figure 1.11.

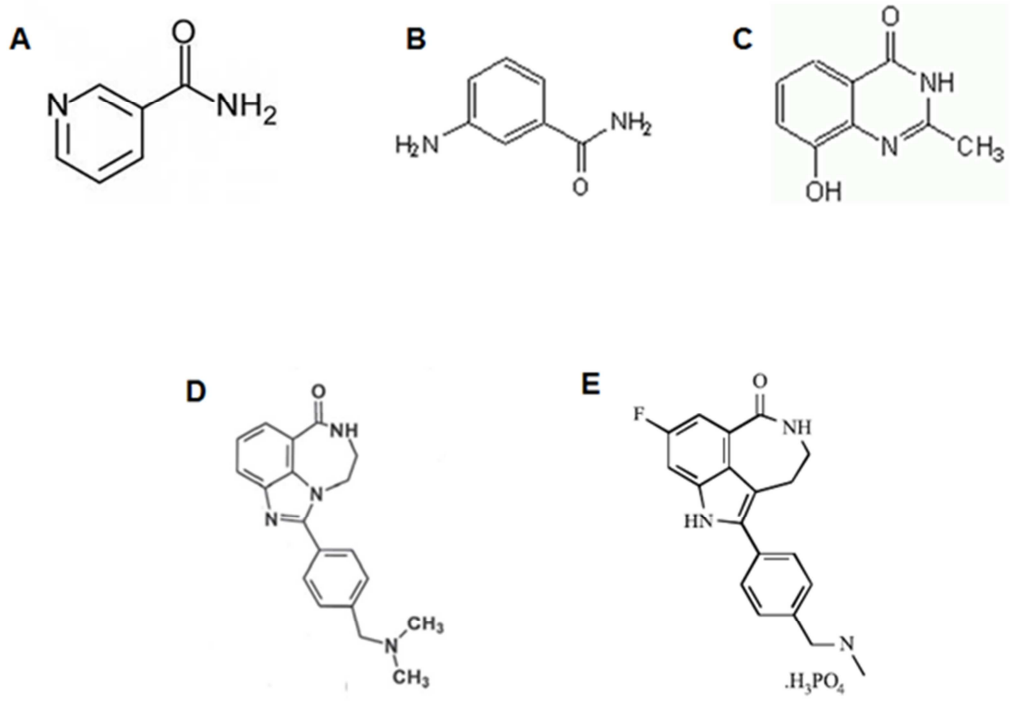

Figure 1.11: Structural basis of PARP-1 inhibitiors
Inhibitors of the PARP-1 enzyme were based upon the structure of the nicotinamide moiety (A). The structure of benzamide based inhibitors, such as 3-AB (B) was optimised to produce cyclic benzamidazoles such as NU1025 (C) and then AG14361 (D) and AG-014699 (E) with improved potency and pharmacokinetics.
Taken from (Calabrese et al., 2004, Thomas et al., 2007, White et al., 2000)

1.3.4.1 Therapeutic potential of PARP inhibitors

There have numerous studies into the clinical uses of PARP inhibitors, both in combination with conventional chemotherapeutic agents, and as stand-alone agents (Drew and Plummer, 2009). These reports have shown many promising and exciting results, and a brief discussion will be undertaken here. The rationale for using PARP inhibitors in combination with radio- or chemo-therapeutic agents, is centred around the hypothesis that inhibition of DNA repair proteins, such as PARP-1, would prevent the repair of the genotoxic lesions caused by these DNA damaging chemotherapies or IR. Therefore, it is possible that the use of DNA repair inhibitors in combination with existing agents may improve the therapeutic index of the chemo-therapeutic agent. Importantly, tumour cells are more likely to undergo apoptosis in response to lower doses of cytotoxic agents, therefore potentially limiting the toxicities associated with many cancer treatments.

A large body of literature has proved that PARP inhibition is efficacious in combination with radiotherapy and chemo-therapeutic agents, including the topoisomerase I poisons and the alkylating agent, temozolomide, all of which are known to induce SSBs, in tumour cell lines and xenograft models (Calabrese et al., 2004, Curtin et al., 2004, Delaney et al., 2000). Topoisomerase I poisons, including camptothecin, prevent the activity of this enzyme which is essential for DNA remodelling by stabilising the enzyme-DNA complex. This then results in the formation of SSBs, however many cancers and leukaemias acquire resistance to these widely used agents. Importantly, Smith *et al.,* (2005) showed that the potent and specific PARP inhibitor, AG14361 sensitised leukaemia cell lines to the effects of the camptothecin (Smith et al., 2005). A large number of studies have shown the cells are sensitised to IR when used in combination with PARP inhibitors (Zaremba and Curtin, 2007). For example, AG14361 increased IR-induced cell death, an effect further enhanced by combined inhibition of DNA-PK activity (Veuger et al., 2003). Tentori *et al.,* (2001) reported that exposure of leukemic cells to temozolomide in combination with a PARP inhibitor, resulted in a marked sensitisation to the alkylating agent (Tentori et al., 2001). These findings were supported using Calebrese e*t al.,* (2004) and others. A further discussion of the literature surrounding the use of PARP inhibitors in combination with temozolomide can be found in section 6.1. Taken together, these data support a clinical relevance for PARP-1 inhibition in conjunction with conventional cancer treatments.

The potent and specific PARP inhibitor, AG-014699 has been shown to be efficacious both *in vitro* and *in vivo* (Daniel et al., 2010, Daniel et al., 2009, Drew et al., 2011, Plummer et al., 2008, Zaremba et al., 2009), and was the first PARP inhibitor to enter clinical trials for cancer therapy. Phase I trials showed that profound and sustained PARP inhibition could be achieved after a single intravenous infusion (Plummer et al., 2005). Phase II trials combining AG-014699 with temozolomide in metastatic melanoma patients showed an improvement in the response rate in comparison with temozolomide alone (Plummer et al., 2008). A number of pharmaceutical companies are now undertaking clinical trials of PARP inhibitors for the treatment of cancer (Drew and Plummer, 2009).

One hugely interesting aspect of DNA repair inhibition, and PARP inhibition in particular, is the possibility of the use of such agents as mono-therapies. It is important to remember that each cell has the ability to repair a single genotoxic lesion *via* more than one pathway, and that this accounts for the relatively low level of oncogenesis within a lifetime. Two seminal papers (Bryant et al., 2005, Farmer et al., 2005) were suggested that PARP-1 inhibitors could be used as stand-alone agents in BRCA2 defective tumours, and were also among the first to introduce the concept of 'synthetic lethality'. This phenomenon is exemplified by the repair of DSBs via HRR, which result from single strand break collapse in the presence of PARP-1 inhibitors. Patients with mutations in the BRCA1 or BRCA2 gene are at an increased risk of developing breast and gynaecological cancers due to their defect in efficient DSB repair. Critically, a selective killing of cell lines defective in the BRCA1 or BRCA2 and Rad51 members of the HRR cascade by PARP-1 inhibitors was demonstrated by a number of groups (Bryant et al., 2005, Drew et al., 2011, Farmer et al., 2005, McCabe et al., 2006). Strikingly, only the BRCA-defective cells are susceptible to PARP inhibition in this case, and therefore selective killing of the tumour cells is achieved with minimum toxicity to normal cells. PARP inhibitors, including AG-014699, are now in clinical trials for BRCA defective breast and ovarian cancer as single agent therapies (www.clinicaltrials.gov). Phase I trials with the AstraZeneca PARP inhibitor, olaparib, have shown that this drug has significant anti-tumour activity in BRCA1 and BRCA2 mutation carriers (Fong et al., 2009, Fong et al., 2010).

Not all clinical development of PARP-1 inhibitors has been focused within the oncology field. For example, reports have shown that PARP-1 activity is increased

during conditions that restrict blood flow to the brain, such as stroke and is in this case is associated with significant NAD^+ depletion and results in neurological injury. In this case, PARP-1 inhibition has an important protective role by preventing cerebral ischemia and limiting the release of associated inflammatory mediators (Haddad et al., 2006). Other uses of PARP inhibitors are described in section 1.5, detailing the role of PARP-1 as a transcriptional regulator. To this end it is important to note that understanding the mechanisms by which PARP-1 regulates other genes and transcription factors is vital to elucidate the effects of PARP-1 inhibitors, and this thesis will undertake the first investigation of the clinically relevant PARP inhibitors in the context of their potential utility as inhibitors of transcriptional activation.

1.4 DNA repair and NF-κB

There is a mounting body of literature which has shown that many DNA damaging agents activate not only damage repair pathways, but also the NF-κB transcriptional cascade in tandem (Janssens and Tschopp, 2006). These observations have led to an increasing number of investigations studying the cross-talk between these two pathways. In particular, the DNA repair proteins, ATM, DNA-PK and PARP-1 have now been implicated in transcriptional regulation both in response to, and in the absence of, DNA damaging agents. The role of both ATM and DNA-PK will be discussed below, whilst an in-depth discussion of PARP-1 as a co-regulator of NF-κB activation is added later (section 1.5).

NF-κB induction following DNA damage is hypothesised to mediate a cell survival effect. Early studies using antioxidant compounds suggested that DNA damage-induced cytoplasmic events were responsible for the induction of NF-κB transcriptional activity independently of any DNA strand breaks. More recently however, studies have demonstrated that DNA repair proteins may mediate cytoplasmic signalling of nuclear DNA damage events which are related to the formation and detection of strand breaks within the genome (Janssens and Tschopp, 2006). It is, however, it is highly likely that the signalling to and effects of NF-κB activation following DNA damage are dependent upon the specific damaging agent used (Strozyk et al., 2006).

1.4.1 The role of ATM in NF-κB regulation

The mammalian cell cycle has a number of key DNA damage response regulators with checkpoint activity and these include the protein kinases, ATM and DNA-PK. ATM and DNA-PK both contain domains which are commonly found in the lipid kinase phosphatidyl-inositol 3-kinase (PI3K) and are often termed 'PI3K-like protein kinases' (PIKKs) (Shiloh, 2003). Both ATM and DNA-PK respond to DNA double strand breaks (DSBs) by phosphorylating a number of key substrates in downstream pathways whilst other PIKK proteins such as ATR respond to UV damage and stalled replication forks (Abraham, 2001).

Wu *et al.,* published a seminal paper in 2006, which provided a great deal of insight into the activation of NF-κB by ATM (Wu et al., 2006). This study showed that following genotoxic stimuli, in particular ionising radiation, the canonical pathway of NF-κB activation, which is dependent on NEMO-IKKβ activation is initiated (Figure 1.12). In particular, Wu *et al.,* (2006) showed that upon DNA damage, NEMO/IKKγ is translocated to the nucleus and is SUMOylated. Importantly however, Huang *et al.,* stated that the addition of the SUMO moiety to NEMO occurs in an ATM-independent manner (Huang et al., 2003). SUMOylation prevents the nuclear export of NEMO and makes it a target for phosphorylation by ATM, as shown in Figure 1.12 (Wu et al., 2003). Following this, the SUMO moiety is displaced by mono-ubiquitination allowing the ubiquitinated NEMO:ATM complex to translocate to the cytoplasm where it can activate the IKK complex (Bartek and Lukas, 2006). Traditionally, DNA repair proteins have been thought to be exclusively nuclear, an event attributed to their DNA associated function. However, immunoprecipitation experiments by Wu *et al.,* demonstrate a multifaceted IKKβ/ATM/NEMO complex essential for NF-κB activation within the cytoplasm of damaged cells (Wu et al., 2006).

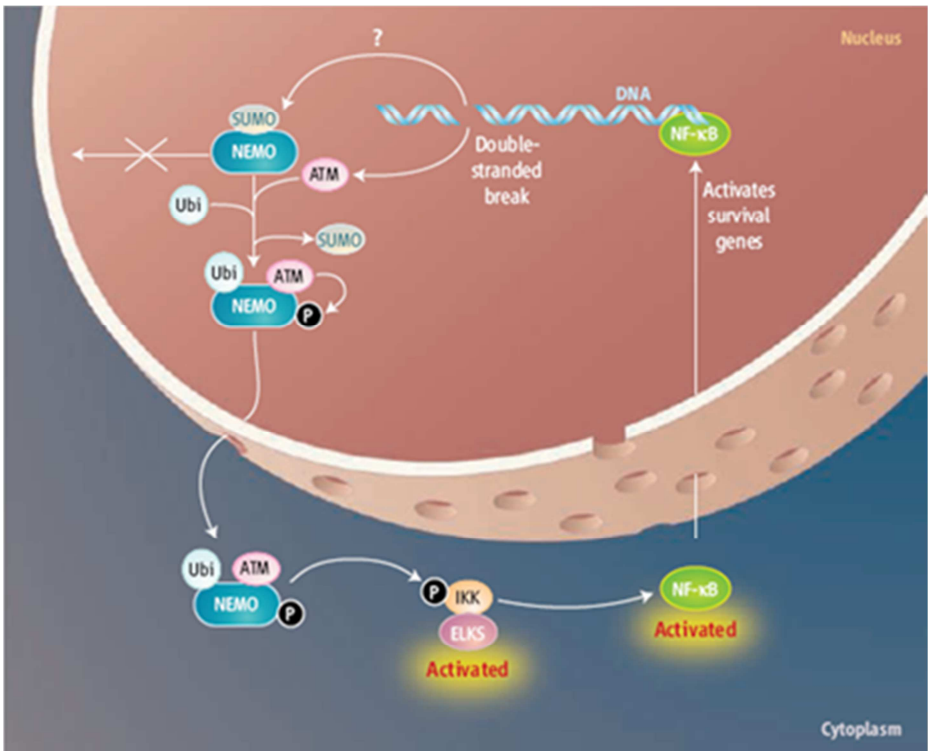

Figure 1.12: The association of NEMO and ATM results in canonical pathway activation
Genotoxic stress which causes DSBs produce a stress signal that prevents NEMO shuttling to the cytoplasm thus making it a target for SUMOylation. SUMOylated NEMO is a target for phosphorylation by ATM. Once phosphorylation has occurred, SUMO is displaced by a ubiquitin moiety and this allows the ATM-NEMO complex to translocate to the cytoplasm. The active IKK complex, which NEMO is a part of, requires ELKS (a protein rich in glutamine (E), leucine (L) lysine, (K) and serine (S)) in order to promote NF-κB translocation to the nucleus and the subsequent activation of target genes.
From: (Bartek and Lukas, 2006)

Data from Wu *et al.*, (2006) suggested that the ATM-dependent activation of NF-κB only occurred in response to DNA damaging agents such as IR or genotoxic stress; however this has been contested by Wuerzberger-Davis *et al*., (2003). This group have suggested that ATM-dependent NF-κB activation can occur in the absence of DNA damage as the SUMOylation of NEMO can occur without DSB-inducing conditions. The combination of electroporation stress (which activates the post-translational SUMOylation of NEMO) and hypotonic shock (which activates ATM) induced, albeit weakly, NF-κB activation. This publication used the PI3K inhibitor, Wortmannin to show that this NF-κB activation could not occur without ATM (Wuerzberger-Davis et al., 2007). It should be noted that Wortmannin is known to inhibit ATM, along with DNA-PK and other members of the PI3K family (Rosenzweig et al., 1997). More

recently, Veuger and Durkacz (2011) reported that the small molecule inhibitor of ATM kinase activity, KU55933 (Hickson et al., 2004) sensitised breast cancer cells to IR *via* the inhibition of NF-κB activation, rather than the widely reported inhibition of DSB repair (Veuger and Durkacz, 2011).

Hinz *et al.,* (2010) further elucidated the mechanism of ATM in the activation of NF-κB once the kinase is translocated to cytoplasm, as first reported by another group (Wu et al., 2006). Using HepG2 hepatocellular carcinoma cells, Hinz e*t al.,* showed that following DNA damage, by either IR or the topoisomerase II poison etoposide, there was a rapid accumulation of ATM in the cytosol and membrane cellular fractions, and that this translocation was calcium-dependent. They then used an RNAi screen, and found that IR-induced NF-κB mediated by ATM required the canonical pathway components TRAF6 and Ubc13, and that in fact ATM contained a TRAF-binding motif. This resulted in the activation of TRAF-6, subsequent Ubc13-mediated polyubiquitination, and recruitment of the cIAP1 protein. This ATM:TRAF6:cIAP1 module then stimulates the canonical pathway protein TAB2, which in turn phosphorylates TAK1, allowing this activated complex to phosphorylate IKKβ. Simultaneously, the ATM:TRAF6:cIAP1 module promotes monoubiquitination of NEMO/ IKKγ at lysine 285, which Hinz *et al.,* state is essential for the activation of NF-κB following genotoxic stress. Once ubquitinated, NEMO/IKKγ can complex with the now activated IKKβ, and also IKKα, and initiate the series of downstream events in the canonical pathway of NF-κB activation (Hinz et al., 2010).

1.4.2 The role of DNA-PK in NF-κB regulation

Panta *et al.,* (2004) proposed a common mechanism by which ATM and DNA-PKcs activate NF-κB through a MEK/extracellular signal-regulated kinase (ERK)/p90^{rsk} signalling pathway in response to some forms of DNA damage (Panta et al., 2004). Mitogen-activated protein kinase (MAPK) pathways including the ERK pathway, were reported to be defected in γ-irradiated A-T cells (Kharbanda et al., 2000) and these pathways have also been implicated in the NF-κB response to DNA damage (Ryan et al., 2000). Panta *et al.,* (2004) found that ATM-proficient cells activated NF-κB when treated with 5μM doxorubicin (DOX), a DSB-inducing agent, whereas ATM-deficient cells showed no NF-κB activation. After treating the ATM-proficient cells with the MEK inhibitor, PD98059 the NF-κB activation no longer occurred, therefore suggesting that ATM activates NF-κB *via* a MEK-dependent mechanism. MEK is phosphorylated

at serines 218 and 222 in an ATM-dependent manner, which results in the sequential phosphorylation of ERK and its downstream target $p90^{rsk}$, which can associate with the IKK complex leading to activation of NF-κB (Panta et al., 2004). They also detail how DNA-PK activates NF-κB induction in the same MEK-to-IKK signalling pathway in response to treatment with 5μM AD288, *N*-benzyladriamycin (a catalytic inhibitor of topoisomerase II) but not in response to DOX as was the case with ATM. Interestingly, catalytic inhibitors of topoisomerase II do not cause DNA damage, unlike classical topoisomerase poisons, such as DOX, suggesting that DNA-PK mediated activation of NF-κB can occur in the absence of DNA damage.

Liu *et al*., (1998) detailed that there are key phosphorylation events by DNA-PK at residues in both the N- and C-termini of IκBα and IκBβ which regulate NF-κB DNA binding (Liu et al., 1998). The N-terminus and ankyrin repeats of the IκB proteins are involved in the cytoplasmic regulation of NF-κB whilst the C-terminus is concerned with nuclear regulation (Luque and Gelinas, 1998) and therefore, the activity of these proteins is regulated by their phosphorylation state. Lui *et al.,* (1998) reported that DNA-PK phosphorylates one of the key sites, serine 36 in the N-terminus that earmarks the IκB proteins for degradation and ultimately results in a translocation of the NF-κB subunits from the cytoplasm to the nucleus. However, they also demonstrated that DNA-PK does not phosphorylate the other key residue, serine 32. Finally, this group illustrated they DNA-PKcs phosphorylates IκBα at threonine 273 and postulate that this event contributes to increased nuclear accumulation of NF-κB, and subsequently NF-κB DNA binding (Liu et al., 1998).

Basu *et al.,* (1998) showed that the activation of NF-κB by DNA-PK was DNA damage dependent. This group used the PI3K inhibitor, Wortmannin at a dose known to inhibit DNA-PK (Rosenzweig et al., 1997) to prove the hypothesis that DNA-PK stimulated NF-κB activation following DNA damage. In response to both the DNA damaging agents, IR and etoposide, the DNA-PK inhibitor prevented the activation of NF-κB, whereas in response to TNF-α Wortmannin had no effect. This suggests that DNA-PK, like ATM is primarily involved in NF-κB activation is response to DNA damage (Basu et al., 1998). Conversely, Ju *et al*.,(2010) demonstrated that the phosphorylation of the p50 subunit of NF-κB by DNA-PKcs, in response to the cytokine, TNF-α, was required for the expression of the NF-κB-dependent gene, VCAM-1, suggesting that DNA-PK is important for the activation of NF-κB in the absence of DNA damage (Ju et al., 2010).

Finally, the DNA repair associated kinase CK2 is involved in an IKK-independent activation of the NF-κB signalling cascade (Loizou et al., 2004). Taken together, these data highlight a critical link between the DNA repair signalling and the activity of the NF-κB transcription factor.

1.5 PARP-1 as a co-activator of NF-κB activation

There have been a number of reports on the role PARP-1 as a co-activator of NF-κB in various cell types and tissues. Many of these studies detail a role for PARP-1 in mediating the inflammatory response via regulation of the transcription factor (Hassa et al., 2001, Hassa et al., 2005, Hassa and Hottiger, 1999, Kauppinen and Swanson, 2005), although some do start to determine whether PARP-1 also regulates NF-κB following DNA damage (Chang and Alvarez-Gonzalez, 2001, Hunter et al., 2011, Stilmann et al., 2009, Veuger et al., 2009).

1.5.1 PARP-1 as a co-activator of NF-κB following inflammatory stimuli

Le Page *et al.,* (1998) were the first to suggest that PARP-1 may act as a co-regulator of NF-κB using the classical PARP inhibitor, 3-AB in the macrophage cell line, 264.7 they showed that NF-κB activation by LPS was reduced in combination with 3-AB. They also showed that transcription of the NF-κB target gene, *iNOS,* was reduced in cells treated with LPS and 3-AB compared with LPS alone (Le Page et al., 1998).

Another group then utilised the PARP knockout mouse model to investigate the role of PARP-1 in the activation of NF-κB following LPS or TNF-α *in vivo.* They showed that PARP-1-proficient mice treated with LPS exhibited rapid NF-κB activation in macrophages whereas PARP-1-deficient mice showed no NF-κB response. Furthermore, this report detailed that PARP-1-deficient cells were more sensitive to TNF-α induced cell death, and that this could be related to an impairment of NF-κB activation in these cells (Oliver et al., 1999b). Hassa and Hottiger (1999) extended this by demonstrating that NF-κB activation could be restored *in vivo* by the expression of PARP-1 in PARP-1-deficient cells. They also reported that PARP-1 and NF-κB could form a stable complex independent of DNA binding (Hassa and Hottiger, 1999).

In 2001, Hassa *et al.,* showed that PARP-1 enzymatic and DNA binding activity were not essential for TNF-α mediated PARP-1 co-activation of NF-κB. They demonstrated that although TNF-α-induced NF-κB activation was attenuated in PARP-deficient cells,

this was unaffected by either expression of a PARP-1 catalytic mutant or PARP inhibition (Hassa et al., 2001). Hassa *et al.,* (2005) then went on to show that the acetylation of PARP-1, by HDAC1 and p300, regulated NF-κB activity (Hassa et al., 2005). These data supported the earlier work by this group, when they illustrated how the physical presence of the PARP-1 C-terminal catalytic domain, but importantly not enzymatic activity, was required for PARP-1 and p300 to synergistically activate NF-κB-dependent transcription following either TNF-α or LPS (Hassa et al., 2003). More recently, Hassa *et al.,* (2008) showed that PARP-1 synergistically co-activates NF-κB gene expression at the macrophage inflammatory protein 2 and human immunodeficiency virus 1 long terminal repeat promoters in concert with the CBP-p300 complex, the coactivator-associated arginine methyltransferase 1 (CARM1) and the protein arginine methyltransferase 1 (PRMT1). PARP-1 and PRMT formed a complex with NF-κB *in vivo* , and it was reported that the methyltransferase activity of PRMT1 was essential for this interaction (Hassa et al., 2008).

Protein acetylation by CBP/p300 is essential for the expression of the NF-κB-dependent genes, ICAM-1 and VCAM-1, in TNF-α treated smooth muscle cells (Zerfaoui et al., 2008). ICAM-1 and VCAM-1 are both adhesion molecules involved in the inflammatory response. However, the interaction between CBP/p300 and PARP-1 was only essential for the activation of ICAM-1, not VCAM-1.

Many reports suggest that PARP inhibitors may be advantageous in inflammatory disorders due to their ability to inhibit transcriptional activation of key genes regulated by NF-κB and other factors, such as AP-1. Numerous reports have assessed the role of PARP-1 in glial models and those of brain injury. Ha *et al.,* (2002) reported that PARP-1 deficient glia exhibited reduced transcription factor binding (NF-κB, AP-1, Sp1 and Oct-1) and associated gene expression (Ha et al., 2002). Another report using rat glial and neuronal cultures showed that the use of PARP inhibitors significantly reduced activation of NF-κB target genes, including *iNOS, IL-1β* and *TNF-α*, resulting in a reduced neuro-inflammation and the neurotoxic potential of activated glia (Chiarugi and Moskowitz, 2003). Zingarilli *et al.,* (2003) used the PARP inhibitors, 3-AB and 1,5-dihydroxyisoquinoline in combination with the inflammatory stimulant 2,4,6-trinitrobenzene sulfonic acid (TNBS) and showed that this combination markedly reduced DNA binding of both NF-κB and AP-1 in a rat model of colitis. This resulted in a reduction in neutrophil infiltration, resolved colonic damage and induced apoptosis

(Zingarelli et al., 2003b). Nakajima *et al.,* (2004) also used cultured murine glial cells to show that the auto-ribosylation of PARP-1 lead to enhanced LPS-induced NF-κB DNA binding and in particular NF-κB p50-dependent gene transcription in this model (Nakajima et al., 2004). Furthermore, PARP-1 inhibition was able to alleviate TNF-α-stimulated NF-κB-dependent MMP-9-mediated neurotoxicity in microglia in a model of brain injury (Kauppinen and Swanson, 2005).

Two groups used cDNA microarrays to determine the role of PARP-1 in the regulation of gene transcription using the PARP-1 knockout mouse model (Carrillo et al., 2004, Zingarelli et al., 2003a). Zingarilli *et al.,* (2003) found that PARP-1 deficient cells expressed 29 apoptosis-related genes differentially compared with PARP-1 wild-type cells. These included many known to be NF-κB regulated, such as the anti-apoptotic gene *Bcl-2*, which were significantly lower in PARP-1 deficient cells. This correlated with reduced activation of the IκB kinase complex and NF-κB DNA binding in these cells, and was thought to contribute to the reduction in myocardial damage observed in PARP-1-deficient mice (Zingarelli et al., 2003a). Carrillo et al., (2004) performed microarray analysis on TNF-α-treated heart endothelial cells from PARP-1 proficient and deficient mice. They reported that the up-regulation of several inflammatory response genes, known to be NF-κB regulated was reduced in PARP-1-deficient cells (Carrillo et al., 2004).

Oumouna-Benachour *et al.,* used a apolipoprotein (ApoE)-deficient mouse model and induced atherosclerosis using a high fat diet before treatment with the PARP inhibitor, thieno[2,3-c]isoquinolin-5-one. They found that PARP inhibition reduced the number and size of atherosclerotic plaques, and that in PARP-1 deficient macrophages LPS-induced NF-κB nuclear translocation was reduced (Oumouna-Benachour et al., 2007). A study of unstable angina (UA) aimed to elucidate the role of PARP-1 in the production of TNF-α and IL-6, both NF-κB regulated genes. In mononuclear cells (MNCs) from UA patients the PARP activity and expression correlated with plasma levels of TNF-α and IL-6. Cultured MNCs from healthy volunteers were used to show that PARP-1 was component of the NF-κB DNA complex. Moreover, PARP inhibition inhibited LPS-mediated NF-κB DNA binding and consequently TNF-α and IL-6 transcription (Huang et al., 2008). Taken together all of these again confirm that PARP-1 is an important regulator of the inflammatory response, and many groups suggest that

PARP inhibitors may be utilised therapeutically in the protection against chronic inflammatory diseases.

1.5.2 PARP-1 as a co-regulator of DNA-damage activated NF-κB

Chang and Alvarez-Gonzalez (2000) were the first to describe a role for PARP-1 in the activation of NF-κB following DNA damage. Using the human cervical adenocarcinoma cell line, Hela, they showed that inactive PARP-1 could bind NF-κB p50 and block its sequence specific DNA binding, resulting in inhibition of transcriptional activation. Following treatment with the DNA damaging agent, H_20_2, PARP-1 was activated and the binding of the p50 subunit was reversed, allowing the subunit to bind DNA and upregulate transcription. Co-incubation with the PARP inhibitor, 3-AB, also significantly reduced H_20_2-induced NF-κB DNA binding (Chang and Alvarez-Gonzalez, 2001).

Two reports from Martin-Oliver *et al.,* (2004 and 2006) using the irritant TPA, illustrate the importance of PARP-1 in the regulation of NF-κB activation in murine papillomas. Susceptibility to papilloma in PARP-1-deficient mice was significantly lower than in PARP-1 proficient animals, and that the development of such lesions had a much longer latency in these mice after treatment with TPA. This was consistent with lower NF-κB activation and gene transcription during the initiation of tumour development in PARP-1 deficient mice (Martin-Oliva et al., 2004). A later study by this group, used TPA in combination with the PARP inhibitor, DPQ, and showed that in this model system, PARP-1 activity did not alter NF-κB activation following TPA treatment (Martin-Oliva et al., 2006).

Veuger *et al.,* (2009) used the breast cancer cell lines, MDA-MB-231 and T47D to investigate the role of PARP-1 in IR-induced NF-κB. They show that activation of the IκB proteins and nuclear translocation of either NF-κB p65 or p50 are unaffected by PARP inhibition, suggesting that the role of PARP-1 is at the DNA binding and transcriptional level. PARP inhibition radio-sensitised p65 proficient but not deficient MEFs and reduced IR-induced XIAP protein expression (Veuger et al., 2009). This work is discussed extensively in chapter 6.

The recent work of Stilmann *et al.* (2009) describes the formation of a PARP-1 signaling scaffold via direct protein-protein interactions with NEMO/IKKγ, PIASγ and

ATM in response to DNA damage, by IR (Figure 1.13). This signalosome formation requires binding with PAR and leads to pro-survival NF-κB activation, and this was the first study to suggest that NF-κB activation following DNA damage was mediated *via* the active form of PARP-1. PARP-1 was essential for DNA damage induced IKK, and subsequent NF-κB activation, and NEMO/IKKγ could interact directly with automodified PARP-1 very quickly following DNA damage. They also showed that PIASγ was also recruited to PARP-1 with NEMO/IKKγ, and used a series of NEMO/IKKγ mutants to find that the association between either PARP-1- or PIASγ- and NEMO/IKKγ, was within the kinase domain of the protein. Stilmann *et al.,* (2009) went on to show that PIASγ contained a C-terminal PAR binding motif (PARBM), which recruited the protein to the PARP-1 signalsome after DNA damage, and that this binding was essential for SUMOylation of NEMO/IKKγ and NF-κB activation (Stilmann et al., 2009). Moreover, they reported that ATM (itself activated upon DNA damage) was a member of this signalosome due to its known PARBM (Haince et al., 2007). Stilmann *et al.,* (2009) postulated that ATM was responsible for the phosphorylation of NEMO/IKKγ, and the subsequent downstream activation of NF-κB, supporting other work in the field (Wu et al., 2006).

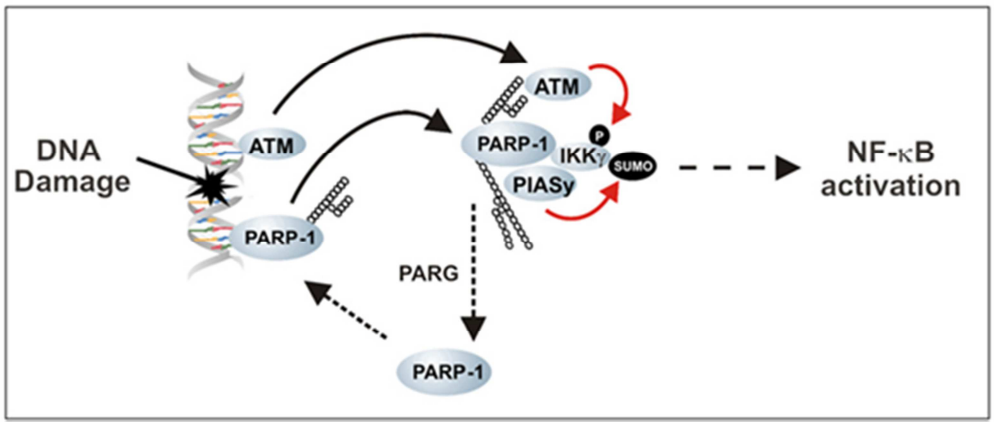

Figure 1.13: The formation of a PARP-1 signaling scaffold *via* direct protein-protein interactions with NEMO/IKKγ, PIASγ and ATM in response to DNA damage, which results in NF-κB activation
Taken from: (Stilmann et al., 2009)

Most recently, Ohanna *et al.,* (2011) reported that senescent melanoma cells develop at a PARP-1 and NF-κB-associated secretome, which they termed PNAS. They show that this secretome has pro-invasive and pro-tumourigenic properties due to the expression of many known NF-κB-dependent inflammatory response genes, in particular the

chemokine, CCL2. Furthermore, they report that the secretion of CCL2 was increased following treatment with either oxidative stress (H_2O_2) or the chemo-therapeutic agent, TMZ, both of which are known to activate PARP-1, and also NF-κB activation using a luciferase reporter assay. Pharmacological inhibition of either PARP-1 using 3-AB, or NF-κB using sulfasalazine, inhibited the secretion of CCL2 induced by H_2O_2 or TMZ, to the same extent. Therefore, the authors concluded that secretome was dependent on the activation of PARP-1 and NF-κB (Ohanna et al., 2011).

1.6 Justification

Following activation by DNA damage the canonical pathway of NF-κB is known to regulate genes involved in apoptosis, cell proliferation, angiogenesis and metastasis. (Ghosh and Karin, 2002). Constitutively active NF-κB is common in many cancers and leukemias (Basseres and Baldwin, 2006) and correlates with increased metastatic potential, more rapid disease progression, a higher proportion of tumour recurrence and therapeutic resistance (Prasad et al., 2010). Cellular NF-κB activity is known to be induced by varying doses of IR and other chemo-therapeutic agents and this differential is likely to be both cell type- and tissue-specific (Brach et al., 1991, Campbell et al., 2006b, Criswell et al., 2003). DNA damage-activated NF-κB induces anti-apoptotic genes, thereby inhibiting apoptosis and contributing to therapeutic resistance in many types of cancer (Barkett and Gilmore, 1999, Wang et al., 1998). For example, aberrant NF-κB contributes to radio- and chemo-resistance in breast tumours (Biswas et al., 2001, Wu and Kral, 2005) and loss or inhibition of NF-κB has been shown to chemo- or radio-sensitize in many different tumour types (Criswell et al., 2003, Hewamana et al., 2008a, Hewamana et al., 2008b, Jung and Dritschilo, 2001, Russo et al., 2001).

Thus, inhibition of NF-κB represents a potential therapeutic strategy in cancer, and there are a number of inhibitors targeting various pathway components in development. These include inhibitors of the IKK complex, such as Parthenolide or proteosomal inhibitors like Bortezomib which may prevent degradation of IκB (Gilmore and Herscovitch, 2006). However, global inhibition of NF-κB can have adverse effects on the cell due to the vital role NF-κB plays in both the immune and inflammatory responses. Therefore, a novel strategy may be to inhibit DNA damage induced NF-κB activity to overcome the toxic or off-target effects often encountered with other NF-κB

inhibitors, since a number of DNA repair proteins, including ATM, DNA-PK and PARP-1, have been implicated in the activation of NF-κB following DNA damage. Thus, the inhibition of DNA damage activated NF-κB using inhibitors of these DNA repair proteins requires much further testing, and specifically the effect on NF-κB-dependent gene expression should be studied closely.

PARP-1 is known to co-regulate a number of transcription factors, including Oct-1, NF-κB, AP-1 and HIF-1α (Gilmore and Herscovitch, 2006, Kraus, 2008, Kraus and Lis, 2003, Martin-Oliva et al., 2006). This may be *via* local modification of chromatin structure (Althaus et al., 1994) and/or modulation of transcription factor activity *via* direct binding to gene regulating sequences, or physical interactions with proteins including transcription factors. Previous work using experimental PARP inhibitors, such as 3-AB, have shown that PARP-1 plays a role in the activation of NF-κB. Unfortunately, it is difficult to confidently conclude that the effects observed on NF-κB in these cases are solely due to PARP-1 as early inhibitors are known to have many off-target effects (Moses et al., 1990). More recently, Veuger *et al.,* (2009) showed that the PARP inhibitor, AG-14361 radio-sensitised p65 proficient but not deficient MEFs and also suggested that the role of PARP-1 in the activation of NF-κB following DNA binding was at the DNA binding and transcriptional level, by showing there was no effect on IκB degradation or subunit translocation to the nucleus (Veuger et al., 2009). However, mechanistic studies were absent in this case.

The potent and specific PARP-1 inhibitor, AG-014699 has been used in Phase I and II clinical trials for solid tumours in combination with standard chemotherapeutics and also as a standalone treatment (Plummer et al., 2008). Studies have also shown that AG-014699 enhances tumour regression in xenograft models (Daniel et al., 2010, Daniel et al., 2009). However the effect of this agent upon NF-κB transcriptional activity remains undetermined.

Importantly, the role of PARP-1 catalytic activity in the activation of NF-κB is somewhat contentious, and is likely to be mainly dependent on stimulus, but also on cell type (Hassa et al., 2001, Hassa and Hottiger, 1999, Hassa and Hottiger, 2002). Therefore, it is necessary to compare two canonical activators of NF-κB, IR and TNF-α and determine whether PARP-1 is differentially required in the induction of NF-κB, in a given model system. Moreover, the recent work of Stilmann *et al.* (2009) describes the

formation of a PARP-1 signalling scaffold via direct protein-protein interactions with NEMO, PIASγ and ATM in response to DNA damage. This signalosome formation requires binding with PAR and leads to pro-survival NF-κB activation (Stilmann et al., 2009).

Although the work of Stilmann *et al.,* (2009) provided a great deal of insight into the mechanism by which NF-κB is activated by PARP-1 in response to DNA damage, there are some caveats associated with it. Firstly, this study used hyper-lethal doses of IR, as high as 80 Gy, in PARP-$1^{-/-}$ MEFs, which are widely reported to be exhibit genomic instability. They are not the only group to use high doses of the DNA damaging agent, as the study by Veuger *et al.,* (2009) used up to 50 Gy in some cases. These doses are not clinically relevant, and studies should be undertaken at lower doses which are as close to mimicking a clinical dose as is possible. Although the study by Stilmann *et al.*, (2009) is purely functional, is does have wider implications for the use of PARP inhibitors, and the inhibition of NF-κB activation is diseases such as cancer. Therefore, an in depth study using a clinically used PARP inhibitor should be undertaken, rather than the classical inhibitor, 3-AB used by Stilmann *et al.,* (2009), as these early compounds have a range of off target effects. Finally, although the model proposed by Stilmann *et al.,* (2009) (Figure 1.13) eludes to the effect of the PARG enzyme on PAR and consequently NF-κB activation, no mechanistic studies were presented to support this, and thus warrant further investigation.

1.7 Aims and hypothesis

Therefore, the overall aims of this thesis are four-fold:

1. To elucidate the underlying molecular mechanisms that transduce signals from DNA damage-activated PARP-1 to the activation of NF-κB using the potent and specific PARP inhibitor, AG-014699 and siRNA targeting of p65 and PARP-1

2. To test the hypothesis that PARP-1 mediates cell survival following DNA damage primarily through activation of NF-κB

3. To undertake preclinical testing of AG-014699 in cancer cell line models in which DNA damage- activated NF-κB mediates therapeutic resistance

4. To undertake preclinical testing of a series of NF-κB subunit DNA binding inhibitors, both in combination with radio-therapy and as stand-alone agents

Chapter 2. Materials and Methods

2.1 Materials

2.1.1 Chemical/reagents

Routinely used chemicals, unless otherwise stated, were either analytical or molecular biology grade, and purchased from Sigma-Aldrich Company Ltd (Poole, UK), and VWR International (Leicestershire, UK), unless otherwise stated.

2.1.2 General equipment

Irradiator; RS320 irradiation system (Gulmay Medical, Surrey, UK)

FacScan (Beckton Dickinson, Oxford, UK)

Spectromax 96-well microtitre plate reader (Molecular Devices, Berks, UK)

Incubator (Heraeus Equipment Ltd., Beds., UK)

Waterbath: Grant Model OLS200 (BDH, Dorset, UK)

Centrifuge; Eppendorf model MSE3000/30001 (Scientific Laboratory Supplies, Nottingham, UK)

Criterion electrophoresis tank and Criterion Blotting module (Bio-Rad, Herts., UK)

Power pack 200 (BioRad, Hertfordshire, UK)

Roller Mixer model SRT1 (Stuart Scientific, Surrey, UK)

Fuji LAS 3000 (Fuji Photo Film Ltd., Japan)

Milipore filtration system (Milipore Corporation, Bedford, Mass., USA)

2.1.3 PARP inhibitor, AG-014699

AG-014699 (8-fluoro-2-(4-((methylamino)methyl)phenyl)-4,5-dihydro-1H-azepino[5,4,3-cd]indol-6(3H)-one) is a PARP-1 inhibitor developed in a collaborative venture between Newcastle University and Pfizer GRD, CA (Thomas et al., 2007). AG-014699 was provided by Pfizer (Surrey, UK). The inhibitor was dissolved in anhydrous DMSO and was stored at a concentration of 10 mM protected from light, at -20°C. The drug was diluted to stock concentrations in the mM range in sterile dimethyl sulphoxide (DMSO) and further diluted in full media (RPMI 1640, 10 % FBS). .AG-014699 was used at 0.4 μM in all assays, a dose known to inhibit PARP activity > 90 %, unless otherwise stated. The structure of AG-014699 is shown in Figure 2.1. It should be noted that when diluted in tissue culture medium, a final concentration of <0.1 % (v/v) DMSO was achieved. For all inhibitors and chemotherapeutic agents used in this thesis, drug free controls were exposed to <0.1 % (v/v) DMSO.

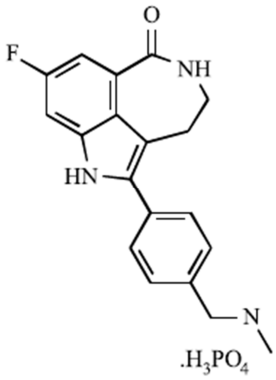

Figure 2.1: Structure of the PARP inhibitor, AG-014699

From: (Thomas et al., 2007)

2.1.4 PARG inhibitor, ADP-HPD

ADP-HPD (Adenosine 5'-diphosphate (hydroxymethyl) pyrrolidinediol) is a commercially available PARG inhibitor, known to be highly specific for PARG over PARP-1 (Slama et al., 1995). ADP-HPD was obtained from ENZO Life Sciences (Exeter, UK). The inhibitor was dissolved in anhydrous DMSO and was stored at a concentration of 10 mM protected from light, at -20°C. The drug was diluted to stock concentrations in the mM range in sterile DMSO and further diluted in full media (RPMI 1640, 10 % FBS). ADP-HPD was used at 1 µM in all assays, unless otherwise stated. The structure of ADP-HPD is shown in Figure 2.2.

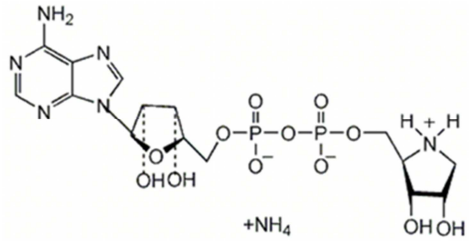

Figure 2.2: Structure of the PARG inhibitor, ADP-HPD

From: (Slama et al., 1995)

2.1.5 NF-κB inhibitors, PBS--1079, PBS-1086, PBS-1088, PBS-1110, PBS-1135, PBS-1169, PBS-1170

A range of NF-κB inhibitors, PBS-1079, PBS-1086, PBS-1088, PBS-1110, PBS-1135, PBS-1169, PBS-1170 were synthesised by Profectus BioSciences Inc. (Baltimore, MD,

USA). These compounds are referred to as Rel inhibitors of NF-κB, specifically meaning that they target the Rel domain of the NF-κB subunits, therefore inhibiting subunit DNA binding and resulting in the inhibition of NF-κB (Oh et al., 2011). These inhibitors were dissolved in anhydrous DMSO and were stored at a concentration of 5 mg/ml protected from light, at -20°C. The inhibitors were diluted to stock concentrations in the mM range in sterile DMSO and further diluted in full media (RPMI 1640, 10 % FBS) for cell treatment at concentrations in the µM range. It should be noted that Profectus BioSciences Inc. have not disclosed the structure of these inhibitors.

2.1.6 Ionising radiation (IR)

Ionising radiation (IR) produces many types of DNA lesions through direct ionisation of the DNA or by hydroxyl radicals. It must be noted that the most common lesions are SSBs and DSBs but can also include base legions and sugar modifications (Lomax et al., 2002). A range of doses of IR were used within this thesis and they were achieved using the RS320 irradiation system (Gulmay Medical), at the dose rate of 2.86 Gy/minute.

2.1.7 Tumour necrosis factor-α (TNF-α)

Mammalian Tumour Necrosis Factor α (TNF-α) was purchased from R & D systems (Abingdon, UK) and resuspended to a final concentration of 10µg/ml in PBS/BSA solution (PBS, 0.1 % w/v BSA) and aliquots were stored at -20°C. Prior to cell treatment, TNF-α was diluted to a final concentration of 10 ng/ml in full media (RPMI 1640, 10 % FBS). Control cells were treated with the BSA/PBS solution in the absence of TNF-α.

2.1.8. Doxorubicin

The anthracycline, doxorubicin (DOX) is often referred to as a topoisomerase II (Topo II) poison due to its ability to intercalate with the DNA, thus inhibiting the progression of the Topo II enzyme. This results in the induction of double stranded DNA breaks, and consequently cell death, hence DOX is widely used in cancer therapeutics for the treatment of breast cancer and haematological malignancies (Hoogstraten et al., 1976). Doxorubicin hydrochloride is commercially available and was obtained from Sigma. It was dissolved in DMSO and was stored at a concentration of 10 mM protected from light, at -20°C. The drug was diluted to stock concentrations in the mM range in sterile

DMSO and further diluted in full media (RPMI 1640, 10 % FBS) for cell treatment at concentrations in the µM range. The structure of doxorubicin hydrochloride is shown in Figure 2.3.

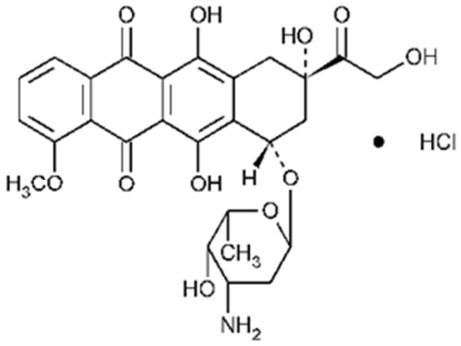

Figure 2.3: Chemical structure of doxorubicin hydrochloride
From:http://www.sigmaaldrich.com/

2.1.9 Temozolomide

The alkylating agent, temozolomide (TMZ) is used for the treatment of glioblastoma and melanoma, as well as other forms of cancer. Alkylation by temozolomide occurs, in the most part at the N-7 position of guanine, and the N-3 position of adenine residues, resulting in single stranded DNA breaks and tumour cell death (Newlands et al., 1997). TMZ is commercially available and was obtained from Sigma. It was dissolved in DMSO and was stored at a concentration of 100 mM protected from light, at -20°C, for a maximum of 14 days. The drug was diluted to stock concentrations in the mM range in sterile DMSO and further diluted in full media (RPMI 1640, 10 % FBS) for cell treatment at concentrations in the µM range. The structure of TMZ is shown in Figure 2.4.

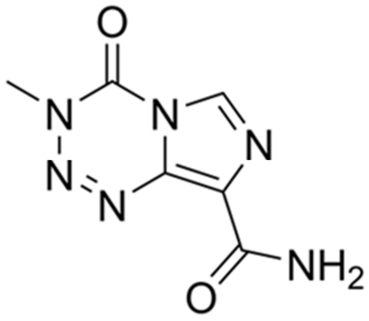

Figure 2.4: Chemical structure of temozolomide
From: (Newlands et al., 1997)

2.2 Mammalian cell culture

Tissue culture plasticware including Petri dishes, and multi-well plates were obtained from Corning (Corning Ltd., UK) or Nunc (VWR International Ltd, UK). Sterile plastic pipettes and filter tips were purchased from and Starlabs (Buckinghamshire, UK), whilst tissue culture media, foetal calf serum and trypin-EDTA were all purchased from Sigma (Poole, Dorset, UK). Sterile PBS was obtained from stores at the Northern Institute for Cancer Research (NICR).

2.2.1 Cell lines

Table 2.1 details the cell lines that were utilised in the studies described;

Cell Line	Details	Reference
$p65^{+/+}$	Spontaneously immortalised mouse embryonic fibroblasts derived from primary cells kindly provided by Professor Ron Hay (Dundee University)	Described in (Wietek et al., 2003)
$p65^{-/-}$	Mouse embryonic fibroblast. Knockout for p65 kindly provided by Professor Ron Hay (Dundee University)	**(Wietek et al., 2003)**
PARP-$1^{+/+}$	Spontaneously immortalised mouse embryonic fibroblasts derived from primary cells kindly provided by Professor Gilbert de Murcia, Ecole Superieure de Biotechnologie de Strasbourg, France.	(Trucco et al., 1998)
PARP-$1^{-/-}$	Mouse embryonic fibroblast. Knockout for PARP-1 through disruption in exon 4 which encodes the DNA binding domain of this enzyme	(Trucco et al., 1998)
p65 null	Mouse embryonic fibroblast. Knockout for p65 kindly provided by Professor Neil Perkins (Newcastle University).	(O'Shea and Perkins, 2010)
p65 WT	Mouse embryonic fibroblast. Knockout for p65, genetically complemented with WT p65, kindly provided by Professor Neil Perkins (Newcastle University).	(O'Shea and Perkins, 2010)
MDA-MB-231	Estrogen-receptor negative epithelial breast cancer cell line initially derived from the mammary gland of a 51-year old female known to have an aggressive adenocarcinoma.	(Walker-Nasir et al., 1982)
T47D	Estrogen-receptor positive adherent breast cancer cell line initially derived from the mammary duct of a 54-year old female with a known ductal carcinoma	(Horwitz et al., 1982)
MCF7	Estrogen-receptor positive breast cancer cell line established from the pleural effusion	(Westley and Rochefort, 1979)

	from a 69-year-old female Caucasian suffering from a breast adenocarcinoma	
U251	Adherent glioblastoma cell line derived from a 44 year old female.	(Quemener et al., 1990)
MO59J	Adherent glioblastoma cell line derived from a 33 year old male. Fibroblastic morphology. Known to lack the DNA repair protein, DNA-PK	(Lees-Miller et al., 1995)
MO59J-Fus1	MO59J cells genetically complemented with chromosome 8, on which DNA-PK is located	(Hoppe et al., 2000)
A549	Adherent lung cancer cell line with epithelial morphology. Initially derived from a 58 year old Caucasian male with lung carcinoma	(Smith, 1977)
H522	Adherent lung cancer cell line initially derived from a 58 year old Caucasian male with non-small cell lung cancer	
U2OS	Adherent osteosarcoma cell line initially derived from a 15 year old Caucasian female	(Kanzaki et al., 1994)

Table 2.1: Cell lines used in these studies

2.2.2 Recovery of cyropreserved cell lines from liquid nitrogen storage

Cell lines, stored in cyrovials, were recovered from long-term storage in liquid nitrogen by warming at 37°C in order to thaw the cell suspension slowly, which was diluted in freezing media (section 2.2.5). Residual DMSO was removed from the cell suspensions via centrifugation and pellets were re-suspended in the appropriate growth media (section 2.2.3) and transferred to sterile tissue culture flasks. Medium was changed daily, to eliminate any traces of residual DMSO, until the cells were ready for subculturing.

2.2.3 Continuous culture of cell lines

All cell lines were cultured as monolayers in plastic tissue culture flask and grown in RPMI-1640 supplemented with 10 % (v/v) FBS, with the exception of the p65 null and p65 WT MEFs which were grown in Dulbeccos modified eagles medium (DMEM) supplemented with 10 % (v/v) foetal calf serum and 2 mM L-glutamine. All lines were sub-cultured twice weekly to maintain the cells in exponential phase of growth and kept at 37°C, 5 % CO_2 in a humidified incubator. During routine sub-culturing, and in experiments, the medium was aspirated from the flask and the cells washed with 1 x sterile phosphate buffer saline (PBS, available from NICR in house stocks). An appropriate volume of Trypsin-EDTA solution was added and the cells incubated in this solution for 5 min at 37°C, 5 % CO_2 . The Trypsin-EDTA solution was neutralised by

addition of an equal volume of full media and the cell suspension centrifuged to remove any further traces of enzyme. The cell pellet was then resuspended in full media.

It should also be noted that the p65 WT (p65 null cell genetically complemented with wild-type p65) and M059J-Fus1 (M059J genetically complemented with chromosome 8) cell lines were maintained under antibiotic selection. In the case of the M059J-Fus1 cells this was by an additional supplement of Gentamicin Sulphate (Gibco, Paisley, Scotland) which was added at a final concentration, in medium, of 200 µg/ml, and for the p65 WT cells this was by supplementation of cell culture media to a final concentration with 4 µg/ml Puromycin (Invivogen, Nottingham, UK).

2.2.4 Counting cells using a Haemocytometer

In all studies described within this thesis cells were counted using a haemocytometer.

2.2.4.1 Principle

A haemocytometer is a slide containing two mirrored chambers of known depth with a grid etched onto its lower surface. When a cover slip is placed over the chambers, the depth is uniform (0.1 mm) across the chambers. When using a Neubauer haemocytometer, the chamber is divided into 9 large 1 mm^2 squares, which is subsequently divided into 16 smaller squares (Figure 2.5). The volume of each large square is (1 mm x 1 mm) x 0.1 mm = 0.1 mm^3. It is given that 1 $mm^3 \equiv 1$ µl, and that the conversion factor for 1ml = x 10^4. Using this information, the cell number per ml of the original suspension can be calculated.

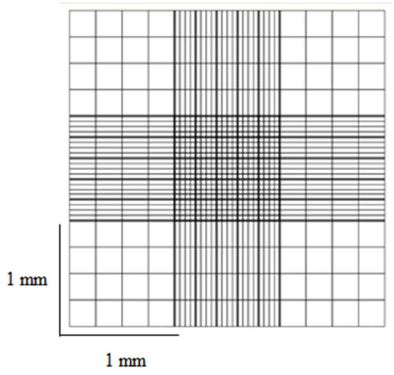

<u>Figure 2.5</u>: Chamber layout of haemocytometer

2.2.4.2 Method

Each sample was diluted 1:1 with 0.4 % v/v Trypan blue (Sigma). This is used as it gives an indication of the viability of the cells, as non-viable cells are stained blue due to them having compromised cell membranes. The cells:trypan blue mix was then loaded into a Neubauer haemocytometer chamber (Sigma) by capillary action. At least 100 cells were counted usually from the 4 corner squares, or if necessary, all large 9 squares. Only viable cell were counted, and all counts were carried out in duplicate.

$$\frac{Mean\ cell\ count}{Number\ of\ squares} \times Dilution\ factor\ = cells/ml\ x\ 10^4$$

2.2.5 Preparation of cell line stocks for long term liquid nitrogen storage

Cells were grown to 70 % confluence in the appropriate medium, washed once with sterile PBS and removed from the plate using Trypsin/EDTA. The trypsin enzyme was neutralised by addition of full media and cells pelleted at 2000rpm for 5 min. The cell pellet was then resuspended in freezing media (RPMI 1640, 20 v/v FBS, 10 % DMSO), to a concentration of 1 x 10^6 cells/ml and 1 ml aliquots of the solution transferred to cryovials. Cell suspensions were initially stored at -80°C then transferred to liquid nitrogen for long-term storage.

2.2.6 Mycoplasma

Mycoplasma is a common contamination of cell culture cells and is not detectable by morphological change in the cells or visual presence in the cell culture medium itself. However, mycoplasma infections can cause abnormal protein and nucleic acid synthesis and are also associated with chromosomal breakage. Cell cultures were periodically certified to be free of mycoplasma by routine testing using the Mycoalert Mycoplasma detection kit (Cambrex, Berkshire, UK) at the NICR, on a six weekly basis.

2.2.7 Clonogenic survival assay

2.2.7.1 Principle

The clonogenic survival- or colony formation-assay is an *in vitro* cell survival assay based on the ability of a single cell to grow into a colony. The colony is defined to consist of at least 50 cells, and it is generally accepted that only viable cells are capable of carrying out the 5-6 rounds of cell division required to form a visible colony.

Therefore, this assay assesses every cell in a known population for the ability to undergo unlimited rounds of cell division, making the clonogenic assay the method of choice when determining cell survival after treatment with known cytotoxic agents. Only a fraction of seeded cells retain the capacity to produce colonies. Cells are exposed to drug for one doubling time (usually 24 h) after which cells are re-plated out at appropriate low cell densities and incubated for 1–3 weeks to allow colony formation. Clonogenic assays show the difference between cytotoxic and cytostatic effects which are not differentiated in growth inhibition assays.

2.2.7.2 Method

Cells were plated onto 6-well plates at a density that gave a final cell number of 3-5 x 10^5 cells/ml on the day of experiment. Drug treatment schedules, regarding siRNA transfection and treatment with IR or drugs are as described in the individual chapters and figure legends. All drugs and inhibitors were added at final concentration of <0.1 % DMSO (v/v) in medium for all experiments. Inhibitors were added prior to either irradiation or drug treatment, at the timepoints described in the individual chapters and figure legends.

For all experiments, cells were exposed to drug for 24 h incubated at 37 ^oC in a humidified atmosphere containing 5% CO_2. Following this, the cells were trypsinised (as described in section 2.2.3) and re-suspended in 5 ml of drug free medium, an aliquot of each cell suspension was then counted using a haemocytometer (see section 2.2.4). Once cell counts had been undertaken, cells were diluted in medium to give suspensions of either 1 x 10^4cells/ml or 1 x 10^3 cells/ml. A volume of the diluted cell suspension corresponding to a number of cells calculated to produce a countable number of colonies (50-200) were then seeded in triplicate onto 92 mm plates in 10 ml of fresh medium. The plates were then incubated for 7-21 days depending on the cell line, to allow for colony formation.

Following the formation of suitably large colonies, the medium was aspirated from the plates and the colonies fixed by the addition of 5 ml Carnoys fixative solution (3:1 Methanol: Acetic acid). After 5 min the fixative was removed and the colonies were allowed to dry in air. Staining was achieved by the addition of 0.4 % (w/v) Crystal violet (Sigma) in water for one minute. Excess stain was gently washed off under running water and the plates allowed to air dry.

2.2.7.3 Analysis of results

Plating efficiency (absolute cell survival) was calculated as the percentage of cells seeded which formed colonies using the following equation

$$Plating\ Efficiency\ = \frac{Number\ of\ colonies}{Number\ of\ cells\ seeded} \times 100$$

Different cell lines have differing plating efficiencies, therefore it is important to determine this with untreated cells in the first instance. For example, the PARP-$1^{+/+}$ MEFs have a plating efficiency of approximately 35 % whereas the PARP-$1^{-/-}$ MEFs have a plating efficiency of <10 %. The relative survival of the treated cells was then expressed as a percentage of untreated controls. The LD_{50} and LD_{90} are defined as the dose of γ-irradiation or drug to give 50 % and 90 % reduction in survival, and from this the potentiation factor at 50% survival (PF_{50}) was calculated as follows:

$$PF_{50} = \frac{LD50\ IR\ alone}{LD50\ IR \pm p65\ siRNA, \pm AG-014699, \pm PARP-1\ siRNA}$$

2.2.7.4 Advantages and disadvantages

The clonogenic survival assay is generally accepted as the gold standard for the determination of cell survival, however there is another method of undertaking this assay, and this involves plating a much lower cell density initially and after an appropriate drug exposure, medium is changed on the cells but no re-plating occurs, therefore any dead cells which would have been aspirated off in the method used here, which are known to release apoptotic/death signals into the medium, perhaps signalling to other cells. However, this other method is less cost effective than the method utilised in this thesis, as it requires a much larger number of plates in the first instance and consequently uses more expensive reagents such as inhibitors and siRNA oligos.

2.2.8 XTT cell proliferation assay

2.2.8.1 Principle

The XTT assay is a measurement of the metabolic activity of the cell and therefore cellular viability in a culture. The assay is based on the ability of viable cells to cleave the yellow tetrazolium salt, XTT, and produce an orange formazan dye (Figure 2.6).

The dye is soluble and is quantifiable by spectrophotometry with a peak absorbance of the formazan dye at ~480 nm. Thus an increase or decrease in cell number (due to increase or decrease in viability) in turn results in an increase or decrease in the mitochondrial dehydrogenase activity within the sample, which directly correlates with the absorbance of the sample as a result of the formazan dye.

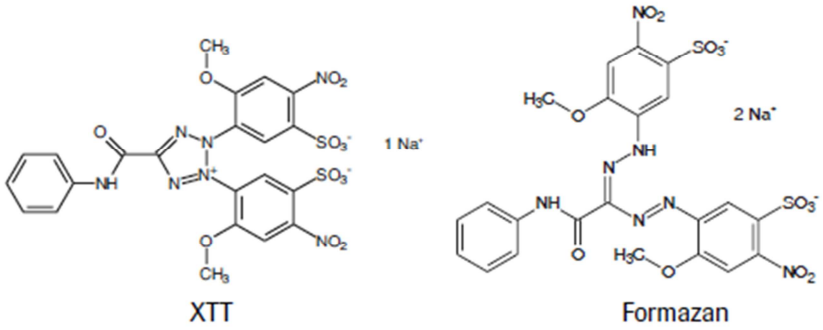

<u>Figure 2.6:</u> Metabolisation of XTT to the water soluble formazan salt, in viable cells
From: http://www.roche.com/index.htm

2.2.8.2 Advantages and disadvantages

Importantly, this assay is very high throughput as it is undertaken in a 96-well format, allowing testing of series of new compounds at a large range of concentrations at any one time. However, the XTT assay measures cellular viability by an indirect method, since the production of the formazan dye depends on the activity of mitochondrial dehydrogenase within the sample. This therefore, does not indicate whether the cells within the sample are destined for apoptosis or whether they are simply arrested in the cell cycle. Cells which have arrested during the cell cycle may continue to replicate cellular contents without division. This can lead to an increase in mitochondrial dehydrogenase activity within the sample that does not correlate to cell proliferation.

2.2.8.3 Method

Exponentially growing U251 cells were trypinised, as described in section 2.2.3, and plated out into 96 well plates at 2 x10^3 cells/well. Cells were seeded in 90 µl of the growth medium and were then incubated at 37 ^oC in humidified atmosphere containing 5% CO_2 for 24 h, which allowed the cells to adhere, before 10 µl of medium containing the relevant drug concentration was added to the appropriate well. Where compounds were dissolved in DMSO, each well contained <0.1% DMSO, including untreated

controls. The 'blank' (control) lane contained 100 µl cell-free medium to allow for background subtraction. Cells were incubated for 5 days at 37 ^{o}C in humidified atmosphere containing 5% CO_2 before addition of the XTT reagent. It should also be noted that all of the outer wells of the 96 well plate contained cell-free medium and were not used as part of the assay itself. These wells often experience evaporation of liquid, and therefore results obtained can be unreliable. This is often referred to as 'edge effect,' and it is for this reason that these wells were excluded from the assay.

The XTT assay was obtained from Roche (Herts, UK), and is often referred to as the Roche Cell Proliferation Kit. The addition of the XTT reagent was as follows: 3.5 ml XTT labelling reagent (1mg/ml XTT (sodium 3'-[1-(phenylaminocarbonyl)- 3,4-tetrazolium]-bis (4-methoxy-6-nitro) benzene sulphonic acid hydrate in RPMI without Phenol red) was mixed with 70 µl electron coupling reagent (1.25 mM PMS (N-methyl dibenzopyrazine methyl sulphate in phosphate buffered saline) for each 96 well plate to be assayed. 50 µl of this mixture was added to each well (final XTT concentration 0.3 mg/ml). Plates were incubated for 4 h in a humidified atmosphere at 37^{o}C, 5% CO_2. The XTT assay plates were read at 450 nm on a Spectromax Spectrophotometer (Molecular Devices, Berks, UK) at room temperature.

Results were analysed using GraphPad Prism 4.0, and the growth inhibition of drug-treated cultures was expressed as a percentage of control culture growth.

2.3 Transient siRNA transfection

2.3.1 Principle of siRNA technology

RNA interference (RNAi) is now a widely used tool in the suppression of gene expression. It is a method of post-transcriptional gene silencing activated by double-stranded RNA (dsRNA) which is homologous in sequence to the gene targeted for silencing (Fire, 1999). The key effectors in RNAi-mediated knockdown of gene expression are small interfering RNAs (siRNAs). These siRNAs are cleaved from a dsRNA silencing trigger, producing the 21-25 nucleotide molecules (Hannon G Nature 2002). The cleavage is by an ATP-dependent enzyme, called DICER, which includes dual RNase-III catalytic domains, an RNA helicase domain and a binding motif (Bernstein et al., 2001). Following this, siRNAs become phosphorylated at their 5'-hydroxyl group and are incorporated into the mutli-subunit protein-RNA complex,

called RISC (RNAi-induced silencing complex). The now activated RISC uses the siRNA as a guide to complex homologous substrate mRNA, and cleaves it exactly 10 nucleotides upstream from the first complementary nucleotide of the 5' end of the siRNA. The newly cleaved mRNA does not contain a poly-A tail, and is therefore quickly degraded by exonucleases, resulting in the loss of RNA transcripts and hence the suppression of gene expression. This is shown in Figure 2.7.

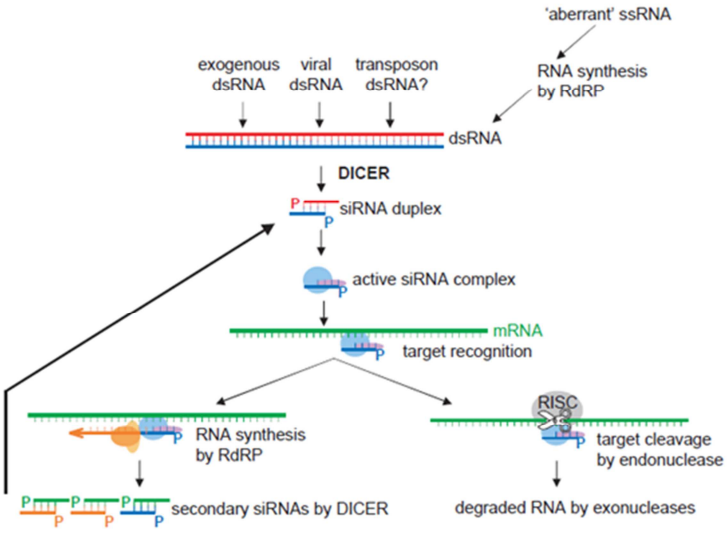

Figure 2.7: Mechanism of gene silencing using siRNA

From: (Plasterk, 2002)

Therefore this technique is widely used in molecular and cellular biology in order to validate potential targets, in the drug discovery process, to classify new functions for existing drugs, and to generate isogenic paired cell lines. This technique relies on the siRNA being imported into the cell using either lipid transfection methods, which can make a minute hole in the cell membrane in order to transport the nucleic acid across, or by electroporation, which uses an electro-static pulse to make the same type of hole in the cell membrane through which the siRNA can pass. In this thesis, lipid transfection methods have been favoured.

2.3.2 Advantages and disadvantages

The major advantage of siRNA technology is the ability to manipulate gene expression *in vitro* and *in* vivo within a relatively short timescale, for example some knockdown of gene expression occurs only 24 h after transfection. This therefore opens up enormous

possibilities for the use siRNAs in a whole range of assays, and even as potential drug candidates in the future. However, knockdown of RNA transcript and therefore expression at the gene and protein levels, can have different effects from small molecule inhibition, and therefore this caveat should always be taken into consideration and will be discussed further in Chapter 3 and 4.

2.3.3 Rehydration of siRNA

Six siRNA molecules were used within this thesis; four were used in order to knockdown expression of murine p65, human p65, murine PARP-1 and human PARP-1 and two were used as control/non-specific siRNAs (murine NS and human NS). The siRNA sequences are shown in Table 2.2.

Target gene	siRNA sequence
Murine p65	GGAGUACCCUGAAGCUAUA
Human p65	GCCCUAUCCCUUUACGUCA
Murine PARP-1	GGAGGAAGGUGUCAACAAA
Human PARP1	AAGCCUCCGCUCCUGAACAAU

Table 2.2: siRNA sequences used in these studies

All siRNA molecules were synthesised by Dharmacon (Cramlington, UK), and required rehydration, which was undertaken according to manufacturers' instructions. Briefly, 1 ml of 1x siRNA buffer (Dharmacon, Cramlington, UK) was added to each individual tube of siRNA and pipetted up and down 5 times to mix. The solution was then placed on an orbital shaker for 30 min at room temperature before the concentration determined using the Nanodrop ND-1000 spectrophotometer (Labtech, East Sussex, UK), reading at OD_{260}. This piece of equipment estimates the concentration of RNA, using only 1 µl of the RNA sample and also gives the 260:280 ratio. This ratio is an indicator of RNA quality and integrity and must be between 1.9 and 2.1.

2.3.4 Transient transfection of siRNA

Cells were plated at 1 x 10^4cells/ well in 6-well plates and then incubated at 37 ^oC in a humidified atmosphere containing 5% CO_2, for 24 h, in order to adhere. Following this, cells were transfected with either 50 nM p65, PARP-1 or NS siRNA. siRNAs were incubated in serum free RPMI for 5 min (this is because serum can be very sticky and can therefore adhere to the siRNA molecules) before mixing with the transfection

reagent, Lipofectamine 2000 (Invitrogen, Paisley, Scotland), also diluted in serum free RPMI. The resultant transfection cocktails were incubated at room temperature for a further 20 min (this allows the siRNA molecules to form complexes with the Lipofectamine 2000, which can then be transported into the cell) before applying to the 6-well plates containing cells. Cells were then incubated at 37 ^{o}C in humidified atmosphere containing 5% $CO_{2,}$ for 5 h, before aspirating this media and replacing with full media (RPMI 1640, 10 % FBS) for a further 48 h at 37 ^{o}C in humidified atmosphere containing 5% $CO_{2.}$ Protein knockdown was assessed by Western blotting (section 2.5) in all silencing experiments of p65 and PARP-1 performed throughout this thesis.

2.4 Quantification of PARP activity from permeabilised cells

PARP activity was measured in whole cells by using the published method by (Plummer et al., 2005) which has been validated to Good Clinical and Laboratory Practise (GCLP) standards, and is currently used in Phase I and II clinical trials. The principle of this technique relies on the incorporation of the ADP-ribose moiety NAD^{+} into acid-insoluble poly (ADP-ribose) (PAR) polymer. The presence of a DNA oligonucleotide (see 2.4.2) activates PARP-1 which uses both itself and intracellular proteins as PAR acceptors. This is quantified against a standard curve of purified PAR (see section 2.4.3) and is detected by immunoblotting (see 2.4.6) with a purified antibody against PAR and in this case chemiluminescence is directly proportional to PARP activity. It should be noted that neither the NAD^{+} or the oligonucleotide can enter intact cells, and therefore the plasma membrane was rendered 'permeabilised' by either hypotonic shock or treatment with digitonin (see 2.4.4). A reaction schematic is shown in Figure 2.8.

2.4.1 Preparation of NAD^{+}

A stock solution of 7 mM NAD^{+} (Sigma) was freshly prepared in dH_2O on the day of each assay. The optical density (OD) at 260 nm of a 1/100 dilution of this stock NAD^{+} solution was measured using spectrophotometer (WPA Biowave, S1200Diode array, Scientific Laboratory Supplies, Nottingham, UK) and a 1 cm silica cuvette. The Molar extinction coefficient (ε) for NAD^{+} at 260 nm is known to be 18000 and therefore 18 OD = 1 mM NAD^{+} (Beer Lambert Law). The absolute molarity of the stock solution was calculated and a working solution of 700 μM NAD^{+} was prepared.

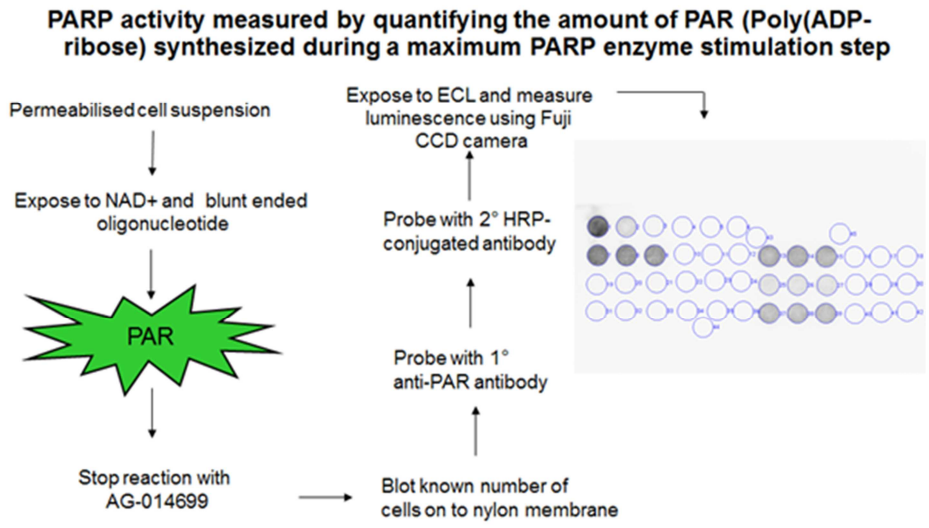

<u>Figure 2.8:</u> Schematic protocol for the quantification of PARP activity from permeabilised cells

2.4.2 Preparation of oligonucleotide

Pellets of a palindromic sequence oligonucleotide (CGGAATTCCG) were purchased from Invitrogen (Paisley, Scotland), and were dissolved in 500 µl 10 mM Tris/EDTA, pipetting vigorously to ensure the pellet is fully re-suspended. This solution is then heated to 60 °C in a waterbath and cooled by 1 °C/min to 24 °C by the addition of ice flakes, in order to ensure correct strand re-annealing. Once this has occurred, a further 1.5 ml of 10 mM Tris/EDTA is added and a 1 in dilution is made (again with 10 mM Tris/EDTA) and the OD is measured at 260 nm. In this case 1 OD unit is equivalent to 50 µg/ml, and the final stock is diluted to 200 µg/ml, and stored at -20 °C until use.

2.4.3 Preparation of PAR standards

Purified PAR is purchased from Biomol (Exeter, UK), as a branched and linear polymer, with an average chain length of 25 ADP-ribose monomers (range 3-300). 100 µl of a 10 µg/ml solution is provided, and it is taken that 1 µl is equivalent to 2000 pmol ADP-ribose monomer. In order to dilute this solution, to use in the assay, it is diluted 1 in 80 in dH_2O to give a stock of 25 pmol of ADP-ribose polymer per 100 µl of solution. This solution is then serially diluted in dH_2O at final concentrations of 25, 5, 1, 0.2, 0.04 and 0 pmol, and this is loaded onto the immuno-blot (see section 2.4.6).

2.4.4 Preparation and use of quality control standards and samples

The murine leukaemic L1210 cells are used as a quality control (QC) for this assay and aliquots provided were frozen down and stored at -80 °C by Dr. Evan Mulligan. On the day of assay, one aliquot was removed from -80 °C storage and thawed gently to room temperature before transferring into a 20 ml universal tube. At this point, samples (e.g. cell lines) to be assayed were trypinised and also transferred to 20 ml universal tubes. All samples, along with the QC were vortexed and pelleted at 500 xg for 5 min at 4 °C, before washing with PBS and this pelleting repeated. Cells were then re-suspended in 50 µl of ice cold 0.15 mg/ml digitonin in dH_2O, in order to permeabilise them, and left on ice for 5 min before the addition of 450 µl of ice cold isotonic buffer (7 mmol/L HEPES, 26 mmol/L KCl, 0.1 mmol/L, dextran, 0.4 mmol/L EGTA, 0.5 mmol/L $MgCl_2$, 45 mmol/L sucrose (pH 7.8)). A small aliquot was mixed in equal volumes with trypan blue and counted using a haemocytometer (see section 2.2.4). In this case, however it is expected that the digitonin/isotonic buffer will have permeabilised the cell membrane and hence the majority of cells should appear blue when visualised by microscopy. More than 90 % of cells must be permeabilised for the assay to continue. Once the count is complete, the cell suspension is diluted to 1.22 x 10^5/ml in ice cold isotonic buffer in preparation for the PARP reaction.

2.4.5 PARP reaction

Firstly, HybondN membrane and 2 pieces of 3 mm Whatman filter paper were soaked in PBS for at least 15 min prior to commencement of the PARP reaction. The oligonucleotide, prepared as described above, was thawed gently on ice and STOP solution, (AG-014699 diluted in PBS to a final concentration of 12.5 µM) was also prepared. Reaction tubes (15 ml falcon tubes) were set up as shown in Table 2.3, note that these tubes are set up in triplicate and set up in the presence or absence of NAD^+ and oligonucleotide, in order to determine stimulated *versus* un-stimulated PARP activity.

Reagent	**Stimulated**	**Un-stimulated**
Oligonucleotide	5 µl	-
NAD^+	5 µl	-
dH_2O	-	10 µl
Reaction buffer	40 µl	40 µl
Cell suspension	50 µl	50 µl
Reaction Total	100 µl	100 µl
STOP solution	400 µl	400 µl
Final volume	500 µl	500 µl

Table 2.3: PARP reaction mix components

Reaction test tubes containing reaction buffer with either oligonucleotide and NAD^+ or sterile water, and 1.5 ml tubes containing the cell suspension (section 2.4.4) were then warmed in a waterbath at 26 °C for 7 min. Following this the cell suspension was vortexed briefly and 50 µl added to each reaction tube. Reaction tubes were replaced in the 26 °C waterbath for a further 6 min, with gentle shaking and the reaction was stopped with the addition of an excess of the pre-prepared STOP solution. Reaction tubes were placed on ice and immunoblotting was undertaken within 1 hr.

2.4.6 Loading of immunoblot manifold and subsequent immunoblotting

Once samples and QCs had undergone the PARP reaction, they were blotted, along with the purified PAR standards, onto HybondN membrane (GE Healthcare, Amersham, UK). This membrane was chosen for its ability to bind up to 600 µg of nucleic acids per cm^2. The membrane, along with two pieces of 3 mm filter paper (Whatman, GE Healthcare, Amersham, UK) were pre-soaked in PBS prior to immuno-blot loading onto the assay manifold (kindly provided by Prof. Nicola Curtin). PAR standards (400 µl), L1210 QC samples (500 µl) and the unknown samples (500 µl) were loaded onto the blot by pipetting. Once all wells were loaded, suction was applied using Vacusafe comfort (IBS integra Biosciences, Nottingham, UK), which was attached to the manifold equipment. Wells were then washed and fixed, firstly with a solution of 10 % Tricholoacetic acid (TCA, Sigma), 2 % Sodium pyrophosphate decahydrate (NaPPi, Sigma), and secondly with a 70 % ethanol solution. Again suction was applied to remove any excess liquid.

The manifold was disassembled and the immuno-blot was washed in PBS to remove any traces of ethanol before blocking in non-fat dried milk dissolved in 0.05 % Tween in PBS (PBS-MT) to prevent nonspecific binding of antibodies to unoccupied sites on the membrane. Tween 20 (polyoxyethylene-sorbitanmonolaureate, Sigma) is a mild ionic detergent used in all buffers throughout immunodetection as it reduces non-specific binding to nitrocellulose and antigens. PBS-MT was also used for the dilution of antibodies in the immunodetection procedure. To this end, the immune-blot was incubated overnight at 4 °C, in primary antibody (10 H, kindly provided by Prof. Alexander Burkle, University of Constanz) at a dilution of 1 in 1000 in PBS-MT. The immuno-blot was then washed with PBS-T before a 1 h incubation with goat-anti mouse HRP-conjugated secondary antibody (diluted 1 in 1000 in PBS-MT), at room temperature. Following this, the blot was washed with PBS-T for a further hour before

detection using ECL (GE Healthcare, Amersham, UK, section 2.5.7). Briefly, reagents were mixed in 1:1 ratio in a volume sufficient to cover the membrane equally which was then transferred onto the blot with a pipette. The blot was left for 1 min before excess reagent was removed. The blot was then wrapped in a plastic document wallet and placed protein side up in the Fuji LAS 3000 and the image captured with an exposure 5 min.

2.4.7 Analysis of results using Aida Image Analyser

Immuno-blot images captured using the Fuji LAS 3000 were analysed using Aida Image Analyser version 3.28.001 using the 2D, densiometric analysis function within the software. Regions of interest (samples or purified PAR standards) were identified and background measurements on unused portions of the immuno-blot were also assigned to allow for background subtraction. The software generates a standard curve from the purified PAR standards, and PARP activity (pmol PAR) of the unknown samples was extrapolated from this.

2.5 Protein analysis

2.5.1 Preparation of whole cell extracts

Cell pellets were re-suspended in an appropriate volume of ice cold lysis buffer (50mM NaF, 20mM HEPES, 450mM Nacl, 25% v/v Glycerol, 200µM EDTA, 500µM DTT) at approximately 1 x 10^7 cells per 200 µl of lysis buffer, in a 1.5 ml microfuge tube. Samples were then lysed by freeze-thawing cycles (3 cycles of 2 minutes on dry ice and 2 minutes in 30°C water bath). Cell lysates were centrifuged at 14,000 rpm for 7 min at 4 °C to remove cell debris and the supernatant removed for analysis. An aliquot from these whole cell lysates was then removed for protein estimation and the remaining volume was then snap frozen and stored at -80°C until use for Western blotting.

2.5.2 Extraction of nuclear and cytoplasmic protein fractions using the Pierce NE PER kit

Adherent cells were trypsinised and pelleted at 3000 rpm for 5 min and washed with PBS. Nuclear and cytoplasmic extracts were the prepared using the NE-PER Nuclear and Cytoplasmic extraction kit, according to manufacturers' instructions (Pierce, Perbio Science UK Ltd., Cramlington, UK). Briefly, cell pellets were re-suspended in the CER I reagent, which was supplemented with protease inhibitor cocktail (Roche, West

Sussex, UK) and allowed to lyse on ice for 10 min, after which CER II reagent was added to facilitate full disruption of the cell membrane and release of cytoplasmic contents. Following centrifugation to isolate the cytoplasmic extract, the nuclear pellet was resuspended in the NER I reagent, supplemented with protease inhibitor cocktail, *via* repeated vortexing for 40 min. The supernatant (nuclear extract) was removed, and a small aliquot was taken for protein estimation, whilst the remaining volume was then snap frozen and stored at -80°C until use in the ELISA-based assays (section 2.9) or Western blotting.

2.5.3 Quantification of protein using the Pierce protein assay

2.5.3.1 Principle

Protein estimation is possible through using the bicinchonic acid (BCA) method which combines the reduction of Cu^{2+} to Cu^{1+} by protein in alkaline conditions with the colorimetric detection of the cuprus cation (Cu^{1+}). In this case the Cu^{1+} ion reacts with bicinchonic acid to form a purple BCA-Cu^{1+} complex product, formed by the chelation of two BCA molecules with one Cu^{1+} ion. This purple-coloured solution is detected spectrophometrically at 562 nm. This method was chosen as the cell lysis method does not interfere with this assay.

2.5.3.2 Method

The BCA protein assay (Pierce, Perbio Science UK Ltd., Cramlington, UK), was used, according to manufacturers' instructions, to estimate the protein content of either whole cell extracts or nuclear and cytoplasmic cellular fractions. Briefly, the Albumin standard provided containing bovine serum albumin (BSA) at 2 mg/ml was used to prepare six standard solutions of 0.2, 0.4, 0.6, 0.8, 1.0 and 1.2 mg/ml. Unknown samples were typically diluted 1:10 with dH_2O. Standards, unknown samples and dH_2O blanks were loaded in quadruplicate in 10 µl volumes onto 96 well plates. BCA reagent A (20 mls) and BCA reagent B (4 mls) were combined and 190 µl of the mixture was added to each well and then mixed on a plate shaker for 30 seconds. The plate was covered and incubated at 37 ºC for 30 minutes. Absorbance at 562 nm was read on the Spectromax plate reader (Molecular Devices, Berks, UK) and unknown protein concentrations were calculated from the standard curve generated by the plate reader, taking into account the 10-fold dilution factor.

2.5.4 Separation of protein extracts by molecular weight by SDS-polyacrylamide gel electrophoresis

2.5.4.1 Principle

Sodium dodecyl sulphate-polyacrylamide gel electrophoresis (SDS-PAGE) is a technique which has allowed the separation and analysis of proteins in a given sample. SDS is an amphiphillic 12 carbon alkyl sulphate molecule which denatures proteins and forms a charged micelle around polypeptide chains. This micelle ablates the native charge of the polypeptide and the SDS-protein aggregate has an equal resultant charge per unit volume dependent upon the size of the micelle which is determined by the size of the polypeptide chain. Thus proteins move through the electrophoresis gel toward the anode according to size.

The polyacrylamide gel is formed from the polymerisation of acrylamide monomers into chains which are cross-linked by bisacrylamide, producing a gel with pores through which polypeptide chains travel. The size of the pores determines the rate at which the proteins travel. A gel with a variable gradient allows proteins of large size to be resolved on the same gel as small proteins which are retarded by higher acrylamide concentrations further down the gel.

The protein expression assessed in this thesis included that of the large protein, DNA-PK, which a molecular weight of 450 kDa, as well as the low molecular weight protein, β-actin (43 kDa). Therefore, the separation of such proteins by PAGE requires specific gel composition. The Criterion XT Tris-acetate gels are based on a Tris-acetate buffer system (pH 7.0). This uses discontinuous acetate and Tricine ion fronts to form moving boundaries to stack and then separate large denatured proteins by molecular weight. XT Tris-acetate gels are made without SDS, allowing the sample buffer and running buffer to dictate the separation mechanism. Protein samples are prepared in a reducing denaturing sample buffer. The sample buffer contains SDS which, along with heat is used to denature the proteins.

2.5.4.2 Method

Whole cell extracts, described in section 2.5.1, were mixed with 4X XT loading buffer (Biorad, Hertfordshire, UK) and fresh extraction buffer (section 2.5.1) to the final required protein concentration of 30 μg in a final volume of 25 μl . Samples were then loaded into a heating block and incubated at 95 °C for 5 min to denature proteins in the

sample. Once allowed to cool, samples were loaded onto an 18 well (30 µl) pre-cast 3-8% Tris-Acetate polyacrylamide gel (13.3 x 8.7 cm, 1mm thick, for electrophoresis (BioRad). HiMark pre-stained high molecular weight marker (Invitrogen, Paisley, Scotland) was also loaded onto the gel in order to estimate protein size in the samples. Gels were placed in a BioRad criterion gel tank according to the manufacturer's guidelines and the electrophoresis tank filled with 1 x Tricine running buffer (Biorad, Herfordshire, UK). Electrophoresis was performed using a constant voltage of 90 V using a PowerPack 200 power supply (Biorad, Herfordshire, UK) and continued until the bromophenol blue in the loading dye had reached the bottom of the gel.

2.5.5 Western blotting

The immobilisation of macromolecules separated by electrophoresis was first performed for DNA (Southern, 1975), but has been extended for both RNA and proteins. In Western blotting, proteins are transferred from polyacrylamide gels onto a protein binding membrane such as nitrocellulose or polyvinylidene difluoride. This transfer is achieved through electro-elution in a transfer buffer. A transfer buffer with a low alcohol content is favoured in order to ensure the transfer of larger (>100 kD) proteins. Immobilisation of proteins onto the membrane is followed by immunodetection by specific antibodies.

2.5.5.1 Method

The electroblotting apparatus was set up as described in the manufacturer's instructions (BioRad, Herfordshire, UK), with components, including the fibre pads, 3 mm filter paper (Whatman, GE Healthcare, Amersham, UK) and HybondC nitrocellulose membrane (GE Healthcare, Amersham, UK) after being soaked in 1.5 x Novex transfer buffer (Invitrogen, Paisley, Scotland) for at least 15 min beforehand. HybondC nitrocellulose membrane was chosen for its protein binding capacity. This membrane has a binding capacity of 80-100 mg/cm2 due to electrostatic and hydrophobic interactions with the nitrocellulose web. The blotting cassette was constructed as shown in Figure 2.9, and care was taken to ensure there were no air bubbles between any of the layers. The transfer of separated proteins from the gel to the nitrocellulose membrane was the achieved by the application of an electric current which passed through the gel in the direction of the membrane, carrying with it the protein. In this case, the proteins were transferred for 1 h using a constant voltage of 100 V, on ice. Once transferred, the cassette was disassembled and the membrane recovered for immunoblotting.

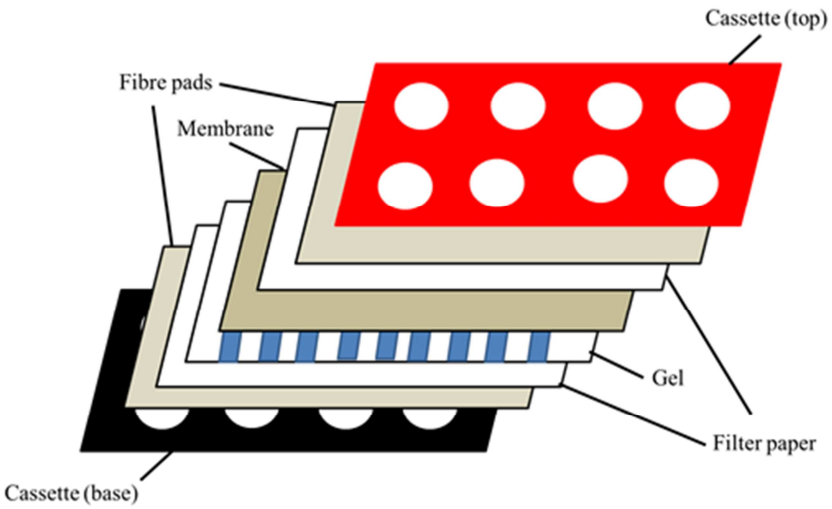

Figure 2.9: Set up of the transfer cassette for Western blotting (Biorad system)

2.5.6 Immunodetection

The nitrocellulose membrane was blocked in non-fat dried milk dissolved in 0.05 % Tween in TBS to prevent nonspecific binding of antibodies to unoccupied sites on the nitrocellulose membrane. Tween 20 (Sigma) is a mild ionic detergent used in all buffers throughout immunodetection as it reduces non-specific binding to nitrocellulose and antigens. 0.05 % Tween in TBS was also used for the dilution of antibodies in the immunodetection procedure. After blocking, the membrane was incubated in a primary antibody specific to the protein of interest, as described along with the relevant conditions in Table 2.4. This was followed by a secondary antibody from a different species raised against the Ig of the first species, also described in Table x. This secondary antibody is conjugated to HRP which catalyses the reaction provided by the ECL system.

Target	Species (raised in)	Manufacturer	Catalogue number	Dilution	Conditions
NF-κB p65	Mouse	Santa Cruz Biotechnology	sc-8008x	1 in 3000	1 h RT
NF-κB p50	Mouse	Santa Cruz Biotechnology	sc-8414	1 in 1000	1 h RT
NF-κB p52	Rabbit	Santa Cruz Biotechnology	sc-298	1 in 1000	o/n 4 °C
NF-κB RelB	Rabbit	Santa Cruz Biotechnology	sc-226	1 in 1000	o/n 4 °C
NF-κB c-Rel	Rabbit	Santa Cruz Biotechnology	sc-71	1 in 1000	o/n 4 °C
PARP-1	Rabbit	Santa Cruz Biotechnology	H-250	1 in 1000	1 h RT

Lamin	Mouse	Santa Cruz Biotechnology	sc-7293	1 in 500	o/n 4 °C
β-actin	Mouse	Calbiochem	CP01	1 in 10000	1 h RT
DNA-PK (ser 2056)	Rabbit	Abcam	Ab18192	1 in 100	o/n 4 °C
DNA-PKcs	Mouse	Thermo-Shandon	MS-370-P	1 in 500	1 h RT
Anti-mouse Ig-HRP	Goat	DAKO	P0447	1 in 1000	1 h RT
Anti-rabbit Ig-HRP	Goat	DAKO	P0448	1 in 1000	1 h RT

Table 2.4: Primary and secondary antibodies used in Western blotting

2.5.7 Enhanced chemiluminesence for protein detection

2.5.7.1 Principle

Enhanced chemiluminesence (ECL) is a light emitting, non-radioactive and highly sensitive system that is able to detect less than 1 pg of antigen on nitrocellulose. ECL requires the oxidation of luminol in the presence of an enhancer (phenol) under alkaline conditions by HRP, shown in Figure 2.10. This oxidation places luminol in an excited state which decays to ground state with the associated emission of light. Phenol increase the light output by 1000-fold and prolongs the time of emission so that peak emission occurs between 2 and 30 min following incubation with reagents. The maximum light emission occurs at 428 nm which can be detected by autoradiography film or charge couple devices such as Fuji LAS 3000.

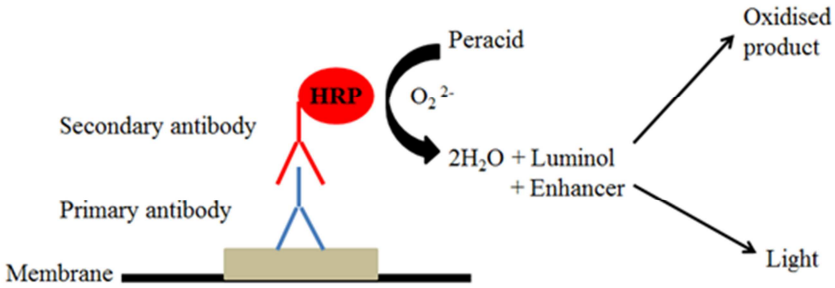

Figure 2.10: The HRP conjugate on the secondary antibody catalyses the formation of $2H_2O + O_2^{2-}$ from peracid, leading to the peroxidase catalysed degradation of Luminol, which in turn produces the luminescence

2.5.7.2 Method

ECL was used as per manufacturer's protocol (GE Healthcare, Amersham, UK). Briefly, luminol enhancer and peroxide reagents were mixed in 1:1 ratio in a volume sufficient to cover the membrane equally which was then transferred onto the blot with

a pipette. The blot was left for 1 min before excess reagent was removed. The blot was then wrapped in a plastic document wallet and placed protein side up in the Fuji LAS 3000 and the image captured with an exposure of the appropriate time.

2.5.8 Quantification using Aida Image Analyser

Immuno-blot images captured using the Fuji LAS 3000 were analysed using Aida Image Analyser version 3.28.001 using the 2D, densiometric analysis function within the software, as described in section 2.4.7.

2.6 Analysis of apoptosis

2.6.1 Annexin V FACs assay

2.6.1.1 Principle

It is widely accepted that loss of plasma membrane integrity is one of the earliest features of apoptosis. In cells undergoing apoptosis, the membrane phospholipid phosphatidylserine (PS) is translocated from the inner to the outer leaflet of the plasma membrane, thereby exposing PS to the external cellular environment. Annexin V is a 35-36 kDa Ca^{2+} dependent phospholipid-binding protein that has a high affinity for PS, and binds to cells with exposed PS, hence identifying cells going through the early stages of apoptosis. Annexin V may be conjugated to fluorochromes including FITC, and still retains its high affinity for PS, therefore serving as a sensitive probe for flow cytometric analysis of cells that are undergoing apoptosis. FITC Annexin V staining precedes the loss of membrane integrity which is associated with the latest stages of cell death, known to result from either apoptotic or necrotic processes. For this reason, staining with FITC Annexin V is typically used in conjunction with a vital dye such as propidium iodide (PI), which can identify nuclear changes such as DNA fragmentation. Viable cells with intact membranes exclude PI, whereas the membranes of dead and damaged cells are permeable to PI. For example, cells that are considered viable are FITC Annexin V and PI negative; cells that are in early apoptosis are FITC Annexin V positive and PI negative; and cells that are in late apoptosis or already dead are positive for both FITC Annexin V and PI.

2.6.1.2 Advantages and disadvantages

The major advantage of this technique, over others which are used to investigate cellular levels of apoptosis is that this assay can differentiate between the stages of apoptosis. It

also a flow cytometric (FACs) based assay, and as with all FACs assays a known number of cells (referred to as 'events') are counted, across all samples, which means that any cell number is constant regardless of treatment status of each sample. An example of an annotated FACs plot is shown in Figure 2.11.

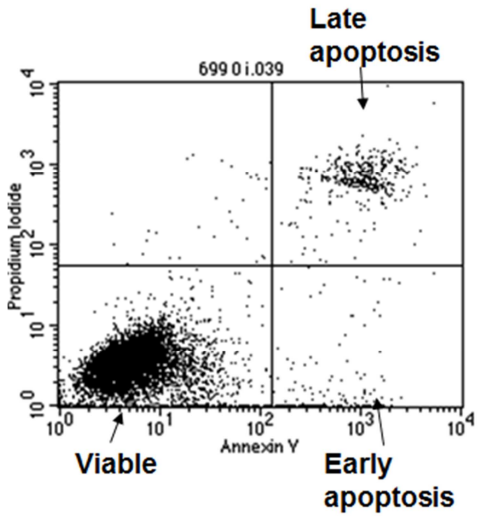

Figure 2.11: An example FACs plot from an annexin V assay

FACs analysis is a technique for counting particles, such as cells and chromosomes, by suspending them in a stream of fluid and passing them by an electronic detection apparatus. It allows simultaneous multiparametric analysis of the physical and/or chemical characteristics of up to thousands of particles per second. Briefly, the principles of FACs analysis are centered around a beam of light (usually from a laser) of a single wavelength which is directed onto a hydrodynamically-focused stream of liquid. A number of detectors are aimed at the point where the stream passes through the light beam: one in line with the light beam (Forward Scatter or FSC) and several perpendicular to it (Side Scatter or SSC) and one or more fluorescent detectors. Each suspended particle from 0.2 to 150 micrometers passing through the beam scatters the ray, and fluorescent chemicals found in the particle or attached to the particle may be excited into emitting light at a longer wavelength than the light source. This combination of scattered and fluorescent light is picked up by the detectors, allowing analysis of the physical and chemical structure of each individual particle. FSC correlates with the cell volume and SSC depends on the inner complexity of the particle (i.e., shape of the nucleus, the amount and type of cytoplasmic granules or the membrane roughness).

2.6.1.3 Method

Cells were plated onto 6-well plates at a density that gave a final cell number of 3-5 x 10^5 cells/ml on the day of experiment. Treatment schedules, regarding siRNA transfection and treatment with IR or drugs are as described in the individual chapters and figure legends. The PARP inhibitor, AG-014699 was added at final concentration of <0.1 % DMSO (v/v) in medium for all experiments. AG-014699 was added 1 h before γ-irradiation as described in the individual chapters and figure legends.

For all experiments, cells were exposed to γ-irradiation then incubated at 37 ^oC in a humidified atmosphere containing 5% CO_2 for 24 h. Following this the cells were trypsinised (as described in section 2.2.3) and counted using a haemocytometer (section 2.2.4). The FITC Annexin V Apoptosis Detection Kit II (BD Biosciences, Oxford, UK), was then used to assess the levels of apoptosis in each sample, according to manufacturers' instructions. Briefly, once counted, samples were re-suspended in 1x Binding buffer (provided) to a concentration of 1 x 10^6cells/ml, and 100 µl of this solution was transferred to a 5 ml FACs tube. 5 µl of FITC Annexin V and 5 µl of PI (both provided) were then added to each tube before vortexing, and incubation for 15 min, at room temperature in the dark. Following this a further 400 µl of 1x Binding buffer was added to each sample and then sample were then analysed using the Becton Dickinson FACScan (Becton Dickinson, Oxford, UK) and Cell Quest Software (Becton Dickinson, Oxford, UK). Results were expressed as a percentage increase in apoptosis of treated sample, compared with untreated controls.

2.6.2 Caspase 3/7 assay

2.6.2.1 Principle

The Caspase-Glo 3/7 Assay is a homogeneous, luminescent assay that measures caspase-3 and -7 activities from Promega (Southampton, UK). The assay provides a luminogenic caspase-3/7 substrate, which contains the tetrapeptide sequence DEVD, in a reagent optimized for caspase activity, luciferase activity and cell lysis. This peptide also contains a site which is cleaved by the caspases 3 and 7. The addition of the Caspase-Glo 3/7 Reagent in results in cell lysis, followed by caspase cleavage of the substrate and generation of a luminescent signal, produced by luciferase (Figure 2.12). The luminescence observed is proportional to the amount of caspase activity present.

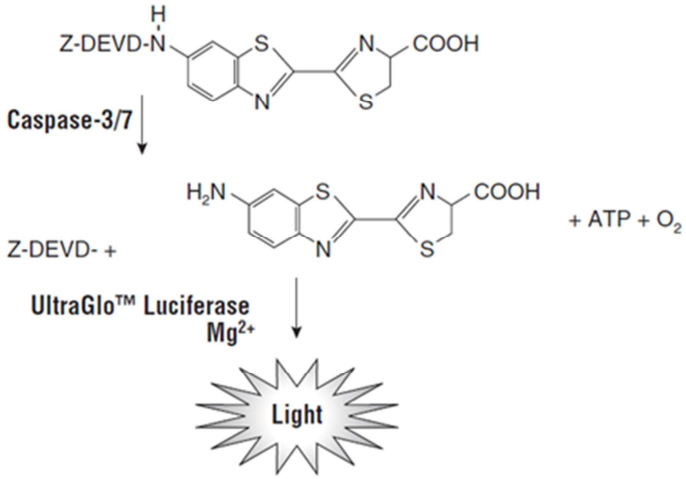

Figure 2.12: Caspase-3/7 cleavage of the luminogenic substrate containing the DEVD sequence. Following caspase cleavage, a substrate for luciferase (aminoluciferin) is released, resulting in the luciferase reaction and the production of light
From:http://www.promega.com/

2.6.2.2 Advantages and disadvantages

This assay is undertaken in 96-well plate format, and hence compared with some other methods used to investigate the induction of apoptosis, it is much higher throughput. The luminescent assay also avoids interference from fluorescence signals, which can be an issue when screening new compounds. This assay also requires fewer cells than many other methods, however the drawback to it is that is relies on the fact that the absolute cell number per well is constant, which may not always be the case in drug treated *versus* control samples.

2.6.2.3 Method

Cells were plated onto 96-well plates at a density that gave a final cell number of 2 x 10^4cells/ml on the day of experiment. Treatment schedules, regarding siRNA transfection and treatment with IR or drugs are as described in the individual chapters and figure legends. The PARP inhibitor, AG-014699 was added at final concentration of <0.1 % DMSO (v/v) in medium for all experiments. AG-014699 was added 1 h before γ-irradiation as described in the individual chapters and figure legends.

For all experiments, cells were exposed to γ-irradiation then incubated at 37 ^oC in a humidified atmosphere containing 5% CO_2 for 24 h. Caspase-Glo 3/7 Reagent was prepared, according to manufacturers' instructions by mixing 10 ml of the Caspase-Glo 3/7 buffer with the Caspase-Glo 3/7 substrate (both provided). This was mixed gently

by inverting before adding it to the culture medium at a 1:1 ratio. Plates were then shaken for 30 s and incubated at room temperature for 2 h. Cell lysates were transferred to a white-walled 96-well plate. Luminescence was measured using a microplate luminometer (Perkin Elmer, Buckinghamshire, UK). Results were expressed as a percentage increase in apoptosis of treated sample, compared with untreated controls.

2.7 Quantification of single stranded DNA breaks following DNA damaging agents

2.7.1 Alkaline Comet assay

2.7.1.1 Principle

The alkaline Comet assay kit (Trevigen, Gaithersberg, MD, USA) is used to analyse the DNA fragmentation associated with DNA damage, in particular damage caused by SSBs. Cells are mixed with low melting point agarose and are pipetted onto specially treated pre-coated slides in order to promote agarose adherence. Alkaline conditions are then used to unwind and relax DNA, which is then able to migrate out of the cell during electrophoresis. DNA can then be visualised using SYBR Green nucleic acid gel stain. Cells that have accumulated DNA damage appear as fluorescent comets with tails of fragmented DNA, whereas, normal undamaged DNA does not migrate far from the origin. This is shown in Figure 2.13.

Figure 2.13: Comet assay workflow
From: http://www.trevigen.com/

2.7.1.2 Advantages and disadvantages

This assay allows analysis of SSBs at the single cell level and therefore allows insight into the extent and diversity of DNA damage across an entire population of cells. It should be noted that although this alkaline Comet assay is used to identify SSBs, it can detect some DSBs and alkali labile sites, therefore it is important to choose doses of

DNA damaging agents (known to activate both SSBs and DSBs), that are reported to activate a greater proportion of SSBs, compared with DSBs. However, there is another version of the Comet assay which uses neutral conditions, which detects primarily DSBs.

2.7.1.3 Method

Cells were plated onto 6-well plates at a density that gave a final cell number of 3-5 x 10^5 cells/ml on the day of experiment and treated with siRNA and IR or drugs are as described in the individual chapters and figure legends. For all experiments, cells were exposed to drug for a given length of time (see individual figure legends) and incubated at 37 ^oC in humidified atmosphere containing 5% CO_2. Following this the cells were trypsinised (secion 2.2.3) and pelleted at 500 xg for 5 min. Cells were washed once with PBS and re-pelleted as before, then counted using a haemocytometer (section 2.2.4). Following this, cells were re-suspended in ice cold PBS to a concentration of 1 x 10^5cells/ml. Cells were then mixed with proprietary low melting point agarose, which had been pre-warmed to 37 °C. This cell/agarose mix was then pipetted on Comet slides and placed at 4 °C in order to gel. Once set, the slides were incubated for 30 min in Comet lysis solution at 4° C in the dark in order to relax the DNA. Slides were protected from light to prevent any further DNA damage, and kept at 4 °C in order to prevent DNA repair. Following this, slides were incubated in Alkaline unwinding solution (300 mM sodium hydroxide, 1 mM EDTA, pH>13), which unwinds the DNA, before being subjected to electrophoresis under alkaline conditions (Alkaline electrophoresis solution: 300 mM sodium hydroxide, 1 mM EDTA, pH>13) at 20 V for 40 min, in the dark, and then fixed, with 70 % ethanol. After drying at room temperature overnight, in the dark, slides were stained with SYBR Green nucleic acid gel stain in TE buffer (10 mM Tris-HCl pH 7.5, 1 mM EDTA).

2.7.2 Fluorescence microscopy to visualise Comet slides and quantification using Komet 5.5

An Olympus BH2-RFCA fluorescence microscope (10x objective) (GX Optical, Suffolk, UK) with Hamamatsu ORCAII BT-1024 cooled CCD camera (Hamamatsu Photonics, Massy, France) was used to capture images. Image Pro Plus (Media Cybernetics, Bethesda, MD, USA) was used for image capture. The software package, Komet 5.5 (Kinetic Imaging, Nottingham, UK), was used to analyse results providing extensive Comet measurements and data including percentage head DNA, percentage

tail DNA, tail length, olive tail moment and Comet optical intensity. Data is represented in two forms, firstly using the Olive Tail Moment (OTM), which is used as a measure of both the smallest detectable size of migrating DNA (reflected in the comet tail length) and the number of relaxed / broken pieces (represented by the intensity of DNA in the tail), and secondly by the percentage DNA in the comet tail, both are recommended by the Comet Assay Interest Group.

2.8 Quantification of NF-κB DNA binding activity

2.8.1 Measurement of NF-κB DNA binding using the Pierce EZ detect p65 DNA binding ELISA

The ability of murine NF-κB p65 or p50 to bind a specific κB consensus sequence was assessed using an EZ-Detect Chemiluminescent Transcription Factor Assay (Pierce, Perbio Science UK Ltd., Cramlington, UK) according to the manufacturer's instructions. Cells were plated onto 6-well plates at a density that gave a final cell number of 3-5 x 10^5 cells/ml on the day of experiment and treated with siRNA and IR or drugs are as described in the individual chapters and figure legends. For all experiments, cells were exposed to drug for 24 h incubated at 37 ^oC in a humidified atmosphere containing 5% CO_2. Following this the cells were trypsinised (as described in section 2.2.3) and harvested at various timepoints (see figure legends) for nuclear extraction. Nuclear lysates of equivalent protein levels, prepared using the NE PER kit (section 2.5.2) were allowed to bind to the consensus sequence (Table 2.5), which was pre-bound to a 96-well Enzyme-linked immunosorbent assay (ELISA) plate provided with the assay in the presence of poly dI•dC and an NF-κB binding buffer for 1 h at room temperature with gentle agitation. Importantly, the poly dI•dC was added to prevent any non-specific binding. Non-specific DNA binding was assessed via incubation of nuclear lysates with mutant or wild type competitor duplexes (Table 2.5), thus providing a robust control for the assay.

κB consensus sequence	**GGGACTTTCC**
Wild-type competitor duplex	5'-CACAGTTGAG**GGGACTTTCC**CAGGC-3' 3'-GTGTCAACTC**CCCTGAAAGG**GTCCG-5'
Mutant competitor duplex	5'-CACAGTTGAG**GCCACTTTCC**CAGGC-3' 3'-GTGTCAACTC**CGGTGAAAGG**GTCCG-5'

Table 2.5: Competitor duplexes for NF-κB DNA binding assay (Pierce)

The plate is then washed three times with the wash buffer provided and incubated with a primary antibody against the p65, or p50, NF-κB subunit for 1 h. Following washes, the plate is then incubated in the presence of an HRP-tagged secondary antibody directed against the anti-p65 or anti-p50 primary antibody for a further hour. Antibody binding is detected via incubation of the plate with a chemiluminescent substrate and read using a Fuji LAS 3000. The reaction scheme is shown in Figure 2.14. Images were analysed using Aida Image Analyser version 3.28.001 using the 2D, densitometric analysis function within the software, as described in section 2.4.7. Values were corrected for background activity and expressed as mean fold values of triplicates.

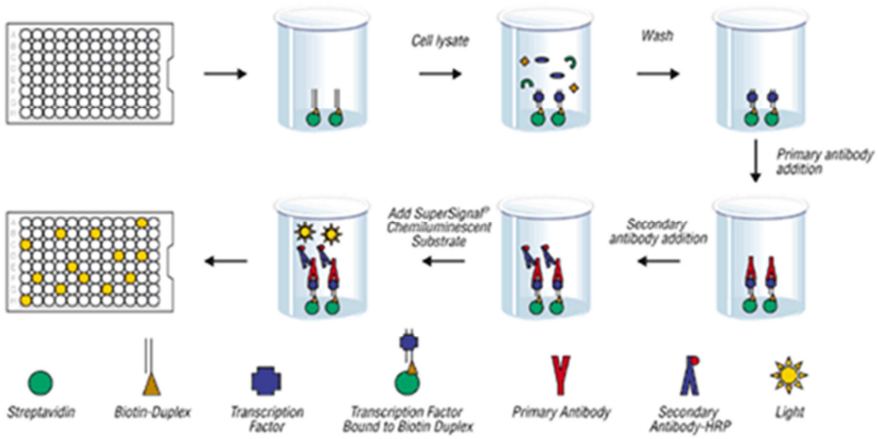

<u>Figure 2.14:</u> Schematic protocol for EZ-Detect NF-κB p50 and NF-κB p65 Transcription Factor Assay Kits.
From: http://www.qcbio.com/pierce/89858.htm

2.8.2 Measurement of NF-κB DNA binding using the TransAM Family ELISA

The ability of human NF-κB p65, p50, p52, RelB or c-Rel to bind a specific κB consensus sequence was assessed using a TransAM Family ELISA Assay (Active Motif, Rixensart, Belgium) according to the manufacturer's instructions. Cell treatment and nuclear extraction was as described in section 2.8.1, for the EZ Detect ELISA Assay. In this case, nuclear lysates of equivalent protein levels, prepared using the NE PER kit (section 2.5.2) were allowed to bind to the consensus sequence, which was pre-bound to a 96-well ELISA plate in the presence of herring sperm DNA and an NF-κB binding buffer for 1 h (both provided) at room temperature with gentle agitation. Once again, non-specific DNA binding was assessed via incubation of nuclear lysates with mutant or wild type competitor duplexes. The plate was then washed three times with the wash buffer provided and incubated with a primary antibody against the p65, p50,

p52, RelB or c-Rel for 1 h. Following washes, the plate was then incubated in the presence of an HRP-tagged secondary antibody directed against the chosen primary antibody for a further hour. Antibody binding was detected *via* a colourimetric reaction, and in this case the plate was incubated with developing solution for 5 min at room temperature until the wells developed a blue colour. This reaction was stopped by the addition of the stop solution containing an acid, which turns the blue colour yellow. Absorbance was then read at 450 nm on the Spectromax plate reader (Molecular Devices, Berks, UK), and values were corrected for background activity and expressed as mean fold values of triplicates.

2.8.4 Advantages and disadvantages

There are other methods used to assess the DNA binding of transcription factors, including the classical gel retardation, or EMSA. Although this assay is highly sensitive, it is not as high throughput as the ELISA-based assays used here. In an EMSA, nuclear extracts are incubated with a radio-active double-stranded oligonucleotide probe containing the transcription factor consensus sequence, therefore if the transcription factor is active, it will bind to the probe. Sample are resolved using electrophoresis on poly-acrylamide gels and probed using methods similar to those described for Western blotting in section 2.5. This method is much more time consuming and also requires the use of radio-chemicals, which therefore make the ELISA assays, a better choice for the assessment of transcription factor DNA binding. Importantly, a large number of DNA binding assays were undertaken as part of this thesis, and therefore the ELISA was the method of choice in these cases due to the fact it is a high-throughput assay, which allowed the direct comparison of a number of extracts within one plate.

2.9 Quantification of NF-κB-dependent gene transcription

2.9.1 Competent cells

Competent cells used for transformation of plasmid DNA were Top10 (purchased from Invitrogen, Paisley, Scotland.)

2.9.2 Bacterial transformations

1-2 µg of plasmid DNA was added to 100µl of competent cells and mixed by gentle pipetting. A control aliquot of competent cells with no DNA added was also transformed in tandem. Cells and DNA mixtures were placed on ice for 20 min, heat

shocked at 37°C for 5 min and then returned to the ice for a further 5 min. 1ml of sterile SOC medium (2 % tryptone, 0.5 % yeast extract, 10 mM NaCl, 2. 5 mM KCl, 10 mM MgCl2, 10 mM MgSO4, 20 mM glucose) was added and cell suspensions were incubated at 37°C for 1 h with agitation. Cells were then spread onto sterile LB-agar plates (Sigma, Poole, Dorset) containing an antibiotic appropriate to the resistance of the plasmid and incubated overnight at 37°C.

2.9.3 Extraction of plasmid DNA using Qiagen MAXI-prep

A single bacterial colony was picked and used to inoculate 200ml LB (2 % Tryptone, 1 % Yeast, 1 % NaCl) containing the appropriate antibiotic for plasmid selection. Cultures were incubated at 37°C at 180 rpm in an orbital shaker overnight until an appropriate cell density was reached. Plasmid DNA was extracted using the Qiagen Maxi Prep Kit (Qiagen, West Sussex, UK) according to the manufacturer's instructions. Bacterial cell pellets were lysed under alkaline conditions, clarified and loaded onto a QIAGEN-tip column. DNA was washed and eluted in an appropriate buffer. Plasmid DNA was precipitated using isopropanol and pellets washed in 70 % ethanol before being resuspended in endotoxin free TE Buffer (10 mM Tris-HCl pH 8. 0, 1 mM EDTA). Plasmid DNA concentration was determined using a NanoDrop ND-1000 spectrophotometer (Labtech, East Sussex, UK), as described previously (section 2.3.3).

2.9.4 Transient transfection of plasmid DNA and siRNA

Cells were seeded at 2 x 10^3 cells/well onto 24-well tissue culture treated plates and incubated at 37 ^oC in humidified atmosphere containing 5% CO_2 to adhere overnight. The following day cells were transfected with 200ng of an NF-κB-luciferase construct containing 3 tandemly repeated NF-κB consensus sequence binding sites in the promoter (kindly provided by Prof. Ron Hay, Dundee University) and 200 ng of a pCMB-β-galactosidase plasmid containing a minimal promoter element up-stream from the β-galactosidase gene as well 50 nM p65, PARP-1 or NS siRNA (described in section 2.3). Plasmid DNA and siRNA were incubated in serum free RPMI for 5 min before mixing with the transfection reagent, Lipofectamine 2000 (Invitrogen, Paisley, Scotland), also diluted in serum free RPMI. The resultant transfection cocktails were incubated at room temperature for a further 20 min before applying to the 24-well plates containing cells. Cells were then incubated at 37 ^oC in humidified atmosphere containing 5% CO_2, for 5 h, before aspirating this media and replacing with full media (RPMI 1640, 10 % FBS) for a further 48 h at 37 ^oC in humidified atmosphere

containing 5% CO_2. This allows the knockdown of the target proteins and to ensure the plasmids are expressing in the cells before a 1 h pre-treatment with AG-014699 prior to treatment with γ-irradiation or TNF-α.

2.9.5 Harvesting cells for luciferase and β-galactosidase assays

Following treatment, cells were washed in PBS at appropriate timepoints (see figure legends) and stored overnight at -20°C, until lysis. Cells were lysed in 100µl Reporter lysis buffer (Promega, Southampton, UK) by scraping with a sterile pipette tip to facilitate full cell lysis. Once cells were fully lysed the cell/Reporter lysis buffer mix was assayed for both β-galactosidase and luciferase activity.

2.9.6 β-galactosidase assay

A control plasmid containing a β-Galactosidase gene which is ubiquitously expressed in transfected cells was co-transfected with reporter constructs to account for discrepancies in transfection efficiencies and cell death between experiments. To assess the β-Galactosidase activity of transfected cells, cell lysate was incubated in a 96 well assay plate with an equal volume of β-Galactosidase buffer (1 mM MgCl2, 45 mM β-mercaptoethanol, 40µg/ml o-nitrophenyl-beta-galactopyranoside solution, 1 mM NaxHyPO4 buffer (pH 7.5)) for approximately 20 min at 37°C until colour developed. The reaction was terminated by the addition of 1M Na_2CO_3 and absorbance read at 450 nM using a Bio-Rad 680 Microplate reader (Bio-Rad Laboratories, Hertfordshire, UK).

2.9.7 Luciferase reporter assay

In order to assess the relative luciferase activity of each sample, cell lysates were loaded in triplicate onto a white walled 96 well assay plate and incubated with luciferase assay buffer (Promega, UK) and read immediately on Micro Beta Plus liquid scintillation counter (Wallac, Millipore, Watford UK). Luciferase values were corrected for β-galactosidase activity and expressed as mean fold values of triplicates.

2.10 Quantification of specific gene transcription

2.10.1 Preparation of RNA for real time reverse transcriptase polymerase chain reaction (qRT-PCR) and gene expression microarray

2.10.1.1 Harvesting cells for RNA extraction

Cells were plated onto 6-well plates at a density that gave a final cell number of 3-5 x 10^6 cells/ml on the day of experiment and treated with siRNA and IR or drugs are as

described in the individual chapters and figure legends. For all experiments, cells were exposed to drug for 24 h incubated at 37 ^{o}C in humidified atmosphere containing 5% CO_2. Following this, the cells washed with ice cold PBS before being gently scraped from the plate using a cell scraper (Corning, UK). It should be noted that scraping was performed on ice in order to minimise RNA degradation. Cells were transferred to 1.5 ml tubes and pelleted at 500 xg for 5 min in a cooled centrifuge. The PBS supernatant was removed and the pellets stored at -80 °C until RNA extraction took place.

2.10.1.2 Extraction of RNA using Qiagen RNeasy Mini Kit

The RNeasy Mini kit (Qiagen, West Sussex, UK) was used to extract RNA from cell pellets. The pellets, collected as above, were defrosted slowly on ice and, all steps were performed on ice or in a cooled centrifuge to minimise RNA degradation. The pellet was loosened before 350 µl RLT buffer was added. This contains guanidine isothiocyanate and β-mercaptoethanol to stabilise the RNA species in the sample. Samples were then homogenised by passing through a 20-gauge needle 5 times, then 1 volume of 70 % ethanol was added to promote binding of RNA to the silica gel membrane in the spin column. The sample was applied to the column and centrifuged at 8000 xG for 15 sec before washing with RW1 buffer and repeated centrifugation. Two subsequent washes with RPE buffer were performed, followed by centrifugation. The flow-through was discarded after each step. After these washes 30 µl of RNase-free H_2O was applied to the column to elute the RNA.

2.10.1.3 Assessing RNA concentration and quality

The RNA concentration in each sample was assessed using the Nanodrop ND-1000 spectrophotometer (Labtech, East Sussex, UK), as described in section 2.3.3.

2.10.2 Reverse transcriptase Real time PCR

2.10.2.1 Polymerase chain reaction

The polymerase chain reaction (PCR) is a method by which large copies of a target DNA sequence can be synthesised. A PCR reaction generally contains; target DNA, primers, the four deoxyribonucleoside triphosphates (dNTPs) and a DNA polymerase that is thermally stable. A standard PCR reaction has 3 steps; denaturation, primer annealing and elongation. The denaturation step heats the PCR mix to 95 °C to denature the DNA into single strands for replication, the primers are then annealed to the target DNA as the PCR mix is rapidly cooled to approximately 60 °C. The primers are

designed such that they are complementary to the two strands flanking the target DNA. The primers are in excess and consequently, the two original DNA strands do not re-anneal. The DNA polymerase finally elongates the primer and produces a complementary strand of DNA by copying the single stranded templates. This process is repeated again, in cycles and as a result the target DNA is amplified (Saiki et al., 1989).

2.10.2.2 Principles of qRT-PCR

qRT-PCR was developed to monitor PCR reactions as they occur due to collection of data as the reaction progresses. It is generally accepted the higher the starting level of target sequence, the sooner a significant level is reached, and with this method the specific PCR product is detected as it accumulates. For experiments described in this thesis, the Taqman (Applied Biosystems, Carlsbad, CA, USA) system was used. This widely used method uses a fluorogenic labelled probe that binds to the target sequence, which is made up of a high energy reporter dye at the 5' end, and a lower energy quencher dye at the 3' end, both of which are in close proximity to one another. The reporter dye, fluorescein (FAM) is excited by the light source, and rather than emitting fluorescence it transfers this energy to the quencher dye (TAMRA) through fluorescence resonance energy transfer (FRET).

The probe is designed to anneal to the target sequence downstream of the primer and as the DNA polymerase (which has a 5'-exonuclease activity) extends the primer it encounters this probe and digests it. This then releases the quencher dye from the probe so the two dyes are no longer in close proximity. When the reporter dye is excited by the light source, fluorescence emissions are considerably higher, and the cleaving of the probe and extension time of the primer increases the overall fluorescence intensity of the reaction. The increase in reporter signal is captured by the sequence detection instrument whilst the rest of the probe is removed from the target sequence allowing primer extension to continue. It should also be noted that probe binding to the target sequence, does not affect the overall PCR reaction. As cycles progress, additional reporter dye molecules are cleaved from the probes increasing the fluorescence intensity proportional to the amount of PCR product (Higuchi et al., 1993). qRT-PCR uses these principles in order to determine the mRNA transcript levels of a chosen gene, however before this reaction can proceed, mRNA must be reverse transcribed into complementary DNA (cDNA). The primers designed to detect cDNA were designed to cross exon-exon boundaries in the mRNA to avoid contaminating DNA from being

amplified in the PCR reaction (Foley et al., 1993). This reaction is described in section 2.10.2.4.1.

2.10.2.3 Advantages and disadvantages of qRT-PCR

qRT-PCR is a fully quantitative technique and is therefore often favoured over traditional PCR assays for the assessment of gene expression. Conventional PCR experiments run for a set number of cycles, usually 40, and the products are separated using agarose-gel electrophoresis. Gels are subsequently stained with ethidum bromide (EtBr), and the end point measures the amount of product, making it only semi-quantitative. EtBR staining makes it more difficult to determine small changes in gene expression, whereas measurements from qRT-PCR assays are taken during the exponential phase of the reaction, allowing greater sensitivity.

2.10.2.4 Quantitative real-time PCR method

2.10.2.4.1 Reverse transcriptase step

In order to generate cDNA for qRT-PCR, a reverse transcriptase step was performed using the High capacity cDNA reverse transcription kit with RNase inhibitor (Applied Biosystems, Carlsbad, CA, USA). 1 µg of RNA was transcribed for each sample, in a final volume of 20 µl (including the master mix). The reaction is summarised in Table 2.6:

Reagent	**Volume (µl)**
10x RT buffer	2.0
25x dNTP mix	0.8
10x RT primers	2.0
Reverse transcriptase	1.0
RNase inhibitor	1.0
Nuclease-free H_2O	3.2
RNA (diluted in nuclease-free H_2O)	10.0

Table 2.6: Reaction mix for reverse transcriptase PCR

The reaction mix was made up in 0.2 ml PCR tubes (Starlabs, Notts, UK) on ice and then transferred to a thermal cycler for the following programme: 25 °C for 10 min, 37 °C for 120 min, 85 °C for 5 min. cDNAs were stored at -20°C until qRT-PCR reactions.

2.10.2.4.2 Quantitative PCR step

The primers and probes used were all from Applied Biosystems (assay on demand) and details are given in the chapters where they are specifically used. All of the results were normalised to a control gene. Firstly, cDNA was diluted 1 in 5 to 10 ng/µl with with nuclease free H_2O, so for a final concentration of 20ng cDNA, each reaction required 2 µl of diluted cDNA. Taqman gene expression, for example the β actin assay reagents, were thawed gently on ice and the reactions set up, in triplicate as described in Table 2.7:

Component	1 x repeat (µl)	3 x repeat (µl)
Taqman master mix	12.5	37.5
Gene expression assay	1.25	3.75
cDNA	2 (10 ng/µl)	6 (10 ng/µl)
Nuclease-free H_2O	9.25	27.75

Table 2.7: Reaction mix for qRT-PCR

Samples were then pipetted into a 96-well qRT-PCR plate (Applied Biosystems), on ice, along with a control which contains no cDNA. Any bubbles were removed using a sterile needle before the plate was covered with a plastic plate sealer (Applied Biosystems). The plate was then loaded onto the 7500 Fast System (Applied Biosystems) and then assayed using the following protocol: 50 °C – 2 min (1 cycle), 95 °C – 10 min (1 cycle), 95 °C – 15 sec then 60 °C – 1 min (for a total of 40 cycles). Results were analysed using the 7500 Fast System Software, which generates an amplification plot, and the ΔΔCt method was used to determine the expression of each gene of interest relative to the β-actin control.

2.11 Statistical analysis

2.11.1 Statistical analysis using GraphPad Prism software

GraphPad Prism software v4.0 (La Jolla, CA, USA) was used to analyse data, undertake statistical testing and represent data graphically.

Chapter 3. Investigation into the role of PARP-1 as a regulator of DNA-damage activated NF-κB

3.1 Introduction

There is an increasing body of evidence suggesting that PARP-1 is a promoter-specific nuclear co-regulator (either a co-activator or co-repressor) of numerous transcription factors, reviewed extensively in section 1.5. This includes the sequence-specific DNA – binding transcriptional regulators, NF-κB, B-Myb, Oct-1, AP-1, Sp1, NFAT, Elk1, HIF-1α and HTLV-Tax-1 (Kraus, 2008, Krishnakumar and Kraus, 2010), however the role of PARP-1 in regulation of these factors can be diverse. PARP-1 may act *via* through local modification of chromatin structure (Althaus et al., 1993, Althaus et al., 1994) and/or modulation of transcription factor activity *via* direct binding to gene regulatory sequences, or physical interactions with proteins including transcription factors(Kraus and Lis, 2003, Martin-Oliva et al., 2006). In some cases, the transcription factor is thought to recruit PARP-1 to the promoters of relevant targets but this is likely to dependent on both the cell type concerned and whether or not PARP-1 enzymatic activity is required for co-activation/-repression. This latter point will be discussed in depth in Chapter 4.

In terms of modifying chromatin structure, Althaus *et al*., (1994) proposed that the large overall negative charge of PAR had the ability to relax the chromatin structure, which is usually extremely tightly wound, and displace histones from DNA. This PAR-induced relaxation would then allow large regions surrounding the DNA strand breaks to become accessible to other proteins, such as p65 (Althaus et al., 1994).

PARP-1 also functions as a co-regulator by mediating the transcriptional complexes assembled at the promoters of target genes. In these cases, PARP-1 functions as a promoter exchange factor that promotes the release of inhibitory factors. For example, Pavri *et al.*, (2005) detailed that PARP-1 was responsible for the exchange of an inactive cdk8-postive mediator for an active cdk8-negative mediator during retinoic acid-regulated activation (Pavri et al., 2005).

Chang and Alvarez-Gonzalez (2000) described the interaction between PARP-1 and NF-κB following DNA damage. They showed that inactive PARP-1 could bind NF-κB p50 and block its sequence specific DNA binding, resulting in inhibition of transcriptional activation in Hela cells. Following treatment with the DNA damaging agent, H_20_2, PARP-1 was activated and the binding of the p50 subunit by PARP-1 was released, allowing the subunit to DNA bind and upregulate transcription. Co-incubation

with the PARP inhibitor, 3-amino-benzamide (3-AB), also significantly reduced H_20_2-induced NF-κB DNA binding (Chang and Alvarez-Gonzalez, 2001).

Most recently, Stilmann *et al.,* (2009) have described the formation of a PARP-1 signaling scaffold *via* direct protein-protein interactions with NEMO, PIASγ and ATM in response to DNA damage, induced by ionising radiation (IR). This signalosome formation requires binding with PAR and leads to pro-survival NF- κB signaling (Stilmann et al., 2009). In particular, this group detail that impaired sumoylation following treatment with the PARP inhibitor, 3-AB, results in reduced IKK activation and therefore inhibition of p65 induction. However, Stilmann *et al.,* (2009) use hyper-lethal doses of IR (80 Gy) in combination with the highly non-specific PARP inhibitor, 3-AB which has been shown by us and others to have many off-target effects (Moses et al., 1990).

3.2 Aims

The aim of this chapter was to test the hypothesis that PARP-1 mediates cell survival following DNA damage primarily through activation of NF-κB. The potent and specific PARP inhibitor (AG-014699) together with mouse embryonic fibroblasts (MEFs) proficient and deficient for NF-κB or PARP-1, and siRNA targeting either p65 or PARP-1 were used. Previous studies investigating the role of PARP-1 in the activation of NF-κB following DNA damage have tended to use hyper-lethal doses of damaging agents, such as IR and classical PARP inhibitors, known to have off-target effects. Hyper-lethal damage refers to large doses of a DNA damaging agent, which are much higher than the clinically relevant dose. For example, the recent study by Stilmann *et al.,* (2009) used singular doses of IR as high as 80 Gy IR, which is forty times the single clinical dose of 2 Gy. Therefore, it is vital to test this hypothesis not only using a potent and highly specific PARP inhibitor, which is in clinical trials, but also at clinically relevant doses of IR.

IR is known to produce both single and double stranded DNA breaks. The majority of these breaks are in the phosphodiester linkages in one of the DNA strands (Lomax et al., 2002), suggesting that SSBs are most prevalent following IR. It has been reported that the ratio of SSB to DSBs is 20 : 1 following IR (Lomax et al., 2002). PARP-1 is vital for the repair of SSBs *via* the BER pathway and hence a further aim of this study was to

determine the effects of PARP inhibition on SSB repair in MEFs proficient and deficient for p65. The widely accepted notion surrounding PARP inhibition is that any radio- or chemo-sensitisation observed is a repair-driven response (Bryant and Helleday, 2004, Calabrese et al., 2004). Hence, the hypothesis that PARP inhibition mediates radio-sensitisation through inhibition of NF-κB activation, rather than inhibition of SSB repair, was also tested within this chapter.

3.3 Results

3.3.1 Characterisation of cell lines

Prior to commencement of any assays used to directly test the hypotheses described in section 3.2, the expression levels of PARP-1, NF-κB p65, NF-κB p50, NF-κB p52, c-Rel and RelB, were determined by Western blotting in whole cell extracts from exponentially growing $p65^{+/+}$, $p65^{-/-}$, $PARP\text{-}1^{+/+}$ and $PARP\text{-}1^{-/-}$ mouse embryonic fibroblasts (MEFs). Briefly, $p65^{+/+}$, $p65^{-/-}$, $PARP\text{-}1^{+/+}$ and $PARP\text{-}1^{-/-}$ MEFs were seeded and harvested 48 h later, whole cell extracts were prepared (as described in section 2.5.1) and protein quantification was undertaken using the Pierce BSA protein assay, according to manufacturers' instructions. The levels of p65, p50, p52, RelB, c-Rel or PARP-1 were determined by Western analyses and the house-keeping protein, β-actin, was used as a loading control.

Figure 3.1 shows that the $p65^{-/-}$ MEFS lacked p65 but expressed levels of PARP-1, p50 and p52 similar to the $p65^{+/+}$ MEFs. $PARP\text{-}1^{-/-}$ MEFs did not express PARP-1 protein but had bands of similar intensity to that of the $PARP\text{-}1^{+/+}$ MEFs for p65, p50 and p52. In all cases the house-keeping protein, β-Actin was used a loading control. RelB and c-Rel were not detectable in any of the cells lines assessed; however this is unsurprising as these two subunits are most commonly found in haematopoietic cells and tissues (Rayet and Gelinas, 1999, Ryseck et al., 1996). Previous studies from our laboratory have shown all four of these cell lines show comparable levels IκBα and IκBβ (Veuger et al., 2009).

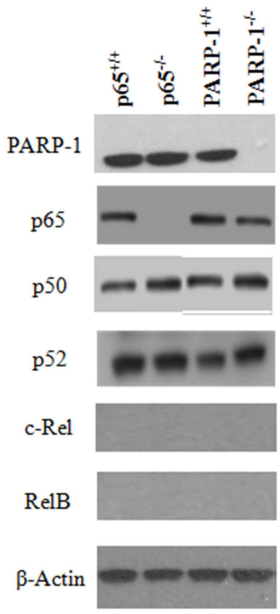

Figure 3.1: Characterisation of cell lines
Western blots of whole cell extracts of untreated $p65^{+/+}$, $p65^{-/-}$, $PARP\text{-}1^{+/+}$ and $PARP\text{-}1^{-/-}$ MEFs; blots were probed using antibodies against PARP-1, p65, p50, p52, c-Rel, RelB and β-actin

This study would be mainly centred around the use of the $p65^{+/+}$ and $p65^{-/-}$ MEFs, and the role of PARP-l in the activation of NF-κB following DNA damage in these cells, hence it was important to ensure these cell lines had similar PARP-1 activity levels, prior to further study. Once, protein expression had been determined, PARP activity was also assessed in the four cell lines using a validated assay (Plummer et al., 2005, Zaremba et al., 2009), this would also confirm that the lack of detectable protein in the $PARP\text{-}1^{-/-}$ cells correlated with an absence of enzymatic activity.

Briefly, basal PARP activity present in cells was measured in $1x10^4$ permeabilized cells that had been incubated with NAD^+ and oligonucleotide (to maximally stimulate PARP activity). The reaction was terminated with excess AG-014699, and replicate samples were blotted onto nitrocellulose membrane. A standard curve of purified PAR (pmol of PAR) was also blotted to aid with quantification. The membrane was probed with PAR-specific antibody and chemiluminescence was detected prior to densiometric analysis. The results shown are the mean of 3 independent experiments.

Figure 3.2 shows stimulated PARP activity, quantified against a standard curve of purified PAR. PARP activity was similar in all cell lines apart from the $PARP\text{-}1^{-/-}$ MEFs

which showed very low (<2%) detectable PARP activity. This low residual PARP activity could be attributable to other members of the PARP superfamily, for example, PARP-2, which like PARP-1 has been implicated in the BER process (Schreiber et al., 2002). Importantly however, the PARP-$1^{+/+}$ cells show significantly higher activity when compared with the PARP-$1^{-/-}$ cells ($p< 0.0001$, unpaired Student's t-test), whereas there is no significant difference in PARP activity between the $p65^{+/+}$ and $p65^{-/-}$ cells ($p=0.105$, unpaired Student's t-test).

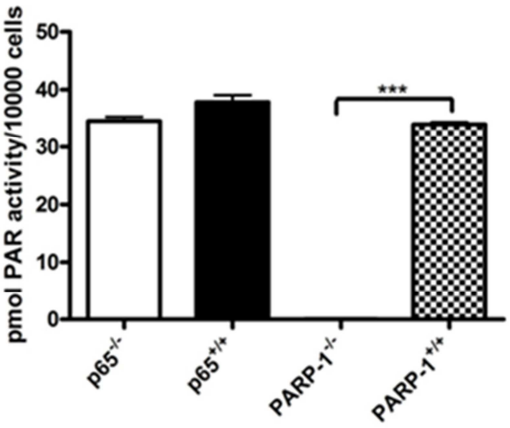

Figure 3.2: Cellular PARP activity
Oligonucleotide and NAD^+-stimulated maximal PARP activity in $p65^{+/+}$, $p65^{-/-}$, PARP-$1^{+/+}$ and PARP-$1^{-/-}$ MEFs. Results shown are the mean + SEM of 3 independent experiments. *** Significance PARP-$1^{+/+}$ versus PARP-$1^{-/-}$ in a Student's unpaired t-test $p<0.001$

3.3.2 Knockdown of target proteins using siRNA technology

Small inhibitory RNA (siRNA) techniques were used to determine optimal conditions for the abrogation both of p65 and PARP-1 expression in the $p65^{+/+}$, $p65^{-/-}$, PARP-$1^{+/+}$ and PARP-$1^{-/-}$ MEFs. Firstly, it was important to determine the optimum timepoint for tranfection, hence $p65^{+/+}$ MEFs were seeded and left for 24 h to adhere before lipid transfection with 50 nM of siRNA oligos targeting either p65 or PARP-1, or a non-specific (NS) control (Table 2.2). The levels of p65 expression were determined at 24, 48, 72 and 96h following lipid transfection. Whole cell extracts were prepared (as described in section 2.5.1) and the levels of p65 or PARP-1 were determined by Western analyses and compared to the house-keeping protein, β-actin.

Figure 3.3A shows that 24 h hours following siRNA transfection, p65 protein was >90 % reduced in the $p65^{+/+}$ MEFs, and that p65 knockdown was maximal (>95 %) 48 h

following transfection. This knockdown persisted for 96 h following transfection. Importantly the control (NS siRNA) had no effect on p65 protein knockdown, compared with mock (vehicle alone) controls. Similarly, Figures 3.3B shows that 24 h hours following siRNA transfection PARP-1 protein was >60 % knockdown in the $p65^{+/+}$ MEFs, and that PARP-1 knockdown was maximal (>95 %) 48 h following transfection. This knockdown persisted for 96 h following transfection, and the control (NS siRNA) had no effect on PARP-1 protein knockdown, compared with mock (vehicle alone) controls. These data suggest that for maximal knockdown of either p65 or PARP-1, the 48 h time-point should be used.

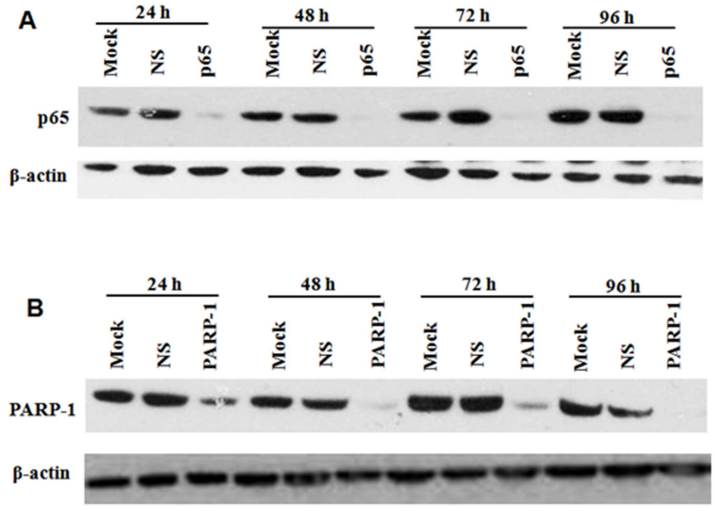

Figure 3.3: Timecourse of siRNA knockdown of NF-κB p65 or PARP-1
(**A**) Western blots of whole cell extracts of $p65^{+/+}$ MEFs at 24, 48, 72 and 96 h after transfection with vehicle alone (Mock), non-specific (NS) siRNA or p65 siRNA. (**B**) Western blots of whole cell extracts of $p65^{+/+}$ MEFs at 24, 48, 72 and 96 h after transfection with vehicle alone (Mock), non-specific (NS) siRNA or PARP-1 siRNA.

keep the conditions as constant as possible. This however, was tested initially using Western blotting analyses. Briefly, $p65^{+/+}$, $p65^{-/-}$, $PARP\text{-}1^{+/+}$ and $PARP\text{-}1^{-/-}$ MEFs were seeded and left for 24 h to adhere before lipid transfection with 50 nM of siRNA oligos targeting p65 or a non-specific (NS) control (Table 2.2). The levels of p65 expression were determined 48 following lipid transfection. Whole cell extracts were prepared (as described in section 2.5.1) and protein quantification was undertaken using the Pierce BSA protein assay, according to manufacturers' instructions. The levels of p65 or PARP-1 were determined by Western analyses and densiometric analysis was used to assess the levels of protein knockdown compared to the house-keeping protein, β-actin.

A reproducible reduction in p65 protein (> 95% knock-down) could be seen 48 h post-transfection using 50 nM siRNA in the $p65^{+/+}$, PARP-$1^{+/+}$ and PARP-$1^{-/-}$ MEFs (Figure 3.4A and 3.4C). Figure 3.4B illustrates that p65 protein levels are significantly reduced by 50 nM p65 siRNA, compared with NS siRNA controls in the $p65^{+/+}$ MEFs ($p<0.0001$, unpaired Student's t-test). Similarly, Figure 3.4D illustrates that p65 protein levels are significantly reduced by 50 nM p65 siRNA, compared with NS siRNA controls in the PARP-$1^{+/+}$ and PARP-$1^{-/-}$ MEFs ($p<0.0001$ and $p<0.0001$, respectively, unpaired Student's t-tests). As expected, p65 siRNA had no effect in the p65 deficient cells (Figure 3.4A). These data show that the optimal conditions for transfection of p65 siRNA in either the $p65^{+/+}$, $p65^{-/-}$, PARP-$1^{+/+}$ or PARP-$1^{-/-}$ MEFs, is the concentration of 50 nM and the 48 h time-point.

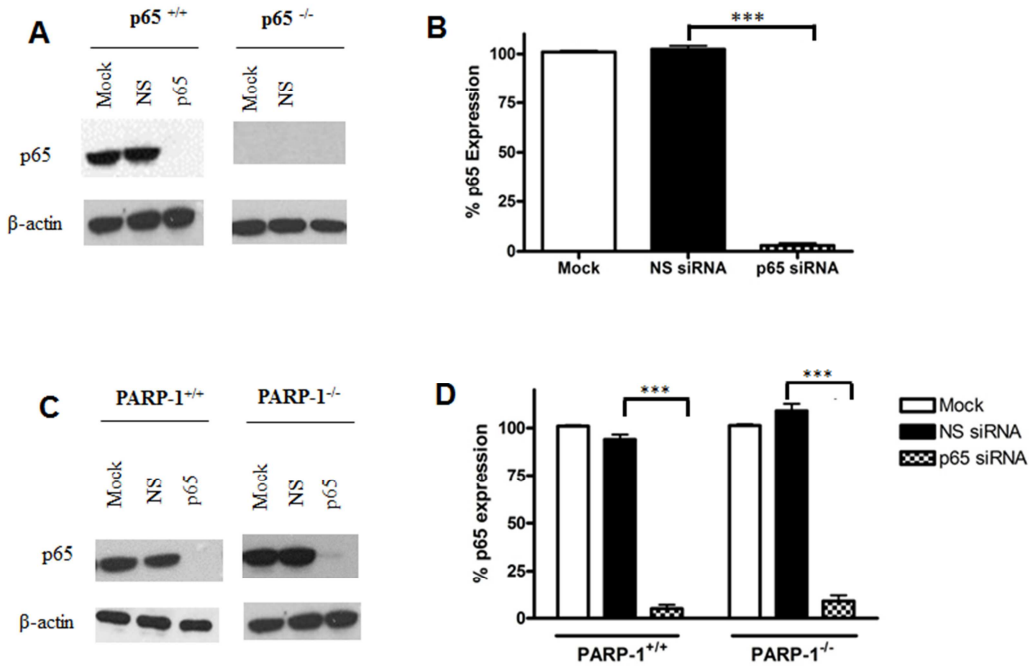

Figure 3.4: siRNA knockdown of NF-κB p65 using optimal conditions
(**A**) Western blots of whole cell extracts of $p65^{+/+}$ and $p65^{-/-}$ MEFs at 48 h after transfection with vehicle alone (Mock), non-specific (NS) siRNA or p65 siRNA. (**B**) p65 protein expression in $p65^{+/+}$ cells expressed as a percentage of NS siRNA treated cells. Results shown are the mean + SEM of 3 independent experiments. (**C**)Western blots of whole cell extracts of PARP-$1^{+/+}$ and PARP-$1^{-/-}$ MEFs at 48 h after transfection with vehicle alone (Mock), non-specific (NS) siRNA or p65 siRNA. (**D**) p65 protein expression in PARP-$1^{+/+}$ and PARP-$1^{-/-}$ cells expressed as a percentage of NS siRNA treated cells. Results shown are the mean + SEM of 3 independent experiments. . *** Significance relative to NS siRNA control was $p<0.0001$ using Student's unpaired t-tests.

It was important to assess the effects of p65 knockdown on the expression of the other NF-κB subunits as p65 is known to dimerise with each one of the other four subunits (Gilmore, 2006), and in particular p50 is the most common hetero-dimeric partner of p65 (Chen et al., 1998). Therefore, Western analyses were used to determine whether siRNA targeting p65 had any effect on p50 or p52, as it had already been confirmed that these cells did not express RelB or c-Rel (Figure 3.1). Using the optimal conditions (described above), $p65^{+/+}$ MEFs were seeded and left for 24 h to adhere before lipid transfection with 50 nM p65 siRNA or NS control (Table 2.2). Whole cell extracts were prepared 48 h following transfection (as described in section 2.5.1) and the levels of p65, p50, p52 or PARP-1 were determined by Western analyses and compared to the house-keeping protein, β-actin.

Figure 3.5 illustrates that knockdown of p65 had no effect on the other NF-κB subunits expressed by the $p65^{+/+}$ MEFs. The expression levels of both p50 and p52 remained constant in cells treated with either vehicle alone (mock), NS siRNA or p65 siRNA. Importantly, the knockdown of p65 did not affect the expression of PARP-1 either.

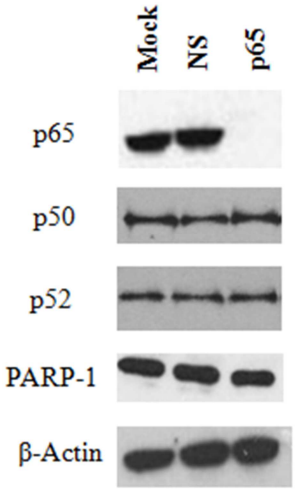

Figure 3.5: Knockdown of NF-κB p65 does not affect expression of other NF-κB subunits
Western blots of whole cell extracts of $p65^{+/+}$ MEFs at 48 h after transfection with vehicle alone (Mock), non-specific (NS) siRNA or p65 siRNA. Blots were probed with antibodies against p65, p50, p52, PARP-1 and β-actin

The data in figure 3.3B suggested that PARP-1 knockdown in the $p65^{+/+}$ MEFs was maximal 48 h following transfection. Taken with the data in Figure 3.4 showing the optimal conditions for all the cell lines regarding p65 siRNA, it was decided to test

these identical conditions for PARP-1 knockdown in all cell lines. This would therefore keep the conditions and nucleic acid ratios as constant as possible across the panel of cell lines. Hence, $p65^{+/+}$, $p65^{-/-}$, $PARP\text{-}1^{+/+}$ and $PARP\text{-}1^{-/-}$ MEFs were seeded and left for 24 h to adhere before lipid transfection with 50 nM of PARP-1 or NS siRNA (Table 2.2). The levels of PARP-1 expression were determined 48 following lipid transfection. Whole cell extracts were prepared (as described in section 2.5.1) and the levels of PARP-1 or p65 were determined by Western analyses and densiometric analysis was used to assess the levels of protein knockdown compared to the house-keeping protein, β-actin.

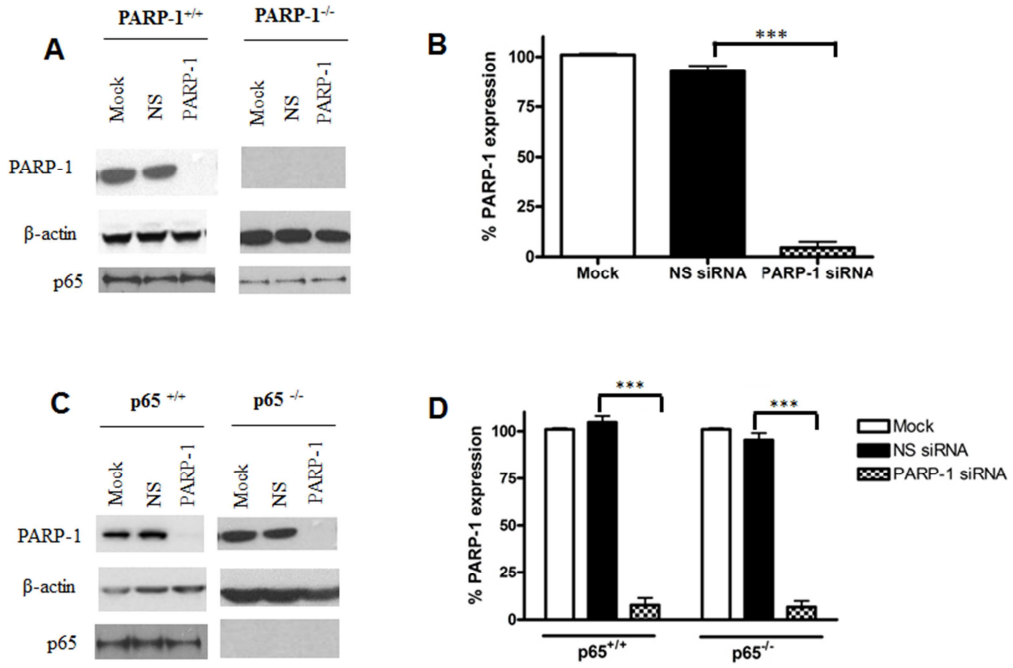

Figure 3.6: siRNA knockdown of PARP-1 using optimal conditions
(**A**) Western blots of whole cell extracts of $PARP\text{-}1^{+/+}$ and $PARP\text{-}1^{-/-}$ MEFs at 48 h after transfection with vehicle alone (Mock), non-specific (NS) siRNA or PARP-1 siRNA. (**B**) PARP-1 protein expression in $PARP\text{-}1^{+/+}$ cells expressed as a percentage of NS siRNA treated cells. Results shown are the mean + SEM of 3 independent experiments. (**C**)Western blots of whole cell extracts of $p65^{+/+}$ and $p65^{-/-}$ MEFs at 48 h after transfection with vehicle alone (Mock), non-specific (NS) siRNA or p65 siRNA. (**D**) PARP-1 protein expression in $p65^{+/+}$ and $p65^{-/-}$ cells expressed as a percentage of NS siRNA treated cells. Results shown are the mean + SEM of 3 independent experiments. *** Significance relative to NS siRNA control was $p<0.0001$ using Student's unpaired t-tests.

A reproducible reduction in PARP-1 protein (> 95% knock-down) could be seen 48 h post-transfection using 50 nM siRNA in the $p65^{+/+}$, $p65^{-/-}$ and $PARP\text{-}1^{+/+}$ MEFs (Figure

3.6A and 3.6C). Figure 3.6B illustrates that PARP-1 protein levels are significantly reduced by 50 nM PARP-1 siRNA, compared with NS siRNA controls in the PARP-$1^{+/+}$ MEFs ($p<0.0001$, unpaired Student's t-test). Similarly, Figure 3.6D illustrates that PARP-1 protein levels are significantly reduced by 50 nM p65 siRNA, compared with NS siRNA controls in the $p65^{+/+}$ and $p65^{-/-}$ MEFs ($p<0.0001$ and $p<0.0001$, respectively, unpaired Student's t-tests). As expected, PARP-1 siRNA had no effect in the PARP-1 deficient cells (Figure 3.6A). These data show that the optimal conditions for transfection of PARP-1 siRNA in either the $p65^{+/+}$, $p65^{-/-}$, PARP-$1^{+/+}$ or PARP-$1^{-/-}$ MEFs, is the concentration of 50 nM and the 48 h time-point. It should also be noted that Figure 3.6A and 3.6C show that PARP-1 siRNA had no effect on p65 protein expression.

In order to confirm PARP knockdown and specificity of the PARP inhibitor, AG-104699, PARP activity was assessed in $p65^{+/+}$ and $p65^{-/-}$ MEFs following transfection with PARP-1 or p65 siRNA, or following treatment with AG-014699 (Figure 3.7). A combination of p65 siRNA and AG-014699 was also assessed, using the validated PARP activity assay (Plummer et al., 2005, Zaremba et al., 2009). Briefly, $p65^{+/+}$ or $p65^{-/-}$ MEFs were seeded and allowed to adhere for 24 h prior to transfection with 50 nM p65, PARP-1 or NS siRNA, or AG-014699. Cells were then incubated for a further 48 h before permeabilisation, and the assay undertaken as described in section 2.4.

Figures 3.7A shows that $p65^{+/+}$ cells treated with AG-014699, or a combination of AG-014699 and p65 siRNA exhibited very low (< 5%) PARP activity ($p=0.03$ and $p=0.02$ respectively, compared with NS siRNA controls, unpaired Student's t-test). Cells treated with PARP-1 siRNA exhibited 25% PARP activity compared with controls ($p=0.04$, $p65^{+/+}$ and $p=0.04$, $p65^{-/-}$, unpaired Student's t-test), in both cell lines (Fiures 3.7A and B), which confirms the results from Western analysis. siRNA targeting p65 did not have any significant effect on PARP-1 activity in either cell line, when compared with NS siRNA controls. It must be noted that there is some reduction in PARP activity when comparing NS siRNA with Mock treated controls. Other groups have documented the effects of transfection on cellular processes including cell viability, proliferation, cell cycle distribution, apoptosis, and migration (Jackson and Linsley, 2004, Tschaharganeh et al., 2007). It is possible that this could perhaps to due to the increased nucleic acid ratio in NS siRNA-treated cells *versus* mock transfected controls, causing the cells some stress.

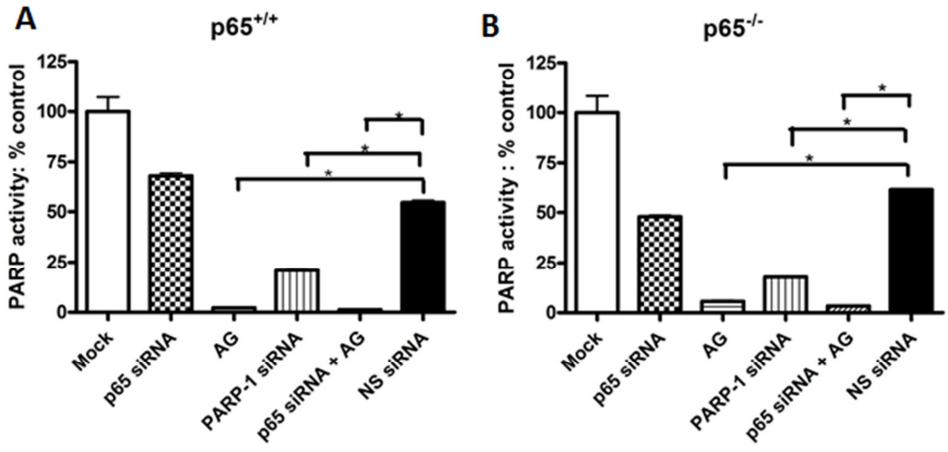

Figure 3.7: PARP activity following PARP-1 siRNA or treatment with AG-014699
(**A**) Bar chart showing PARP activity, measured using a validated immunoblot assay which quantifies PAR formation, in $p65^{+/+}$ MEFs after transfection with vehicle alone (mock), p65 siRNA, AG-014699 (AG), PARP-1 siRNA, a combination of p65 siRNA + AG or NS siRNA. (**B**) PARP activity in $p65^{-/-}$ MEFs following transfection with vehicle alone (mock), p65 siRNA, AG, PARP-1 siRNA, a combination of p65 siRNA + AG or NS siRNA. Data are represented as the mean ± SEM of three independent experiments. *Significance relative to NS siRNA control was $p<0.05$ using unpaired Student's t-test.

3.3.3 Radio-sensitisation by p65 knockdown, PARP-1 knockdown or AG-014699

Once the knockdown of p65 and PARP-1 could be reproducibley achieved, and the specificity of AG-014699 verified, the ability of p65 knockdown, PARP-1 knockdown or AG-014699 to sensitise $p65^{+/+}$ and $p65^{-/-}$ MEFs, and PARP-$1^{+/+}$ and PARP-$1^{-/-}$ MEFs to IR was assessed using colony forming assays (section 2.2.7). In this particular assay $p65^{+/+}$ or $p65^{-/-}$ MEFs were plated and left to adhere for 24 h before transfection with 50 nM p65 PARP-1 or NS siRNA, (or vehicle control). Cells were then left for 48 h, and pre-treated with AG-014699, or DMSO control 1 h prior to treatment with increasing doses of IR before being re-plated after a further 24 h and allowed to form colonies for 7-21 days. (Figure 3.8).

Previous work from the group showed that the $p65^{-/-}$ MEFs were 1.3-fold more sensitive to IR alone compared with $p65^{+/+}$ MEFs (Veuger et al., 2009) when comparing PF_{50} values. PF_{50} values (potentiation factor at 50% cell kill) were calculated from the ratio of the individual LD_{50} (lethal dose producing 50% cell kill) values:- i.e., LD_{50} divided by LD_{50} in the presence of AG-014699. This is consistent with NF-κB conferring radio-resistance (Biswas et al., 2001, Wu and Kral, 2005) and is also illustrated here in Figure 3.8A *versus* 3.8B. Furthermore, Figure 3.8A illustrates that co-incubation with IR and

either AG-014699, p65 siRNA or PARP-1 siRNA reduced survival of the $p65^{+/+}$ cells compared with IR alone or in combination with NS siRNA, resulting in a 1.3-fold potentiation factor. Statistical analysis using an unpaired Student's t-test confirm that, at the LD_{50} values AG-014699, p65 or PARP-1 siRNA significantly radio-sensitised the $p65^{+/+}$ cells compared with IR in combination with NS siRNA (p=0.017, p=0.031 and p=0.038, respectively, unpaired Student's t-test). Importantly, a co-incubation with p65 and AG-014699 in combination with IR, did not further reduce $p65^{+/+}$ cell survival compared with either agent alone, consistent with existing reports that NF-κB and PARP-1 are mechanistically linked in a common pathway (Chang and Alvarez-Gonzalez, 2001, Hassa et al., 2001, Hassa and Hottiger, 1999, Martin-Oliva et al., 2004, Stilmann et al., 2009, Veuger et al., 2009).

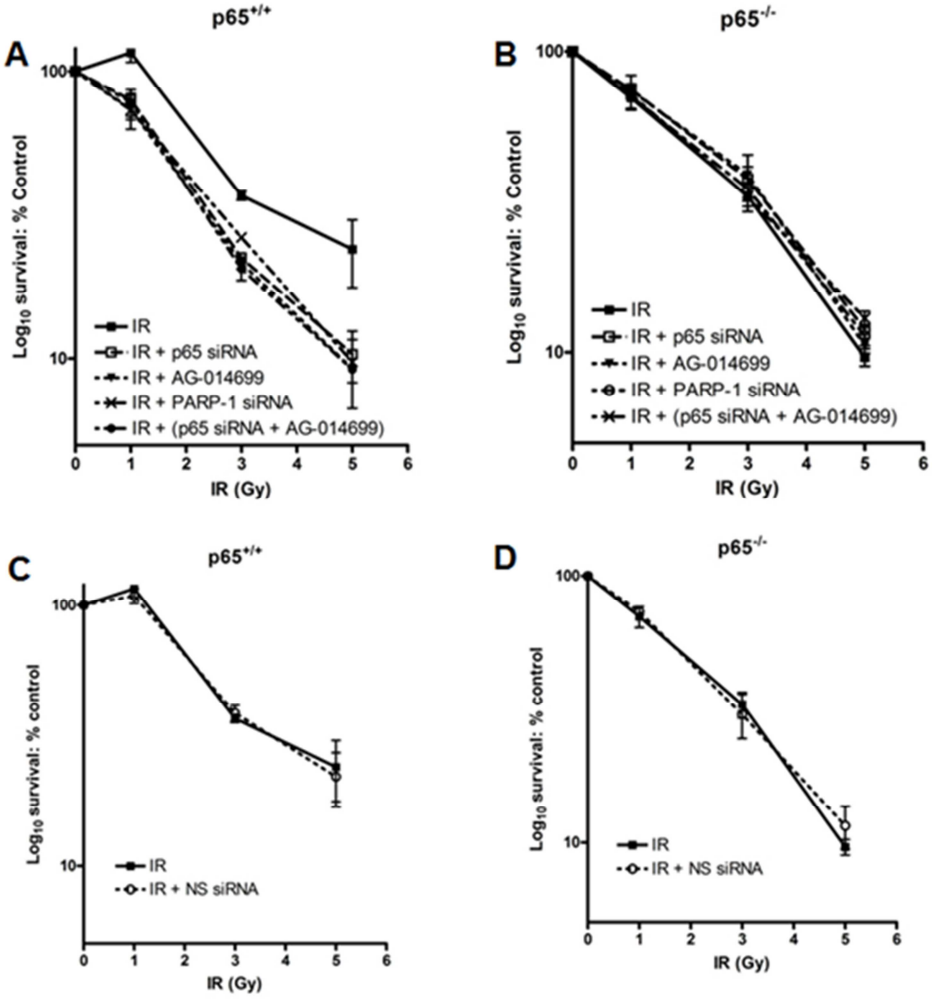

<u>Figure 3.8:</u> Radio-sensitisation by p65 knockdown, PARP-1 knockdown or AG-014699
The effects of increasing doses of IR either alone, or co-incubated with p65 siRNA, AG-014699, PARP-1 siRNA or a combination of p65 siRNA and AG-014699, on cell survival were assessed using the clonogenic survival assay in (**A)** $p65^{+/+}$ MEFs, (**B)** $p65^{-/-}$ MEFs. Cells were treated with relevant siRNA, (or vehicle control), left for 48 h, pre-treated with AG-014699, or DMSO control 1 h prior to IR then re-plated after a further 24 h and allowed to form colonies for 7-21 days. The effects of increasing doses of IR either alone, or co-incubated with NS siRNA on cell survival were assessed using the clonogenic survival assay in (**C**) $p65^{+/+}$ MEFs or (**D**) $p65^{-/-}$ MEFs. Results shown are the mean + SEM of three independent experiments

Furthermore, Figure 3.8B shows that, co-incubation with either AG-014699, p65 siRNA or PARP-1 siRNA had no effect in $p65^{-/-}$ MEFs (p=0.665, p=0.584 and p=0.233, respectively, unpaired Student's t-test on LD_{50} values). Importantly, Figures 3.8C and 3.8D show that a combination of IR and NS siRNA had no significant effects on the survival of the $p65^{+/+}$ or $p65^{-/-}$ MEFs when compared with IR alone (p=0.778 and p=0.853, respectively, unpaired Student's t-test).

The survival curves in Figure 3.8 indicate that PARP-1 and NF-κB are mechanistically linked in a common pathway, and importantly that radio-sensitisation by the PARP inhibitor, AG-014699 or PARP-1 was only achievable in cells containing NF-κB p65. Therefore, it was important to confirm these data using the PARP-1 proficient and deficient in order to further demonstrate the role of PARP-1 on cell survival in the activation of NF-κB following DNA damage. In order to do this clonogenic assays were performed using $PARP\text{-}1^{+/+}$ or $PARP\text{-}1^{-/-}$ MEFs, as described above.

Similarly, the clonogenic assays shown in Figures 3.9A and 3.9B illustrated that the $PARP\text{-}1^{-/-}$ MEFs were 2.7-fold more sensitive to IR compared with $PARP\text{-}1^{+/+}$ MEFs. This is consistent with reports that PARP-1 knockout animals are hyper-sensitive to irradiation due to their compromised DNA repair response (Masutani et al., 2005). Moreover, $PARP\text{-}1^{+/+}$ MEFs exhibited a 1.3-fold sensitisation to IR by AG-014699, p65 knockdown or PARP-1 knockdown, compared with IR alone or in combination with NS siRNA (Figure 3.9A). Statistical analysis using an unpaired Student's t-test confirm that, at the LD_{50} values, AG-014699, p65 or PARP-1 siRNA significantly radio-sensitised the $PARP\text{-}1^{+/+}$ cells compared with IR in combination with NS siRNA (p=0.009, p=0.030 and p=0.048, respectively, unpaired Student's t-test). Importantly, the combination of p65 and AG-014699 in combination with IR, did not further reduce $PARP1^{+/+}$ cell survival compared with either agent alone, once again suggesting that PARP-1 and NF-κB are mechanistically linked. Furthermore, Figure 3.9B shows that, co-incubation with either AG-014699, p65 siRNA or PARP-1 siRNA had no effect in $PARP\text{-}1^{-/-}$ MEFs (p=0.328, p=0.479 and p=0.415, respectively, unpaired Student's t-test on LD_{50} values). Importantly, Figures 3.9C and 3.9D show that a combination of IR and NS siRNA had no significant effects on the survival of the $PARP\text{-}1^{+/+}$ or $PARP\text{-}1^{-/-}$ MEFs when compared with IR alone (p=0.869 and p=0.924, respectively, unpaired Student's t-test). Therefore these data corroborate the results observed in the $p65^{+/+}$ and $p65^{-/-}$ MEFs.

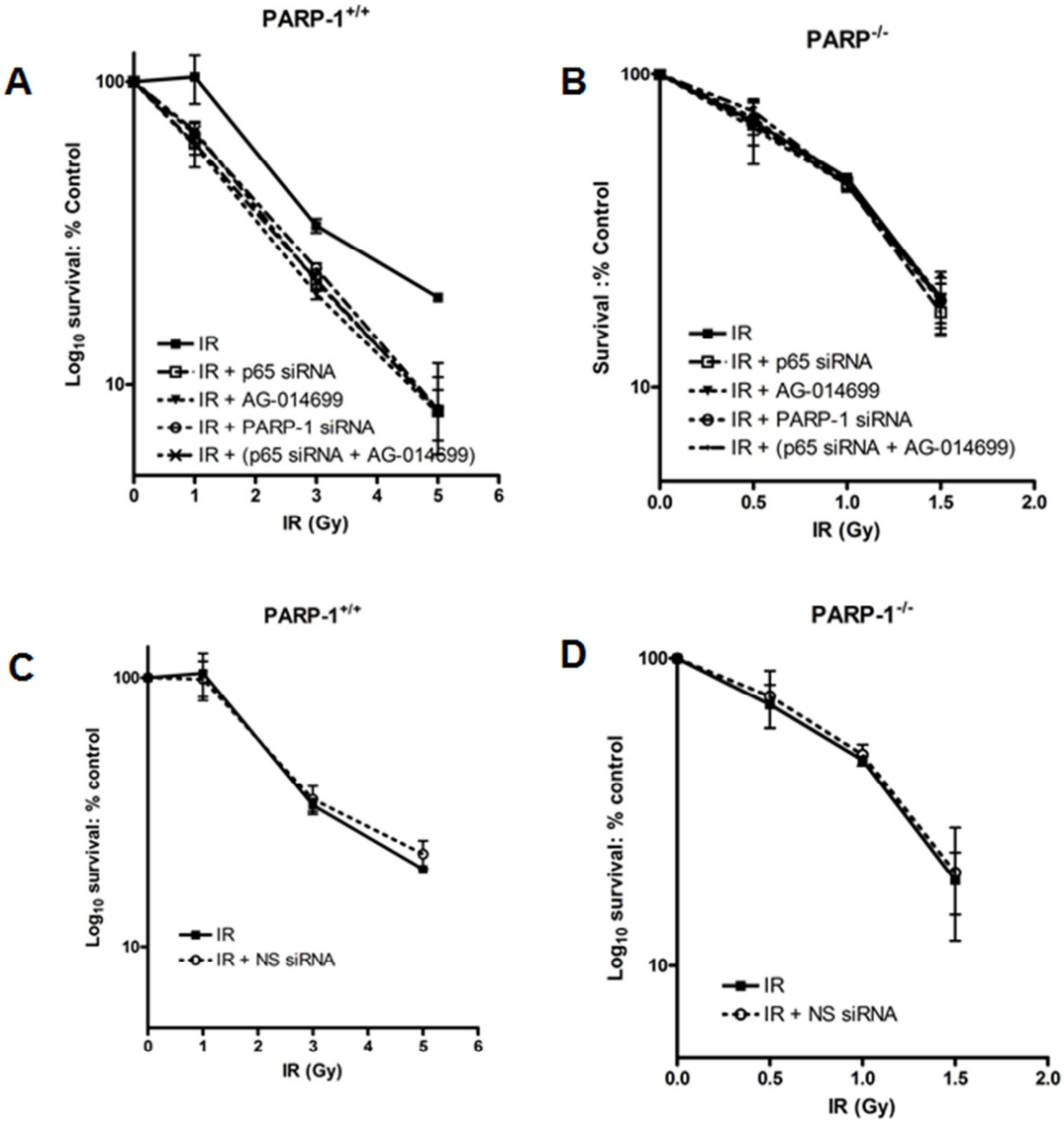

<u>Figure 3.9:</u> Radio-sensitisation by p65 knockdown, PARP-1 knockdown or AG-014699 The effects of increasing doses of IR either alone, or co-incubated with p65 siRNA, AG-014699, PARP-1 siRNA or a combination of p65 siRNA and AG-014699, on cell survival were assessed using the clonogenic survival assay in (**A)** PARP-$1^{+/+}$ MEFs, (**B)** PARP-$1^{-/-}$ MEFs. Cells were treated with relevant siRNA, (or vehicle control), left for 48 h, pre-treated with AG-014699, or DMSO control 1 h prior to IR then re-plated after a further 24 h and allowed to form colonies for 7-21 days. The effects of increasing doses of IR either alone, or co-incubated with NS siRNA on cell survival were assessed using the clonogenic survival assay in (**C**) PARP-$1^{+/+}$ MEFs or (**D**) PARP-$1^{-/-}$ MEFs. Results shown are the mean + SEM of three independent experiments

Spontaneous immortalisation of primary MEFs frequently leads to mutations in p53 meaning that the p65 proficient and deficient MEFs may not be a truly isogenic pair. For example, it has been reported that the $p65^{-/-}$ MEFs have mutant p53 (Gilmore), and

this is also known to be the case for the PARP-$1^{+/+}$ MEFs (Trucco et al., 1998). Hence, to truly confirm the results on cell survival observed in the p65 paired MEFs, colony forming assays with IR alone, or in combination with AG-014699, in $p65^{-/-}$ cells that had been genetically complemented with wild-type (WT) p65, and in relevant control cells were also undertaken.

The data in Figures 3.10A and 3.10B support that shown in Figures 3.8 and 3.9, by illustrating firstly that the cells containing WT p65 were more radio-resistant than their p65 null counterparts, and, secondly that AG-014699 radio-sensitised cells containing WT p65 but not the p65 null cells. Moreover, this radio-sensitisation was statistically significant, when unpaired Student's t-tests were performed on LD_{50} values (p=0.046, LD_{50} IR alone: 2.31 Gy, compared with LD_{50} IR in combination with AG-014699: 1.76 Gy).

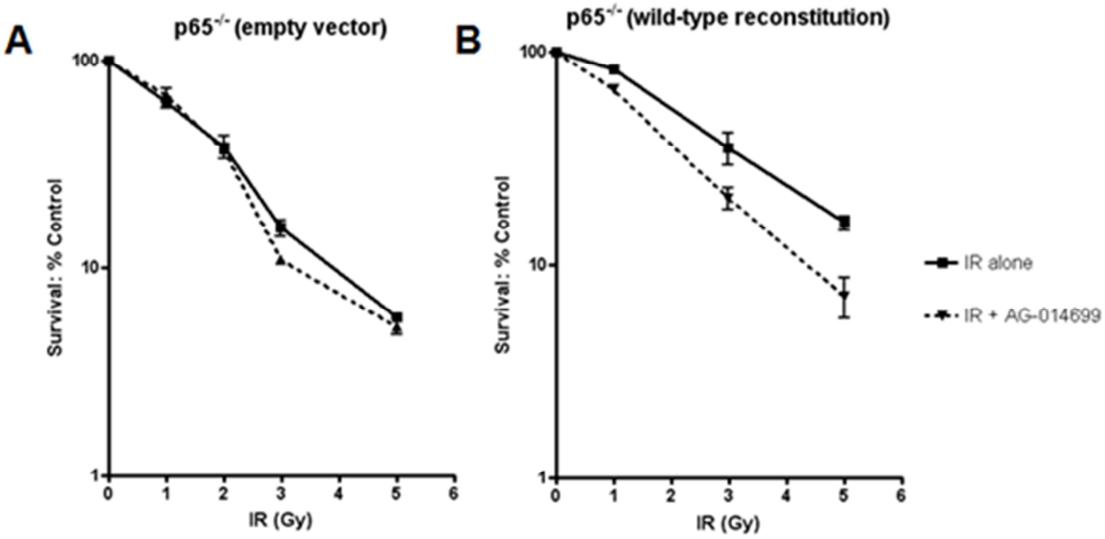

<u>Figure 3.10</u>: Radio-sensitisation of reconstituted $p65^{-/-}$ MEFs by AG-014699
The effects of increasing doses of IR either alone, or co-incubated with AG-014699, on cell survival were assessed using the clonogenic survival assay. Cells were treated with AG-014699, or control 1 h prior to IR then re-plated after a further 24 h and allowed to form colonies for 7-21 days. (Survival curve (**A)** shows $p65^{-/-}$MEFs, (**B)** p65 WT MEFs,) Results shown are mean+ SEM of three independent experiments

3.3.4 p65 knockdown, PARP-1 knockdown or AG-014699 is associated with the induction of apoptosis following ionising radiation

In order to be confident that the effects observed on cell survival in the both the $p65^{+/+}$ (Figure 3.8) and PARP-$1^{+/+}$ cells (Figure 3.9) were associated with the induction of

apoptosis, assays assessing the effects of IR in combination with either AG-014699 or p65 siRNA were undertaken. NF-κB is known to affect the transcription of a number of genes associated with apoptosis (Pahl, 1999). Furthermore, following DNA damage it has been reported that NF-κB induces the transcription of genes such as *XIAP* and *Bcl-xL*, known to be associated with the protection against apoptosis (Stehlik et al., 1998, You et al., 1999). Thus in view of the survival data in Figures 3.8 and 3.9, it could therefore be hypothesised that knockdown of p65 or inhibition of PARP-1 would further activate IR-induced apoptosis, due to the inhibition of NF-κB-dependent transcriptional activation.

In order to assess the effects on apoptosis in the $p65^{+/+}$ and $p65^{-/-}$ MEFs, FITC-conjugated Annexin, which has a high affinity for membrane phospholipid phosphatidylserine was used. Briefly, cells were transfected with p65 siRNA (or vehicle control) 48 h prior to 1 h pre-treatment with AG-014699 and subsequent irradiation. Cells were harvested and the FITC Annexin V Apoptosis Detection Kit I and used according to manufacturers' guidelines (section 2.6.1).

Firstly, it was found that $p65^{-/-}$ MEFs have a 3-fold higher intrinsic levels of apoptosis following IR, compared with $p65^{+/+}$ (33.73 ± 3.1 for $p65^{-/-}$ *versus* 12.60 ± 2.7 for $p65^{+/+}$). These data were used to calculate percentage increase in apoptosis, shown in Figure 3.11. This is consistent with reports that NF-κB activation increases survival following DNA damage (Criswell et al., 2003, Russo et al., 2001). The levels of apoptosis were measured following IR (2 Gy or 5 Gy) in combination with either p65 knockdown or AG-014699 in $p65^{+/+}$ and $p65^{-/-}$ MEFs (Figure 3.11A *versus* 3.11B). A combination of p65 siRNA and AG-014699 were also assessed. Compared to IR alone (mock), both p65 knockdown and AG-014699 significantly increased apoptosis following 2 Gy IR (approx 2.5-fold) in the $p65^{+/+}$ MEFs ($p=0.03$ and $p=0.04$, respectively, unpaired Student's t-test). Importantly, when AG-014699 was used in conjunction with p65 knockdown, there was no change in the level of apoptosis in the $p65^{+/+}$ MEFs, compared to either agent alone. No increase in apoptosis was observed in the $p65^{-/-}$ MEFs (Figure 3.11B) with any of the treatments, compared with IR alone.

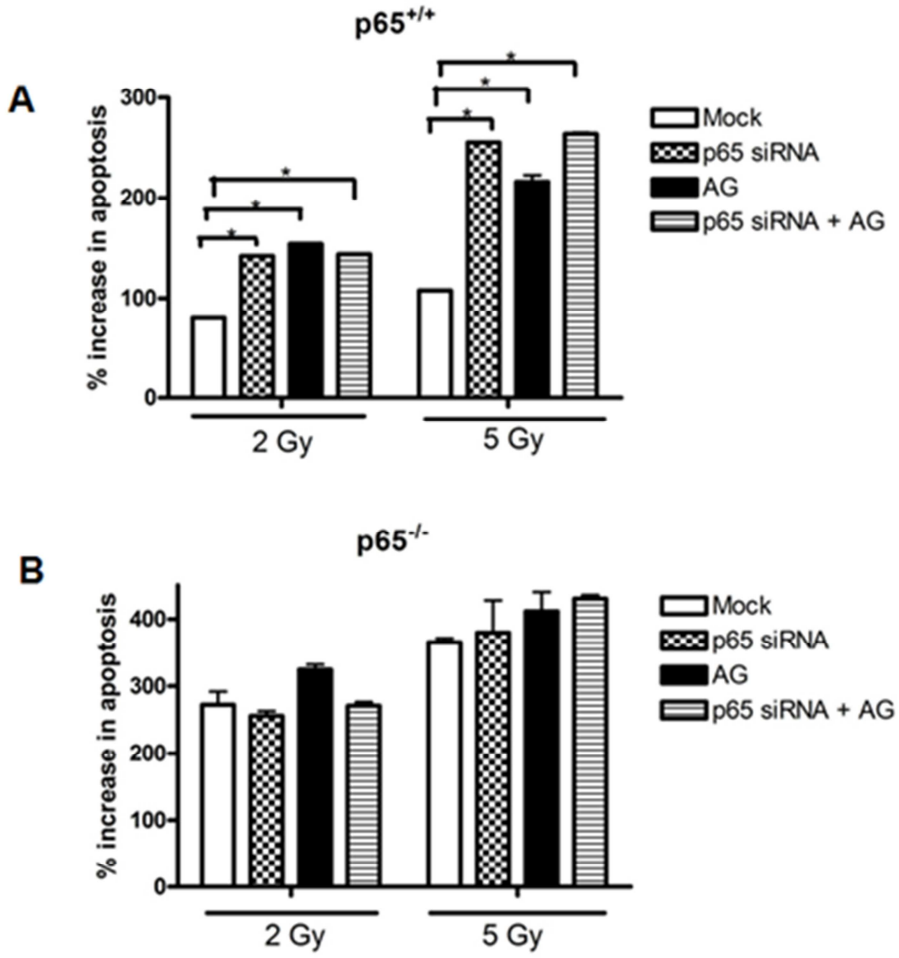

Figure 3.11: The induction of apoptosis measured using the Annexin V FACs assay
The effect of IR alone (mock, white bar) ± p65 siRNA (hatched bar) ± AG-104699 (AG alone, black bar, AG + p65 siRNA, striped bar) on the induction of apoptosis in $p65^{+/+}$ (**A**) and $p65^{-/-}$ MEFs (**B**). Cells were treated with relevant siRNA, or control left for 48 h, pre-treated with AG-014699, or control 1 h prior to IR then allowed to repair for a further 24 h before harvesting and assessment of the induction of apoptosis by Annexin V FACs analysis. Results shown are calculated as a percentage increase of the untreated controls. All data shown are represented as the mean ±SEM of three independent experiments. *Significance relative to mock treated control was $p<0.05$ using unpaired Student's t-test.

These data were confirmed using a caspase 3/7 activity assay. The proteases, caspase-3 and caspase-7, are frequently activated, by proteolytic cleavage, during mammalian cell apoptosis (Nicholson and Thornberry, 1997). Caspase-3, in particular, plays a very important role in the survival of many cell types, demonstrated by the development of caspase-3 knockout mice. These animals are born in low litter numbers, and have a striking phenotype in which there are skull defects due to etopic masses of supernumerary cells, representing a failure of programmed cell death during brain

development, and resulting in mice dying only a few weeks after birth (Kuida et al., 1996). Caspase-3 has also been reported to be essential for apoptotic chromatin condensation and DNA fragmentation (Porter and Janicke, 1999). Caspase-3 activity was determined using the Caspase-Glo 3/7 kit (described in section 2.6.2). $p65^{+/+}$ or $p65^{-/-}$ MEFs were transfected with 50 nM p65 siRNA (or vehicle control) and incubated for 48 h. Cells were then pre-treated with AG-014699 for 1 h before IR and allowed to recover at 37°C, 5 %CO_2 for 24 h before apoptosis was assessed using the Caspase-Glo 3/7 assay.

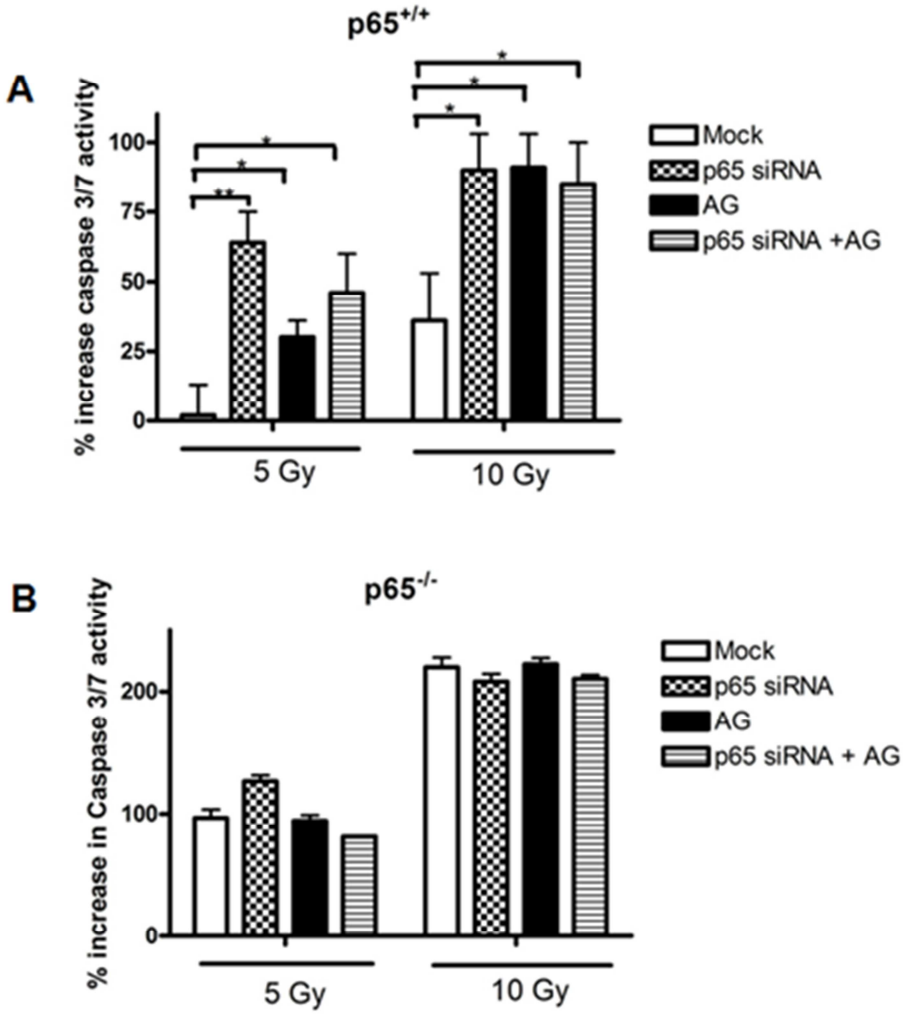

Figure 3.12: The induction of apoptosis measured using the caspase 3/7 assay The effect of IR alone (mock, white bar) ± p65 siRNA (hatched bar) ± AG-104699 (AG alone, black bar, AG + p65 siRNA, striped bar) on the induction of apoptosis in $p65^{+/+}$ (**A**) and $p65^{-/-}$ MEFs (**B**). Cells were treated with relevant siRNA, or control left for 48 h, pre-treated with AG-014699, or control 1 h prior to IR then allowed to repair for a further 24 h before harvesting and assessment of the induction of apoptosis by caspase 3/7 activation. Results shown are normalised to untreated controls.
All data shown are represented as the mean ±SEM of three independent experiments. *Significance relative to mock treated control was $p<0.05$ using unpaired Student's t-test.

The data generated using the caspase3/7 assay required slightly higher doses of IR (5 Gy and 10 Gy) to induce apoptosis, when compared with the Annexin V assay (2 Gy and 5 Gy), and this will be discussed further in section 3.4. Figure 3.12A *versus* Figure 3.12B confirmed the findings from the Annexin V assay, showing that the $p65^{-/-}$ MEFs have higher intrinsic levels of apoptosis, measured by caspase 3/7 cleavage, following IR, compared with $p65^{+/+}$ MEFs. Furthermore, when compared with IR alone (mock), both p65 knockdown and AG-014699 significantly increased caspase 3/7 activation following 5 Gy IR in the $p65^{+/+}$ MEFs ($p=0.0086$ and $p=0.044$ respectively, Student's unpaired t-test). Importantly, when AG-014699 was used in conjunction with p65 knockdown, there was no further increase in caspase 3/7 activity in the $p65^{+/+}$ MEFs, compared to either agent alone. It should be noted here that following 5 Gy IR, it appears that p65 siRNA has a greater effect on the induction of apoptosis in the $p65^{+/+}$ MEFs, compared with AG-014699, even though these two agents have a similar effect on survival (Figures 3.8 and 3.9). However, when an unpaired Student's t-test was performed on p65 siRNA *versus* AG-014699 following 5 Gy IR, there was no significant difference on apoptosis induction ($p=0.209$). Importantly, no increase in apoptosis was observed in the $p65^{-/-}$ MEFs (Figure 3.12B) with any of the treatments, compared with IR alone, confirming the Annexin V results (Figure 3.11).

3.3.5 AG-014699 inhibits Single strand break (SSB) repair to a similar extent regardless of cellular NF-κB status

The results observed from the survival and apoptosis assays suggested that PARP-1 and NF-κB are mechanistically in a common pathway, thus supporting existing work (Chang and Alvarez-Gonzalez, 2001, Hassa et al., 2001, Hassa and Hottiger, 1999, Martin-Oliva et al., 2004, Stilmann et al., 2009, Veuger et al., 2009). The data presented in this chapter also postulate that the radio-sensitisation observed with the PARP inhibitor, AG-014699, is mediated *via* NF-κB. However, PARP-1 is most widely known for its role in the repair of SSBs *via* the BER pathway. Hence, it was important to determine the effects of PARP inhibition on SSB repair in the $p65^{+/+}$ and $p65^{-/-}$ MEFs. The widely accepted notion surrounding PARP inhibition is that any radio- or chemo-sensitisation observed is a repair-driven response (Bryant and Helleday, 2004, Calabrese et al., 2004), and not mediated through the inhibition of NF-κB activation. Hence, the alkaline Comet assay was used to test the hypothesis that PARP inhibition

mediates radio-sensitisation through inhibition of NF-κB activation, rather than inhibition of SSB repair.

The alkaline Comet assay was used to examine IR-induced SSB formation and repair at the individual cell level in the $p65^{+/+}$ and $p65^{-/-}$ cells. The method is described in detail in section 2.7, however, briefly, $p65^{+/+}$ or $p65^{-/-}$ cells were plated and allowed to adhere overnight before pre-treated with AG-014699 (or DMSO control) 1 h prior to treatment with 10 Gy IR. Cells harvested at various timepoints following IR (0, 15, 30, 60 min) and the assay undertaken as described in section 2.7. Data is represented in two forms, firstly using the Olive Tail Moment (OTM), which is used as a measure of both the smallest detectable size of migrating DNA (reflected in the comet tail length) and the number of relaxed / broken pieces (represented by the intensity of DNA in the tail), and secondly by the percentage DNA in the comet tail, both are recommended by the Comet Assay Interest Group. It should be noted that in each scatter diagram, one dot represents one individual cell. All data were shown to exhibit a Gaussian distribution and the lines shown on the scatter plots in Figure 3.13A-D indicate the mean of the data plotted.

Figure 3.13A, 3.13B, 3.13C and 3.13D show that immediately following 10 Gy IR, both the $p65^{+/+}$ and the $p65^{-/-}$ cell lines had the same initial level of SSBs as demonstrated by both OTM and percentage Comet tail DNA. These scatter plots also illustrate how, in both cell lines, the number of SSB are repaired over time. Markedly, there was no significant difference in the SSB levels remaining in the two cell lines 60 min post-IR, with > 85 % of breaks rejoined despite the difference in radio-sensitivity (shown in Figures 3.8A and 3.8B). Most importantly however, AG-014699 inhibited SSB repair (as demonstrated by increased residual SSB levels at all time-points post-IR) to the same extent in both cell lines, regardless of the p65 status, and despite the observed radio-potentiation by AG-014699 in $p65^{+/+}$ cells, not the $p65^{-/-}$ cells.

The kinetics of SSB repair in both cells line are illustrated in Figures 3.13E and 3.13F by line graphs. These clearly show that the SSBs generated by IR are repaired rapidly over time (solid black line), and that in both cells line the kinetics of repair were very similar. The broken line shows how cells pre-treated with AG-014699 prior to treatment with IR, have slower repair kinetics in both cell lines, regardless of p65 status.

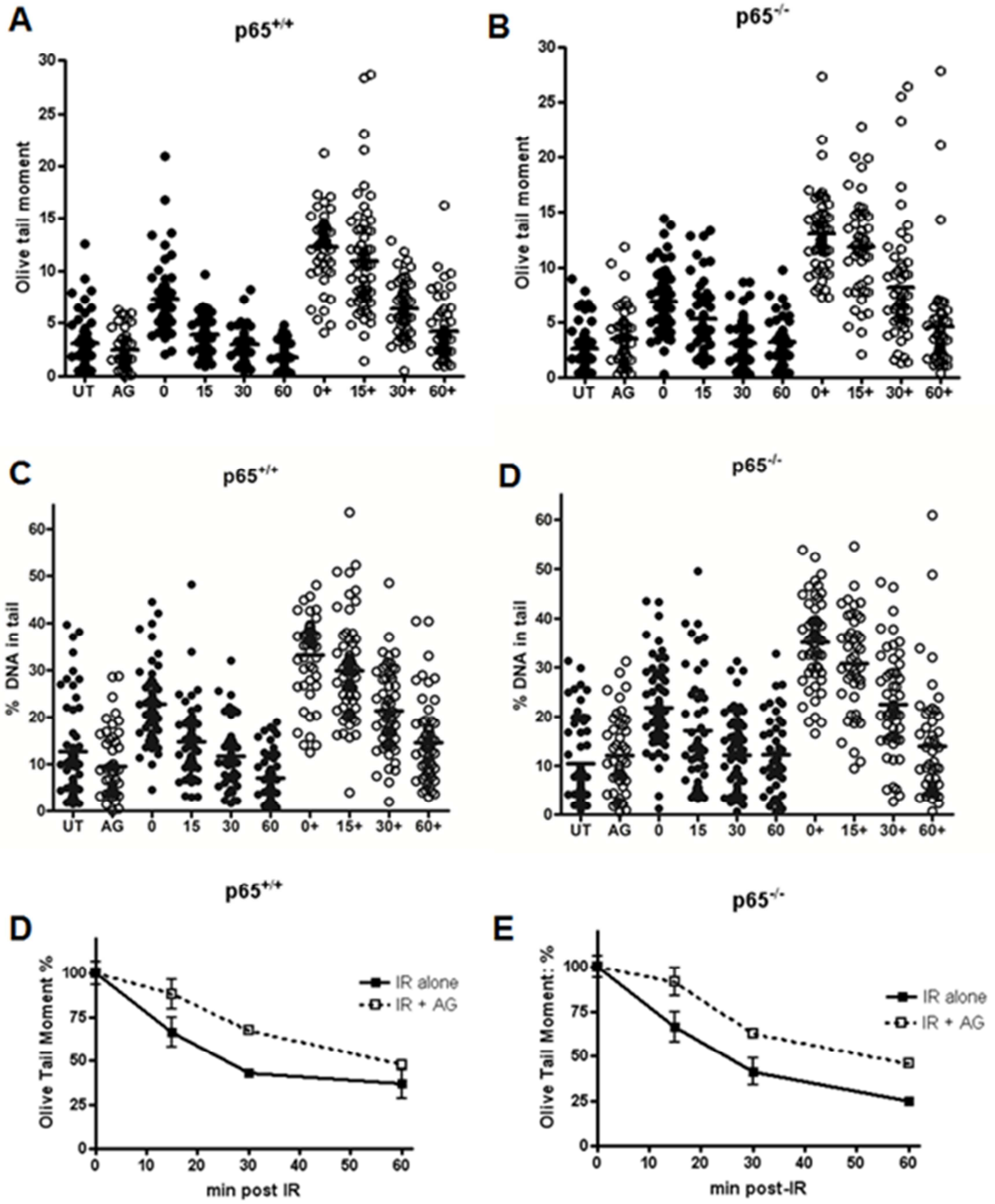

<u>Figure 3.13:</u> AG-014699 inhibits SSB repair to a similar extent regardless of cellular NF-κB status Scatter diagrams showing the extent of single strand breaks (SSBs) in $p65^{+/+}$ and $p65^{-/-}$ MEFs treated with 10 Gy IR ± AG-014699 (AG, denoted by +) and allowed to repair (0 min, 15 min, 30 min and 60 min). (**A**) and (**B**) represent OTM and (**C**) and (**D**) represent % Tail DNA. Line graph showing the kinetics of single strand break repair in $p65^{+/+}$ (**E**) and $p65^{-/-}$ MEFs (**F**). Data was normalised to relevant controls and in both cases solid black lines represent repair over time of cells treated with 10 Gy IR, and dotted lines represent repair over time of cells treated with 10 Gy IR + AG-014699.

To further confirm these findings, these experiments were repeated in $p65^{-/-}$ cells that had been genetically complemented with WT p65, and also in p65 null controls, for the reasons discussed in section 3.3.3. Once again the alkaline Comet assay was undertaken for these experiments. Figure 3.14A, 3.14B, 3.14C and 3.14D show that immediately following 10 Gy IR, both the p65 WT and the p65 null control cell lines had the same initial level of SSBs as demonstrated by both OTM and percentage Comet tail DNA, which is exactly what had been observed in the $p65^{+/+}$ and $p65^{-/-}$ cells. These scatter plots also illustrate how, in both the p65 WT and p65 null control cells, the number of SSB are repaired over time. Importantly, there was no significant difference in the SSB levels remaining in the two cell lines 60 min post-IR, with > 85 % of breaks rejoined, as seen in the $p65^{+/+}$ and $p65^{-/-}$ cells. Once again the SSB repair kinetics and the extent of SSB inhibition by AG-014699 were very similar in both the p65 WT and p65 null control cells (Figure 3.10A and 3.10B). The kinetics of SSB repair in both cells line are illustrated in Figures 3.14E and 3.14F by line graphs. These clearly show that the SSBs generated by IR are repaired rapidly over time (solid black line), and that in both cells line the kinetics of repair were very similar. The broken line shows how cells pre-treated with AG-014699 prior to treatment with IR, have slower repair kinetics in both cell lines, regardless of p65 status. These data corroborate the data generated in the $p65^{+/+}$ and $p65^{-/-}$ MEFs, thus confirming the hypothesis that radio-sensitisation by AG-014699 is mediated solely *via* the inhibition of NF-κB and is therefore independent of the widely reported inhibition of SSB repair.

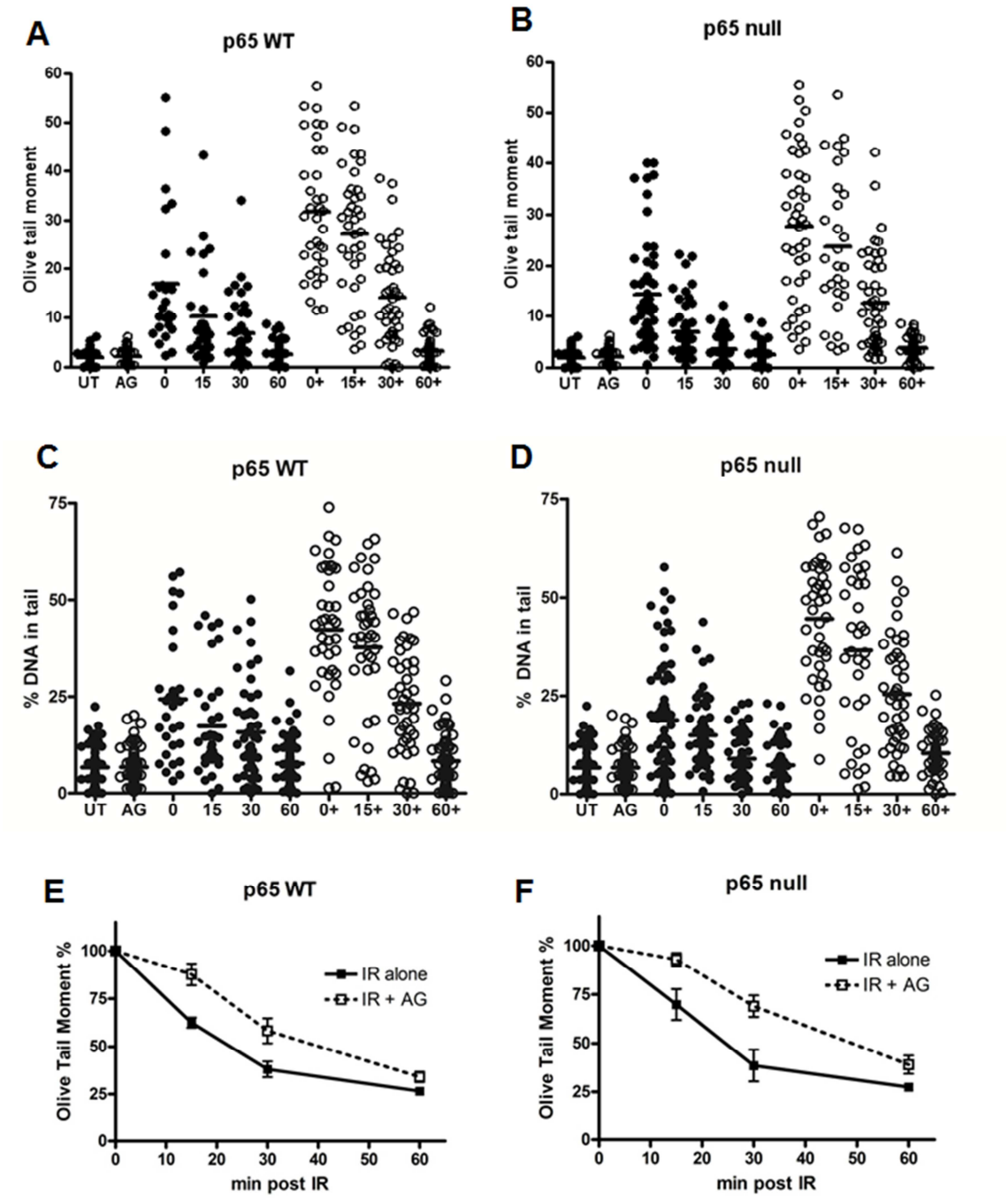

<u>Figure 3.14:</u> AG-014699 inhibits SSB repair to a similar extent regardless of cellular NF-κB status Scatter diagrams showing the extent of single strand breaks (SSBs) in p65WT and p65 null MEFs treated with 10 Gy IR ± AG-014699 (AG, denoted by +) and allowed to repair (0 min, 15 min, 30 min and 60 min). (**A**) and (**B**) represent OTM and (**C**) and (**D**) represent % Tail DNA. Line graph showing the kinetics of single strand break repair in p65WT (**E**) and p65null MEFs (**F**). Data was normalised to relevant controls and in both cases solid black lines represent repair over time of cells treated with 10 Gy IR, and dotted lines represent repair over time of cells treated with 10 Gy IR + AG-014699.

3.4 Discussion

This investigation has demonstrated that PARP-1 knockdown and the PARP inhibitor, AG-014699 significantly decreased survival and induced apoptosis following IR in $p65^{+/+}$ MEFs whilst having no effect in $p65^{-/-}$ MEFs. Radio-sensitisation was 1.3-fold and importantly occurred at clinically relevant doses of IR. A combination of AG-014699 and p65 knockdown did not further enhance this response, which is consistent with reports that PARP-1 and NF-κB are mechanistically linked in a common pathway (Chang and Alvarez-Gonzalez, 2001, Hassa et al., 2001, Hassa and Hottiger, 1999, Martin-Oliva et al., 2004, Stilmann et al., 2009, Veuger et al., 2009). This is also consistent with reports that loss or inhibition of NF-κB has been shown to chemo- or radio-sensitise in many different tumour types (Criswell et al., 2003, Hewamana et al., 2008a, Hewamana et al., 2008b, Jung and Dritschilo, 2001, Russo et al., 2001). However, is it important to note that the dose of IR required to active NF-κB may be cell type or tissue-dependent. For example, Brach *et al.,* (1991) showed that the clinically relevant dose of 2 Gy could induce NF-κB activation in the myeloid cell line, KG-1 (Brach et al., 1991). Furthermore, in the EBV-transformed 244B human lymphoblastoid cell line, 0.5 Gy IR was shown to activate NF-κB activation (Sahijdak et al., 1994). Whereas, other studies such as Stilmann *et al.* (2009), used hyper-lethal doses, of 80 Gy IR when studying the NF-κB response of other cell lines. Importantly, the doses of IR used within this study are low and as close to a clinically relevant dose as possible. The clinical single dose of 2 Gy IR was used in both the clonogenic and annexin V flow cytometry assays. A slightly higher dose of 5 Gy IR was required for the caspase 3/7 assay, as this assay did not appear as sensitive as the FACs based method. The FACs assay counts a maximum of 10,000 events whilst the caspase assay also requires that the absolute cell numbers are constant between the control and treated wells. In reality this is much more difficult to control, since the clonogenic assay data shows that p65 siRNA or AG-014699 both reduce cell survival compared with controls, and hence there could be a lower cell number in these wells.

Moreover, the work of Stilmann *et al.,* (2009) used hyper-lethal doses of IR (80 Gy) in the $PARP\text{-}1^{+/+}$ and $PARP\text{-}1^{-/-}$ MEFs however they did not study survival following such doses of IR, just the induction of apoptosis (Stilmann et al., 2009). The survival data shown within this investigation illustrate that the $PARP\text{-}1^{-/-}$ MEFs are very radio-sensitive at low doses of IR (LD_{50} value: 0.9 Gy *versus* 2.3 Gy in $PARP\text{-}1^{+/+}$ cells). This is consistent with many other reports that loss or inhibition of PARP-1 is associated

with chemo-and radio-sensitisation due to inhibition of efficient DNA repair (Calabrese et al., 2004, de Murcia et al., 1997, Masutani et al., 2005). PARP-$1^{-/-}$ cells have also been shown to have high genomic instability (Wang et al., 1997), hence the use of such high doses of IR, by Stilmann *et al.*, (2009) is likely to exacerbate this phenotype.

Many reports into the role of PARP-1 in the activation of NF-κB have used classical PARP inhibitors such 3-AB and nicotinamide derivatives (Chang and Alvarez-Gonzalez, 2001, Martin-Oliva et al., 2006, Martin-Oliva et al., 2004, Stilmann et al., 2009). However, reports have shown that these compounds have many off target effects at the concentrations used (Moses et al., 1990). Early compounds, such as 3-AB showed selectivity problems, due to their weak inhibition of the enzyme, and having to be used at physiologically non-specific concentrations, usually in the millimolar range. This investigation not only used the potent PARP inhibitor, AG-014699, at a sub-micromolar concentration, known to be a highly potentcy for PARP (K_i 1.4 nmol/L) (Thomas et al., 2007), but PARP-1 siRNA as a direct comparison in order to verify the results seen with the PARP inhibitor.

It is widely accepted that use of small molecule inhibitors should be compared directly with siRNA knockdown of a target protein, if this is a viable option. Loss-of-function data obtained at the single-cell level is now achievable through siRNA molecules which are now readily available and affordable. This technology has provided a complementary approach to more traditional pharmacological procedures, *via* small molecule inhibition, and other methods including the generation of genetic knockout animals, which are generally in whole organisms rather than single cells. For example, p65/RelA knockout animals were found to be embryonic lethal at E15-16 due to massive liver degeneration as a consequence of chronic inflammation and subsequently apoptosis (Beg et al., 1995). The generation of chemical agents which target protein-protein or protein-DNA interactions, such as those of transcription factors, like NF-κB, have been more challenging than pharmacological approaches that target proteins which have a defined substrate, such as PARP-1 or kinases, for example DNA-PK or ATM. In this case, use of p65 siRNA in comparison or in combination with the PARP inhibitor, AG-014699, has allowed a direct assessment of the role of PARP-1 in the regulation of NF-κB.

The use of siRNA targeting PARP-1 as a direct comparison to the use of AG-014699, has shown that regulation of DNA-damage activated NF- κB is mediated by PARP-1, and not any of the other PARP superfamily proteins. Although inhibition of other PARP family proteins (such as PARP-2) by AG-014699 cannot be rigorously excluded, the consistency in the data obtained from both the inhibitor studies and PARP-1 knockdown studies indicate that this is not the case. Furthermore, Cohausz and Althaus (2009) have shown that PARP-1 but not PARP-2 is required for expression of genes involved in regulation of apoptosis (Cohausz and Althaus, 2009), supporting the survival and apoptosis data within this investigation which has shown that AG-014699 radio-sensitizes cells *via* inhibition of PARP-1, not PARP-2.

There have been reports which show divergence between enzymatic inhibition and protein knockdown. These include studies into Aurora kinase inhibitors and siRNA targeting Aurora kinase B. The Aurora kinases, A, B and C, are highly conserved mitotic regulators. The 'polar' kinase, Aurora A, is required for biopolar spindle assembly and therefore localizes to spindle poles and the centrosome during mitosis. The 'equatorial' kinase, Aurora B, first localizes to the centromeres and the kinetochores during the early stages of mitosis acting as a chromosome passenger (Keen and Taylor, 2004). Small molecule Aurora kinase inhibitor studies showed that Aurora B function was vital for checkpoint signaling following checkpoint activation. These showed that in inhibitor treated cells, the checkpoint response to paclitaxel was lost, whereas this checkpoint was activated when microtubule polymerization was prevented with nocodazole. Knockdown of Aurora B using siRNA also showed a compromised checkpoint response, however in this case this was following both paclitaxel and nocodezole (Biggins and Murray, 2001, Ditchfield et al., 2003, Hauf et al., 2003). The lack of congruence illustrated with these, and other data, highlight how loss of enzymatic activity can have very different effects from the loss of protein expression. However, the consistencies shown in the survival and apoptosis data in this chapter, suggest that both the physical presence of the PARP-1 protein and the catalytic activity are required to activate NF-κB, following ionising radiation. It is possible, that in this case PARP-1 may facilitate a structural role in the NF-κB transcriptional complex, as illustrated by Hassa *et al.,* (2005) using TNF-α as an activator of NF-κB, and demonstrating that the acetylation of PARP-1 (by HDAC1 and p300) regulated NF-κB activity. However, this theory is less likely to be true following treatment with IR, as the data using the PARP inhibitor (Figures 3.8 and 3.9) has shown that enzymatic inhibition

generates the same reduction in cell survival as PARP-1 siRNA, and in this case PARP-1 protein is still available to act as a scaffold for protein-protein interactions.

It has been documented that non-specific/scrambled siRNA controls can have effects on cellular processes including cell viability, proliferation, cell cycle distribution, apoptosis, and migration (Jackson and Linsley, 2004, Tschaharganeh et al., 2007), when compared with 'mock/transfection reagent alone' controls. Although the Western analyses show that the non-specific (NS) siRNA molecules used here have no effects on the expression of the target proteins, p65 or PARP-1, or those downstream, there appears to be some effect when used in the PARP activity assay but not for the cell survival or apoptosis assays.

The levels of SSBs in $p65^{+/+}$ and $p65^{-/-}$ MEFs induced by IR were similar and both were equally proficient at their repair. AG-014699 was also able to increase the level of breaks to the same extent in both cell lines, consistent with the known role of PARP-1 in BER (Durkacz et al., 1980). Thus, these novel observations have led to the conclusion that the potentiating effect of AG-104699 when used in conjunction with IR is perhaps not primarily due to the widely reported transient inhibition of SSB repair but a consequence of PARP-1 downstream signaling to NF-κB. This is consistent with the observation that cells severely compromised in DNA repair (e.g. PARP-$1^{-/-}$) are able to divide and go on to survive despite having consistently higher levels of breaks compared to their wild type counterparts, even in the absence of exogenous damage (Trucco et al., 1998). These data are very novel and very much against the widely accepted dogma that the inhibition of DNA repair by PARP inhibition is the reason for the observed cytotoxicity. Therefore it is vital that these experiments are undertaken in other cell lines, perhaps using p65 siRNA to knockdown p65 expression, and with other DNA damaging agents, such as temozolomide, which has been shown to be sensitised by PARP inhibition (Calabrese et al., 2004, Chalmers, 2009, Chalmers, 2010, Daniel et al., 2009).

There is evidence that the effects shown within this chapter, using the Comet assay are likely to be due to SSBs, even though the alkaline Comet assay can detect a small amount of DSBs as well as SSBs, as discussed in section 2.7.1.2. Firstly, Ogorek and Bryant (1985) showed that at the low doses of IR as used in our experiments, the ratio

of SSB to DSB is approximately 20:1 (Ogorek and Bryant, 1985a, Ogorek and Bryant, 1985b). Furthermore, previous work has shown that PARP-1 has a minor role in the repair of DSBs by NHEJ in the absence of DNA-PK (Veuger et al., 2003). However the $p65^{+/+}$ and $p65^{-/-}$ cells used here have functional DNA-PK, and thus any DSBs would be repaired by NHEJ, with AG-014699 being solely responsible for the inhibition of SSBs.

It is however, important to note that IR does induces a combination of SSBs and DSBs. The overall impact of PARP inhibition, in this case and others in the literature (Chalmers et al., 2004, Schlicker et al., 1999), is one of modest radio-sensitisation, and some studies have reported very minimal sensisation in certain cell lines (Noel et al., 2006), therefore it is important to consider other factors and roles that PARP-1 may be playing in the cell, other than just SSB repair. Although the data here suggests a clear mechanistic link between PARP-1 and NF-κB, other factors, which have not been assayed for should be considered, such as the role of PARP-1 in DSB repair, discussed previously in section 1.3.2.2. In replicating cells the unrepaired SSBs generate collapsed replication forks which could give rise to potentially lethal DSBs, and recent data suggests that it is these DSBs that are responsible for the cytotoxicity of PARP inhibitors (Chalmers 2009). Hence, future work could include assays for DSB repair such as the γH2AX foci assay, and also some cell synchronisation assays to discover which phase of the cell cycle is crucial in this particular case.

PARP-1 is known to regulate many transcription factors (Kraus, 2008, Kraus and Lis, 2003, Krishnakumar and Kraus, 2010) and therefore it is important to note that this may then involve the cross-talk, in this case between NF-κB and other transcription factors activated by IR, such as p53. It has been shown previously that NF-κB and p53 share the transcriptional co-activators, CBP and p300 as transcriptional coactivators (Webster and Perkins, 1999) and furthermore that the acetylation of PARP-1 by CBP and p300 is associated the regulation of the NF-κB transcriptional response (Hassa et al., 2005).

The spontaneous immortalisation of MEFs can often lead to mutations in p53, meaning that the p65 proficient and deficient MEFs may not be a truly isogenic pair. In order to address this $p65^{-/-}$ cells that had been genetically complemented with wild-type p65 protein were used (Figures 3.10 and 3.14). These data support the original findings that the extent of the inhibition of SSB repair by AG-014699 is the same, regardless of the p65 status, and that inhibiting SSB repair with AG-014699 does not lead to radio-

sensitisation in the absence of NF-κB. Hence, this now allows the conclusion that the radio-sensitisation observed with AG-014699 is mediated *via* inhibition of NF-κB activation, and not the widely reported transient inhibition of SSBs.

Inhibition of NF-κB is clearly an attractive target for cancer therapeutics although, as previously mentioned, the direct inhibition of a transcription factor, is very challenging in terms of drug discovery. Most pharmacological approaches have concentrated on inhibition of proteosomal degradation, or the IKK complex (Gilmore and Herscovitch, 2006). However, global inhibition using these types of agents may have some negative aspects. For example, NF-κB plays a vital role in the inflammatory response, and thus complete inhibition of NF-κB, for example with an IKK inhibitor, may have adverse effects. The IKK complex has many known functions within the cell (Chariot, 2009, Criollo et al., 2010), and inhibition may be cytotoxic. Long-term NF-κB inhibition may also increase the likelihood of immunodeficiency, since it plays a pivotal role in the innate and adaptive immune response, and can possibly delay bone marrow recovery due to some reports of chemotherapeutic induced apoptosis of hematopoietic progenitors (Grossmann et al., 1999, Turco et al., 2004). The data here suggest that AG-014699 specifically inhibits IR-induced NF-κB activation and thus may overcome these potential toxicities. It is important to note that the effects on NF-κB when using AG-014699, are very much a transient (i.e. during and in the short period following DNA damage), thus it would be fair to hypothesise that AG-014699 would not affect the NF-κB induced by inflammatory stimuli, and hence the NF-κB mediated inflammatory response, which is known to be hugely important to the cell. However, this requires further investigation into the role of PARP-1 and other activators of NF-κB (Chapters 4 and 5). Importantly however, therapeutic inhibition of PARP has been shown by many to be relatively non-toxic to normal cells (Drew and Plummer, 2009).

AG-014699 has been shown to be efficacious both *in vitro* and *in vivo* (Daniel et al., 2010, Daniel et al., 2009, Drew et al., 2011, Plummer et al., 2008, Zaremba et al., 2009). Moreover, AG-014699 was the first PARP inhibitor to enter clinical trials for cancer therapy and Phase I trials showed that profound and sustained PARP inhibition could be achieved after a single intravenous infusion (Plummer et al., 2005). Phase II trials combining AG-014699 with temozolomide in metastatic melanoma patients showed an improvement in the response rate in comparison with temozolomide alone (Plummer et al., 2008). Furthermore, AG-014699 is currently in phase II trials for

BRCA defective breast and ovarian cancer as a single agent (www.clinicaltrials.gov). A number of pharmaceutical companies are now undertaking clinical trials of PARP inhibitors for the treatment of cancer (Drew and Plummer, 2009); however, the data here represent the first investigation of the clinically relevant PARP inhibitors in the context of their potential utility as inhibitors of DNA-damage induced NF-κB activation, and these data are now published in Oncogene (Hunter et al., 2011).

3.5 Summary and future work

The data in this chapter, using AG-014699 and siRNA targeting NF-κB p65 and MEFs proficient and deficient for NF-κB p65, show that inhibition of PARP-1 modulates the apoptotic response to IR, and that the potentiation of IR-induced cytotoxicity by PARP-1 inhibition is due to the loss of NF-κB activation. Strikingly, the Comet assay data are the first to demonstrate that radio-sensitisation by PARP inhibition is exclusively due to inhibition of NF-κB, and not due to the widely reported prevention of DNA repair.

However, these data do highlight further questions regarding the use of PARP inhibitors for the inhibition of NF-κB. The work in this chapter has concentrated on the activation of NF-κB by the DNA damaging agent, ionising radiation, and the role PARP-1 plays in the context of NF-κB following this stimulus. It would therefore be interesting to determine whether PARP-1 is required for the activation of NF-κB following other known stimulators of NF-κB, such as TNF-α, and furthermore, whether any activation is dependent on PARP-1 enzymatic function. The literature suggests that PARP-1 catalytic activity may be dispensable for TNF-α induced NF-κB activation (Hassa et al., 2001) leading to the hypothesis that AG-014699 may specifically inhibit DNA-damage induced NF-κB activation and therefore overcome toxicity obstacles seen with other NF-κB inhibitors. In order to test this, it will be important to investigate the role of PARP-1 in the activation of NF-κB dependent gene transcription after both inflammatory and DNA-damaging stimuli. These studies will be undertaken as part of this thesis (Chapter 4 and 5).

Moreover, it is well documented that the activation of NF-κB is dependent on the cell type and stimulus, and therefore it would be important to investigate the role of PARP-1 in the co-activation of NF-κB in other cell lines and contexts. The data within this chapter suggest that the PARP inhibitor AG-014699, may have a potential uses in cancers in order to overcome NF-κB mediated therapeutic resistance. To this end it is

vital to discover which types of cancer would benefit from this type of therapeutic intervention, and to investigate whether PARP inhibition can re-sensitise cancer cell lines to DNA-damaging agents (IR and perhaps, other chemo-therapeutic agents) *via* the inhibition of NF-κB. This study will be undertaken as part of this thesis (Chapter 6).

Chapter 4. PARP-1 is differentially required in the activation of NF-κB

4.1 Introduction

Although there is a mounting body of evidence describing a role for PARP-1 in the co-activation of NF-κB, the role of PARP-1 catalytic activity in NF-κB activation is somewhat contentious. This is discussed at length in section 1.5. Some groups have reported that PARP-1 enzymatic activity directly influences NF-κB dependent transcription after DNA damage (Chang and Alvarez-Gonzalez, 2001, Chiarugi and Moskowitz, 2003, Nakajima et al., 2004, Stilmann et al., 2009, Veuger et al., 2009, Zingarelli et al., 2003b)whilst others have described how PARP-1 protein alone is required for NF-κB activation following inflammatory stimuli (Hassa et al., 2001, Hassa and Hottiger, 1999, Martin-Oliva et al., 2004). It is highly likely that the differential requirements reported in the literature are both cell-type and stimulus-dependent.

Le Page *et al.*, (1998) used the classical PARP inhibitor, 3-AB in the macrophage cell line, 264.7 and showed that NF-κB activation by LPS was reduced in combination with 3-AB. They also showed that transcription of the NF-κB target gene, *iNOS*, was reduced in cells treated with LPS and 3-AB compared with LPS alone (Le Page et al., 1998). This was the first indication that inhibition of PARP-1 could modulate NF-κB-dependent gene expression. Chang and Alvarez-Gonzalez, 2001, demonstrated that pre-incubation with 3-AB inhibited H_20_2 activated NF-κB p50 DNA binding and activation. A report using rat glial and neuronal cultures showed that the use of PARP inhibitors significantly reduced activation of NF-κB target genes, including *iNOS*, *IL-1β* and *TNF-α*, resulting in a reduced neuro-inflammation and the neurotoxic potential of activated glia (Chiarugi and Moskowitz, 2003). Zingerilli *et al.*, (2003) used the PARP inhibitors, 3-AB and 1,5-dihydroxyisoquinoline in combination with the inflammatory stimulant 2,4,6-trinitrobenzene sulfonic acid (TNBS) and showed that this combination markedly reduced DNA binding of both NF-κB and AP-1 in a rat model of colitis (Zingarelli et al., 2003b). Nakajima *et al.*, (2004) also used cultured murine glial cells to show that the auto-ribosylation of PARP-1 led to enhanced LPS-induced NF-κB DNA binding and in particular NF-κB p50-dependent gene transcription in this model (Nakajima et al., 2004). Furthermore, PARP-1 inhibition was able to alleviate TNF-α-stimulated NF-κB-dependent MMP-9-mediated neurotoxicity in microglia in a model of brain injury (Kauppinen and Swanson, 2005).

More recently, Stilmann *et al* (2009) showed that a PARP-1 signalling scaffold via direct protein-protein interactions with NEMO, PIASγ and ATM formed in response to DNA damage (Figure 1.13). In particular, this group detail that impaired sumoylation following treatment with the PARP inhibitor, 3-AB, results in reduced IKK activation and therefore inhibition of p65 induction. They describe the formation of a signalosome which relies on binding with PAR and leads to pro-survival NF-κB activation (Stilmann et al., 2009).

A different approach was taken by, Hassa *et al.,* (2001) which demonstrated that TNFα-mediated PARP-1 co-activation of the NF-κB transcription factor was attenuated in PARP-1 null cells, but was unaffected by over-expression of a PARP-1 catalytic mutant (Hassa et al., 2001). A later study by Martin-Oliver *et al.*, (2006 Cancer Res), used the carcinogen, TPA ((12-O-tetradecanoyl-phorbol-13-acetate) in combination with the PARP inhibitor, DPQ, and showed that in a model system of murine papillomas, PARP-1 activity did not alter NF-κB activation following TPA treatment.

4.2 Aims

Studies to date have concentrated on the role of PARP-1 in the activation of NF-κB following either an inflammatory stimulus or a DNA-damaging agent. However, head-to-head studies in one model system are absent. Hence, this chapter aims to directly compare activation by the inflammatory cytokine, TNF-α and the DNA-damaging agent, ionising radiation, and thus determine whether PARP-1 is differentially required in the activation of NF-κB and importantly whether this is stimulus-dependent. Furthermore, these studies will test the hypothesis that any differential observed would be dependent on the ability of the stimuli to activate PAR.

The potent and specific PARG inhibitor, Adenosine 5'-diphosphate (hydroxymethyl) pyrrolidinediol, referred to hereafter as, ADP-HPD (Slama et al., 1995) will also be used to investigate the role of PAR r in the activation of NF-κB following DNA damage. PARG is the major enzyme responsible for the catabolism of PAR (Bonicalzi et al., 2005), and therefore PARG inhibition results in a reduction in PAR degradation. Hence, the ADP-HPD is a very useful tool for testing the hypothesis that DNA-damage-activated NF-κB is mediated *via* PAR.

4.3 Results

4.3.1 IR or TNF-α induced nuclear translocation of NF-κB is unaffected by AG-014699 or PARP-1 knockdown

NF-κB subunits are held inactive in the cytoplasm through their interaction with IκB proteins. Upon stimulus, by DNA damage or inflammatory cytokines, the canonical pathway of NF-κB activation is induced and signalling cascades converge at the IKK complex which phosphorylates IκBα, targeting this for degradation and promoting nuclear translocation of the p65/p50 heterodimer, activating transcription of many genes (Ghosh and Karin, 2002). One method of investigating whether an NF-κB subunit is activated by a particular stimulus, is to assess the nuclear translocation by Western blotting. Previous reports would suggest that both IR and TNF-α would induce the nuclear translocation of the p65 subunit (Beg and Baltimore, 1996, Veuger et al., 2009), and moreover that IR-induced p65 nuclear translocation would be unaffected by PARP inhibition (Veuger et al., 2009). However, it was important in this study to assess the activation of p65 following either stimuli in the $p65^{+/+}$ MEFs. To this end it was also interesting to determine whether p65 siRNA, AG-014699, PARP-1 siRNA or a combination of p65 siRNA and AG-014699 had any effect on the nuclear translocation of p65 following either IR or TNF-α.

Briefly, $p65^{+/+}$ MEFs were transfected with 50 nM p65 siRNA, 50 nM PARP-1 siRNA , 50 nM NS siRNA (optimised previously, Chapter 3), or vehicle alone control. Cells were then incubated for a further 48 h prior to treatment with either 10 Gy IR or 10 mg/ml TNF-α (or 0.1 % BSA diluted in PBS control). Cells were harvested 1 h later and nuclear extracts prepared using the NE PER kit, (section 2.5.2). The levels of p65, Lamin or β-actin were determined by Western analyses in nuclear extracts. Densiometric analysis was used to assess the levels of p65 compared to the nuclear protein, Lamin. β-actin was used as a control in order to ensure that there was no cytoplasmic contamination of the nuclear extracts.

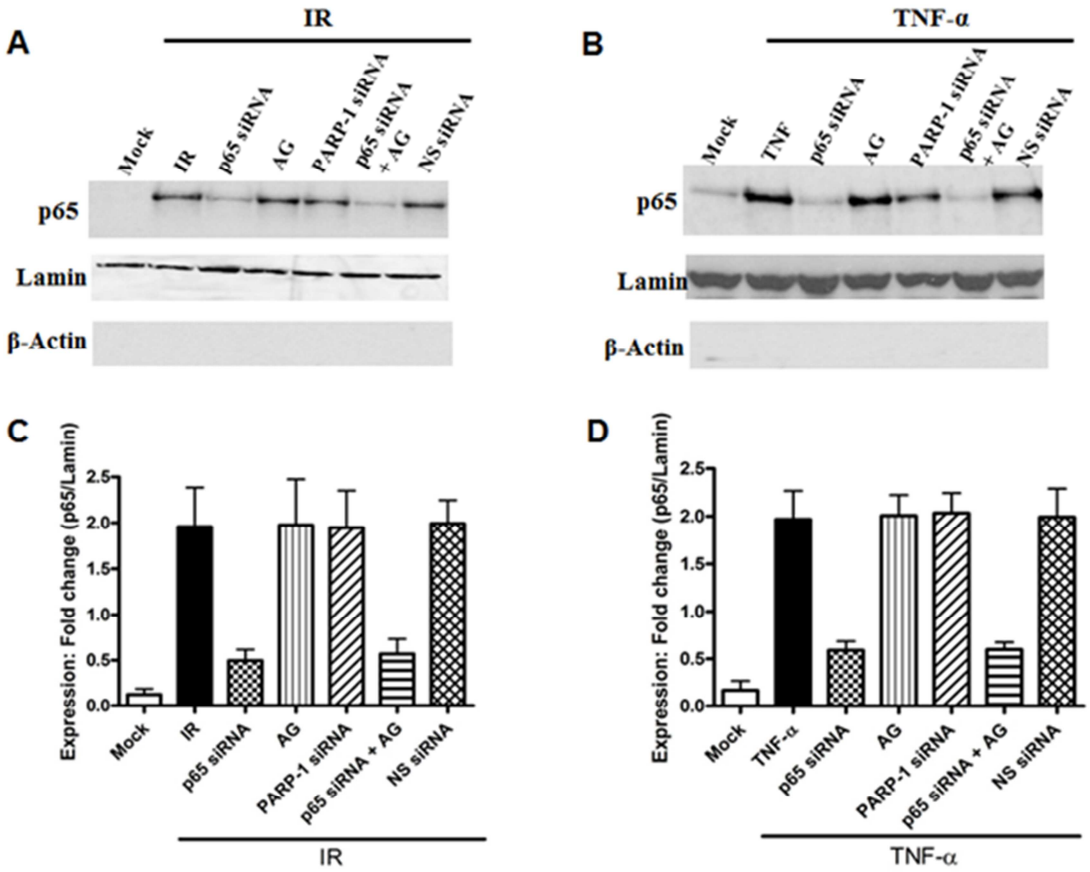

<u>Figure 4.1</u>: p65 nuclear translocation is unaffected by AG-014699 or PARP-1 siRNA

Western blotting data showing nuclear translocation of p65 following (**A**) IR or TNF-α (**B**) ± p65 siRNA ± AG-014699 (AG) ± PARP-1 siRNA ± (p65 siRNA + AG-014699) ± NS siRNA control, in $p65^{+/+}$ MEFs. Bar charts showing densiometric analysis of Western blotting data (**C**) IR and (**D**) TNF-α. Cells were treated with relevant siRNA, or control, left for 48 h, pre-treated with AG-014699, or control 1 h prior to IR and harvested 1 h post-IR. Loading was normalised to lamin nuclear loading control in all cases. Nuclear extracts were shown to be free of any cytoplasmic contamination by blotting with β-Actin antibody.

Figure 4.1A and 4.1B show the nuclear translocation of p65 1 hour following treatment with either IR or TNF-α in nuclear extracts of the $p65^{+/+}$ MEFs. The effect of co-incubation with either stimulus and p65 siRNA, AG-014699, PARP-1 siRNA or a combination of p65 siRNA and AG-014699 was also assessed at this timepoint. The bar charts representing that densiometric analysis Figures 4.1C and 4.1D show that nuclear translocation of p65 was induced to a similar extent by either 10 Gy IR or 10 ng/ml TNF-α,compared to controls, as the blots shown following TNF-α treatment were exposed for longer than those following treatment with IR. Importantly, this IR- or TNF-α-induced translocation was unaffected by AG-014699 or PARP-1 siRNA ($p=0.854$ and $p=0.721$, respectively IR; $p=0.542$ and $p=0.399$, respectively, TNF-α,

unpaired Student's t-tests). It should also be noted that although the PARP-1 siRNA does appear to have a slight effect on p65 translocation following TNF-α, this is not the case as the Lamin control indicates under loading of the protein extract in this case (Figure 4.1B). Knockdown of p65, either alone or in combination resulted in the loss of p65 protein, hence no nuclear translocation was observed following either stimulus. Loading was normalised to Lamin, and to ensure the nuclear extracts had no contamination of cytoplasmic proteins blots were probed for β-actin, and showed no presence of this protein. These data suggest that PARP-1 does not affect nuclear translocation, and must be acting further downstream in the activation cascade, perhaps at the DNA binding or transcriptional level.

4.3.2 IR or TNF-α induced NF-κB DNA binding in a time dependent manner

The data in Figure 4.1 illustrated that PARP-1 inhibition or siRNA did not affect p65 nuclear translocation, and hence PARP-1 must be acting further downstream in the activation of NF-κB, perhaps at the DNA binding or transcriptional level. In order to determine whether this was the case, an assessment of p65 DNA binding, using an ELISA-based assay was undertaken. However, the timepoint at which maximal DNA binding occurred following either 10 Gy IR or 10 ng/ml TNF-α had to be determined before any further investigation could take place.

The ELISA-based assay, described in detail in section 2.8.1 was utilised. Briefly, $p65^{+/+}$ MEFs were plated and left to adhere for 24 h prior to treatment with 10 Gy IR or 10 ng/ml TNF-α. Cells were then harvested at various timepoints (0, 1, 2, 4, 6, 8 24 h) and DNA binding of nuclear extracts assessed using the ELISA assay. Figures 4.2A and 4.2B illustrate that DNA binding of p65 following either IR or TNF-α increased after 1 h when compared with untreated controls ($p=0.0091$ and $p=0.0007$, respectively, unpaired Student's t-test). Moreover, in the case of both stimuli DNA binding was maximal 2 h following treatment ($p<0.0001$ and p0.0001, compared with untreated controls, unpaired Student's t-test). DNA binding of p65 was still significantly increased 4 h after treatment with 10 Gy IR and 10 ng/ml TNF-α, and in both cases DNA binding activity returned to basal levels 24 h post treatment.

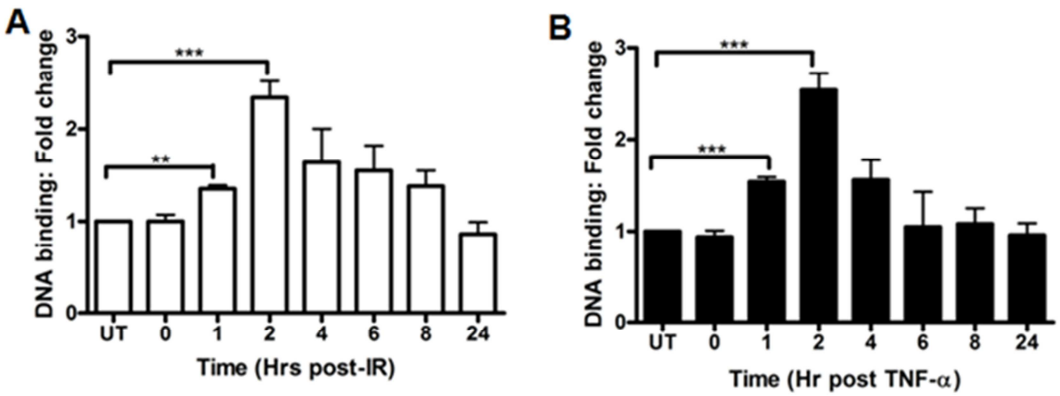

Figure 4.2: Maximal activation of NF-κB by either IR or TNF-α is 2 h post-treatment Bar chartshowing the effect of IR or TNF-α over time on NF-κB DNA binding activity, measured using an ELISA-based assay, in $p65^{+/+}$ MEFs. All results are the mean of three independent experiments with SEM. Significance relative to mock treated control using unpaired Student's t-test *** $p<0.001$, ** $p<0.01$

4.3.3 NF-κB DNA binding requires PARP protein and enzymatic activity following IR, but PARP-1 protein alone following TNF-α

Once it had been determined that DNA binding of p65 was maximal 2 h following treatment with 10 Gy IR or 10 ng/ml TNF-α, the ELISA was utilised to assess the effects of AG-014699, p65 or PARP-1 siRNA on IR- and TNF-α-induced NF-κB DNA binding. In this case, $p65^{+/+}$ MEFs were transfected with 50 nM p65, PARP-1 or NS siRNA (or vehicle control). Cells were then left for 48 h, and pre-treated with AG-014699, or DMSO control 1 h prior to treatment with 10 Gy IR or 10 ng/ml TNF-α. Cells harvested 2 h later and nuclear extracts were prepared before running on the ELISA as described in 4.3.2.

The open bars in Figure 4.3 show that 10 Gy IR increased DNA binding activity 2-fold compared with Mock treated $p65^{+/+}$ cells. Also, siRNA targeting p65 or a combination of p65 siRNA and AG-014699 reduced IR-induced DNA binding > 85% following IR in $p65^{+/+}$ cells ($p=0.006$ and $p=0.008$, compared to IR in combination with NS siRNA, respectively, unpaired Student's t-tests). PARP-1 siRNA inhibited DNA binding by approximately 60% ($p=0.02$, compared to IR in combination with NS siRNA, unpaired Student's t-test). Significantly, AG-014699 also reduced IR-induced DNA binding to levels comparable with untreated controls ($p=0.03$, compared to IR in combination with NS siRNA, unpaired Student's t-test). Non-specific siRNA had no effect on DNA-binding following IR. The black bars in Figure 4.3 illustrate that 10 ng/µl TNF-α

increased p65 DNA binding activity 2.3-fold compared with Mock treated $p65^{+/+}$ cells. p65 siRNA or a combination of p65 siRNA and AG-014699 reduced DNA binding to levels relative to Mock treated controls, following TNF-α (p=0.01 and p=0.008, compared to TNF-α in combination with NS siRNA, respectively, unpaired Student's t-tests). Importantly, PARP-1 siRNA also reduced DNA binding after TNF-α treatment (p=0.02, compared to TNF-α in combination with NS siRNA, unpaired Student's t-test). In marked contrast, AG-014699 had no effect on p65 DNA binding following TNF-α.

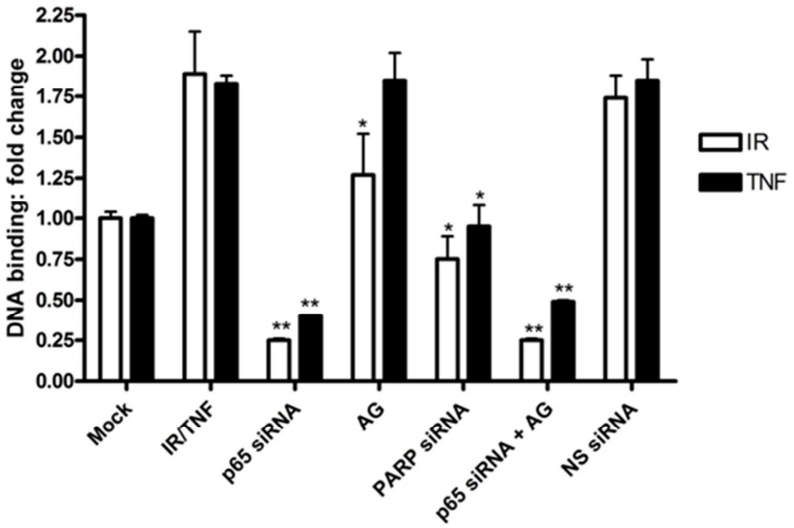

Figure 4.3: PARP activity is essential for NF-κB DNA binding following IR, not TNF-α Bar chart showing the effect of IR or TNF-α ± p65 siRNA ± AG-014699 (AG) ± PARP-1 siRNA ± (p65 siRNA + AG-014699) ±Non-specific (NS) siRNA control on NF-κB DNA binding activity, measured using an ELISA-based assay in $p65^{+/+}$ MEFs. Open bars IR, black bars TNF-α. All results are the mean of three independent experiments with SEM. Significance relative to NS siRNA control using unpaired Student's t-test *** $p<0.001$, ** $p<0.01$

4.3.4 IR or TNF-α induced NF-κB-dependent gene transcription in a time dependent manner

The data in Figure 4.3 illustrated that PARP-1 inhibition or siRNA inhibited IR-induced p65 DNA binding but that PARP-1 protein alone was required for p65 DNA binding following TNF-α treatment. Hence, it was vital to determine the role of PARP-1 in the activation of NF-κB-dependent gene transcription following both stimuli. For this a luciferase reporter assay was utilised. However, the timepoint at which luciferase activity was maximal following either 10 Gy IR or 10 ng/ml TNF-α had to be determined before any further investigation could take place.

Briefly, $p65^{+/+}$ MEFs were seeded and incubated for 24 h before transient transfection with 200 ng of an NF-κB-luciferase construct and 200 ng of a pCMB-β-galactosidase plasmid (section 2.9). Following further 48 h incubation, cells were treated with either 10 Gy IR or 10 ng/ml TNF-α. Cells were lysed after 0, 2, 4, 6, 8 or 24 h and assayed for luciferase activity using the Promega Luciferase assay system, according to the manufacturer's instructions. Luciferase activity was corrected for β-galactosidase activity as described previously (Brady et al., 1999), and relative activities expressed as fold changes.

Figures 4.4A and 4.4B illustrate that luciferase reporter activity increased steadily following either IR or TNF-α when compared with untreated controls. Four hours after either stimuli, luciferase reporter activity was significantly increased when compared with untreated controls ($p=0.0086$; IR and $p=0.0071$; TNF-α, respectively, unpaired Student's t-test). Moreover, in the case of both stimuli NF-κB-dependent luciferase activity was maximal 8 h following treatment ($p=0.0005$; IR and $p=0.0008$; TNF-α, compared with untreated controls, unpaired Student's t-test). Luciferase reporter activity returned to basal levels 24 h post treatment with either stimulus.

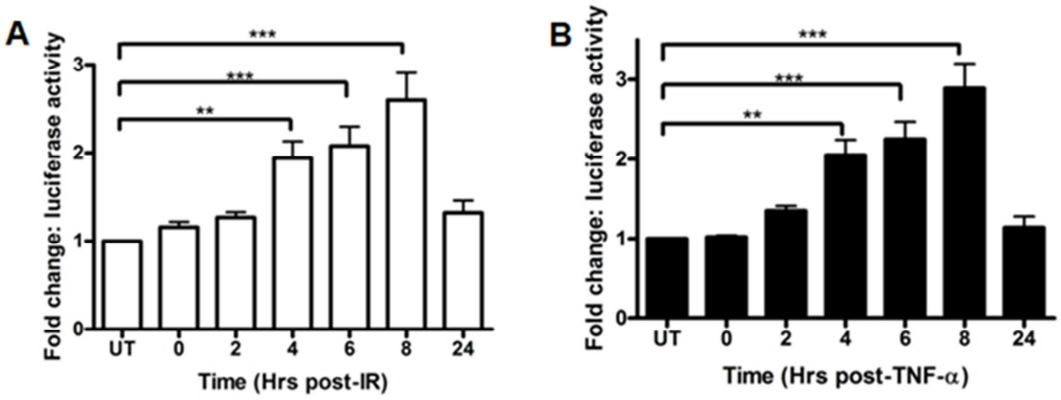

<u>Figure 4.4:</u> Maximal activation of NF-κB-dependent gene transcription by either IR or TNF-α is 8 h post-treatment. Bar chart showing the effect of IR or TNF-α over time on NF-κB-dependent gene transcription, measured using a luciferase reporter assay, in $p65^{+/+}$ MEFs. All results are the mean of three independent experiments with SEM. Significance relative to mock treated control 001 using unpaired Student's t-test *** $p<0.001$ ** $p<0.01$

4.3.5 NF-κB-dependent gene transcription requires PARP protein and enzymatic activity following IR, but PARP-1 protein alone following TNF-α

Once it had been determined that NF-κB-dependent luciferase activiation was maximal 8 h following treatment with 10 Gy IR or 10 ng/ml TNF-α, the luciferase reporter assay

was utilised to assess the effects of AG-014699, p65 or PARP-1 siRNA on IR- and TNF-α-induced NF-κB-dependent gene transcription. In this case, $p65^{+/+}$ MEFs were seeded and incubated for 24 h before transient transfection 200 ng of an NF-κB-luciferase construct and 200 ng of a pCMB-β-galactosidase plasmid (section 2.9). siRNA transfection was undertaken simultaneously in this case. Following a further 48 h incubation, cells were assayed for luciferase actiavity expressed as fold changes.

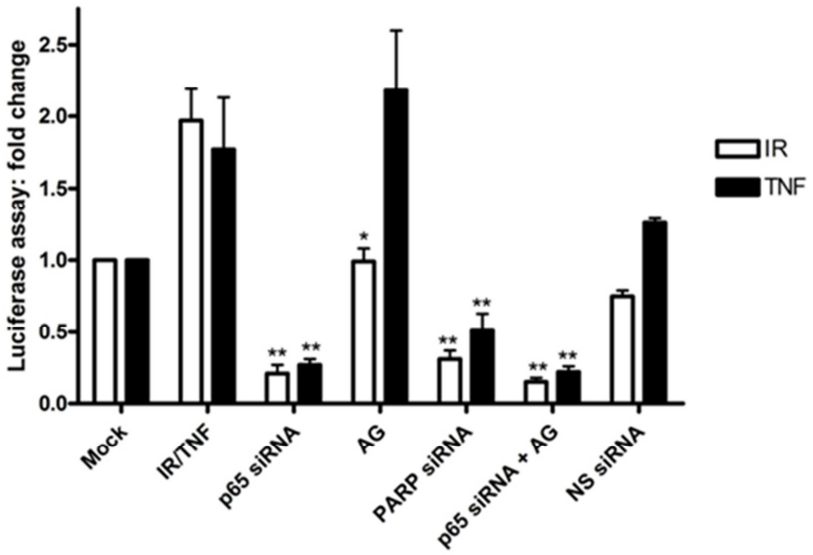

<u>Figure 4.5:</u> PARP activity is essential for NF-κB-dependent gene transcription following IR, not TNF-α Bar chart showing the effect of IR or TNF-α ± p65 siRNA ± AG-014699 (AG) ± PARP-1 siRNA ± (p65 siRNA + AG-014699) ±Non-specific (NS) siRNA control on NF-κB-dependent transcriptional activation, measured using a luciferase reporter assay, in $p65^{+/+}$ MEFs. Open bars IR, black bars TNF-α. All results are the mean of three independent experiments with SEM. Significance relative to NS siRNA control using unpaired Student's t-test ** $p<0.01$, * $p<0.05$

Consistent with the increased DNA binding (Figure 4.3), following either 10 Gy IR or 10 ng/ml TNF-α, luciferase activity was increased 2- and 2.5-fold respectively, compared to Mock treated controls (Figure 4.5). Also, siRNA targeting p65 or a combination of p65 siRNA and AG-014699 reduced luciferase activity > 80% following IR alone or in combination with NS siRNA ($p=0.01$ and $p=0.007$, respectively, unpaired Student's t-tests) or TNF-α alone or in combination with NS siRNA ($p=0.009$ and $p=0.01$, respectively, unpaired Student's t-tests) in $p65^{+/+}$ MEFs. PARP-1 siRNA inhibited luciferase activity by approximately 70%, following either stimulus ($p=0.03$ compared to IR, $p=0.05$ compared to TNF-α, unpaired Student's t-tests). Significantly, AG-014699 also reduced IR-induced luciferase reporter activity to levels comparable with untreated controls ($p=0.04$, unpaired Student's t-test). However, AG-014699 had no effect on luciferase activity following TNF-α compared with TNF-α alone, consistent

with other reports which have shown that a NF-κB transcriptional activation was attenuated in PARP-1 null cells but unaffected by over-expression of a PARP-1 catalytic mutant (Hassa et al., 2001).

4.3.6 IR, not TNF-α stimulates PAR formation

The p65 DNA binding and NF-κB-dependent transcriptional activation results have shown that PARP-1 activity and protein is required for NF-κB activation following IR, whereas PARP-1 protein alone is essential for NF-κB activation following treatment with TNF-α. It is well documented that PARP-1 is activated following DNA, resulting in the automodification of the protein and formation of PAR (Jagtap and Szabo, 2005). However, there are no reports in the literature investigating the activation of PARP-1 following the cytokine, TNF-α. Therefore, in order to determine whether PARP-1 was activated by IR or TNF-α, PARP activity was assessed in the $p65^{+/+}$ MEFs using a validated assay (Plummer et al., 2005, Zaremba et al., 2009). Briefly, $p65^{+/+}$ MEFs were plated and allowed to adhere for 24 h before treatment with increasing doses of either IR (0–20 Gy) or TNF-α (0-50 ng/ml). Cells were permeabilised immediately following IR or TNF-α treatment and PARP activity assay undertaken (section 2.4)

Figure 4.6A shows that IR-induces PAR formation in a dose-dependent manner. After treatment with as little as 2 Gy IR, PARP activity is significantly increased (p=0.011, unpaired Student's t-test). Statistical analysis using unpaired Student's t-tests, show that at all doses tested, PARP-1 activity is significantly increased (p=0.0023; 5 Gy, p=0.0017; 10 Gy, p=0.0002; 20 Gy, respectively). However, Figure 4.6B illustrates that a range of concentrations of TNF-α (5 – 50 ng/ml) fail to stimulate PARP-1 activity compared with untreated controls in the $p65^{+/+}$ MEFs. Statistical analysis using unpaired Student's t-tests, show that at all doses tested, PARP-1 activity was not significantly different from untreated cells (p=0.109; 5 ng/µl, p=0.112; 10 ng/µl, p=0.578; 20 ng/µl, p=0.765; 50 ng/µl respectively). These data suggest that PAR formation is vital in the IR-induced NF-κB.

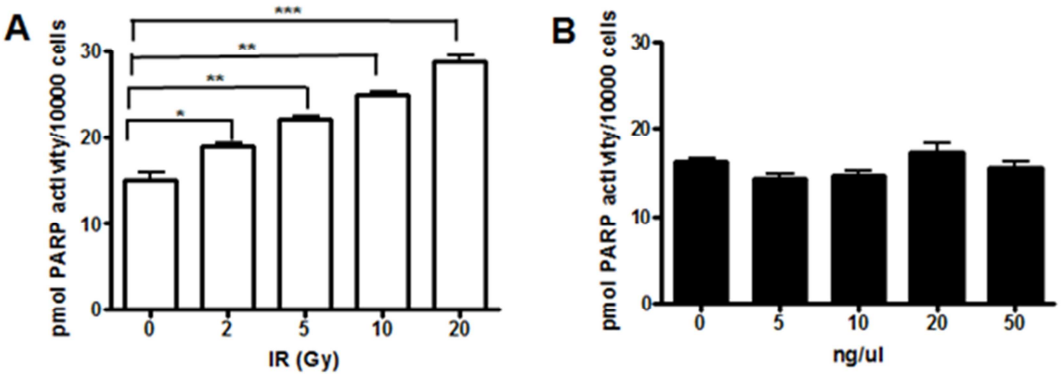

Figure 4.6: PARP-1 is activated following IR, not TNF-α
Bar chart showing PARP activity, measured using a validated immunoblot assay which quantifies PAR formation, in $p65^{+/+}$ MEFs after increasing doses of IR (**A**) and TNF-α (**B**) All results are the mean of three independent experiments with SEM. All results are the mean of three independent experiments with SEM. Significance relative to mock treated control using unpaired Student's t-test *** $p<0.001$, ** $p<0.01$,* $p<0.05$

4.3.7 The PARG inhibitor, ADP-HPD, prevents degradation of PAR

The PARP-1 activity assay data suggested that PAR formation is important in mediating the IR-induced NF-κB response, this observation required further testing. PARG is the enzyme responsible for the catabolism of the PAR. It is ubiquitously expressed at low levels in all cells and tissues (Bonicalzi et al., 2005). Hence, ADP-HPD, a commercially available potent PARG inhibitor (Slama et al., 1995) was used in order to further investigate the importance of the PAR in IR-induced NF-κB activation.

In this case the validated PARP activity assay (Plummer et al., 2005, Zaremba et al., 2009) was utilised in order to determine whether specific inhibition of the PARG enzyme would prevent degradation of the PAR. It must noted that ADP-HPD is highly specific for PARG and does not inhibit PARP, even if used at millimolar concentrations (Slama et al., 1995). Briefly, $p65^{+/+}$ MEFs were plated and allowed to adhere for 24 h before a 1 h pre-treatment with 1 µM ADP-HPD prior to treatment with 10 Gy IR. Cells were permeabilised at various timepoints following IR (0, 15, 30, 60, 120, 240 min) and the reaction undertaken as in section 2.4.

The open bars in Figure 4.7 represent $p65^{+/+}$ MEFs treated with 10 Gy IR and the black bars represent $p65^{+/+}$ MEFs treated with 10 Gy IR and ADP-HPD. Figure 4.7 illustrates that co-incubation with ADP-HPD results in increased stability of the PAR in IR-treated cells. PAR formation is significantly increased following treatment with IR ($p<0.0001$, unpaired Student's t-test). However, polymer is degraded rapidly and returns to basal

levels 1-2 hours following IR. In cells treated with both IR and ADP-HPD treated cells PAR was further activated compared with IR alone treated cells, all time-points investigated. Significantly, in the presence of ADP-HPD, PAR formation persists for upto 4-hours post-IR treatment (p=0.023, compared with untreated controls, unpaired Student's t-test).

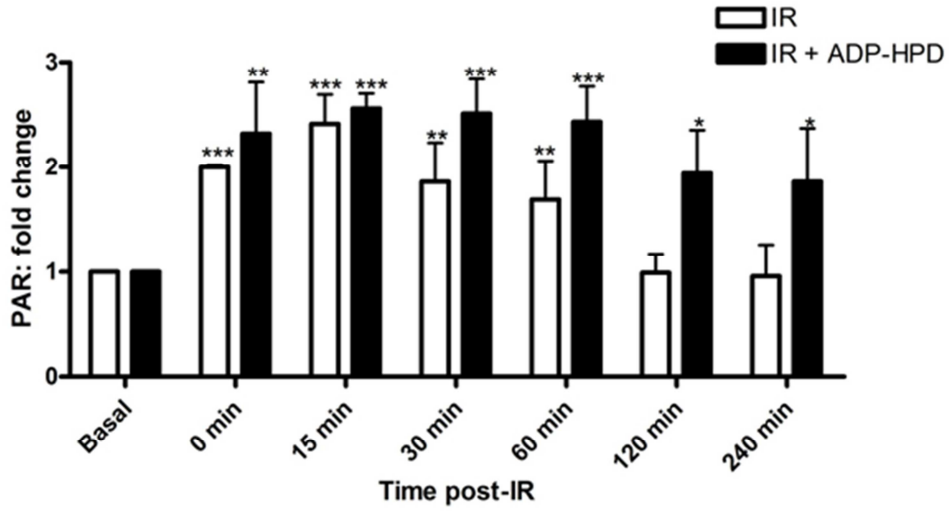

Figure 4.7: PARG inhibition leads to increased PAR stability
Bar chart showing PARP activity timecourse, measured using a validated immunoblot assay which quantifies PAR formation, in $p65^{+/+}$ MEFs following 10 Gy IR ± ADP-HPD (open bars IR, black bars IR + ADP-HPD). All results are the mean of three independent experiments with SEM. Significance relative to mock treated control using unpaired Student's t-test *** $p<0.001$, ** $p<0.01$,* $p<0.05$

4.3.8 PARG inhibition results in the persistence of IR-induced NF-κB DNA binding

Figure 4.7 showed that the PARG inhibitor, ADP-HPD resulted in the persistence of PAR formation following IR. Hence, it was therefore vital to assess the effects of this extended polymer presence on NF-κB DNA binding. The DNA binding ELISA (section 2.8.1) was used for this. Briefly, $p65^{+/+}$ MEFs were plated and left to adhere for 24 h before pre-treatment with ADP-HPD (or DMSO control) 1 h prior to treatment with 10 Gy IR. Cells harvested 2 h later and nuclear extracts were before running on the ELISA as described in 4.3.2. The results shown are the mean of three independent experiments.

Figure 4.8 illustrates that polymer stability correlates with a persistence in NF-κB DNA binding. The open bars represent represent $p65^{+/+}$ MEFs treated with 10 Gy IR and the black bars represent $p65^{+/+}$ MEFs treated with 10 Gy IR and ADP-HPD. IR significantly increased p65 DNA binding 2 h following treatment ($p<0.0001$, compared with untreated controls, unpaired Student's t-test). After this time-point, however, p65 DNA rapidly decreased and returned to basal levels by 8 h. Markedly, $p65^{+/+}$ MEFs treated

with a combination of IR and ADP-HPD, DNA binding was also maximal 2 h following treatment (p=0.0078, compared with untreated controls, unpaired Student's t-test). However, DNA binding persists for upto 8 hours following IR and ADP-HPD, and statistical analysis using Student's unpaired t-test confirm that this is significant (p=0.0019, compared with untreated controls).

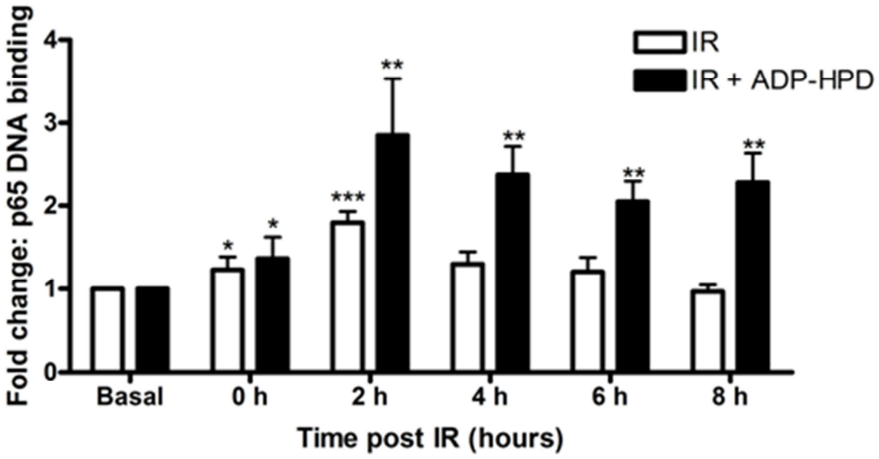

Figure 4.8: Persistence of NF-κB DNA binding following PARG inhibition
Bar chart showing NF-κB DNA binding timecourse measured using an ELISA-based method following IR ± ADP-HPD (open bars IR, black bars IR + ADP-HPD). All results are the mean of three independent experiments with SEM. Significance relative to mock treated control using unpaired Student's t-test *** p<0.001, ** p<0.01, * p<0.05

4.3.9 The effect of ADP-HPD in combination with ionising radiation on cell survival

The DNA binding data using the PARG inhibitor, ADP-HPD confirmed that a persistence of the PAR resulted in prolonged p65 DNA binding, and hence it was therefore important to determine whether this increased NF-κB activation had any effect on cell survival. Thus, the effect of ADP-HPD on cell survival following IR was assessed in the $p65^{+/+}$ and $p65^{-/-}$ MEFs was assessed using colony forming assays. In this case, $p65^{+/+}$ or $p65^{-/-}$ cells were plated and left for 24 hours to adhere before being treated with ADP-HPD or a DMSO control for 1 h prior to increasing doses of IR.

Figure 4.9A shows that co-incubation with IR and ADP-HPD protects against IR-induced cell kill in the $p65^{+/+}$ MEFs compared with IR alone. Furthermore, sstatistical analysis using an unpaired Student's t-test confirmed that, at the LD_{50} values, cells treated with ADP-HPD exhibited a significant radio-protective effect in the $p65^{+/+}$ MEFs compared with IR alone (p=0.024). Markedly, Figure 4.9B shows that IR in

combination with ADP-HPD had no effect on cell survival in the $p65^{-/-}$MEFs compared with IR alone (p=0.914, unpaired Student's t-test).

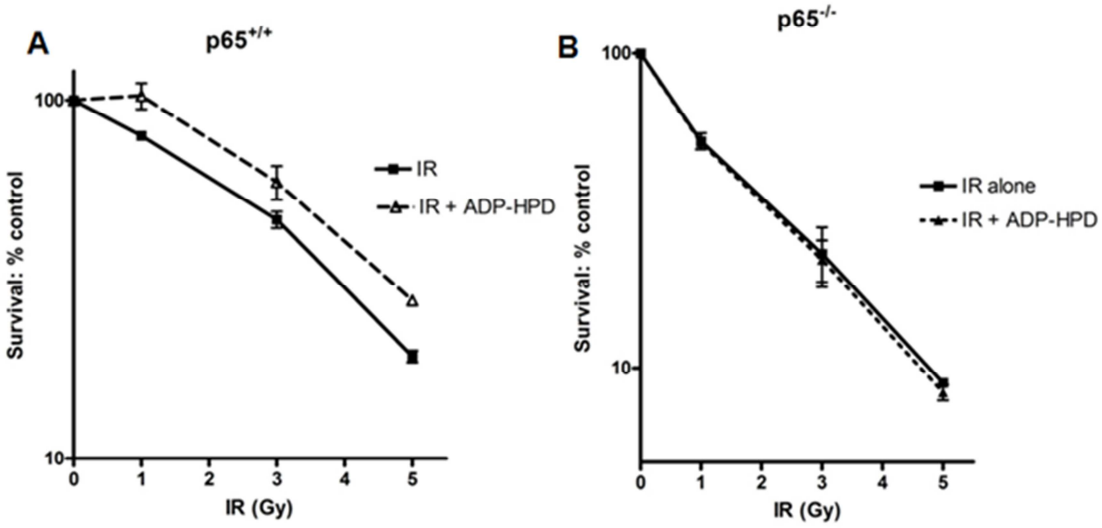

Figure 4.9: ADP-HPD has a radio-protective effect in the $p65^{+/+}$, but not $p65^{-/-}$ MEFs
The effects of increasing doses of IR on cell survival, either alone (solid line) or co-incubated with ADP-HPD (dashed line) were assessed using the clonogenic survival in $p65^{+/+}$ and $p65^{-/-}$ MEFs. Cells were pre-treated with ADP-HPD, or control 1 h prior to IR then re-plated after a further 24 h and allowed to form colonies for 7-21 days. All results are the mean of three independent experiments with SEM.

4.3.10 The effect of ADP-HPD in combination with IR on the transcription of NF--κB-dependent anti-apoptotic genes

In order to demonstrate that the DNA binding (Figure 4.8) and survival data (Figure 4.9) obtained using ADP-HPD, were physiologically relevant it was important to determine whether PARG inhibition by ADP-HPD, and subsequent persistence of PAR, leads to an increase of the expression of some known NF-κB-mediated anti-apoptotic genes following IR. The genes chosen to investigate were; *Bcl-xL* (Lee et al., 1999b), *cFLAR* (Kreuz et al., 2001) and *XIAP* (Turner et al., 2007) in the $p65^{+/+}$ MEFs.

This method is described in detail in 2.10. In this particular case, $p65^{+/+}$ MEFs were seeded and left for 24 h to adhere before a 1 h pre-treatment with 1 μM ADP-HPD prior to treatment with 10 Gy IR. Cells were then harvested at various timepoints (0 – 6 h) and RNA extracted using the RNeasy kit, and subsequently transcribed into cDNA using the High Capacity cDNA reverse transcription kit. cDNA was then used in a qRT-

PCR reaction using Taqman primers to confidently quantify the mRNA levels of either *Bcl-xL*, *cFLAR* or *XIAP* in each sample.

Figure 4.10A shows that treatment with IR significantly increases expression of *Bcl-xL* at 2h after treatment (p=0.041 compared with untreated controls, unpaired Student's t-test) and importantly, that co- incubation with ADP-HPD significantly increased IR-induced *Bcl-xL* expression at this timepoint (p=0.0089 compared with ADP-HPD alone controls, unpaired Student's t-test). *cFLAR* expression (Figure 4.10B) was also increased following IR although this was not statistically significant (p=0.103, 0 h, compared to untreated controls, unpaired Student's t-test) and this again was increased further by co-incubation with ADP-HPD at the 4 h timepoint (p=0.0098, unpaired Student's t-test). A similar trend was also observed with *XIAP* expression, however this was not statistically significant (Figure 4.10C).

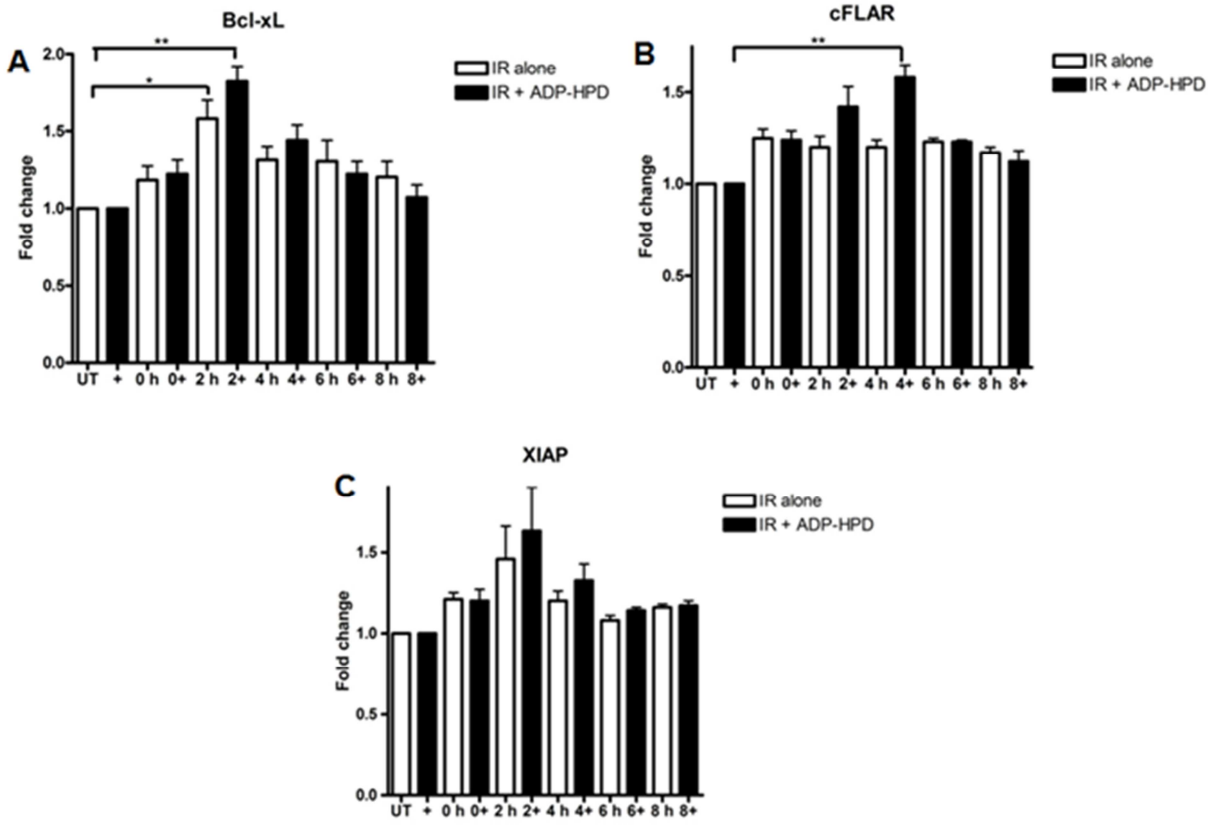

Figure 4.10: ADP-HPD increases the transcription of NF-κB-dependent anti-apoptotic genes following IR Bar chart showing the effect of IR ± ADP-HPD (Denoted as +) over time on the expression of the anti-apoptotic genes (**A**) Bcl-xL, (**B**) cFLAR and (**C**) XIAP. All results are the mean of three independent experiments with SEM. Significance compared to relevant control using unpaired Student's t-test was **p<0.01, * p<0.05.

4.4 Discussion

In this chapter, PARP-1 knockdown and the PARP inhibitor, AG-014699 were used to investigate the role of PARP-1 in the activation of NF-κB, following treatment with either IR or TNF-α. While knockdown of the PARP-1 protein abrogated NF-κB activation following the inflammatory stimulus, PARP-1 enzymatic inhibition had no effect. In contrast, PARP-1 protein and activity were necessary to inhibit the IR-induced NF-κB response. Therefore, the data presented here illustrate that PARP-1 is differentially required in the induction of NF-κB, and this is dependent on the activation stimulus and the ability of such stimuli to activate PAR.

It has been documented that TNF-α stimulation induces an NF-κB response approximately 20 minutes following treatment in some model systems. The data obtained within this study illustrated that NF-κB DNA binding was maximal 2 hours following either TNF-α or IR. However, other reports in the literature suggest that this phenomenon is cell type-dependent. For example, Nelson *et al.,* (2004) showed the oscillatory nature of p65 in and out of the nucleus following TNF-α treatment in HeLa and SK-N-AS cells, and that the first oscillation is clearly seen 100 minutes following a TNF-α pulse of 10 ng/ml (the same concentration used within this chapter). This leads to an NF-κB response by up-regulating early-response genes, with subsequent oscillations then resulting in the activation of mid- and late-response NF-κB dependent genes (Nelson et al., 2004). Furthermore, Criswell *et al.,* (2003) comprehensively reviewed the activation of transcription factors by IR and found that the IR-induced NF-κB is consistently reported to peak 0.5-2 hours following damage (Criswell et al., 2003). Hence, the literature and these data presented within this chapter concur, suggesting that the time-points used here are the optimum for the chosen cell line model.

The role of PARP-1 protein rather its catalytic activity as a co-activator of NF-κB is contentious. The data here are consistent with some studies which have shown that PARP-1 enzymatic activity is not required for NF-κB activation (Hassa et al., 2001, Hassa and Hottiger, 1999, Martin-Oliva et al., 2004), however, others, for example, Kauppinen and Swanson, (2005), have shown that PARP-1 inhibition was able to alleviate TNF-α-stimulated NF-κB-dependent MMP-9-mediated neurotoxicity in microglia in a model of brain injury. This differential is highly likely to be cell line or model system dependent and may also vary depending on the activation and the levels of other NF-κB subunits. For example, ongoing work in this institute, has shown that

subunit activation is a complex balance in CLL (Mulligan EA et al., 2010). This work showed that constitutive activation of the p65 and p50 subunits in CLL correlated closely and predicted shorter time to first treatment (TTFT) and overall survival (OS). p52 and c-Rel activation correlated with p65 and p50 activation. However although high p65 and p50 activation predicted shorter OS and TTFT, increased p52 and c-Rel activation were associated with a longer TTFT. Moreover, activation of RelB was absent is all cases unless there was an ATM mutation, which is known to confer poor prognosis and resistance to treatment. Hence, demonstrating the complex crosstalk between the different NF-κB subunits in CLL.

The data shown here suggesting that PARP-1 protein alone is required for TNF-α-induced NF-κB activation, supports reports that PARP-1 can act as a transcriptional co-regulator *via* direct interaction and protein-protein interactions. It is possible that PARP-1 may facilitate a structural role in the NF-κB transcriptional complex, following TNF-α in the $p65^{+/+}$ MEFs. This is consistent with the work of Hassa *et al.*, (2003), which illustrated how the physical presence of the PARP-1 C-terminal catalytic domain, but not its enzymatic activity, was required for PARP-1 and p300 to synergistically activate NF-κB-dependent transcription following either TNF-α or LPS (Hassa et al., 2003). Further work by this group also found that the acetylation of PARP-1, by HDAC1 and p300 was in key in the regulation of NF-κB activity by PARP-1 (Hassa et al., 2005).

Nuclear translocation of p65 was similar following both stimuli, and this was unaffected by either AG-014699 or PARP-1 knockdown. This therefore suggests that the differential requirements of PARP-1 for IR- and TNF-α-activated NF-κB must occur at the DNA binding and transcription stage. The requirement of PAR in DNA damage-activated NF-κB has been demonstrated (Stilmann et al., 2009) and this is consistent with our data that IR, but not TNF-α stimulates polymer formation. Stilmann *et al.* (2009) clearly identified a novel mechanism of pro-survival NF-κB activation mediated *via* PAR. This group showed that a PARP-1 signalling scaffold via direct protein-protein interactions with NEMO, PIASγ and ATM formed in response to DNA damage. In particular, this report details that impaired sumoylation following treatment with the PARP inhibitor, 3-AB, which resulted in reduced IKK activation and therefore inhibition of p65 induction. Furthermore, this report also describe the formation of a signalosome (Figure 1.13) which relies on binding with PAR and leads to pro-survival NF-κB activation.

Based on the observations within this chapter, a further mechanism detailing the role of PAR in DNA-damage-induced NF-κB activation can be proposed (Figure 4.11). Ghosh *et al.,* (1999) reported that the DNA binding interface of p65 is buried until a conformational change is induced, usually when p65 is in close proximity to the negatively charged region of its DNA consensus sequence (Ghosh, 1999), and importantly PAR is known to have a large overall negative charge (Ueda and Hayaishi, 1985). The increase in DNA binding observed following IR could be due to that either a persistence of p65 on the DNA, to promote transcription, or a greater concentration of p65 molecules. Importantly, the Western blot data showed increased nuclear p65 levels following DNA damage, as well as following TNF-α treatment (Figure 4.1). The DNA binding ELISA showed that p65 binding increased upon stimulation of polymer formation. Taken together, these data support the concept that DNA damage stimulates upstream pathways to free p65 for activation. Markedly, the amount of p65 in the nucleus was unaffected by AG-014699. Thus, it can be postulated that the negative charge on the polymer induces a conformational change in p65, similar to the one described by Ghosh *et al.,* (1999), which would lead to the increased binding and transcriptional activation observed in Figures 4.8 and 4.10, in the presence of ADP-HPD.

Althaus *et al.,* (1994) proposed that the large overall negative charge of PAR had the ability to relax the chromatin structure, which is usually extremely tightly wound, and displace histones from DNA. This PAR-induced relaxation would then allow large regions surrounding the DNA strand breaks to become accessible to other repair proteins; however it is very plausible that this theory can be extended to other proteins, such as p65 (Althaus et al., 1994). Hence, the mechanism described in Figure 4.11, corroborates the work of Althaus *et al.,* (1994), by suggesting that PARP-1 regulates IR-induced NF-κB, in part by chromatin structure remodelling. Moreover, a recent study has investigated the promoter recruitment of PARP-1, using ChIP-chip techniques, and has shown that peaks of promoter-proximal PARP-1 binding can be upto 3kb shoulder-to-shoulder (Krishnakumar et al., 2008). This study further supports the hypothesis that PARP-1 activation (by virtue of PAR formation) has the ability to relax the chromatin structure, and allows transcription factors to access the DNA, as postulated in the model shown in Figure 4.11.

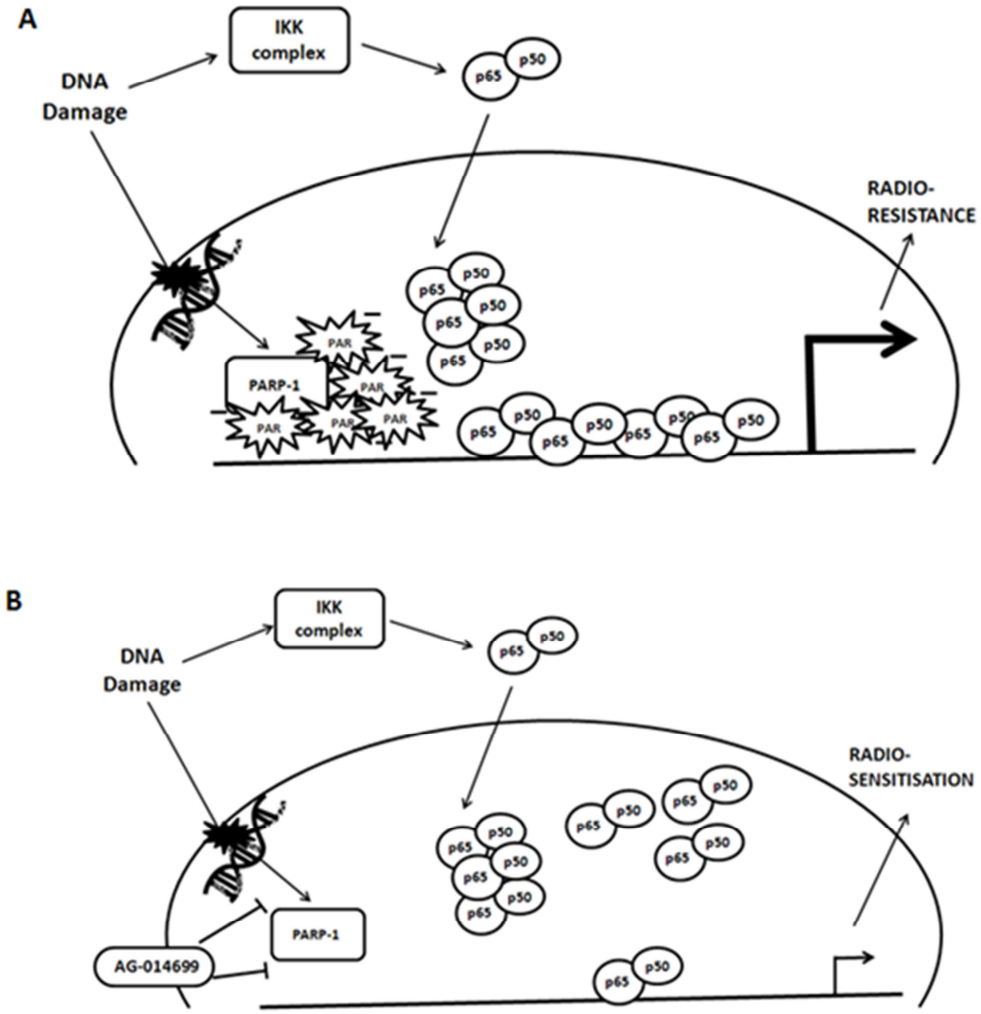

Figure 4.11: PAR is essential for DNA damage activated NF-κB
(**A**) DNA damage, such as IR, activates PARP-1, recruiting it to the site of damaged DNA. This results in formation of negatively charged PAR. The NF-κB p65-p50 heterodimer is also translocated to the nucleus following DNA damage via activation of the canonical pathway of NF-κB activation. When in proximity to regions with overall negative charge, such as that of PAR, a conformational change in p65 can be induced, exposing the positively charged DNA binding interface of p65. Thus, negatively charged PAR has the ability to attract p65 to DNA bind, (as PARP-1 and the polymer are recruited to sites of damaged DNA), up-regulating transcription of NF-κB-dependent genes, protecting against apoptosis and conferring radio-resistance.
(**B**) When the PARP inhibitor, AG-014699 is present, PARP-1 is no longer active and cannot form the polymer. Hence in this case, there is reduced DNA binding and transcriptional activation following IR, with induction of apoptosis and ultimately radio-sensitisation.

Stilmann *et al.*, (2009) reported that impaired sumoylation following treatment with the PARP inhibitor, 3-AB, resulted in reduced IKK activation and therefore inhibition of p65 induction. Stilmann *et al.*, (2009) use the non-specific PARP inhibitor, 3-AB, which has been shown to have many off target effects (Moses et al., 1990), and this group report a reduced nuclear translocation of p65 following use of 3-AB in combination

with IR. However, Western blotting data presented here (Figure 4.1) showed that p65 translocation was unaffected by AG-014699 in combination with IR, when compared with IR alone. This suggests that the phenomenon reported by Stilmann *et al.,* (2009) could be due to the off target effects of 3-AB, which was used at millimolar concentrations. However, a further explanation for this discrepancy could be that Stilmann *et al.,* (2009) used hyper-lethal doses of IR (80 Gy), whereas the doses used within this study are more clinically relevant. Stilmann *et al.,* (2009) utilised a different cell line model, and the activation of NF-κB has shown to be very cell type and stimulus dependent. Importantly, however, the data presented within this chapter not only agree with the major findings of Stilmann *et al.,* (2009) (i.e. that PAR formation is essential in the activation of NF-κB) but also extend these data by showing a further way in which PAR is specifically involved in NF-κB DNA binding and activation, importantly, by using a highly specific PARP inhibitor that is currently in clinical trials. Significantly, the overall consequences of both the Stilmann hypothesis and the model proposed here in Figure 4.11 are the same; a reduction in NF-κB-dependent gene expression. However, the slightly different, yet complementary mechanisms do highlight the importance of determining the role of PARP-1, and subsequently the formation of PAR, in the regulation of NF-κB, in different cell types and tissues.

The data presented here using the PARG inhibitor, ADP-HPD, also further support the model shown in Figure 4.11. PARG is ubiquitously expressed, at low levels in all cells and tissues, and is responsible for the catabolism of PAR (Bonicalzi et al., 2005). Increased polymer stability following IR, by virtue of inhibition of polymer degradation by using ADP-HPD, led to a persistence of NF-κB DNA binding, increased expression of anti-apoptotic genes and a protection against IR-induced cell death. These data not only confirm a role for PAR in the activation of NF-κB following DNA damage, but they show that the findings here are physiologically relevant as they demonstrate a direct impact of poly(ADP-ribosylation) on the transcription of key genes involved in apoptosis.

Using a similar approach, Majewski *et al.,* (2010) used over-expression of PARG to support their findings that that NF-κB and PARP-1 work co-operatively in the TNF-α induced inhibition of PHEX, which is expressed in osteoblasts and known to contribute to bone mineralisation. Inhibition of PHEX has been linked with the loss of bone mass density in chronic inflammatory diseases, such as inflammatory bowel disease.

Following treatment with TNF-α, the RelA/p50 NF-κB complex interacted with two cis-elements of the PHEX promoter and found that PARP-1 could bind immediately upstream of the NF-κB sites. Furthermore, TNF-α induced poly(ADP-ribosyl)ation of RelA when bound to the PHEX promoter, which was abrogated *in vitro* by overexpression of PARG (Majewski et al., 2010).

4.5 Summary and future work

The data shown within this chapter using AG-014699 and siRNA targeting PARP-1 illustrate that PARP-1 is differentially required in the activation of NF-κB, and that this differential is stimulus dependent. While knockdown of the PARP-1 protein abrogated NF-κB activation following the inflammatory stimulus, TNF-α, PARP-1 enzymatic inhibition had no effect. Conversely, PARP-1 protein and catalytic activity were necessary to inhibit the IR-induced NF-κB response. Furthermore, these data have shown that the differential requirements of PARP-1 are also dependent on the ability of the activation stimuli to activate PAR.

There is one major caveat associated with this study and that is the use of the DNA binding ELISA. Although this method has been favoured here, and in many other studies, in most cases because it is a high throughput method, it does not give a true indication of what is happening *in vivo* within the cell. Therefore, any future work should include chromatin immunoprecipitation (ChIP) assays in order to ascertain how NF-κB is DNA binding to the promoter region of individual genes following DNA damage.

The data shown here using the PARG inhibitor, ADP-HPD showed that increased polymer stability following IR, by virtue of inhibition of polymer degradation by using ADP-HPD, led to a persistence of NF-κB DNA binding, increased expression of anti-apoptotic genes and a protection against IR-induced cell death. Importantly, the qRT-PCR data presented using the PARG inhibitor, ADP-HPD, indicate that these findings do have physiological relevance, although this should be further confirmed. It is well documented that inhibition of NF-κB is an attractive target for cancer therapeutics (Gilmore and Herscovitch, 2006). However, global inhibition may also have some negative aspects. For example, NF-κB plays a vital role in the inflammatory response, and thus complete inhibition of NF-κB, for example with an IKK inhibitor, may have

adverse effects. The IKK complex has many known functions within the cell (Carrillo et al., 2004, Chariot, 2009), and inhibition may be cytotoxic. Long-term NF-κB inhibition may also increase the likelihood of immunodeficiency, since it plays a pivotal role in the innate and adaptive immune response, and can possibly delay bone marrow recovery due to some reports of chemotherapeutic induced apoptosis of hematopoietic progenitors (Grossmann et al., 1999, Turco et al., 2004). The data here suggest that AG-014699 inhibits IR-induced NF-κB activation but not an inflammatory stimulus and thus may overcome these potential toxicities. It is important to ascertain whether the effects seen within this and the previous chapter translate to the gene expression level. Currently these data these data suggest that blockade of DNA-damage activated NF-κB by AG-014699 could represent a viable therapeutic strategy, since the data has demonstrated that the survival function of NF-κB can be directly inhibited without compromising other functions, such as the immune response. A possible strategy for determining the effects of AG-014699 on NF-κB-dependent gene expression, following either IR or TNF-α, would be to undertake a microarray study, and subsequent confirmation by qRT-PCR, to ensure that vital inflammatory responses, known to be regulated by TNF-α-induced NF-κB activation, are still intact following treatment with AG-014699. This study will be performed as part of this thesis (Chapter 5).

The model developed from this investigation present a novel mechanism for PARP-1 in the regulation of NF-κB and importantly these data highlight important new therapeutic avenues for the use of PARP inhibitors. However, determining the potential utility in other model systems is vital, but must also proceed with caution. Although the model described within this chapter and the one proposed by Stilmann *et al.*, (2009) are very complementary, they do have some differences, thus highlighting the importance of defining a clear mechanism within a certain cell type or tissue before these data can be used in clinical models. Radio-therapy is the most widely used treatment for cancer, and is the main-stay of therapy for glioblastoma, breast and lung cancers. Importantly aberrantly active NF-κB, known to mediate therapeutic resistance, has been reported in cell line models and primary material of each of these types of cancer. Hence, when investigating the utility of AG-014699 in combination with IR, in order to inhibit DNA-damage activated NF-κB activation, these model systems could well provide an interesting starting point and most definitely warrant further investigation. This study will be performed as part of this thesis (Chapter 6).

It would also be important to investigate the role of PARP-1 in the activation of NF-κB after other chemo-therapeutic agents, known to damage the DNA. For example, PARP inhibitors have previously been shown to potentiate the cytotoxic effects of temozolomide (Calabrese et al., 2004, Chalmers, 2009, Chalmers, 2010), and it would be interesting to determine whether these effects are mediated via the inhibition of NF-κB. Other agents, such as the topoisomerase II poison, doxorubicin are known to activate NF-κB (Campbell et al., 2006a), and there is a report from Munoz-Gamez *et al.*, (2005) showing that PARP inhibitors can sensitise breast cancer cells to this agent, although it is now known whether this phenomenon is mediated via NF-κB (Munoz-Gamez et al., 2005).

Other more classically known activators of NF-κB would also be of interest in order to further this study. These data presented here are a head-to-head comparison of TNF-α and IR, however it would provide further insight into the mechanism by which PARP-1 is acting if other agents, such as LPS were used. Some groups have used LPS (Le Page et al., 1998, Nakajima et al., 2004), but not in direct comparison with a DNA damaging agent.

Furthermore, the activation of the NF-κB in leukaemias, such as CLL, along with how chemotherapeutic agents are inducing an NF-κB response in patients with the disease, is currently being studied by this research group and others. CD40 ligand is used to induce proliferation of primary CLL cells in culture (Weston et al., 2010) and it is also known to activate NF-κB (Hayden and Ghosh, 2004). Recently, Weston *et al.*, (2010), have suggested the use of PARP inhibitors as a potential novel therapeutic strategy in patients with ATM mutant CLL after using CD40 ligand to induce cell proliferation in culture (Weston et al., 2010). They suggest a possible mechanism of synthetic lethality, similar to that observed with PARP inhibitors in BRCA mutant backgrounds (Bryant et al., 2005, Farmer et al., 2005). However, it would be important to elucidate whether the effects observed by PARP inhibitors in ATM mutant CLL were due to the effect on homologous recombination repair as postulated, or whether the inhibition of CD40 ligand-induced NF-κB activation by PARP-1 is also playing a role.

Chapter 5. Investigation into the effects of AG-014699 on NF-κB-dependent gene transcription following IR and TNF-α

5.1 Introduction

The stress-inducible transcription factor, NF-κB has the ability to both induce and repress gene expression (Perkins, 2007) and plays a crucial role in many biological processes. There are a number of genes regulated by NF-κB, including those controlling apoptosis, cell adhesion, inflammation, proliferation, immune responses, cellular stress and tissue remodelling (Bonizzi and Karin, 2004, Hayden and Ghosh, 2004, Pahl, 1999). NF-κB is sometimes referred to as 'the central mediator of the immune response' because it regulates the expression of inflammatory chemokines, cytokines, immune-receptors and cell adhesion molecules (Pahl, 1999).

Activated NF-κB is known to promote the expression of hundreds of target genes (Pahl, 1999). It should be noted however, that the transcriptional response is directly attributable to the activation stimuli. For example, a number of bacteria, bacterial proteins, viruses and inflammatory cytokines are known to activate NF-κB. These include the bacterial product LPS (Sen and Baltimore, 1986), the Epstein Barr Virus (EBV) (Hammarskjold and Simurda, 1992) and the inflammatory cytokine, TNF-α (Israel et al., 1989a, Osborn et al., 1989). Hence, the majority of proteins encoded by NF-κB target genes participate in the host immune response. These include numerous different cytokines and chemokines, such as TNF-α (Collart et al., 1990, Shakhov et al., 1990) and IL-6 (Libermann and Baltimore, 1990, Shimizu et al., 1990), as well as receptors required for immune recognition, including those which recognise major histocompatibility complex (MHC) proteins (Israel et al., 1989a, Israel et al., 1989b, Johnson and Pober, 1994). NF-κB also regulates that expression of genes which are associated with antigen presentation and proteins required for neutrophil adhesion and transmigration across blood vessel walls, for example, VCAM-1 (Iademarco et al., 1992). Taken together, these data suggest that that NF-κB activation is vital for the inflammatory and immune responses.

As well as being a hugely important mediator of the immune response, NF-κB is also known to respond to both physiological stress conditions, such as ischemia/reperfusion, liver regeneration and haemorrhagic shock, and also physical stresses, such as irradiation and oxidative stress. It is widely accepted that the genes activated following these stimuli differ from those activated following the inflammatory stimuli, discussed above. For example, it has been documented that NF-κB activation following IR induces the expression of the anti-apoptotic genes, Bfl1/A1 (Grumont et al., 1999, Zong

et al., 1999), Bcl-xL (Lee et al., 1999a) and the inhibitor of apoptosis proteins (IAPs) (Stehlik et al., 1998, You et al., 1999), resulting in cell survival. Jeremias *et al.*, (1998), were the first to report that NF-κB inhibition could restore drug-induced apoptosis sensitivity to resistant leukaemic cell lines and primary samples, suggesting that the inhibition of NF-κB activation induced by DNA-damaging drugs could provide a potential therapeutic strategy in leukaemia and cancers (Jeremias et al., 1998). Conversely, TNF-α-induced NF-κB activation is known to up-regulate the expression of the Fas receptor (Chan et al., 1999) and its ligand (Matsui et al., 1998), which induce apoptosis. Thus it is important to establish which genes are affected by each individual stimulus, and most importantly their role in the cell.

It is therefore also very important to assess the effect of NF-κB inhibitors on the transcriptional response, after different stimuli. Complete or global inhibition of NF-κB, for example with an IKK inhibitor, may have adverse effects, as this may result in the inhibition of genes known to have vital roles in the inflammatory response. There have been two reports suggesting that long-term NF-κB inhibition may have a negative impact on the haematopoietic system, in particular, due the pivotal role NF-κB plays in the innate and adaptive immune response, the first indicating that this increases the likelihood of immunodeficiency, and the second reporting that this can delay bone marrow recovery due to chemotherapeutic induced apoptosis of hematopoietic progenitors (Grossmann et al., 1999, Turco et al., 2004). However, NF-κB is an attractive therapeutic target, particularly in cancer as in this context, and specifically after activation by DNA-damaging chemo- or radio-therapy, it is known to up-regulate genes associated with the protection against apoptosis, cell proliferation, angiogenesis and metastasis (Ghosh and Karin, 2002), thus contributing to disease progression and severity.

Hence, it is vitally important to develop inhibitors of NF-κB which target these aspects of NF-κB-dependent gene transcription, without compromising its essential role in the inflammatory response. Data from chapters 3 and 4 in this thesis suggest that AG-014699 inhibits IR-induced NF-κB activation but not an NF-κB activation following an inflammatory stimulus. Therefore targeted inhibition of DNA-damage-activated NF-κB using a PARP inhibitor may overcome the potential toxicities observed with other NF-κB inhibitors, however it is important to assess the effect of AG-014699 on NF-κB-dependent gene transcription following either stimuli in order to confirm the findings.

5.2 Aims

The data within chapters 3 and 4 here currently suggest that blockade of DNA-damage activated NF-κB by AG-014699 could represent a viable therapeutic strategy, since the data has demonstrated that the survival function of NF-κB can be directly inhibited without compromising other NF-κB activation stimulated by the inflammatory cytokine, TNF-α. These data require confirmation, and therefore the first aim of this chapter is to utilise gene expression arrays to assess to change in gene expression in cells treated with IR *versus* cells treated with TNF-α. NF-κB-dependent genes regulated by TNF-α are widely known and include a range of cytokines, chemokines and cell adhesion molecules, all known to have a vital role in the inflammatory response, whereas NF-κB-dependent genes regulated by IR are not so well documented. Hence, this head-head-comparison will potentially identify novel IR-induced-NF-κB-dependent genes. Any genes identified in the array studies will subsequently be confirmed using qRT-PCR.

The second aim of this chapter is to assess the effects of the PARP inhibitor, AG-014699 in combination with both of each of stimuli, IR or TNF-α. It would be expected that the genes regulated by TNF-α were associated with the inflammatory and immune responses, and hence hypothesised that genes would not be affected by co-incubation with AG-014699. Furthermore, it would be hypothesised that NF-κB-dependent genes activated by IR, would be inhibited by co-incubation with AG-014699 thus supporting the data from chapter 4 which showed that NF-κB activated following DNA damage required PARP-1 protein and enzymatic activity, whereas TNF-α induced NF-κB activation required PARP-1 protein alone. Any genes of interest identified during this portion of the study would also be confirmed using qRT-PCR, along with siRNA targeting p65 or PARP-1 and the pan-IKK inhibitor, BAY-117082 in order to confirm any findings.

5.3 Materials and Methods

5.3.1 Gene expression microarrays

5.3.1.1 The general principle of gene expression microarrays

Gene expression microarrays allow the simultaneous genome wide analysis of transcript expression. Sample RNA is labelled with the water-soluble B-complex vitamin, biotin and then this labelled copy RNA (cRNA) is allowed to hybridise to the microarray. cRNA hybridises to specific probes for each gene, and any excess unbound cRNA is

washed from the chip. The bound biotinylated cRNA is stained with fluorescent tagged streptavidin complexes to visualise the extent of hybridisation to individual sequence specific probes on the array. Photometric scanning of the arrays is then used to capture the relative fluorescence intensities and the relative amount of each transcript is estimated from the intensity values.

5.3.1.2 Illumina MouseWG-6 v2.0 Expression BeadChip array

Illumina MouseWG-6 v2.0 Expression BeadChip was used for this study. The Illumina MouseWG-6 is a murine genome wide array that contains probes for the analysis of more than 45,200 different transcripts. Illumina MouseWG-6 content is derived from the National Center for Biotechnology Information Reference Sequence (NCBI RefSeq) database, supplemented with probes derived from the Mouse Exonic Evidence Based Oligonucliotide set and exemplar protein-coding sequences described in the RIKEN FANTOM2 database. Furthermore, six samples can be analysed simultaneously on a single BeadChip, reducing the inter-BeadChip variation.

5.3.1.3 Probe sets

In standard microarrays, probes are synthesised and then attached via surface engineering to a solid surface by a covalent bond to a chemical matrix. The solid surface tends to be glass or a silicon chip, whereas, in this case, the Illumina array platform uses microscopic beads, instead of the large solid support. Candidate probe sequences for use in the Illumina MouseWG-6 undergo extensive bioinformatic screening prior to selection. 50-mer gene-specific probe sequences are coupled with "address" sequences which are immobilised on a bead along with hundreds of thousands of probes of the same sequence. The major advantage of having multiple probes for each transcript is that this therefore allows multiple independent measurements for each transcript.

5.3.1.4 Advantages and disadvantages of gene expression microarrays

There a number of techniques that can be used to examine global gene expression. These include spotted DNA microarrays, oligonucleotide arrays, and serial analysis of gene expression (SAGE). The advent of next-generation sequencing has made sequence based expression analysis an increasingly popular alternative to microarrays. The major advantage of using platforms such as Illumina or Affymetrix is that several probes are used for one transcript, giving more reliable data. However, the ability to analyse six

samples simultaneously on the Illumina MouseWG-6, eliminates the requirement for technical replicates with this platform, when compared with the Affymetrix platform.

However, one of the disadvantages of examining global gene expression patterns, in general, not just with the platform described here, is the reliability of the results at the lower end of the confidence scale (i.e. when the probe signal is weak, or perhaps it has reached saturation). There can be discrepancies between various gene lists derived from different studies, and this in part may be attributed to the differential sensitivities between the different platforms or different methods used to examine whole genome expression. However, the major drawback is that changes in transcript level do not always reflect what is occurring at the protein level: for example proteins may be subject to post-translational modifications, or targeted for degradation.

5.3.2 Planning and designing gene expression microarray experiments

Previous data in this thesis has shown that both PARP-1 activity and protein are required for the activation of NF-κB following IR, but that PARP-1 protein alone is required following TNF-α. Hence, it was hypothesised that PARP-1 inhibition could overcome the toxicities observed with more global inhibition of NF-κB, by transiently inhibiting DNA damage activated NF-κB, and not affecting its vital role in the inflammatory response. Therefore, the major aim of this study was to determine the effects of the PARP inhibitor, AG-014699, on IR- or TNF-α-induced gene expression in the $p65^{+/+}$ MEFs.

It was decided to determine the changes in gene expression at two timepoints following treatment with either IR or TNF-α. To determine early changes in gene expression, as the DNA damage response in particular, is known to be fairly rapid, samples were harvested 2 h following treatment with either agent. A number of reports in the literature suggested that the TNF-α-induced expression of some NF-κB-dependent genes, including VCAM1 and IL-6, was also maximal 2 h following treatment (Shu et al., 1993, Ulich et al., 1991). Cells were also harvested 8 h following treatment as the luciferase assays (section 4.3.4), showed that NF-κB-dependent gene transcription was maximal at this time-point following either agent. The experimental plan is shown in Figure 5.1.

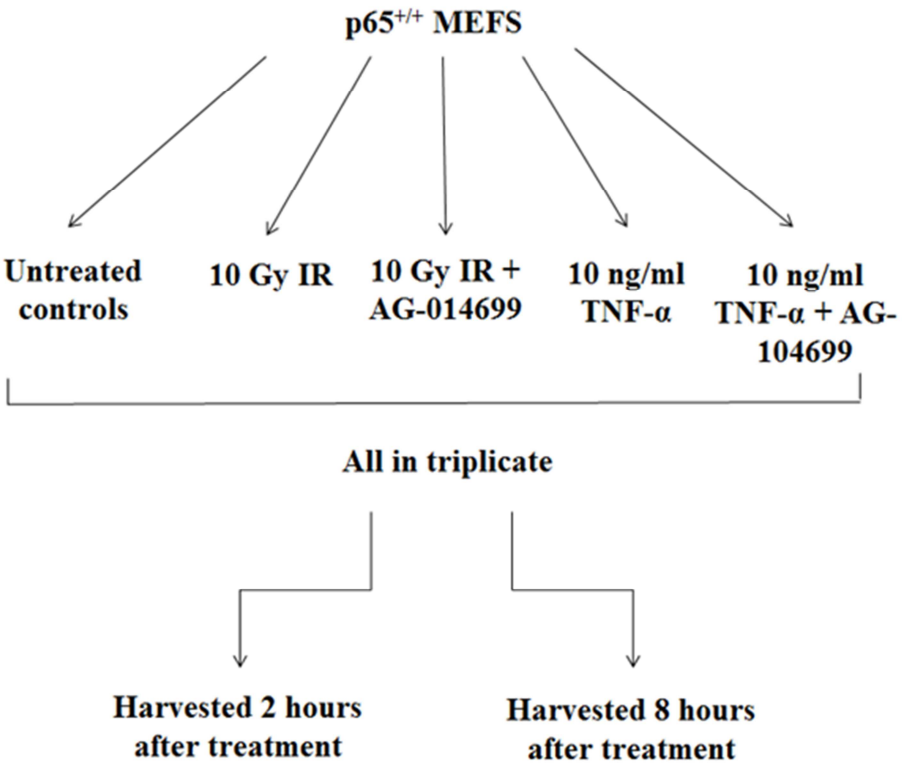

Figure 5.1: Microarray experimental plan The changes in gene expression in $p65^{+/+}$ MEFs will be assessed at two timepoints (2 hours or 8 hours) after treatment with either IR or TNF-α, alone or in combination with AG-014699

5.3.2.1 Replicates

Replicates are defined as either technical or biological replicates. Technical replicates for gene expression microarray studies determine the variation in RNA preparation, handling, hybridisation and inter -assay/-chip variations. Importantly, the ability to analyse six samples simultaneously on the Illumina MouseWG-6, eliminates the requirement for technical replicates with this platform. However, an additional check of RNA quality was undertaken prior to amplification at the Cambridge Genomics Service (Section 5.3.3.2).

Biological replicates include testing independent samples and repeating the treatment with AG-014699 (or DMSO control), IR or TNF-α. The Illumina platform was chosen, as it is the most well characterised platform for the study of the mouse genome, it has been thoroughly tested, standardised and validated and therefore, in this case biological variation outweighs any variation caused by technique. All IR or TNF-α (alone or in combination with AG-014699, see Figure 5.1) were performed in triplicate to obtain

biological analysis. The use of triplicates of each sample would also allow for a more robust statistical analysis and interpretation of data.

5.3.3 Protocol for Illumina MouseWG-6 v2.0 Expression BeadChip array

This section very briefly describes the standard protocol used at the Cambridge Genomics Service for Illumina MouseWG-6 v2.0 Expression BeadChip arrays and is based on information detailed at http://www.cgs.path.cam.ac.uk/services/genexpression/wg-gex.html

5.3.3.1 RNA extraction from samples

Cells were seeded and allowed to adhere for 24 h before to a 1 h pre-treatment with AG-014699 (or DMSO control) prior to treatment with either 10 Gy IR or 10 ng/µl TNF-α. Cells were then harvested for RNA extraction either 2 h or 8 h following treatment. RNA extraction was carried out using the RNeasy midi kit (Qiagen) according to manufacturers' instructions, as described in section 2.10.1.2. It is important to note here that the DNase step was omitted from the RNeasy procedure, as this is not recommended by Illumina. Before RNA samples were sent to for labelling and microarray experiments at the Cambridge Genomics Service (http://www.cgs.path.cam.ac.uk/), the RNA was quantified, and the quality checked using the Nanodrop spectrophotometer (using methods described previously section 2.3.3). In total 30 samples were sent to the Cambridge Genomic Service for microarray analysis.

5.3.3.2 RNA integrity analysis

It is vital to assess the RNA integrity in order to obtain meaningful gene expression array data. Therefore the quality of the 30 RNA samples to be used for the gene expression arrays were examined on a 2100 Bioanalyser (Agilent) by the Cambridge Genomics Service. This technique uses electrophoretic separation on micro-fabricated chips, in which RNA samples can be separated and then detected using laser induced fluorescence detection. The software then generates an electropherogram which allows visual assessment of the RNA quality, and calculates an RNA Integrity Number (RIN) based on a software algorithm. An example of four electropherograms, with varying RIN scores, are shown in Figure 5.2. A sample with a RIN score of 10 (Figure 5.2A) is regarded as containing high quality intact RNA which has not undergone any degradation. RNA degradation is a gradual process is observed in Figure 5.2B, 5.2C and

5.2D. As this proceeds an increase in the base-line signal between the peaks at 18S and 26S, and the lower marker is observed. A decrease in the ratio between the 18S and the 26S bands is also visible. RIN scores for each of the 30 samples sent for array analysis were generated by the Cambridge Genomic Service and are detailed in Table 5.1. The RIN scores from all the samples indicated that all of the samples contained high quality RNA, and that could be subsequently used for array analysis.

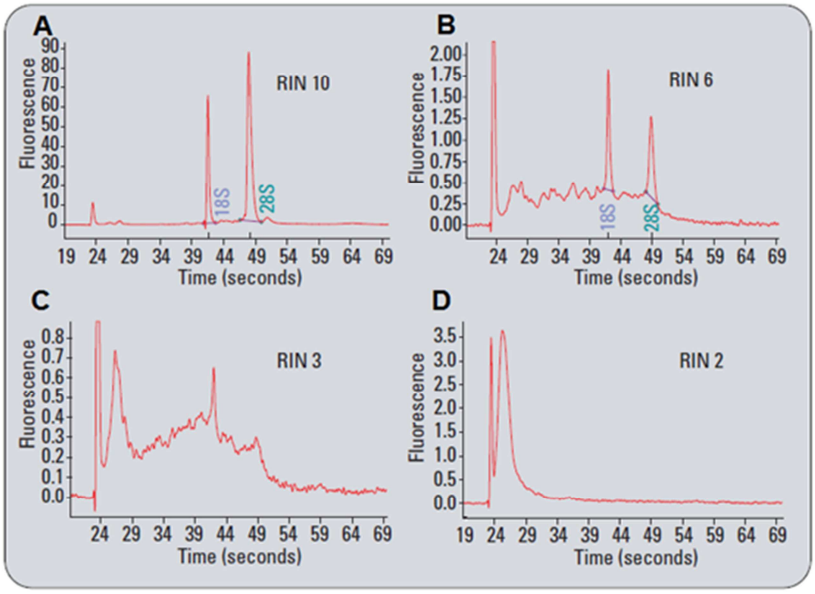

Figure 5.2: Example RNA Integrity electropherograms One showing a RIN score of 10 (**A**) and the others showing RNA which has degraded (**B**, **C** and **D**), and hence have lower RIN scores, depending on the extent of the degradation. From:http://www.agilent.com/about/newsroom/lsca/background/rna_integrity.pdf

Sample ID	Sample name	RIN
1	Control 2 h 1	9.90
2	Control 2 h 2	9.70
3	Control 2 h 3	10.00
4	IR 2 h 1	9.90
5	IR 2 h 2	10.00
6	IR 2 h 3	10.00
7	IR + AG 2 h 1	10.00
8	IR + AG 2 h 2	10.00
9	IR + AG 2 h 3	9.80
10	TNF-α 2 h 1	10.00
11	TNF-α 2 h 2	10.00
12	TNF-α 2 h 3	10.00
13	TNF-α + AG 2 h 1	10.00
14	TNF-α + AG 2 h 2	10.00
15	TNF-α + AG 2 h 3	10.00

16	Control 8 h 1	10.00
17	Control 8 h 2	10.00
18	Control 8 h 3	10.00
19	IR 8 h 1	8.10
20	IR 8 h 2	10.00
21	IR 8 h 3	8.40
22	IR + AG 8 h 1	10.00
23	IR + AG 8 h 2	10.00
24	IR + AG 8 h 3	8.30
25	TNF-α 8 h 1	10.00
26	TNF-α 8 h 2	10.00
27	TNF-α 8 h 3	10.00
28	TNF-α + AG 8 h 1	10.00
29	TNF-α + AG 8 h 2	10.00
30	TNF-α + AG 8 h 3	10.00

Table 5.1: RIN scores for each of the samples provided for microarray analysis
30 RNA samples to be used for the gene expression arrays were examined on a 2100 Bioanalyser (Agilent) by the Cambridge Genomics Service, and all scores >8, indicating RNA of high integrity

5.3.3.3 Amplification of RNA

Once the integrity of the RNA had been verified, the samples were amplified using the Illumina TotalPrep96 RNA Amplification Kit (Ambion). Described in Figure 5.3. The procedure begins with reverse transcription with an oligo(dT) primer bearing a T7 promoter. The cDNA then undergoes second strand synthesis and clean up to become a template for in vitro transcription with T7 RNA Polymerase. Hunderds to thousands of biotinylated, antisense RNA copies of each mRNA are generated in each sample, and this is generally referred to as cRNA. The labelled cRNA produced is then used for hybridisation with Illumina MouseWG-6 BeadChip arrays.

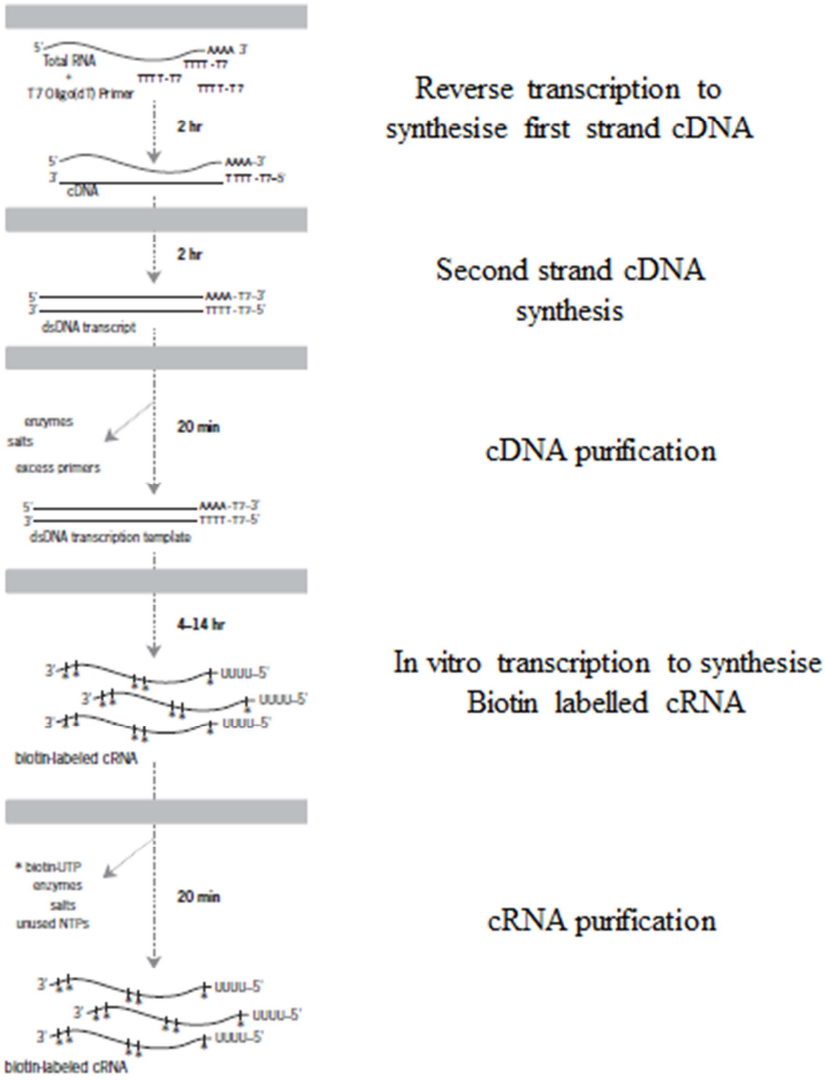

Figure 5.3: Workflow of RNA processing steps using the Illumina TotalPrep96 RNA Amplification Kit (Ambion)
From: http://www.ambion.com/techlib/prot/fm_4393543.pdf

5.3.3.4 Hybridisation and scanning

Biotin labelled cRNA was hybridised to the Illumina MouseWG-6 v2.0 Expression BeadChip arrays using the Illumina Direct Hybridization Assay (Figure 5.4). Each bead has a 50-base gene specific probe immobilised onto it *via* a short 'address' sequence. This probe is then used to directly hybridise the labelled cRNA. The arrays were then washed, blocked and stained with streptavidin-Cy3 and run on the iScan and Autoloader 2 system (Illumina), which measured fluorescence emission by Cy3, which allowed quantitative downstream analysis.

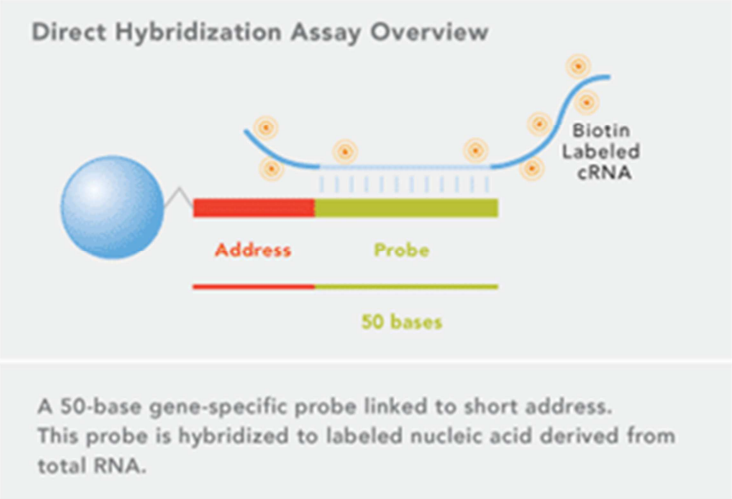

Figure 5.4: Direct hybridization Assay overview
From: http://www.illumina.com/technology/direct_hybridization_assay.ilmn

5.3.4 Analysis of array data received from the Cambridge Genomics Service

This section very briefly describes the bioinformatics processes used by Dr Dan Swan at the Newcastle University Bioinformatics Service in order to interpret and analyse the array data received from the Cambridge Genomics Service. Two software packages were utilised and these were Genespring GX 11, to generate gene lists, and Ingenuity Pathway Analysis, to indenify processes and pathways affected by either IR or TNF-α, in the presence or absence of AG-014699.

5.3.4.1 Genespring GX 11

Data exported from Illumina Bead Studio in a GeneSpring compatible format was loaded into GeneSpring GX 11 for analysis and analysed using the Illumina.SingleColor.MouseWG-6_V2_0_R2_11278593_A technology annotation package. Expression values below 1 were thresholded to 1.0 on import and transformed to log base 2 prior to analysis. Quantile normalisation was applied across the samples with a baseline transformation to the median of all samples. To support flag based filtering, detection p-values <0.6 were marked as 'absent' and p-values >0.8 marked as 'present'. Detection p-values >0.6 but <0.8 were marked as 'marginal'.

Of 45281 entities, 22125 remained after filtering on flags so that 80 of the samples across the experiment had 'present' or 'marginal' flags associated with each probe.

Differential gene expression analysis was performed using ANOVA in GeneSpring (Benjamini-Hochberg FDR multiple testing correction applied) where probes had a corrected p-value of <0.05 and a fold change of >1.2 to be considered significantly differentially expressed.

5.3.4.2 Ingenuity Pathway Analysis (IPA)

Pathway analysis was carried out with Ingenuity Pathway Analysis 8 (Ingenuity Systems http://www.ingenuity.com) on probesets differentially expressed on selenium treatment. Canonical pathways analysis and biological process analysis identified the pathways and processes from the Ingenuity library that were most significant to the data set.

The significance of the association between the data set and the canonical pathway/process was measured in 2 ways:

1) A ratio of the number of molecules from the data set that map to the pathway/process divided by the total number of molecules that map to the canonical pathway/process is displayed.

2) Fisher's exact test was used to calculate a p-value determining the probability that the association between the genes in the dataset and the canonical pathway/process is explained by chance alone.

5.3.5 Microarray validation experiments using qRT-PCR

The genes selected for validation by qRT-PCR are listed in Table 5.2, alongside the details of the primers and probes from Applied Biosystems. The method for qRT-PCR is described in detail in section 2.10. Seven genes were validated as those that were regulated following IR treatment; *AURKA*, *AURKB, BIRC6, CDC20, PLK1*, *PLK2* and *TOP2A*. Two inflammatory response genes were validated as those regulated following TNF-α; *CCL5* and *CXCL10*. Three genes were validated as those regulated following both IR and TNF-α; *IRF1*, *JUNB* and *TNIP1*. Levels of the housekeeping gene, *ACTN* were also assessed by qRT-PCR.

Gene name	Assay reference	Probes
AURKA	Mm01248179_g1	FAM
AURKAB	Mm01718146_g1	FAM
BIRC6	Mm00464380_m1	FAM
CCL5	Mm01302427_m1	FAM
CDC20	Mm00650983_g1	FAM
CXCL10	Mm00445235_m1	FAM

FAS	Mm00433237_m1	FAM
IRF-1	Mm01288580_m1	FAM
JUNB	Mm01251660 _s1	FAM
PLK1	Mm00440924_g1	FAM
PLK2	Mm01306047_g1	FAM
TNIP1	Mm00457957_m1	FAM
TOP2A	Mm01296339_g1	FAM
ACTN	Mm02619580_g1	FAM

Table 5.2: Details of primers and probes from Applied Biosystems (FAM=fluorescein)

5.4 Results

5.4.1 Differentially expressed genes 2 hours following treatment with IR

One of the main aims of this chapter was to assess the different types, and functions of the genes up- or down-regulated following treatment with either IR or TNF-α at an early timepoint after either agent. It is well documented that TNF-α induces NF-κB activation, and in particular a transcriptional response associated with the induction of inflammatory- or immune-responses (Pahl, 1999). However, although there have been reports in the literature suggesting that DNA damage, in particular IR, up-regulates NF-κB-dependent genes associated with the protection against apoptosis (Grossmann et al., 1999, Lee et al., 1999a, Stehlik et al., 1998, You et al., 1999, Zong et al., 1999), information about other genes are less common. Hence, it was decided to undertake a head-to-head comparison of the genes regulated by IR or TNF-α in the $p65^{+/+}$ MEFs, using an array based approach, within this chapter.

Once the array data was received from the Cambridge Genomics Service, Genespring GX 11 was utilised by Dr Dan Swan in order to generate to lists of genes differentially expressed 2 hours after treatment with 10 Gy IR, compared with controls. Table 5.3 details a list of genes differentially expressed following treatment with IR as well as the accession/identification number and the fold change.

Gene	Symbol	ID	Fold change
Aminoadipate-semiadlehyde dehydrogenase	*AADDH*	NM_173765.2	1.218
ADP-ribosylation factor 2	*Arf2*	NM_007477.4	1.258
ADP-ribosylation factor like-6 interacting protein	*ARL6IP1*	NM_019419.1	1.355
Aurora kinase A	*AURKA*	NM_011497.3	2.283
Baculoviral IAP repeat containing 6	*BIRC6*	AK038699	1.285

cDNA sequence BC003965	*BRPF1*	NM_030178.1	-1.203
Chromosome 10 open reading frame 34	*C13orf34*	NM_175265.4	1.559
Chromosome 1 open reading frame 51	*C1orf51*	NM_001033302.1	-1.313
Chromosome 6 open reading frame 211	*C6orf211*	NM_24261.2	1.214
Chromosome 9 open reading frame 100	*C9orf100*	NM_131404.3	1.924
Chromosome 9 open reading frame 140	*C9orf140*	NM_130053.2	1.975
Coiled-coil domain containing 99	*CCDC99*	NM_027411.1	1.424
Cyclin B1	*Ccnb1*	NM_172301.3	1.497
Cyclin F	*CCNF*	NM_007634.2	1.625
Cell division cycle 20 homolog	*CDC20*	NM_023223.1	1.468
Cell division cycle 6 homolog	*CDC6*	NM_011799.2	-1.692
Cell division cycle associated 2	*CDCAA2*	NM_175384.2	1.702
Cyclin-dependent kinase inhibitor 1A (p21)	*CDKN1A*	NM_007669.2	1.501
Cyclin-dependent kinase inhibitor 2C (p18)	*CDKN2C*	AK087461	1.311
Cyclin-dependent kinase inhibitor 2D (p19)	*CDKN2D*	NM_009878.3	1.351
Chromatin licencing and DNA replication factor	*CDT1*	NM_026014.3	1.454
Centromere protein L	*CENPL*	NM_027429.2	2.179
Cation transport regulator homolog 1	*CHAC1*	NM_026929.3	1.374
Cysteine rich hydrophobic domain 2	*CHIC2*	AK015681	-1.275
Choline kinase alpha	*CHKA*	AK014174	1.517
CAP-GLY domain containing linker protein family 4	*CLIP4*	NM_030179.2	1.239
Component of oligomeric golgi complex 8	*COG8*	NM_139229.2	1.239
Cleavage stimulating factor	*CSTF1*	NM_139229.2	1.237
DBF4 homolog	*DBF4*	NM_013726.2	1.284
DEAD box polypeptide	*DDX11/DDX12*	NM_128714.3	1.224
DEP domain containing 1B	*DEPDC1B*	NM_178683.4	1.459
Enoyl CoA hydratase short chain 1	*ECHS1*	AK086762	1.274
ERI1 exoribonuclease family member 2	*ER12*	NM-027698.4	1.311
v-ets erythroblastosis virus E26 oncogene	*ETS1*	NM_011809.2	-1.271
Family with sequence similarity 110, member A	*FAM110A*	NM_028666.2	-1.321
Family with sequence similarity 13, member C	*FAM13C*	NM_024244.2	-1.279
Family with sequence similarity 83, member D	*FAM83D*	NM_027975.1	2.144

FERM domain containing 4A	*FRMD4A*	AK089210	1.260
G2/M-phase specific E3 ligase	*G2E3*	NM_00105099.1	1.466
Growth arrest and DNA damage inducible beta	*GADD45B*	NM_008655.1	1.586
Growth arrest specific 2 like 3	*GAS2L3*	NM_001079876.1	1.827
GATS-protein like 2	*GatsL2*	NM_030719.3	-1.238
Glutathione peroxidase 8	*GPX8*	NM_027127.1	1.208
GTP binding protein 2	*GTPBP2*	NM_019581.2	1.324
G-2 and S phase expressed 1	*GTSE1*	NM_013882.1	1.737
Homo-cysteine inducible endoplasmic reticulum 1	*HERPUD1*	NM_022331.1	-1.454
Histone cluster 1, H2ae	*HIST1H2AB*	NM_178182.1	1.716
Histone cluster 1, H2ac	*HIST1H2AC*	NM_175659.1	1.667
Histone cluster 2, H2ab	*HIST2H2AB*	NM_178213.3	1.613
Heterogeneous nuclear ribonuclear protein D-like	*HNRPDL*	NM_0166690.2	1.380
Immediate early response 3	*IER3*	NM_133662.2	1.380
Inner centromere antigens 135/155 kDa	*INCENP*	NM_016692.1	1.268
Inversin	*INVS*	AK040307	1.298
Interferon regulatory factor 1	*IRF1*	NM_008390.1	-1.584
Kinesin family member 11	*KIF11*	NM_001615.1	1.401
Kinesin family member 18A	*KIF18A*	NM_139303.1	1.900
Kinesin family member 18B	*KIF18B*	NM_197959.1	1.834
JunB proto-oncogene	*JUNB*	NM_008416.1	1.643
Kinesin family member 20B	*KIF20B*	NM_183046.1	1.712
Kinesin family member 22	*KIF22*	NM_145588.1	1.452
Kinesin family member 2C	*KIF2C*	NM_134471.3	1.572
Kinesin family member C1	*KIFC1*	NM_001479207.1	1.796
Kruppel like factor 16	*KLF16*	NM_078477.1	-1.356
Kruppel like factor 4	*KLF4*	NM_001081150.1	-1.409
LON peptidase N-terminal domain and ring finger	*LONRF1*	NM_001081150.1	-1.207
LIM domain contained preferred translocation peptide	*LPP*	AK051937	1.367
Minixsome maintanience complex component 10	*MCM10*	NM_027290.1	1.395
Meis homobox 1	*MEIS1*	NM_010789.2	-1.257
MIS18 binding protein 1	*MIS18BP1*	NM_172578.2	1.570
Nuclear autoantigenic sperm protein	*NASP*	NM_016777.3	-1.363
Nuclear factor 1/X	*NFIX*	NM_001081981.1	1.216
OMA1 homolog	*OMA1*	NM_025909.1	1.277
Pre-B cell leukemia homolog 1	*PBX1*	AK037006	1.442
PHD finger protein 15	*PHF15*	NM_199299.3	1.211
PIF1 5’-3’DNA helicase homolog	*PIF1*	NM_172453.1	3.122
Polo-like kinase 1	*PLK1*	NM_011121.3	1.651
Protein regulator of cytokinesis	*PRC1*	NM_145150.1	1.345
Proline rich 11	*PRR11*	NM_175563.3	1.210
Pseudouridylate synthase 7 homolog	*PUS7L*	NM_172437.2	1.210

Receptor accessory protein 4	*REEP4*	NM_180588.1	1.276
Ribosomal protein S24	*Rps24*	AK052480	1.397
Sestrin 2	*SESN2*	NM_144907.1	-1.347
SH3 and PX domain 2B	*SH3PXD2B*	AK043324	1.244
Shugoshin like 1	*SG0L1*	NM_028232.1	1.433
Shugoshin like 2	*SGOL2*	NM_199007.1	1.445
Seven in absentia homolog 1	*SIAH1*	NM_009172.1	-1.203
Spindle and kinetochore associated complex subtype 2	*SKA2*	NM_0253771	1.243
Solute carrier family 30	*SLC30A1*	NM_009579.3	1.390
Slit homlog 2	*SLIT2*	AK053913	1.575
Structural maintenance of chromosomes 4	*SMC4*	AK10848	1.429
Sperm associated antigen 5	*SPAG5*	NM_017407.1	1.371
SPC25, NDC80 kinetochore complex component	*SPC25*	NM_025565.1	1.288
splA/ryanodine receptor domain and SOCs box	*SPSB1*	NM_029035.2	-1.457
Telomeric repeat binding factor 1	*TERF1*	AK036615	1.346
Transducin-like enhancer of split 4	*TLE4*	NM_011600.2	-1.316
Tousled like kinase 1	*TLK1*	NM_172664.2	-1.205
Topoisomerase (DNA) II alpha 170 kDa	*TOP2A*	AK028218	1.659
TNFAIP3 interacting protein 1	*TNIP1*	NM_021327.1	1.846
Trafficking protein particle complex 2	*TRAPPC2*	AK034967	1.213
Tribbles homolog 3	*TRIB3*	NM_175093.2	-1.297
Tastin	*TROAP*	XM_912265.2	1.682
Trichorhinophalangeal syndrome 1	*TRPS1*	AK036590	1.461
Vascular endothelial growth factor	*VEGFA*	NM_009505	1.413
Exportin 4	*XPO4*	NM_20506.1	-1.201
Zinc finger, SWIM-type containing 4	*ZSWIM 4*	NM_172503.3	-1.259

Table 5.3: Differentially expressed genes 2 hours following treatment with IR in $p65^{+/+}$ MEFs, compared with untreated controls

This list of genes of was then entered into the pathway analysis software, IPA, in order to determine the key pathways and processes affected by treatment with IR in the $p65^{+/+}$ MEFs. Interestingly, the most frequent functional annotations given by the software were associated with cellular assembly and organisation. A network diagram, produced by IPA, is shown in Figure 5.5. This shows the genes up- (in red) or down- (in green) regulated by IR that associated with that particular network. It also shows the known

interactions between any two molecules with a solid line, and any putative interactions with a broken line. These data are derived from literature searches and algorithms built into the software package.

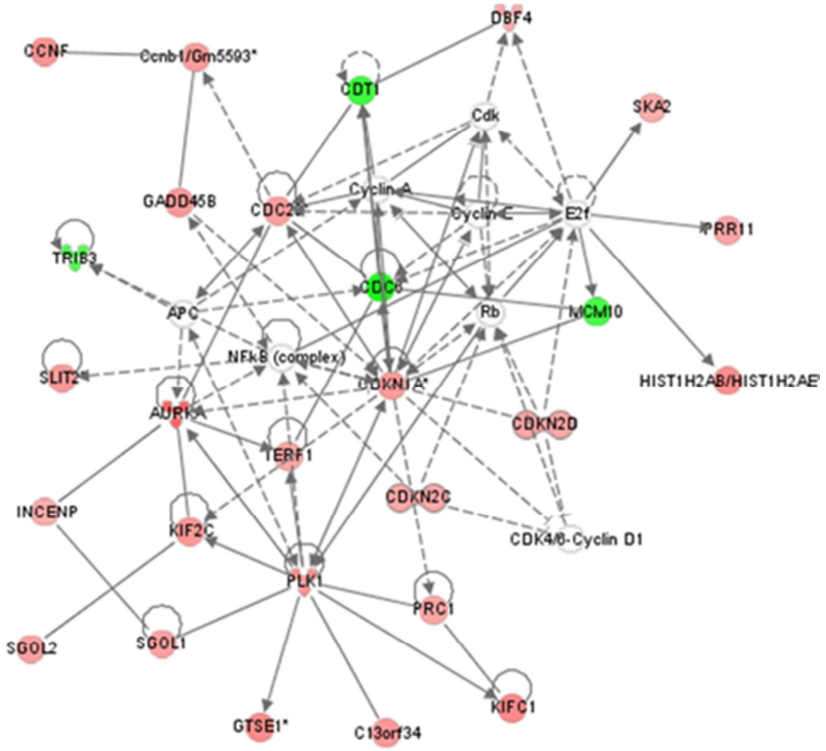

Figure 5.5: Genes associated with the cell cycle, cellular movement, cellular assembly and organisation Network generated by IPA with genes that were up-regulated (shown here in red) or down-regulated (shown here in green) in $p65^{+/+}$ MEFs 2 hours after treatment with 10 Gy IR

IPA assigns functional annotations to sets of molecules known to be associated within a certain cellular pathway or process, and lists the genes within these annotations. For example one of the genes up-regulated by IR, aurora kinase A (which had one of the greatest fold changes, increasing by 2.2-fold) was associated with the alignment of chromosomes, as well as being involved in the amplification of the centrosome and the mitotic spindle. A range of kinesin family (KIF) proteins were also up-regulated and are known to be associated with the alignment and congression of chromosomes, along with being involved in the formation of the mitotic spindle and the organisation of spindle fibres. Polo-like kinase 1 (*PLK-1*) was up-regulated 1.6-fold and is known to involved in the formation of the mitotic spindle as well having other roles with the centrosome. Both PLK1 and Aurora kinase A (*AURKA*) have been shown to be over-expressed in

different forms of cancer (Goepfert et al., 2002, Musacchio and Salmon, 2007, Sakakura et al., 2001, Tanaka et al., 1999b), and there are known targeted inhibitors for these proteins in development as potential cancer therapeutics (Dar et al., 2010, Degenhardt and Lampkin, 2010). This will be discussed in detail later in this chapter. A summary of the functional annotations from the IPA software, the associated molecules and p-values are shown in Table 5.4. The significance of the association between the molecules within the data set and the pathway/process was measured, by the software algorithms, using a Fisher's exact test to calculate a p-value determining the probability that the association between the genes in the dataset and the pathway/process is not explained by chance alone.

Functional annotations	P value	Molecules
Alignment of chromosomes	2.43E-11	*AURKA, KIF18A, KIF22, KIF2C, KIF1C, SMC4, PLK1*
Chromosomal congression of chromosomes	8.71E-10	*SGOL2, KIF18A, KIF2C, KIFC1*
Segregation of chromosomes	1.67E-08	*DDX11/DDX12, INCENP, KIF2C, SGOL1, SMC4, SKA2, SPC25, TOP2A*
Quantity of mitotic spindle	2.51E-07	*AURKA, KIF11, PLK1, SPC25*
Organisation of spindle fibres	7.47E-07	*C13orf34, KIF11, KIFC1, SPC25, SIAH1(-)*
Amplification of centrosome	9.96E-06	*AURKA, KIF1C, PLK1, KLF4(-)*
Organisation of mitotic spindle	1.66E-05	*C13orf34, KIF11, SPC25, SIAH1(-)*
Replication of DNA	6.37E-05	*CDKN1A, DBF4, PUS7L, TERF1, CDC6(-), CDT1(-), MCM10(-), NASP(-)*
Formation of mitotic spindle	1.65E-04	*KIF11, KIF2C, KIFC1, PLK1*
Elongation of mitotic spindle	2.14E-04	*PRC1, SPC25*
Quality of centrosome	3.43E-04	*AURKA, CDKN1A, PLK1*

Table 5.4: Functional annotations associated with cellular assembly and organisation assigned by IPA Summary of the functional annotations from the IPA software, the associated molecules and p-values (-) denotes a gene which was down-regulated 2 hours after treatment with 10 Gv IR

Table 5.4 indicates that a large proportion of the gene expression altered following IR treatment in the $p65^{+/+}$ MEFs is associated with cellular organisation and assembly, and this is something which warrants further investigation. There is a very little literature detailing the regulation of gene transcription associated with cellular assembly by NF-κB, however one group have shown the polo like kinase 3 (*PLK3*) is an NF-κB regulated gene (Li et al., 2005). The data here suggests that *PLK1* could therefore perhaps be an NF-κB target gene. It is up-regulated 1.6-fold following IR, and other

associated proteins are also up-regulated following treatment with IR. PLK1 is involved in the metaphase to anaphase transition, and also mitotic exit (shown in Figure 5.6), along with *CDC20, Cyclin B* and *PRC1*, all of which are up-regulated after treatment with 10 Gy IR in the $p65^{+/+}$ cells. Therefore, this warrants further investigation, by qRT-PCR, to determine whether any of these genes are novel NF-κB regulated genes following DNA damage. It will also be essential to assess whether co-incubation with the PARP inhibitor, AG-014699, in combination with IR, had an effect on any of these, or other genes known to be associated with cellular assembly that were up-regulated with treatment with IR alone. Based on the observations from chapter 3 and 4, it would be reasonable to hypothesise that if a gene was regulated by NF-κB, treatment with PARP inhibitor prior to IR would inhibit the expression of that particular gene, compared with IR alone.

Another group have shown that *CDKN1A*/p21 (a cyclin dependent kinase) is an NF-κB target gene (Hinata et al., 2003). *CDKN1A*/p21 is up-regulated 1.5-fold in the array data presented here, and is also known to have a role in the both the G1/S and G2/M cell cycle checkpoints (Niculescu et al., 1998). *CDKN1A*/p21 is the primary downstream target in p53-mediated damage response. DNA damage, such as IR is known to activate kinases ATM and ATR, which phosphorylate and activate the Chk effector kinases. These kinases go on to stabilise p53 through a series of phosphorylation events resulting in the increased transcription of its target p21 (Bartek and Lukas, 2001) hence it is perhaps not surprising that the transcription of *CDKN1A*/p21 is induced following treatment with IR, but further investigation into whether this is, mediated wholly, or in part by NF-κB, should be undertaken. In particular the effect of TNF-α treatment on *CDKN1A* expression should be noted, as TNF-α is not known to induce a DNA damage response, hence if increased expression of this gene is observed after treatment with this agent, it is most likely to be due to an NF-κB response in this particular cell line.

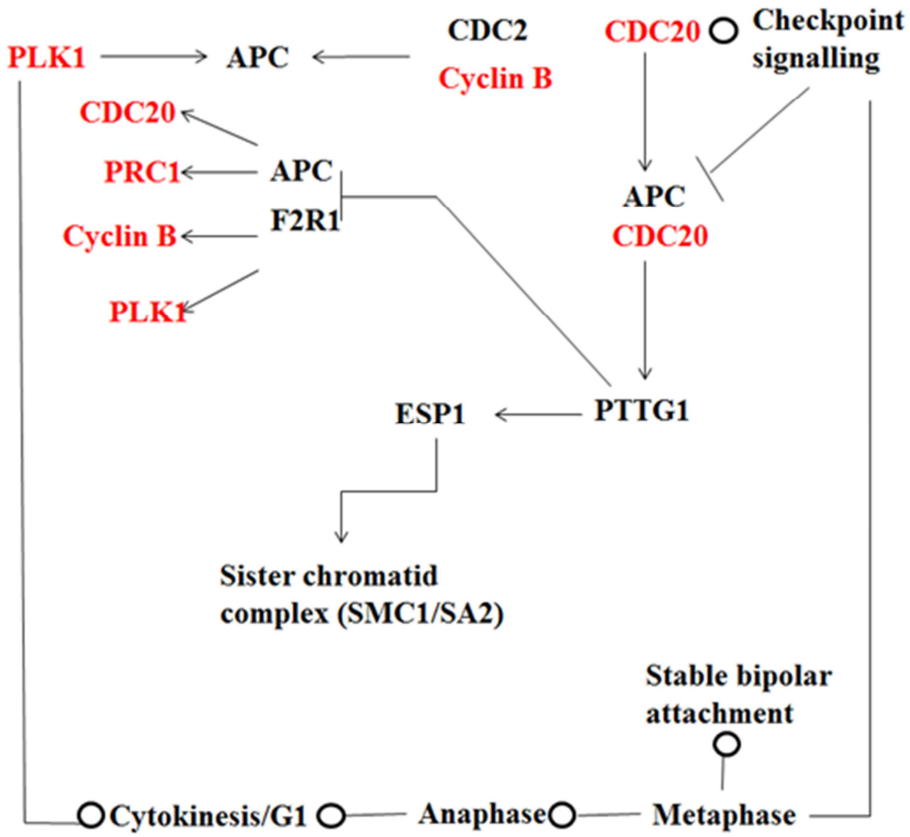

Figure 5.6: Metaphase to anaphase transition and mitotic exit
Genes which were identified as up-regulated 2 hours after treatment with 10 Gy IR are in red, those unaffected are in black. Adapted from Ingenuity Pathway analysis (IPA)

Similarly, the *TOP2A* gene, which encodes the topoisomerase II alpha protein, was up-regulated following treatment with IR. Topoisomerase II is a nuclear enzyme which controls and alters the topologic states of DNA during transcription and replication. It is involved in processes such as chromosome condensation, chromatid separation, and the relief of torsional stress that occurs during DNA transcription and replication. It catalyses the transient breaking and rejoining of two strands of DNA thus allowing the strands to pass through one another, and altering the topology of DNA. There are many known inhibitors of the enzyme currently used in cancer therapeutics (Liu and D'Arpa, 1992). Although the *TOP2A* gene has not previously been shown to be regulated by NF-κB, it could be something to further investigate. Topoisomerase II poisons are often used in combination with radio-therapy for the treatment of cancers, such as breast (Hoogstraten et al., 1976) and are widely used for the treatment of acute myeloid leukaemia (AML). Reports have also shown that doxorubicin, daunorubicin and mitoxantrone induce NF-κB activity (Campbell et al., 2006a), hence it is possible that

there is a feedback loop occurring with NF-κB inducing the *TOP2A* gene, perhaps resulting in the acquired resistance sometimes observed with these types of treatments.

Other genes of interest up-regulated following IR, include the proto-oncogene JunB, which has previously been shown to be regulated by NF-κB after induction with the inflammatory cytokine, IL-6 (Brown et al., 1995). However, this gene has not been shown to be regulated by NF-κB following treatment with a DNA damaging agent. Furthermore, TNFAIP3 interacting protein 1 (*TNIP1*) gene is also shown to be up-regulated following treatment with IR. *TNIP1* encodes the protein ABIN1 and interacts with the putative tumour suppressor TNFAIP3/A20 (Compagno et al., 2009, Heyninck et al., 1999). TNIP1 is regulated by NF-κB following treatment with TNF-α, and is associated with TNF-α mediated apoptosis, in concert with TNFAIP3 (Hymowitz and Wertz, 2010), therefore it would interesting to determine whether this gene is regulated by NF-κB following IR, and its function in this context.

5.4.2 Differentially expressed genes 2 hours following treatment with IR versus IR in combination with AG-014699

Following on from the section studying the genes which were differentially expressed following IR treatment compared with controls, it was decided to directly compare IR treated $p65^{+/+}$ MEFs with $p65^{+/+}$ MEFs treated with a combination of IR and AG-014699. A number of genes which were up-regulated after IR treatment were associated with cellular assembly and organisation, which are not widely known as NF-κB-regulated genes. Hence, it was important to assess the expression of these genes, and others following IR with co-incubation with the PARP inhibitor, AG-014699. Previous data, presented in chapters 3 and 4 of this thesis, have shown that radio-sensitisation by the AG-014699 is mediated *via* NF-κB, and is independent of SSB repair. This leads to the hypothesis that genes, such as PLK1 which were up-regulated following treatment with IR, would be down-regulated by co-incubation with a PARP inhibitor, if they were regulated by NF-κB. Hence, Genespring GX 11 was utilised by Dr Dan Swan in order to generate to a list of genes differentially expressed following treatment with 10 Gy IR, compared with 10 Gy IR in combination with AG-014699. These genes are listed in Table 5.5 along with the accession/identification number and the fold change.

Gene	Symbol	ID	Fold change
Rho/Rac guanine nucleotide exchange factor 2	*ARHGEF2*	AK035683	-1.716

Atonal homolog 8	*ATOH8*	NM_153778.3	1.247
Aurora kinase A	*AURKA*	NM_011497.3	-1.853
Baculoviral IAP repeat containing 6	*BIRC6*	AK038699	-1.200
Cell division cycle 20 homolog	*CDC20*	NM_023223.1	-1.288
Cyclin-dependent kinase inhibitor 2D (p19)	*CDKN2D*	NM_009878.3	-1.221
Cation transport regulator homolog 1	*CHAC1*	NM_026929.3	-1.240
FERM domain containing 4A	*FRMD4A*	AK089210	-1.268
Inversin	*INVS*	AK040307	-1.238
Importin 5	*IPOS*	AK017701	-1.165
Interferon regulator factor 1	*IRF1*	NM_008390.1	1.563
Jun proto-oncogene	*JUN*	NM_010591.1	-1.305
Katanin p60 subunit A like 1	*KATNAL1*	NM_135572.7	-1.277
Mitogen activated kinase 11	*MAPK11*	NM_011161.4	-1.253
Polo like kinase 1	*PLK1*	NM_011121.3	-1.468
Protease, serine 8	*PRSS8*	NM_13351.1	1.238
Ribosomal protein S24	*Rps24*	AK052480	-1.428
Slit homlog 2	*SLIT2*	AK053913	-1.328
Stabilin 1	*STAB1*	AK087634	-1.414
TNFAIP3 interacting protein 1	*TNIP1*	NM_021327.1	-1.273
Topoisomerase (DNA) II alpha 170 kDa	*TOP2A*	AK028218	-1.207

Table 5.5: Differentially expressed genes 2 hours following treatment with IR + AG-014699 in p65$^{+/+}$ MEFs, compared with IR alone

Interestingly, Table 5.5 shows that a number of the genes up-regulated following IR, including TOP2A, PLK1, AURKA, CDC20, and others which are all known to play a role in cellular organisation and assembly, are down-regulated in the presence of AG-014699. This is summarised in the subsequent Table 5.6, along with the fold change following IR alone, and the fold change of IR in combination with AG-014699, allowing a direct comparison.

Gene	**Symbol**	**Fold change (IR)**	**Fold change (IR + AG-014699)**
Aurora kinase A	*AURKA*	2.2832	-1.853
Baculoviral IAP repeat containing 6	*BIRC6*	1.285	-1.200
Cell division cycle 20 homolog	*CDC20*	1.468	-1.288
Cyclin-dependent kinase inhibitor 2D (p19)	*CDKN2D*	1.351	-1.221
Cation transport regulator homolog 1	*CHAC1*	1.374	-1.240
FERM domain containing 4A	*FRMD4A*	1.260	-1.268
Inversin	*INVS*	1.298	-1.238

Interferon regulator factor 1	*IRF1*	-1.584	1.563
Jun proto-oncogene	*JUN*	1.643	-1.305
Polo like kinase 1	*PLK1*	1.651	-1.468
Ribosomal protein S24	*Rps24*	1.397	-1.428
Slit homlog 2	*SLIT2*	1.575	-1.328
TNFAIP3 interacting protein 1	*TNIP1*	1.846	-1.273
Topoisomerase (DNA) II alpha 170 kDa	*TOP2A*	1.659	-1.207

Table 5.6: Fold changes of genes which were up-regulated following IR, and subsequently down-regulated in the presence of IR and AG-014699

The data here shows that the baculoviral IAP (inhibitor of apoptosis) repeat containing 6 gene (*BIRC6*) is induced 1.3-fold following IR in the $p65^{+/+}$ MEFs, however this induction is abrogated in the presence of AG-104699. This is an anti-apoptotic gene and therefore supports existing literature from two groups stating that NF-κB activation following IR induces the expression of the anti-apoptotic genes, including the IAPs (Stehlik et al., 1998, You et al., 1999), resulting in cell survival. These data should be further confirmed using qRT-PCR.

Interestingly, the gene encoding interferon regulatory factor 1 (*IRF-1*) was down-regulated 1.6-fold by IR, however this fold change was reversed by co-incubation with AG-014699. Previous literature has shown that this gene is regulated by NF-κB following the inflammatory stimuli TNF-α and interferon-γ (IFN-γ) (Harada et al., 1994, Robinson et al., 2006). These data suggest that IRF-1 is also regulated by IR following DNA damage. It has been suggested that IRF-1 has a role as a tumour suppressor, and there has been one report showing that IRF-1 promotes apoptosis following DNA damage (Clarke et al., 2003), however the data presented here indicate that IR alone inhibits the transcription of this gene, whereas the PARP inhibitor induces mRNA expression of IRF-1. IRF-1 is a transcription factor itself and it has recently been shown that NF-κB p65 is a transcriptional target of IRF-1 (Ning et al., 2010), suggesting the presence of the feedback loop between the two transcription factors. Furthermore, there have a number of reports suggesting that over-expression, or induction of IRF-1 by IFNγ induces apoptosis and inhibits tumourigenesis, particularly in breast cancers (Bouker et al., 2005, Bowie et al., 2004, Pizzoferrato et al., 2004). These data therefore indicate that the inhibition of IRF-1 expression by IR and the subsequent induction of the gene by AG-014699, requires further investigation. It is well documented that NF-κB can repress gene transcription (Perkins, 2007), therefore in

this case the expression of IRF-1 could be inhibited by IR-induced NF-κB activation and the inhibition of NF-κB by AG-014699, restores expression of IRF-1.

Genes associated with cellular assembly and organisation, including *AURKA, PLK-1*, *TOP2A* and *CDC20* were all up-regulated following treatment with IR (2.2-fold, 1.6-fold, 1.7-fold and 1.5-fold, respectively). The expression of these genes was inhibited when $p65^{+/+}$ cells were pre-treated with AG-014699 prior to IR treatment. This therefore suggests that these genes may be regulated by NF-κB following DNA damage, and indicate that these genes require further validation using qRT-PCR. As previously mentioned the proto-oncogene, *Jun* and the *TNIP-1* gene (both known to be regulated by NF-κB, following inflammatory stimuli (Brown et al., 1995, Compagno et al., 2009, Heyninck et al., 1999, Tian et al., 2005)) were also found to be up-regulated following treatment with IR. This up-regulation was abrogated in the presence of AG-014699, and therefore these genes also warrant further investigation. A list of the interesting genes identified from the gene expression study on IR alone, and IR in combination with AG-014699 are in Table 5.7.

Gene	Symbol	Fold change (IR)	Fold change (IR + AG-014699)
Aurora kinase A	*AURKA*	2.283	-1.853
Baculoviral IAP repeat containing 6	*BIRC6*	1.285	-1.200
Cell division cycle 20 homolog	*CDC20*	1.468	-1.288
Interferon regulator factor 1	*IRF1*	-1.584	1.563
Jun proto-oncogene	*JUN*	1.643	-1.305
Polo like kinase 1	*PLK1*	1.651	-1.468
TNFAIP3 interacting protein 1	*TNIP1*	1.846	-1.273
Topoisomerase (DNA) II alpha 170 kDa	*TOP2A*	1.659	-1.207

Table 5.7: A list of the interesting genes identified from the data on IR alone, and IR in combination with AG-014699

5.4.3 Differentially expressed genes 2 hours following treatment with TNF-α

Once Genespring GX 11 and IPA had been used to assess the different types, and functions of the genes up- or –down-regulated following treatment with IR, these software packages were used again, by Dr Dan Swan, to determine the types or genes and canonical pathways regulated following treatment with 10 ng/ml TNF-α in the $p65^{+/+}$ MEFs. It is well documented that TNF-α induces NF-κB activation, and in particular a transcriptional response associated with the induction of inflammatory- or

immune-responses (Pahl, 1999). Hence, it is possible to hypothesise that this would be the transcriptional response observed with the data obtained from the arrays undertaken at the Cambridge Genomics Service. This would be very different from the response observed following IR, in the $p65^{+/+}$ MEFs, which showed that the majority of genes up-regulated after IR were associated with cellular organisation and assembly. Table 5.8 details a list of genes differentially expressed following treatment with TNF-α as well as the accession/identification number and the fold change.

Gene	Symbol	ID	Fold change
AE binding protein 2	*AEBP2*	AK04538	1.354
Adhesion molecule interacts with CXADR antigen 1	*AMICA1*	NM_001005421.3	-1.336
BAH domain and coiled coil containing 1	*BAHCC1*	NM_198423.3	2.010
BCL2 binding component 3	*BBC3*	NM_133234.1	1.304
B-cell CLL/lymphoma 10	*BCL10*	NM_009740.1	1.337
B-cell CLL/lymphoma 3	*BCL3*	NM_033601.1	1.394
BCL6 co-repressor	*BCOR*	NM_175045.2	1.334
Basic helix-loop-helix family member e40	*BHLHE40*	NM_011498.4	1.523
BH3 interacting domain death agonist	*BID*	NM_007544.3	1.859
Bone morphogenic protein 4	*BMP4*	NM_007554.2	-1.613
Chromosome 5 open reading frame 13	*C5orf13*	NM_053078.3	-1.214
Chromosome 6 open reading frame 203	*C6orf203*	NM_026411.1	-1.350
Chemokine (C-C motif) ligand 13	*CCL13*	NM_011333.3	5.503
Chemokine (C-C motif) ligand 5	*CCL5*	NM_013653.2	2.981
CCR4 carbon catabolite repression-4-like	*CCRN4L*	NM_009834.1	1.464
CD47 molecule	*CD47*	NM_175169.2	1.445
Cyclin dependent kinase 5 regulatory subunit associated protein 1	*CDK5RAP1*	NM_025876.2	-1.163
Cyclin dependent kinase inhibitor 3	*CDKN3*	NM_919022.2	-1.255
Cyclin-dependent kinase inhibitor 1A (p21)	*CDKN1A*	NM_007669.2	1.597
Cation transport regulator homolog 1	*CHAC1*	NM_026929.3	1.274
Chemokine (C-XC motif) ligand 10	*CXCL10*	NM_021274.1	3.771
DAB2 interacting protein	*DAB21P*	NM_001001602	1.241
Deafness, autosomal dominant 5	*DFNA5*	NM_018769.3	-1.213
Dolichyl pyrophosphate phosphatase 1	*DOLPP1*	NM_020329.3	-1.229
EH domain containing 1	*END1*	NM_010119.5	1.360
Family with sequence similarity 102 member A	*FAM102A*	NM_153560.4	-1.375

Family with sequence similarity 13 member C	*FAM13A*	NM_024244.3	1.413
F-box protein 40	*FBXO40*	NM_156083.3	-1.143
Fibroblast growth factor 7	*FGF7*	NM_008008.3	1.313
Four jointed box 1	*FJX1*	NM_010218.2	1.293
FERM domain containing 4A	*FRMD4A*	AK089210	1.282
Growth arrest and DNA damage inducible beta	*GADD45B*	NM_008655.1	1.759
Glial cell derived neutotrophic factor	*GDNF*	NM_010275.3	1.399
Histocompatibility 2, Q region locus 5	*H2-Q5*	NM_010393.3	1.533
Human immunodeficiency virus type I enhancer binding protein 3	*HIVEP3*	NM_010657	1.290
Major histocompatibility complex, class I, C	*HLA-C*	NM_010380.3	1.243
Intercellular adhesion molecule 1	*ICAM1*	NM_010439.2	1.532
Inhibitor of DNA binding 1	*ID1*	NM_010495.2	-1.601
Inhibitor of DNA binding 4	*ID4*	NM_031166.2	-1.671
Immediate early response 3	*IER3*	NM_133662.2	1.689
Immediate early response like 5	*IERL5*	NM_030244.3	-1.379
Immunoglobulin superfamily member 9	*IGSF9*	NM_033608.2	1.572
Interleukin 1 receptor like 1	*IL1RL1*	NM_010743.1	1.695
Immunity related GTPase family Q	*IRGQ*	NM_153134.2	1.431
Interferon regulatory factor 1	*IRF1*	NM_008390.1	2.845
Interferon regulatory factor 5	*IRF5*	NM_012057.3	1.792
JunB proto-oncogene	*JUNB*	NM_008416.1	1.867
Leukemia inhibitory factor	*LIF*	NM_001039537.1	1.458
Lysophosphatidic acid receptor 6	*LPAR6*	NM_175116.2	-1.474
Mastermind-like 2	*MAML2*	XM_001481278.2	1.290
Mitogen activated protein kinase kinase kinase 11	*MAPK311*	NM_022012.3	1.312
Mitogen activated protein kinase 11	*MAPK11*	NM_011161.4	1.215
Mitogen activated protein kinase 6	*MAPK6*	NM_027418.1	1.363
Meis homobox 1	*MEIS1*	NM_010789.2	-1.298
Malignant fibrous histio-cytoma amplified sequence 1	*MFAHAS1*	NM_001081279.1	1.738
Myotubularin related protein 4	*MTMR14*	NM_026849.1	1.246
N-myc downstream regulator 1	*NDRG1*	NM_008681	1.569
Nuclear factor of activated T-cells, calcineurin-dependent 4	*NFATC4*	NM_023699.3	-1.303
Nuclear factor (erythroid derived 2)-like 1	*NFE2L1*	NM_008686.2	1.281
Nuclear factor of kappa light polypeptide gene enhancer in B cells (p49/p100)	*NFKB2*	NM_019408.1	1.635
Nuclear factor of kappa light polypeptide gene enhancer inhibitor epsilon	*NFKBIE*	NM_008690.2	2.125
NIPA-like domain containing 1	*NIPAL1*	NM_001081205.1	1.736

Neuregulin 1	*NRG1*	NM_178591.2	1.490
OCIA domain containing 2	*OCIAD2*	NM_026950.3	-1.209
Opitneurin	*OPTN*	NM_181848.3	1.346
Photocadherin 7	*PCDH7*	NM_018764.1	1.419
Platelet derived growth factor beta polypetptide	*PDGFB*	NM_011057.2	2.426
Platelet derived growth factor receptor like	*PDGLRL*	NM_026840.2	1.218
6-phosphofructo-2-kinase	*PFKFB4*	NM_173019.5	-1.206
Pleckstrin homology-like domain, family B, member 1	*PHLDB1*	NM-153537.3	1.784
Paroxysmal nonkinosigenc dyskinesia	*PNKD*	NM_019999.3	1.579
Plasminogen activator, tissue	*PLAT*	NM_008872	1.219
Peroxisome proliferator activated receptor gamma, coactivator-related 1	*PPRC1*	NM_001081214.1	1.165
Proline rich 7	*PPR7*	NM_001030296.3	1.311
Proteosome 26S subunit, non-ATPase, 10	*PSMD10*	NM_016883.3	1.203
RAB32, member RAS oncogene family	*RAB32*	NM_026405.3	1.572
RAB3A, member RAS oncogene family	*RAB3A*	NM_009001.3	-1.255
Ras associated domain family (N-terminal) member 7	*RASSF7*	NM_025886.3	1.244
Receptor interacting serine-threonine kinase 2	*RIPK2*	NM_138952.3	1.515
Ring finger protein 19B	*RNF19B*	XM_910375.2	1.770
Shroom family member 2	*SHROOM2*	NM_172441.2	-1.317
SMAD family member 3	*SMAD3*	NM_016769.2	1.449
Solute carrier family 44, member 1	*SLC44A1*	AK008866.1	1.122
Smg-7 homolog	*SMG7*	NM_001005507.1	1.266
Sorting nexin 16	*SNX16*	NM_029068.2	-1.206
SplA/ryanodine receptor domain and SOCS box containing 1	*SPSB1*	NM_029035.2	1.724
Syntaxin 11	*STX11*	NM_203312.6	3.259
TAP binding protein like	*TAPBPL*	NM_145391.1	1.424
T-box 3	*TBX3*	NM_0011535.2	1.417
T-cell immune regulator 1	*TCIRG1*	NM_016921.2	1.607
Toll like receptor 4	*TLR4*	NM_021297.1	-1.216
TNF-alpha-induced protein 2	*TNFAIP2*	NM_009396.1	2.969
TNF-alpha-induced protein 3	*TNFAIP3*	NM_009397.2	3.351
TNFAIP3 interacting protein 1	*TNIP1*	NM_021327.1	2.284
TNF receptor associated factor 1	*TRAF1*	AK089281	-1.738
Vascular cell adhesion molecule 1	*VCAM1*	AK030195	1.730
Zinc finger protein36, C3H type homolog	*ZFP36*	NM_011756.4	1.810
Zinc finger protein36, C3H type-like 1	*ZFP36L1*	NM_007564.2	1.388
Zinc finger, SWIM-type containing 4	*ZSWIM 4*	NM_172503.3	-1.624

Table 5.8: Differentially expressed genes 2 hours following treatment with TNF-α in p65$^{+/+}$ MEFs, compared with untreated controls

In order to clearly to determine whether there were differentially expressed genes following IR and TNF-α, a Venn diagram (Figure 5.7) was generated comparing the genes which were up- or down-regulated following either agent compared with controls.

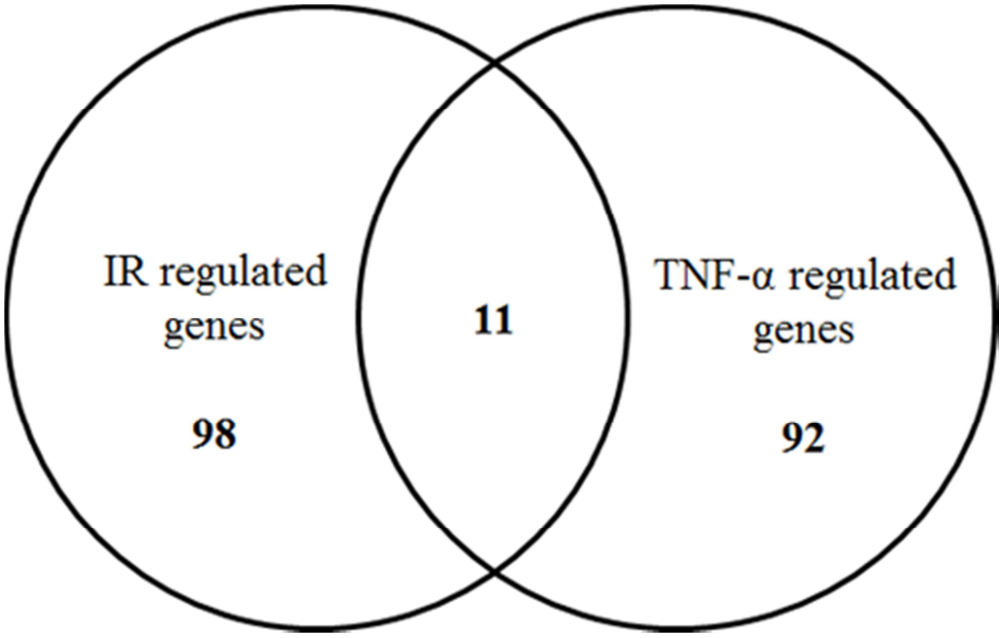

Figure 5.7: Venn Diagram showing the number of gene differentially expressed following either IR or TNF-α compared with untreated controls in the $p65^{+/+}$ MEFs, and importantly the number of common genes which were regulated following both stimuli.

The Venn diagram in Figure 5.7 shows that, using the parameters set in Genespring GX11 (section 5.3.4.1), there were 103 genes with a fold change greater than 1.2-fold following TNF-α treatment, and 109 genes with a fold change greater than 1.2-fold in cells treated with IR. However, of these genes, only 11 common genes were found to be regulated by both agents. These are listed, along with their fold changes after either agent, in Table 5.9. The table also details whether it is known if these genes are NF-κB regulated. This information was obtained by cross-referencing with the website from the laboratory of Dr. Thomas Gilmore (Boston University) http://www.bu.edu/nf-kb/the-gilmore-lab/home/, and where appropriate, references have been included.

Gene	Symbol	Fold Change (IR)	Fold change (TNF-α)	NF-κB regulated?	Reference
Cyclin-dependent kinase inhibitor 1A (p21)	CDKN1A	1.501	1.597	Yes	(Hinata et al., 2003)
Cation transport	CHAC1	1.374	1.274	No	

regulator homolog 1					
Growth arrest and DNA damage inducible beta	GADD45B	1.586	1.759	Yes	(De Smaele et al., 2001)
FERM domain containing 4A	FRMD4A	1.260	1.282	No	
Immediate early response 3	IER3	1.380	1.689	Yes	(Wu et al., 1998)
Interferon regulatory factor 1	IRF1	-1.584	2.845	Yes	(Harada et al., 1994)
JunB proto-oncogene	JUNB	1.643	1.867	Yes	(Brown et al., 1995)
Meis homobox 1	MEIS1	-1.257	-1.298	No	
splA/ryanodine receptor domain and SOCs box	SPSB1	-1.457	1.724	No	
TNFAIP3 interacting protein 1	TNIP1	1.846	2.211	Yes	(Tian et al., 2005)
Zinc finger, SWIM-type containing 4	ZSWIM 4	-1.259	-1.624	No	

Table 5.9: Information regarding fold change on the 11 genes which were differentially expressed following both IR and TNF-α in the $p65^{+/+}$ MEFs
Information regarding whether any of these genes are known to be regulated by NF-κB regulated following either stimulus is also included

Table 5.9 shows the 11 genes up- or down- regulated by treatment with either IR or TNF-α, and also that 6 of these genes are known to be regulated by NF-κB. In the case of *CDKN1A, TNIP1, JUNB, IER3* and *IRF-1* these genes have been shown to regulated by NF-κB following inflammatory stimuli (Brown et al., 1995, Harada et al., 1994, Hinata et al., 2003, Tian et al., 2005, Wu et al., 1998), and not by DNA damage. Hence, further investigation into some of these genes in order to confirm the array findings would be advantageous.

The Venn diagram in figure 5.7, shows that of the 103 genes with altered expression following TNF-α, there were 92 genes which showed altered expression, different from those differentially expressed following IR treatment in the same $p65^{+/+}$ MEFs. IPA pathway analysis software showed (Figure 5.5 and Table 5.4) that the networks and functional annotations assigned to the differentially expressed genes following IR were cellular assembly and organisation, which also has cross-talk with the cell cycle and cellular movement. Therefore, it was important to perform the same analysis with the

gene list (Table 5.8) generated for TNF-α regulated genes in IPA, in order to determine which pathways and cellular processes were involved with the differentially expressed genes following this stimulus.

It is well documented that TNF-α induces NF-κB dependent transcription of genes associated with the inflammatory and immune responses, including numerous different cytokines and chemokines, such as *CXCL10* (Hein et al., 1997) and *IL-8* (Kunsch and Rosen, 1993), as well as receptors required for immune recognition, including those which recognise MHC proteins (Israel et al., 1989a, Israel et al., 1989b, Johnson and Pober, 1994). NF-κB also regulates that expression of genes which are associated with antigen presentation and proteins required for neutrophil adhesion and transmigration across blood vessel walls, for example, *VCAM-1* (Iademarco et al., 1992). Hence, it was perhaps unsurprising that the top canonical pathways and functional annotations assigned to the list of genes regulated by TNF-α within this study were associated with the inflammatory response and the cell mediated immune response.

A summary of the functional annotations, associated molecules and p-values generated by the IPA software from the list of genes in Table 5.9, the are shown in Table 5.10. Table 5.10 details the genes assigned to functional annotations associated with the inflammatory response and also with the cell mediated immune response by IPA. The significance of the association between the molecules within the data set and the canonical pathway/process was measured, by the software algorithms, using a Fisher's exact test to calculate a p-value determining the probability that the association between the genes in the dataset and the canonical pathway/process is not explained by chance alone.

Functional annotations	**P value**	**Molecules**
Accumulation of lymphocytes	4.17E-09	*BCL10, BCL3, CCL13, CCL5, CXCL10, ICAM1, IER3, VCAM1*
Quantity of phagocytoes	1.02E-08	*BID, CCL13, CD47, CXCL10, FGF7, ICAM1, IRF1, MIES1(-), NFKB2, PLAT, SMAD3, TRL4(-)*
Immune response	3.79E-08	*BCL10, BCL3, BID, CCL13, CCL5, CD47, CDKN1A, CXCL10, HLA-C, ICAM1, IER3, IL1RL1, IRF1, JUNB, NDRG1, NFATC4, NFE2L1, NFKB2, PDGFB, PNKD, RIPK2, SMAD3, TC1RG1, TLR4(-), TNFAIP3, VCAM1, ZPF36*
CD4 T-cell response	3.95E-08	*BCL3, CCL13, CCL5, CXCL10, ICAM1,*

		IL1RL1, IRF1, RIPK2, TLR4(-)
Inflammation	1.10E-07	*BID, CCL13, CCL5, CD47, CXCL10, ICAM1, IL1RL1, JUNB, NFE2L1, PNKD, SMAD3, TLR4(-), TNFAIP3, VCAM1, ZPF36*
CD4 T-cell response of organism	1.34E-07	*BCL3, CCL13, CCL5, CXCL10, IL1RL1, IRF1, TLR4(-)*
Activation of leukocytes	5.82E-07	*BCL10, BCl3, BID, CCL13, CCl5, CD47, CDKN1A, CXCL10, HLA-C, ICAM1, ILR1L1, NDRG1, NFKB2, SMAD3, TLR4(-), VCAM1*
T-cell development	4.10E-10	*BBC3, BCL10, BID, BMP4(-), CCL13, CCL5, CD47, CDKN1A, HLA-C, ICAM1, ID1(-), IER3, ILR1L1, IRF1, JUNB, LIF, RIPK2, DMAD3, TLR4(-), TRAF1*
Apoptosis of T lymphocytes	4.26E-08	*BBC3, BCL10, BCL3, BID, BMP4(-), CCL13, CCL5, CD47, CDKN1A, ICAM1, IER3, TRAF1*
Differentiation of T lymphocytes	9.44E-06	*BCL3, BMP4(-), HLA-C, ICAM1, ID1(-), ILR1L1, IRF1, JUNB, LIF, RIPK2, SMAD3*
Chemotaxis of Th1 cells	1.09E-05	*CCL13, CCL5, CXCL10*
Recruitment of T lymphocytes	1.09E-05	*CCL13, CCL5, CXCL10, ICAM1, VCAM1*
Differentiation of helper T lymphocytes	3.00E-05	*BCL3, ICAM1, ILR1L1, IRF1, JUNB, RIPK2, SMAD3*
NK cell migration	8.41E-05	*CCL13, CCL5, CXCL10, VCAM1*

Table 5.10: Functional annotations associated with the inflammatory and immune responses assigned by IPA. Summary of the functional annotations from the IPA software, the associated molecules and p-values (-) denotes a gene which was down-regulated 2 hours after treatment with 10 ng/ml TNF-α

As anticipated, the functional annotations assigned by IPA to the genes up-or down-regulated by TNF-α were associated with both the inflammatory and immune response, with many genes, such as the chemokines *CCL13, CCL5* and *CXCL10* associated with many of the different functions identified by the software. It should also be noted that some of the greatest fold changes were also associated with these genes. For example, *CCL13* was up-regulated 5.5-fold, which is much higher than any of the genes activated by IR (see Table 5.3). Moreover, as expected, a number of these genes are also known to regulated by NF-κB, when cross-referenced with the website http://www.bu.edu/nf-kb/the-gilmore-lab/. These include those previously mentioned, such as *CXCL10* (Hein et al., 1997), *IRF1* (Harada et al., 1994, Robinson et al., 2006), *JUNB* (Brown et al., 1995), and *VCAM1* (Iademarco et al., 1992), as well as others including *CCL5*

(Wickremasinghe et al., 2004), *RIPK2* (Matsuda et al., 2003), *TRAF1* (Schwenzer et al., 1999) and *BCL3* (Brocke-Heidrich et al., 2006), along with many of the other genes listed in Table 5.10.

Both TRAF1 and BCL3 are associated with the activation of NF-κB, and the subsequent activation or repression of gene transcription. The former is a TNF-receptor associated factor known to mediate the signals from the cytokine receptor to their downstream effectors, whilst the latter is a known co-activator for the NF-κB subunits p50 and p52 (Perkins, 2007). There is a large body of literature which suggests that the activation of NF-κB is known to up-regulate the transcription of genes which encode proteins related to the NF-κB activation pathway, and many of these are known to be vital for both the inflammatory and immune responses. For example, *NFKB2* (which encodes the p100 NF-κB subunit precursor protein) is shown to be up-regulated 1.6-fold following treatment with TNF-α, in these $p65^{+/+}$ MEFs (Table 5.8), and the IPA software package assigns it to functions associated with the immune response and the activation of leukocytes (Table 5.10). Once again, it is a known NF-κB target gene (Lombardi et al., 1995). Furthermore, the gene (*NFKBIE*) which encodes the inhibitor of kappaB (IKK) subunit IKKε protein is also shown be up-regulated 2.1-fold (Table 5.8), highlighting the complex feedback loops associated with the activation of NF-κB and associated pathway components.

IPA software generates networks based on the transcriptional response observed, and it is perhaps unsurprising that the network it has produced from the gene list in Table 5.8, is one which highlights the complex cross-talk of both the activation of NF-κB and immunological signalling (Figure 5.8). This shows the genes up- (in red) or down- (in green) regulated by TNF-α that are associated with gene expression, antigen presentation and immunological cell signalling.

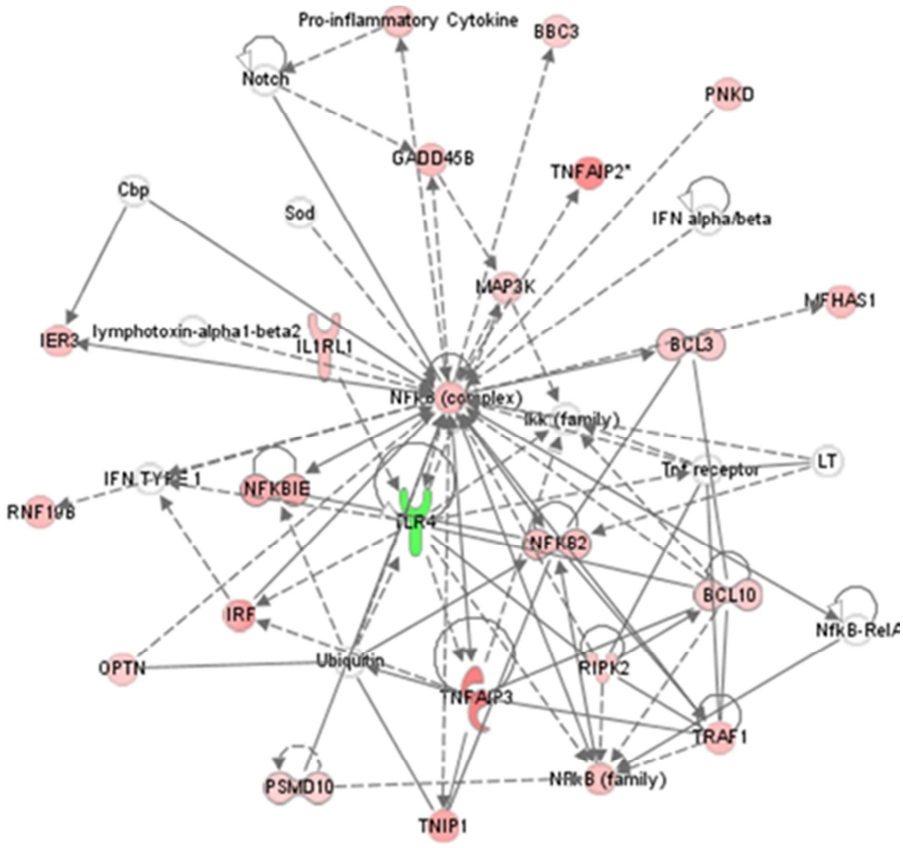

<u>Figure 5.8:</u> Genes associated with gene expression, antigen presentation and immunological cell signalling. Canonical network generated by IPA with genes that were up-regulated (shown here in red) or down-regulated (shown here in green) in $p65^{+/+}$ MEFs 2 hours after treatment with 10 ng/ml TNF-α

This network diagram shows that NF-κB signalling is vital for a functional inflammatory and immune response within a cell, and once again highlights how challenging drug discovery is in the context of the inhibition of NF-κB. It shows that the activation of NF-κB by an inflammatory stimulus, such as TNF-α, is essential for the transcription of numerous pro-inflammatory cytokines, which are known to function primarily in the host immune response (Table 5.10). Therefore, complete or global inhibition of NF-κB may have a detrimental effect on the cell, as this may result in the inhibition of these genes known to have vital roles in the inflammatory response. Hence, it is vital to assess the effect of the PARP inhibitor, on the transcription of these inflammatory response genes following TNF-α, in order to determine whether the use of a PARP inhibitor is a viable therapeutic strategy when targeting NF-κB, as suggested by the previous data in Chapter 4.

5.4.4 Differentially expressed genes 2 hours following treatment with TNF-α versus TNF-α in combination with AG-014699

The data in Chapter 4 of this thesis has shown that the PARP inhibitor, AG-014699, had no effect on TNF-α-induced NF-κB DNA binding or NF-κB-dependent gene transcription (measured using a luciferase reporter assay in $p65^{+/+}$ MEFs) whereas PARP-1 siRNA inhibited TNF-α-induced DNA binding and luciferase activity in the same cells. These data indicated that PARP-1 protein, but not its enzymatic activity was important in activating NF-κB following the inflammatory stimulus. However, these data also showed that AG-014699 attenuated the observed IR-induced NF-κB DNA binding and transcriptional activation in the $p65^{+/+}$ MEFs, suggesting that the PARP inhibitor would be a viable therapeutic strategy in inhibiting DNA-damage-induced NF-κB, which is known to drive therapeutic resistance in cancer (Prasad et al., 2010), without comprising the vital inflammatory functions of the transcription factor. This hypothesis therefore warranted much further testing, using the array based approach within this chapter. A small number of genes have been shown to be induced by IR, and this induction was abrogated in the presence of AG-014699 (Table 5.7). A number of the genes up-regulated by TNF-α treatment alone (Table 5.8) were associated with the inflammatory and immune responses, hence it was vital to determine the expression of these genes was altered in the presence of AG-016499. In order to do this it was decided to directly compare TNF-α treated $p65^{+/+}$ MEFs with $p65^{+/+}$ MEFs treated with a combination of TNF-α and AG-014699.

Genespring GX 11 was utilised by Dr Dan Swan in order to generate to lists of genes differentially expressed following treatment with 10 ng/ml TNF-α, compared with TNF-α in combination with AG-014699. Table 5.11 details a list of genes differentially expressed following treatment with TNF-α + AG-014699 as well as the accession/identification number and the fold change.

Gene	Symbol	ID	Fold change
Family with sequence similarity 165, member B	*FAM165B*	NM_138743.2	-1.205
Nicastrin	*NCSTN*	NM_021607.2	1.226
Transducin (beta)-like 1X linked	*TBL1X*	NM_0206301.2	-1.477

Table 5.11: Differentially expressed genes 2 hours following treatment with TNF-α + AG-014699 in $p65^{+/+}$ MEFs, compared with TNF-α alone

Table 5.11 shows that there were only three genes differentially expressed in the presence of AG-014699, when compared with TNF-α alone. This therefore suggests that AG-014699 in combination with TNF-α has no effect on any of the inflammatory or immune response associated genes compared with TNF-α, thus supporting the data in Chapter 4, which showed that AG-014699 had no effect on TNF-α-induced NF-κB DNA binding or NF-κB-dependent gene transcription. This should be confirmed using qRT-PCR, to assess the effect of PARP-1 siRNA on known NF-κB regulated genes which were induced in this this array study. Therefore, a selection of NF-κB-dependent inflammatory and immune response genes, including *CCL5* and *CXCL10*, which showed large fold changes following TNF-α treatment in the $p65^{+/+}$ MEFs, were chosen for further investigation in this manner. These are detailed in section 5.4.9

The three genes identified as being differentially expressed when comparing TNF-α treated $p65^{+/+}$ MEFs and TNF-α in combination with the PARP inhibitor, AG-014699 included the *TBL1X* gene, which encodes the transducin β-like 1X-linked protein. Array data indicated that transcription was decreased in the presence of AG-014699. A related protein family member, transducin β-like protein 1 (TBL1) has sequence similarity with F-box and WD-40-domain containing proteins (Guenther et al., 2000, Li et al., 2000), and is reported to play a role in the ubiquitin-conjugating/19S proteosome complex that mediates the exchange of co-repressors for co-activators by some nuclear receptors and transcription factors, including NF-κB (Perissi et al., 2004). Most recently, one group reported that TBL1 was required for the recruitment of NF-κB p65 to NF-κB target gene promoters, using TBL1 siRNA. Moreover, this group illustrated that TBL1 knockdown in the MDA-MB-231 breast cancer cell line decreased invasion through inhibition of NF-κB-dependent gene transcription (Ramadoss et al., 2011).

Another gene, *NCSTN*, which encodes the nicistrin protein, was up-regulated in the presence of AG-014699, compared with TNF-α alone. Nicastrin is part of the gamma secretase protein complex, along with presenilin, anterior pharynx-defective 1 (APH-1), and presenilin enhancer 2 (PEN-2). Together these proteins are involved in processing amyloid precursor protein (APP) to the short Alzheimer's disease-associated peptide amyloid beta (Kaether et al., 2006). Presenilin is catalytically active subunit, whereas nicastrin promotes the maturation and proper trafficking of the other proteins in the complex, all of which undergo significant post-translational modification before becoming active in the cell (Zhang et al., 2005b).

5.4.5 Differentially expressed genes 8 hours following treatment with IR

One of the main aims of this chapter was to assess the different types, and functions of the genes up- or –down-regulated following treatment with either IR or TNF-α at the 8 hour timepoint. This time-point was chosen because previous data, presented in chapter 4, using a luciferase reporter assay, found that NF-κB-dependent gene transcription was maximal following either IR or TNF-α at this timepoint. Data obtained at the early (2 hour) timepoint during this array study (section 5.4.3) has shown that, in concordance with the literature, TNF-α induced the transcription of many genes associated with the induction of inflammatory- or immune-responses (Pahl, 1999). Interestingly, the genes regulated following treatment with IR at the 2 hour timepoint were in the most part associated with cellular assembly and organisation, therefore it would be interesting to determine whether the expression of these genes is still up-regulated 8 hours following IR treatment, or whether others involved in new cellular process and pathways are affected.

In order to do this, the array data received from the Cambridge Genomics Service was input into Genespring GX 11 by Dr Dan Swan in order to generate to lists of genes differentially expressed 8 hours following treatment with 10 Gy IR, compared with controls. Table 5.12 details a list of genes differentially expressed following treatment with IR as well as the accession/identification number and the fold change.

Gene	Symbol	ID	Fold change
Amiloride-sensitive cation channel 2, neuronal	*ACCN2*	NM_009597.1	-1.305
Acyl-CoA synthetase family member 3	*ACFS3*	NM_144932.3	-1.249
Acyl-CoA synthetase long chain family member 3	*ACSL3*	NM_028817.2	1.260
Acidic nuclear phosphoprotein 32 family member A	*ANP32A*	NM_009672.2	1.254
Rho GTPase activating protein 18	*ARHGAP18*	NM_176837.2	1.203
Aurora kinase B	*AURKAB*	NM_011496.1	1.251
Chromosome 20 open reading frame 194	*C20orf194*	NM_029432.1	-1.237
Chromosome 5 open reading frame 13	*C5orf13*	NM_053078	1.320
Cell division cycle 20 homolog	*CDC20*	NM_023223.1	1.293
Cyclin dependent kinase inhibitor 3	*CDKN3*	NM_919022.2	1.228
Cellular retinoic acid binding protein 2	*CRABP2*	NM_007759.2	-1.239
Cullin 7	*CUL7*	NM_025611.5	1.250
Dickkopf homolog 3	*DKK3*	NM_015814.2	1.236

Ecotrophoic viral integration site 2A	*EVI2A*	NM_010161.3	-1.413
Family with sequence similarity 104, member A	*FAM104A*	NM_138598.5	1.221
Histone cluster 1, H1c	*HIST1H1C*	NM_015768	1.846
Histone cluster 1, H2bk	*HIST1H2BK*	NM_023422.3	1.408
Histone cluster 1, H2be	*HIST1H2BE*	NM_178195.1	1.202
Major histocompatibility complex, class 1C	*HLA-C*	NM_010380.3	-1.236
Meis homobox 2	*MEIS2*	NM_010825.3	1.249
Nuclear autoantigenic sperm protein	*NASP*	NM_016777.2	1.204
Neuroblastoma, suppression of tumorigenicity 1	*NBL1*	NM_008675.1	-1.224
Nestin	*NES*	NM_016701.3	-1.305
Nuclear respiratory factor 1	*NRF1*	NM_010938.3	1.313
Osteoglycin	*OGN*	NM_008760.2	1.582
Platelet derived growth factor receptor alpha polypeptide	*PDGFRA*	NM_011058.2	1.259
Prolactin family 2, subfamily C, member 2	*Prl2cl*	NM_011118.1	-1.295
Ras associated domain family member 1	*RassF1*	NM_019713.3	-1.368
Retinoblastoma binding protein 4	*RBBP4*	NM_009030.3	1.227
Structural maintenance of chromosomes 4	*SMC4*	AK10848	1.569
Sorting nexin 16	*SNX16*	NM_099068.2	1.271
Stromal antigen 1	*STAG1*	NM_009282.3	1.234
Ubiquitin-like with PHD and ring finger domains 1	*UHRF1*	NM_010931.2	1.239
Exportin 4	*XPO4*	NM_20506.1	-1.203
Zinc finger protein36, C3H type-like 1	*ZFP36L1*	NM_007564.2	1.318

Table 5.11: Differentially expressed genes 8 hours following treatment with IR in p65$^{+/+}$ MEFs, compared with untreated controls

The gene list generated from the differentially expressed genes 8 hours after treatment with IR in Table 5.11 contains a very different list of genes compared with those regulated 2 hours post IR treatment (section 5.4.1). There are only four genes which are present in both lists; *NASP*, *XPO4*, *SMC4* and *CDC20*. Interestingly, *CDC20* was identified as a potential gene of interest and selected for future study previously (section 5.4.2), due the effects observed following treatment with AG-014699. Two hours following treatment with IR, CDC20 expression was up-regulated 1.5-fold, and this up-regulation was abrogated in the presence of AG-014699. It will be interesting to see whether this is also the case at the later, 8 hour, timepoint.

SMC4, the gene which encodes the protein structural maintenance of chromosomes 4 was up-regulated 1.6-fold at the late timepoint and 1.4-fold at the early timepoint. This

gene is known to be involved in cellular assembly and organisation and was assigned such functional annotations by the IPA analysis used at on the IR-early time-point gene lists. It does not appear that any of the other genes assigned these functions are differentially expressed in the list in Table 5.11. *AURKA* was up-regulated at the 2 hour timepoint and interestingly, *AURKB*, which encodes the aurora kinase B protein is up-regulated, although modestly at 1.3-fold, at 8 hours after IR treatment in the $p65^{+/+}$ MEFs. This protein is also associated with cellular organisation and assembly.

In order to gain insight into the other canonical pathways and processes involved with the genes in Table 5.11, the list was uploaded into IPA software by Dr Dan Swan, as previously stated in section 5.3.4.2. Once again, the network associated with cellular assembly and organisation, DNA replication, recombination and repair, and the cell cycle were identified by the software. Figure 5.9 shows the network generated by IPA in this case.

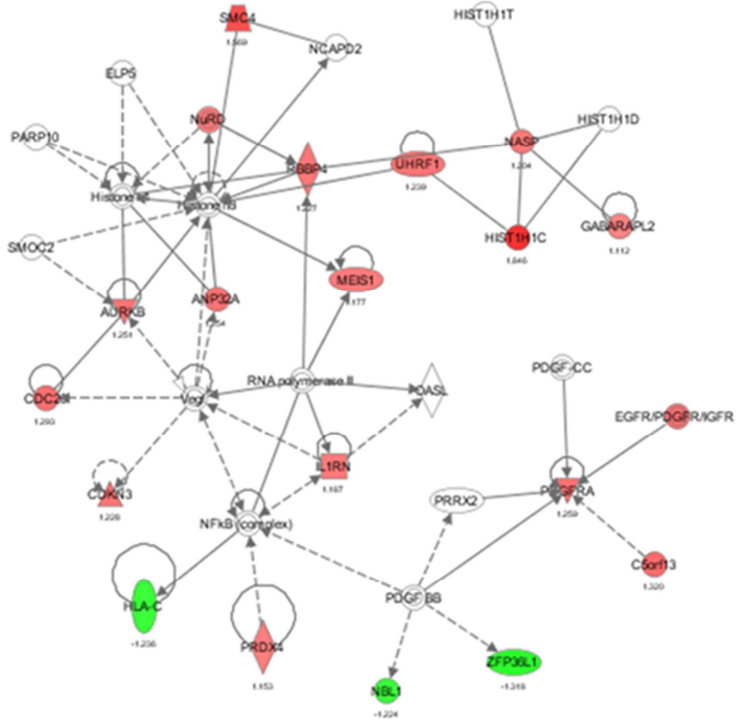

<u>Figure 5.9:</u> Genes associated with cellular assembly and organisation, DNA replication, recombination and repair, and the cell cycle. Network generated by IPA with genes that were up-regulated (shown here in red) or down-regulated (shown here in green) in $p65^{+/+}$ MEFs 8 hours after treatment with 10 Gy IR

Interestingly, many of these genes were also associated with cellular proliferation and were assigned this functional annotation by the IPA software package. These are listed in Table 5.12. The significance of the association between the molecules within the data

set and the canonical pathway/process was measured, by the software algorithms, using a Fisher's exact test to calculate a p-value determining the probability that the association between the genes in the dataset and the canonical pathway/process is not explained by chance alone.

Functional Annotation	P value	Molecules
Cellular proliferation	2.91E-03	*ANP32A, AURKA, C5orf13, CDC20, CDKN3, CUL7(-), NASP, NRF1, PDGFRA, Prl2c1, RBBP4, UHRF1, ZFP36L1*

Table 5.12: Functional annotations associated with proliferation assigned by IPA
Summary of the functional annotations from the IPA software, the associated molecules and p-values (-) denotes a gene which was down-regulated 8 hours after treatment with 10 Gy IR

NF-κB is known to regulate genes involved in a number of cellular processes, including apoptosis, angiogenesis, metastasis and cellular proliferation (Ghosh and Karin, 2002). It is also known to contribute to therapeutic resistance (Prasad et al., 2010). Hence, it is unsurprising that, following IR, the genes which are up-regulated are associated with cell proliferation. It is plausible that these cells are evading cell death by inducing the transcription of a number of genes with known roles in cell proliferation, in response to the DNA damaging agent. Two of the genes associated with cell proliferation in Table 5.12 are known to be regulated by NF-κB; *PDGFRA* (Khachigian et al., 1995) and *RBBP4* (Pacifico et al., 2007). Therefore, it is possible some of the others listed could perhaps be novel genes regulated by NF-κB following IR.

5.4.6 Differentially expressed genes 8 hours following treatment with IR versus IR in combination with AG-014699

It was decided to directly compare IR treated $p65^{+/+}$ MEFs with $p65^{+/+}$ MEFs treated with a combination of IR and AG-014699 harvested at the 8 hour timepoint. A number of the genes which were up-regulated 8 hours after with IR treatment were associated with cellular assembly and organisation, and also cell proliferation. Hence, it was important to assess the expression of these genes, and others following IR with co-incubation with the PARP inhibitor, AG-014699. Data in section 5.4.2 of this array study showed that there were a number of genes up-regulated 2 hours after IR, in which the effects seen were attenuated in the presence of AG-014699 at this timepoint. Therefore, it was essential to determine whether the same effects were seen with the any

of the genes listed in section 5.4.5, which explored genes regulated 8 hours after IR treatment. Dr Dan Swan used Genespring GX 11 software in order to generate to a list of genes differentially expressed 8 hours following treatment with 10 Gy IR, compared with 10 Gy IR in combination with AG-014699. These genes are listed in Table 5.13 along with the accession/identification number and the fold change.

Gene	Symbol	ID	Fold change
Bcl-2 binding component 3	*BBC3*	NM_133234.1	1.305
Cell division cycle 20 homolog	*CDC20*	NM_023223.1	-1.296
Prolactin family 2, subfamily C, member 2	*Prl2cl*	NM_011118.1	1.260

Table 5.13: Differentially expressed genes 8 hours following treatment with IR + AG-014699 in p65$^{+/+}$ MEFs, compared with IR alone

Table 5.13 shows that there were only three genes which were identified as being differentially expressed when comparing cells harvested 8 hours after treatment with IR and those harvested 8 hours after treatment of IR in combination with AG-014699. One of these genes, *CDC20* was up-regulated 1.3-fold 8 hours after treatment with IR, and then array data showed that the presence of AG-014699 resulted in the gene being down-regulated 1.3-fold. This gene was also identified as a potential gene of interest in section 5.4.2, when a similar regulation of the gene was observed 2 hours after IR treatment. The *Prl2c1* gene which encodes the prolactin family 2, subfamily C, member 2 protein is down-regulated 1.3-fold 8 hours after treatment with IR, and then array data showed that the presence of AG-014699 resulted in the gene being up-regulated 1.3-fold, however there is little literature on this gene, however it appears to be primarily murine.

The fold changes observed 8 hours after IR (Table 5.11, section 5.4.5) were very subtle. Genes associated with cellular assembly and organisation, including *AURKB* and *CDC20* were up-regulated following treatment with IR (1.2-fold and 1.3-fold, respectively). The expression of CDC20 was inhibited when p65$^{+/+}$ cells were pre-treated with AG-014699 prior to IR treatment at this timepoint. This therefore suggests that these genes may be regulated by NF-κB following DNA damage, and indicate that this gene, in particular requires further validation using qRT-PCR, especially as this mirrors the regulation observed with CDC20 at the earlier (2 hour) timepoint.

Interestingly, the gene that encodes aurora kinase A was up-regulated 2 hours after IR treatment whereas the gene which encodes the aurora kinase B protein was up-regulated

8 hours after IR treatment. The Aurora kinases, A, B and C, are highly conserved mitotic regulators. The 'polar' kinase, Aurora A, is required for biopolar spindle assembly and therefore localizes to spindle poles and the centrosome during mitosis. The 'equatorial' kinase, Aurora B, first localizes to the centromeres and the kinetochores during the early stages of mitosis acting as a chromosome passenger (Keen and Taylor, 2004). Small molecule Aurora kinase inhibitor studies showed that Aurora B function was vital for checkpoint signaling following checkpoint activation (Biggins and Murray, 2001, Ditchfield et al., 2003, Hauf et al., 2003). Hence, as aurora kinase A was identified due to the down-regulation of the gene in presence of AG-014699 at the early timepoint, it was decided to also further investigate aurora kinase B by qRT-PCR. A full list of the gene chosen for further study is in section 5.4.9.

5.4.7 Differentially expressed genes 8 hours following treatment with TNF-α

Once Genespring GX 11 and IPA had been used to assess the different types, and functions of the genes up- or –down-regulated 8 hours after treatment with IR, these software packages were used again, by Dr Dan Swan, to determine the types or genes and networks regulated 8 hours after treatment with 10 ng/ml TNF-α in the $p65^{+/+}$ MEFs. Data obtained at the early (2 hour) timepoint during this array study (section 5.4.3) has shown that, in concordance with the literature, TNF-α induced the transcription of many genes associated with the induction of inflammatory- or immune-responses (Pahl, 1999). Therefore it would be interesting to determine whether the expression of these genes is still up-regulated 8 hours following TNF-α treatment, or whether others involved in new cellular process and pathways are affected. Table A.1, which contains a list of genes of over 400 genes differentially expressed following treatment with TNF-α, as well as the accession/identification number and the fold change, is in Appendix A.

IPA pathway analysis software showed (Figure 5.9 and Table 5.12) that the networks functions associated with the genes differentially expressed 8 hours after treatment with IR were cellular assembly and organisation, and also cellular proliferation. Therefore, it was important to perform the same analysis with the gene list (Table A.1) generated 8 hours after treatment with TNF-α using IPA software, in order to determine which pathways and cellular processes were involved with the differentially expressed genes following this stimulus. It was perhaps unsurprising that here the top networks and functional annotations assigned to the list of genes regulated by TNF-α, 8 hours after

treatment, were also associated with the inflammatory response and the cell mediated immune response. A summary of the functional annotations generate by the IPA software from the list of genes in Table A.1, the associated molecules and p-values are shown in Table 5.14. Table 5.14 details the genes assigned to functional annotations associated with the cell mediated immune response by IPA. The significance of the association between the molecules within the data set and the canonical pathway/process was measured, by the software algorithms, using a Fisher's exact test to calculate a p-value determining the probability that the association between the genes in the dataset and the canonical pathway/process is not explained by chance alone.

Functional annotation	P value	Molecule
Immune response	9.75E-09	*Abcb1b, ASS1, BCL211, C3, CASP4, CCL13, CCL17, CCL5, CCL7, CD151, CD74, CDKN1A, CXCL10, CXCL2, DCN, EGIR3(-), F2R(-), FAS, FOS(-), GBP2, GRN(-), HBP1(-), HADC5(-), HLA-B, HLA-C, HLA-G, IER3, IFNGR2, IL1RL1, IRF1, ITGBS(-), MMP9, MRC1, NFATC4, NFKB2, NFKBIA, NUPR(-), PLSCR1, PML(-), PNKD, PPARD, PPBP, PSMB10, PSMBB, PSME1, PTPN22, RAP1GAP(-), RELA, RELB, SLC11A1, SOCS2, SPHK1(-), SPON2(-), SPP1, STAB1(-), TAPBP, TLR4(-), TNC, TNFAIP3, TNFRSF11B, TNFRSF9, WAS1(-)*
Activation of antigen presenting cells	1.82E-05	*C3, CCL5, CCL7, CD74, CXCL10, FAS, HBP1(-),. HLA-C, IL1RL1, PSMBB, PSME1, RELB, SLC11A1, SPON2(-), TLR4(-)*
Infiltration of granulocytes	2.61E-05	*C3, CCL5, CXCL10, CXCL2, F2R(-), FAS, IL1RL1, NFKBIA, PPBP, RELA, SPP1(-), TLR4(-), TNFAIP3, TNFRSF9*
Activation of leukocytes	4.48E-05	*C3, CCL5, CCL13, CCL17, CCL7, CD74, CDKN1A, CXCL10, EGR3(-), FAS, FOS, HBP1(-), HDAC5(-), HLA-C, IL1RL1, NFKB2, PSMBB, PSME1, PTPN22, RELA, RELB, SLC11A1, SOCS2, SPON2(-), SPP1(-), TLR4(-), TNC, TNFRSF9*
Inflammation	8.18E-05	*C3, CASP4, CAV1(-), CCL13, CCL5, CXCL10, CXCL2, F2R(-), FAS, GRN(-), IL1RL1, MMP9, NFKBIA, PNKD, PPARD, RELA, RELB, SLC11A1, SPHK1, SPP1(-), TLR4(-), TNFAIP3, TNFRSF9*

Table 5.14: Functional annotations associated with cell mediated immune response assigned by IPA. Summary of the functional annotations from the IPA software, the associated molecules and p-values (-) denotes a gene which was down-regulated 8 hours after treatment with 10 ng/ml TNF-α

As anticipated, the functional annotations assigned by IPA to the genes up-or down-regulated by TNF-α were associated with both the inflammatory and immune response, with many genes, such as the chemokines *CCL13, CCL5, CCL7, CCL17, CXCL2* and *CXCL10* associated with many of the different function identified by the software. It should also be noted the some of the greatest fold changes were also associated with these genes, as was the case with chemokines up-regulated 2 hours after treatment with TNF-α. At this later tiempoint, the chemokine *CCL5* was up-regulated 6.5-fold. It is also noteworthy that the expression of the three chemokines which was up-regulated 2 afters after TNF-α treatment; *CCL13, CCL5* and *CXCL10*, remained high 8 hours after treatment with this stimulus. Moreover, as expected a number of these genes are also known to regulated by NF-κB, when cross-referenced with the website http://www.bu.edu/nf-kb/the-gilmore-lab/. These include those mentioned in section 5.4.4, as well as others including, the complement pathway component, C3, which is known to be essential for the cellular immune response (Moon et al., 1999), and also FAS and CASP4, both of which are known to have pro-apoptotic roles (Chan et al., 1999, Schauvliege et al., 2002).

As previously mentioned (section 5.1), the TNF-α-induced NF-κB response is known to be very important in the induction of cell death through the induction of genes such as FAS and CASP4. Once again, Dr Dan Swan used IPA software to generate networks based on the transcriptional response observed. In this particular case the network produced from the gene list in Table A.1, highlights the activation of cell death and immunological signalling (Figure 5.10). Hence it is important to follow up these results by assessing the effect of AG-014699 or PARP-1 siRNA on inflammatory genes such as FAS, following TNF-α in the qRT-PCR validation of these data.

The network in Figure 5.10 and the gene list in Table A.1 support the data obtained at the early timepoint following TNF-α treatment, in that there appears to be an up-regulation of the genes encoding the NF-κB subunits and pathway components 8 hours after TNF-α treatment. For example, at this later timepoint *NFKB2* is shown to be up-regulated 1.7-fold following treatment with TNF-α, whilst *RELB* is shown to up-regulated 2-fold, once again highlighting the complex feedback loops associated with the activation of NF-κB and associated pathway components.

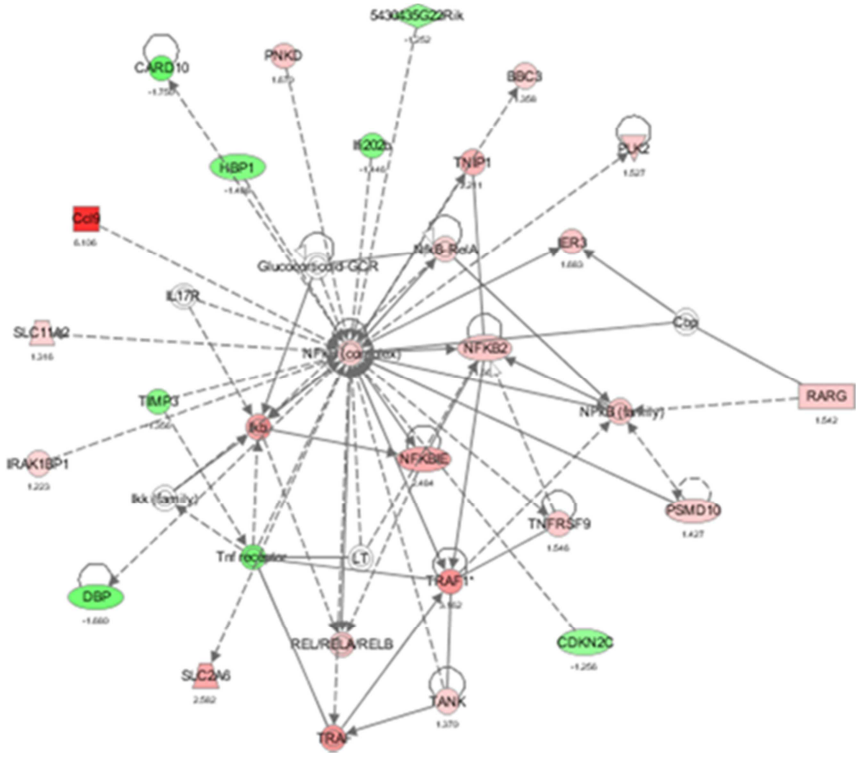

Figure 5.10: Genes associated with activation of cell death and immunological signalling. Canonical network generated by IPA with genes that were up-regulated (shown here in red) or down-regulated (shown here in green) in $p65^{+/+}$ MEFs 8 hours after treatment with 10 ng/ml TNF-α

Interestingly, the gene *PLK2*, which encodes the polo-like kinase 2 protein is up-regulated 1.5-fold 8 hours after treatment with TNF-α whereas the gene which encodes its family member polo-like kinase 1 was shown to be up-regulated 1.6-fold 2 hours after IR treatment. In the case of the latter the up-regulation observed was abrogated in the presence of AG-014699, suggesting that *PLK1*, like *PLK3* (Li et al., 2005), could be an NF-κB target gene. Therefore, further investigation into the induction of PLK2 using qRT-PCR should be undertaken.

5.4.8 Differentially expressed genes 8 hours following treatment with TNF-α versus TNF-α in combination with AG-014699

The data in Chapter 4 of this thesis has shown that the PARP inhibitor, AG-014699, had no effect on TNF-α-induced NF-κB DNA binding or NF-κB-dependent gene transcription, measured using a luciferase reporter assay in $p65^{+/+}$ MEFs, whereas PARP-1 siRNA inhibited TNF-α-induced DNA binding and luciferase activity in the same cells. Indicating that PARP-1 protein, but not its enzymatic activity was important

in activating NF-κB following the inflammatory stimulus. However, these data also showed that AG-014699 attenuated the observed IR-induced NF-κB DNA binding and transcriptional activation in the $p65^{+/+}$ MEFs, suggesting that the PARP inhibitor would be a viable therapeutic strategy in inhibiting DNA-damage-induced NF-κB, which is common in cancers, and is known to mediate therapeutic resistance (Prasad et al., 2010), without comprising the vital inflammatory functions of the transcription factor. This hypothesis was therefore tested at an early timepoint (2 hours) following treatment with TNF-α, (section 5.4.4) and it was found that that there were only three genes differentially expressed in the presence of AG-014699, when compared with TNF-α alone. This therefore suggests that AG-014699 in combination with TNF-α had no effect on any of the inflammatory or immune response associated genes compared with TNF-α, at this early timepoint, thus supporting the data in chapter 4. However, it was also important to test this hypothesis once more, at a later timepoint when the inflammatory gene expression was still found to be high (5.4.7).

Genespring GX 11 was utilised by Dr Dan Swan in order to generate to lists of genes differentially expressed 8 hours following treatment with 10 ng/ml TNF-α, compared with TNF-α in combination with AG-014699. Table 5.15 details a list of genes differentially expressed following treatment with TNF-α + AG-014699 as well as the accession/identification number and the fold change.

Gene	Symbol	ID	Fold change
Post-GPI attachment to proteins 2	*Pgap2*	NM_145583.2	1.290
Zinc finger, SWIM-type containing 3	*ZSWIM3*	NM_178375	-1.316

Table 5.15: Differentially expressed genes 8 hours following treatment with TNF-α + AG-014699 in $p65^{+/+}$ MEFs, compared with TNF-α alone

Table 5.15 shows that there were only two genes differentially expressed in the presence of AG-014699, when compared with TNF-α, in cells harvested 8 hours after treatment with the cytokine. This therefore suggests that AG-014699 in combination with TNF-α has no effect on any of the inflammatory or immune response associated genes compared with TNF-α, thus supporting the data in Chapter 4, and section 5.4.4 of this chapter, which showed that AG-014699 had no effect on TNF-α-induced NF-κB DNA binding or NF-κB-dependent gene transcription. It is however to further confirm these data using qRT-PCR, and assess the effect of PARP-1 siRNA on known NF-κB

regulated genes which were induced in this this array study. Therefore, a selection of NF-κB-dependent inflammatory and immune response genes, which showed large fold changes following TNF-α treatment in the $p65^{+/+}$ MEFs, were chosen for further investigation in this manner. Some of these genes showed an up-regulation at both timepoints after TNF-α treatment, and others at either the early or late timepoint. These are all listed in section 5.4.9.

5.4.9 Genes of interest identified for qRT-PCR validation

Table 5.16 details the genes of interest identified from the microarray analysis performed by Dr Dan Swan using Genespring GX 11 and IPA. The reasons for choosing each gene is discussed in the relevant sections (5.4.1-8), but is also briefly explained in Table 5.16.

Gene symbol	Timepoint	Reason
AURKA	2 h	Up-regulated expression 2 hours after IR treatment, which was abrogated in the presence of AG-014699
AURKAB	8 h	Up-regulated expression 8 hours after IR treatment. Interesting as associated family gene (AURKA) also up-regulated by IR
BIRC6	2 h	Up-regulated expression 2 hours after IR treatment, which was abrogated in the presence of AG-014699. IAP proteins are known to be NF-κB regulated following DNA damage (Stehlik et al., 1998, You et al., 1999)
CCL5	2 h/8 h	Up-regulated following TNF-α treatment, unaffected by AG-014699. Known NF-κB regulated gene (Wickremasinghe et al., 2004) Would PARP-1 siRNA alter TNF-α expression of this gene?
CDC20	2 h/ 8 h	Up-regulated expression 2 hours after IR treatment, which was abrogated is the presence of AG-014699
CXCL10	2 h/8 h	Up-regulated following TNF-α treatment, unaffected by AG-014699. Known NF-κB regulated gene (Hein et al., 1997) Would PARP-1 siRNA alter TNF-α expression of this gene?
FAS	8 h	Up-regulated following TNF-α treatment, unaffected by AG-014699. Known NF-κB regulated gene following TNF-α (Chan et al., 1999) Would PARP-1 siRNA alter TNF-α expression of this gene?
IRF-1	2 h	Down-regulated expression 2 hours after IR treatment, which was reversed in the presence of AG-014699. Up-regulated following TNF-α, but unaffected by AG-014699 after this stimulus. IRF1 is known to be NF-κB regulated following TNF-α, not DNA damage (Harada et al., 1994)
JUNB	2 h	Up-regulated expression 2 hours after IR treatment, which was abrogated in the presence of AG-014699. Also up-regulated following TNF-α, but unaffected by

		AG-014699 after this stimulus. JUNB is known to NF-κB regulated following inflammatory stimuli, not DNA damage (Brown et al., 1995)
PLK1	2 h	Up-regulated expression 2 hours after IR treatment, which was abrogated in the presence of AG-014699
PLK2	8 h	Up-regulated expression 8 hours after TNF-α treatment. Interesting as associated family gene (PLK1) was up-regulated by IR
TNIP1	2 h/ 8 h	Up-regulated expression 2 hours after IR treatment, which was abrogated in the presence of AG-014699 Up-regulated by TNF-α at both timepoints but unaffected by AG-014699 following this stimulus. Known NF-κB regulated gene following TNF-α (Heyninck et al., 1999)
TOP2A	2 h	Up-regulated expression 2 hours after IR treatment, which was abrogated in the presence of AG-014699

Table 5.16: A list of the interesting genes identified from the microarray data, with brief justifications

5.4.10 qRT-PCR validation of microarray genes of interest

In order to validate the microarray findings, the genes of interest (shown in Table 5.16, section 5.4.9) were also investigated using q-RT-PCR. Specifically, the induction or down-regulation of the chosen genes were assessed at the timepoints shown in Table 5.16 following either 10 Gy IR or 10 ng/ml TNF-α in the presence or absence of the PARP inhibitor, AG-014699 in the $p65^{+/+}$ MEFs. To further confirm whether the genes are truly regulated by NF-κB, siRNA targeting p65 or the pan IKK inhibitor, BAY11-7082 (Mori et al., 2002), was assessed as a direct comparison to AG-014699. Existing data, presented in Chapter 4 of this thesis showed that the physical presence of the PARP-1 protein is vital for the activation of NF-κB following TNF-α, hence PARP-1 siRNA or a non-specific (NS) control siRNA was also used in the qRT-PCR assays presented here. The knockdown of either p65 or PARP-1 in the $p65^{+/+}$ MEFs were previously optimised (Chapter 3).

This method is described in detail in section 2.10. For these assays; $p65^{+/+}$ MEFs were seeded and left for 24 h to adhere prior to transfection with 50 nM p65, PARP-1 or NS siRNA (or vehicle control). Cells were incubated left for 48 h, and pre-treated with either 0.4 μM AG-014699 or 10 μM BAY11-7082, (or DMSO control) for 1 h prior to treatment with 10 Gy IR or 10 ng/ml TNF-α. Cells were then harvested at the timepoints stated in Table 5.16 and RNA extracted using the RNeasy kit. RNA was subsequently transcribed into cDNA using the High Capacity cDNA reverse transcription kit,

according to manufacturers' instructions. cDNA was then used in a qRT-PCR reaction using Taqman primers to confidently quantify the mRNA levels of either *AURKA, AURKB, BIRC6, CDC20, CCL5, CXCL10, FAS, IRF1, JUNB, PLK1, PLK2, TNIP1, TOP2A* and the housekeeping gene *ACTN*, which encodes the β-actin protein, in each sample. All results shown are the mean of three independent experiments.

Table 5.17 briefly details the results from all of the qRT-PCR validation assays, and includes the fold change from the gene expression microarray, and also whether each gene was up- or down-regulated by either IR or TNF-α using qRT-PCR. Moreover, Table 5.17 the significance level (p value), obtained using unpaired Student's t-tests, for any up- or down-regulation is also included. The effect of p65 siRNA, AG-014699, BAY11-7082 or PARP-1 siRNA is also explained, where relevant. In all cases the qRT-PCR assays for the genes of interest that were validated have been included in Appendix A.

Gene	Array fold change	qRT-PCR fold change (IR)	qRT-PCR fold change (TNF-α)	Notes
AURKA	2.2 (IR 2 h)	2 (p=0.0006)	No change	IR induced expression of AURKA significantly inhibited in the presence of BAY11-7082
AURKB	1.2 (IR 8 h)	No change	No change	AURKB not regulated by NF-κB following either stimuli
BIRC6	1.2 (IR 2 h)	1.2 (p=0.027)	No change	IR induced expression of BIRC6 inhibited by p65 siRNA, AG-014699, BAY11-7082 or PARP-1 siRNA, although this was not significant
CCL5	3 (TNF-α 2 h) 6.5 (TNF-α 8 h)	No change at either timepoint	5 (p<0.0001) (2 h) 5.5 (p=0.0001) (8 h)	TNF-α induced expression of CCL5 significantly inhibited by p65 siRNA, BAY11-7082 or PARP-1 siRNA, but unaffected by AG-014699 at both timepoints
CXCL10	3.7 (TNF-α 2 h) 6 (TNF-α 8 h)	No change at either timepoint	6.5 (p=0.0005) (2 h) 5.5 (p=0.0002) (8 h)	TNF-α induced expression of CXCL10 significantly inhibited by p65 siRNA, BAY11-7082 or PARP-1 siRNA, but unaffected by AG-014699 at both timepoints
CDC20	1.5 (IR 2 h) 1.3 (IR 8 h)	1.4 (p=0.0016) (2 h) 1.4 (p=0.0257) (8 h)	No change at either timepoint	IR induced expression of CDC20 significantly inhibited by p65 siRNA, AG-014699, BAY11-7082 or PARP-1 siRNA, at the 2 h timepoint
FAS	3.6 (TNF-α 8 h)	No change	2.4 (p=0.027)	TNF-α induced expression of FAS inhibited by p65 siRNA, BAY11-7082 or PARP-1 siRNA (not significant), but unaffected by AG-014699
IRF1	-1.5 (IR 2 h) 2.8 (TNF-α 2 h)	-1.4 (p=0.0004)	2 (p=0.0003)	Reduction in IRF1 mRNA observed following treatment with IR alone or in combination with p65 siRNA or BAY11-7082, however IR in combination with AG-014699 or PARP-1 siRNA increased IRF1 expression back to levels comparable to untreated controls. TNF-α induced expression of IRF1 inhibited by p65 siRNA, BAY11-7082 or PARP-1 siRNA, but

				unaffected by AG-014699
JUNB	1.6 (IR 2 h) 1.9 (TNF-α 2 h)	No change	1.6 (p=0.041)	TNF-α induced expression of JUNB inhibited by p65 siRNAor BAY11-7082(not significant), but unaffected by AG-014699or PARP-1 siRNA
PLK1	1.6 (IR 2 h)	1.5 (p=0.0001)	No change	IR induced expression of PLK1 significantly inhibited by p65 siRNA, AG-014699, BAY11-7082 or PARP-1 siRNA
PLK2	1.5 (TNF-α 8 h)	No change	No change	PLK2 not regulated by NF-κB following either stimuli
TNIP1	1.6 (IR 2 h) 2.8 (TNF-α 2 h)	No change	2 (p=0.0046)	TNF-α induced expression of TNIP1 inhibited by p65 siRNA, BAY11-7082 or PARP-1 siRNA (not significant), but unaffected by AG-014699
TOP2A	1.6 (IR 2 h)	No change	No change	TOP2A not regulated by NF-κB following either stimuli

Table 5.17: Summary of qRT-PCR validation assays

Genes of interest identified from the gene expression microarray study, and the associated fold change from this study. Also the effect of either IR or TNF-α on these genes assessed using qRT-PCR and were relevant, the significance level (p value), obtained using unpaired Student's t-tests, for any up- or down-regulation is also included. The effect of p65 siRNA, AG-014699, BAY11-7082 or PARP-1 siRNA is also explained

5.5 Discussion

Gene expression profiling was utilised here in order to assess any changes in gene expression in $p65^{+/+}$ cells treated with IR *versus* cells treated with TNF-α, and furthermore to investigate the effect of the PARP inhibitor, AG-014699 on the transcriptional response to each agent. Two software packages, Genespring GX 11 and IPA were used by Dr Dan Swan at the Bioinformatics Service (Newcastle University) to aid in the identification of genes which were differentially expressed after treatment with either IR or TNF-α, and also assign functional information in the form of canonical pathways/processes which were affected by the transcriptional outcome of either agent.

It is well documented that inflammatory cytokines, such as TNF-α and IL-1β, induce an NF-κB-dependent transcriptional response associated with the up-regulation of many genes known to be essential for the immune and inflammatory responses (Pahl, 1999), and the array data in sections 5.3.3 and 5.3.7 support this existing literature. The canonical pathways and processes identified by IPA analysis included networks associated with immunological signalling and functional annotations, such as those involved in the immune response or inflammation were assigned. Importantly, further computational analysis indicated that these genes, including many cytokines and chemokines, were unaffected by co-incubation with AG-014699, suggesting that PARP inhibition did not affect the vital inflammatory functions of NF-κB transcriptional activation following TNF-α stimulation. This supported that data in chapter 4 of this thesis which found that PARP-1 protein was required for the activation of NF-κB p65 DNA binding and transcriptional activation following TNF-α treatment, whereas both PARP-1 protein and enzymatic activity were required for NF-κB activation following IR.

However, in order to further confirm these data, qRT-PCR analysis was performed on a selection of genes including the cytokines *CCL5* and *CXCL10*. In this case siRNA targeting either p65 or PARP-1 and the pan-IKK inhibitor BAY11-7082 (Mori et al., 2002) were used as a direct comparison to the PARP inhibitor, AG-014699, to assess the effects these other treatment would have on NF-κB-dependent gene expression. It must be noted that both array and qRT-PCR data show that the inflammatory response genes were unaffected by treatment with IR at the dose tested here. Importantly, the qRT-PCR data shows an induction of the known NF-κB-dependent inflammatory

response genes, including *CCL5* and *CXCL10* following treatment with TNF-α, supporting the both the array data and existing literature (Hein et al., 1997, Wickremasinghe et al., 2004). These data also show that TNF-α induced expression of these genes is inhibited by either p65 siRNA or the pan-IKK inhibitor, BAY11-7082, which has been shown to inhibit NF-κB activation *via* inhibition of the IKK complex components (Mori et al., 2002), further confirming that these genes are regulated by NF-κB in response to TNF-α stimulation. Markedly, PARP-1 siRNA is found to inhibit the TNF-α-induced expression of *CCL5* and *CXCL10* whereas the PARP inhibitor, AG-014699 had no effect, thus confirming the hypothesis that PARP-1 protein alone is essential for TNF-α-induced NF-κB activation perhaps facilitating a structural role in the NF-κB transcriptional complex. This is consistent with the work of Hassa *et al.*, (2001), which illustrated how the physical presence of the PARP-1 C-terminal catalytic domain, but not its enzymatic activity, was required for PARP-1 and p300 to synergistically activate NF-κB-dependent transcription following either TNF-α or LPS (Hassa et al., 2001).

The qRT-PCR data investigating the activation of *CXCL10* following TNF-α illustrated that PARP-1 protein knockdown could inhibit the TNF-α-induced up-regulation of this gene, suggesting that physical presence of PARP-1 at the *CXCL10* promoter facilitates the transcription of this particular gene. Interestingly, another group have reported that PARP-1 can regulate the transcription of known cytokines through sequence-specific binding to DNA regulatory elements. Amiri e*t al.,* (2006) found that inactive PARP-1 could bind to a DNA element in the *CXCL1* promoter and in this case act to block NF-κB to an adjacent element, thus repressing the transcription in this case. Furthermore, they showed that activation of PARP-1 (as has been shown to occur by DNA damage, but not by TNF-α in Chapter 4 of this thesis), leads to a loss of PARP-1 binding and enhanced *CXCL1* expression by virtue of increased access of NF-κB to the DNA (Amiri et al., 2006). Inactive PARP-1 in this case in the literature is analogous to the use of AG-014699 within this chapter, which was found to have no effect on a related family gene, CXCL10. This could be explained by the fact that two genes have related, but still distinct functions, as well as the fact that the data generated by Amiri and collegues was in a different cell line background, multiple myeloma, and it is well documented that NF-κB activation and consequently effects on gene transcription are very dependent on the stimulus and model system used.

The finding from the array study and the qRT-PCR analysis of key inflammatory cytokines has important implications for the wider use of AG-014699 in the inhibition of NF-κB activation for the treatment of cancer. These data have shown that the genes associated with the inflammatory response induced by NF-κB are unaffected by AG-014699. NF-κB inhibition is an attractive target for cancer therapeutics however, global inhibition for example with an IKK inhibitor, may have adverse effects. The IKK complex has many known functions within the cell (Carrillo et al., 2004, Chariot, 2009), meaning that inhibition of NF-κB in this manner might be cytotoxic. Moreover, long-term complete NF-κB inhibition may also increase the likelihood of immunodeficiency, since it plays a pivotal role in the innate and adaptive immune response, and can possibly delay bone marrow recovery due to some reports of chemotherapeutic induced apoptosis of hematopoietic progenitors (Grossmann et al., 1999, Turco et al., 2004). This could be even more of an issue in cancer patients which may already have a compromised immune system due to the nature of other therapeutic agents. The data here corroborate the data in Chapter 3 and 4 which suggested that blockade of DNA-damage activated NF-κB by AG-014699 could represent a viable therapeutic strategy, since the data has demonstrated that the survival function of NF-κB can be directly inhibited without compromising other functions, such as the immune response. The gene expression profiling and and subsequent confirmation by qRT-PCR within this chapter have shown that the vital inflammatory responses, known to be regulated by TNF-α-induced NF-κB activation, are still intact following treatment with AG-014699.

Interestingly, the array data here (sections 5.3.1 and 5.3.5) has shown that genes associated with cellular organisation and assembly, including those encoding the mitotic kinases, aurora kinase A (*AURKA*), aurora kinase B (*AURKB*), polo-like kinase 1 (*PLK1)* and polo-like kinase 2 (*PLK2*), (as well as many others) were up-regulated following treatment with IR. These genes have not previously been shown to be regulated by NF-κB, and were thus investigated further within this study. *AUKRA*, *PLK1* and also cell division cycle 20 (*CDC20*) were also investigated as these were up-regulated in $p65^{+/+}$ MEFs harvested after treatment with 10 Gy IR, and this affect was abrogated in the presence of AG-014699, suggesting that these might be novel NF-κB regulated genes following DNA damage. The associated kinases, *AURKB* and *PLK2* were up-regulated by IR and TNF-α, respectively, but unaffected by co-incubation with AG-014699 nonetheless these genes were investigated further due to their close functional relationships to other genes of interest.

Aurora kinase A is known to regulates a number of events from late S- to M-phase of the cell cycle, including centrosome maturation, separation and assembly, mitotic entry and exit, cytokinesis and bipolar spindle assembly (Berdnik and Knoblich, 2002, Hirota et al., 2003, Marumoto et al., 2003). Its kinase function is tightly regulated during the cell cycle, however overexpression or amplification of the *AURKA* gene is frequent in many tumour types (Goepfert et al., 2002, Sakakura et al., 2001, Tanaka et al., 1999b) and correlates with poor prognosis (Jeng et al., 2004). The oncogenic potential of *AURKA* activation was reported by Zhou *et al.*, (1998) who showed that the gene had transforming abilities both *in vitro* and *in vivo*, and also induced multipolar mitotic spindles resulting in genomic instability (Zhou et al., 1998).

Aurora kinase B is known to regulate kinetochore-microtubule attachment and also ensure faithful chromosome separation (Biggins and Murray, 2001). *AURKB* is also overexpressed in cancers including prostate, breast, lung and kidney (Katayama et al., 1999) and is known to be associated with errors in chromosomal segregation and cytokinesis, and chromosomes lagging in metaphase, thus contributing to carcinogenesis (Ota et al., 2002). Therefore aurora kinase inhibitors are generating a lot of interest in the field of cancer therapeutics, and the array data here indicated that *AURKA*, in particular, might be regulated *via* NF-κB following DNA damage, and consequently inhibited using AG-014699. However, although the qRT-PCR data showed that *AURKA* was up-regulated 2-fold following IR, co-incubation with AG-014699 did not inhibit the expression of this gene. Knockdown of p65 or PARP-1 also had no effect on the IR-induced expression of *AURKA*, but interestingly the pan-IKK inhibitor BAY11-7082 significantly decreased *AURKA* expression following IR. BAY11-7082 has been shown to inhibit all of the NF-κB subunits to some extent (Mori et al., 2002), and therefore it is plausible that *AURKA* is not a p65 target gene, but the target of perhaps of one of the one of the other NF-κB subunits. For example, E2F3a is known to be a target of c-Rel (Cheng et al., 2003). Another explanation for this phenomenon is that this is the result of an off target effect of BAY11-7082, which has been suggested previously (Mahadevan et al., 2011). This warrants further investigation, as discussed in section 5.6.

The polo-like- and aurora- kinases are cell cycle regulated, and in particular play vital roles in promotion in M-phase. It is therefore possible that in this study IR has arrested these $p65^{+/+}$ cells at the point, in late G_{2}- or early M-phase of the cell cycle, where both

PLK1 and AURKA are known to be highest, thus accounting for the increased mRNA levels of both of these genes. This does not however explain the effects observed by treatment with p65 siRNA or AG-014699 in the case of PLK1, or BAY11-7082 in the case of AURKA. Nevertheless, it would be interesting to determine whether in this case IR has arrested these the $p65^{+/+}$ MEFs at the timepoints chosen for this study, perhaps using FACs analysis.

CDC20, a homolog of *Saccharomyces cerevisiae* cell division cycle 20 protein, is vital in controlling the spindle checkpoint (Fang et al., 1998). Mammalian CDC20 interacts with the anaphase-promoting complex/cyclosome (APC/C), and is involved in anaphase onset and late mitotic events (Fung and Poon, 2005). A number of groups have shown that overexpression of CDC20 at the mRNA level is common in cancer (Kidokoro et al., 2008, Kim et al., 2005, Mondal et al., 2007). Furthermore, siRNA knockdown of CDC20 of various cancer cell lines resulted in a G_2/M arrest and consequently growth arrest (Kidokoro et al., 2008). The array data here indicated that *CDC20*, might be regulated *via* NF-κB following DNA damage, and consequently inhibited using AG-014699. The qRT-PCR support that array data in that they show that *CDC20* is up-regulated 2 hours after treatment with IR, and this up-regulation is attenuated by co-incubation with either p65 siRNA, BAY11-7082, AG-104699 or PARP-1 siRNA. Therefore, these data strongly indicate that *CDC20* is a novel NF-κB regulated gene following DNA damage at early timepoints. It should be noted that this phenomenon was not observed at the later, 8 hour, timepoint, as it had been in the array data. This warrants further investigation, and is discussed in section 5.6.

The family of polo-like kinases are also attractive targets for cancer therapeutics with a number of compounds in pre-clinical and clinical development (Degenhardt and Lampkin, 2010). They are a family of serine-threonine kinases associated with many of the functions associated with mitosis not only through phosphorylation activities but also *via* protein-protein interactions (Golsteyn et al., 1995). Overexpression of *PLK1* is common in cancer (Ito et al., 2004, Takahashi et al., 2003, Yamamoto et al., 2006), making it the main target for drug discovery at the moment, especially given that *PLK1* is only expressed in dividing cells (Golsteyn et al., 1995). Overexpression of *PLK1* is known to promote proliferation and has also been described as oncogenic as it has the ability to promote chromosome instability and aneuploidy *via* the regulation of cell cycle checkpoints (Musacchio and Salmon, 2007). Importantly, another member of

polo-like kinase family, *PLK3*, has been shown to be regulated by NF-κB (Li et al., 2005). The array data here indicated that *PLK1*, in particular might be regulated *via* NF-κB following DNA damage, and consequently inhibited using AG-014699. The qRT-PCR support that array data in that they show that *PLK1* is up-regulated following treatment with IR, and this up-regulation is attenuated by co-incubation with either p65 siRNA, BAY11-7082, AG-104699 or PARP-1 siRNA. Therefore, these data strongly indicate that PLK1 is a novel NF-κB regulated gene following DNA damage, and perhaps that through its inhibitory effects on NF-κB, AG-014699 is also reducing the DNA-damage-induced expression of the putative oncogene. This warrants further investigation, which is discussed in section 5.6.

Although array analyses showed that 8 hours after IR or TNF-α the expression of *AURKB* and *PLK2*, respectively, was induced, this was not corroborated when using qRT-PCR analyses. The dose of IR given to these $p65^{+/+}$ MEFs is very transient and it is well documented that the DNA damage response (DDR) is induced very quickly after treatment with this agent. For example, there have been a number of reports showing that the DDR is activated as quickly as 15 minutes or 1 hour after treatment with IR (Elliott et al., 2011). Therefore, the up-regulation observed in the array may perhaps be explained by the point of the cell cycle these cells were in at the time, as it has been demonstrated that the levels of the polo-like kinases oscillate during cell cycle progression (Golsteyn et al., 1995).

Array analysis also indicated that genes associated with the protection against apoptosis, such as *BIRC6*, encoding one of IAP family proteins, are up-regulated by IR. This was consistent with other reports suggesting that associated genes were regulated by NF-κB following IR (Stehlik et al., 1998, You et al., 1999). Furthermore, the array data showed that the up-regulation of *BIRC6* was attenuated in the presence of the PARP inhibitor AG-014699. These data were confirmed by the qRT-PCR validation assays, although the inhibition of IR-induced *BIRC6* by co-incubation with either p65 siRNA, BAY11-7082, AG-014699 or PARP-1 siRNA, was not statistically significant. These data highlight that AG-014699 inhibits DNA-damage-induced NF-κB anti-apoptotic gene transcription, thus supporting the survival data presented with this inhibitor in chapter 3.

NF-κB is also known to regulate genes associated with the induction of apoptosis, particularly following stimulation by TNF-α, and therefore it was important to determine whether AG-014699 was having an effect on these genes following treatment

with the cytokine. Previous reports have shown that TNF-α-induced NF-κB activation up-regulated the expression of the Fas receptor (Chan et al., 1999) and its ligand (Matsui et al., 1998), both of which are known induce apoptosis. Data from the gene expression profiling showed that the *FAS* gene was unaffected by treatment with IR alone, or in combination with AG-014699 but, that as expected, TNF-α induced the expression of the pro-apoptotic gene. Importantly the induction of this gene was unaffected in the presence of AG-014699. These data were also corroborated by the qRT-PCR validation, with TNF-α inducing the expression of *FAS*, and this induction being inhibited by co-incubation with p65 siRNA, BAY11-7082 or PARP-1 siRNA. Once again, AG-014699 had no effect, supporting the previous finding that PARP inhibition does not affect TNF-α-induced NF-κB-dependent gene transcription, and most markedly in this case, AG-014699 does not inhibit the induction of vital pro-apoptotic genes.

IRF1 is a nuclear transcription factor which is known to regulate genes associated with the inflammatory and immune responses (Kroger et al., 2002), and also genes which promote apoptosis, including the caspases 3, 7 and 8 (Bouker et al., 2005, Sanceau et al., 2000). Microarray data showed that *IRF1* gene expression was up-regulated following TNF-α treatment (section 5.3.4) but down-regulated following treatment with IR (section 5.3.1). Validation using qRT-PCR assays supported the microarray data following TNF-α, showing that IRF1 expression was induced following stimulation by the cytokine. Furthermore, co-incubation with either p65 siRNA or BAY11-7082 attenuated the TNF-α-induced up-regulation of *IRF1*, thus corroborating the existing literature which states that IRF1 is an NF-κB-regulated gene following inflammatory stimuli (Harada et al., 1994, Robinson et al., 2006).

Validation of the microarray data which showed that *IRF1* expression was down-regulated 2 hours after treatment with IR (section 5.4.1) but up-regulated following co-incubation with AG-014699, supported these data to some extent. qRT-PCR assays illustrated that there was a small but significant decrease in *IRF1* expression following treatment with IR. Interestingly, a report in the literature states that the IRF1 transcription factor is activated following DNA-damage and promotes apoptosis through the up-regulation of caspase-1 in T lymphocytes (Tamura et al., 1995). The qRT-PCR data here also show that the IR-induced decrease in IRF1 expression was unaffected by co-incubation with p65 siRNA or BAY11-7082, suggesting that this gene

is not regulated by NF-κB following DNA damage. Importantly, IR in combination with AG-014699 or PARP-1 siRNA significantly increased the transcript levels of IRF1 compared with IR alone, suggesting that PARP-1 protein and activity are important for the activation of this gene. One explanation is that *IRF1* may be under the transcriptional control of one of the other transcription factors, for which PARP-1 is known to have a role as a co-activator. For example, there is one report suggesting that *IRF1* expression may be regulated by Sp1 (Sanceau et al., 1995), and other reports have suggested that PARP-1 is a co-activator of the transcription factor, Sp1 (Zaniolo et al., 2007).

Microarray data showed that the *JUNB* gene expression was up-regulated following TNF-α treatment (section 5.3.4) and also following treatment with IR (section 5.3.1). Validation using qRT-PCR assays supported the microarray data following TNF-α, showing that *JUNB* expression was induced following stimulation by the cytokine. Furthermore, co-incubation with either p65 siRNA or BAY11-7082 inhibited this TNF-α-induced up-regulation of *JUNB*, although this was not statistically significant. These data do support the existing literature which shows that *JUNB* is an NF-κB-regulated gene following inflammatory stimuli (Brown et al., 1995). However, qRT-PCR validation assays did not support the microarray data following IR, as they showed that *JUNB* expression was unaffected following the DNA damaging agent.

Microarray data (section 5.4.1) showed that the gene *TOP2A* which encodes the topoisomerase (DNA) II alpha was up-regulated 1.6-fold 2 hours after treatment with IR, but appeared to be unaffected by treatment with TNF-α. However, although qRT-PCR analysis showed that *TOP2A* expression was unaffected was TNF-α in the $p65^{+/+}$ MEFs, qRT-PCR data did not corroborate the microarray data following IR, suggesting that the expression of *TOP2A* was unchanged following DNA damage. The discordance of these results may be explained by the decreased sensitivity of the microarray *per se* or by the relatively low expression levels of this gene in the initial array analysis.

5.6 Summary and future work

Interestingly, this study has identified genes which could potentially be novel NF-κB regulated genes following IR, however these data require much further confirmation. Intriguingly, these genes include *PLK1*, *CDC20* and *AURKA*, all of which are

associated with the cellular assembly and organisation. The most interesting genes are *PLK1* and *CDC20,* both of which have been implicated in the progression of cancer (Kidokoro et al., 2008, Kim et al., 2005, Mondal et al., 2007, Musacchio and Salmon, 2007) which were both up-regulated following IR. This up-regulation was reduced in the presence of either p65 siRNA, BAY11-7082, AG-014699 or PARP-1 siRNA. However, in order to further confirm these results chromatin immune-precipitation (ChIP) assays should be undertaken to determine whether NF-κB can interact with the promoters of the *PLK1* or *CDC20* genes.

Analysis of the protein expression of PLK1 and CDC20 following IR alone or in combination with p65 siRNA, BAY11-7082, AG-014699 or PARP-1 siRNA should also be undertaken. This is essential, because one of the major limitations of gene expression profiling can be that changes at the mRNA levels do not always translate to the protein level, as proteins may be subject to post-translational modifications, or targeted for degradation. To this end the fold changes observed within this study are relatively small (approximately 1.5-fold for these genes of interest), and thus observing this at the protein level might be difficult.

The other gene of interest which was identified was AURKA, which encodes the aurora kinase B protein. In this case the qRT-PCR data illustrated that this gene was up-regulated 2-fold following IR treatment and intriguingly that this affect abrogated in the presence of BAY11-7082, but not p65 siRNA, AG-014699 or PARP-1 siRNA. In order to determine whether this is a true NF-κB-mediated affect, and not a result of BAY11-7082 having off target effects, knockdown of the other NF-κB subunits should be undertaken and the qRT-PCR assay repeated using following this. This should provide insight into whether AURKA is a target of one of the other NF-κB subunits, for example p52, rather than p65, following DNA damage.

The gene expression profiling and subsequent confirmation by qRT-PCR within this chapter have shown that the vital inflammatory responses, known to be regulated by TNF-α-induced NF-κB activation, are still intact following treatment with AG-014699. These data have very important implications for the wider use of AG-014699 in the inhibition of NF-κB activation for the treatment of cancer, due to the fact that NF-κB inhibition is an attractive target for cancer therapeutics. Reports have suggested that long-term global inhibition for example with an IKK inhibitor, may have adverse

effects, such as increased likelihood of immunodeficiency (Grossmann et al., 1999, Turco et al., 2004), which could be a significant problem for cancer patients which may already have a compromised immune system due to the nature of other therapeutic agents. Importantly, the data here support that in Chapter 3 and 4 which suggest that blockade of DNA-damage activated NF-κB by AG-014699 could represent a viable therapeutic strategy, since the data have demonstrated that the survival function of NF-κB can be directly inhibited, using AG-014699, without compromising other functions, such as the immune response.

Chapter 6: Investigation into the potential utility of AG-014699 inhibiting DNA-damage-induced NF-κB activation in cancer cell line models

6.1 Introduction

There have been numerous reports that have detailed the use of PARP inhibitors to chemo- and radio-sensitise cancer cell lines, xenograft models and primary samples (Drew and Plummer, 2009). It is widely accepted that these effects are due to the inhibition of DNA repair, specifically single strand break repair. This is very likely to be the case in terms of the use of PARP inhibitors as a mono-therapy for BRCA-deficient or –mutant breast or ovarian cancers (Bryant et al., 2005, Farmer et al., 2005). However, data in chapter 3 of this thesis suggests that PARP inhibition by AG-014699, can re-sensitise cells to irradiation and that this is mediated directly *via* NF-κB, rather than the widely reported inhibition of SSB repair. These data were generated using $p65^{+/+}$ and $p65^{-/-}$ MEFs and this therefore needs to be further investigated within this chapter using other model systems and in the context of the existing literature.

Radio-therapy is widely used in many major therapeutic regimens used in the treatment of cancers, including glioblastoma, breast and lung cancer. IR induces both SSBs and double strand breaks, thus activating PARP-1, and consequently activating cellular DNA repair pathways. Hence, the ability of PARP inhibitors to radio-sensitise cancer cells has been assessed by a number of groups. Studies have shown radio-sensitisation *in vitro* in a wide range of cell types including human colorectal cancer, lung cancer and murine sarcoma (Albert et al., 2007, Brock et al., 2004, Calabrese et al., 2004, Donawho et al., 2007). *In vivo* radio-sensitisation has also been observed in xenograft models of glioblastoma, lung cancer and colon cancer (Calabrese et al., 2004, Donawho et al., 2007).

The ability of PARP inhibitors to chemo-sensitise has been assessed using a variety of agents. Combination studies using various PARP inhibitors with the alkylating agent temozolomide (TMZ) have been undertaken in a range of cellular backgrounds, including human lung cancer cell lines, colorectal cancer cell lines and glioblastoma and medulloblastoma cell lines and xenografts (Calabrese et al., 2004, Chalmers, 2009, Chalmers, 2010, Daniel et al., 2009). These studies have shown pronounced chemo-sensitisation *in vitro* and tumour growth inhibition *in vivo*. PARP inhibitors have also been used in combination with the topoisomerase I poisons, topotecan and irinotecan, and similar results to those seen with TMZ have been reported, in lung, colorectal, breast, and ovarian cancer cell lines, as well as lung, colorectal, ovarian and prostate cancer xenograft models (Cheng et al., 2005, Smith et al., 2005). A synergism between

the Abbott laboratories PARP inhibitor, ABT-888, was observed with cisplatin, carboplatin and cyclophosphamide in murine melanoma, rat glioma, human B-cell lymphoma and breast cancer cells (Donawho et al., 2007).

Many of the model systems used to investigate the role of PARP inhibitors in chemo- or radio-sensitisation are known to have constitutive- or inducible- NF-κB activation. For example, aberrant activation of NF-κB is known to play a role in the tumourigenesis of both diffuse and high-grade gliomas (Kanzawa et al., 2003, Wang et al., 2004). Elevated NF-κB DNA binding activity has been demonstrated both in breast cancer cell lines and primary breast cancer tissues (Biswas et al., 2004, Nakshatri et al., 1997, Sovak et al., 1997), and shown to contribute to malignant progression through the regulation of gene expression. Constitutive NF-κB activation in all of these tumours types has been associated with chemo- and radio-resistance as well as an increased metastatic potential (Prasad et al., 2010). Thus, inhibition of NF-κB represents a promising therapeutic strategy for many different types of cancer.

6.2 Aims

Data presented in Chapter 3 of this thesis suggests that PARP inhibition by AG-014699 can re-sensitise cells to irradiation and that this is mediated, in part, *via* NF-κB, rather than just by the inhibition of SSB repair, as previously thought. These data were generated with $p65^{+/+}$ and $p65^{-/-}$ MEFs, and there are caveats associated with using these cells lines, not least that these are murine and not human cells. Therefore one aim of this chapter was to further investigate the hypothesis that radio-sensitisation observed with AG-014699 is due, in part, to the inhibition of NF-κB activation. In order to do this, cancer cell line models will be utilised that have previously been shown to be radio-sensitised by PARP inhibition. This chapter will therefore also explore potential tumour models in which the use of PARP inhibitors may be beneficial, for example tumours in which radio-therapy is a major part of the therapeutic regimen. It is also important to investigate the role of PARP-1 in NF-κB activation following other DNA-damaging agents, such as TMZ. PARP inhibition has been shown to sensitise cells to this agent (Calabrese et al., 2004, Daniel et al., 2009). Hence, this chapter will investigate the potential for AG-014699 to inhibit TMZ-induced NF-κB activation in a cell line model, in which this chemo-therapeutic agent is widely used, both alone and in combination with radio-therapy.

6.3 Results

6.3.1 IR-induced nuclear translocation of NF-κB p65 in glioblastoma cell lines

Initially, it was important to choose a type of cancer in which to study the effects of AG-014699 on DNA-damage-induced NF-κB activation. Glioblastoma was chosen because there are a number of reports that detail both radio- and chemo-sensitisation by PARP inhibitors, in both cell line and xenograft models of the disease (Chalmers, 2010). However, these reports showed that this was due to the inhibition of SSB repair, and other mechanistic investigations were not undertaken. There are also reports which suggested that aberrant activation of NF-κB played an important role in the tumourigenesis of both diffuse and high-grade gliomas (Kanzawa et al., 2003, Wang et al., 2004). Taken together, this made glioblastoma, in which cell line models were readily available, an obvious choice for further study in this chapter.

Firstly, it was essential to determine whether any of the three cell lines, U251, MO59J or MO59J-Fus-1, had constitutive activation of NF-κB p65, and most importantly whether p65 was further inducible by treatment with IR. At this stage, it was decided that concentrating on the p65 subunit was most relevant as all of the other data generated the Chapter 3 and 4 of this thesis had centred on p65, by virtue of access to the $p65^{+/+}$ and $p65^{-/-}$ MEFs. In order to investigate the activation of NF-κB p65 by IR, an assessment of p65 nuclear translocation following the DNA-damaging agent was undertaken. Briefly, U251, MO59J or MO59J-Fus-1 cells were seeded and allowed to adhere for 24 h before treatment with either 2 Gy or 10 Gy IR. Previous data (Chapter 4) would suggest that the response to IR would be rapid, hence cells were harvested at early timepoints (0 and 2 h). Nuclear extracts were prepared (section 2.5.2) and the levels of p65, Lamin or β-actin were determined by Western analyses in nuclear extracts from all three cell lines. Densiometric analysis was used to assess the levels of p65 compared to the nuclear protein, Lamin. β-actin was used as a control in order to ensure that there was no cytoplasmic contamination of the nuclear extracts.

Figure 6.1A illustrates that p65 is translocated to the nucleus of U251 cells at early timepoints following IR, and that this translocation is concentration-dependent. Nuclear translocation of p65 in these cells is induced 1.8-fold immediately following 10 Gy IR, and approximately 2.2-fold 2 h following 10 Gy IR. The blots shown are representative of three experiments whilst the densiotometry data is the mean of three, hence allowing statistical analysis to be performed. Unpaired Student's t-tests indicated that there is a

significant increase of p65 in the nucleus of U251 following 10 Gy IR at the 0 h and 2 h timepoints (p=0.0016 and p=0.024, respectively). Figure 6.1B shows that p65 nuclear translocation was induced by both 2 Gy and 10 Gy in the MO59J-Fus-1 cells, but that the greatest increase in nuclear p65 levels was observed immediately after treatment with IR (2.2-fold following 2 Gy IR and 2.6-fold following 10 Gy). Unfortunately, due to time constraints, the experiments with the MO59J and Fus-1 cells were not repeated, therefore statistical analyses could not be performed. Interestingly, p65 nuclear translocation following IR was not observed in the MO59J cells (Figure 6.1C), although this is not surprising. The MO59J cells lack DNA-PK (Lees-Miller et al., 1995), and this protein is not only vital for the DNA-damage response (Smith and Jackson, 1999) but has also been implicated in the activation of NF-κB (Basu et al., 1998, Ju et al., 2010, Liu et al., 1998, Panta et al., 2004). This is will be discussed later.

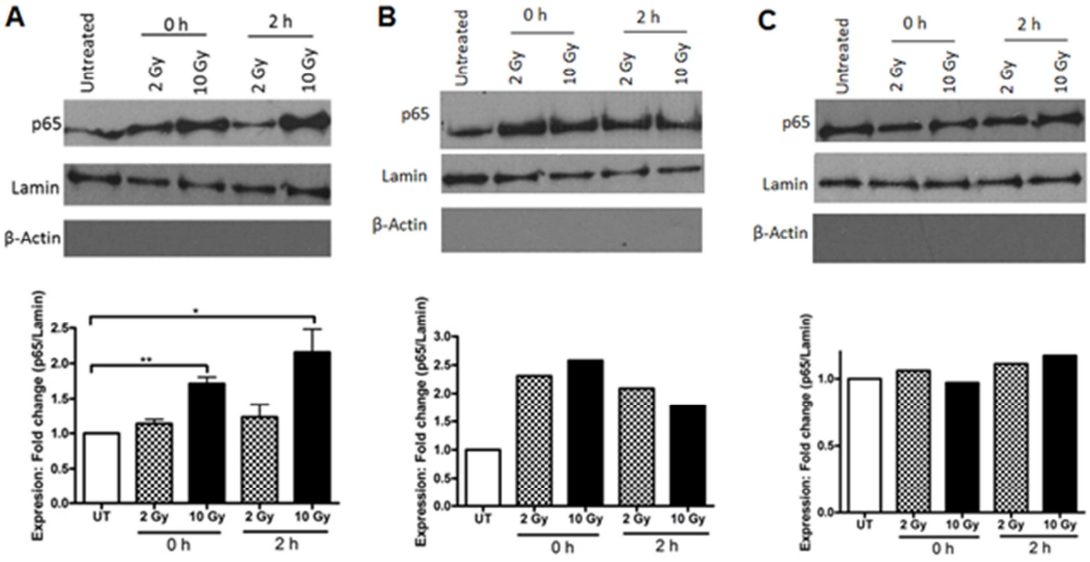

Figure 6.1: p65 nuclear translocation by IR in gliobastoma cells
Western blotting data and bar charts showing nuclear translocation of p65 and densiometric analysis, following IR in three glioblastoma cell lines (**A**) U251, (**B**) MO59J-Fus-1 and (**C**) MO59J. Cells were harvested 0 or 2 h post-IR and nuclear extracts prepared. Loading was normalised to lamin nuclear loading control in all cases. Nuclear extracts were shown to be free of any cytoplasmic contamination by blotting with β-Actin antibody. Densiotometry was used to assess the levels of p65 compared to the nuclear protein and fold change in p65 expression levels are shown in the bar charts below the relevant Western blot

6.3.2 Knockdown of target proteins using siRNA technology in U251 cells

Since p65 nuclear translocation was significantly induced by IR in U251 cells (Figure 6.2), this cell line was used to further investigate the role of PARP-1 in the activation of NF-κB, for a number of reasons. The MO59J cells did not show any p65 activation

following IR and are from a glioblastoma tumour lacking DNA-PK (Lees-Miller et al., 1995). The role of DNA-PK in the DNA-damage and NF-κB-responses is also discussed in section 6.3.1, suggesting that this cell line model was not suitable for further study in this chapter. The MO59J-Fus-1 cells (Hoppe et al., 2000) are a derivative of the MO59J cells in which chromosome 8, (on which DNA-PK is located, (Sipley et al., 1995)), has been re-introduced, in its entirety. Hence, these cells are likely to have multiple copies of many genes found on chromosome 8, and are not be optimal for this study, the U251 cells were used.

siRNA targeting either p65 or PARP-1 were used to silence each of the proteins in the U251 cells, in order to use knockdown of p65 or PARP-1 in direct comparison with AG-01699, as had been done previously in the $p65^{+/+}$, $p65^{-/-}$, $PARP\text{-}1^{+/+}$ and $PARP\text{-}1^{-/-}$ MEFs. U251 cells were incubated for 24 h prior to lipid transfection with 50 nM of siRNA oligos targeting either p65 or PARP-1, or a non-specific (NS) control (Table 2.2). Cells were harvested 48 h later and whole cell extracts were prepared (section 2.5.1) It should be noted that this concentration of siRNA and timepoint were chosen as these conditions had been optimal in other cell lines (Chapter 3). The levels of p65 or PARP-1 were determined by Western analyses and densiometric analysis was used to assess the knockdown compared to β-actin.

Figure 6.2A shows that a reproducible significant reduction in p65 protein expression (> 95%) was observed in the U251 cells ($p<0.0001$, compared with untreated controls, unpaired Student's t-test). Similarly, a reproducible knockdown of PARP-1, (> 97 %), was achieved ($p<0.0001$) (Figure 6.2B). Importantly, there were no significant differences in p65 or PARP-1 protein expression between the control NS siRNA and untreated control cell extracts.

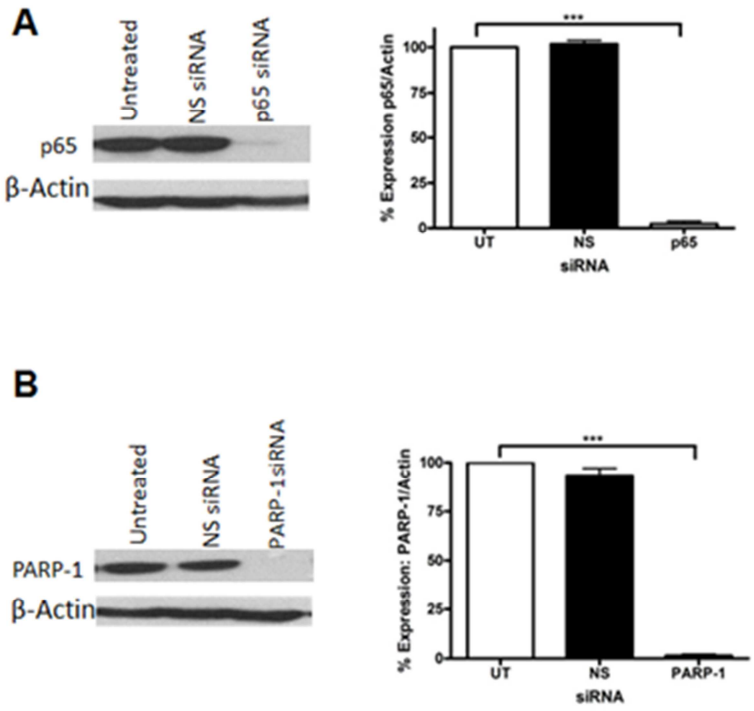

<u>Figure 6.2:</u> siRNA knockdown of p65 and PARP-1 in U251 cells
(**A**) Western blot and quantification of densiotometry of whole cell extracts of U251 cells at 48 h after transfection with vehicle alone (untreated), non-specific (NS) siRNA or p65 siRNA. p65 protein expression in U251 cells expressed as a percentage of Mock treated cells. (**B**)Western blot of whole cell extracts of U251 cells at 48 h after transfection with vehicle alone (untreated), NS siRNA or PARP-1 siRNA. PARP-1 protein expression in U251 cells expressed as a percentage of Mock treated cells.
Results shown are the mean + SEM of 3 independent experiments. *** Significance relative to Mock transfected control was $p<0.0001$ using Student's unpaired t-tests.

6.3.3 Radio-sensitisation by p65 knockdown, PARP-1 knockdown or AG-014699

It was important to determine what effects these treatments, and AG-104699 had on cell survival, in combination with IR. Previous data (Chapter 3) and other reports using a PARP inhibitor in glioblastoma cells (Chalmers et al., 2004, Cheng et al., 2005, Dungey et al., 2009) suggest that a radio-sensitisation would be expected. Therefore, this was investigated using classical colony forming assays (section 2.2.7). This assay would use a range of doses of IR and compare this to either to a fixed concentration of AG-014699, or siRNA in combination with IR.

U251 cells were incubated for 24 h before transfection with 50 nM p65 or 50 nM PARP-1 siRNA, (or vehicle control). Cells were then left for 48 h, and pre-treated with AG-014699, or DMSO control 1 h prior to treatment with increasing doses of IR before

being re-plated after a further 24 h and allowed to form colonies for 7-21 days (Figure 6.3).

The data here show that the U251 cells are quite resistant to IR alone, consistent with reports that the aberrant activation of NF-κB can lead to radio-resistance (Criswell Oncogene 2003). Furthermore, Figure 6.3 illustrates that co-incubation with IR and either AG-014699, p65 siRNA or PARP-1 siRNA reduced survival of the U251 cells by 2.5-fold compared with IR alone. The unpaired Student's t-test confirm that, at the LD_{50} values (lethal dose which reduces survival to 50 %) AG-014699, p65 or PARP-1 siRNA significantly radio-sensitised the U251 cells compared with IR alone ($p=0.0002$, $p<0.0001$ and $p=0.0004$, respectively). Importantly, a co-incubation with p65 and AG-014699 in combination with IR, did not further reduce U251 cell survival compared with either agent alone, confirming previous data (Chapter 3), suggesting that NF-κB and PARP-1 are mechanistically linked in a common pathway.

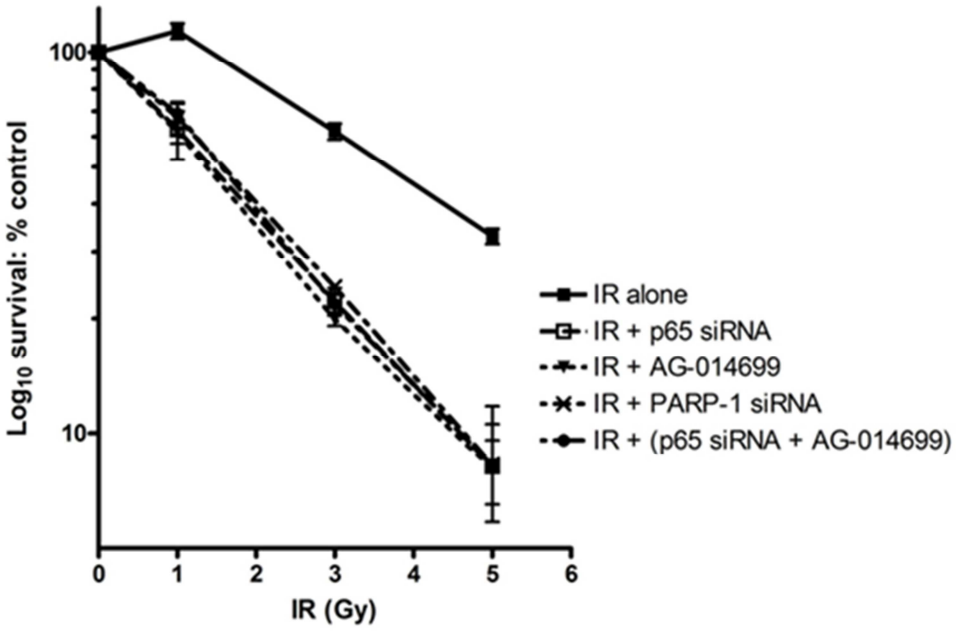

Figure 6.3: Radio-sensitisation of U251 cells by p65 knockdown, PARP-1 knockdown or AG-014699

The effects of increasing doses of IR either alone, or co-incubated with p65 siRNA, AG-014699, PARP-1 siRNA or a combination of p65 siRNA and AG-014699, on cell survival were assessed using the clonogenic survival assay. Cells were treated with relevant siRNA, (or vehicle control), incubated for 48 h, pre-treated with AG-014699, or DMSO control 1 h prior to IR then re-plated after a further 24 h and allowed to form colonies for 7-21 days. Results shown are the mean + SEM of three independent experiments

6.3.4 NF-κB activation following IR in U251 cells is time dependent

In order to confirm that the results observed in the clonogenic assays (Figure 6.3) were in fact due to the effect of AG-014699 on NF-κB activation, the effects of AG-104699, p65 siRNA and PARP-1 siRNA on NF-κB DNA binding were assessed. Although a timecourse for the activation of IR-induced p65 DNA binding had been determined for the MEFs (Chapter 4), it was necessary to determine the peak activation of both p65 and p50 following 10 Gy IR (the dose shown to induce nuclear translocation of p65 at early timepoints, section 6.3.1).

Exponentially growing U251 cells treated with 10 Gy IR. Cells were harvested at various timepoints (0, 2, 4, 6,8 24 h), and nuclear extracts were prepared and assessed on the ELISA assay (section 2.8).

Figures 6.4A and 6.4B illustrate that DNA binding of both p65 and p50 increased immediately following IR when compared with untreated controls (p=0.044 and p=0.0087, respectively, unpaired Student's t-test). Moreover, in the case of both p65 and p50, DNA binding was maximal 2 h following treatment with IR (p=0.0006 and p=0.0093, compared with untreated controls, unpaired Student's t-test). DNA binding of both subunits was still significantly increased 4 h after treatment with 10 Gy IR and in both cases DNA binding activity returns to basal levels 24 h post treatment.

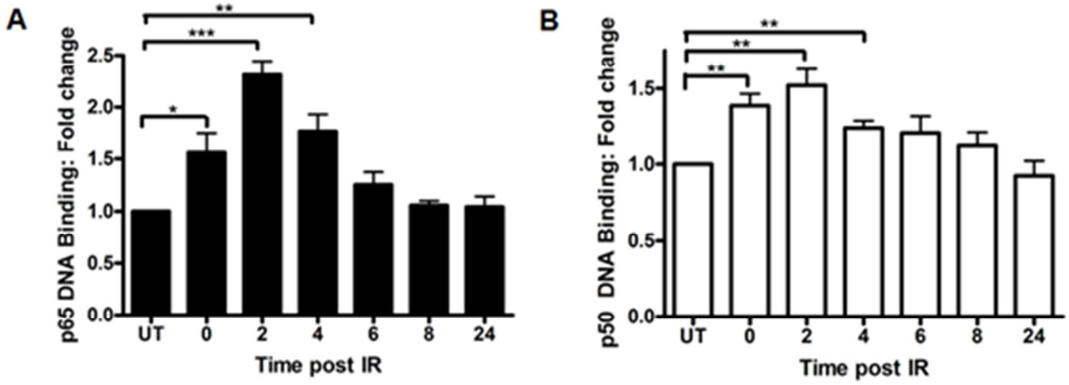

Figure 6.4: Maximal activation of NF-κB p65 or p50 by IR is 2 h post-treatment
Bar charts showing the effects of IR over time on NF-κB p65 (**A**) or p50 (**B**) DNA binding activity in U251 cells. Cells were treated with 10 Gy IR and nuclear extract prepared at various timepoints before measurement in an ELISA-based assay. All results are the mean of three independent experiments with SEM. Significance relative to mock treated control using unpaired Student's t-test *** $p<0.001$, ** $p<0.01$, * $p<0.05$

6.3.5 NF-κB p65 DNA binding requires PARP protein and enzymatic activity following IR, whereas p50 DNA binding requires PARP-1 protein alone

The ELISA was utilised to assess the effects of AG-014699, p65 or PARP-1 siRNA on IR-induced NF-κB DNA binding. U251 cells were incubated for 24 h prior to transfection with 50 nM p65, PARP-1 or NS siRNA (or vehicle control). Cells were then left for 48 h, and pre-treated with AG-014699, or DMSO control 1 h prior to treatment with 10 Gy IR. Cells were harvested 2 h later, nuclear extracts were prepared and loaded onto the ELISA-plates.

Figure 6.5A shows that 10 Gy IR significantly increased p65 DNA binding compared with mock treated controls (p=0.0012, unpaired Student's t-test), and that co-incubation with p65 siRNA, AG-014699 or PARP-1 siRNA reduced this IR-dependent increase in p65 DNA binding (p65 siRNA; p=0.0002, AG-014699; p=0.0043, PARP-1 siRNA; 0.0035, compared to IR). Markedly, a combination of p65 siRNA and AG-014699 did not further decrease IR-induced p65 DNA binding compared to either agent alone, confirming the survival data which suggested that NF-κB and p65 are linked in a common pathway. Importantly, NS siRNA had no effect on IR-induced p65 DNA binding when compared with IR alone (p=0.981).

Figure 6.5B shows that 10 Gy IR significantly increased p50 DNA binding compared with mock treated controls (p=0.016, unpaired Student's t-test). Both p65 and PARP-1 siRNA clearly inhibit IR-induced p50 DNA binding, but the outcome is just below the level of significance (p=0.078 and p=0.076, compared to IR in combination with NS siRNA). This observation is not due to the transfection process, since NS siRNA had no effect on IR-induced p50 DNA binding when compared with IR alone (p=0.641). Interestingly, AG-014699 alone or in combination with p65 siRNA had no effect on IR-induced p50 DNA binding when compared with IR in combination with NS siRNA (p=0.653 and p=0.834, respectively).

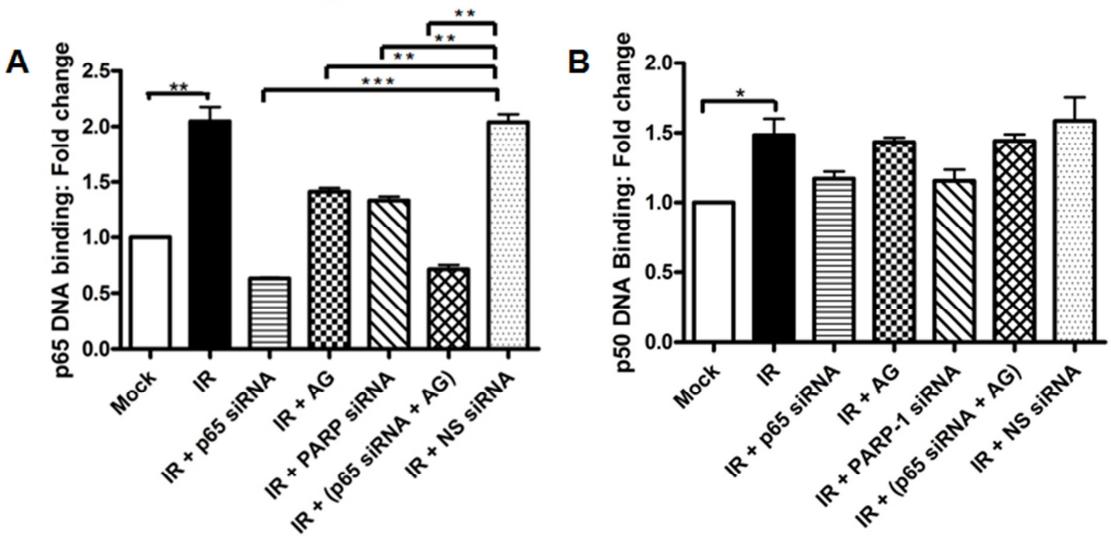

Figure 6.5: PARP-1 protein and enzymatic activity are required for activation of p65 DNA binding following IR whereas p65 or PARP-1 protein knockdown inhibit IR-induced p50

Bar chart showing the effect of IR ± p65 siRNA ± AG-014699 ± PARP-1 siRNA ± Non-specific (NS) siRNA control on IR-induced NF-κB (A) p65 or (B) p50 DNA binding, measured using an ELISA-based assay, in U251 cells. All results are the mean of three independent experiments with SEM. Significance relative to NS siRNA control using unpaired Student's t-test *** $p<0.001$, ** $p<0.01$

6.3.6 AG-014699 inhibits Single strand break (SSB) repair to a similar extent regardless of cellular NF-κB status in U251 cells

Previous data (Chapter 3), generated using the $p65^{+/+}$ and $p65^{-/-}$ MEFs, showed that both of those cell lines had the same level of SSBs immediately following IR, and that the repair of SSBs kinetics were identical in both sets of MEFs (section 3.3.5), regardless of their differing p65 status. Most importantly however, AG-014699 inhibited SSB repair to the same extent in both of these cell lines but radio-sensitisation by the PARP inhibitor was only observed in the $p65^{+/+}$ cells. This leads to the hypothesis that radio-sensitisation by AG-014699 was mediated by inhibition of NF-κB activation, and independent of the role PARP inhibitors play in the inhibition of DNA repair. In order to confirm these novel data, it was decided to undertake a similar approach in the U251 cells, utilising p65 siRNA (shown in Figure 6.7).

The alkaline Comet assay was used to measure SSB as described previously (section 2.7). U251 cells were incubated overnight before transfection with 50 nM p65 siRNA or vehicle control. Cells were then left for 48 h, and pre-treated with AG-014699, or DMSO control 1 h prior to treatment with 10 Gy IR. Cells were harvested at various

timepoints following IR and the alkaline comet assay undertaken as described in section 2.7.

Figure 6.6A *versus* 6.6B shows that the number of SSBs is greatest immediately following IR, and importantly that the olive tail moment is very similar, regardless of the p65 status of the cells. These scatter plots also illustrate that all breaks are repaired 30 minutes following irradiation. Markedly, there was no significant difference in the SSB levels remaining in the presence of absence of p65 siRNA 30 min post-IR, with > 90 % of breaks repaired. AG-014699 inhibited SSB repair (as demonstrated by increased residual SSB levels at all time-points post-IR) to the same extent regardless of whether p65 was present or not. The kinetics of SSB repair clearly show that the SSBs generated by IR are repaired rapidly over time and that in both cell populations the kinetics of repair were very similar. Furthermore, regardless of p65 status, cells pre-treated with AG-014699 prior to treatment with IR, have slower repair kinetics, thus supporting the earlier observations in the $p65^{+/+}$ and $p65^{-/-}$ MEFs.

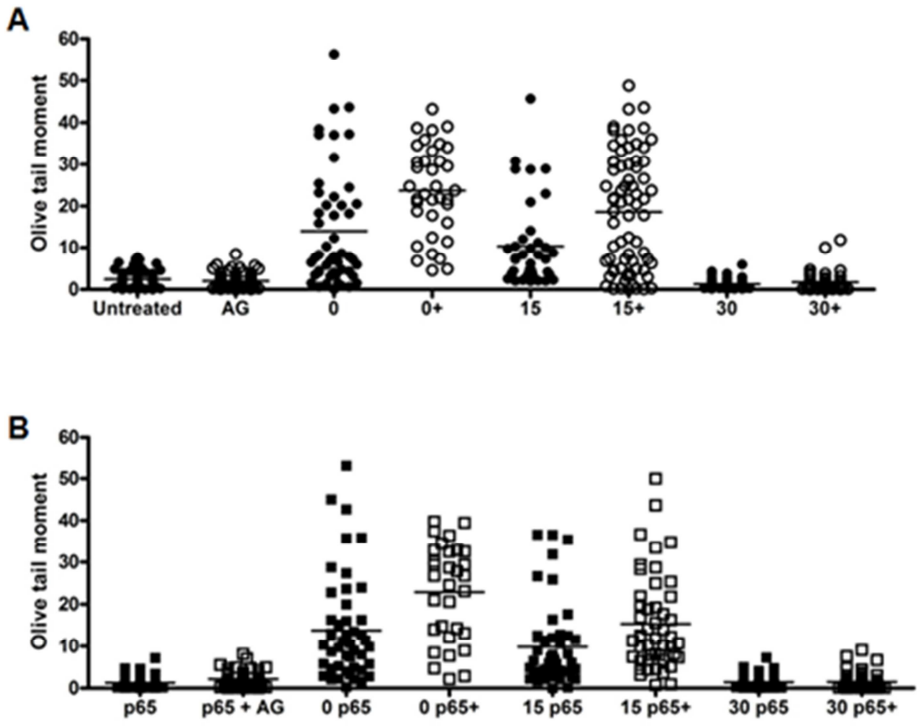

Figure 6.6: AG-014699 inhibits SSB repair to a similar extent regardless of cellular NF-κB status

(A) Scatter diagramshowing the extent of single strand breaks (SSBs) in U251cells treated with 10 Gy IR ± AG-014699 (AG, denoted by +) and allowed to repair (0 min, 15 min, 30 min).

(B) Scatter diagramshowing the extent of single strand breaks (SSBs) in U251cells treated with 10 Gy IR ± AG-014699 ±p65 siRNA and allowed to repair (0 min, 15 min, 30 min).

6.3.7 The effect of temozolomide alone, or in combination with IR on U251 cell viability

The data presented thus far in this chapter, using IR to assess the role of PARP-1 in the activation of NF-κB following DNA, has supported the results in Chapter 3 and 4. However, it was important to investigate the role of PARP-1 in the activation of NF-κB following a different DNA-damaging agents. The alkylating agent, TMZ, was chosen because there have been a number of reports showing that PARP inhibitors potentiate TMZ-induced cytotoxicity in various tumour types (Calabrese et al., 2004, Chalmers, 2009, Chalmers, 2010, Daniel et al., 2009) as this agent is known to induce SSBs. Also, TMZ is used alone and in combination with radio-therapy in the treatment of glioblastoma (Danson and Middleton, 2001), hence the U251 cell line is an appropriate model system. Moreover, a direct comparison between TMZ alone and TMZ in combination with IR could be undertaken, as these two agents are used in conjunction in the treatment of glioblastoma. This could generate therapeutically relevant data, whilst importantly gaining further insight into the role of PARP-1 in DNA-damage activated NF-κB.

The effect of TMZ alone, and in combination with a low dose of IR was assessed using the Roche XTT Cell Proliferation assay, (section 2.2.6). This is a high throughtout method used to determine a GI_{50} values for a chemo-therapeutic agent, such as TMZ. The use of such assays allowing the simultaneous assessment of a large variation of drug concentrations, something which cell survival assay, such as the clonogenic assay do not allow with such ease. U251 cells were incubated overnight before a 1 h pre-treatment with AG-014699, or DMSO control, prior to treatment with TMZ or DMSO control, and where relevant 2 Gy IR. This dose of IR was chosen as it the single dose used clinically. After treatment, the cells were incubated for a further 72 h before a further 4 h incubation in the presence of XTT labelling solution. Absorbance at 450 nm was then measured and results shown are the mean of three independent experiments.

Figure 6.7A shows the growth inhibition of U251 cells following increasing doses of TMZ (0.5- 500 μM) in the presence or absence of AG-014699. The GI_{50} values indicate that AG-014699 sensitises U251 cells to TMZ; GI_{50} TMZ alone, 32.5 μM compared with GI_{50} value TMZ in combination with AG-014699, 20.5 μM, a potentiation factor of 1.6-fold ($p=0.019$, unpaired Student's t-test).

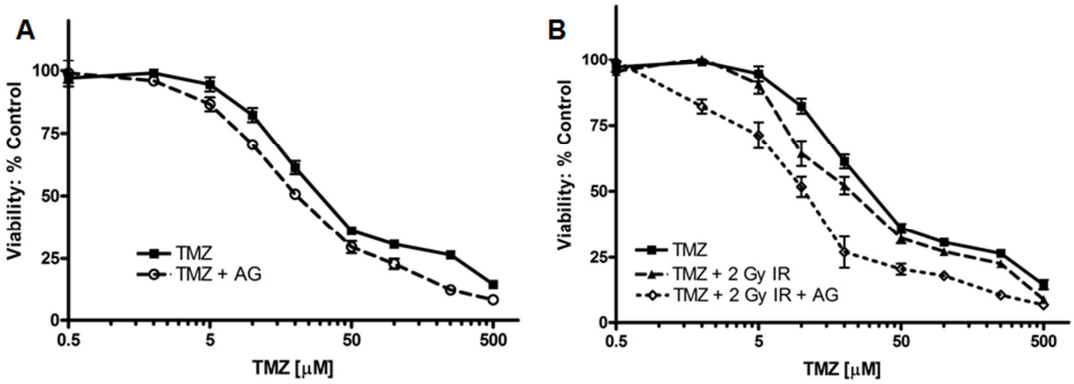

Figure 6.7: Growth inhibitory effects of temozolomide in the presence or absence of a fixed concentration of IR and AG-014699

(A) U251 cells were treated with increasing concentrations of temozolomide (0.5-500 μM) in the absence (solid line) or presence (dotted line) of AG-014699.

(B) U251 cells were treated with increasing concentrations of temozolomide (0.5-500 μM) ± 2 Gy IR ± AG-014699. After 72 h of exposure, cells were stained with XTT and OD_{450nm} was quantified. Results shown are the mean of three independent experiments ± SEM.

The effects of a combination of IR and TMZ on U251 cell viability were assessed as a direct comparison to TMZ alone. Figure 6.7B shows the growth inhibitory effects of increasing doses of TMZ alone (0.5- 500 μM), TMZ in combination with 2 Gy IR, and also TMZ in combination with both 2 Gy IR and AG-014699. The combination of TMZ and IR reduces cell viability compared with TMZ alone, although when comparing the GI_{50} values (22.8 μM and 32.5 μM, respectively), this was not statistically significantly ($p=0.094$, unpaired Student's t-test). However, that the potentiation factor here was 1.6-fold, which is the same as what was previously observed with TMZ in combination with AG-014699. Markedly, AG-04699 in combination with IR and TMZ significantly potentiated the effects of TMZ alone or IR in combination with TMZ ($p=0.0061$ and $p=0.021$, respectively). Importantly, AG-014699 in combination with IR and TMZ potentiated the effects of TMZ alone 3.3-fold, and the effects of IR and TMZ 2.3-fold. These data suggest that a combination of TMZ and IR, which is used in the clinic for treatment of glioblastoma, is more efficacious than TMZ alone, and moreover that the addition of the PARP inhibitor, AG-014699 may provide further therapeutic benefit in the disease.

6.3.8 The effect of temozolomide alone, or in combination with IR on U251 cell survival

Once the effects of TMZ alone or in combination with IR on cell viability had been assessed, it was important to determine the effects on these agents on cell survival. For this the clonogenic survival assay (section 2.2.7). U251 cells were plated and left to adhere for 24 h before pre-treatment with AG-014699, or DMSO control 1 h prior to treatment with increasing doses of TMZ, and where appropriate 2 Gy IR. Figure 6.8A shows the effect of 0, 10 and 30 µM TMZ alone or in combination with 2 Gy IR. This survival data confirms the growth inhibition data by showing that the combination of IR and TMZ reduces U251 cell survival to a greater extent than TMZ alone. When comparing the percentage cell survival following 10 µM TMZ alone (35.5 %) *versus* IR in combination with TMZ (22.0 %) these values are significantly different (p=0.031, unpaired Student's t-test). Since the curves are very steep, with very low percentage of surviving cells at 30 µM TMZ, these experiments could be repeated with lower concentrations of TMZ. Sincetime constraints meant that this was not possible for this thesis, the 10 µM concentration has been used for future comparisons in this Chapter.

These data are also represented in the bar chart in Figure 6.8B, which directly compares untreated U251 cells, or those treated with either 2 Gy IR, 10 µM TMZ or a combination of 2 Gy IR and 10 µM TMZ. Figure 6.8B shows that 2 Gy IR significantly reduced U251 cell survival by 30 % compared to untreated cells (p=0.0003, unpaired Student's t-test). Treatment with 10 µM TMZ significantly reduced cell survival by >55% compared with untreated controls (p<0.0001). Importantly, a combination of IR and TMZ further reduced U251 cell survival compared with either agent alone suggesting the two are additive (p=0.0002 IR v*ersus* IR in combination with TMZ, p=0.0019 TMZ *versus* IR in combination with TMZ, unpaired Student's t-tests). Furthermore, overall cell survival was reduced by 75 % compared with untreated controls, with this combination therapy. Taken together these data support the growth inhibition data in section 6.3.7 and also support the simultaneous use of both radio-therapy and TMZ in a clinical setting.

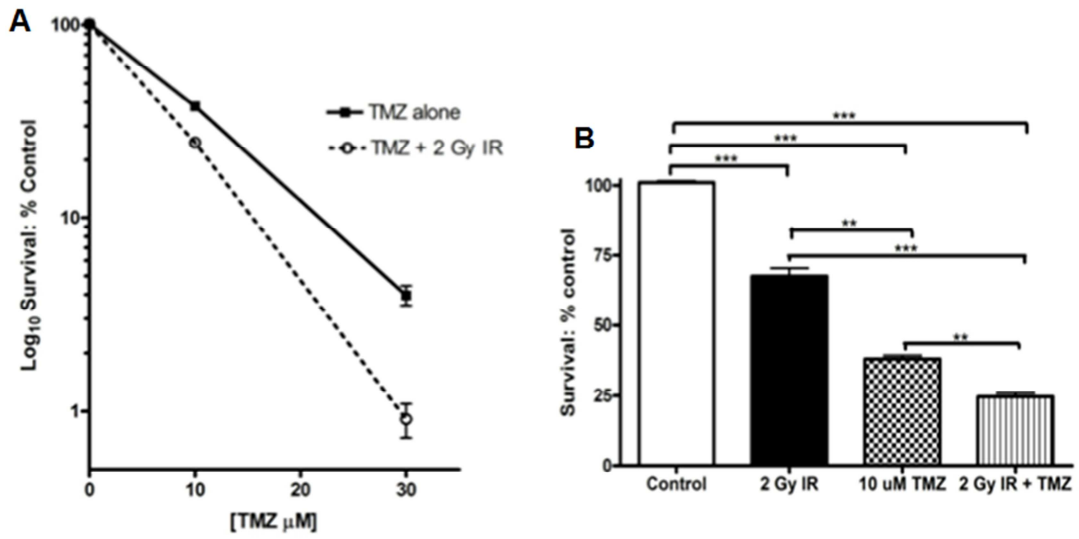

<u>Figure 6.8:</u> U251 cell survival following either IR or temozolomide or a combination of IR and temozolomide.
(A) U251 cells were treated with increasing concentrations of temozolomide (0-30 μM) in the absence (solid line) or presence of 2 Gy IR (dotted line).
(B) U251 cells were treated 2 Gy IR ± 10 μM TMZ ± AG-014699. Results shown are the mean of three independent experiments ± SEM.

6.3.9 Potentiation of temozolomide cytotoxicity either by p65 knockdown, PARP-1 knockdown or AG-014699

Once the cell survival of U251 cells in response to 10 μM TMZ and 2 Gy IR had been determined it was important to investigate whether there were any further effects on cell survival using AG-014699, p65 siRNA or PARP-1 siRNA, as had been observed (section 6.3.3). Knockdown of p65 and PARP-1 could be reproducibly achieved, in the U251 cells, hence it was decided to investigate this using classical colony forming assays (section 2.2.7). This assay used a fixed dose of both TMZ (10 μM) and IR (2 Gy) and compare this to either to a fixed concentration of AG-014699, or p65 or PARP-1 siRNA in combination with either IR or TMZ, or a combination of the two DNA-damaging agents.

Figure 6.9 shows six data sets, each containing four individual bars – one for control cells (open bars), one treated with IR (black bars), one treated with TMZ (hatched bars) and one treated with a combination with IR and TMZ (striped bars). The six sets are categorised by the presence or absence of siRNA or inhibitor used in combination with the four treatments. These six sets include p65 siRNA, AG-014699, PARP-1 siRNA,

NS siRNA, a combination of p65 siRNA and AG-014699, or cells without any of these siRNAs or inhibitors. All statistical analyses were performed using Student's unpaired t-tests, and are summarised in Table 6.1.

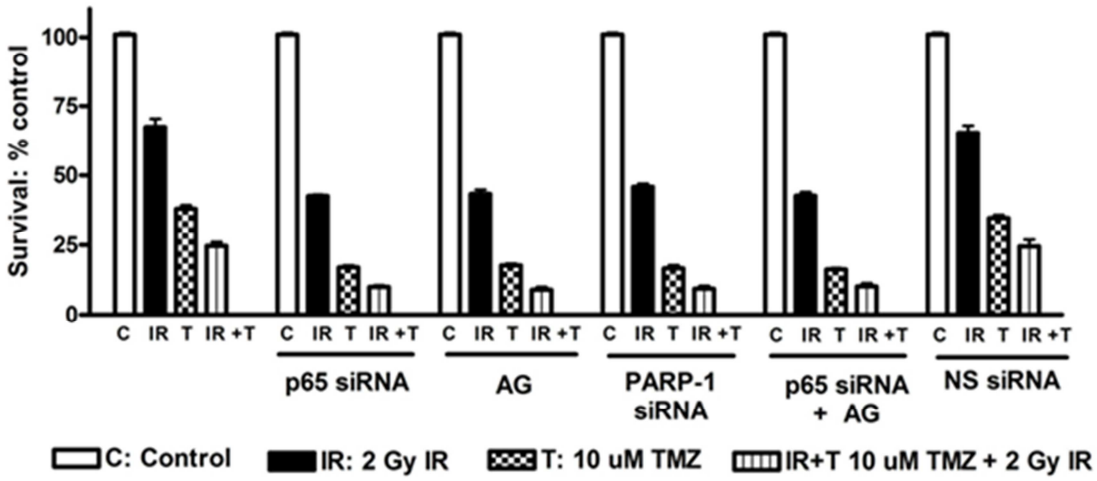

Figure 6.9: Chemo- and radio-sensitisation of U251 cells by p65 knockdown, PARP-1 knockdown or AG-014699
U251 cells were treated 2 Gy IR ± 10 µM TMZ ± p65 siRNA ± AG-014699 (AG) ± PARP-1 siRNA ± NS siRNA. Cells were treated with relevant siRNA, (or vehicle control), incubated for 48 h, pre-treated with AG-014699, or DMSO control 1 h prior to IR then re-plated after a further 24 h and allowed to form colonies for 7-21 days. Results shown are the mean + SEM of three independent experiments

Firstly, Figure 6.9 shows U251 cells without any siRNA or inhibitor treatment, and this set of bars set the bench-mark for any comparisons drawn with each of the siRNAs or inhibitor combinations used. In this case, 2 Gy IR reduced cell survival by 30 % compared to untreated cells, whereas treatment with 10 µM TMZ significantly reduced cell survival by 58% compared with untreated controls. Importantly, a combination of IR and TMZ further reduced U251 cell survival (compared with either agent alone) by 75 % compared with untreated controls.

It should be noted that all p-values (shown in Table 6.1) were generated by comparing each data set to the first set of bars (U251 cells without any siRNA or inhibitor), after it had been established that there were no significant differences between U251 cells transfected with NS siRNA and U251 cells without any siRNA or inhibitor. To this end, the final data set in Figure 6.9 shows U251 cells treated with NS siRNA 48 h prior to treatment with IR, TMZ or a combination of IR and TMZ. When comparing these data to the first set of bars (U251 cells without any siRNA or inhibitor), it is clear that NS

siRNA has no effect on cell survival in combination with IR, TMZ or a combination of IR and TMZ, compared with these DNA-damaging agents alone. Similarly, U251 cell survival was unchanged with NS siRNA in conjunction with TMZ, compared with TMZ alone. NS siRNA in combination with IR and TMZ, was not significantly different from cells treated with IR and TMZ alone.

The second data set in Figure 6.9 shows U251 cells treated with p65 siRNA 48 h prior to treatment with IR, TMZ or a combination of IR and TMZ. p65 siRNA significantly reduced cell survival further in combination with IR, TMZ or a combination of IR and TMZ, compared with these DNA-damaging agents alone. U251 cell survival was significantly decreased with p65 siRNA in conjunction with TMZ, compared with TMZ alone, or in combination with IR and TMZ, compared with IR and TMZ alone.

The third data set in Figure 6.9 show U251 cells treated with AG-014699 1 h prior to treatment with IR, TMZ or a combination of IR and TMZ. In this case, treatment with the PARP inhibitor significantly reduced cell survival further in combination with IR, TMZ or a combination of IR and TMZ, compared with these DNA-damaging agents alone. AG-014699 in combination with IR significantly decreased U251 colony forming ability compared with U251 cells treated with IR alone. U251 cell survival was significantly decreased with AG-014699 in conjunction with TMZ, compared with TMZ alone or in combination with IR and TMZ, compared with IR and TMZ alone.

The fourth set of bars on Figure 6.9 show U251 cells treated with PARP-1 siRNA 48 h prior to treatment with IR, TMZ or a combination of IR and TMZ. It is clear that treatment with the PARP-1 siRNA reduced cell survival further in combination with IR, TMZ or a combination of IR and TMZ, compared with these DNA-damaging agents alone. PARP-1 siRNA in combination with IR significantly decreased U251 colony forming ability compared with U251 cells treated with IR alone ($p=0.0022$). Similarly, U251 cell survival was significantly decreased with PARP-1 siRNA in conjunction with TMZ, compared with TMZ alone or in combination with IR and TMZ, compared with IR and TMZ alone.

The fifth data set in Figure 6.9 show U251 cells treated with a combination of p65 siRNA and AG-014699 prior to treatment with IR, TMZ or a combination of IR and TMZ. When comparing these to the controls, it is clear that treatment with this

combination of p65 siRNA and the PARP inhibitor reduced cell survival further in combination with IR, TMZ or a combination of IR and TMZ, compared with these DNA-damaging agents alone. The combination of p65 siRNA and AG-014699 in conjunction with IR significantly decreased U251 colony forming ability compared with U251 cells treated with IR alone. Similarly, U251 cell survival was significantly decreased with p65 siRNA and AG-014699 in conjunction with TMZ, compared with TMZ alone, or in combination with IR and TMZ, compared with IR and TMZ alone (p=0.001, unpaired Student's t-test). Most importantly however, there is no difference between U251 cells treated with the combination of p65 siRNA and AG-014699, compared with either of these agents alone, in combination any of the DNA-damaging agents, supporting the existing data, that PARP-1 and NF-κB are mechanistically linked in a common pathway, and that that radio- or chemo-sensitisation by the PARP inhibitor, AG-014699 is mediated *via* NF-κB.

	IR alone	**TMZ**	**IR + TMZ**
p65 siRNA +IR	0.0010 **		
p65 siRNA + T		0.0001 ***	
p65 siRNA + (IR +T)			0.0005 ***
AG + IR	0.0018 **		
AG + T		0.0001 ***	
AG + IR + T (IR +T)			0.0007 ***
PARP-1 siRNA + IR	0.0022 **		
PARP-1 siRNA + T		0.0003 ***	
PARP-1 siRNA + (IR + T)			0.0008 ***
(p65 siRNA + AG) + IR	0.0014 **		
(p65 siRNA + AG) + T		<0.0001 ***	
(p65 siRNA + AG) + (IR + T)			0.001 **
NS siRNA + IR	0.6096 ns		
NS siRNA + T		0.1151 ns	
NS siRNA + (IR + T)			0.9484 ns

Table 6.1: Statistical analysis of data sets represented in Figure 6.9
Statistical analysis perfomed using Student's unpaired t-tests generated by comparing each data set to the first set of bars (U251 cells without any siRNA or inhibitor), shown in Figure 6.12. ***Significance relative to suitable control p<0.001 **Significance relative to suitable control was p<0.01 using unpaired Student's t-test. Ns Not-significant

6.3.10 TMZ induced-NF-κB DNA binding is time-dependent

In order to confirm that the results observed in the clonogenic assays (Figure 6.9) were in fact due to the effect of AG-014699 on NF-κB activation, the effects of AG-104699,

p65 siRNA and PARP-1 siRNA on NF-κB DNA binding were assessed. Firstly, a timecourse for the activation of TMZ-induced, or TMZ + IR-induced p65 DNA binding was determined following 10 μM TMZ (the concentration used in the clonogenic assays in section 6.3.9) using the DNA binding ELISA. Figures 6.10A and 6.10B illustrate that DNA binding of both p65 and p50 increased immediately following TMZ when compared with untreated controls, although this was only statistically significant for p65 DNA binding ($p=0.017$, unpaired Student's t-tests). Moreover, in the case of both p65 and p50, DNA binding was maximal 2 h following treatment with TMZ ($p<0.0001$ and $p=0.0037$). DNA binding of the p65 subunit was still significantly increased 4 h after treatment with 10 μM TMZ and in both cases DNA binding activity returned to basal levels 24 h post treatment.

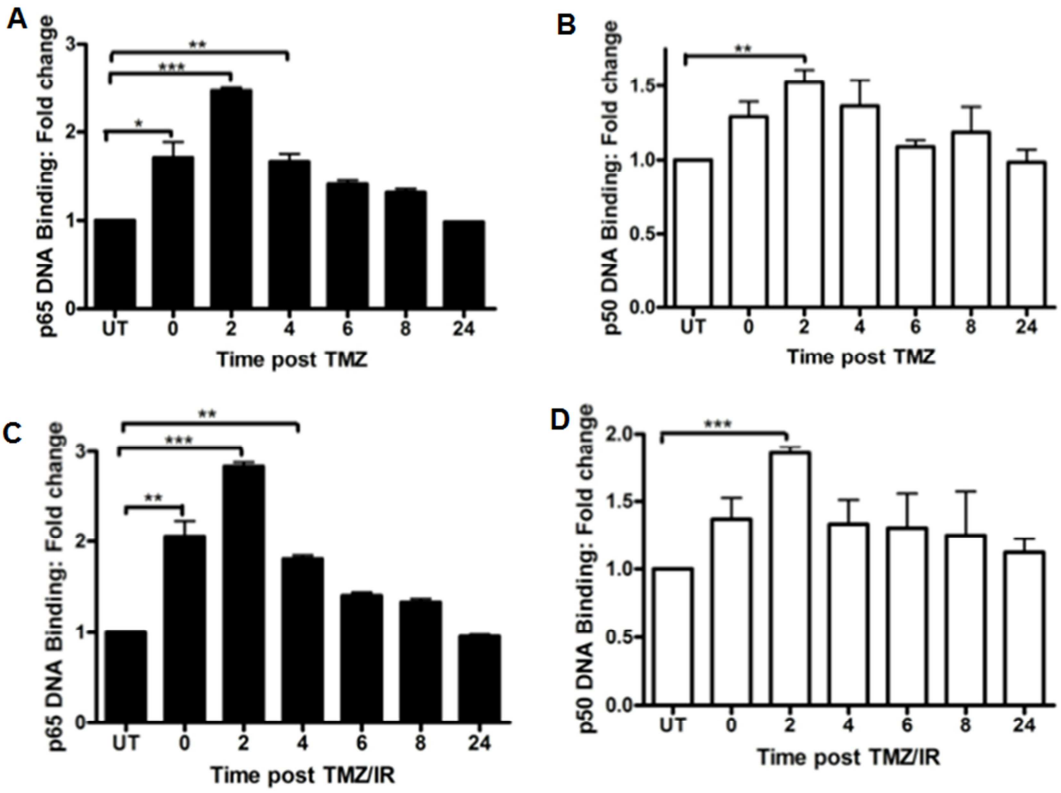

<u>Figure 6.10:</u> Maximal activation of NF-κB p65 or p50 by TMZ, or TMZ+IR is 2 h post-treatment

Bar charts showing the effects of TMZ over time on NF-κB p65 (**A**) or p50 (**B**) DNA binding activity, or TMZ + IR over time on p65 (**C**) or p50 (**D**) DNA binding activity in U251 cells. Cells were treated with 10 μM TMZ ± IR and nuclear extract prepared at various timepoints before measurement in an ELISA-based assay. All results are the mean of three independent experiments with SEM. Significance relative to mock treated control using unpaired Student's t-test *** $p<0.001$, ** $p<0.01$

Figures 6.10C and 6.10D illustrate that DNA binding of both p65 and p50 increased immediately following TMZ in combination with IR when compared with untreated controls, (significant for p65 DNA binding (p=0.0033, unpaired Student's t-tests)). In the case of both p65 and p50 DNA binding was maximal 2 h following treatment with a combination of TMZ and IR ($p<0.0001$ and $p<0.0001$). DNA binding of the p65 subunit was still significantly increased 4 h after treatment with 10 μM TMZ and 2 Gy IR and in both cases DNA binding activity returns to basal levels 24 h post treatment. These assays were undertaken simultaneously with TMZ-induced DNA binding timecourse ELISA assays (Figures 6.10A and B), and are therefore directly comparable. Thus, all timepoints tested a combination of 10 μM TMZ and 2 Gy IR induced a greater level of both p65 and p50 DNA binding compared to 10 μM TMZ alone.

6.3.11 NF-κB p65 DNA binding requires PARP protein and enzymatic activity following TMZ alone or in combination with IR

The ELISA was utilised to assess the effects of AG-014699, p65 or PARP-1 siRNA on IR-induced NF-κB DNA binding, as previously described in section 6.3.5. Figure 6.11A shows that 10 μM TMZ significantly increased p65 DNA binding compared with mock treated controls (p=0.012, unpaired Student's t-test). Co-incubation with p65 siRNA, AG-014699 or PARP-1 siRNA reduced this TMZ-dependent increase in p65 DNA binding (p=0.0042, p=0.027, p=0.041, respectively,compared to TMZ in combination with NS siRNA). Markedly, a combination of p65 siRNA and AG-014699 did not further decrease TMZ-induced p65 DNA binding compared to either agent alone, confirming the survival data which suggested that NF-κB and p65 are linked in a common pathway. Importantly, NS siRNA had no effect on TMZ-induced p65 DNA binding when compared with TMZ alone (p=0.788, unpaired Student's t-test).

Figure 6.11B shows that a combination of 10 μM TMZ and 2 Gy IR significantly increased p65 DNA binding compared with mock treated controls (p=0.0047, unpaired Student's t-test). Furthermore, Figure 6.15B illustrates that co-incubation with p65 siRNA reduced this TMZ and IR-increase in p65 DNA binding (p=0.0027). Treatment with AG-014699 or PARP-1 siRNA decreased DNA-damage-induced p65 activation, although this was not statistically significant (AG-014699; p=0.182, PARP-1 siRNA; 0.084, compared to TMZ + IR in combination with NS siRNA). Markedly, a combination of p65 siRNA and AG-014699 did not further decrease TMZ and IR-

induced p65 DNA binding compared to p65 siRNA alone, confirming the survival data which suggested that NF-κB and p65 are linked in a common pathway. Importantly, NS siRNA had no effect on TMZ and IR-induced p65 DNA binding when compared with TMZ and IR-alone (p=0.950, unpaired Student's t-test).

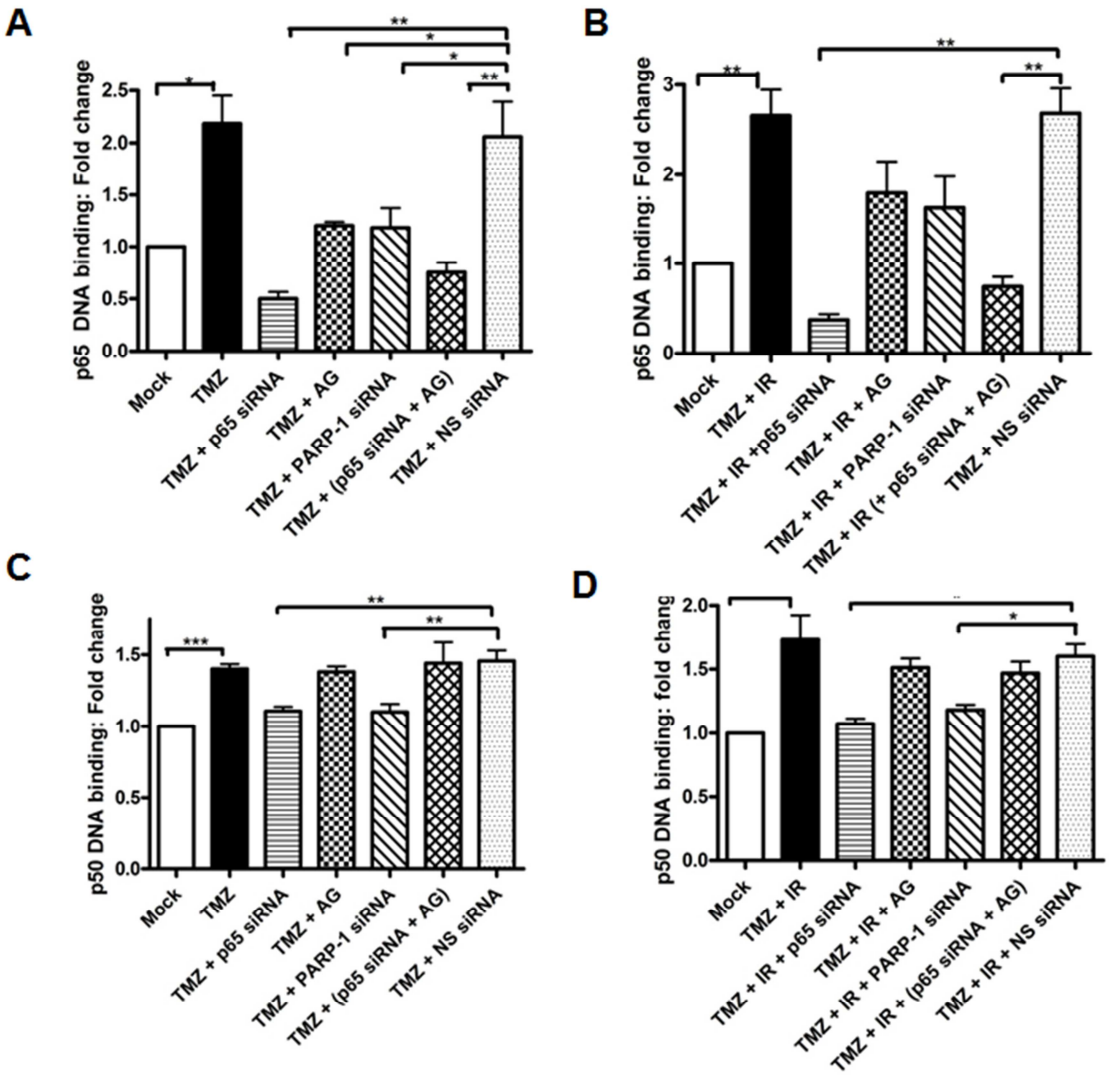

<u>Figure 6.11</u>: PARP-1 protein and enzymatic activity are required for activation of p65 DNA binding following TMZ alone, or in combination with IR

Bar charts showing the effect of TMZ ± IR ± p65 siRNA ± AG-014699 ± PARP-1 siRNA ± Non-specific (NS) siRNA control on IR-induced NF-κB p65 DNA binding, measured using an ELISA-based assay, in U251 cells. (**A**) TMZ alone, (**B**) TMZ in combination with IR.

Bar charts showing the effect of TMZ ± IR ± p65 siRNA ± AG-014699 ± PARP-1 siRNA ± Non-specific (NS) siRNA control on IR-induced NF-κB p50 DNA binding, measured using an ELISA-based assay, in U251 cells. (**C**) TMZ alone, (**D**) TMZ in combination with IR.

All results are the mean of three independent experiments with SEM. Significance relative to NS siRNA control using unpaired Student's t-test ** $p<0.01$, * $p<0.05$

Figure 6.11C shows that 10 µM TMZ significantly increased p50 DNA binding compared with mock treated controls (p=0.0004, unpaired Student's t-test). In this case, both p65 and PARP-1 siRNA significantly inhibited TMZ-induced p50 DNA binding (p=0.0057 and p=0.0099, compared to TMZ in combination with NS siRNA). It is unlikely that this observation is due to the transfection process since NS siRNA had no effect on TMZ-induced p50 DNA binding when compared with IR alone (p=0.520). Interestingly, AG-014699 alone or in combination with p65 siRNA had no effect on TMZ-induced p50 DNA binding when compared with TMZ in combination with NS siRNA (p=0.696 and p=0.887, respectively).

Figure 6.11D shows that a combination of 10 µM TMZ and 2 Gy IR significantly increased p50 DNA binding compared with mock treated controls (p=0.020). Both p65 and PARP-1 siRNA significantly inhibited TMZ-induced p50 DNA binding (p=0.033 and p=0.05, compared to TMZ + IR in combination with NS siRNA). Again, it is unlikely that this observation is due to the transfection process as NS siRNA had no effect on TMZ-induced p50 DNA binding when compared with IR alone (p=0.641). Interestingly, AG-014699 alone or in combination with p65 siRNA had no effect on TMZ-induced p50 DNA binding when compared with TMZ alone (p=0.389 and p=0.257, respectively).

6.3.12 Investigation into the induction of single strand breaks following temozolomide

Previous data showed that regardless of the p65 status of U251 cells, the numbers of SSBs were very similar following IR, and that in cells pre-treated with AG-014699 prior to treatment with IR, the repair kinetics were similar. This data supports the conclusion drawn in Chapter 3 that radio-sensitisation by AG-014699 was mediated solely by inhibition of NF-κB activation, and independent of the role AG-014699 is known to play in the inhibition of SSB repair. This very novel observation therefore requires further testing with another DNA damaging agent. Therefore, it was decided to undertake a similar set of experiments in the U251 cells, utilising p65 siRNA in combination with TMZ.

The induction of SSBs following treatment with TMZ was determined using the alkaline Comet assay (section 2.7). U251 cells were incubated overnight prior to treatment with 10 µM TMZ, the dose used for all other assays within this study. Cells were incubated with TMZ and harvested at various timepoints (0, 2, 4, 6 h) and

resuspended in ice-cold PBS before performing the Comet assay (section 7.3.6). Analysis was performed as described in section 2.7. The scatter plot in Figure 6.12 shows that the induction of SSBs following TMZ is time dependent. The maximal number of SBBs was observed 2 h following treatment with TMZ, and this persisted 4 h after treatment, but then decreased 6 h following TMZ treatment. The 2 h timepoint was selected to use for future Comet assay using TMZ, i.e., cells would be exposed to TMZ for 2 h, then the media on cells changed and the repair of SSBs assessed over a short time-course (0-30 mins), as previously used for IR (Section 6.3.6).

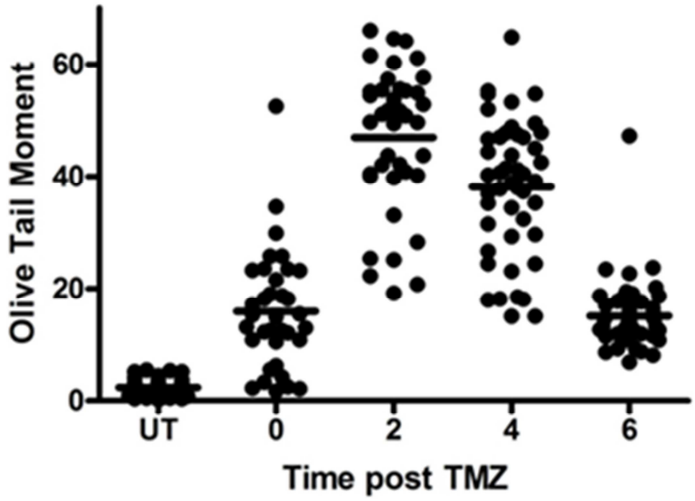

Figure 6.12: Single strand DNA breaks are maximal 2 h following TMZ treatment
Scatter diagram showing the extent of single strand breaks (SSBs) in U251cells treated with 10 μM TMZ at for various exposure times (0, 2, 4, 6 h).

6.3.13 AG-014699 inhibits temozolomide induced-single strand breaks to a similar extent in U251 cells regardless of cellular NF-κB status

The alkaline Comet assay was utilised to assess the effects of p65 siRNA, AG-014699 or a combination of the two agents on TMZ-induced SSB repair kinetics. U251 cells were plated and allowed to adhere overnight before transfection with 50 nM p65 siRNA or vehicle control. Cells were then left for 48 h, and pre-treated with AG-014699, or DMSO control 1 h prior to treatment with 10 μM TMZ alone or in combination with IR. Cells harvested at various timepoints following IR (0, 15, 30 min) and resuspended in ice-cold PBS before performing the Comet assay (section 7.3.6). Analysis was performed as described in section 2.7.

Figure 6.13A *versus* 6.13B shows that immediately following treatment with 10 µM TMZ the number of SSBs is greatest, and importantly that the olive tail moments are very similar, regardless of the p65 status of the cells. These scatter plots also illustrate that all breaks are repaired 30 minutes following TMZ treatment. Markedly, there was no significant difference in the SSB levels remaining in the presence of absence of p65 siRNA 30 min post-treatment with TMZ, with > 85 % of breaks remaining (shown in Figures 6.13A and 6.13B). Most importantly however, AG-014699 inhibited SSB repair (as demonstrated by increased residual SSB levels at all time-points post-TMZ) to the same extent regardless of whether p65 was present or not. The kinetics of SSB repair in cells with or without p65 clearly show that the SSBs generated by TMZ are repaired rapidly over time and that in both cell populations the kinetics of repair were very similar. Furthermore, regardless of p65 status, cells pre-treated with AG-014699 prior to treatment with TMZ, have slower repair kinetics, thus supporting the observations in Chapter 3.

Furthermore, figures 6.13C *versus* 6.13D also illustrate that immediately following treatment with a combination of 10 µM TMZ and 2 Gy IR, the number of SSBs is once again greatest. Importantly, the numbers of breaks are also very similar, regardless of the p65 status of the cells. These scatter plots illustrate that all breaks are repaired 30 minutes following TMZ treatment. Markedly, there was no significant difference in the SSB levels remaining in the presence of absence of p65 siRNA 30 min post-TMZ treatment, with 80% of breaks still remaining (shown in Figures 6.13C and 6.13D).

Most importantly however, AG-014699 inhibited SSB repair to the same extent regardless of the p65 status. The kinetics of SSB repair in cells with or without p65 clearly show that the SSBs generated by TMZ are repaired rapidly over time and that in both cell populations the kinetics of repair were very similar. Importantly, the assays investigating TMZ alone and in combination with IR were carried out simultaneously, making them directly comparable. Hence, it should also be noted here that there was an increase in the OTM observed in cells treated with TMZ and IR compared with TMZ alone. For example, the mean OTM at 0 h in the case of TMZ alone was 18.6 compared with a mean OTM of 27.3 for TMZ + IR, suggesting that the two DNA damaging agents used in combination induce more SSBs than either agent alone.

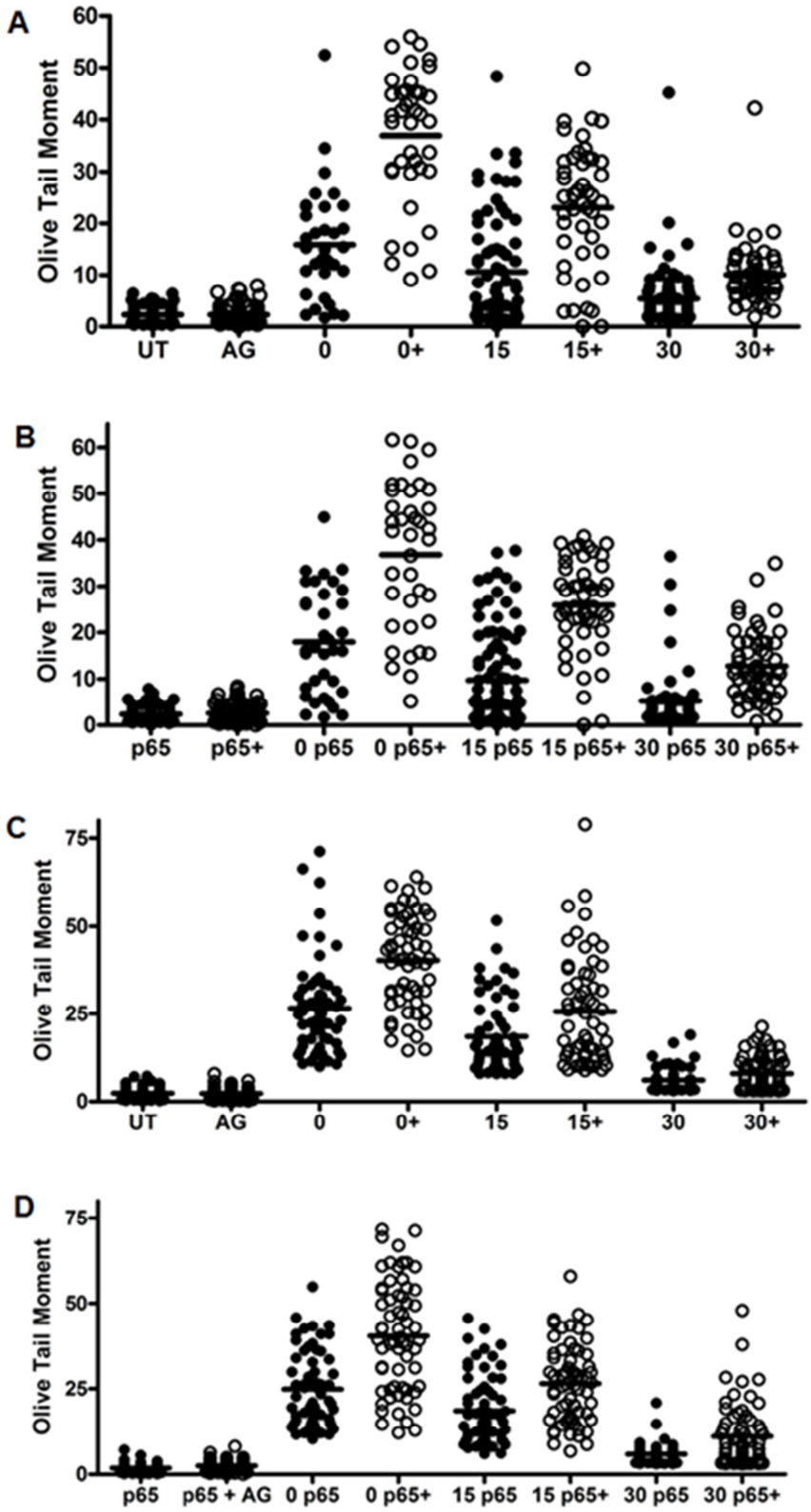

<u>Figure 6.13</u>: AG-014699 inhibits SSB repair to a similar extent regardless of cellular NF-κB status

Scatter diagramshowing the extent of SSBs in U251cells treated with 10 μM TMZ ± IR ± AG-014699 (AG, denoted by +) and allowed to repair (0 min, 15 min, 30 min). (**A**) TMZ ± AG, (**B**) TMZ + p65 siRNA ± AG, (**C**) TMZ + IR ± AG, (**B**) TMZ + IR + p65 siRNA ± AG

6.3.14 Investigation into IR-induced nuclear translocation of NF-κB p65 in cancer cell line models

Once the effects of IR or TMZ (alone or in combination) on NF-κB activity in the glioblastoma U251 cells had been determined, it was decided that a screen a series of other cell lines, in a similar manner to that described in section 6.3.1, to find any other model systems that may warrant further study. Six cell lines were chosen – two lung cancer, one sarcoma and three breast cancer. The rationale behind choosing the lung cancer cell lines, H522 and A549 was three fold; firstly radio-therapy is a main-stay of lung cancer treatment (Bleehen and Cox, 1985), secondly, there have reports which have shown that a PARP inhibitor may have a therapeutic benefit in combination with either radio- or chemo-therapy in the disease (Calabrese et al., 2004) and finally the literature suggests that both lung cancer cell line models and primary tissues have aberrantly active NF-κB (Tang et al., 2006). The sarcoma cell line, U2OS, was chosen because a number of groups use this as a model system for studying NF-κB and have reported that activation of the subunits after DNA-damaging agents (Campbell et al., 2006a).

The three breast cancer cell lines, MDA-MB-231, MCF7 and T47D were chosen because there is a large body of evidence which details the potential utility of PARP inhibitors in breast cancers, and clinical trials with AG-014699 and other compounds have been initiated based on these data (Bryant et al., 2005, Drew et al., 2011, Farmer et al., 2005, Veuger et al., 2009). Moreover, elevated NF-κB DNA binding activity has been demonstrated both in breast cancer cell lines and primary breast cancer tissues (Biswas et al., 2001, Nakshatri et al., 1997, Sovak et al., 1997) where it is known to contribute to malignant progression through the regulation of gene expression. Furthermore, constitutive NF-κB activation is also associated with chemo- and radio-resistance and also increased metastasis of breast tumours (Biswas et al., 2001, Wu and Kral, 2005). Most recently, however, a study was published which showed that PARP-1 activity was vital for NF-κB activation following IR using the MDA-MB-231 and T47D cell lines, and the small molecule inhibitor of PARP-1, AG-14361 (Veuger et al., 2009).

Firstly, constitutive activation of NF-κB p65 and inducible activation by treatment with IR was assessed by measuring p65 nuclear translocation following the DNA-damaging agent. Briefly, H522, A549, U2OS, MDA-MB-231, MCF7 or T47D cells were seeded and allowed to adhere for 24 h before treatment with either 2 Gy or 10 Gy IR. Previous

data (Chapter 4) suggested that the response would be rapid, hence cells were harvested at early timepoints (0 and 2 h). The levels of p65, Lamin or β-actin were determined by Western analyses in nuclear extracts from all three cell lines. Densiometric analysis was used to assess the levels of p65 compared to the nuclear protein, Lamin. β-actin was used as a control in order to ensure that there was no cytoplasmic contamination of the nuclear extracts.

Figure 6.14A illustrates that p65 is translocated to the nucleus of A549 cells at immediately following IR, and that this translocation is concentration-dependent. Nuclear translocation is induced 3.2-fold immediately following 10 Gy IR but these levels return to basal 2 h after treatment with IR. Figure 6.14B shows that p65 nuclear translocation was immediately induced by both 2 Gy (1.4-fold) and 10 Gy in the H522 cells (2.2-fold), but that once again p65 levels return to basal 2 h following IR treatment. Figure 6.14C illustrates that p65 is translocated to the nucleus of U2OS cells at early timepoints following IR, and that this translocation is concentration-dependent (1.6-fold immediately following 10 Gy IR, and approximately 1.7-fold 2 h following 10 Gy IR). Interestingly, maximal translocation was observed 2 h after treatment with 2 Gy IR in the U2OS cells, in which a 2.1-fold increase was observed. Taken together these data suggest that further investigation into the use of AG-014699 as a combination therapeutic agent with radio-therapy in order to overcome NF-κB-mediated therapeutic in lung cancers and sarcomas, are warranted.

Figures 6.14D, 6.14E and 6.14F show that there was no induction of p65 translocation at any of the IR doses tested in the MDA-MB-231, MCF7 and T47D cells, respectively. In all cases the nuclear extracts were not contaminated with any cytoplasmic proteins, as shown by the negative β-actin western blots. These results are somewhat unexpected as data generated by Veuger *et al.,* (2009) showed nuclear translocation and activation of NF-κB p65 and p50 DNA-binding in both the MDA-MB-231 and T47D cell lines following IR. This therefore warrants further investigation.

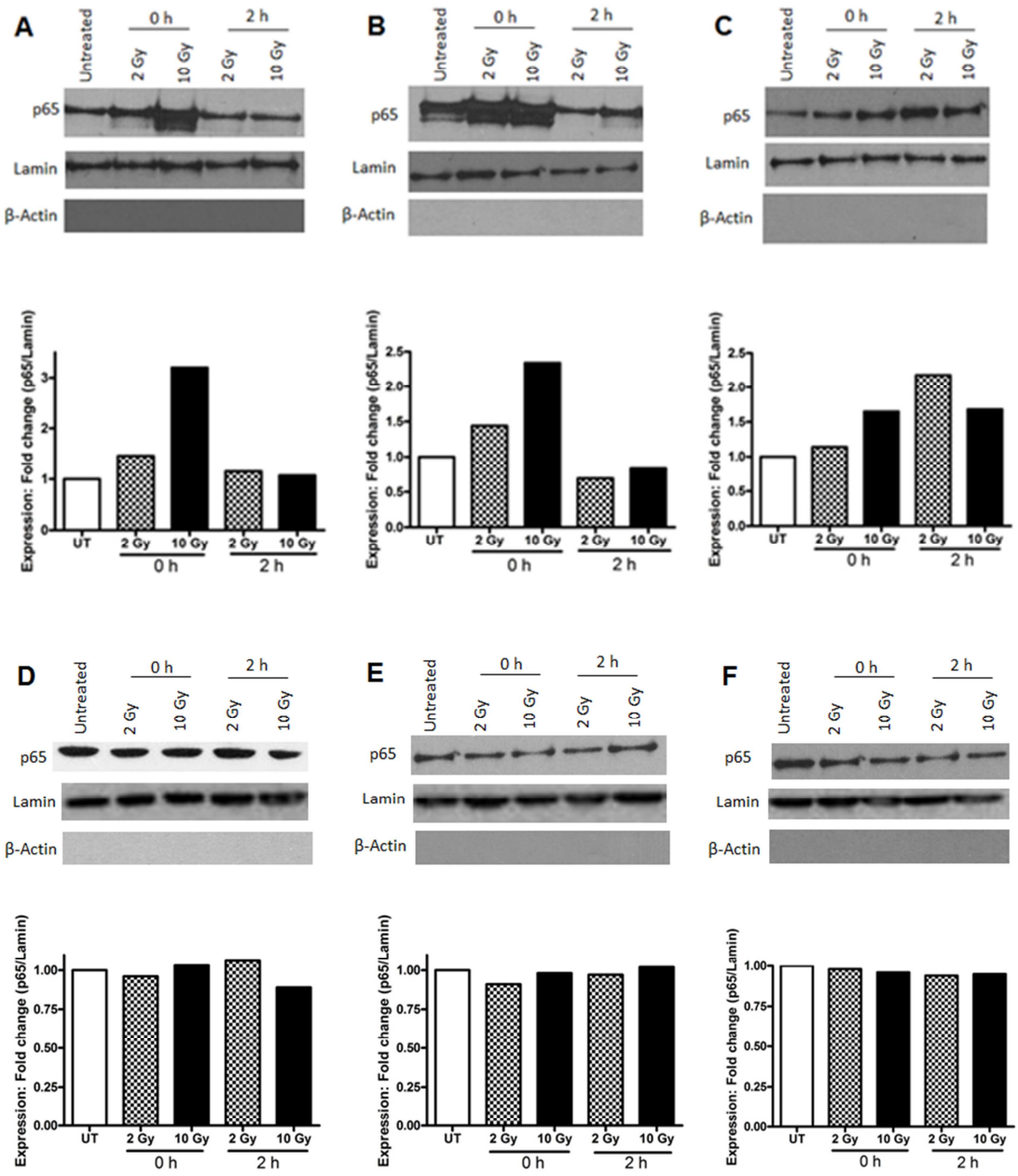

Figure 6.14: p65 nuclear translocation by IR in cancer cell line models
Western blotting data and bar charts showing nuclear translocation of p65 and densiometric analysis, following IR in cancer cell lines (**A**) A549, (**B**) H522 (**C**) U2OS, (**D**) MDA-MB-231, (**E**) MCF7 and (**F**) T47D. Cells were harvested 0 or 2 h post-IR and nuclear extracts prepared. Loading was normalised to lamin nuclear loading control in all cases. Nuclear extracts were shown to be free of any cytoplasmic contamination by blotting with β-Actin antibody. Densiotometry was used to assess the levels of p65 compared to the nuclear protein and fold change in p65 expression levels are shown in the bar charts below the relevant blotting data.

6.3.15 Investigation into the role of PARP-1 in the activation of NF-κB following IR using the MDA-MB-231 and T47D cell lines, and the small molecule inhibitor of PARP-1, AG-14361

A previous study performed in the most part by Dr Stephany Veuger using the analogue and predecessor to AG-014699 (AG-14361) and the breast cancer cell lines, MDA-MB-231 and T47D, showed that PARP-1 activity was vital for NF-κB activation following IR in these cell lines (Veuger et al., 2009). Hence, these cell lines were chosen for further study with the clinically used inhibitor, AG-014699. A summary of the data generated by Dr Veuger and to a lesser extent as part of this thesis, using the MDA-MB-231 and T47D will now be presented here.

Firstly, Veuger *et al.*, (2009) found that the MDA-MB-231 cells had higher nuclear expression of both the p65 and p50 subunits compared with the T47D cell line. This is consistent with the data presented here (Chapter 7) and reports in the literature (Nakshatri et al., 1997). Figure 6.15A and 6.15B shows the induction of p50 and p65 nuclear translocation, respectively, following 20 Gy IR in the T47D cells, suggesting perhaps that the dose of IR used previously in section 6.3.14 of this chapter was too low. However, this figure does indicate that this translocation was unaffected by pre-treatment with the PARP inhibitor, AG-14361, supporting the data shown in Chapter 4 of this thesis.

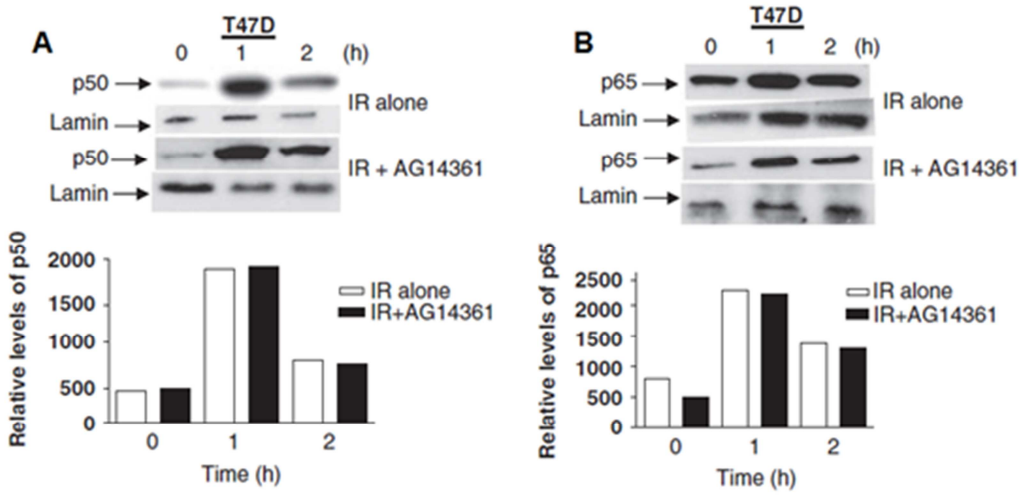

Figure 6.15: Kinetics of p50 and p65 nuclear translocation following IR in T47D cells
Western blots of nuclear extracts prepared from T47D cells treated with 20 Gy IR ± AG-14361. Blots were probed for (**A**) p50 and (**B**) p65. Bar charts show densitometry normalised to Lamin loading controls
Taken from: (Veuger et al., 2009)

Dr Veuger also observed that treatment with IR induced DNA binding of both p65 and p50 in the MDA-MB-231 and T47D cells and that the PARP inhibitor, AG-14361 abrogated induction of DNA binding. The ELISA-based assay (described in section 2.8.1) revealed that high doses of IR were required to induce an NF-κB response in these cell lines, for example, 20 Gy IR was sufficient to activate p65 or p50 in the MDA-MB-231 cells whereas a dose of 50 Gy was required to activate DNA binding in the T47D cells (Figures 6.16A *versus* 6.16B. Consistent with these data, Dr Veuger also reported that maximal luciferase activity in the MDA-MB-231 cells occurred at a lower dose compared with the T47D cell line (10 *versus* 50 Gy, respectively) using a luciferase reporter assay (described in section 2.9). Moreover, AG-14361 inhibited this IR-induced transcriptional activation by at least 80% at all IR doses tested (Figure 6.16C *versus* 6.16D).

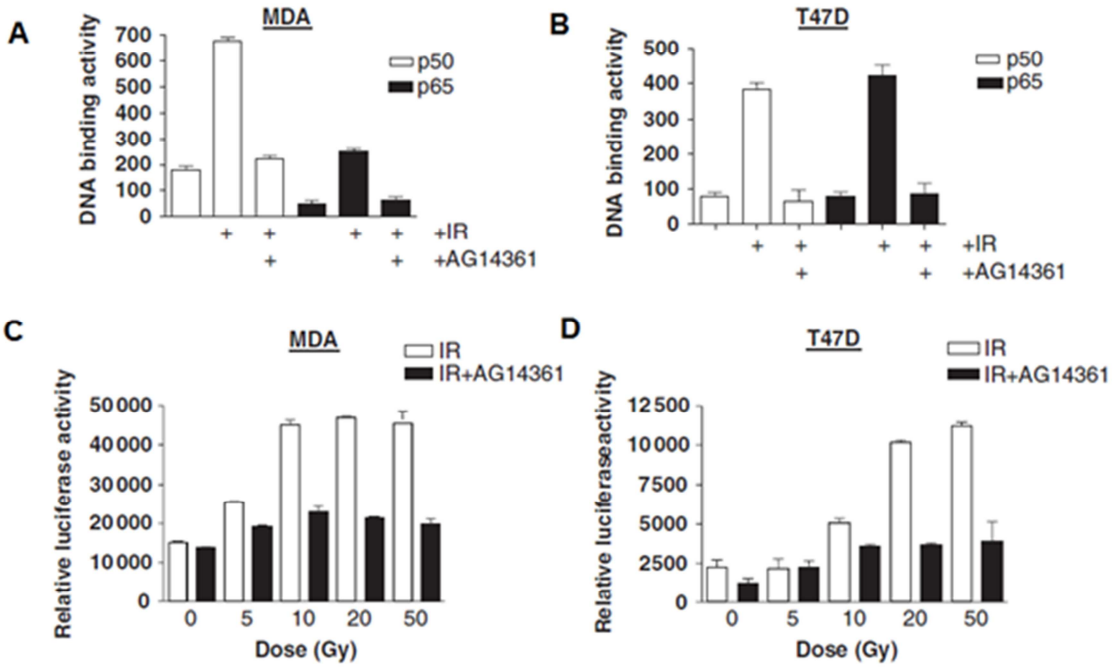

<u>Figure 6.16</u>: AG-14361 inhibits IR-induced NF-κB DNA binding and transcriptional activation

Bar chart showing the effect of IR ± AG-14361 NF-κB p65 and p50 DNA binding, measured using an ELISA-based assay, in MDA-MB-231 (20 Gy) (**A**) and T47D (50 Gy) (**B**) cells. Bar chart showing the effect of IR ± AG-14361 NF-κB transcriptional activation, measured using a luciferase reporter assay, in MDA-MB-231 (**C**) and T47D (**D**) cells.

Similar to the work presented in this thesis using the clinical PARP inhibitor (AG-014699, used in the $p65^{+/+}$ and $p65^{-/-}$ MEFs, PARP-$1^{+/+}$ and PARP-$1^{-/-}$ MEFs and the U251 cells), Dr Veuger showed that AG-14361 radio-sensitised both the MDA-MB-231

and T47D cells. In order to confirm these data for the subsequent publication of our joint data in Oncogene (Veuger et al., 2009), studies were also undertaken as a contribution to this thesis. To this end, it was essential to confirm the results of the survival data generated by Dr Veuger, to demonstrate an induction of apoptosis in the breast cancer cell lines. Caspase-3 activity is up-regulated in cells with reduced NF-κB activity (Cardoso and Oliveira, 2003), hence caspase-3 activity assays were to undertaken following IR alone, and in combination with AG-14361. However, to further confirm these data, it was decided to directly compare AG-14361 with p65 siRNA in this case in order to strengthen the existing body of data by Dr Veuger.

It was important to ascertain whether knockdown of p65 was achievable in the MDA-MB-231 and T47D cells. Thus, siRNA targeting p65 were used to silence this protein in these cells, in order to use knockdown of p65 in direct comparison with AG-14361, as had been done previously in the $p65^{+/+}$, $p65^{-/-}$, PARP-$1^{+/+}$ and PARP-$1^{-/-}$ MEFs. Briefly, MDA-MB-231 or T47D cell were seeded and left for 24 h to adhere before lipid transfection with 50 nM of siRNA oligos targeting p65, or a non-specific (NS) control (Table 2.2). Cells were harvested 48 h later, whole cell extracts were prepared (as described in section 2.5.2). The levels of p65 were determined by Western analyses and densiometric analysis was used to assess the levels of protein knockdown compared to the house-keeping protein, β-actin.

Figure 6.17 shows that there is a reproducible reduction in p65 protein expression, (>95%) in both the MDA-MB-231 and T47D cells, and when compared with untreated control cells, using an Unpaired Student's t-test, there was a significant knockdown in both cell lines ($p<0.0001$, MDA-MB-231 and $p<0.0001$, T47D). (Figures 6.17A and 6.17B). Importantly, there were no significant differences in p65 or PARP-1 protein expression between the control NS siRNA and untreated control cell extracts. Blots shown are representative of three independent experiments.

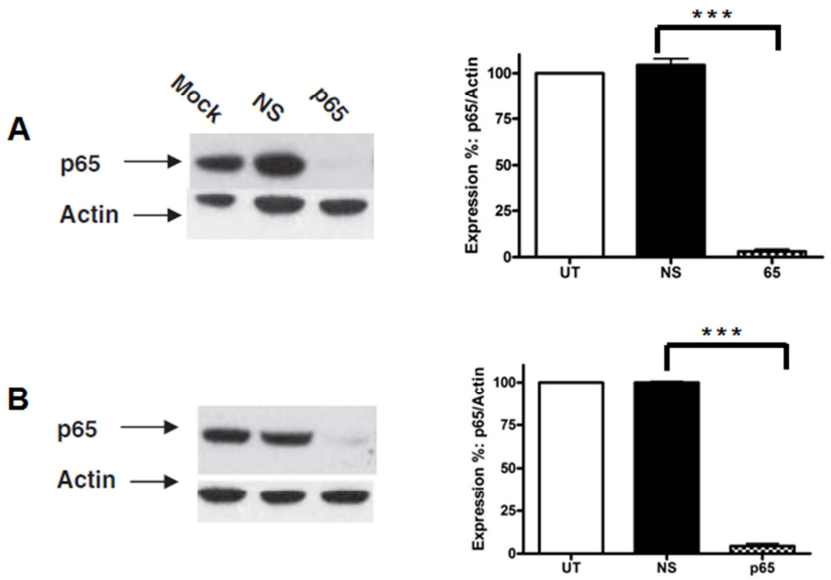

Figure 6.17: siRNA knockdown of p65 and PARP-1 in breast cancer cells
(**A**) Western blots (left panel) of whole cell extracts of MDA-MB-231 cells at 48 h after transfection with vehicle alone (Mock), non-specific (NS) siRNA or p65 siRNA. p65 protein expression in MDA-MB-231 cells expressed as a percentage of NS siRNA cells (right panel). (**B**)Western blots of whole cell extracts of T47D cells at 48 h after transfection with vehicle alone (Mock), NS siRNA or p65 siRNA. P65 protein expression in T47Dcells expressed as a percentage of NS siRNA cells. Results shown are the mean + SEM of 3 independent experiments. *** Significance relative to NS siRNA control was $p<0.0001$ using Student's unpaired t-tests.

Once p65 knockdown was reproducibly achieved in both cell lines, caspase-3 assays were undertaken, as described in section 2.6.2. Briefly, MDA-MB-231 or T47D cells were incubated for 24 h. Cells were then transfected with 50 nM p65 siRNA, 50 nM NS siRNA or vehicle alone control (mock-treated cells) and incubated for 48 h. Cells were pre- treated with AG14361 for 1 h prior to treatment with 20 Gy IR and allowed to recover at 37 5 % CO_2 for 24 h before the Caspase-Glo 3/7 assay was performed. Data were normalised to mock treated controls.

Figure 6.18A shows that when compared with IR alone (mock), both p65 knockdown and AG-14361 significantly increased caspase 3/7 activation following 20 Gy IR in the MDA-MB-231 cell line ($p=0.007$ and $p=0.008$, respectively, unpaired Student's t-test). Importantly, when AG-14361 was used in conjunction with p65 knockdown, there was no further increase in caspase 3/7 activity in the MDA-MB-231 cells, compared to either agent alone. These results were echoed in the T47D cells (Figure 6.18B); when compared with IR alone (mock), both p65 knockdown and AG-14361 significantly increased caspase 3/7 activation following 20 Gy IR in the T47D cell line ($p<0.0001$ and $p=0.0008$, respectively). When AG-14361 was used in conjunction with p65

knockdown, there was no further increase in caspase 3/7 activity in the T47D cells, compared to either agent alone. Furthermore, no increase in apoptosis was observed when NS siRNA was used in combination with IR, compared with IR alone, in either cell line (p=0.879, MDA-MB-231 and p=0.115, T47D). Taken together, the data generated by Dr Veuger here, and as part of this thesis, demonstrate that PARP-1 activity was vital for NF-κB activation following IR using the MDA-MB-231 and T47D cell lines, when using the PARP inhibitor, AG-14361.

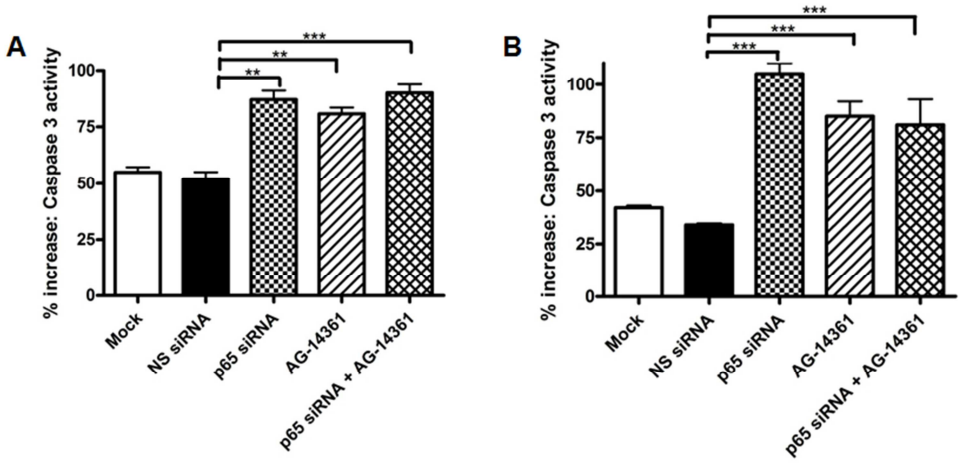

Figure 6.18: Induction of caspase-3 activity following IR in breast cancer cell lines
The effect of IR ± AG14361 ± p65 siRNA on the induction of caspase-3 activity at 24 h

6.3.16 Investigation into the nuclear translocation of p65 in breast cancer cell lines following TNF-α

The data presented in section 6.3.18 (Veuger et al., 2009), provided a clear rationale for further investigation into the use of AG-014699 in breast cancer cell lines. However, the Western blotting data in section 6.3.17, using MDA-MB-231, MCF7 and T47D cells showed that induction of p65 nuclear translocation was not achievable at relatively low doses of IR (Figures 6.14D, 6.14E and 6.14F). In the other studies within this thesis, the dose of IR has been low, with the maximum dose used being 10 Gy, however, data from the study by Dr Veuger suggests that higher doses of IR may be required. This is not considered to be clinically relevant, since 2 Gy is the used as a single dose in the clinic and sequential dosing results in an increased cumulative dose. Therefore, before testing p65 translocation following high doses of IR, it was decided to determine whether p65 nuclear translocation was achievable at low concentrations of TNF-α, such as the 10 ng/ml used previously in Chapter 4. The cytokine, TNF-α, is widely considered to be the most classical activator of NF-κB (Perkins, 2007), and is therefore used as a reference point for many studies measuring activity the transcription factor.

Western blotting was used in order to determine whether TNF-α could induce p65 nuclear translocation in the breast cancer cell lines. MDA-MB-231, MCF7 or T47D cells were incubated for 24 h before treatment with10 ng/ml TNF-α. Previous data (Chapter 4) suggested that the response to TNF-α would be rapid, hence cells were harvested at early timepoints (0 and 2 h) and nuclear extracts were prepared from all three cell lines before the levels of p65, Lamin or β-actin were determined by Western. Figure 6.19 shows that p65 is translocted to the nucleus of MDA-MB-231, MCF7 and T47D cells with a fold increase of 3.1-, 2.5- or 2.1-fold, respectively, 2 hours after treatment with TNF-α. These data clearly show that translocation of p65 to the nucleus of all of the breast cancer cell lines was achievable at low concentrations of TNF-α, warranting further investigations with higher concentrations of IR and perhaps other DNA damaging agents.

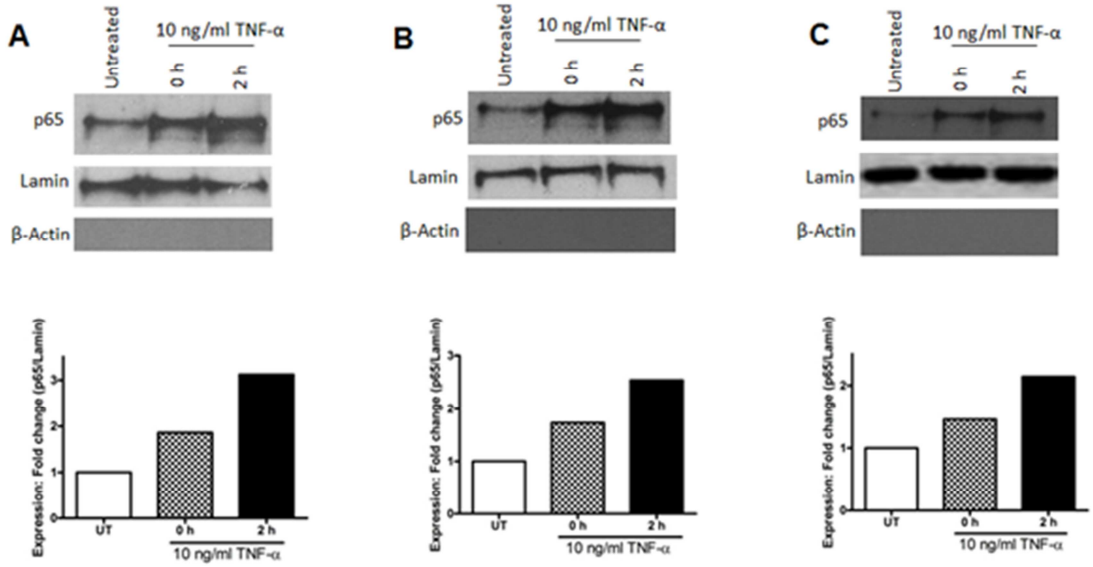

<u>Figure 6.19</u>: p65 nuclear translocation by TNF-α in breast cancer cell line models
Western blotting data and bar charts showing nuclear translocation of p65 and densiometric analysis, following TNF-α in three breast cancer cell lines (**A**) MDA-MB-231, (**B**) MCF7 and (**C**) T47D. Cells were harvested 0 or 2 h post-TNF-α and nuclear extracts prepared. Loading was normalised to lamin nuclear loading control in all cases. Nuclear extracts were shown to be free of any cytoplasmic contamination by blotting with β-Actin antibody. Densiotometry was used to assess the levels of p65 compared to the nuclear protein and fold change in p65 expression levels are shown in the bar charts below the relevant blotting data.

6.3.17 Investigation into the activation of NF-κB following DNA damaging agents in breast cancer cell lines

Once it had been shown that low concentrations of TNF-α could induce nuclear translocation of p65, it was decide to investigate further using a higher dose of IR (20 Gy), as this dose had been utilised in the study by Dr Veuger (2009). Another DNA damaging agent, the topoisomerase II poision, doxorubicin (DOX) was also studied because it is one of the most widely used treatments for breast cancer (Hoogstraten et al., 1976), and it has also been shown to induce an NF-κB response (Campbell et al., 2006a). Both IR and DOX are known to induce a DNA damage response (DDR) in cells, and therefore these agents were used to confirm that the breast cancer cells had an intact DDR, in parallel with Western blotting to measure p65 translocation. It has been well documented that the DNA-PK undergoes automodification following DNA damage and a marker of this is phosphorylation of the serine residue at 2056 (S2056) (Chen et al., 2005a). Therefore, Western blots would be probed with antibodies against phosphorylated-DNA-PK (S2056) and full length protein (DNA-PK).

MDA-MB-231, or T47D cells were incubated 24 h before treatment with either 20 Gy or 1 μM DOX. Previous data (Chapter 4) suggested that the response to IR would be rapid (Chapter 4), however, in this case a range of time-points were investigated (0, 2, 6 and 24 h) to ensure no activation was missed. The levels of p65, DNA-PK (S2056), DNA-PK, Lamin or β-actin were determined by Western analyses in nuclear extracts from all three cell lines. β-actin was used as a control in order to ensure that there was no cytoplasmic contamination of the nuclear extracts.

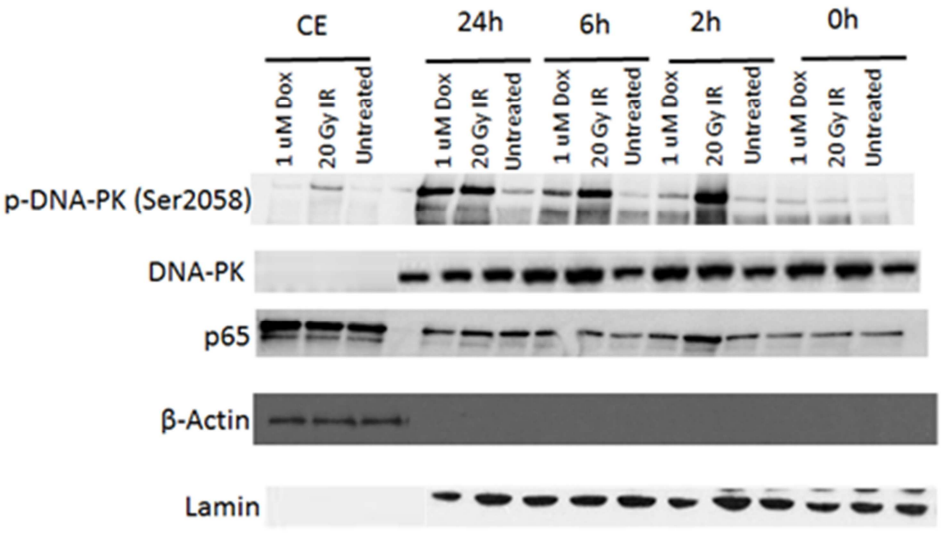

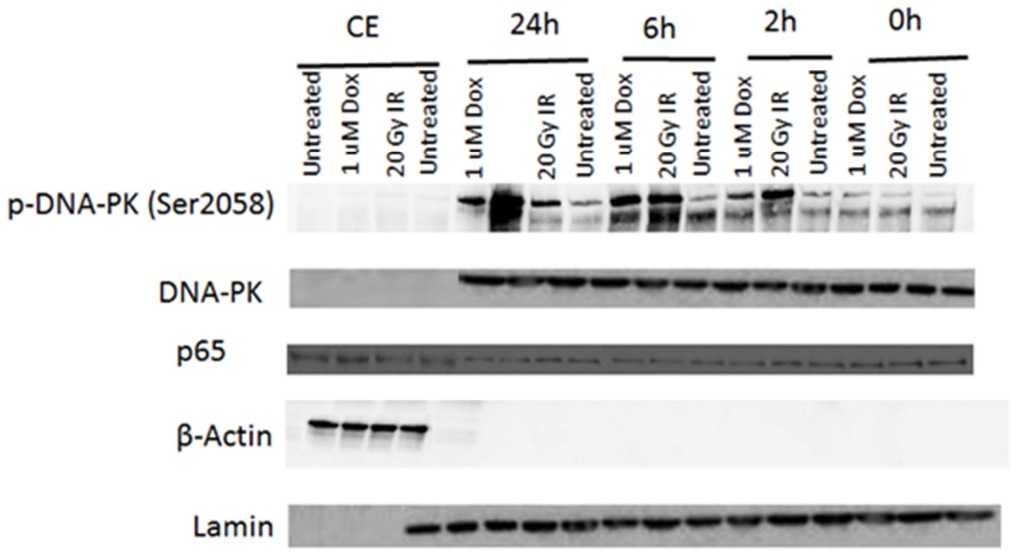

<u>Figure 6.20</u>: Investigation into the activation of NF-κB following DNA damaging agents in MDA-MB-231 and T47D cells. Western blotting data showing nuclear translocation of p65 and phosphorylation of DNA-PK, following IR or DOX in MDA-MB-231 (**A)** and T47D (**B**) cells. Cells were harvested 0, 2, 6 or 24 h post-IR or DOX and nuclear extracts prepared. Loading was normalised to lamin nuclear loading control in all cases. Nuclear extracts were shown to be free of any cytoplasmic contamination by blotting with β-Actin antibody.

Figures 6.20A and 6.20B show the results from MDA-MB-231 and T47D cells, respectively. The nuclear levels of p65 appear to be constant in both of these cell lines regardless of the treatment they had received or the time-point at which they were harvested. This indicates that p65 is not translocated to the nucleus of these cells following DNA damage. These blots have cytoplasmic extracts alongside the nuclear extracts of interest and it is clearly visible that there is no contamination of the nuclear fraction with cytoplasmic proteins, by virtue of the absence of β-actin in the nuclear extracts. Similarly, there were no nuclear proteins leftover during the cytoplasmic fractionation, as indicted by the fact that no Lamin or DNA-PK, was present in these lanes. Moreover, treatment with either 20 Gy IR or 1 µM DOX induced a DDR at all time-points tested, as indicated by an increase in the phosphorylation of DNA-PK at serine 2056, compared with untreated controls. This shows that these cells have an intact DDR, and the lack of NF-κB activation by DNA damaging agent cannot be attributed to a non-functional DDR.

It was thought that any change in the expression of p65 following DNA may be too subtle to view by Western blotting, hence it was decided to run the extracts that had also been used in Western blotting, and others prepared independently, on the DNA binding

ELISA. Using this method any effect on the other subunits, p52, RelB or c-Rel could be assessed simultaneously. In this case, MDA-MB-231 or T47D cells incubated for 24 h prior to treatment with 1 µM DOX or 20 Gy IR. Cells were harvested at various timepoints (0, 2, 6, and 24 h), the nuclear extracts were prepared and DNA binding binding was assessed using the TransAM NF-κB family ELISA kits (section 2.8.2).

Each one of the five bar charts in Figure 6.21 represent the DNA binding activity of the MDA-MB-231 cells over time of each individual subunit, p65, p50, p52, RelB and c-Rel. In all cases, the open bars represent untreated cells, the black bars represent cells treated with 20 Gy IR, and the hatched bars represent cells treated with 1 µM DOX. The data presented indicates that there is no induction of DNA binding, in any of the five subunits, at any of the time-points tested, by either of the DNA damaging agents tested. These data support the Western blotting data shown in Figures 6.20B. Similar data was obtained using the T47D cell line (Figure 6.22).

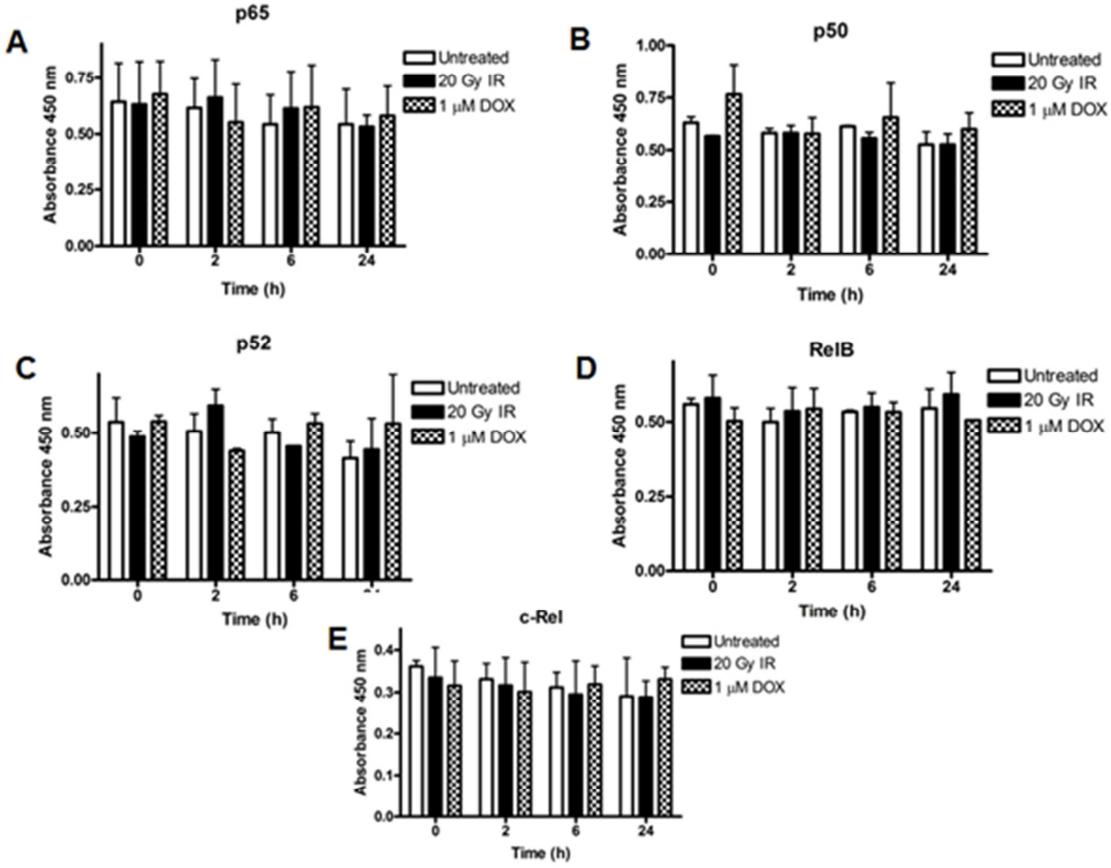

Figure 6.21: Investigation into the activation of NF-κB DNA binding following DNA damaging agents in MDA-MB-231 cells. Bar charts showing DNA binding of p65 (**A**), p50 (**B**), p52 (**C**), RelB (**D**) and c-Rel (**E**), following IR or DOX in MDA-MB-231 cells.

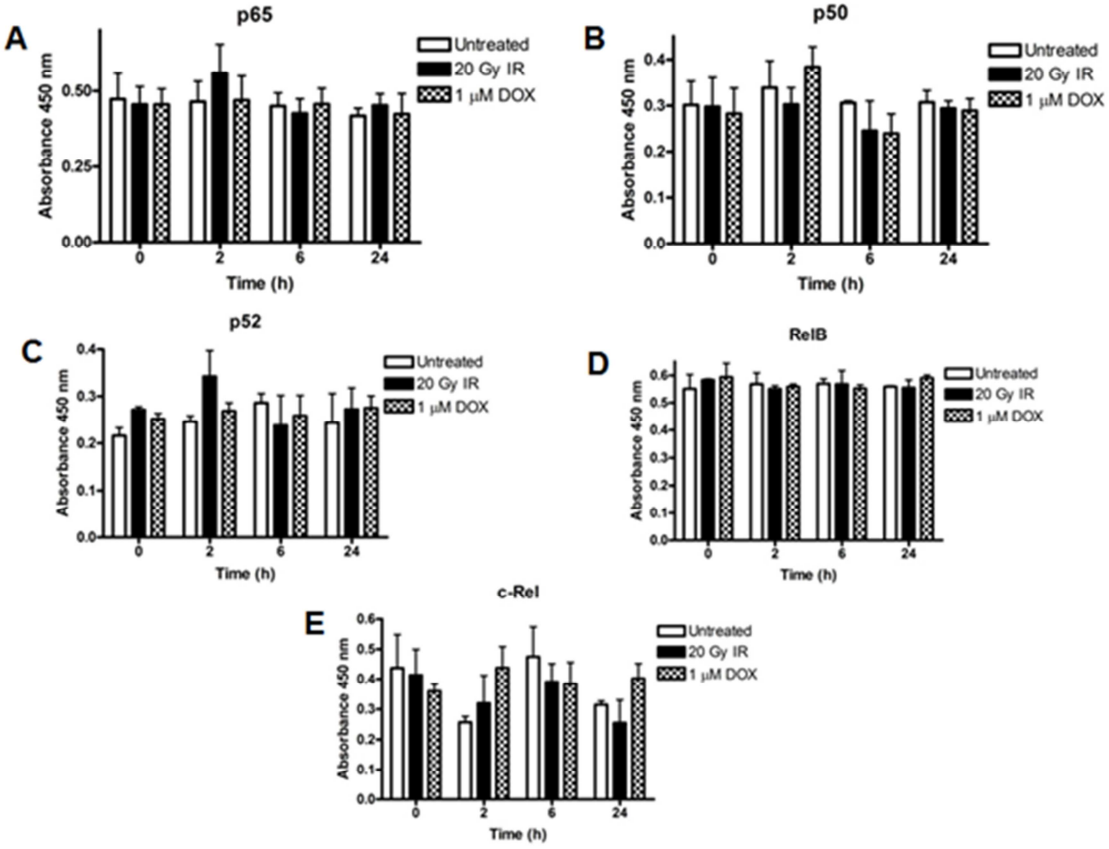

Figure 6.22: Investigation into the activation of NF-κB DNA binding following DNA damaging agents in T47D cells. Bar charts showing DNA binding of p65 (**A**), p50 (**B**), p52 (**C**), RelB (**D**) and c-Rel (**E**), following IR or DOX in T47D cells.

6.4 Discussion

Previous work within this thesis has demonstrated that PARP-1 knockdown and the PARP inhibitor, AG-014699 significantly decreased survival and induced apoptosis following IR in $p65^{+/+}$ MEFs whilst having no effect in $p65^{-/-}$ MEFs. A combination of AG-014699 and p65 knockdown did not further enhance this response, which is consistent with reports that PARP-1 and NF-κB are mechanistically linked in a common pathway (Chang and Alvarez-Gonzalez, 2001, Hassa et al., 2001, Hassa and Hottiger, 1999, Martin-Oliva et al., 2004, Stilmann et al., 2009, Veuger et al., 2009). Moreover, the very novel observations in Chapter 3, detail how the levels of IR-induced SSBs in $p65^{+/+}$ and $p65^{-/-}$ MEFs were similar and that both cell lines were equally proficient at their repair. AG-014699 was also able to increase the level of breaks to the same extent in both cell lines, consistent with the known role of PARP-1 in base excision repair (Durkacz et al., 1980). Thus, these data lead to the conclusion that the potentiating effect of AG-104699 when used in conjunction with IR is, in part, a consequence of PARP-1 downstream signaling to NF-κB. However, all of these data were generated

using MEFs, and it was vital to determine the potential utility in cancer model systems, and also test the hypothesis that PARP inhibitors would not only inhibit IR-induced NF-κB activation, but also NF-κB activation by other clinically-used DNA damaging agents.

The choice of model in which to study the effects of AG-014699 on DNA-damage-induced NF-κB activation was important. Glioblastoma was selected. Firstly, because there had been a number of reports that had detailed both radio- and chemo-sensitisation by PARP inhibitors, in both cell line and xenograft models of the disease (Chalmers, 2010). However, these reports showed that this sensitisation was due to the inhibition of SSB repair, and other mechanistic investigations were not undertaken. Secondly, there were also reports in the literature which suggested that aberrant activation of NF-κB played an important role in the tumourigenesis of both diffuse and high-grade gliomas (Kanzawa et al., 2003, Wang et al., 2004). Taken, together this made glioblastoma, in which cell line models were readily available, an obvious choice for further study.

The initial screen of three glioblastoma cell lines, showed that all three had constitutively nuclear p65, consistent with reports that NF-κB is aberrantly active in this tumour type (Kanzawa et al., 2003, Wang et al., 2004). Importantly, in two of the three cell lines, p65 activation, by virtue of its nuclear translocation, was further induced by relatively low doses of IR. However, only the U251 cell line was chosen for further investigation. The MO59J line was derived from a glioma tumour lacking DNA-PK (Lees-Miller et al., 1995), and in this case p65 nuclear translocation was not inducible following IR in this cell line. DNA-PK is vital for the DNA damage response (Zhou and Elledge, 2000), in particular mediating the repair of double stranded DNA breaks *via* the non-homologous end joining pathway (Sancar et al., 2004). Moreover, DNA-PK has been implicated in the activation of NF-κB following DNA damage (Basu et al., 1998, Ju et al., 2010, Liu et al., 1998, Panta et al., 2004), as discussed in section 1.4.2.

There is an increasing body of evidence in the literature which details how PARP inhibitors may be of therapeutic value in glioblastoma (Chalmers et al., 2004, Cheng et al., 2005, Dungey et al., 2009). However, in general, studies lack a clear mechanistic aspect, something which has been addressed in this chapter by investigating the use of a PARP inhibitor in glioblastoma in the context of the inhibition of NF-κB. Glioblastoma multiforme (GBM) tumours are the most common and most aggressive primary brain

tumours. Current treatment comprises surgical resection followed by radio-therapy with concomitant and subsequent adjuvant TMZ, and despite such an aggressive treatment regimen, median survival in the UK is only 1 year (Chalmers, 2009). Hence, the decision to investigate the role of the PARP inhibitor, AG-014699 following IR or TMZ, or the combination of both DNA damaging agents, as novel treatment strategies was justified.

The data presented here are in concordance with existing data that the addition of a PARP inhibitor can sensitise glioblastoma cells to either radio- or chemo-therapy. It is however, the first study in GBM to investigate the combination of IR, TMZ and a PARP inhibitor and show that the addition of this type of agent, in this case AG-014699, clearly sensitises U251 cells to this treatment regimen. Although the side effects of radio-therapy and TMZ, currently given concomitantly for GBM, can be severe, current reports from clinical trials using AG-014699 show it has a very low toxicity profile (Plummer et al., 2005, Plummer et al., 2008). Taken together these data strongly suggest that the use of AG-014699 in GBM would represent a potential therapeutic avenue. Furthermore, aberrant activation of NF-κB is known to play a role in the tumourigenesis of both diffuse and high-grade gliomas (Kanzawa et al., 2003, Wang et al., 2004).

GBM is unique in that tumours exhibit high proliferation rates while the surrounding normal tissue dividing at an altogether much lower rate (Chalmers, 2009). Radio-therapy is the main-stay of GBM treatment, and therefore it is necessary to treat large volumes of normal brain tissue which can result in irreversible neurotoxicity (Griebel et al., 1991), thus any agent used in combination with radio-therapy must by highly tumour specific, which is the case for AG-014699 has been proven against PARP (Plummer et al., 2008). Moreover, AG-014699 has been shown to have the ability to cross the blood-brain-barrier (Daniel et al., 2009), something which is essential in the treatment of GBM. Interestingly, a study performed by Dungey *et al.,* (2008) showed that the radio-sensitising effects of the KuDOS/AstraZeneca PARP inhibitor, KU-0059436, were specific to cells undergoing DNA replication (Dungey et al., 2008), hence providing further rationale for the use of PARP inhibitors as radio-sensitising agents in GBM.

The data presented here illustrating that AG-014699 sensitises cells to TMZ treatment are important. At least half of all GBM tumours are refractory to TMZ treatment

because they express the repair protein methyl guanine methyl transferase (MGMT) (Chalmers, 2009). One report showed that PARP inhibition increased TMZ sensitivity in cells expressing MGMT (Plummer et al., 2005), therefore the addition of AG-014699 may open up a new therapeutic avenue, for the treatment of poor prognosis patients, in which current treatments remain ineffective.

Importantly, this study is also the first to investigate the role of PARP in DNA-damage-activated NF-κB in GBM. Reports in the literature suggested that aberrant activation of NF-κB played an important role in the tumourigenesis of both diffuse and high-grade gliomas (Kanzawa et al., 2003, Wang et al., 2004). Therefore, it was important to determine whether the observations in Chapter 3 and 4 of the thesis, showing that radio-sensitisation by AG-014699 was mediated *via* NF-κB, was also the case in the U251 glioblastoma cell line. The use of p65 siRNA, AG-014699, PARP siRNA or a combination of p65 siRNA and AG-014699 in the clonogenic survival assays following IR alone, TMZ alone or a combination of IR and TMZ clearly indicate that radio- or chemo-sensitisation observed with the PARP inhibitor was mediated *via* the inhibition of DNA-damaged activated NF-κB p65, supporting the existing data in this thesis.

The Comet assay data generated within this chapter supported the novel findings in Chapter 3 that the potentiating effects of AG-104699 when used in conjunction with DNA damaging agents are, in part, a consequence of PARP-1 downstream signaling to NF-κB. These observations have greatly strengthened the data generated using the p65 paired MEFs, and add to weight to the conclusion that chemo- or radio-sensitisation by AG-014699 is mediated, in part, by inhibition of NF-κB activation. The p65 DNA binding in the U251 cells also supports the finding described in Chapter 4, showing that both PARP-1 protein and enzymatic activity were required for DNA-damage induced p65 DNA binding. IR alone, TMZ alone or a combination of both of these agents induced p65 DNA binding and this was abrogated by co-incubation with either p65 siRNA, PARP-1 siRNA or AG-014699. Importantly, the combination of p65 siRNA and AG-014699 had no further effect on p65 DNA binding compared with either agent alone, thus supporting the proposed mechanism in Chapter 4. These data suggesting that p65 DNA binding requires the catalytic function of PARP-1 are consistent with other reports in the literature (Chang and Alvarez-Gonzalez, 2001, Chiarugi and Moskowitz, 2003, Nakajima et al., 2004, Stilmann et al., 2009, Veuger et al., 2009, Zingarelli et al., 2003b). Importantly, the inhibitor used here is highly potent and specific for PARP,

compared with the use of classical compounds, such as 3-AB, which are known to have off target effects (Moses et al., 1990). Also the direct comparison with PARP-1 siRNA showed that the effects observed are mediated solely by PARP-1.

However, p50 DNA binding following IR, TMZ or a combination of IR and TMZ, has provided some interesting observations. All of these damaging agents induced p50 DNA binding, however this effect was mitigated by the addition of p65 siRNA or PARP-1 siRNA. AG-014699 alone or in combination with p65 siRNA had no effect on DNA-damage induced p50 DNA binding. It is perhaps not surprising that loss of p65 protein results in an inhibition of DNA-damage induced p50 DNA binding, and in this case p50 has lost its most common hetero-dimeric partner (Chen et al., 1998). Interesting, the inhibition of DNA-damage induced p50 DNA binding by co-incubation with PARP-1 siRNA suggests that p50 DNA binding requires PARP-1 protein but not enzymatic activity, in line with reports from other research groups (Hassa et al., 2001, Martin-Oliva et al., 2006). These data suggest that that PARP-1 may facilitate a structural role in the p50 transcriptional complex, following IR, TMZ or a combination of both agents in the U251 cells. This is consistent with the work of Hassa *et al.,* (2003 JBC), which illustrated how the physical presence of the PARP-1 C-terminal catalytic domain, but not its enzymatic activity, was required for PARP-1 and p300 to synergistically activate NF-κB-dependent transcription following either TNF-α or LPS, although this report did not investigate NF-κB activation following DNA damage, as has been undertaken here.

The absence of any p65 nuclear translocation or NF-κB subunit DNA binding in response to DNA damaging agents in the breast cancer cells lines is somewhat puzzling. It is well documented that elevated NF-κB DNA binding activity in both breast cancer cell lines and primary breast cancer tissues contributes to malignant progression and resistance to treatment (Biswas et al., 2004, Nakshatri et al., 1997, Sovak et al., 1997). There have also been a number of reports in the literature which have shown that DNA damaging agents can induce an NF-κB response in various breast cancer cell lines, and consequently that therapeutic intervention with an NF-κB inhibitor can inhibit such an NF-κB response. For example, Wang *et al.,* (2005) demonstrated that as little as 5 Gy IR was necessary to induce NF-κB DNA binding, measured using an electrophoretic mobility shift assay (EMSA), and also NF-κB-dependent gene transcription, measured using a luciferase reporter assay (Wang et al., 2005), similar to the one used in this

thesis. This data is supported by that of Guo *et al.,* (2003), which showed that a there was a 2-fold induction of NF-κB-dependent gene transcription following 5 Gy IR, which was abrogated in the presence of the IκB super repressor (Guo et al., 2003). Furthermore, Madhusoodhanan *et al.,* (2010) illustrated induction of an NF-κB response in MCF7 cells using an EMSA by as little as 2 Gy IR (Madhusoodhanan et al., 2010). These data suggest that NF-κB activation should have been observed in the MCF7 cells especially as in this case the doses of IR tested included were higher than that described in the literature. Many different batches of these cells were use for the assays undertaken here and in order to rule out the possibility that the cell line may have 'drifted' during continuous culture.

An investigation using either DOX or TNF-α to activate NF-κB in the MDA-MB-231 cells was undertaken by Ho *et al.,* (2005) who showed that low doses of TNF-α induced NF-κB DNA binding at early time-points. The data shown within this chapter illustrated that p65 was translocated to the nucleus 1 h following treatment with the cytokine. Chi Ho et al., observed that 5 μmol/L DOX also induced NF-κB DNA binding in MDA-MB-231 cells, however the kinetics of this were slightly slower, with maximal activation noted 3 h following treatment (Ho et al., 2005). Moreover, Munoz-Gamez *et al.,* (2005) showed that PARP inhibition using the PARP inhibitor, ANI (4-amino-1,8-naphthalimide) sensitised MDA-MB-231 cells to 1 μM DOX, the same concentration tested in this chapter. This group found that NF-κB activation by DOX was maximal 24 h after treatment, but interestingly that co-incubation with ANI had no effect on DOX-induced NF-κB DNA binding (Munoz-Gamez et al., 2005). These data suggest that activation of NF-κB following DOX should have been achievable in the MDA-MB-231 cells, at the concentrations and time-points tested, especially taken with the data presented here which illustrates that these cells have a functional DDR. However, the report from Munoz-Gamez *et al.,* (2005) which showed that PARP inhibition had no effect on DOX-induced NF-κB activation, is perhaps expected. DOX is primarily an agent which induces double stranded DNA breaks (Lyu et al., 2007) and PARP-1 is known to be activated, in the main, by SSBs, hence activation of PARP-1 and subsequent single strand repair pathways is unlikely with DOX. However, it is noteworthy that DSBs are actually the most potent activator of PARP-1 activity.

The published work by Dr Veuger (Veuger et al., 2009) and as part of this chapter showed that PARP-1 activity was vital for NF-κB activation following IR using the

MDA-MB-231 and T47D cell lines, and the small molecule inhibitor of PARP-1, AG-14361. Dr Veuger showed that nuclear translocation of both p65 and p50 occurred following 20 Gy IR in the T47D cells, something which could not be repeated in the studies for this thesis. Moreover, the data from Dr Veuger's publication also detailed how 20 Gy IR was required to activate p65 or p50 DNA binding in the MDA-MB-231 cells whereas a dose of 50 Gy was required to activate DNA binding in the T47D cells. However, DNA binding of all subunits, which was assessed as part of this chapter (following 20 Gy IR) was not inducible. It was decided not to use the dose of 50 Gy, as this is 25 times the single clinically relevant dose. In all of the initial assays the batches of the MDA-MB-231 and T47D cells were from stocks frozen down by Dr Veuger, and subsequent assays utilised other stocks from the Northern Institute for Cancer Research's cell line bank, suggesting that the cell line is not an issue and has not 'drifted' in continuous culture. One explanation for the discrepancy between the data from Dr Veuger's study and that obtained within this thesis could be the irradiator used. Although the same equipment was used for both studies, there were some technical issues with calibration of the instrument during the course of study. Therefore some variation in dose given is possible.

6.5 Summary and future work

The data shown within this chapter using AG-014699 and siRNA targeting NF-κB p65 in the U251 glioblastoma cell line, supports the data generated from chapters 3 and 4 using the p65 proficient and deficient MEFs. The studies in this chapter have shown that inhibition of PARP-1 modulates the apoptotic response not just to IR but also to the mono-functional alkylating agent, TMZ, and most importantly that the potentiation of cytotoxicity by PARP-1 inhibition is due to the loss of NF-κB activation. Strikingly, the Comet assay data demonstrates that both chemo- and radio-sensitisation by PARP inhibition is due to inhibition of NF-κB, and not the prevention of DNA repair. These data not only support the existing literature which suggests that the addition of a PARP inhibitor to current therapeutic regimen would be an advantageous (Chalmers et al., 2004, Cheng et al., 2003, Dungey et al., 2009), but also they show the mechanism by which PARP inhibition functions, namely *via* the inhibition of DNA-damage-induced NF-κB activation. Since this study was undertaken in the most part in just one glioblastoma cell line, it would be advantageous to repeat such experiments in further cell line models of the disease and also importantly, in xenograft models.

The data within this thesis suggested that other cancers may warrant further investigation, but unfortunately in the time-scale this was not possible in this thesis. There is clear rationale for future studies in lung cancer in particular. Studies have shown radio-sensitisation *in vitro* models of the disease and *in vivo* radio-sensitisation has also been observed in xenograft models (Albert et al., 2007, Brock et al., 2004, Calabrese et al., 2004, Donawho et al., 2007). Combination studies using various PARP inhibitors with TMZ have been undertaken in human lung cancer cell lines and xenografts (Calabrese et al., 2004), and these studies have shown pronounced chemo-sensitisation *in vitro* and tumour growth inhibition *in vivo*. Moreover, groups have also described the aberrant activation of NF-κB in lung cancer cell line models and primary samples, and shown that this contributes to poor prognosis and disease progression (Basseres et al., 2010, Tang et al., 2006).

Interestingly, it appears in figures 6.5A, 6.5B, 6.11A, 6.11B, 6.11C, 6.11D and 6.18A that AG-014699 antagonises the effects of p65 siRNA following DNA damage. This is something which warrants further investigation. It is plausible that in this case one or more of the other NF-κB subunits is compensating for the loss of p65 and inhibition *via* AG-014699. Therefore it would be interesting to assay which dimers were present, and active, in these cells following p65 siRNA or the combination of p65 siRNA and AG-014699.

The interesting observations showing that p65 nuclear translocation was not inducible following DNA damage in the DNA-PK deficient MO59J cells but inducible in the DNA-PK proficient MO59J-Fus-1 cells, warrants further study. DNA-PK has been implicated in the activation of NF-κB following DNA damage by a number of groups (Basu et al., 1998, Ju et al., 2010, Liu et al., 1998, Panta et al., 2004). Interestingly, Panta *et al.,* (2004) reported that DNA-PKcs activates NF-κB induction in the MEK/ ERK/p90^{rsk} to IKK signalling pathway in response to treatment with 5μM AD288, a catalytic inhibitor of topoisomerase II *N*-benzyladriamycin but not in response to DOX. Catalytic inhibitors of topoisomerase II do not cause DNA damage, unlike topoisomerase II poisons, such as DOX, suggesting that DNA-PK can activate NF-κB in the absence of DNA damage, something which would be interesting to study further.

The inability to activate NF-κB in the three breast cancer cell lines was somewhat surprising, and as a consequence it meant that further study into the effects of AG-

014699 on NF-κB activation were not applicable. However, these data require further investigation, and the Northern Institute for Cancer Research has recently acquired a piece of imaging equipment which allows the visualisation and quantification of protein translocation at the single cell level. This would allow observation of the shuttling of p65, for example, from cytoplasm to nucleus, in real-time following DNA damage. It could be the case that nuclear translocation is occurring in only a small percentage of the breast cancer cells treated following DNA damage, and this method would gain insight into such phenomenon.

Chapter 7: Preclinical testing of a series of NF-κB subunit DNA binding inhibitors, both in combination with radio-therapy and as stand-alone agents

7.1 Introduction

NF-κB has been implicated in both inflammatory disease and cancer, therefore making inhibition of the transcription factor an attractive target for therapy. To date, there are over 750 known inhibitors of the NF-κB pathway and these can be divided into broad categories depending on which points of the NF-κB activation pathway they target. For example, there are naturally occurring substances or chemical inhibitors that act at the receptor or adaptor level or those which directly target the IKK complex, such as parthenolide. Proteosomal inhibitors, for example bortezomib, which is licensed for use in multiple myeloma, inhibit the degradation of IκB, whilst other compounds prevent the nuclear translocation or DNA binding of NF-κB (Gilmore and Herscovitch, 2006).

Many chemical NF-κB inhibitors, such as those which target proteosmal degradation, do not specifically target the NF-κB pathway alone. Although bortezomib has demonstrated considerable efficacy against multiple myeloma both i*n vitro a*nd i*n vivo* (Adams, 2004), it is not clear whether these anti-tumour effects are mediated entirely by the inhibition of NF-κB (Hideshima et al., 2009). Many other proteins are targeted for proteosomal degradation, including the tumour suppressor p53 (Asher and Shaul, 2005), so it is possible that the efficacy of bortezomib and other proteasome inhibitors is due to the stabilisation of other key proteins with known roles in cancer, other than NF-κB.

Moreover, NF-κB plays a vital role in the inflammatory response and it is well documented that the IKK subunit, IKKβ is the primary participant in the production of pro-inflammatory stimuli associated with NF-κB activation (Aupperle et al., 1999, Tak and Firestein, 2001). For example, Aupperle *et al.,* (1999) showed that IKKβ is expressed in fibroblast-like synoviocytes and has a crucial role in NF-κB activation following either TNF-α or IL-1. Thus, complete inhibition of the IKK complex, with derivatives of the naturally occurring compounds like parthenolide (Yip et al., 2004), or even specific IKKβ inhibitors, may have adverse effects by compromising the vital immune functions mediated by NF-κB. Furthermore, the IKK complex has many other functions within the cell, including the regulation of autophagy (Carrillo et al., 2004, Chariot, 2009). Therefore, IKK inhibitors may not be specifically targeting the NF-κB pathway and may have undesirable side effects.

Profectus Biosciences Inc., (Baltimore, MD) have recently developed several families of NF-κB inhibitors. One of these compounds, PBS-1086 was found to be a Rel

inhibitor of NF-κB DNA binding, specifically meaning that this compound targets the Rel domain of the NF-κB subunits, therefore inhibiting the DNA binding of all of the subunits, resulting in the inhibition of NF-κB. PBS-1086 has been reported as a more potent inhibitor of both RelA and RelB DNA binding than the widely known NF-κB inhibitors, parthenolide and DHMEQ (Oh et al., 2011). Oh *et al.,* (2010), reported that PBS-1086 suppressed spontaneous lympho-proliferation and inhibited the production of pro-inflammatory cytokines in PBMCs from HTLV-I–associated myelopathy/tropical spastic paraparesis (HAM/TSP) patients *via* the inhibition of NF-κB DNA binding. To this end, PBS-1086 was shown to be a Rel inhibitor and therefore inhibit the DNA binding of p65, p50 and RelB as well as luciferase expression in a 293/NF-κB-luciferase reporter cell line (Oh et al., 2011).

7.2 Aims and hypothesis

The aims of this chapter were to screen a panel of NF-κB inhibitors (provided by Profectus Biosciences Inc) in p65 proficient MEFs in order to determine which were the most potent and specific, and, efficacious *in vitro,* and to investigate the utility of such compounds as radio-sensitising agents. The hypothesis that any radio-sensitisation would be mediated *via* the canonical pathway would also be tested by using siRNA targeting the p65 subunit of NF-κB as a direct comparison with the most promising compounds.

Furthermore, the potential utility for use of these compounds as mono-therapies would also be investigated using a panel of breast cancer cell lines. Elevated NF-κB DNA binding activity has been demonstrated both in breast cancer cell lines and primary breast cancer tissues (Biswas et al., 2004, Nakshatri et al., 1997, Sovak et al., 1997). Constitutive NF-κB activation has been shown to contribute to malignant progression through the regulation of gene expression. Therefore the hypothesis that inhibition of NF-κB DNA binding would induce cell death in breast cancer cells expressing aberrantly active NF-κB would be tested.

Furthermore, constitutive NF-κB has been associated with chemo- and radio-resistance and also increased metastasis of breast tumours (Biswas et al., 2001, Wu and Kral, 2005). Radio-therapy is one of the main-stays of breast cancer treatment, and there have also been a number of reports detailing the activation of NF-κB by IR breast cancer cell

lines (Guo et al., 2003, Veuger et al., 2009, Wang et al., 2005) Thus, the addition of an NF-κB inhibitor to the current therapeutic regimen represents a promising therapeutic strategy for breast cancers. Hence, the hypothesis that inhibitors of NF-κB DNA binding would radio-sensitise breast cancer cells, would also be rigorously tested within this chapter.

7.3 Results

7.3.1 Assay development

The clonogenic assay (section 2.2.7) was used to assess which of the seven compounds from Profectus Biosciences Inc was the most potent radio-sensitising agent in MEFs proficient for NF-κB p65, in the first instance, with a view to determining subunit specificity using $p65^{-/-}$ MEFs. Previous work (Chapter 3) using the PARP inhibitor, AG-014699 and siRNA targeting p65 or PARP-1 demonstrated that either AG-014699, p65 siRNA or PARP-1 siRNA radio-sensitised $p65^{+/+}$ but not $p65^{-/-}$ MEFs (Hunter et al., 2011). Using the data from the survival curves of $p65^{+/+}$ MEFs treated with IR alone, a fixed dose of IR which kills approximately 50% of $p65^{+/+}$cells is 2.5 Gy. A standard clonogenic assay uses a range of doses of a DNA damaging agent (e.g. IR) and compares this to a fixed dose of an inhibitor in combination with the DNA damaging agent (section 2.2.7). However, a concentration range for these inhibitors was provided by Profectus Biosciences (0.1, 0.3, 1, 3, 10, 30 μM) and since the toxicity of these compounds was unknown in this system, it was decided to use a 'window of potentiation' method. Essentially, the concentration range provided for the inhibitor was used in combination with a fixed dose of IR (known to kill 50% of the $p65^{+/+}$ MEFs). Briefly, cells were incubated for 24 hours before being treated with the inhibitors (or DMSO control) for 15 min prior to treatment with IR then re-plated after a further 24 h and allowed to form colonies for 7-21 days. All treatments or doses used were normalised to the relevant controls – for example, the inhibitor alone treated cells were normalised to a DMSO control of $p65^{+/+}$ MEFs, whereas for the inhibitor in combination with IR, these were normalised to cells treated with both IR and the DMSO control.

Prior to commencing work with the Profectus Biosciences compounds, the 'window of potentiation' clonogenic assay was tested in the $p65^{+/+}$ MEFs using a dose range of the PARP inhibitor, AG-014699 alone or in combination with one fixed dose of IR. Cells

were incubated for 24 h before treatment with AG-014699 (or DMSO control) 1 hour treatment prior to treatment with IR then re-plated after a further 24 h and allowed to form colonies for 7-21 days. Figure 7.1 shows that there is a significant difference ($p<0.0001$, unpaired Student's t-test) between the LD_{50} values (lethal dose producing 50% cell kill) of AG-014699 alone (LD_{50} of 0.82 µM) and AG-014699 in combination with 2.5 Gy IR (LD_{50} of 0.05 µM). The visible large difference ('window of potentiation') between the solid line of AG-014699 alone, and the dotted line of AG-014699 in combination with IR, makes it very clear that this method of the clonogenic assay is robust and reproducible in the $p65^{+/+}$ MEFs. Moreover, this method illustrates that at low concentrations of AG-014699, the compound is relatively non-toxic, as has been shown in other studies (Calabrese et al., 2004, Daniel et al., 2010, Daniel et al., 2009, Zaremba et al., 2009). If a compound is very toxic at low concentrations, the slope of the survival curve would be much steeper at the top which would also indicate whether the Profectus Biosciences compounds may have any stand-alone toxicity at lower concentrations, or the concentration used in the combination experiments.

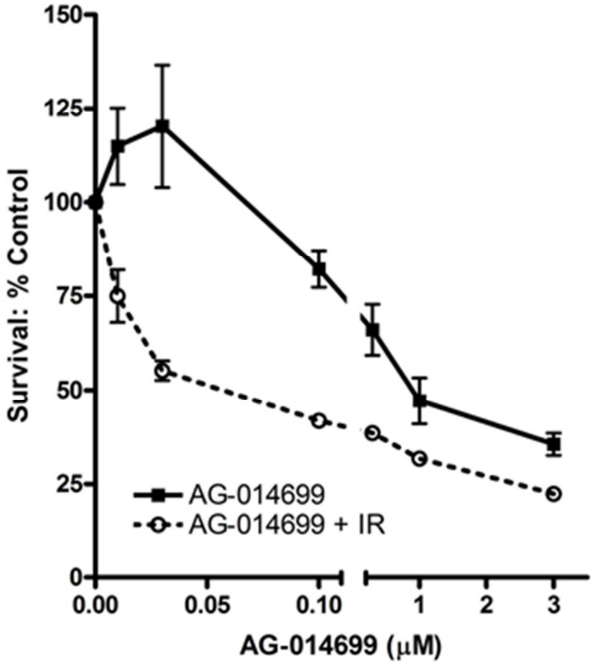

Figure 7.1: Survival of $p65^{+/+}$ cells following treatment with increasing doses of AG-014699 and 2.5 Gy IR. The effects of increasing doses of AG-014699 (0 – 3 µM) AG-014699, alone (solid line) or in combination with one fixed dose of IR (2.5 Gy) (dotted line), on cell survival was assessed in $p65^{+/+}$ MEFs. Cells were treated with AG-014699 or DMSO control for 1 h prior to IR (if relevant) then re-plated after a further 24 h and allowed to form colonies for 7-21 days.

7.3.2 Window of potentiation studies with five Profectus Biosciences NF-κB inhibitors

Once confident with the experimental design, five inhibitors from Profectus Biosciences were screened:- PBS-1079, PBS-1086, PBS-1088, PBS-1110 and PBS-1135. The dose range used for each compound was 0-30 μM (0, 0.1, 0.3, 1, 3, 10, 30 μM), in combination with a fixed dose of IR (2.5 Gy) to give an indication of which of these NF-κB inhibitors might radio-sensitise the $p65^{+/+}$ MEFs. $p65^{+/+}$ cells were incubated for 24 hours before being treated with either inhibitors (or DMSO control) for 15 min prior to IR then re-plated after a further 24 h and allowed to form colonies for 7-21 days. All survival curves shown are the mean of three independent experiments.

Figure 7.2A shows the survival curve of the $p65^{+/+}$ MEFs following increasing doses of PBS-1079 alone or in combination with 2.5 Gy IR. The 'window of potentiation' observed in Figure 7.1, using AG-014699 is not as large with PBS-1079. In this case, the inhibitor alone has a greater effect on cell survival at low concentration when compared with PBS-1079 in combination with IR. The LD_{50} value for PBS-1079 alone is 0.57 μM whereas the LD_{50} value for PBS-1079 in combination with IR is 1.04 μM, although the difference between these two values is not statistically significant (p=0.11, unpaired Student's t-test).

The survival curve of $p65^{+/+}$ MEFs treated with increasing doses of PBS-1086 alone or in combination with 2.5 Gy IR (Figure 7.2B) showed that there is a significant difference (p=0.0016, unpaired Student's t-test) between the LD_{50} values of PBS-1086 alone (LD_{50} of 3.58 μM) and PBS-1086 in combination with 2.5 Gy IR (LD_{50} of 1.4 μM). Furthermore, at low concentrations, PBS-1086 was relatively non-toxic alone, as seen previously with AG-014699 (Figure 7.1), yet there was a pronounced radio-sensitisation with 2.5 Gy IR at these doses. These data suggest that this compound warrants further investigation as a radio-sensitising agent.

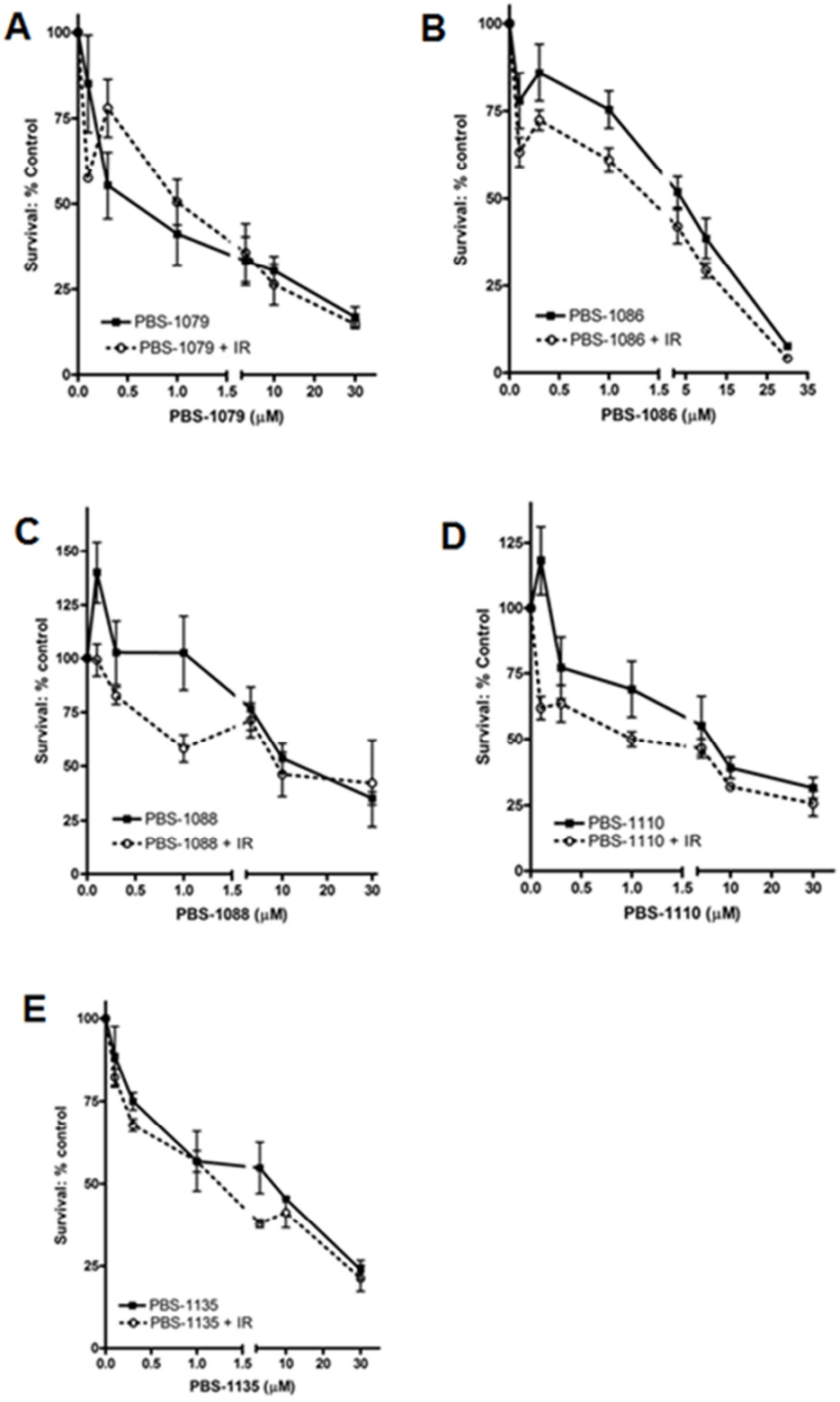

<u>Figure 7.2:</u> Survival of p65$^{+/+}$ following treatment with increasing doses of Profectus Biosciences inhibitors and 2.5 Gy IR

The effects of increasing doses of (**A**) PBS-1079, (**B**) PBS-1086, (**C**) PBS-1088, (**D**) PBS-1110 or (**E**) PBS-1135 (0 – 30 μM) PBS-1086, alone (solid line) or in combination with one fixed dose of IR (2.5 Gy) (dotted line), on cell survival was assessed in p65$^{+/+}$ MEFs. Cells were treated with PBS inhibitor or DMSO control for 15 min prior to IR (if relevant) then re-plated after a further 24 h and allowed to form colonies for 7-21 days.

Figure 7.2C shows PBS-1088 alone or in combination with 2.5 Gy IR. At the low concentrations tested the inhibitor is clearly radio-sensitised in the presence of the fixed dose of IR used and there is a visible window of potentiation. This echoed in the doses which reduce survival by 25 % (LD_{25}) with this compound alone (LD_{25} value of 3.39 µM) compared with PBS-1088 in combination with IR (LD_{25} value of 0.48 µM, p=0.031). However at higher concentrations, for example LD_{50} values observed with PBS-1088, there was no significant differences observed (p=0.39), and the survival curves of PBS-1088 alone or in combination with 2.5 Gy IR overlap.

The survival curve of $p65^{+/+}$ MEFs treated with PBS-1110 alone or in combination with 2.5 Gy IR (Figure 7.2D) showed that there is a significant difference (p=0.038, unpaired Student's t-test) between the LD_{50} values of PBS-1110 alone (LD_{50} of 5.05 µM) and PBS-1110 in combination with 2.5 Gy IR (LD_{50} of 0.99 µM). These data would suggest that this compound should be further investigated as a potential radio-sensitising agent. Figure 7.2E shows that there is little difference between PBS-1135 alone or the combination of PBS-1135 and IR, however a small window of potentiation is seen at the LD_{50} values. Although there is approximately 3-fold difference between the LD_{50} of PBS-1135 alone (7.01 µM) and that of PBS-1135 in combination with IR (1.26 µM), this difference is not significant when tested using an unpaired Student's t-test (p=0.169).

It is very important to note that when used at higher concentrations (10 and 30 µM), two of the inhibitors, PBS-1079 and PBS-1088 appeared to have had a profound effect on the growth of these cells. The colonies formed by the $p65^{+/+}$ cells are usually discrete and uniform in shape (Figure 7.3A). However, high concentrations of PBS-1079 or PBS-1088, alone or in combination with IR, have forced the colonies to be become elongated and appear fibroblastic, suggesting that this compound is having an effect on the cells morphology and growth (Figure 7.3A *versus* 7.3B*)*. This therefore suggests that these inhibitors are quite toxic to these particular cells and taken together these data suggest that PBS-1079 and PBS-1086 may not be good candidates for use as radio-sensitising agents.

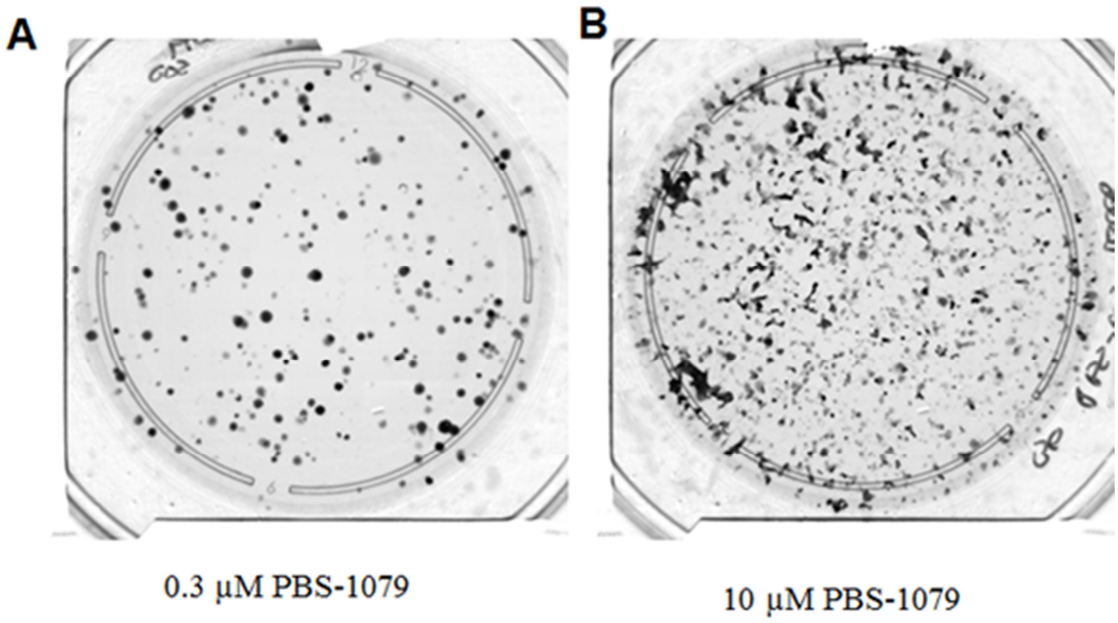

Figure 7.3: Cellular growth and morphology of p65$^{+/+}$ MEFs treated with either 0.3 or 10 µM PBS-1079. The colonies formed by the p65$^{+/+}$ cells are usually discrete and uniform in shape and this continued at low concentrations of PBS-1079 (**A**). However, high concentrations of PBS-1079, alone or in combination with IR, have forced the colonies to be become elongated and appear fibroblastic (**B**).

Table 7.3 summarises the LD_{50} values of each of the Profectus Biosciences inhibitors, alone or in combination with 2.5 Gy IR. This table also includes the PF_{50} values for each of these agents, where appropriate. The PF_{50} value is the (potentiation factor at 50% cell kill) and was calculated from the ratio of the individual LD_{50} values:- for example, LD_{50} of PBS-1086 alone divided by LD_{50} of PBS-1086 in the presence of IR. These data indicate that the most promising compounds in terms of their ability to radio-sensitise the p65$^{+/+}$ MEFs are PBS-1086 (2.5-fold PF_{50} value), PBS-1110 (5-fold PF_{50} value) and PBS-1135 (5.5-fold PF_{50} value). However, PBS-1110 was found to have a profound effect on cellular growth, morphology and colony formation, and although there was a small window of potentiation at the LD_{50} values of the PBS-1135 survival curve, this was not seen at the other concentrations tested. It was therefore decided that any further studies should be undertaken with PBS-1086.

Compound	LD_{50} (μM)	LD_{50} +IR (μM)	PF_{50}
PBS-1079	0.57	1.04	0.5-fold
PBS-1086	3.58	1.40	2.5-fold
PBS-1088	13.49	8.76	1.5-fold
PBS-1110	5.05	0.99	5-fold
PBS-1135	7.01	1.26	5.5-fold

Table 7.1: LD_{50} values calculated from survival curves of $p65^{+/+}$ cells treated with various Profectus Biosciences inhibitors Table 7.1 summarises the LD_{50} values of each of the Profectus Biosciences inhibitors, PBS-1079, PBS-1086, PBS-1088, PBS-1110 or PBS-1135 alone or in combination with 2.5 Gy IR. PF_{50} values (potentiation factor at 50% cell kill) are expressed as fold changes.

PBS-1086, a compound which has been rigorously tested by Profectus Biosciences is an inhibitor of Rel DNA binding. The compound is known to covalently modify the cysteine-38 residue in the Rel domain of the NF-κB subunits (Jie Zhang personal communication). Moreover, Oh *et al.*, (2010) have shown that PBS-1086 inhibits DNA binding of p65, p50 and RelB as well as luciferase expression in a 293/NF-κB-luciferase reporter cell line. Furthermore, PBS-1086 was also found to inhibit TNF-alpha induced Il-6 and Il-8 release in MDA-MB-231 cells (Jie Zhang, personal communication). Therefore, this compound was chosen for further investigation within this chapter.

7.3.3 Investigation into the effects of PBS-1086 as a radio-sensitising agent in NF-κB proficient and deficient MEFs

The initial screen of the seven compounds identified PBS-1086 as a potential radio-sensitising agent. Table 7.1 and Figure 7.2 illustrate that a combination of PBS-1086 and IR reduced cell survival in the $p65^{+/+}$ MEFs to a greater extent when compared with PBS-1086 alone. Moreover, PBS-1086 appeared to be relatively non-toxic as a mono-therapy at low doses in the $p65^{+/+}$ MEFs. Therefore, it was decided to investigate the ability of PBS-1086 to sensitise $p65^{+/+}$ and $p65^{-/-}$ MEFs to IR using classical colony forming assays (section 2.2.7). To determine whether any potential radio-sensitisation observed was mediated *via* the p65 subunit of NF-κB, p65 siRNA was used. PBS-1086 is known to be a Rel inhibitor and therefore inhibit DNA binding of all five NF-κB subunits (Oh et al., 2011). Thus, $p65^{+/+}$ or $p65^{-/-}$ MEFs were plated and left to adhere for 24 h before transfection with 50 nM p65 or NS siRNA, (or vehicle control). It should be noted that this concentration of siRNA had been optimised previously in these cells (Chapter 3), and known to reduce p65 expression by > 95 %. Cells were then left for 48 h, and pre-treated with PBS-1086, (or DMSO control) 15 min prior to treatment with

increasing doses of IR before being re-plated after a further 24 h and allowed to form colonies for 7-21 days. All survival curves shown are the mean of three independent experiments.

It should be noted that a fixed dose of 1 μM PBS-1086 was used in these experiments, as this dose was shown to reduce cell survival in combination with IR but to be relatively non-toxic alone (Figure 7.2B). This concentration reduced cell survival by approximately 80 % (Figure 7.2B). The data presented here (Figure 7.4) illustrate, that co-incubation with IR and either PBS-1086 or p65 siRNA reduced survival of the $p65^{+/+}$ MEFs compared with IR alone. At the LD_{75} values (lethal dose which reduces survival be 75 %) PBS-1086 or p65 siRNA significantly radio-sensitised the $p65^{+/+}$ MEFs compared with IR alone (p=0.026 and p=0.034, respectively). It is also clear from Figure 7.4 that NS siRNA in combination IR had no effect cell survival compared with IR alone in the $p65^{+/+}$ MEFs (p=0.876). Markedly, Figure 7.4 shows that IR in combination with PBS-1086, p65 siRNA or NS siRNA had no effect on cell survival in the $p65^{-/-}$MEFs compared with IR alone (p=0.542, p=0.489 and p=0.613 respectively). Taken together these data suggest that radio-sensitisation by PBS-1086 is mediated *via* NF-κB p65.

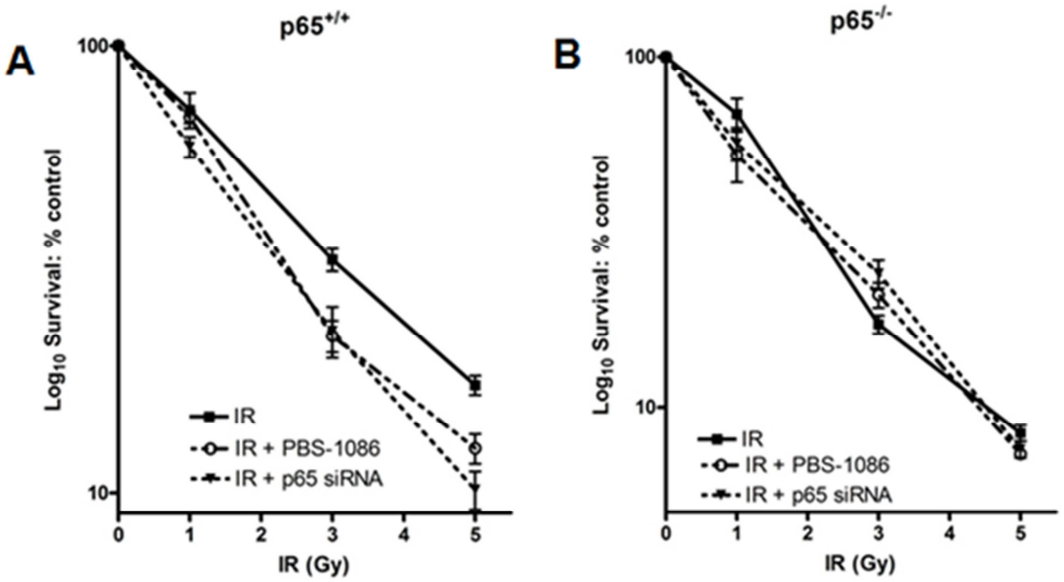

Figure 7.4: Radio-sensitisation by PBS-1086 is mediated *via* p65
The effects of increasing doses of IR either alone, or co-incubated with PBS-1086 or p65 siRNA on cell survival were assessed using the clonogenic survival assay. Cells were treated with relevant siRNA, (or vehicle control), left for 48 h, pre-treated with PBS-1086, or DMSO control for 15 min prior to IR then re-plated after a further 24 h and allowed to form colonies for 7-21 days. (Survival curve (**A)** shows $p65^{+/+}$ MEFs and (**B)** $p65^{-/-}$ MEFs). All results are the mean of three independent experiments with SEM.

7.3.4 Investigation into the effects of PBS-1086 as a radio-sensitising agent in PARP-1 proficient and deficient MEFs

It appeared, from the clonogenic assays detailed in section 7.3.3, that PBS-1086 radio-sensitisation was mediated *via* the p65 NF-κB subunit. Previous work in this thesis has shown that radio-sensitisation by the PARP inhibitor, AG-014699 is mediated *via* NF-κB p65 (Hunter et al., 2011). Thus, from the previous work (Chapters 3 and 4) demonstrating the role of PARP-1 in the activation of NF-κB p65, and results using PBS-1086 in the $p65^{+/+}$ and $p65^{-/-}$ MEFs, it would be expected that radio-sensitisation would only be achieved using an NF-κB inhibitor, such as PBS-1086, in the PARP-$1^{+/+}$ cells.In order to test this hypothesis and confirm both the work with AG-014699 and that presented here with PBS-1086, the classical clonogenic assays were performed using increasing doses of IR in combination with one fixed dose of PBS-1086 (1 μM) in the PARP-$1^{+/+}$ and PARP-$1^{-/-}$ MEFs.

Figure 7.5 shows that co-incubation with IR and PBS-1086 reduced survival of the PARP-$1^{+/+}$ MEFs compared with IR alone. It should be noted that the PARP-$1^{-/-}$ MEFs were 2.7-fold more sensitive to IR compared with PARP-$1^{+/+}$ MEFs. This is consistent with reports that PARP-1 knockout animals are hyper-sensitive to irradiation due to their compromised DNA repair response (Masutani et al., 2005). Furthermore, statistical analysis using an unpaired Student's t-test confirm that, at the LD_{50} values PBS-1086 significantly radio-sensitised the PARP-$1^{+/+}$ MEFs compared with IR alone ($p=0.015$). Markedly, Figure 7.5 shows that IR in combination with PBS-1086 had no effect on cell survival in the PARP-$1^{-/-}$MEFs compared with IR alone ($p=0.924$). Taken together these data support the finding in section 6.3.3, and those in Chapters 3 and 4, and confirm that radio-sensitisation by PBS-1086 is mediated *via* NF-κB p65, and that only PARP-1 proficient cells would be sensitised to IR by an NF-κB inhibitor, such as PBS-1086. Moreover, these data show that PARP-1 is required for radio-sensitistation.

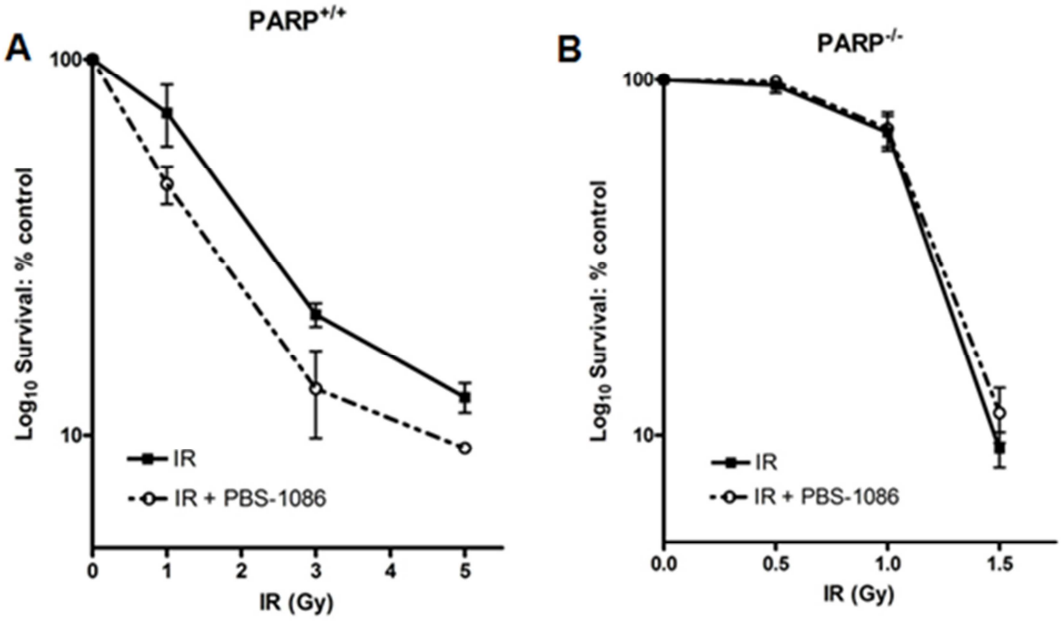

Figure 7.5: Investigation into the effects of PBS-1086 as a radio-sensitising agent in PARP-1 proficient and deficient MEFs. The effects of increasing doses of IR either alone, or co-incubated with PBS-1086 or p65 siRNA on cell survival were assessed using the clonogenic survival assay. Cells were treated with relevant siRNA, (or vehicle control), left for 48 h, pre-treated with PBS-1086, or DMSO control for 15 min prior to IR then re-plated after a further 24 h and allowed to form colonies for 7-21 days. (Survival curve (**A)** shows PARP-$1^{+/+}$ MEFs and (**B)** PARP-$1^{-/-}$ MEFs). All results are the mean of three independent experiments with SEM.

7.3.5 Assessment of the effects of PBS-1086 as a novel inhibitor of IR-induced- NF-κB DNA binding

In order to be confident that the effects observed on cell survival in the both the $p65^{+/+}$ (Figure 7.4) and PARP-$1^{+/+}$ cells (Figure 7.5) were mediated by the inhibition of Rel DNA binding, ELISA-based assays were undertaken in the $p65^{+/+}$ MEFs. Specifically, the inhibition of p65 and p50 DNA binding was investigated. siRNA targeting p65 or a non-specific control (section 3.3.1) was assessed as a direct comparison to PBS-1086. In this case, the p65 siRNA would not only allow insight into the mechanism of action, and specificity of the compound, but also serve as a control for the p65-specific DNA binding ELISA. For these experiments, $p65^{+/+}$ cells were plated and left to adhere for 24 h prior to transfection with 50 nM p65 or NS siRNA (or vehicle control). Cells were incubated left for 48 h, and pre-treated with PBS-1086, (or DMSO control) 15 min prior to treatment with 10 Gy IR. Cells were harvested 2 h later, nuclear extracts prepared and DNA binding assessed using the ELISA.

Firstly, Figures 7.6A and 7.6B show that 1 µM PBS-1086 alone inhibited both p65 and p50 DNA binding compared with basal levels (p=0.052 and p=0.098, respectively),

supporting the data of Oh *et al.,* (2010) which shows that PBS-1086 is a potent and specific inhibitor of NF-κB DNA binding. Moreover, Figures 7.6A and 7.6B illustrate that 10 Gy IR increased DNA binding of either p65 or p50, 2-fold compared with basal levels ($p<0.0001$ and $p=0.002$, respectively). Importantly, co-incubation with PBS-0186 significantly reduced IR-induced p65 and p50 DNA binding, compared with IR in combination with NS siRNA ($p=0.0011$ and $p=0.043$, respectively). The effect of p65 siRNA was assessed following IR in $p65^{+/+}$ MEFs, and it was found that knockdown of the p65 subunit significantly inhibited IR-induced p65, but not p50 DNA binding ($p<0.0001$ compared to IR in combination with NS siRNA). Importantly, Non-specific (NS) siRNA had no effect on DNA-binding of either subunit following IR.

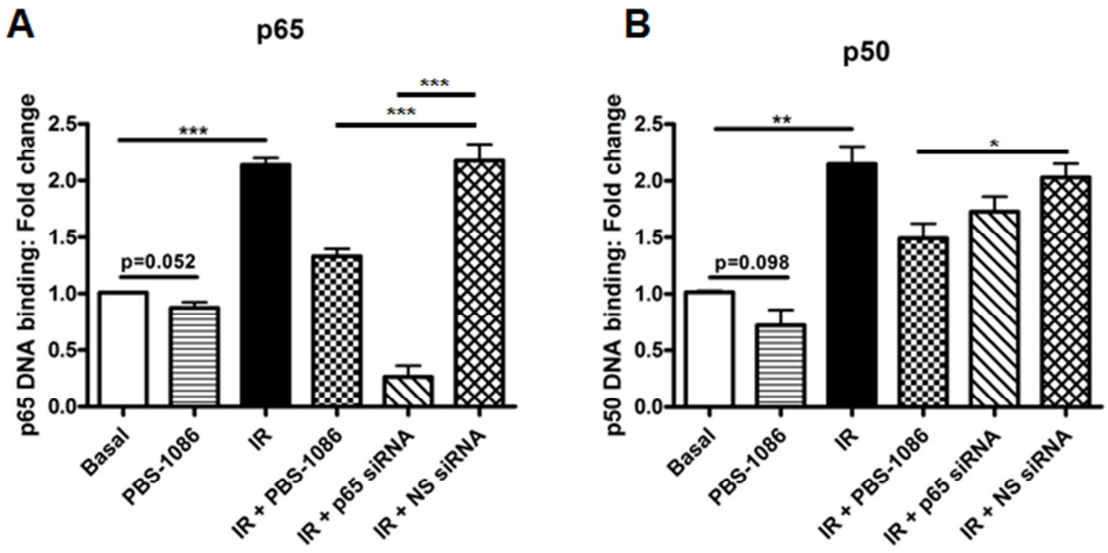

<u>Figure 7.6:</u> PBS-1086 is a novel inhibitor of IR-induced-NF-κB DNA binding
Bar chart showing the effect of IR ± PBS-1086 ± p65 siRNA ±Non-specific (NS) siRNA control on NF-κB p65 and p50 DNA binding activity, measured using an ELISA-based assay (**A**) and (**B**) in $p65^{+/+}$ MEFs. All results are the mean of three independent experiments with SEM. Significance relative to NS siRNA control using unpaired Student's t-test *** $p<0.0001$ ** $p<0.001$, * $p<0.05$

7.3.6 Investigation into the effects of PBS-1086 as a novel inhibitor of IR-induced-NF-κB transcriptional activation

Once the inhibition of p65 and p50 DNA binding by PBS-1086 was confirmed and it could be concluded that PBS-1086 mediated radio-sensitisation *via* the p65 subunit, it was important to determine any effects the compound was having on NF-κB-dependent gene transcription. Furthermore, Oh *et al.,* (2010) reported that that PBS-1086 inhibited TNF-α-induced luciferase expression in a 293/NF-κB-luciferase reporter cell line.

Hence, the inhibitory effects of PBS-1086 on NF-κB activation were further assessed using a luciferase reporter assay in the $p65^{+/+}$ MEFs. siRNA targeting p65 or a non-specific control (section 3.3.1) was assessed as a direct comparison to PBS-1086. Cells were incubated for 24 h before transient transcfection with 200 ng of an NF-κB-luciferase construct and 200 ng of a pCMB-β-galactosidase plasmid (section 2.9). Following further 48 h incubation, cells were treated with either 10 Gy IR or 10 ng/ml TNF-α. Cells were lysed after 0, 2, 4, 6, 8 or 24 h and assayed for luciferase activity using the Promega Luciferase assay system, according to the manufacturer's instructions. Luciferase activity was corrected for β-galactosidase activity as described previously (Brady et al., 1999), and relative activities expressed as fold changes.

Figures 7.7 illustrates that 1 μM PBS-1086 alone inhibited NF-κB-dependent gene transcription compared with basal levels, however this trend was not significant ($p=0.117$, unpaired Student's t-test). Consistent with the increased DNA binding (Figure 7.6), following 10 Gy IR, luciferase activity was increased 2.3-fold, compared to basal levels ($p<0.0001$). PBS-1086 reduced IR-induced luciferase reporter activity to levels comparable with untreated controls although this was not statistically significant when compared to IR in combination with NS siRNA ($p=0.066$). Also, siRNA targeting p65 reduced luciferase activity > 80% following IR ($p=0.03$, compared to IR in combination with NS siRNA), whereas as NS siRNA had no effect on IR-induced luciferase reporter activity compared with IR alone ($p=0.356$).

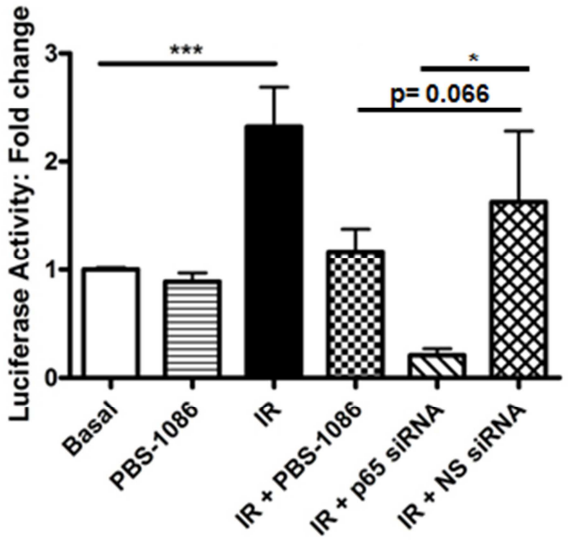

Figure 7.7: PBS-1086 is a novel inhibitor of IR-induced-NF-κB-dependent gene transcription. Bar chart showing the effect of IR ± PBS-1086 ± p65 siRNA ±Non-specific (NS) siRNA control on NF-κB-dependent transcriptional activation, measured using a luciferase reporter assay, in $p65^{+/+}$ MEFs. All results are the mean of three independent experiments with SEM. Significance relative to NS siRNA control using unpaired Student's t-test *** $p<0.001$, * $p<0.05$

7.3.7 PBS-1086 inhibits the transcription of NF-κB-dependent anti-apoptotic genes

In order to demonstrate that the DNA binding (Figure 7.6), luciferase activity (Figure 7.7) and survival data (Figure 7.4) were physiologically relevant it was important to determine whether NF-κB inhibition by PBS-1086 leads to an inhibition of the expression of some known NF-κB-mediated anti-apoptotic genes. The genes chosen to investigate were; *Bcl-xL* (Lee et al., 1999b), *cFLAR* (Kreuz et al., 2001) and *XIAP* (Turner et al., 2007) in the $p65^{+/+}$ MEFs. This method is described in detail in section 2.10. $p65^{+/+}$ MEFs were incubated for 24 h before a 15 min pre-treatment with 1 µM PBS-1086 prior to treatment with 10 Gy IR. Cells were then harvested at various timepoints (0 – 6 h) and RNA extracted using the RNeasy kit and subsequently transcribed into cDNA using the High Capacity cDNA reverse transcription kit. cDNA was then used in a qRT-PCR reaction using Taqman primers to confidently quantify the mRNA levels of either *Bcl-xL*, *cFLAR* or *XIAP* in each sample.

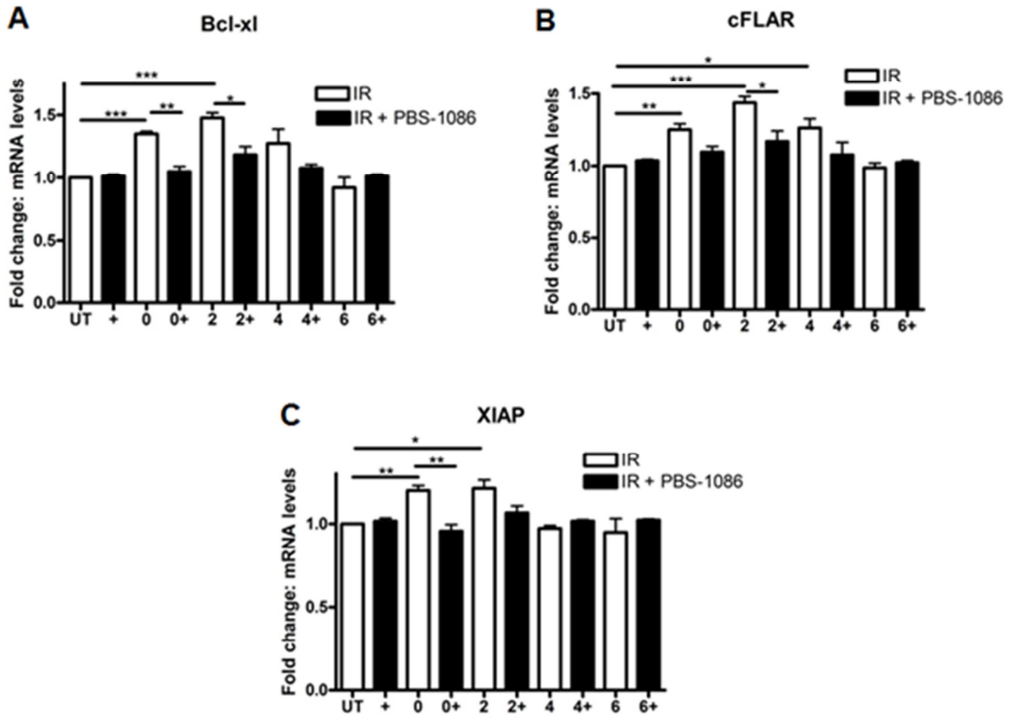

<u>Figure 7.8:</u> PBS-1086 inhibits the transcription of NF-κB-dependent anti-apoptotic genes. Histogram showing the effect of IR ± PBS-1086 (Denoted as +) over time on the expression of the anti-apoptotic genes (**A**) Bcl-xL, (**B**) cFLAR and (**C**) XIAP. All results are the mean of three independent experiments with SEM. Significance relative to mock treated control using unpaired Student's t-test *** $p<0.001$ ** $p<0.01$, * $p<0.05$

Figure 7.8A shows that treatment with IR significantly increases expression of Bcl-xL at early timepoints ($p<0.0001$ (0 h post IR), $p=0.0004$ (2 h post IR), compared with untreated controls) and importantly, that co- incubation with PBS-1086 inhibited IR-induced *Bcl-xL* expression at these timepoints ($p=0.002$ (0 h post IR) and $p= 0.019$ (2 h post IR)) (Figure 7.8A). *cFLAR* expression (Figure 7.8B) was also increased following IR ($p=0.0047$, 0 h, $p=0.0007$ 2 h, $p=0.016$ 4 h, compared to untreated controls) and this again was inhibited by co-incubation with PBS-1086 at the 2 h timepoint ($p=0.034$). A similar trend was aslo observed with *XIAP* expression, which was increased by IR ($p=0.003$ 0 h, $p=0.014$ 2 h) and inhibited by PBS-1086 ($p=0.007$) (Figure 7.8C).

7.3.8 PBS-1086 radio-sensitises breast cancer cells

The data presented in this chapter demonstrate that PBS-1086 is a potent and specific inhibitor of NF-κB DNA binding, and consequently transcriptional activation. As a result of NF-κB inhibition, data presented here also illustrate that PBS-1086 can radio-sensitise cells, *via* the inhibition of p65 DNA binding, and that this radio-sensitisation is likely to be due to the inhibition of IR-induced transcription of anti-apoptotic genes known to be specifically regulated by NF-κB. However, thus far the main body of these data have been in one model system; the p65 proficient and deficient MEFs. Therefore, it was important to determine whether PBS-1086 would have the same effects in another model system.

A panel of breast cancer cell lines was chosen to further investigate the potential utility of PBS-1086 as a radio-sensitising agent. Radio-therapy is one of the main-stays of breast cancer therapy and elevated NF-κB DNA binding activity has been demonstrated both in breast cancer cell lines and primary tissues (Biswas et al., 2004, Nakshatri et al., 1997, Sovak et al., 1997). Constitutive NF-κB activation has been associated with chemo- and radio-resistance and also increased metastasis of breast tumours (Biswas et al., 2001, Wu and Kral, 2005). Inhibition of NF-κB activation *via* inhibition of PARP-1 has also been shown to radio-sensitise two breast cancer cells, MDA-MB-231 and T47D (Veuger et al., 2009). Therefore, the ability of PBS-1086 to sensitise the breast cancer cells to IR using colony forming assays was assessed. Three breast cancer cells lines were chosen for this part of the study; MDA-MB-231, T47D and MCF7, and these are described in detail in section 2.2.7.

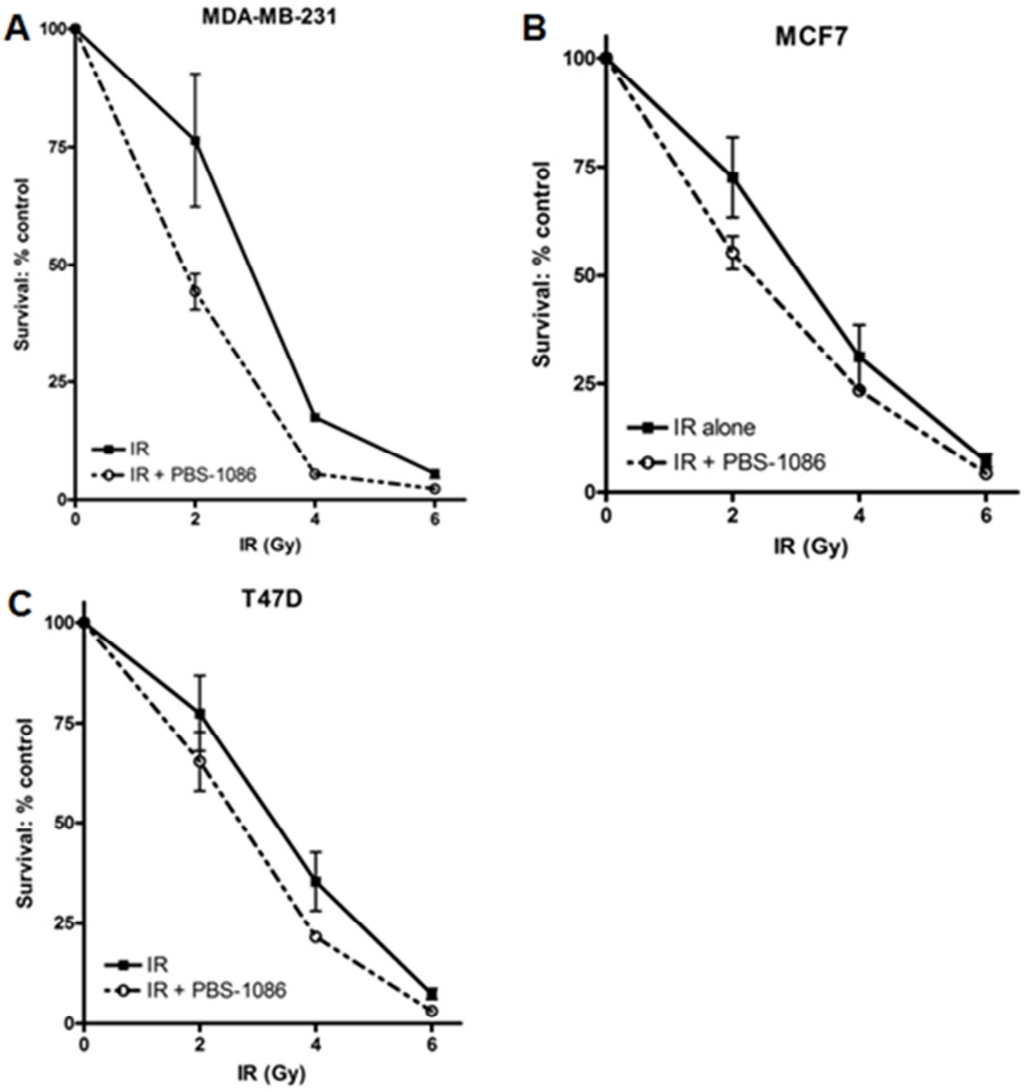

Figure 7.9: PBS-1086 radio-sensitises breast cancer cells. The effects of increasing doses of IR either alone, or co-incubated with PBS-1086, on cell survival were assessed using the clonogenic survival assay. Cells were treated with PBS-1086 or DMSO control then re-plated after a further 24 h and allowed to form colonies for 7-21 days. (Survival curve (**A)** shows MDA-MB-231 cells, (**B**) shows MCF7 cells and (**C)** T47D cells). All results are the mean of three independent experiments with SEM.

Figure 7.9 shows that co-incubation with 1 μM PBS-1086 radio-sensitised all three cell lines compared to cells treated with IR alone (Figures 7.9A-C). Figure 7.9A shows that co-incubation with IR and PBS-1086 reduced survival of the MDA-MB-231 compared with IR alone (LD_{50} value of 2.85 Gy IR alone, compared with an LD_{50} value of 1.70 Gy, IR in combination with PBS-1086 ($p=0.031$). Markedly, Figure 7.9B and 7.9C also shows that IR in combination with PBS-1086 radio-sensitised both the MCF7 cells ($p=0.022$) and T47D cells ($p=0.041$), at the LD_{50} values. Taken together these data

expand the findings in section 6.3.3 and suggest that PBS-1086 has therapeutic potential as radio-sensitising agent for the treatment of breast cancer cells.

7.3.9 Characterisation of the NF-κB status of breast cancer cell lines

Section 7.3.8 showed that the three breast cancer cell lines tested, MDA-MB-231, MCF7 and T47D, were differentially sensitised to IR by PBS-1086. Hence, it was important to assess the NF-κB status of these cell lines, both at the protein and DNA binding levels. This would determine whether any of these cell lines had any constitutive activation of any of the NF-κB subunits. Therefore nuclear extracts were prepared for each of the three cell lines using the NE-PER kit (section 2.5.2). After protein quantification using the Pierce BSA protein assay (section 2.5.3), nuclear extracts were loaded onto the NF-κB DNA binding TransAM Family ELISA (as described in detail, Chapter 2.8.2) and binding of all five subunits was assessed. Expression of the NF-κB subunits p65, p50, p52. RelB and c-Rel proteins was also assessed by Western blotting (section 2.5), and normalised to the nuclear loading control Lamin. Western blots were also probed for β-actin, a protein only found in the cytoplasm, to ensure the nuclear extracts were free from any contamination.

Both the Western analysis (Figure 7.10) and the DNA-binding data (Figure 7.11) illustrate that the MDA-MB-231 cells have the highest protein expression and DNA binding activity of the p65, p50 and RelB subunits. The MCF7 cells have intermediate protein expression and DNA binding activity of these subunits and the T47D cells have the lowest protein expression and DNA binding activity. Statistical analysis using an unpaired Student's t-test shows that MDA-MB-231 cells have significantly higher p65 DNA binding compared with both the MCF7 and T47D cells ($p=0.0006$ and $p=0.046$, respectively). This is also the case for the p50 subunit ($p=0.003$ MDA-MB-231 compared with MCF7, and $p<0.0001$, MDA-MB-231 compared with T47D), and in the case of p50, MCF7 cells show significantly higher DNA binding activity compared with the T47D cells ($p=0.0007$). Furthermore, MDA-MB-231 cells have significantly higher RelB DNA binding activity compared with the MCF7 and T47D cells ($p=0.014$ and $p<0.0001$, respectively), and MCF7 cells have higher RelB binding activity compared with T47D cells ($p=0.013$). DNA binding activity of p52 (Figure 7.11) was highest in the MDA-MB-231 cells, and lowest in the MCF7 cells ($p=0.013$, MDA-MB-231 compared with MCF7). Both the ELISA and Western blotting data shows that the protein levels of p52 are very similar in both the T47D and MCF7 cells. Western

analyses and DNA binding data (Figures 7.10 and 7.11) indicate that c-Rel expression and DNA binding are very similar across all three breast cancer cell lines.

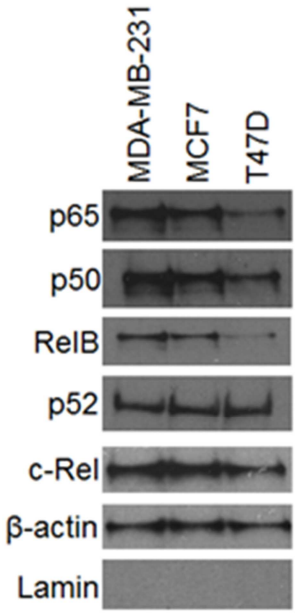

Figure 7.10: NF-κB subunit protein expression in nuclear extracts from untreated breast cancer cell lines. Western blots of nuclear extracts of MDA-MB-231, MCF7 and T47D showing protein expression of p65, p50, p52, RelB and c-Rel. Loading was normalised to lamin nuclear loading control and blots were probed for the β-actin to ensure no cytoplasmic contamination of nuclear extracts.

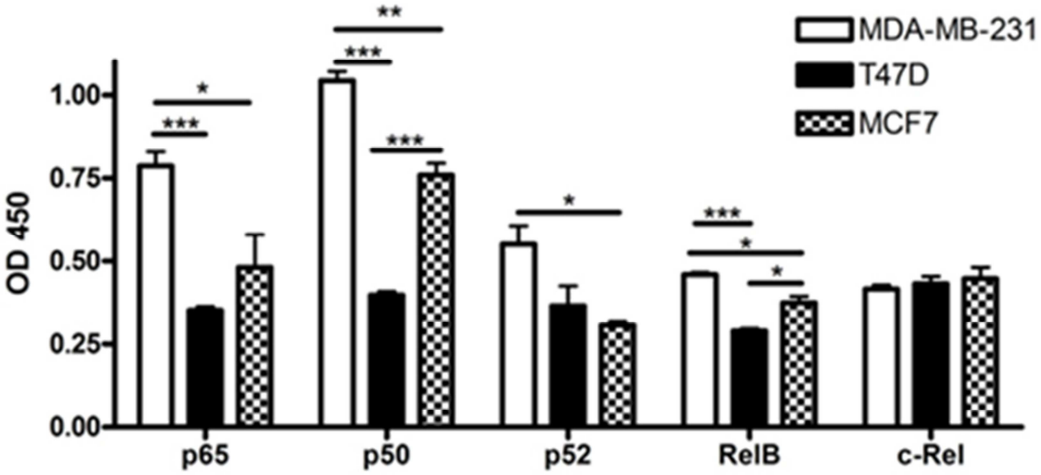

Figure 7.11: NF-κB DNA binding in untreated breast cancer cell lines. Bar chart showing DNA binding of p65, p50, p52, RelB and c-Rel in untreated MDA-MB-231, MCF7 and T47D cells, measured using an ELISA-based assay. All results are the mean of three independent experiments with SEM. Significance relative to mock treated control using unpaired Student's t-test *** $p<0.001$ ** $p<0.01$, * $p<0.05$

7.3.10 PBS-1086 as a mono-therapy in breast cancer expressing aberrantly active NF-κB

The DNA binding and Western blotting data from untreated breast cancer cell lines illustrated that all of these cells had some constitutive NF-κB activity, and previous data (section 6.3.2), suggested that PBS-1086 may have some potential activity against NF-κB as a mono-therapy in MEFs expressing p65. Therefore, it was important to determine whether PBS-1086 alone had any effect on survival in the MDA-MB-231, MCF7 and T47D cells. Clonogenic assays were used in which cells were plated and incubated for 24 h. Following this cells were treated with increasing doses of PBS-1086 (0 – 10 μM) and left for a further 24 h. Cells were re-plated and allowed for form colonies for 7-21 days.

Figure 7.12 shows that PBS-1086 is cytotoxic as a mono-therapy at all doses tested (0.1 – 10 μM) in all three cells lines, however the cell lines did show differential sensitivity. LD_{50} values detailed in Table 7.2 show that the MDA-MB-231 cells (which have been found to have the highest NF-κB expression and DNA binding activity of the cell lines tested), were the most sensitive to PBS-1086 (LD_{50} value of 0.39 μM). MDA-MB-231 were almost 10-fold more sensitive than the T47D cells (LD_{50} value of 3.13 μM), and 17-fold more sensitive than the MCF7 cells (LD_{50} value of 6.68 μM). The table also includes the NF-κB status, as summarised from the data in section 6.3.9. Statistical analyses on LD_{50} values confirmed that MDA-MB-231 cells were significantly more sensitive to PBS-1086 compared with T47D and MCF7 cells ($p<0.0001$ and $p<0.0001$, respectively). The T47D cells were also more sensitive to PBS-1086 compared with the MCF7 cell, although this was not statistically significant ($p=0.082$).

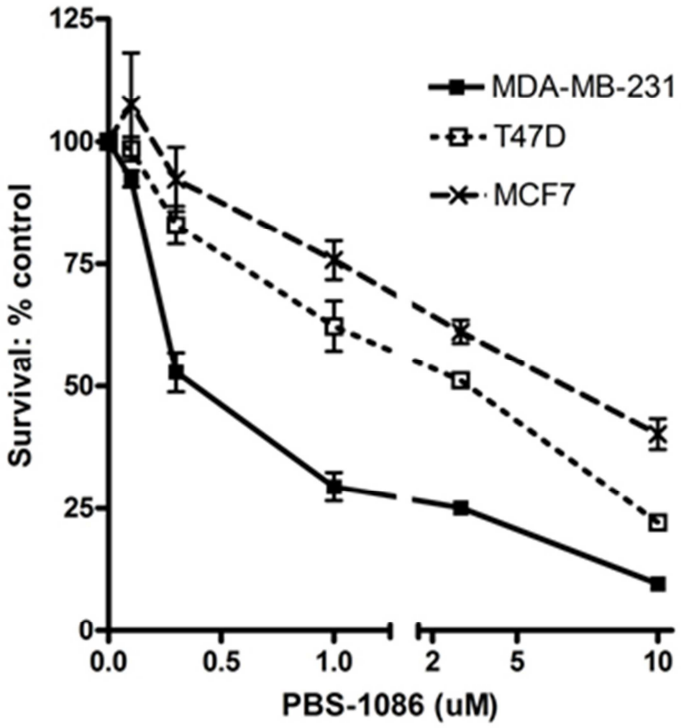

Figure 7.12: Clonogenic survival of three breast cancer cell lines following treatment with PBS-1086. The effects of increasing doses of PBS-1086 (0 – 10 µM) PBS-1086 on cell survival was assessed in MDA-MB-231, T47D and MCF7 cells (**C**). Cells were treated with PBS-1086 or DMSO control then re-plated after a further 24 h and allowed to form colonies for 7-21 days. All results are the mean of three independent experiments with SEM.

Cell line	LD_{50} (µM)	NF-κB status
MDA-MB-231	0.39	+++
T47D	3.10	+
MCF7	6.68	++

Table 7.2: LD_{50} values calculated from survival curves of breast cancer cell lines treated with PBS-1086 Table 7.2 summarises the LD_{50} values of each of the breast cancer cell lines, MDA-MB-231, T47D and MCF7 treated with increasing doses of PBS-1086. NF-κB status is summarised; +++ denotes high constitutive activation, ++ denoted intermediate constitutive activation and + denotes low constitutive activation (as determined in Figure 7.11).

7.3.11 PBS-1086 inhibits NF-κB DNA binding in breast cancer cell lines

In order to confirm that the results obtained in the clonogenic assays (section 7.3.10) were due to the inhibition of NF-κB DNA binding by PBS-1086, a series of NF-κB DNA binding ELISA assays in the presence or absence of PBS-1086 were undertaken in the breast cancer cell lines. This would also confirm the potential utility of the compound as a single agent therapy in breast cancer. Oh *et al.*, (2010) reported that 10

µM PBS-1086 suppressed spontaneous lympho-proliferation and inhibited the production of pro-inflammatory cytokines in PBMCs from HTLV-I–associated myelopathy/tropical spastic paraparesis (HAM/TSP) patients *via* the inhibition of NF-κB DNA binding. Hence, it was decided to use this concentration (10 µM), and the 1 µM PBS-1086 concentration that had been used previously in this study (as a combination therapy), and assess the effects of these concentrations on NF-κB subunit DNA binding in the three breast cancer cell lines. MDA-MB-231, MCF7 or T47D cells were incubated for 24 h prior to treatment with 1 µM or 10 µM PBS-1086 or a DMSO control. Cells were harvested 24 h later, to duplicate the timecourse of the clonogenic assays (section 6.3.10) and nuclear extracts were prepared and DNA binding assessed using the ELISA assay.

Figure 7.13A shows that 1 µM PBS-1086 significantly inhibited p65 DNA binding in the MDA-MB-231 cells (p=0.028, compared with untreated controls), and this trend was echoed in both the MCF7 and T47D cells, although this was not statistically significant. Moreover, 10 µM PBS-1086 further inhibited p65 DNA binding in the MDA-MB-231 and T47D cells (p=0.001 and p=0.014, respectively, compared to untreated controls). 10 µM PBS-1086 also further inhibited p65 DNA binding in the MCF7 cells (p=0.062). PBS-1086 also inhibited DNA binding of the other canonical subunit p50 (Figure 7.13B). 1 µM PBS-1086 significantly inhibited p50 DNA binding in the MDA-MB-231 cells (p=0.032), and this trend was echoed in both the MCF7 and T47D cells, although this was not statistically significantly. Moreover, 10 µM PBS-1086 further inhibited p50 DNA binding in all of the cell lines tested (p=0.0001 (MDA-MB-231), p=0.0004 (T47D) and p=0.0076 (MCF7)). Figure 7.13C shows that PBS-1086 inhibited binding of the non-canonical subunit, RelB when used at the 10 µM concentration, consistent with the report of Oh *et al.* (2010). RelB DNA binding was significantly inhibited in both the MDA-MB-231 and T47D cells (p=0.0034, and p=0.029, respectively). PBS-1086 had no effect on RelB DNA binding in the MCF7 cells at any of the concentrations tested. PBS-1086 also inhibited p52 DNA binding in both the MDA-MB-231 and T47D cells, compared to untreated controls (Figure 7.13D), although this was not statistically significant. However, both concentrations of PBS-1086 tested increased p52 DNA binding in the MCF7 cells (p=0.013). Figure 7.13E shows that PBS-1086 had no effect on c-Rel DNA binding in the breast cancer cells, at any of the doses tested.

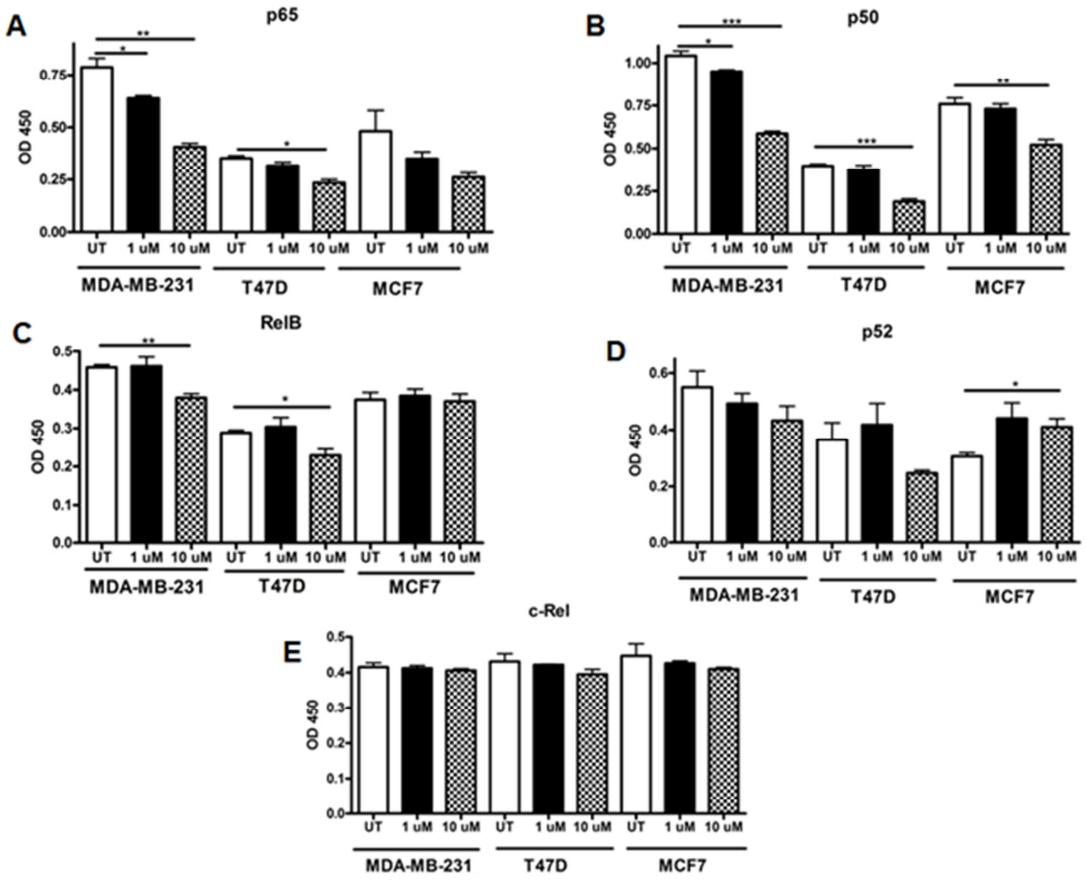

Figure 7.13: The effect of PBS-1086 on NF-κB DNA binding in breast cancer cells. The effect of a 24 h exposure of PBS-1086 on (**A**) p65, (**B**) p50, (**C**) RelB, (**D**) p52 and (**E**) c-Rel DNA binding in MDA-MB-231, MCF7 and T47D cells, measured using an ELISA-based assay. Open bars denote untreated controls (UT), black bars denote cells treated with 1 µM PBS-1086 and hatched bars denote cells treated with 10 µM PBS-1086. All results are the mean of three independent experiments with SEM. Significance relative to mock treated control using unpaired Student's t-test *** $p<0.001$ ** $p<0.01$, * $p<0.05$

7.3.12 Window of potentiation studies with two further Profectus Biosciences NF-κB inhibitors

For the duration of this study, PBS-1086 was the lead compound in the NF-κB inhibitor programme at Profectus Biosciences Inc, however further families of compounds were synthesised by the company during this time and two further compounds of interest were identified. These inhibitors were PBS-1169 and PBS-1170, and they underwent the 'window of potentiation' study, described in section 7.3.2 of this chapter. The survival curve of $p65^{+/+}$ MEFs treated with increasing doses of PBS-1169 alone or in combination with 2.5 Gy IR (Figure 7.14A) shows that there is very little difference when comparing the inhibitor alone or in combination with IR. The LD_{50} value for PBS-1169 alone is 1.33 µM whereas the LD_{50} values for PBS-1169 in combination with IR is

1.72 µM, although the difference between these two values is not statistically significant (p=0.413).

The survival curve of $p65^{+/+}$ MEFs treated with increasing doses of PBS-1170 alone or in combination with 2.5 Gy IR (Figure 7.14B) shows that there is a clear window of potentiation observed between treatment with the inhibitor alone and the inhibitor in combination with IR, at all doses tested. A significant difference (p=0.023) was observed between the LD_{50} values of PBS-1170 alone (LD_{50} of 9.55 µM) and PBS-1086 in combination with 2.5 Gy IR (LD_{50} of 0.75 µM). Furthermore, at low concentrations, PBS-1170 was relatively non-toxic alone, something had been seen previously with AG-014699 (Figure 7.1), yet there was a pronounced radio-sensitisation with 2.5 Gy IR at these doses. These data suggest that this compound warrants further investigation as a radio-sensitising agent.

Table 7.3 summarises the LD_{50} values of each of the Profectus Biosciences inhibitors, PBS-1169 or PBS-1170 alone or in combination with 2.5 Gy IR. This table also includes the PF_{50} values for each of these agents, where appropriate. These data indicate that the most promising compound in terms of its ability to radio-sensitise the $p65^{+/+}$ MEFs was PBS-1170 (12-fold PF_{50} value). These data suggest that PBS-1170 warrants much further investigation as an NF-κB inhibitor.

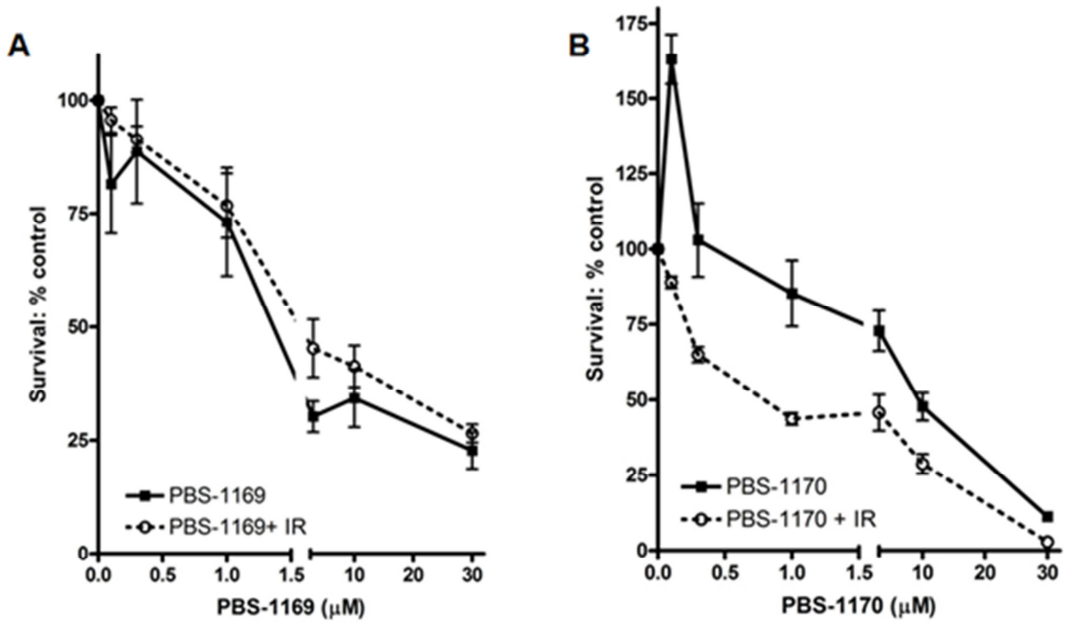

Figure 7.14: Survival of $p65^{+/+}$ following treatment with increasing doses of Profectus Biosciences inhibitors and 2.5 Gy IR. The effects of increasing doses of (**A**) PBS-1169 or (**B**) PBS-1170 (0 – 30 µM) PBS-1086, alone (solid line) or in combination with one fixed dose of IR (2.5 Gy) (dotted line), on cell survival was assessed in $p65^{+/+}$ MEFs (**A**). Cells were treated with PBS inhibitor or DMSO control for 15 min prior to IR (if relevant) then re-plated after a further 24 h and allowed to form colonies for 7-21 days.

Compound	LD_{50} (μM)	LD_{50} +IR (μM)	PF_{50}
PBS-1169	1.33	1.72	0.75-fold
PBS-1170	9.55	0.75	12-fold

Table 7.3: LD_{50} values calculated from survival curves of $p65^{+/+}$ cells treated with two Profectus Biosciences inhibitors. Table 7.3 summarises the LD_{50} values of each of the Profectus Biosciences inhibitors, PBS-1169 or PBS-1170 alone or in combination with 2.5 Gy IR. PF_{50} values (potentiation factor at 50% cell kill) are expressed as fold changes.

7.4 Discussion

The initial screen of a panel of NF-κB inhibitors used p65 proficient MEFs in order to determine which were the most potent and specific identified four of the seven compounds as potential radio-sensitising agents when using LD_{50} values as a determinant (Tables 7.1 and 7.3). However, PBS-1110 was found to have a profound effect on cellular growth, morphology and colony formation, and although there was a small window of potentiation at the LD_{50} values of the PBS-1135 survival curve, this was not seen at the other concentrations tested. The largest fold potentiation (12-fold) was observed with PBS-1170, whilst a 2.5-fold potentiation was seen with PBS-1086.

PBS-1086, a compound which has been rigorously tested by Profectus Biosciences is an inhibitor of Rel DNA binding. The compound is known to covalently modify the cysteine-38 residue in the Rel domain of the NF-κB subunits (Jie Zhang personal communication). Moreover, Oh *et al.,* (2010) have shown that PBS-1086 inhibits DNA binding of p65, p50 and RelB as well as luciferase expression in a 293/NF-κB-luciferase reporter cell line. Furthermore, PBS-1086 was also found to inhibit TNF-alpha induced Il-6 and Il-8 release in MDA-MB-231 cells (Jie Zhang, personal communication). Therefore, this compound was chosen for further investigation within this chapter.

The data presented here demonstrates that the Rel inhibitor, PBS-1086 and siRNA targeting p65 both significantly decreased survival following IR in $p65^{+/+}$ MEFs whilst having no effect in $p65^{-/-}$ MEFs. This sensitisation was 1.4-fold and importantly occurred at clinically relevant doses of IR. Furthermore, PBS-1086 inhibited IR-induced DNA binding of both the p65 and p50 subunits of NF-κB, and that PBS-1086 inhibited IR-induced NF-κB luciferase reporter activity. Importantly, results illustrate that these

findings are physiologically relevant by demonstrating that co-incubation with PBS-1086 decreased the DNA-damage induced transcription of key anti-apoptotic genes, known to be regulated by NF-κB. Moreover, the data also go on to highlight new therapeutic avenues for the development of specific NF-κB subunit inhibitors in breast cancers expressing constitutively active NF-κB. Therefore, this work illustrates that PBS-1086 could be used either as a stand-alone agent or as in combination with radio-therapy in a panel of breast cancer cell lines.

To investigate the mechanism by which PBS-1086 radio-sensitised cells, p65 knockdown and $p65^{-/-}$ MEFs were used as direct comparison for PBS-1086. Results show that radio-sensitisation by PBS-1086 is mediated *via* the p65 subunit of NF-κB, consistent with reports that DNA damaging agents activate the canonical pathway (Hunter et al., 2011). The clonogenic survival data assessing the effect of PBS-1086 in PARP-1 proficient and deficient MEFs, supports the work in chapters 3 and 4, and gives an insight into the types of tumours and inflammatory diseases in which this inhibitor may be active. PBS-1086 radio-sensitises the $PARP\text{-}1^{+/+}$ but not $PARP\text{-}1^{-/-}$ MEFs, supporting the previous work in this thesis, by illustrating that the presence of PARP-1 in essential for any radio-sensitisation mediated *via* NF-κB. Furthermore, these data suggest that PBS-1086 may useful agents in cancers which over express PARP-1. For example, there are some reports which suggest that gain of chromosome 1q, on which PARP-1 is located, is a frequent event in aggressive breast cancers (Farabegoli et al., 2004) Hence, inhibition of NF-κB activation (shown here to be driven by PARP-1 activation, (Hunter et al., 2011)) may be of therapeutic benefit in such breast tumours, and therefore agents such as PBS-1086 the ideal candidate for such treatment benefit. Conversely, the survival data in PARP-1 -proficient and -deficient MEFs suggests that PBS-1086 may not be an ideal radio- or chemo-sensitising agent in cells or tissues lacking PARP-1. It has been reported that PARP-1 null mice develop low-frequency spontaneous tumours in multiple organs, including the mammary glands (Tong et al., 2002, Tong et al., 2001), however it has also been shown that PARP-1 null cells display reduced NF-κB-dependent transcriptional activation (Oliver et al., 1999b).

At low concentrations, PBS-1086 inhibited both p65 and p50 DNA binding in the $p65^{+/+}$ MEFs compared with basal levels, although this was not statistically significant. Importantly, PBS-1086 inhibited IR-induced-DNA binding of both subunits. Unfortunately, the binding of the other subunits could not assessed in the MEFs as the

antibodies provided with the ELISA assay are not compatible with murine p52, RelB or c-Rel, because they are raised against the human forms of these proteins only. It should be noted that although p65 siRNA inhibited IR-induced p65 DNA binding, as would be expected, there was a small, but not significant decrease in IR-induced p50 DNA binding also. It is possible that this is due to the loss of the p65-p50 heterodimer. The p65 subunit is the most common heterodimeric partner of p50 (Chen et al., 1998), and together these subunits make up the most common NF-κB dimer. Moreover, this heterodimer has previously been shown to be frequently activated following DNA damage (Perkins, 2007).

The work in this chapter illustrates that the MDA-MB-231 cells are highly sensitive to PBS-1086 compared with other breast cancer cell lines. Moreover, the data suggest that this correlates with MDA-MB-231 cells having the highest DNA binding activity and protein expression of all of the subunits, except c-Rel, which was found to be constant across all three cell lines. This is consistent with other reports that high NF-κB DNA binding activity correlates with sensitivity to NF-κB inhibition (Hewamana et al., 2008a, Lopez-Guerra et al., 2009). However, clonogenic survival data showed that the cell line that had the lowest DNA binding and NF-κB expression, T47D, was not the least sensitive to PBS-1086. The cell line that was the least sensitive was in fact the cell line with intermediate binding and expression, MCF7. One explanation for this is that 10 μM PBS-1086 markedly inhibited DNA binding of all subunits (except c-Rel) in the T47D cells, whereas in MCF7 significant inhibition of DNA binding was only observed in the canonical subunits, p65 and p50.

Previous work has shown that there is a delicate balance and complex interplay between the NF-κB subunits in CLL (Mulligan EA et al., 2010), and this is undoubtedly the case in breast cancer. The basal levels of NF-κB subunit DNA binding varies from cell line to cell line, and inhibition of individual subunit by PBS-1086 also varies. For example, PBS-1086 shows modest inhibition of p52 DNA binding in both the MDA-MB-231 and T47D cells, however 10 μM PBS-1086 significantly increased p52 DNA binding in the MCF7 cells. It is therefore possible that these cells are addicted to non-canonical pathway activation, mediated in part by p52 and its subsequent downstream signalling. Hence, it is possible that MCF7 cells could be evading cell death by PBS-1086 through increased p52 activation. Further evidence for this is provided in results for RelB, another non-canonical subunit. PBS-1086 significantly inhibited RelB DNA binding in

the MDA-MB-231 and the T47D cells but it had no effect DNA binding in the MCF7 cells, again suggesting that MCF7 are reliant to some extent on non-canonical pathway signalling. Moreover, clonogenic survival data (Figure 7.12) shows a greater fold radio-potentiation by PBS-1086 in both the MDA-MB-231 and T47D cells compared with the MCF7 cells. These data are consistent with the report from Mineva *et al.*, (2009), detailing that the inhibition of RelB is important in sensitising cells to IR. This group reported that RelB promoted the survival of breast cancer cells following both IR and doxorubicin, and moreover than specific targeting of RelB either by siRNA or 1,25-Dihydroxyvitamin D_3 radio-sensitised these cells (Mineva et al., 2009).

The MDA-MB-231 cells have the highest NF-κB subunit DNA binding activity and protein expression and are radio-sensitised to the greatest extent by PBS-1086. However, the MCF7 cells exhibited intermediate DNA binding and protein expression but the radio-sensitisation by PBS-1086 was lower in these cells than it was in the T47D cells, which had the lowest NF-κB subunit DNA binding and protein expression. One explanation for this is that in the MCF7 cells it appears that NF-κB activation is not directly correlated with the cellualar response to IR, and that in this case other factors may contribute to the cytotoxicity observed in this cell line. Furthermore, the single agent concentration of PBS-1086 at which these radio-sensitisation clonogenic assays were performed should also be discussed. A concentration of 1 μM was used as this concentration had been shown previously, in the $p65^{+/+}$ MEFs, to be relatively non-toxic alone. However, when a dose range of PBS-1086 was undertaken in the breast cancer cells, it appeared that this concentration had a profound effect on cell survival alone in all three cell lines. Therefore, it would be advantageous to repeat the radio-sensitisation assays in combination with lower concentrations of PBS-1086. To this end, however, it must also be noted that when the effects of subunit DNA binding following a prolonged exposure to either 1 μM or 10 μM PBS-1086 were assessed in the breast cancer cell lines, the lower concentration only significantly inhibited DNA binding of p65 or p50, whereas the 10 μM DNA binding of all subunits of c-Rel, to some extent. Hence, it would be important to assess any effects on subunit DNA binding with the concentration used in combination with IR in the clonogenic assays.

The data presented here shows that the MDA-MB-231 breast cancer cells have the highest protein expression and DNA binding activity of both of the canonical subunits, p65 and p50, and that these cells are most sensitive to PBS-1086 mono-therapy. This

supports the recent data of Lui *et al.,* (2010) which illustrated, by using the IκBα super repressor (IκBαSR), that the canonical pathway was responsible for the development of murine mammary tumourigenesis. This work also went on to show that NF-κB activity in such tumours maintained the expansion of progenitor cells (measured by CD44 positivity), and that IκBαSR expression reduced the proportion of CD44 positive cells by approximately 50 % (Liu et al., 2010). Furthermore, another group have shown that compounds known to inhibit NF-κB activation, preferentially target breast cancer stem cells (Zhou et al., 2008). Taken together these data suggest that be using a potent and specific inhibitor, such as PBS-1086, may in fact target this stem cell niche.

Mutations in Ras are common in many cancers, including lung and breast, and are associated with poor prognosis and therapeutic resistance (Bos, 1989); hence targeting Ras has become an attractive approach in cancer. It has been reported that 20 % of non-small cell lung cancers have Ras mutations (Mascaux et al., 2005). Two recent reports have suggested that the NF-κB and Ras activation pathways are intimately linked (Barbie et al., 2009, Basseres et al., 2010). Both studies, in lung cancer cell lines and xenograft models, found that NF-κB inhibition is hyper-lethal to cells with mutant K-Ras and may provide an alternative method for the pharmacological targeting of oncogenic K-Ras. Basseres *et al.,* (2010) use a specific inhibitor of IKKβ and conclude that is it the p65 subunit that is vital for K-Ras induced tumorigenesis. The survival data using PBS-1086 as a mono-therapy in the breast cancer cell lines furthers these existing data, by showing that the MDA-MB-231 breast cancer cell line with a G13D K-Ras mutation (Barbie et al., 2009), Sanger cell line Cosmic database), not only has the highest activity and expression of p65 but also is most sensitive to PBS-1086 (almost 10-fold more sensitive compared with the K-Ras wild-type breast cancer cell lines tested). Therefore, this may suggest that there is a co-dependency between the Ras and NF-κB pathways in cancer, which could be potentially be exploited as a mechanism of synthetic lethality.

7.5 Summary and future work

In summary, this chapter demonstrates that a very potent and specific Rel inhibitor, PBS-1086, can sensitise cells to irradiation and that this is mediated directly *via* the inhibition of NF-κB. To this end, PBS-1086 may prove useful in overcoming NF-κB-mediated therapeutic resistance in breast, and other cancers. The use of PBS-1086,

which directly targets the Rel DNA binding functions of the NF-κB subunits (Jie Zhang, personal communication) may overcome toxicities observed with other inhibitors of the NF-κB pathway. For example, the IKK complex is known to have many functions within the cell (Carrillo et al., 2004, Chariot, 2009), and thus global inhibition using IKK inhibitors, may be cytotoxic, due effects on pathways other than just that of NF-κB. Moreover, the data presented within this chapter highlight the potential use for PBS-1086 as a stand-alone agent in breast cancers which express aberrantly NF-κB, something which warrants much further investigation.

The work here has concentrated on the inhibition of NF-κB activation by PBS-1086 in breast cancer cell lines, therefore the further pre-clinical studies should be undertaken in xenograft models and primary tissues of this disease. The role of PBS-1086 as a radio-sensitising agent has been assessed here, however many other DNA damaging agents are used in the treatment of breast cancer. For example, the topoisomerase II poison, doxorubicin, is widely used and also known to activate NF-κB (Campbell et al., 2006a). Hence, it would be predicted that PBS-1086 would chemo-sensitise cells to this agent, and others that act *via* NF-κB activation. Moreover, aberrantly active NF-κB has been reported in many different types of cancers and leukaemia (Basseres and Baldwin, 2006). Therefore, this agent has wide ranging potential in the treatment of many cancers, although this must be rigorously tested in the different types of the disease both *in vitro* and *in vivo*.

Importantly, it was not only PBS-1086 that exhibited potential as a radio-sensitiser in the initial screen undertaken; PBS-1170 showed a 12-fold potentiation (Table 7.3). Due to time constraints, it was not possible to pursue this compound further. It is therefore important to undertake future work with PBS-1170. This compound is known to inhibit p65, without effecting RelB or c-Rel (Jie Zhang, personal communication), and therefore it would be predicted that this compound would be a potent radio-sensitiser, as indicated in the data from the second compound screen (Figure 7.14B).

The potential to exploit a putative mechanism for synthetic lethality in terms of the co-dependency between the Ras and NF-κB pathways in cancer (as described by Barbie *et al.,* (2009) and Basseres *et al.,* (2010) is also something which requires much further investigation. The data presented here supports the existing reports demonstrating that the K-Ras mutation cell line, MDA-MB-231 were the most sensitive to PBS-1086 as a

single agent, however more work is required. A wide range of cell lines containing Ras mutations should be tested to screen for sensitivity to NF-κB inhibition. This approach was used by Bryant *et al.*, (2005) and Farmer *et al.*, (2005) to confirm synthetic lethality of PARP-1 inhibition in BRCA-defective cells. However, to further confirm the hypothesis that NF-κB inhibitors will be particularly effective in a Ras mutated background, and isogenic paired cell line containing cells that are either WT or Ras mutated should be used and would provide a huge amount of insight into the cross-talk between the NF-κB and Ras pathways. Moreover, for true synthetic lethality, the NF-κB inhibitor would have no effect in normal cells, and only those which contain a Ras mutation. It would therefore be essential to develop a very potent and specific NF-κB inhibitor, which could be used at low, non-toxic concentrations.

Chapter 8. Conclusions and future study

The aims of this thesis were to test the hypothesis that PARP-1 mediates cell survival following DNA damage primarily through activation of NF-κB. The potent and specific PARP inhibitor, AG-014699 and siRNA knockdown of either p65 or PARP-1, as well as MEFs proficient or deficient for either NF-κB p65 or PARP-1 were used to elucidate the underlying molecular mechanisms that transduce signals from DNA damage-activated PARP-1 to the activation of NF-κB. Furthermore, it was also hoped that these data could aid in the determination of new therapeutic avenues for use of AG-014699 in cancers in which aberrantly active NF-κB mediates therapeutic resistance.

8.1 The role of PARP and NF-κB in radiosensitivity

Briefly, clonogenic survival and apoptosis assays showed that $p65^{-/-}$ MEFs were more sensitive to IR than $p65^{+/+}$ MEFs, consistent with reports that NF-κB confers radio-resistance (Biswas et al., 2001, Wu and Kral, 2005). Co-incubation with p65 siRNA, PARP siRNA or AG-014699 radio-sensitised $p65^{+/+}$, but not $p65^{-/-}$ MEFs, demonstrating that PARP-1 mediates its effects on survival *via* NF-κB. Furthermore, a combination of p65 siRNA and AG-014699 radio-sensitised $p65^{+/+}$ MEFs to the same extent as either agent alone, strongly indicating that PARP-1 and NF-κB are mechanistically linked, supporting existing data in the literature (Chang and Alvarez-Gonzalez, 2001, Hassa et al., 2001, Hassa and Hottiger, 1999, Kauppinen and Swanson, 2005, Martin-Oliva et al., 2004, Stilmann et al., 2009, Veuger et al., 2009).

PARP-1 is known to be vital for the repair of SSBs. SSB repair kinetics, and the effect SSB repair inhibition by AG-014699 were similar in $p65^{+/+}$ and $p65^{-/-}$ cells. Since inhibition of SSB repair did not radio-sensitise $p65^{-/-}$ cells, these data show that radio-sensitisation by AG-014699 is due, in part, to downstream inhibition of NF-κB activation. However, further work should be undertaken to thoroughly test this hypothesis, and other functional roles of PARP-1 within the cell, such as it's role in DSB repair, should be considered.

8.2 The role of PAR in the activation of NF-κB

PARP-1 catalytic activity was essential for IR-induced p65 DNA binding and NF-κB-dependent gene transcription, whereas for TNF-α treated cells, PARP-1 protein alone was sufficient, in line with the report from Hassa *et al.*, (2001). It can therefore be

hypothesised that this stimulus-dependent differential is mediated *via* stimulation of PAR, which was induced following IR, not TNF-α. PARG is the major enzyme responsible for the catabolism of PAR (Bonicalzi et al., 2005). In order to inhibit degradation of PAR a potent and specific PARG inhibitor, ADP-HPD, was used (Slama et al., 1995). In this case, increased polymer stability following IR, by virtue of inhibition of polymer degradation, led to the persistence of NF-κB DNA binding, an increase in anti-apoptotic gene expression and protection against IR-induced cell death. These data confirm a role for PAR in the activation of NF-κB following DNA damage, thus supporting the work of Stilmann *et al.*, (2009).

As previously discussed, Stilmann *et al.*, (2009), proposed an elegant model which detailed how DNA-damage induced NF-κB activation was mediated by PAR (Figure 1.13). The caveats associated with this study have also been discussed at length as part of this thesis. An extended, complementary model for the activation of NF-κB, which is mediated by PAR following DNA damage, has been proposed in section 4.4. Briefly, DNA damage, such as IR, activates PARP-1, recruiting it to the site of damaged DNA. This results in formation of negatively charged PAR (Ueda and Hayaishi, 1985). The NF-κB p65-p50 heterodimer is also translocated to the nucleus following DNA damage *via* activation of the canonical pathway of NF-κB activation. When in proximity to regions with overall negative charge, such as that of PAR, a conformational change in p65 can be induced, exposing the positively charged DNA binding interface of p65 (Ghosh, 1999). Thus, negatively charged PAR has the ability to attract p65 to bind DNA (as PARP-1 and the polymer are recruited to sites of damaged DNA) up-regulating transcription of NF-κB-dependent genes, protecting against apoptosis and conferring radio-resistance. However, in the presence of the PARP inhibitor, AG-014699, PARP-1 is no longer active and cannot form the polymer. Hence in this case, there is reduced DNA binding and transcriptional activation following IR, with induction of apoptosis and ultimately radio-sensitisation.

However, more experiments, which were beyond the scope of this thesis should be undertaken to further confirm this proposed mechanism. To this end, it would be important to perform some key immunofluorescence assays, similar to those described by (El-Khamisy et al., 2003) which were used to show that PAR recruits the BER protein XRCC1 to micro-sites of DNA damage. The aim of these experiments would be to determine whether p65 is recruited to the DNA through the electrostatic attraction

generated in the presence of PAR. In order to do this, a fluorescent-tagged p65 could be introduced into cells, and then these cells damaged using a laser, so that only a microscopic area had damaged DNA, and therefore PAR formation. Cells could then be stained with a PAR antibody and co-localisation studies could be undertaken, in this case to determine whether p65 is attracted to the negative charge of PAR. It would be important to use micro-sites of damage in this case as large areas of damage will result in a large amount of PAR formation and may mask any signal with p65. Another method of investigating the interaction between PAR and p65 following DNA damage would be to use fluorescence resonance energy transfer (FRET) (Zhang and Rudkevich, 2007). This principle is used to describe the energy transfer between two chromophores, and is centered around the fact that a fluorophore labelled-donor chromophore, initially in its electronic excited state, may transfer energy to an fluorophore labelled-acceptor chromophore in close proximity (typically less than 10 nm). This technique can not only be used to assess protein-protein interactions, but also for monitoring protein conformational changes, and could therefore be utilised to analyse the proposed conformational change in p65 in the presence of PAR.

It is important to take into account the Histone shuttling model, which states that the large overall negative charge of PAR has the ability to relax the chromatin structure, which is usually extremely tightly wound, and displaces histones from DNA. This PAR-induced relaxation would then allow large regions surrounding the DNA strand breaks to become accessible to other repair proteins (Althaus et al., 1993, Althaus et al., 1994); however it is very plausible that this theory can be extended to other proteins, such as p65. The mechanism proposed in Chapter 4, corroborates the histone shuttling model, by suggesting that PARP-1 regulates IR-induced NF-κB, in part by chromatin structure remodelling. Moreover, histone associated proteins have been shown to interact with p65 and alter the transcriptional response. In particular, phosphorylation of p65 at threonine 505 (Thr-505) in response to the DNA crosslinking agent, cisplatin, has been shown to inhibit p65 transactivation, in turn increasing the association between p65 and HDAC1. This can then result in the repression of NF-κB target genes, such as the anti-apoptotic factor, Bcl-xL. The phosphorylation of p65 at Thr-505 was shown to require the checkpoint kinase, Chk1 and was induced by the p14/ARF tumour suppressor protein. Interestingly, this phosphorylation was observed in the U2OS cancer cell line model, following treatment with cisplatin, but not by other agents known to activate Chk1 (Campbell et al., 2006b, Rocha et al., 2005). These data, once again, highlight the

complex crosstalk between the DNA damage and NF-κB pathways, and suggest that the observed response is highly likely to be both cell type- and stimulus- dependent.

8.3 PARP inhibition as a method of inhibiting transcriptional activation

Microarray analysis showed that the TNF-α driven transcription of NF-κB-dependent inflammatory and immune response genes was unaffected by AG-014699, suggesting that targeting DNA-damage activated NF-κB using AG-014699 may overcome toxicity observed with classical NF-κB inhibitors without compromising other vital inflammatory functions. These data are very encouraging in the context of the potential use of AG-014699 in inhibiting DNA-damage activated NF-κB in cancer, as previously discussed. However, there have been a number of reports which have implicated PARP-1 in the development of both acute and chronic inflammatory diseases. For example, PARP-1 null mice or mice treated with PARP inhibitors have exhibited resistance to numerous different types of inflammation, including LPS-induced septic shock and streptozotocin-induced diabetes (Burkart et al., 1999, Mabley et al., 2001, Oliver et al., 1999a). It is therefore very important to assess the effect on AG-014699 on inflammatory response genes after stimuli other than TNF-α, as other inflammatory mediators, such as LPS are known to initiate NF-κB signalling cascades. However, these studies should proceed with caution as LPS has been shown to induce oxidative stress, which is also known to induce SSBs and therefore activate PARP-1. Hence, it may be difficult to tease apart any effects PARP inhibitors were having on transcriptional activation from there role in the inhibition of SSB repair in this case.

Reports have shown that PARP inhibitors may be advantageous for the treatment of neurological and inflammatory disorders. It is important to note that studies using PARP inhibitors in neurological disorders, have not just assessed the effect on these inhibitors on NF-κB activation, but also that of other transcription factors known to be regulated by PARP-1, such as AP-1. Reports have shown that PARP-1 deficient glia exhibited reduced binding and associated gene expression of NF-κB, AP-1, Sp1 and Oct-1 (Ha et al 2002 PNAS). Another report using PARP inhibitors in rat glial and neuronal cultures found that the expression of genes including *iNOS, IL-1β* and *TNF-α* was reduced, resulting in a reduced neuro-inflammation and the neurotoxic potential of activated glia (Chiarugi and Moskowitz, 2003). It is important to recognise that these genes are not solely regulated by NF-κB. Zingerilli *et al.,* (2003) found that PARP inhibition in

concert with the inflammatory stimulant 2,4,6-trinitrobenzene sulfonic acid markedly reduced DNA binding of both NF-κB and AP-1 in a rat model of colitis. This resulted in a reduction in neutrophil infiltration, reduced colonic damage and induced apoptosis (Zingarelli et al., 2003b). These studies highlight the importance of investigating the effects on PARP inhibition, not just on one transcription factor, but on others too, as PARP-1 is a known co-regulator of at least nine transcription factors. However, the studies undertaken as part of this thesis not only used the potent and specific PARP inhibitor, AG-014699 and PARP-1 siRNA, they also used siRNA targeting p65, and p65 proficient and deficient MEFs, and therefore the conclusions drawn can be confidently attributed to the effects of PARP-1 on DNA-damage-induced NF-κB activation, it would be prudent, and also very interestingly to assess the effects on AG-014699 on other transcription factors. In particular, those which are closely related to NF-κB, such as AP-1, which is also activated by TNF-α and IL-1β (Dutta et al., 2006) and NFAT (Jain et al., 1992).

An investigation into the role of PARP-1 in DNA damage activated NF-κB activation in glioblastoma cells was also undertaken as part of this thesis in order to assess the potential utility of AG-014699 in tumour types known to express constitutively active NF-κB. PARP-1 activity was vital for both radio- and chemo-sensitisation of U251 glioblastoma cells, and mediated its effects on survival following either IR or temozolomide *via* NF-κB in these cells. Importantly, these data confirmed the earlier findings in the MEFs by demonstrating that radio- or chemo-sensitisation by AG-014699 is due to downstream inhibition of NF-κB activation, and independent of SSB repair inhibition. Moreover, these data highlight the potential of PARP-1 inhibitors to overcome NF-κB-mediated therapeutic resistance and widens the spectrum of cancers in which these agents may be utilised. These findings are very encouraging, and together with data which showed that NF-κB p65 translocation was induced following DNA damage in cell lines derived from other tumours types, such as lung adenocarcinoma (Chapter 6), they do suggest that the targeting of DNA-damage induced-NF-κB activation with a PARP inhibitor is a viable therapeutic strategy. However, further work and validation using a range of model systems is required. Most important is the use of preclinical modelling to assess the effects of AG-016499 on DNA-damage activated NF-κB *in vivo*.

8.4 Crosstalk between the mitotic spindle, DNA damage and NF-κB

An interesting observation from the microarray study was that the genes up-regulated following treatment with IR were those associated with the mitotic spindle and cellular organisation and assembly. Furthermore, it also appeared, after qRT-PCR validation assays, that a subset of these genes, including *PLK-1*, *AUKRA* and *CDC20* could potentially be regulated by NF-κB following DNA damage. Although some associated genes, such as PLK-3 are known to be NF-κB regulated (Li et al., 2005), the three genes identified as part of the gene expression profiling within this thesis could be novel targets, and as discussed in Chapter 5, require further investigation. However, there have been other reports in the literature which have postulated a link between either NF-κB or members of the PARP superfamily and the mitotic spindle. (Briassouli et al., 2007) demonstrated that aurora kinase A could regulate NF-κB activation through phosphorylation of IκBα at ser32 or ser36, however it is unclear whether this is a direct phosphorylation event or a result of downstream signalling. Aurora kinase inhibition has also been shown to sensitise a range of human tumour cell line to commonly used chemo-therapeutic agents *via* the down-regulation of NF-κB activation (Briassouli et al., 2007, Sun et al., 2007). These data, taken with the observations within this thesis, mean that a feedback loop between aurora kinase A and NF-κB could exist. It could be postulated that the over-expression of aurora kinase A, which is common in cancer and known to contribute to poor prognosis (Goepfert et al., 2002, Jeng et al., 2004, Sakakura et al., 2001, Tanaka et al., 1999b), in turn drives NF-κB activation, known to correlate with increased metastatic potential and therapeutic resistance, through the regulation of target genes (Prasad et al., 2010), one of which is the *AURKA* gene, which encodes the aurora kinase A protein.

Members of the PARP superfamily have also been implicated in regulation of cellular division and assembly. Both PARP-1 and PARP-2 localise to the centromeres where they interact with key kinetochore associated proteins (Saxena et al., 2002a, Saxena et al., 2002b)). Most recently, PARP-3 has been implicated in the stabilisation of the mitotic spindle and in the regulation of telomeric integrity (Boehler et al., 2011) and the phosphorylation of the PARP superfamily member Tankyrase 1 (TNKS1) by PLK-1, has been shown to regulate TNKS1 function at telomeres and during mitosis (Ha et al., 2011) The significance of this association is still somewhat unclear, however, like the array study here, it links the DNA damage signalling network with that of the mitotic fidelity checkpoint. Moreover, other reports show that aurora kinase B is a target for

poly(ADP-ribosyl)ation in response to DNA damage *via* the interaction between PARP-1 and spindle checkpoint component, BUBR1 (Monaco et al., 2005). A further interplay between the spindle checkpoint and DNA damage and repair, was reported by Sourisseau T *et al*., (2010) when they showed that the expression of aurora kinase A inhibited the recruitment of the HRR protein, RAD51 to DSBs. This impairment of RAD51 function was shown to be dependent on the inhibition of Chk1 by PLK-1. This ultimately resulted in the cells with high expression of aurora kinase A having a compromised DSB repair response, and being sensitive to PARP inhibition (Sourisseau et al., 2010), in a similar manner to the synthetic lethality described with the use of PARP inhibitors in BRCA-defective breast and ovarian tumours (Bryant et al., 2005, Farmer et al., 2005). Together with data presented in Chapter 5 of this thesis, it follows that PARP inhibition may be a novel therapeutic approach to cancers with de-regulated mitotic spindle checkpoint signalling, and importantly, NF-κB-regulated gene expression could be a key link between DNA damage and mitotic spindle networks.

The DNA repair kinase, DNA-PK, has also been implicated in the regulation of NF-κB (Basu et al., 1998, Ju et al., 2010, Liu et al., 1998, Panta et al., 2004). Interestingly, the activation of NF-κB by DNA-PK does not appear to be dependent on DNA damage. For example, it has been reported that the phosphorylation of the p50 NF-κB subunit by DNA-PKcs, in response to TNF-α was required for the expression of the NF-κB-dependent gene, *VCAM-1* (Ju et al., 2010), and most interestingly that DNA-PK activates NF-κB in a MEK-to-IKK signalling pathway in response to treatment with AD288 (*N*-benzyladriamycin), a catalytic inhibitor of topoisomerase II but not in response to the topoisomerase II poison, DOX (Panta et al., 2004). Catalytic inhibitors of topoisomerase II do not cause DNA DSBs, unlike classical topoisomerase poisons, such as DOX, but in contrast the mechanism of action and result on the cell, is similar to the effects of the microtubule poisons, another group of chemotherapeutic agents. Intriguingly, there have been two recent reports that have suggested a role for DNA-PK outside its usual remit of DNA repair. These have shown that DNA-PK is required for cell cycle progression through mitosis, and that inhibition of DNA-PK can result in spindle disruption and mitotic catastrophe (Lee et al., 2011, Shang et al., 2010). These data, once again provide an intriguing link between the DNA-damage signalling networks and those associated with cellular organisation and assembly, in line with gene expression profiling study in Chapter 5. These data suggest that NF-κB is involved in

this signalling, and therefore an investigation in to the role of DNA-PK in the activation of NF-κB, and in the context of the spindle checkpoint, is merited.

8.5 The use of DNA repair inhibitors to target NF-κB activation

The use of DNA-damage repair inhibitors as a means of targeting NF-κB is becoming increasingly more interesting following the emergence of studies which have elucidated the mechanism by which proteins such as ATM (Hinz et al., 2010, Wu et al., 2006) and PARP-1 (Hunter et al., 2011, Stilmann et al., 2009, Veuger et al., 2009) activate the transcription factor following DNA damage. However, there are caveats associated with using inhibitors of such enzymes. There have been a number of studies which have shown that targeting DNA repair proteins in cancer cell lines and xenograft models can sensitise cells to DNA damaging chemo-therapeutic agents (Plummer, 2010), but whether this sensitisation is solely due the inhibition of NF-κB remains to be seen. Proteins such as ATM are involved in a huge range of cellular processes, such as gene regulation, apoptosis, DNA repair, and cell cycle checkpoint activation (Kurz and Lees-Miller, 2004). It is therefore essential to determine the precise role of ATM in the cell before the addition of an ATM kinase inhibitor. ATM is known to phosphorylate and activate the p53 tumour suppressor protein in response to DNA damage, resulting in the initiation of the apoptotic response (Ashcroft et al., 1999). Hence, it is likely that there is a delicate balance between the pro-apoptotic gene expression in cancer cells with functional p53 and the anti-apoptotic genes induced by NF-κB-dependent gene transcription in response to DNA damage.

Recently, Veuger and Durkacz (2011) showed that the small molecule inhibitor of ATM kinase activity, KU55933 (Hickson et al., 2004) sensitised breast cancer cells to IR *via* the inhibition of NF-κB activation, and as part of this work they also postulated that ATM inhibition could be used as a stand-alone therapy in cancers which expressed NF-κB p65 that was constitutively nuclear. To this end, it was reported that a prolonged exposure to KU55933 in the MDA-MB-231 cells resulted in an inhibition of NF-κB DNA binding, in the absence of DNA-damage (Veuger and Durkacz, 2011). It is highly likely that this is an off target effect of the ATM inhibitor, as it would be thought that the kinase activity of ATM would have to be induced for KU55933 to have any effect. However another group have suggested that ATM-dependent NF-κB activation can occur in the absence of DNA damage as the SUMOylation of NEMO can occur without

DSB-inducing conditions. Importantly, in this case, electroporation stress was found to induce the post-translational SUMOylation of NEMO, and hypotonic shock, which weakly activates ATM induced NF-κB activation (Wuerzberger-Davis et al., 2007). In this case however, ATM was active, though not through the classical means of DNA-damage. Other mechanisms known to induce ATM activity include oxidative stress (Guo et al., 2010).

The work in this thesis suggests that the activation of PARP-1 is essential for the activation of NF-κB following DNA, hence AG-014699 is only effective in inhibiting NF-κB which has been induced by DNA damage, and not by TNF-α. However, cells do undergo oxidative damage and produce reactive oxygen species in some disease states (Schreiber et al., 2006b), which can result in the activation of PARP-1 in the absence of DNA damage. If, in such cells, NF-κB dimers were constitutively nuclear in location (which they often are in tumour cells), it is plausible to suggest that poly(ADP-ribosyl)ated PARP-1 in this case could facilitate NF-κB DNA binding, as suggested in the model in Chapter 4. In this case, AG-014699 could perhaps be utilised as a mono-therapy in order to inhibit NF-κB activation, however this hypothesis is very speculative, and requires much more investigation before any conclusions could be drawn.

The potential use of PARP inhibitors as single agents for the treatment of BRCA-mutated or defective breast and ovarian cancers has been well documented (Bryant et al., 2005, Drew et al., 2011, Farmer et al., 2005, Fong et al., 2009, Fong et al., 2010). Recently, Gottipati *et al.,* (2010) demonstrated that cells which were defective in, or lacking, any proteins associated with HRR, such as BRCA2, WRN or RAD52, had hyper-activated PARP-1, as illustrated by an increased PAR formation. They also showed that these cells were sensitive to PARP inhibition, suggesting a synthetic lethality mechanism between PARP-1 and other defective HRR proteins, not just BRCA1 or BRCA2 (Gottipati et al., 2010). Data presented in this thesis has shown that PAR is key in mediating NF-κB following DNA damage, which corroborates the work of others (Stilmann et al., 2009). Therefore, it would be interesting to determine whether HRR-defective cells, which are reported as having high levels of PAR in the absence of DNA damage, also have an increased NF-κB DNA binding compared with cells which are known to have a fully functional HRR pathway. In this was in fact the case, it

further adds weight to therapeutic potential of PARP inhibitors as mono-therapeutic agents for the treatment of HRR-defective tumours.

8.6 The use of targeted NF-κB inhibitors *versus* the use of DNA repair inhibitors to inhibit NF-κB activation

The targeting of NF-κB in a more direct fashion was also assessed as part of this thesis in order to determine the therapeutic potential of a potent inhibitor of NF-κB subunit DNA binding, PBS-1086, in the NF-κB $p65^{+/+}$ and $p65^{-/-}$ MEFs and the MDA-MB-231, T47D and MCF7 breast cancer cell lines. Briefly, DNA binding and luciferase reporter assays showed that PBS-1086 inhibited IR-induced p65 and p50 DNA binding and NF-κB-dependent gene transcription in $p65^{+/+}$ cells. Co-incubation with PBS-1086 or p65 siRNA radio-sensitised $p65^{+/+}$, but not $p65^{-/-}$ cells, demonstrating that PBS-1086 mediates radio-sensitisation *via* the p65 NF-κB subunit. Gene expression analysis showed that PBS-1086 inhibited IR-induced transcription of known NF-κB-regulated anti-apoptotic genes. MDA-MB-231 cells were found to have the highest constitutive levels of DNA binding of all NF-κB subunits. PBS-1086 radio-sensitised all three breast cancer cell lines. In survival assays, all of the breast cancer cell lines tested were also sensitive to PBS-1086, however, the MDA-MB-231 cells were the most sensitive to PBS-1086 alone. These data therefore suggest that high NF-κB DNA binding activity appears to correlate with sensitivity to PBS-1086.

The compound used here, PBS-1086 is an early lead compound in the drug discovery pipeline from Profectus BioSciences Inc, and is now undergoing SAR (structural activity relationship) chemistry to optimise properties of this molecule. PBS-1086 is is known to covalently modify the cysteine-38 residue in the Rel domain of the NF-κB subunits (Jie Zhang personal communication) and has been shown to inhibit p65, p50 and RelB DNA binding as well as luciferase expression in a 293/NF-κB-luciferase reporter cell line (Oh et al., 2011). Other compounds which target this cysteine residue, such as epoxyquinone A monomer, a synthetic derivative of the natural product epoxyquinol A, have also been shown to inhibit IKKβ through modification of the cysteine-179 residue (Liang et al., 2006). Moreover, both IKKα and IKKβ have this conserved cysteine residue in the activation loop of their catalytic domain (Kapahi et al., 2000), and this should be taken into account when interpreting results. For example,

PBS-0186 achieved cell kill as a stand-alone therapy in each of the three breast cancer cell lines tested, and although this appears to correlate with the inhibition of constitutive NF-κB activation, the possibility that this compound may have some activity against the IKK complex as well as direct subunit DNA binding should be considered. This is especially the case in the clonogenic assays in which PBS-1086 was used in combination with IR, as the IKK would have been activated by the DNA damaging agent and hence some of the cell kill observed may be attributable to IKK inhibition. A subunit specific inhibitor, such as PBS-1170, which targets p65 alone, and used in later experiments in Chapter 7, may be a more suitable approach for targeting NF-κB, as this should only target canonical pathway signalling.

Targeting NF-κB is an attractive therapeutic avenue, not just in cancer but also in inflammatory diseases, such as rheumatoid arthritis. However, there is one underlying caveat associated with globally inhibiting the NF-κB pathway, that being that this transcription factor is essential for the immune and inflammatory response of the cell, as previously discussed. Personally speaking, targeting one type of NF-κB activation, for example DNA-damage activated NF-κB would be a favoured option. Although the use of DNA repair inhibitors may be a much less direct way of target the transcription factor, they do appear to have numerous benefits over traditional NF-κB pathway inhibitors. The main advantage would be avoiding potential toxicity associated with any effects on the essential immune functions of NF-κB, which has been associated with an increase likelihood of immunodeficiency and the delayed bone marrow recovery due to some reports of chemotherapeutic induced apoptosis of hematopoietic progenitors (Grossmann et al., 1999, Turco et al., 2004). Furthermore, IKK inhibition has been associated with defects in lymphopoiesis, hepatotoxicity and an increased risk of infection, this is exemplified by the use of anti-TNF-α biologics which have been associated with increased reactivation of latent tuberculosis infection (Strnad and Burke, 2007). The data presented here, involving the inhibition of DNA-damage activated NF-κB using a PARP inhibitor, has shown that the vital inflammatory functions of NF-κB are unaffected, thus helping to overcome the toxicities associated with specific NF-κB inhibitors. To this end, it should also be noted that during clinical trials, PARP inhibitors have been found to have low toxicity profiles (Drew and Plummer, 2009). Furthermore, a DNA repair inhibitor, such as AG-014699 affords a ‘double-hit’ to a cancer cell as it not only inhibits key DNA repair pathways (which tumour cells use as a

method of evading cell death) but also inhibits the NF-κB transcriptional response, which is known to contribute to malignant progression.

8.7 Statistical analysis

Throughout this thesis statistical analyses have been performed, and the most part these have been unpaired Student's t-tests that have demonstrated statistical differences in the data. It is therefore necessary to consider the possibility that some of these tests were false positives, and this can be done using the Bonferroni correction. Of the 147 t-tests that have been performed, and assuming a 95 % confidence rate, this correction would assume that 7 of these outcomes would be false positives. However, the consistent trends seen within the data from the different assays used, for example the statististical differences observed in both the DNA binding and luciferase assays, suggest that the outcomes observed are bone fide, and are therefore unlikely to be false positives.

8.8 Summary

Collectively the data in this thesis highlight the potential of modulating NF-κB activity, either by PARP-1, or directly *via* inhibition of subunit DNA binding, to restore radio- and chemo-sensitivity in cancers with aberrantly active NF-κB and to overcome NF-κB-mediated therapeutic resistance. These data also further the existing knowledge and understanding of how signals from DNA-damage activated PARP-1 mediate the activation of NF-κB and importantly suggest that the potent and specific PARP inhibitor, AG-014699 mediates cell survival following DNA damage primarily through activation of NF-κB, and independent of the role PARP inhibitors play in the inhibition of DNA repair. Furthermore, this thesis shows that PARP and NF-κB inhibitors may prove useful in overcoming NF-κB-mediated therapeutic resistance, an important goal in cancer therapy.

Chapter 9. References

Abraham, R. T. (2001) 'Cell cycle checkpoint signaling through the ATM and ATR kinases', *Genes & development*, 15, (17), pp. 2177-96.

Adams, J. (2004) 'The development of proteasome inhibitors as anticancer drugs', *Cancer cell*, 5, (5), pp. 417-21.

Albert, J. M., Cao, C., Kim, K. W., Willey, C. D., Geng, L., Xiao, D., Wang, H., Sandler, A., Johnson, D. H., Colevas, A. D., Low, J., Rothenberg, M. L. and Lu, B. (2007) 'Inhibition of poly(ADP-ribose) polymerase enhances cell death and improves tumor growth delay in irradiated lung cancer models', *Clinical cancer research : an official journal of the American Association for Cancer Research*, 13, (10), pp. 3033-42.

Althaus, F. R., Hofferer, L., Kleczkowska, H. E., Malanga, M., Naegeli, H., Panzeter, P. and Realini, C. (1993) 'Histone shuttle driven by the automodification cycle of poly(ADP-ribose)polymerase', *Environmental and molecular mutagenesis*, 22, (4), pp. 278-82.

Althaus, F. R., Hofferer, L., Kleczkowska, H. E., Malanga, M., Naegeli, H., Panzeter, P. L. and Realini, C. A. (1994) 'Histone shuttling by poly ADP-ribosylation', *Molecular and cellular biochemistry*, 138, (1-2), pp. 53-9.

Althaus, F. R. and Richter, C. (1987) 'ADP-ribosylation of proteins. Enzymology and biological significance', *Molecular biology, biochemistry, and biophysics*, 37, pp. 1-237.

Alvarez-Gonzalez, R. and Mendoza-Alvarez, H. (1995) 'Dissection of ADP-ribose polymer synthesis into individual steps of initiation, elongation, and branching', *Biochimie*, 77, (6), pp. 403-7.

Ame, J. C., Spenlehauer, C. and de Murcia, G. (2004) 'The PARP superfamily', *BioEssays : news and reviews in molecular, cellular and developmental biology*, 26, (8), pp. 882-93.

Amiri, K. I., Ha, H. C., Smulson, M. E. and Richmond, A. (2006) 'Differential regulation of CXC ligand 1 transcription in melanoma cell lines by poly(ADP-ribose) polymerase-1', *Oncogene*, 25, (59), pp. 7714-22.

Andreone, T. L., O'Connor, M., Denenberg, A., Hake, P. W. and Zingarelli, B. (2003) 'Poly(ADP-ribose) polymerase-1 regulates activation of activator protein-1 in murine fibroblasts', *Journal of immunology*, 170, (4), pp. 2113-20.

Ashburner, B. P., Shackelford, R. E., Baldwin, A. S., Jr. and Paules, R. S. (1999) 'Lack of involvement of ataxia telangiectasia mutated (ATM) in regulation of nuclear factor-kappaB (NF-kappaB) in human diploid fibroblasts', *Cancer research*, 59, (21), pp. 5456-60.

Ashcroft, M., Kubbutat, M. H. and Vousden, K. H. (1999) 'Regulation of p53 function and stability by phosphorylation', *Molecular and cellular biology*, 19, (3), pp. 1751-8.

Asher, G. and Shaul, Y. (2005) 'p53 proteasomal degradation: poly-ubiquitination is not the whole story', *Cell cycle*, 4, (8), pp. 1015-8.

Ataian, Y. and Krebs, J. E. (2006) 'Five repair pathways in one context: chromatin modification during DNA repair', *Biochemistry and cell biology = Biochimie et biologie cellulaire*, 84, (4), pp. 490-504.

Audebert, M., Salles, B. and Calsou, P. (2004) 'Involvement of poly(ADP-ribose) polymerase-1 and XRCC1/DNA ligase III in an alternative route for DNA double-strand breaks rejoining', *The Journal of biological chemistry*, 279, (53), pp. 55117-26.

Aupperle, K. R., Bennett, B. L., Boyle, D. L., Tak, P. P., Manning, A. M. and Firestein, G. S. (1999) 'NF-kappa B regulation by I kappa B kinase in primary fibroblast-like synoviocytes', *Journal of immunology*, 163, (1), pp. 427-33.

Bales, K. R., Du, Y., Dodel, R. C., Yan, G. M., Hamilton-Byrd, E. and Paul, S. M. (1998) 'The NF-kappaB/Rel family of proteins mediates Abeta-induced neurotoxicity and glial activation', *Brain research. Molecular brain research*, 57, (1), pp. 63-72.

Barbie, D. A., Tamayo, P., Boehm, J. S., Kim, S. Y., Moody, S. E., Dunn, I. F., Schinzel, A. C., Sandy, P., Meylan, E., Scholl, C., Frohling, S., Chan, E. M., Sos, M. L., Michel, K., Mermel, C., Silver, S. J., Weir, B. A., Reiling, J. H., Sheng, Q., Gupta, P. B., Wadlow, R. C., Le, H., Hoersch, S., Wittner, B. S., Ramaswamy, S., Livingston, D. M., Sabatini, D. M., Meyerson, M., Thomas, R. K., Lander, E. S., Mesirov, J. P., Root, D. E., Gilliland, D. G., Jacks, T. and Hahn, W. C. (2009) 'Systematic RNA interference reveals that oncogenic KRAS-driven cancers require TBK1', *Nature*, 462, (7269), pp. 108-12.

Barkett, M. and Gilmore, T. D. (1999) 'Control of apoptosis by Rel/NF-kappaB transcription factors', *Oncogene*, 18, (49), pp. 6910-24.

Bartek, J. and Lukas, J. (2001) 'Mammalian G1- and S-phase checkpoints in response to DNA damage', *Current opinion in cell biology*, 13, (6), pp. 738-47.

Bartek, J. and Lukas, J. (2006) 'Cell biology. The stress of finding NEMO', *Science*, 311, (5764), pp. 1110-1.

Basak, S., Kim, H., Kearns, J. D., Tergaonkar, V., O'Dea, E., Werner, S. L., Benedict, C. A., Ware, C. F., Ghosh, G., Verma, I. M. and Hoffmann, A. (2007) 'A fourth IkappaB protein within the NF-kappaB signaling module', *Cell*, 128, (2), pp. 369-81.

Basseres, D. S. and Baldwin, A. S. (2006) 'Nuclear factor-kappaB and inhibitor of kappaB kinase pathways in oncogenic initiation and progression', *Oncogene*, 25, (51), pp. 6817-30.
Basseres, D. S., Ebbs, A., Levantini, E. and Baldwin, A. S. (2010) 'Requirement of the NF-kappaB subunit p65/RelA for K-Ras-induced lung tumorigenesis', *Cancer research*, 70, (9), pp. 3537-46.
Basu, S., Rosenzweig, K. R., Youmell, M. and Price, B. D. (1998) 'The DNA-dependent protein kinase participates in the activation of NF kappa B following DNA damage', *Biochemical and biophysical research communications*, 247, (1), pp. 79-83.
Beg, A. A. and Baltimore, D. (1996) 'An essential role for NF-kappaB in preventing TNF-alpha-induced cell death', *Science*, 274, (5288), pp. 782-4.
Beg, A. A., Sha, W. C., Bronson, R. T., Ghosh, S. and Baltimore, D. (1995) 'Embryonic lethality and liver degeneration in mice lacking the RelA component of NF-kappa B', *Nature*, 376, (6536), pp. 167-70.
Benezra, M., Chevallier, N., Morrison, D. J., MacLachlan, T. K., El-Deiry, W. S. and Licht, J. D. (2003) 'BRCA1 augments transcription by the NF-kappaB transcription factor by binding to the Rel domain of the p65/RelA subunit', *The Journal of biological chemistry*, 278, (29), pp. 26333-41.
Benjamin, R. C. and Gill, D. M. (1980) 'Poly(ADP-ribose) synthesis in vitro programmed by damaged DNA. A comparison of DNA molecules containing different types of strand breaks', *The Journal of biological chemistry*, 255, (21), pp. 10502-8.
Berdnik, D. and Knoblich, J. A. (2002) 'Drosophila Aurora-A is required for centrosome maturation and actin-dependent asymmetric protein localization during mitosis', *Current biology : CB*, 12, (8), pp. 640-7.
Berglund, P. and Landberg, G. (2006) 'Cyclin e overexpression reduces infiltrative growth in breast cancer: yet another link between proliferation control and tumor invasion', *Cell cycle*, 5, (6), pp. 606-9.
Berlin, A. L., Paller, A. S. and Chan, L. S. (2002) 'Incontinentia pigmenti: a review and update on the molecular basis of pathophysiology', *Journal of the American Academy of Dermatology*, 47, (2), pp. 169-87; quiz 188-90.
Bernstein, E., Caudy, A. A., Hammond, S. M. and Hannon, G. J. (2001) 'Role for a bidentate ribonuclease in the initiation step of RNA interference', *Nature*, 409, (6818), pp. 363-6.
Bhatia, K., Pommier, Y., Giri, C., Fornace, A. J., Imaizumi, M., Breitman, T. R., Cherney, B. W. and Smulson, M. E. (1990) 'Expression of the poly(ADP-ribose) polymerase gene following natural and induced DNA strand breakage and effect of hyperexpression on DNA repair', *Carcinogenesis*, 11, (1), pp. 123-8.
Bieche, I., Nogues, C. and Lidereau, R. (1999) 'Overexpression of BRCA2 gene in sporadic breast tumours', *Oncogene*, 18, (37), pp. 5232-8.
Biggins, S. and Murray, A. W. (2001) 'The budding yeast protein kinase Ipl1/Aurora allows the absence of tension to activate the spindle checkpoint', *Genes & development*, 15, (23), pp. 3118-29.
Biswas, D. K., Dai, S. C., Cruz, A., Weiser, B., Graner, E. and Pardee, A. B. (2001) 'The nuclear factor kappa B (NF-kappa B): a potential therapeutic target for estrogen receptor negative breast cancers', *Proceedings of the National Academy of Sciences of the United States of America*, 98, (18), pp. 10386-91.
Biswas, D. K., Shi, Q., Baily, S., Strickland, I., Ghosh, S., Pardee, A. B. and Iglehart, J. D. (2004) 'NF-kappa B activation in human breast cancer specimens and its role in cell proliferation and apoptosis', *Proceedings of the National Academy of Sciences of the United States of America*, 101, (27), pp. 10137-42.
Bleehen, N. M. and Cox, J. D. (1985) 'Radiotherapy for lung cancer', *International journal of radiation oncology, biology, physics*, 11, (5), pp. 1001-7.
Boehler, C., Gauthier, L. R., Mortusewicz, O., Biard, D. S., Saliou, J. M., Bresson, A., Sanglier-Cianferani, S., Smith, S., Schreiber, V., Boussin, F. and Dantzer, F. (2011) 'Poly(ADP-ribose) polymerase 3 (PARP3), a newcomer in cellular response to DNA damage and mitotic progression', *Proceedings of the National Academy of Sciences of the United States of America*, 108, (7), pp. 2783-8.
Boehm, J. S., Zhao, J. J., Yao, J., Kim, S. Y., Firestein, R., Dunn, I. F., Sjostrom, S. K., Garraway, L. A., Weremowicz, S., Richardson, A. L., Greulich, H., Stewart, C. J., Mulvey, L. A., Shen, R. R., Ambrogio, L., Hirozane-Kishikawa, T., Hill, D. E., Vidal, M., Meyerson, M., Grenier, J. K., Hinkle, G., Root, D. E., Roberts, T. M., Lander, E. S., Polyak, K. and Hahn, W. C. (2007) 'Integrative genomic approaches identify IKBKE as a breast cancer oncogene', *Cell*, 129, (6), pp. 1065-79.
Bonicalzi, M. E., Haince, J. F., Droit, A. and Poirier, G. G. (2005) 'Regulation of poly(ADP-ribose) metabolism by poly(ADP-ribose) glycohydrolase: where and when?', *Cellular and molecular life sciences : CMLS*, 62, (7-8), pp. 739-50.

Bonizzi, G. and Karin, M. (2004) 'The two NF-kappaB activation pathways and their role in innate and adaptive immunity', *Trends in immunology*, 25, (6), pp. 280-8.
Bortner, D. M. and Rosenberg, M. P. (1997) 'Induction of mammary gland hyperplasia and carcinomas in transgenic mice expressing human cyclin E', *Molecular and cellular biology*, 17, (1), pp. 453-9.
Bos, J. L. (1989) 'ras oncogenes in human cancer: a review', *Cancer research*, 49, (17), pp. 4682-9.
Bouchard, V. J., Rouleau, M. and Poirier, G. G. (2003) 'PARP-1, a determinant of cell survival in response to DNA damage', *Experimental hematology*, 31, (6), pp. 446-54.
Bouker, K. B., Skaar, T. C., Riggins, R. B., Harburger, D. S., Fernandez, D. R., Zwart, A., Wang, A. and Clarke, R. (2005) 'Interferon regulatory factor-1 (IRF-1) exhibits tumor suppressor activities in breast cancer associated with caspase activation and induction of apoptosis', *Carcinogenesis*, 26, (9), pp. 1527-35.
Bours, V., Bentires-Alj, M., Hellin, A. C., Viatour, P., Robe, P., Delhalle, S., Benoit, V. and Merville, M. P. (2000) 'Nuclear factor-kappa B, cancer, and apoptosis', *Biochemical pharmacology*, 60, (8), pp. 1085-9.
Bours, V., Franzoso, G., Azarenko, V., Park, S., Kanno, T., Brown, K. and Siebenlist, U. (1993) 'The oncoprotein Bcl-3 directly transactivates through kappa B motifs via association with DNA-binding p50B homodimers', *Cell*, 72, (5), pp. 729-39.
Bowie, M. L., Dietze, E. C., Delrow, J., Bean, G. R., Troch, M. M., Marjoram, R. J. and Seewaldt, V. L. (2004) 'Interferon-regulatory factor-1 is critical for tamoxifen-mediated apoptosis in human mammary epithelial cells', *Oncogene*, 23, (54), pp. 8743-55.
Brach, M. A., Gruss, H. J., Kaisho, T., Asano, Y., Hirano, T. and Herrmann, F. (1993) 'Ionizing radiation induces expression of interleukin 6 by human fibroblasts involving activation of nuclear factor-kappa B', *The Journal of biological chemistry*, 268, (12), pp. 8466-72.
Brach, M. A., Hass, R., Sherman, M. L., Gunji, H., Weichselbaum, R. and Kufe, D. (1991) 'Ionizing radiation induces expression and binding activity of the nuclear factor kappa B', *The Journal of clinical investigation*, 88, (2), pp. 691-5.
Bradley, J. R. and Pober, J. S. (2001) 'Tumor necrosis factor receptor-associated factors (TRAFs)', *Oncogene*, 20, (44), pp. 6482-91.
Brady, M. E., Ozanne, D. M., Gaughan, L., Waite, I., Cook, S., Neal, D. E. and Robson, C. N. (1999) 'Tip60 is a nuclear hormone receptor coactivator', *The Journal of biological chemistry*, 274, (25), pp. 17599-604.
Briassouli, P., Chan, F., Savage, K., Reis-Filho, J. S. and Linardopoulos, S. (2007) 'Aurora-A regulation of nuclear factor-kappaB signaling by phosphorylation of IkappaBalpha', *Cancer research*, 67, (4), pp. 1689-95.
Brock, W. A., Milas, L., Bergh, S., Lo, R., Szabo, C. and Mason, K. A. (2004) 'Radiosensitization of human and rodent cell lines by INO-1001, a novel inhibitor of poly(ADP-ribose) polymerase', *Cancer letters*, 205, (2), pp. 155-60.
Brocke-Heidrich, K., Ge, B., Cvijic, H., Pfeifer, G., Loffler, D., Henze, C., McKeithan, T. W. and Horn, F. (2006) 'BCL3 is induced by IL-6 via Stat3 binding to intronic enhancer HS4 and represses its own transcription', *Oncogene*, 25, (55), pp. 7297-304.
Brown, R. T., Ades, I. Z. and Nordan, R. P. (1995) 'An acute phase response factor/NF-kappa B site downstream of the junB gene that mediates responsiveness to interleukin-6 in a murine plasmacytoma', *The Journal of biological chemistry*, 270, (52), pp. 31129-35.
Bryant, H. E. and Helleday, T. (2004) 'Poly(ADP-ribose) polymerase inhibitors as potential chemotherapeutic agents', *Biochemical Society transactions*, 32, (Pt 6), pp. 959-61.
Bryant, H. E., Schultz, N., Thomas, H. D., Parker, K. M., Flower, D., Lopez, E., Kyle, S., Meuth, M., Curtin, N. J. and Helleday, T. (2005) 'Specific killing of BRCA2-deficient tumours with inhibitors of poly(ADP-ribose) polymerase', *Nature*, 434, (7035), pp. 913-7.
Burkart, V., Wang, Z. Q., Radons, J., Heller, B., Herceg, Z., Stingl, L., Wagner, E. F. and Kolb, H. (1999) 'Mice lacking the poly(ADP-ribose) polymerase gene are resistant to pancreatic beta-cell destruction and diabetes development induced by streptozocin', *Nature medicine*, 5, (3), pp. 314-9.
Burke, J. R., Pattoli, M. A., Gregor, K. R., Brassil, P. J., MacMaster, J. F., McIntyre, K. W., Yang, X., Iotzova, V. S., Clarke, W., Strnad, J., Qiu, Y. and Zusi, F. C. (2003) 'BMS-345541 is a highly selective inhibitor of I kappa B kinase that binds at an allosteric site of the enzyme and blocks NF-kappa B-dependent transcription in mice', *The Journal of biological chemistry*, 278, (3), pp. 1450-6.
Burkle, A., Beneke, S., Brabeck, C., Leake, A., Meyer, R., Muiras, M. L. and Pfeiffer, R. (2002) 'Poly(ADP-ribose) polymerase-1, DNA repair and mammalian longevity', *Experimental gerontology*, 37, (10-11), pp. 1203-5.
Burns, K. A. and Martinon, F. (2004) 'Inflammatory diseases: is ubiquitinated NEMO at the hub?', *Current biology : CB*, 14, (24), pp. R1040-2.

Calabrese, C. R., Almassy, R., Barton, S., Batey, M. A., Calvert, A. H., Canan-Koch, S., Durkacz, B. W., Hostomsky, Z., Kumpf, R. A., Kyle, S., Li, J., Maegley, K., Newell, D. R., Notarianni, E., Stratford, I. J., Skalitzky, D., Thomas, H. D., Wang, L. Z., Webber, S. E., Williams, K. J. and Curtin, N. J. (2004) 'Anticancer chemosensitization and radiosensitization by the novel poly(ADP-ribose) polymerase-1 inhibitor AG14361', *Journal of the National Cancer Institute*, 96, (1), pp. 56-67.

Caldecott, K. W., Aoufouchi, S., Johnson, P. and Shall, S. (1996) 'XRCC1 polypeptide interacts with DNA polymerase beta and possibly poly (ADP-ribose) polymerase, and DNA ligase III is a novel molecular 'nick-sensor' in vitro', *Nucleic acids research*, 24, (22), pp. 4387-94.

Campbell, K. J., O'Shea, J. M. and Perkins, N. D. (2006a) 'Differential regulation of NF-kappaB activation and function by topoisomerase II inhibitors', *BMC cancer*, 6, pp. 101.

Campbell, K. J., Rocha, S. and Perkins, N. D. (2004) 'Active repression of antiapoptotic gene expression by RelA(p65) NF-kappa B', *Molecular cell*, 13, (6), pp. 853-65.

Campbell, K. J., Witty, J. M., Rocha, S. and Perkins, N. D. (2006b) 'Cisplatin mimics ARF tumor suppressor regulation of RelA (p65) nuclear factor-kappaB transactivation', *Cancer research*, 66, (2), pp. 929-35.

Cao, Z., Xiong, J., Takeuchi, M., Kurama, T. and Goeddel, D. V. (1996) 'TRAF6 is a signal transducer for interleukin-1', *Nature*, 383, (6599), pp. 443-6.

Cardoso, S. M. and Oliveira, C. R. (2003) 'Inhibition of NF-kB renders cells more vulnerable to apoptosis induced by amyloid beta peptides', *Free radical research*, 37, (9), pp. 967-73.

Carrillo, A., Monreal, Y., Ramirez, P., Marin, L., Parrilla, P., Oliver, F. J. and Yelamos, J. (2004) 'Transcription regulation of TNF-alpha-early response genes by poly(ADP-ribose) polymerase-1 in murine heart endothelial cells', *Nucleic acids research*, 32, (2), pp. 757-66.

Cervellera, M. N. and Sala, A. (2000) 'Poly(ADP-ribose) polymerase is a B-MYB coactivator', *The Journal of biological chemistry*, 275, (14), pp. 10692-6.

Chalmers, A., Johnston, P., Woodcock, M., Joiner, M. and Marples, B. (2004) 'PARP-1, PARP-2, and the cellular response to low doses of ionizing radiation', *International journal of radiation oncology, biology, physics*, 58, (2), pp. 410-9.

Chalmers, A. J. (2009) 'The potential role and application of PARP inhibitors in cancer treatment', *British medical bulletin*, 89, pp. 23-40.

Chalmers, A. J. (2010) 'Overcoming resistance of glioblastoma to conventional cytotoxic therapies by the addition of PARP inhibitors', *Anti-cancer agents in medicinal chemistry*, 10, (7), pp. 520-33.

Chambon, P., Weill, J. D. and Mandel, P. (1963) 'Nicotinamide mononucleotide activation of new DNA-dependent polyadenylic acid synthesizing nuclear enzyme', *Biochemical and biophysical research communications*, 11, pp. 39-43.

Chan, H., Bartos, D. P. and Owen-Schaub, L. B. (1999) 'Activation-dependent transcriptional regulation of the human Fas promoter requires NF-kappaB p50-p65 recruitment', *Molecular and cellular biology*, 19, (3), pp. 2098-108.

Chang, W. J. and Alvarez-Gonzalez, R. (2001) 'The sequence-specific DNA binding of NF-kappa B is reversibly regulated by the automodification reaction of poly (ADP-ribose) polymerase 1', *The Journal of biological chemistry*, 276, (50), pp. 47664-70.

Chariot, A. (2009) 'The NF-kappaB-independent functions of IKK subunits in immunity and cancer', *Trends in cell biology*, 19, (8), pp. 404-13.

Chatterjee, S. and Berger, N. A. (2000) 'X-ray-induced damage repair in exponentially growing and growth arrested confluent poly(adenosine diphosphate-ribose) polymerase-deficient V79 chinese hamster cell line', *International journal of oncology*, 17, (5), pp. 955-62.

Chen, B. P., Chan, D. W., Kobayashi, J., Burma, S., Asaithamby, A., Morotomi-Yano, K., Botvinick, E., Qin, J. and Chen, D. J. (2005a) 'Cell cycle dependence of DNA-dependent protein kinase phosphorylation in response to DNA double strand breaks', *The Journal of biological chemistry*, 280, (15), pp. 14709-15.

Chen, E. and Li, C. C. (1998) 'Association of Cdk2/cyclin E and NF-kappa B complexes at G1/S phase', *Biochemical and biophysical research communications*, 249, (3), pp. 728-34.

Chen, F. E., Huang, D. B., Chen, Y. Q. and Ghosh, G. (1998) 'Crystal structure of p50/p65 heterodimer of transcription factor NF-kappaB bound to DNA', *Nature*, 391, (6665), pp. 410-3.

Chen, J., Odenike, O. and Rowley, J. D. (2010) 'Leukaemogenesis: more than mutant genes', *Nature reviews. Cancer*, 10, (1), pp. 23-36.

Chen, L. F. and Greene, W. C. (2004) 'Shaping the nuclear action of NF-kappaB', *Nature reviews. Molecular cell biology*, 5, (5), pp. 392-401.

Chen, L. F., Williams, S. A., Mu, Y., Nakano, H., Duerr, J. M., Buckbinder, L. and Greene, W. C. (2005b) 'NF-kappaB RelA phosphorylation regulates RelA acetylation', *Molecular and cellular biology*, 25, (18), pp. 7966-75.

Chen, Y., Vallee, S., Wu, J., Vu, D., Sondek, J. and Ghosh, G. (2004) 'Inhibition of NF-kappaB activity by IkappaBbeta in association with kappaB-Ras', *Molecular and cellular biology,* 24, (7), pp. 3048-56.

Chen, Z. J. (2005) 'Ubiquitin signalling in the NF-kappaB pathway', *Nature cell biology,* 7, (8), pp. 758-65.

Cheng, C. L., Johnson, S. P., Keir, S. T., Quinn, J. A., Ali-Osman, F., Szabo, C., Li, H., Salzman, A. L., Dolan, M. E., Modrich, P., Bigner, D. D. and Friedman, H. S. (2005) 'Poly(ADP-ribose) polymerase-1 inhibition reverses temozolomide resistance in a DNA mismatch repair-deficient malignant glioma xenograft', *Molecular cancer therapeutics,* 4, (9), pp. 1364-8.

Cheng, S., Hsia, C. Y., Leone, G. and Liou, H. C. (2003) 'Cyclin E and Bcl-xL cooperatively induce cell cycle progression in c-Rel-/- B cells', *Oncogene,* 22, (52), pp. 8472-86.

Cherney, B. W., McBride, O. W., Chen, D. F., Alkhatib, H., Bhatia, K., Hensley, P. and Smulson, M. E. (1987) 'cDNA sequence, protein structure, and chromosomal location of the human gene for poly(ADP-ribose) polymerase', *Proceedings of the National Academy of Sciences of the United States of America,* 84, (23), pp. 8370-4.

Chiarugi, A. (2002) 'Inhibitors of poly(ADP-ribose) polymerase-1 suppress transcriptional activation in lymphocytes and ameliorate autoimmune encephalomyelitis in rats', *British journal of pharmacology,* 137, (6), pp. 761-70.

Chiarugi, A. and Moskowitz, M. A. (2003) 'Poly(ADP-ribose) polymerase-1 activity promotes NF-kappaB-driven transcription and microglial activation: implication for neurodegenerative disorders', *Journal of neurochemistry,* 85, (2), pp. 306-17.

Clarke, R., Liu, M. C., Bouker, K. B., Gu, Z., Lee, R. Y., Zhu, Y., Skaar, T. C., Gomez, B., O'Brien, K., Wang, Y. and Hilakivi-Clarke, L. A. (2003) 'Antiestrogen resistance in breast cancer and the role of estrogen receptor signaling', *Oncogene,* 22, (47), pp. 7316-39.

Cleaver, J. E., Bodell, W. J., Morgan, W. F. and Zelle, B. (1983) 'Differences in the regulation by poly(ADP-ribose) of repair of DNA damage from alkylating agents and ultraviolet light according to cell type', *The Journal of biological chemistry,* 258, (15), pp. 9059-68.

Cohausz, O. and Althaus, F. R. (2009) 'Role of PARP-1 and PARP-2 in the expression of apoptosis-regulating genes in HeLa cells', *Cell biology and toxicology,* 25, (4), pp. 379-91.

Cohen-Armon, M., Visochek, L., Rozensal, D., Kalal, A., Geistrikh, I., Klein, R., Bendetz-Nezer, S., Yao, Z. and Seger, R. (2007) 'DNA-independent PARP-1 activation by phosphorylated ERK2 increases Elk1 activity: a link to histone acetylation', *Molecular cell,* 25, (2), pp. 297-308.

Coll, R. C. and O'Neill, L. A. (2010) 'New insights into the regulation of signalling by toll-like receptors and nod-like receptors', *Journal of innate immunity,* 2, (5), pp. 406-21.

Collart, M. A., Baeuerle, P. and Vassalli, P. (1990) 'Regulation of tumor necrosis factor alpha transcription in macrophages: involvement of four kappa B-like motifs and of constitutive and inducible forms of NF-kappa B', *Molecular and cellular biology,* 10, (4), pp. 1498-506.

Compagno, M., Lim, W. K., Grunn, A., Nandula, S. V., Brahmachary, M., Shen, Q., Bertoni, F., Ponzoni, M., Scandurra, M., Califano, A., Bhagat, G., Chadburn, A., Dalla-Favera, R. and Pasqualucci, L. (2009) 'Mutations of multiple genes cause deregulation of NF-kappaB in diffuse large B-cell lymphoma', *Nature,* 459, (7247), pp. 717-21.

Courtois, G., Smahi, A., Reichenbach, J., Doffinger, R., Cancrini, C., Bonnet, M., Puel, A., Chable-Bessia, C., Yamaoka, S., Feinberg, J., Dupuis-Girod, S., Bodemer, C., Livadiotti, S., Novelli, F., Rossi, P., Fischer, A., Israel, A., Munnich, A., Le Deist, F. and Casanova, J. L. (2003) 'A hypermorphic IkappaBalpha mutation is associated with autosomal dominant anhidrotic ectodermal dysplasia and T cell immunodeficiency', *The Journal of clinical investigation,* 112, (7), pp. 1108-15.

Criollo, A., Senovilla, L., Authier, H., Maiuri, M. C., Morselli, E., Vitale, I., Kepp, O., Tasdemir, E., Galluzzi, L., Shen, S., Tailler, M., Delahaye, N., Tesniere, A., De Stefano, D., Younes, A. B., Harper, F., Pierron, G., Lavandero, S., Zitvogel, L., Israel, A., Baud, V. and Kroemer, G. (2010) 'The IKK complex contributes to the induction of autophagy', *The EMBO journal,* 29, (3), pp. 619-31.

Criswell, L. A., Moser, K. L., Gaffney, P. M., Inda, S., Ortmann, W. A., Lin, D., Chen, J. J., Li, H., Gray-McGuire, C., Neas, B. R., Rich, S. S., Harley, J. B., Behrens, T. W. and Seldin, M. F. (2000) 'PARP alleles and SLE: failure to confirm association with disease susceptibility', *The Journal of clinical investigation,* 105, (11), pp. 1501-2.

Criswell, T., Leskov, K., Miyamoto, S., Luo, G. and Boothman, D. A. (2003) 'Transcription factors activated in mammalian cells after clinically relevant doses of ionizing radiation', *Oncogene,* 22, (37), pp. 5813-27.

Culver, C., Sundqvist, A., Mudie, S., Melvin, A., Xirodimas, D. and Rocha, S. (2010) 'Mechanism of hypoxia-induced NF-kappaB', *Molecular and cellular biology,* 30, (20), pp. 4901-21.

Curtin, N. J., Wang, L. Z., Yiakouvaki, A., Kyle, S., Arris, C. A., Canan-Koch, S., Webber, S. E., Durkacz, B. W., Calvert, H. A., Hostomsky, Z. and Newell, D. R. (2004) 'Novel poly(ADP-ribose) polymerase-1 inhibitor, AG14361, restores sensitivity to temozolomide in mismatch repair-deficient cells', *Clinical cancer research : an official journal of the American Association for Cancer Research,* 10, (3), pp. 881-9.

Cusack, J. C., Jr., Liu, R. and Baldwin, A. S., Jr. (2000) 'Inducible chemoresistance to 7-ethyl-10-[4-(1-piperidino)-1-piperidino]-carbonyloxycamptothe cin (CPT-11) in colorectal cancer cells and a xenograft model is overcome by inhibition of nuclear factor-kappaB activation', *Cancer research,* 60, (9), pp. 2323-30.

D'Amours, D., Desnoyers, S., D'Silva, I. and Poirier, G. G. (1999) 'Poly(ADP-ribosyl)ation reactions in the regulation of nuclear functions', *The Biochemical journal,* 342 (Pt 2), pp. 249-68.

Daniel, R. A., Rozanska, A. L., Mulligan, E. A., Drew, Y., Thomas, H. D., Castelbuono, D. J., Hostomsky, Z., Plummer, E. R., Tweddle, D. A., Boddy, A. V., Clifford, S. C. and Curtin, N. J. (2010) 'Central nervous system penetration and enhancement of temozolomide activity in childhood medulloblastoma models by poly(ADP-ribose) polymerase inhibitor AG-014699', *British journal of cancer,* 103, (10), pp. 1588-96.

Daniel, R. A., Rozanska, A. L., Thomas, H. D., Mulligan, E. A., Drew, Y., Castelbuono, D. J., Hostomsky, Z., Plummer, E. R., Boddy, A. V., Tweddle, D. A., Curtin, N. J. and Clifford, S. C. (2009) 'Inhibition of poly(ADP-ribose) polymerase-1 enhances temozolomide and topotecan activity against childhood neuroblastoma', *Clinical cancer research : an official journal of the American Association for Cancer Research,* 15, (4), pp. 1241-9.

Danson, S. J. and Middleton, M. R. (2001) 'Temozolomide: a novel oral alkylating agent', *Expert review of anticancer therapy,* 1, (1), pp. 13-9.

Dantzer, F., de La Rubia, G., Menissier-De Murcia, J., Hostomsky, Z., de Murcia, G. and Schreiber, V. (2000) 'Base excision repair is impaired in mammalian cells lacking Poly(ADP-ribose) polymerase-1', *Biochemistry,* 39, (25), pp. 7559-69.

Dantzer, F., Schreiber, V., Niedergang, C., Trucco, C., Flatter, E., De La Rubia, G., Oliver, J., Rolli, V., Menissier-de Murcia, J. and de Murcia, G. (1999) 'Involvement of poly(ADP-ribose) polymerase in base excision repair', *Biochimie,* 81, (1-2), pp. 69-75.

Dar, A. A., Goff, L. W., Majid, S., Berlin, J. and El-Rifai, W. (2010) 'Aurora kinase inhibitors--rising stars in cancer therapeutics?', *Molecular cancer therapeutics,* 9, (2), pp. 268-78.

Darnell, J. E., Jr. (2002) 'Transcription factors as targets for cancer therapy', *Nature reviews. Cancer,* 2, (10), pp. 740-9.

Davis, R. E., Brown, K. D., Siebenlist, U. and Staudt, L. M. (2001) 'Constitutive nuclear factor kappaB activity is required for survival of activated B cell-like diffuse large B cell lymphoma cells', *The Journal of experimental medicine,* 194, (12), pp. 1861-74.

de Murcia, G. and Menissier de Murcia, J. (1994) 'Poly(ADP-ribose) polymerase: a molecular nick-sensor', *Trends in biochemical sciences,* 19, (4), pp. 172-6.

de Murcia, J. M., Niedergang, C., Trucco, C., Ricoul, M., Dutrillaux, B., Mark, M., Oliver, F. J., Masson, M., Dierich, A., LeMeur, M., Walztinger, C., Chambon, P. and de Murcia, G. (1997) 'Requirement of poly(ADP-ribose) polymerase in recovery from DNA damage in mice and in cells', *Proceedings of the National Academy of Sciences of the United States of America,* 94, (14), pp. 7303-7.

De Smaele, E., Zazzeroni, F., Papa, S., Nguyen, D. U., Jin, R., Jones, J., Cong, R. and Franzoso, G. (2001) 'Induction of gadd45beta by NF-kappaB downregulates pro-apoptotic JNK signalling', *Nature,* 414, (6861), pp. 308-13.

Degenhardt, Y. and Lampkin, T. (2010) 'Targeting Polo-like kinase in cancer therapy', *Clinical cancer research : an official journal of the American Association for Cancer Research,* 16, (2), pp. 384-9.

Delaney, C. A., Wang, L. Z., Kyle, S., White, A. W., Calvert, A. H., Curtin, N. J., Durkacz, B. W., Hostomsky, Z. and Newell, D. R. (2000) 'Potentiation of temozolomide and topotecan growth inhibition and cytotoxicity by novel poly(adenosine diphosphoribose) polymerase inhibitors in a panel of human tumor cell lines', *Clinical cancer research : an official journal of the American Association for Cancer Research,* 6, (7), pp. 2860-7.

DeLuca, C., Kwon, H., Lin, R., Wainberg, M. and Hiscott, J. (1999) 'NF-kappaB activation and HIV-1 induced apoptosis', *Cytokine & growth factor reviews,* 10, (3-4), pp. 235-53.

Dickson, C., Fantl, V., Gillett, C., Brookes, S., Bartek, J., Smith, R., Fisher, C., Barnes, D. and Peters, G. (1995) 'Amplification of chromosome band 11q13 and a role for cyclin D1 in human breast cancer', *Cancer letters,* 90, (1), pp. 43-50.

Ditchfield, C., Johnson, V. L., Tighe, A., Ellston, R., Haworth, C., Johnson, T., Mortlock, A., Keen, N. and Taylor, S. S. (2003) 'Aurora B couples chromosome alignment with anaphase by targeting BubR1, Mad2, and Cenp-E to kinetochores', *The Journal of cell biology,* 161, (2), pp. 267-80.

Donawho, C. K., Luo, Y., Penning, T. D., Bauch, J. L., Bouska, J. J., Bontcheva-Diaz, V. D., Cox, B. F., DeWeese, T. L., Dillehay, L. E., Ferguson, D. C., Ghoreishi-Haack, N. S., Grimm, D. R., Guan, R., Han, E. K., Holley-Shanks, R. R., Hristov, B., Idler, K. B., Jarvis, K., Johnson, E. F., Kleinberg, L. R., Klinghofer, V., Lasko, L. M., Liu, X., Marsh, K. C., McGonigal, T. P., Meulbroek, J. A., Olson, A. M., Palma, J. P., Rodriguez, L. E., Shi, Y., Stavropoulos, J. A., Tsurutani, A. C., Zhu, G. D., Rosenberg, S. H., Giranda, V. L. and Frost, D. J. (2007) 'ABT-888, an orally active poly(ADP-ribose) polymerase inhibitor that potentiates DNA-damaging agents in preclinical tumor models', *Clinical cancer research : an official journal of the American Association for Cancer Research*, 13, (9), pp. 2728-37.

Drew, Y., Mulligan, E. A., Vong, W. T., Thomas, H. D., Kahn, S., Kyle, S., Mukhopadhyay, A., Los, G., Hostomsky, Z., Plummer, E. R., Edmondson, R. J. and Curtin, N. J. (2011) 'Therapeutic potential of poly(ADP-ribose) polymerase inhibitor AG014699 in human cancers with mutated or methylated BRCA1 or BRCA2', *Journal of the National Cancer Institute*, 103, (4), pp. 334-46.

Drew, Y. and Plummer, R. (2009) 'PARP inhibitors in cancer therapy: two modes of attack on the cancer cell widening the clinical applications', *Drug resistance updates : reviews and commentaries in antimicrobial and anticancer chemotherapy*, 12, (6), pp. 153-6.

Dungey, F. A., Caldecott, K. W. and Chalmers, A. J. (2009) 'Enhanced radiosensitization of human glioma cells by combining inhibition of poly(ADP-ribose) polymerase with inhibition of heat shock protein 90', *Molecular cancer therapeutics*, 8, (8), pp. 2243-54.

Dungey, F. A., Loser, D. A. and Chalmers, A. J. (2008) 'Replication-dependent radiosensitization of human glioma cells by inhibition of poly(ADP-Ribose) polymerase: mechanisms and therapeutic potential', *International journal of radiation oncology, biology, physics*, 72, (4), pp. 1188-97.

Durkacz, B. W., Omidiji, O., Gray, D. A. and Shall, S. (1980) '(ADP-ribose)n participates in DNA excision repair', *Nature*, 283, (5747), pp. 593-6.

Dutta, J., Fan, Y., Gupta, N., Fan, G. and Gelinas, C. (2006) 'Current insights into the regulation of programmed cell death by NF-kappaB', *Oncogene*, 25, (51), pp. 6800-16.

El-Khamisy, S. F., Masutani, M., Suzuki, H. and Caldecott, K. W. (2003) 'A requirement for PARP-1 for the assembly or stability of XRCC1 nuclear foci at sites of oxidative DNA damage', *Nucleic acids research*, 31, (19), pp. 5526-33.

Elliott, S. L., Crawford, C., Mulligan, E., Summerfield, G., Newton, P., Wallis, J., Mainou-Fowler, T., Evans, P., Bedwell, C., Durkacz, B. W. and Willmore, E. (2011) 'Mitoxantrone in combination with an inhibitor of DNA-dependent protein kinase: a potential therapy for high risk B-cell chronic lymphocytic leukaemia', *British journal of haematology*, 152, (1), pp. 61-71.

Fang, G., Yu, H. and Kirschner, M. W. (1998) 'The checkpoint protein MAD2 and the mitotic regulator CDC20 form a ternary complex with the anaphase-promoting complex to control anaphase initiation', *Genes & development*, 12, (12), pp. 1871-83.

Farabegoli, F., Hermsen, M. A., Ceccarelli, C., Santini, D., Weiss, M. M., Meijer, G. A. and van Diest, P. J. (2004) 'Simultaneous chromosome 1q gain and 16q loss is associated with steroid receptor presence and low proliferation in breast carcinoma', *Modern pathology : an official journal of the United States and Canadian Academy of Pathology, Inc*, 17, (4), pp. 449-55.

Farmer, H., McCabe, N., Lord, C. J., Tutt, A. N., Johnson, D. A., Richardson, T. B., Santarosa, M., Dillon, K. J., Hickson, I., Knights, C., Martin, N. M., Jackson, S. P., Smith, G. C. and Ashworth, A. (2005) 'Targeting the DNA repair defect in BRCA mutant cells as a therapeutic strategy', *Nature*, 434, (7035), pp. 917-21.

Feuillard, J., Schuhmacher, M., Kohanna, S., Asso-Bonnet, M., Ledeur, F., Joubert-Caron, R., Bissieres, P., Polack, A., Bornkamm, G. W. and Raphael, M. (2000) 'Inducible loss of NF-kappaB activity is associated with apoptosis and Bcl-2 down-regulation in Epstein-Barr virus-transformed B lymphocytes', *Blood*, 95, (6), pp. 2068-75.

Filippova, M., Song, H., Connolly, J. L., Dermody, T. S. and Duerksen-Hughes, P. J. (2002) 'The human papillomavirus 16 E6 protein binds to tumor necrosis factor (TNF) R1 and protects cells from TNF-induced apoptosis', *The Journal of biological chemistry*, 277, (24), pp. 21730-9.

Fire, A. (1999) 'RNA-triggered gene silencing', *Trends in genetics : TIG*, 15, (9), pp. 358-63.

Foley, K. P., Leonard, M. W. and Engel, J. D. (1993) 'Quantitation of RNA using the polymerase chain reaction', *Trends in genetics : TIG*, 9, (11), pp. 380-5.

Fong, P. C., Boss, D. S., Yap, T. A., Tutt, A., Wu, P., Mergui-Roelvink, M., Mortimer, P., Swaisland, H., Lau, A., O'Connor, M. J., Ashworth, A., Carmichael, J., Kaye, S. B., Schellens, J. H. and de Bono, J. S. (2009) 'Inhibition of poly(ADP-ribose) polymerase in tumors from BRCA mutation carriers', *The New England journal of medicine*, 361, (2), pp. 123-34.

Fong, P. C., Yap, T. A., Boss, D. S., Carden, C. P., Mergui-Roelvink, M., Gourley, C., De Greve, J., Lubinski, J., Shanley, S., Messiou, C., A'Hern, R., Tutt, A., Ashworth, A., Stone, J., Carmichael, J., Schellens, J. H., de Bono, J. S. and Kaye, S. B. (2010) 'Poly(ADP)-ribose polymerase

inhibition: frequent durable responses in BRCA carrier ovarian cancer correlating with platinum-free interval', *Journal of clinical oncology : official journal of the American Society of Clinical Oncology*, 28, (15), pp. 2512-9.

Franzoso, G., Carlson, L., Poljak, L., Shores, E. W., Epstein, S., Leonardi, A., Grinberg, A., Tran, T., Scharton-Kersten, T., Anver, M., Love, P., Brown, K. and Siebenlist, U. (1998) 'Mice deficient in nuclear factor (NF)-kappa B/p52 present with defects in humoral responses, germinal center reactions, and splenic microarchitecture', *The Journal of experimental medicine*, 187, (2), pp. 147-59.

Frosina, G., Fortini, P., Rossi, O., Carrozzino, F., Raspaglio, G., Cox, L. S., Lane, D. P., Abbondandolo, A. and Dogliotti, E. (1996) 'Two pathways for base excision repair in mammalian cells', *The Journal of biological chemistry*, 271, (16), pp. 9573-8.

Fujimura, S., Hasegawa, S., Shimizu, Y. and Sugimura, T. (1967) 'Polymerization of the adenosine 5'-diphosphate-ribose moiety of nicotinamide-adenine dinucleotide by nuclear enzyme. I. Enzymatic reactions', *Biochimica et biophysica acta*, 145, (2), pp. 247-59.

Fukuhara, N., Tagawa, H., Kameoka, Y., Kasugai, Y., Karnan, S., Kameoka, J., Sasaki, T., Morishima, Y., Nakamura, S. and Seto, M. (2006) 'Characterization of target genes at the 2p15-16 amplicon in diffuse large B-cell lymphoma', *Cancer science*, 97, (6), pp. 499-504.

Fung, T. K. and Poon, R. Y. (2005) 'A roller coaster ride with the mitotic cyclins', *Seminars in cell & developmental biology*, 16, (3), pp. 335-42.

Gaurnier-Hausser, A., Patel, R., Baldwin, A. S., May, M. J. and Mason, N. J. (2011) 'NEMO-Binding Domain Peptide Inhibits Constitutive NF-{kappa}B Activity and Reduces Tumor Burden in a Canine Model of Relapsed, Refractory Diffuse Large B-Cell Lymphoma', *Clinical cancer research : an official journal of the American Association for Cancer Research*, 17, (14), pp. 4661-71.

Gerondakis, S., Grossmann, M., Nakamura, Y., Pohl, T. and Grumont, R. (1999) 'Genetic approaches in mice to understand Rel/NF-kappaB and IkappaB function: transgenics and knockouts', *Oncogene*, 18, (49), pp. 6888-95.

Ghosh, G., Huang D., Huxford T. (1999) 'Structural insights into NF-κB/IκB signaling.', *Genes therapy & molecular biology*, 4, pp. 75-82.

Ghosh, S. and Karin, M. (2002) 'Missing pieces in the NF-kappaB puzzle', *Cell*, 109 Suppl, pp. S81-96.

Gilmore, T. D. (1999) 'Multiple mutations contribute to the oncogenicity of the retroviral oncoprotein v-Rel', *Oncogene*, 18, (49), pp. 6925-37.

Gilmore, T. D. (2006) 'Introduction to NF-kappaB: players, pathways, perspectives', *Oncogene*, 25, (51), pp. 6680-4.

Gilmore, T. D. and Herscovitch, M. (2006) 'Inhibitors of NF-kappaB signaling: 785 and counting', *Oncogene*, 25, (51), pp. 6887-99.

Goepfert, T. M., Adigun, Y. E., Zhong, L., Gay, J., Medina, D. and Brinkley, W. R. (2002) 'Centrosome amplification and overexpression of aurora A are early events in rat mammary carcinogenesis', *Cancer research*, 62, (14), pp. 4115-22.

Golsteyn, R. M., Mundt, K. E., Fry, A. M. and Nigg, E. A. (1995) 'Cell cycle regulation of the activity and subcellular localization of Plk1, a human protein kinase implicated in mitotic spindle function', *The Journal of cell biology*, 129, (6), pp. 1617-28.

Gottipati, P., Vischioni, B., Schultz, N., Solomons, J., Bryant, H. E., Djureinovic, T., Issaeva, N., Sleeth, K., Sharma, R. A. and Helleday, T. (2010) 'Poly(ADP-ribose) polymerase is hyperactivated in homologous recombination-defective cells', *Cancer research*, 70, (13), pp. 5389-98.

Gradwohl, G., Menissier de Murcia, J. M., Molinete, M., Simonin, F., Koken, M., Hoeijmakers, J. H. and de Murcia, G. (1990) 'The second zinc-finger domain of poly(ADP-ribose) polymerase determines specificity for single-stranded breaks in DNA', *Proceedings of the National Academy of Sciences of the United States of America*, 87, (8), pp. 2990-4.

Gretarsdottir, S., Thorlacius, S., Valgardsdottir, R., Gudlaugsdottir, S., Sigurdsson, S., Steinarsdottir, M., Jonasson, J. G., Anamthawat-Jonsson, K. and Eyfjord, J. E. (1998) 'BRCA2 and p53 mutations in primary breast cancer in relation to genetic instability', *Cancer research*, 58, (5), pp. 859-62.

Greten, F. R., Eckmann, L., Greten, T. F., Park, J. M., Li, Z. W., Egan, L. J., Kagnoff, M. F. and Karin, M. (2004) 'IKKbeta links inflammation and tumorigenesis in a mouse model of colitis-associated cancer', *Cell*, 118, (3), pp. 285-96.

Griebel, M., Friedman, H. S., Halperin, E. C., Wiener, M. D., Marks, L., Oakes, W. J., Hoffman, J. M., DeLong, G. R., Schold, S. C., Hockenberger, B. and et al. (1991) 'Reversible neurotoxicity following hyperfractionated radiation therapy of brain stem glioma', *Medical and pediatric oncology*, 19, (3), pp. 182-6.

Griffin, R. J., Curtin, N. J., Newell, D. R., Golding, B. T., Durkacz, B. W. and Calvert, A. H. (1995) 'The role of inhibitors of poly(ADP-ribose) polymerase as resistance-modifying agents in cancer therapy', *Biochimie*, 77, (6), pp. 408-22.

Gringhuis, S. I., Garcia-Vallejo, J. J., van Het Hof, B. and van Dijk, W. (2005) 'Convergent actions of I kappa B kinase beta and protein kinase C delta modulate mRNA stability through phosphorylation of 14-3-3 beta complexed with tristetraprolin', *Molecular and cellular biology*, 25, (15), pp. 6454-63.

Grossmann, M., Metcalf, D., Merryfull, J., Beg, A., Baltimore, D. and Gerondakis, S. (1999) 'The combined absence of the transcription factors Rel and RelA leads to multiple hemopoietic cell defects', *Proceedings of the National Academy of Sciences of the United States of America*, 96, (21), pp. 11848-53.

Grumont, R. J., Rourke, I. J. and Gerondakis, S. (1999) 'Rel-dependent induction of A1 transcription is required to protect B cells from antigen receptor ligation-induced apoptosis', *Genes & development*, 13, (4), pp. 400-11.

Guenther, M. G., Lane, W. S., Fischle, W., Verdin, E., Lazar, M. A. and Shiekhattar, R. (2000) 'A core SMRT corepressor complex containing HDAC3 and TBL1, a WD40-repeat protein linked to deafness', *Genes & development*, 14, (9), pp. 1048-57.

Guo, G., Yan-Sanders, Y., Lyn-Cook, B. D., Wang, T., Tamae, D., Ogi, J., Khaletskiy, A., Li, Z., Weydert, C., Longmate, J. A., Huang, T. T., Spitz, D. R., Oberley, L. W. and Li, J. J. (2003) 'Manganese superoxide dismutase-mediated gene expression in radiation-induced adaptive responses', *Molecular and cellular biology*, 23, (7), pp. 2362-78.

Guo, Z., Kozlov, S., Lavin, M. F., Person, M. D. and Paull, T. T. (2010) 'ATM activation by oxidative stress', *Science*, 330, (6003), pp. 517-21.

Guttridge, D. C., Albanese, C., Reuther, J. Y., Pestell, R. G. and Baldwin, A. S., Jr. (1999) 'NF-kappaB controls cell growth and differentiation through transcriptional regulation of cyclin D1', *Molecular and cellular biology*, 19, (8), pp. 5785-99.

Ha, G. H., Kim, H. S., Go, H., Lee, H., Seimiya, H., Chung, D. H. and Lee, C. W. (2011) 'Tankyrase-1 function at telomeres and during mitosis is regulated by Polo-like kinase-1-mediated phosphorylation', *Cell death and differentiation*.

Ha, H. C., Hester, L. D. and Snyder, S. H. (2002) 'Poly(ADP-ribose) polymerase-1 dependence of stress-induced transcription factors and associated gene expression in glia', *Proceedings of the National Academy of Sciences of the United States of America*, 99, (5), pp. 3270-5.

Haddad, M., Rhinn, H., Bloquel, C., Coqueran, B., Szabo, C., Plotkine, M., Scherman, D. and Margaill, I. (2006) 'Anti-inflammatory effects of PJ34, a poly(ADP-ribose) polymerase inhibitor, in transient focal cerebral ischemia in mice', *British journal of pharmacology*, 149, (1), pp. 23-30.

Haince, J. F., Kozlov, S., Dawson, V. L., Dawson, T. M., Hendzel, M. J., Lavin, M. F. and Poirier, G. G. (2007) 'Ataxia telangiectasia mutated (ATM) signaling network is modulated by a novel poly(ADP-ribose)-dependent pathway in the early response to DNA-damaging agents', *The Journal of biological chemistry*, 282, (22), pp. 16441-53.

Hammarskjold, M. L. and Simurda, M. C. (1992) 'Epstein-Barr virus latent membrane protein transactivates the human immunodeficiency virus type 1 long terminal repeat through induction of NF-kappa B activity', *Journal of virology*, 66, (11), pp. 6496-501.

Han, Z., Boyle, D. L., Manning, A. M. and Firestein, G. S. (1998) 'AP-1 and NF-kappaB regulation in rheumatoid arthritis and murine collagen-induced arthritis', *Autoimmunity*, 28, (4), pp. 197-208.

Hanahan, D. and Weinberg, R. A. (2000) 'The hallmarks of cancer', *Cell*, 100, (1), pp. 57-70.

Hanahan, D. and Weinberg, R. A. (2011) 'Hallmarks of cancer: the next generation', *Cell*, 144, (5), pp. 646-74.

Harada, H., Kondo, T., Ogawa, S., Tamura, T., Kitagawa, M., Tanaka, N., Lamphier, M. S., Hirai, H. and Taniguchi, T. (1994) 'Accelerated exon skipping of IRF-1 mRNA in human myelodysplasia/leukemia; a possible mechanism of tumor suppressor inactivation', *Oncogene*, 9, (11), pp. 3313-20.

Hart, L. A., Krishnan, V. L., Adcock, I. M., Barnes, P. J. and Chung, K. F. (1998) 'Activation and localization of transcription factor, nuclear factor-kappaB, in asthma', *American journal of respiratory and critical care medicine*, 158, (5 Pt 1), pp. 1585-92.

Hassa, P. O., Buerki, C., Lombardi, C., Imhof, R. and Hottiger, M. O. (2003) 'Transcriptional coactivation of nuclear factor-kappaB-dependent gene expression by p300 is regulated by poly(ADP)-ribose polymerase-1', *The Journal of biological chemistry*, 278, (46), pp. 45145-53.

Hassa, P. O., Covic, M., Bedford, M. T. and Hottiger, M. O. (2008) 'Protein arginine methyltransferase 1 coactivates NF-kappaB-dependent gene expression synergistically with CARM1 and PARP1', *Journal of molecular biology*, 377, (3), pp. 668-78.

Hassa, P. O., Covic, M., Hasan, S., Imhof, R. and Hottiger, M. O. (2001) 'The enzymatic and DNA binding activity of PARP-1 are not required for NF-kappa B coactivator function', *The Journal of biological chemistry*, 276, (49), pp. 45588-97.

Hassa, P. O., Haenni, S. S., Buerki, C., Meier, N. I., Lane, W. S., Owen, H., Gersbach, M., Imhof, R. and Hottiger, M. O. (2005) 'Acetylation of poly(ADP-ribose) polymerase-1 by p300/CREB-binding

protein regulates coactivation of NF-kappaB-dependent transcription', *The Journal of biological chemistry*, 280, (49), pp. 40450-64.

Hassa, P. O. and Hottiger, M. O. (1999) 'A role of poly (ADP-ribose) polymerase in NF-kappaB transcriptional activation', *Biological chemistry*, 380, (7-8), pp. 953-9.

Hassa, P. O. and Hottiger, M. O. (2002) 'The functional role of poly(ADP-ribose)polymerase 1 as novel coactivator of NF-kappaB in inflammatory disorders', *Cellular and molecular life sciences : CMLS*, 59, (9), pp. 1534-53.

Hatada, E. N., Nieters, A., Wulczyn, F. G., Naumann, M., Meyer, R., Nucifora, G., McKeithan, T. W. and Scheidereit, C. (1992) 'The ankyrin repeat domains of the NF-kappa B precursor p105 and the protooncogene bcl-3 act as specific inhibitors of NF-kappa B DNA binding', *Proceedings of the National Academy of Sciences of the United States of America*, 89, (6), pp. 2489-93.

Hauf, S., Cole, R. W., LaTerra, S., Zimmer, C., Schnapp, G., Walter, R., Heckel, A., van Meel, J., Rieder, C. L. and Peters, J. M. (2003) 'The small molecule Hesperadin reveals a role for Aurora B in correcting kinetochore-microtubule attachment and in maintaining the spindle assembly checkpoint', *The Journal of cell biology*, 161, (2), pp. 281-94.

Hayden, M. S. and Ghosh, S. (2004) 'Signaling to NF-kappaB', *Genes & development*, 18, (18), pp. 2195-224.

Hayden, M. S., West, A. P. and Ghosh, S. (2006) 'NF-kappaB and the immune response', *Oncogene*, 25, (51), pp. 6758-80.

Hein, H., Schluter, C., Kulke, R., Christophers, E., Schroder, J. M. and Bartels, J. (1997) 'Genomic organization, sequence, and transcriptional regulation of the human eotaxin gene', *Biochemical and biophysical research communications*, 237, (3), pp. 537-42.

Hertlein, E., Wang, J., Ladner, K. J., Bakkar, N. and Guttridge, D. C. (2005) 'RelA/p65 regulation of IkappaBbeta', *Molecular and cellular biology*, 25, (12), pp. 4956-68.

Hewamana, S., Alghazal, S., Lin, T. T., Clement, M., Jenkins, C., Guzman, M. L., Jordan, C. T., Neelakantan, S., Crooks, P. A., Burnett, A. K., Pratt, G., Fegan, C., Rowntree, C., Brennan, P. and Pepper, C. (2008a) 'The NF-kappaB subunit Rel A is associated with in vitro survival and clinical disease progression in chronic lymphocytic leukemia and represents a promising therapeutic target', *Blood*, 111, (9), pp. 4681-9.

Hewamana, S., Lin, T. T., Jenkins, C., Burnett, A. K., Jordan, C. T., Fegan, C., Brennan, P., Rowntree, C. and Pepper, C. (2008b) 'The novel nuclear factor-kappaB inhibitor LC-1 is equipotent in poor prognostic subsets of chronic lymphocytic leukemia and shows strong synergy with fludarabine', *Clinical cancer research : an official journal of the American Association for Cancer Research*, 14, (24), pp. 8102-11.

Hewamana, S., Lin, T. T., Rowntree, C., Karunanithi, K., Pratt, G., Hills, R., Fegan, C., Brennan, P. and Pepper, C. (2009) 'Rel a is an independent biomarker of clinical outcome in chronic lymphocytic leukemia', *Journal of clinical oncology : official journal of the American Society of Clinical Oncology*, 27, (5), pp. 763-9.

Heyninck, K., De Valck, D., Vanden Berghe, W., Van Criekinge, W., Contreras, R., Fiers, W., Haegeman, G. and Beyaert, R. (1999) 'The zinc finger protein A20 inhibits TNF-induced NF-kappaB-dependent gene expression by interfering with an RIP- or TRAF2-mediated transactivation signal and directly binds to a novel NF-kappaB-inhibiting protein ABIN', *The Journal of cell biology*, 145, (7), pp. 1471-82.

Hibi, K., Liu, Q., Beaudry, G. A., Madden, S. L., Westra, W. H., Wehage, S. L., Yang, S. C., Heitmiller, R. F., Bertelsen, A. H., Sidransky, D. and Jen, J. (1998) 'Serial analysis of gene expression in non-small cell lung cancer', *Cancer research*, 58, (24), pp. 5690-4.

Hickson, I., Zhao, Y., Richardson, C. J., Green, S. J., Martin, N. M., Orr, A. I., Reaper, P. M., Jackson, S. P., Curtin, N. J. and Smith, G. C. (2004) 'Identification and characterization of a novel and specific inhibitor of the ataxia-telangiectasia mutated kinase ATM', *Cancer research*, 64, (24), pp. 9152-9.

Hideshima, T., Ikeda, H., Chauhan, D., Okawa, Y., Raje, N., Podar, K., Mitsiades, C., Munshi, N. C., Richardson, P. G., Carrasco, R. D. and Anderson, K. C. (2009) 'Bortezomib induces canonical nuclear factor-kappaB activation in multiple myeloma cells', *Blood*, 114, (5), pp. 1046-52.

Higuchi, R., Fockler, C., Dollinger, G. and Watson, R. (1993) 'Kinetic PCR analysis: real-time monitoring of DNA amplification reactions', *Bio/technology*, 11, (9), pp. 1026-30.

Hinata, K., Gervin, A. M., Jennifer Zhang, Y. and Khavari, P. A. (2003) 'Divergent gene regulation and growth effects by NF-kappa B in epithelial and mesenchymal cells of human skin', *Oncogene*, 22, (13), pp. 1955-64.

Hinz, M., Stilmann, M., Arslan, S. C., Khanna, K. K., Dittmar, G. and Scheidereit, C. (2010) 'A cytoplasmic ATM-TRAF6-cIAP1 module links nuclear DNA damage signaling to ubiquitin-mediated NF-kappaB activation', *Molecular cell*, 40, (1), pp. 63-74.

Hirota, T., Kunitoku, N., Sasayama, T., Marumoto, T., Zhang, D., Nitta, M., Hatakeyama, K. and Saya, H. (2003) 'Aurora-A and an interacting activator, the LIM protein Ajuba, are required for mitotic commitment in human cells', *Cell*, 114, (5), pp. 585-98.

Ho, W. C., Dickson, K. M. and Barker, P. A. (2005) 'Nuclear factor-kappaB induced by doxorubicin is deficient in phosphorylation and acetylation and represses nuclear factor-kappaB-dependent transcription in cancer cells', *Cancer research*, 65, (10), pp. 4273-81.

Hoeijmakers, J. H. (2001) 'Genome maintenance mechanisms for preventing cancer', *Nature*, 411, (6835), pp. 366-74.

Hoogstraten, B., George, S. L., Samal, B., Rivkin, S. E., Costanzi, J. J., Bonnet, J. D., Thigpen, T. and Braine, H. (1976) 'Combination chemotherapy and adriamycin in patients with advanced breast cancer. A Southwest Oncology Group study', *Cancer*, 38, (1), pp. 13-20.

Hoppe, B. S., Jensen, R. B. and Kirchgessner, C. U. (2000) 'Complementation of the radiosensitive M059J cell line', *Radiation research*, 153, (2), pp. 125-30.

Horwitz, K. B., Mockus, M. B. and Lessey, B. A. (1982) 'Variant T47D human breast cancer cells with high progesterone-receptor levels despite estrogen and antiestrogen resistance', *Cell*, 28, (3), pp. 633-42.

Houldsworth, J., Olshen, A. B., Cattoretti, G., Donnelly, G. B., Teruya-Feldstein, J., Qin, J., Palanisamy, N., Shen, Y., Dyomina, K., Petlakh, M., Pan, Q., Zelenetz, A. D., Dalla-Favera, R. and Chaganti, R. S. (2004) 'Relationship between REL amplification, REL function, and clinical and biologic features in diffuse large B-cell lymphomas', *Blood*, 103, (5), pp. 1862-8.

Hsu, H., Shu, H. B., Pan, M. G. and Goeddel, D. V. (1996) 'TRADD-TRAF2 and TRADD-FADD interactions define two distinct TNF receptor 1 signal transduction pathways', *Cell*, 84, (2), pp. 299-308.

Huang, D., Yang, C. Z., Yao, L., Wang, Y., Liao, Y. H. and Huang, K. (2008) 'Activation and overexpression of PARP-1 in circulating mononuclear cells promote TNF-alpha and IL-6 expression in patients with unstable angina', *Archives of medical research*, 39, (8), pp. 775-84.

Huang, H. and Tindall, D. J. (2006) 'FOXO factors: a matter of life and death', *Future oncology*, 2, (1), pp. 83-9.

Huang, T. T., Kudo, N., Yoshida, M. and Miyamoto, S. (2000) 'A nuclear export signal in the N-terminal regulatory domain of IkappaBalpha controls cytoplasmic localization of inactive NF-kappaB/IkappaBalpha complexes', *Proceedings of the National Academy of Sciences of the United States of America*, 97, (3), pp. 1014-9.

Huang, T. T., Wuerzberger-Davis, S. M., Wu, Z. H. and Miyamoto, S. (2003) 'Sequential modification of NEMO/IKKgamma by SUMO-1 and ubiquitin mediates NF-kappaB activation by genotoxic stress', *Cell*, 115, (5), pp. 565-76.

Huang, W. C., Ju, T. K., Hung, M. C. and Chen, C. C. (2007) 'Phosphorylation of CBP by IKKalpha promotes cell growth by switching the binding preference of CBP from p53 to NF-kappaB', *Molecular cell*, 26, (1), pp. 75-87.

Hunter, J. E., Willmore, E., Irving, J. A., Hostomsky, Z., Veuger, S. J. and Durkacz, B. W. (2011) 'NF-kappaB mediates radio-sensitization by the PARP-1 inhibitor, AG-014699', *Oncogene*.

Huxford, T., Huang, D. B., Malek, S. and Ghosh, G. (1998) 'The crystal structure of the IkappaBalpha/NF-kappaB complex reveals mechanisms of NF-kappaB inactivation', *Cell*, 95, (6), pp. 759-70.

Hymowitz, S. G. and Wertz, I. E. (2010) 'A20: from ubiquitin editing to tumour suppression', *Nature reviews. Cancer*, 10, (5), pp. 332-41.

Iademarco, M. F., McQuillan, J. J., Rosen, G. D. and Dean, D. C. (1992) 'Characterization of the promoter for vascular cell adhesion molecule-1 (VCAM-1)', *The Journal of biological chemistry*, 267, (23), pp. 16323-9.

Ikejima, M., Noguchi, S., Yamashita, R., Ogura, T., Sugimura, T., Gill, D. M. and Miwa, M. (1990) 'The zinc fingers of human poly(ADP-ribose) polymerase are differentially required for the recognition of DNA breaks and nicks and the consequent enzyme activation. Other structures recognize intact DNA', *The Journal of biological chemistry*, 265, (35), pp. 21907-13.

Israel, A., Le Bail, O., Hatat, D., Piette, J., Kieran, M., Logeat, F., Wallach, D., Fellous, M. and Kourilsky, P. (1989a) 'TNF stimulates expression of mouse MHC class I genes by inducing an NF kappa B-like enhancer binding activity which displaces constitutive factors', *The EMBO journal*, 8, (12), pp. 3793-800.

Israel, A., Yano, O., Logeat, F., Kieran, M. and Kourilsky, P. (1989b) 'Two purified factors bind to the same sequence in the enhancer of mouse MHC class I genes: one of them is a positive regulator induced upon differentiation of teratocarcinoma cells', *Nucleic acids research*, 17, (13), pp. 5245-57.

Ito, Y., Miyoshi, E., Sasaki, N., Kakudo, K., Yoshida, H., Tomoda, C., Uruno, T., Takamura, Y., Miya, A., Kobayashi, K., Matsuzuka, F., Matsuura, N., Kuma, K. and Miyauchi, A. (2004) 'Polo-like

kinase 1 overexpression is an early event in the progression of papillary carcinoma', *British journal of cancer*, 90, (2), pp. 414-8.
Jackson, A. L. and Linsley, P. S. (2004) 'Noise amidst the silence: off-target effects of siRNAs?', *Trends in genetics : TIG*, 20, (11), pp. 521-4.
Jagtap, P. and Szabo, C. (2005) 'Poly(ADP-ribose) polymerase and the therapeutic effects of its inhibitors', *Nature reviews. Drug discovery*, 4, (5), pp. 421-40.
Jain, J., McCaffrey, P. G., Valge-Archer, V. E. and Rao, A. (1992) 'Nuclear factor of activated T cells contains Fos and Jun', *Nature*, 356, (6372), pp. 801-4.
Janssens, S. and Tschopp, J. (2006) 'Signals from within: the DNA-damage-induced NF-kappaB response', *Cell death and differentiation*, 13, (5), pp. 773-84.
Jemal, A., Bray, F., Center, M. M., Ferlay, J., Ward, E. and Forman, D. (2011) 'Global cancer statistics', *CA: a cancer journal for clinicians*, 61, (2), pp. 69-90.
Jeng, Y. M., Peng, S. Y., Lin, C. Y. and Hsu, H. C. (2004) 'Overexpression and amplification of Aurora-A in hepatocellular carcinoma', *Clinical cancer research : an official journal of the American Association for Cancer Research*, 10, (6), pp. 2065-71.
Jenkins, C., Hewamana, S., Gilkes, A., Neelakantan, S., Crooks, P., Mills, K., Pepper, C. and Burnett, A. (2008) 'Nuclear factor-kappaB as a potential therapeutic target for the novel cytotoxic agent LC-1 in acute myeloid leukaemia', *British journal of haematology*, 143, (5), pp. 661-71.
Jeremias, I., Kupatt, C., Baumann, B., Herr, I., Wirth, T. and Debatin, K. M. (1998) 'Inhibition of nuclear factor kappaB activation attenuates apoptosis resistance in lymphoid cells', *Blood*, 91, (12), pp. 4624-31.
Jin, X. M., Kim, H. N., Lee, I. K., Park, K. S., Kim, H. J., Choi, J. S., Juhng, S. W. and Choi, C. (2010) 'PARP-1 Val762Ala polymorphism is associated with reduced risk of non-Hodgkin lymphoma in Korean males', *BMC medical genetics*, 11, pp. 38.
Johnson, D. R. and Pober, J. S. (1994) 'HLA class I heavy-chain gene promoter elements mediating synergy between tumor necrosis factor and interferons', *Molecular and cellular biology*, 14, (2), pp. 1322-32.
Ju, J., Naura, A. S., Errami, Y., Zerfaoui, M., Kim, H., Kim, J. G., Abd Elmageed, Z. Y., Abdel-Mageed, A. B., Giardina, C., Beg, A. A., Smulson, M. E. and Boulares, A. H. (2010) 'Phosphorylation of p50 NF-kappaB at a single serine residue by DNA-dependent protein kinase is critical for VCAM-1 expression upon TNF treatment', *The Journal of biological chemistry*, 285, (52), pp. 41152-60.
Jung, M. and Dritschilo, A. (2001) 'NF-kappa B signaling pathway as a target for human tumor radiosensitization', *Seminars in radiation oncology*, 11, (4), pp. 346-51.
Kaether, C., Haass, C. and Steiner, H. (2006) 'Assembly, trafficking and function of gamma-secretase', *Neuro-degenerative diseases*, 3, (4-5), pp. 275-83.
Kameshita, I., Matsuda, Z., Taniguchi, T. and Shizuta, Y. (1984) 'Poly (ADP-Ribose) synthetase. Separation and identification of three proteolytic fragments as the substrate-binding domain, the DNA-binding domain, and the automodification domain', *The Journal of biological chemistry*, 259, (8), pp. 4770-6.
Kanzaki, S., Hilliker, S., Baylink, D. J. and Mohan, S. (1994) 'Evidence that human bone cells in culture produce insulin-like growth factor-binding protein-4 and -5 proteases', *Endocrinology*, 134, (1), pp. 383-92.
Kanzawa, T., Ito, H., Kondo, Y. and Kondo, S. (2003) 'Current and Future Gene Therapy for Malignant Gliomas', *Journal of biomedicine & biotechnology*, 2003, (1), pp. 25-34.
Kapahi, P., Takahashi, T., Natoli, G., Adams, S. R., Chen, Y., Tsien, R. Y. and Karin, M. (2000) 'Inhibition of NF-kappa B activation by arsenite through reaction with a critical cysteine in the activation loop of Ikappa B kinase', *The Journal of biological chemistry*, 275, (46), pp. 36062-6.
Karin, M. (2006) 'Nuclear factor-kappaB in cancer development and progression', *Nature*, 441, (7092), pp. 431-6.
Katayama, H., Ota, T., Jisaki, F., Ueda, Y., Tanaka, T., Odashima, S., Suzuki, F., Terada, Y. and Tatsuka, M. (1999) 'Mitotic kinase expression and colorectal cancer progression', *Journal of the National Cancer Institute*, 91, (13), pp. 1160-2.
Kauppinen, T. M. and Swanson, R. A. (2005) 'Poly(ADP-ribose) polymerase-1 promotes microglial activation, proliferation, and matrix metalloproteinase-9-mediated neuron death', *Journal of immunology*, 174, (4), pp. 2288-96.
Keen, N. and Taylor, S. (2004) 'Aurora-kinase inhibitors as anticancer agents', *Nature reviews. Cancer*, 4, (12), pp. 927-36.
Khachigian, L. M., Resnick, N., Gimbrone, M. A., Jr. and Collins, T. (1995) 'Nuclear factor-kappa B interacts functionally with the platelet-derived growth factor B-chain shear-stress response element in vascular endothelial cells exposed to fluid shear stress', *The Journal of clinical investigation*, 96, (2), pp. 1169-75.

Khanna, K. K. and Jackson, S. P. (2001) 'DNA double-strand breaks: signaling, repair and the cancer connection', *Nature genetics*, 27, (3), pp. 247-54.

Kharbanda, S., Pandey, P., Yamauchi, T., Kumar, S., Kaneki, M., Kumar, V., Bharti, A., Yuan, Z. M., Ghanem, L., Rana, A., Weichselbaum, R., Johnson, G. and Kufe, D. (2000) 'Activation of MEK kinase 1 by the c-Abl protein tyrosine kinase in response to DNA damage', *Molecular and cellular biology*, 20, (14), pp. 4979-89.

Kidokoro, T., Tanikawa, C., Furukawa, Y., Katagiri, T., Nakamura, Y. and Matsuda, K. (2008) 'CDC20, a potential cancer therapeutic target, is negatively regulated by p53', *Oncogene*, 27, (11), pp. 1562-71.

Kim, H. J., Hawke, N. and Baldwin, A. S. (2006) 'NF-kappaB and IKK as therapeutic targets in cancer', *Cell death and differentiation*, 13, (5), pp. 738-47.

Kim, J. M., Sohn, H. Y., Yoon, S. Y., Oh, J. H., Yang, J. O., Kim, J. H., Song, K. S., Rho, S. M., Yoo, H. S., Kim, Y. S., Kim, J. G. and Kim, N. S. (2005) 'Identification of gastric cancer-related genes using a cDNA microarray containing novel expressed sequence tags expressed in gastric cancer cells', *Clinical cancer research : an official journal of the American Association for Cancer Research*, 11, (2 Pt 1), pp. 473-82.

Klungland, A. and Lindahl, T. (1997) 'Second pathway for completion of human DNA base excision-repair: reconstitution with purified proteins and requirement for DNase IV (FEN1)', *The EMBO journal*, 16, (11), pp. 3341-8.

Knudson, A. G., Jr. (1971) 'Mutation and cancer: statistical study of retinoblastoma', *Proceedings of the National Academy of Sciences of the United States of America*, 68, (4), pp. 820-3.

Kontgen, F., Grumont, R. J., Strasser, A., Metcalf, D., Li, R., Tarlinton, D. and Gerondakis, S. (1995) 'Mice lacking the c-rel proto-oncogene exhibit defects in lymphocyte proliferation, humoral immunity, and interleukin-2 expression', *Genes & development*, 9, (16), pp. 1965-77.

Krappmann, D. and Scheidereit, C. (2005) 'A pervasive role of ubiquitin conjugation in activation and termination of IkappaB kinase pathways', *EMBO reports*, 6, (4), pp. 321-6.

Kraus, W. L. (2008) 'Transcriptional control by PARP-1: chromatin modulation, enhancer-binding, coregulation, and insulation', *Current opinion in cell biology*, 20, (3), pp. 294-302.

Kraus, W. L. and Lis, J. T. (2003) 'PARP goes transcription', *Cell*, 113, (6), pp. 677-83.

Kreuz, S., Siegmund, D., Scheurich, P. and Wajant, H. (2001) 'NF-kappaB inducers upregulate cFLIP, a cycloheximide-sensitive inhibitor of death receptor signaling', *Molecular and cellular biology*, 21, (12), pp. 3964-73.

Krishnakumar, R., Gamble, M. J., Frizzell, K. M., Berrocal, J. G., Kininis, M. and Kraus, W. L. (2008) 'Reciprocal binding of PARP-1 and histone H1 at promoters specifies transcriptional outcomes', *Science*, 319, (5864), pp. 819-21.

Krishnakumar, R. and Kraus, W. L. (2010) 'The PARP side of the nucleus: molecular actions, physiological outcomes, and clinical targets', *Molecular cell*, 39, (1), pp. 8-24.

Kroger, A., Koster, M., Schroeder, K., Hauser, H. and Mueller, P. P. (2002) 'Activities of IRF-1', *Journal of interferon & cytokine research : the official journal of the International Society for Interferon and Cytokine Research*, 22, (1), pp. 5-14.

Kuida, K., Zheng, T. S., Na, S., Kuan, C., Yang, D., Karasuyama, H., Rakic, P. and Flavell, R. A. (1996) 'Decreased apoptosis in the brain and premature lethality in CPP32-deficient mice', *Nature*, 384, (6607), pp. 368-72.

Kumar, A., Takada, Y., Boriek, A. M. and Aggarwal, B. B. (2004) 'Nuclear factor-kappaB: its role in health and disease', *Journal of molecular medicine*, 82, (7), pp. 434-48.

Kunsch, C. and Rosen, C. A. (1993) 'NF-kappa B subunit-specific regulation of the interleukin-8 promoter', *Molecular and cellular biology*, 13, (10), pp. 6137-46.

Kurosaki, T., Ushiro, H., Mitsuuchi, Y., Suzuki, S., Matsuda, M., Matsuda, Y., Katunuma, N., Kangawa, K., Matsuo, H., Hirose, T. and et al. (1987) 'Primary structure of human poly(ADP-ribose) synthetase as deduced from cDNA sequence', *The Journal of biological chemistry*, 262, (33), pp. 15990-7.

Kurz, E. U. and Lees-Miller, S. P. (2004) 'DNA damage-induced activation of ATM and ATM-dependent signaling pathways', *DNA repair*, 3, (8-9), pp. 889-900.

Lane, D. P. (1992) 'Cancer. p53, guardian of the genome', *Nature*, 358, (6381), pp. 15-6.

Langelier, M. F., Servent, K. M., Rogers, E. E. and Pascal, J. M. (2008) 'A third zinc-binding domain of human poly(ADP-ribose) polymerase-1 coordinates DNA-dependent enzyme activation', *The Journal of biological chemistry*, 283, (7), pp. 4105-14.

Lania, L., Majello, B. and De Luca, P. (1997) 'Transcriptional regulation by the Sp family proteins', *The international journal of biochemistry & cell biology*, 29, (12), pp. 1313-23.

Lavrik, O. I., Prasad, R., Sobol, R. W., Horton, J. K., Ackerman, E. J. and Wilson, S. H. (2001) 'Photoaffinity labeling of mouse fibroblast enzymes by a base excision repair intermediate.

Evidence for the role of poly(ADP-ribose) polymerase-1 in DNA repair', *The Journal of biological chemistry*, 276, (27), pp. 25541-8.

Le Page, C., Sanceau, J., Drapier, J. C. and Wietzerbin, J. (1998) 'Inhibitors of ADP-ribosylation impair inducible nitric oxide synthase gene transcription through inhibition of NF kappa B activation', *Biochemical and biophysical research communications*, 243, (2), pp. 451-7.

Lee, H. H., Dadgostar, H., Cheng, Q., Shu, J. and Cheng, G. (1999a) 'NF-kappaB-mediated up-regulation of Bcl-x and Bfl-1/A1 is required for CD40 survival signaling in B lymphocytes', *Proceedings of the National Academy of Sciences of the United States of America*, 96, (16), pp. 9136-41.

Lee, K. J., Lin, Y. F., Chou, H. Y., Yajima, H., Fattah, K. R., Lee, S. C. and Chen, B. P. (2011) 'Involvement of DNA-dependent protein kinase in normal cell cycle progression through mitosis', *The Journal of biological chemistry*, 286, (14), pp. 12796-802.

Lee, R. M., Gillet, G., Burnside, J., Thomas, S. J. and Neiman, P. (1999b) 'Role of Nr13 in regulation of programmed cell death in the bursa of Fabricius', *Genes & development*, 13, (6), pp. 718-28.

Lees-Miller, S. P., Godbout, R., Chan, D. W., Weinfeld, M., Day, R. S., 3rd, Barron, G. M. and Allalunis-Turner, J. (1995) 'Absence of p350 subunit of DNA-activated protein kinase from a radiosensitive human cell line', *Science*, 267, (5201), pp. 1183-5.

Lenormand, P., Brondello, J. M., Brunet, A. and Pouyssegur, J. (1998) 'Growth factor-induced p42/p44 MAPK nuclear translocation and retention requires both MAPK activation and neosynthesis of nuclear anchoring proteins', *The Journal of cell biology*, 142, (3), pp. 625-33.

Li, J., Wang, J., Nawaz, Z., Liu, J. M., Qin, J. and Wong, J. (2000) 'Both corepressor proteins SMRT and N-CoR exist in large protein complexes containing HDAC3', *The EMBO journal*, 19, (16), pp. 4342-50.

Li, Q., Lu, Q., Hwang, J. Y., Buscher, D., Lee, K. F., Izpisua-Belmonte, J. C. and Verma, I. M. (1999a) 'IKK1-deficient mice exhibit abnormal development of skin and skeleton', *Genes & development*, 13, (10), pp. 1322-8.

Li, Q., Van Antwerp, D., Mercurio, F., Lee, K. F. and Verma, I. M. (1999b) 'Severe liver degeneration in mice lacking the IkappaB kinase 2 gene', *Science*, 284, (5412), pp. 321-5.

Li, Z., Niu, J., Uwagawa, T., Peng, B. and Chiao, P. J. (2005) 'Function of polo-like kinase 3 in NF-kappaB-mediated proapoptotic response', *The Journal of biological chemistry*, 280, (17), pp. 16843-50.

Liang, M. C., Bardhan, S., Pace, E. A., Rosman, D., Beutler, J. A., Porco, J. A., Jr. and Gilmore, T. D. (2006) 'Inhibition of transcription factor NF-kappaB signaling proteins IKKbeta and p65 through specific cysteine residues by epoxyquinone A monomer: correlation with its anti-cancer cell growth activity', *Biochemical pharmacology*, 71, (5), pp. 634-45.

Libermann, T. A. and Baltimore, D. (1990) 'Activation of interleukin-6 gene expression through the NF-kappa B transcription factor', *Molecular and cellular biology*, 10, (5), pp. 2327-34.

Lindahl, T., Satoh, M. S., Poirier, G. G. and Klungland, A. (1995) 'Post-translational modification of poly(ADP-ribose) polymerase induced by DNA strand breaks', *Trends in biochemical sciences*, 20, (10), pp. 405-11.

Lindahl, T. and Wood, R. D. (1999) 'Quality control by DNA repair', *Science*, 286, (5446), pp. 1897-905.

Liu, L., Kwak, Y. T., Bex, F., Garcia-Martinez, L. F., Li, X. H., Meek, K., Lane, W. S. and Gaynor, R. B. (1998) 'DNA-dependent protein kinase phosphorylation of IkappaB alpha and IkappaB beta regulates NF-kappaB DNA binding properties', *Molecular and cellular biology*, 18, (7), pp. 4221-34.

Liu, L. F. and D'Arpa, P. (1992) 'Topoisomerase-targeting antitumor drugs: mechanisms of cytotoxicity and resistance', *Important advances in oncology*, pp. 79-89.

Liu, M., Sakamaki, T., Casimiro, M. C., Willmarth, N. E., Quong, A. A., Ju, X., Ojeifo, J., Jiao, X., Yeow, W. S., Katiyar, S., Shirley, L. A., Joyce, D., Lisanti, M. P., Albanese, C. and Pestell, R. G. (2010) 'The canonical NF-kappaB pathway governs mammary tumorigenesis in transgenic mice and tumor stem cell expansion', *Cancer research*, 70, (24), pp. 10464-73.

Lockett, K. L., Hall, M. C., Xu, J., Zheng, S. L., Berwick, M., Chuang, S. C., Clark, P. E., Cramer, S. D., Lohman, K. and Hu, J. J. (2004) 'The ADPRT V762A genetic variant contributes to prostate cancer susceptibility and deficient enzyme function', *Cancer research*, 64, (17), pp. 6344-8.

Loizou, J. I., El-Khamisy, S. F., Zlatanou, A., Moore, D. J., Chan, D. W., Qin, J., Sarno, S., Meggio, F., Pinna, L. A. and Caldecott, K. W. (2004) 'The protein kinase CK2 facilitates repair of chromosomal DNA single-strand breaks', *Cell*, 117, (1), pp. 17-28.

Lomax, M. E., Gulston, M. K. and O'Neill, P. (2002) 'Chemical aspects of clustered DNA damage induction by ionising radiation', *Radiation protection dosimetry*, 99, (1-4), pp. 63-8.

Lombardi, L., Ciana, P., Cappellini, C., Trecca, D., Guerrini, L., Migliazza, A., Maiolo, A. T. and Neri, A. (1995) 'Structural and functional characterization of the promoter regions of the NFKB2 gene', *Nucleic acids research*, 23, (12), pp. 2328-36.

Lopez-Guerra, M., Roue, G., Perez-Galan, P., Alonso, R., Villamor, N., Montserrat, E., Campo, E. and Colomer, D. (2009) 'p65 activity and ZAP-70 status predict the sensitivity of chronic lymphocytic leukemia cells to the selective IkappaB kinase inhibitor BMS-345541', *Clinical cancer research : an official journal of the American Association for Cancer Research,* 15, (8), pp. 2767-76.

Lord, C. J., Garrett, M. D. and Ashworth, A. (2006) 'Targeting the double-strand DNA break repair pathway as a therapeutic strategy', *Clinical cancer research : an official journal of the American Association for Cancer Research,* 12, (15), pp. 4463-8.

Loser, D. A., Shibata, A., Shibata, A. K., Woodbine, L. J., Jeggo, P. A. and Chalmers, A. J. (2010) 'Sensitization to radiation and alkylating agents by inhibitors of poly(ADP-ribose) polymerase is enhanced in cells deficient in DNA double-strand break repair', *Molecular cancer therapeutics,* 9, (6), pp. 1775-87.

Luque, I. and Gelinas, C. (1998) 'Distinct domains of IkappaBalpha regulate c-Rel in the cytoplasm and in the nucleus', *Molecular and cellular biology,* 18, (3), pp. 1213-24.

Lyu, Y. L., Kerrigan, J. E., Lin, C. P., Azarova, A. M., Tsai, Y. C., Ban, Y. and Liu, L. F. (2007) 'Topoisomerase IIbeta mediated DNA double-strand breaks: implications in doxorubicin cardiotoxicity and prevention by dexrazoxane', *Cancer research,* 67, (18), pp. 8839-46.

Mabley, J. G., Jagtap, P., Perretti, M., Getting, S. J., Salzman, A. L., Virag, L., Szabo, E., Soriano, F. G., Liaudet, L., Abdelkarim, G. E., Hasko, G., Marton, A., Southan, G. J. and Szabo, C. (2001) 'Anti-inflammatory effects of a novel, potent inhibitor of poly (ADP-ribose) polymerase', *Inflammation research : official journal of the European Histamine Research Society ... [et al.],* 50, (11), pp. 561-9.

Mabley, J. G., Pacher, P., Bai, P., Wallace, R., Goonesekera, S., Virag, L., Southan, G. J. and Szabo, C. (2004) 'Suppression of intestinal polyposis in Apcmin/+ mice by targeting the nitric oxide or poly(ADP-ribose) pathways', *Mutation research,* 548, (1-2), pp. 107-16.

Madhusoodhanan, R., Natarajan, M., Singh, J. V., Jamgade, A., Awasthi, V., Anant, S., Herman, T. S. and Aravindan, N. (2010) 'Effect of black raspberry extract in inhibiting NFkappa B dependent radioprotection in human breast cancer cells', *Nutrition and cancer,* 62, (1), pp. 93-104.

Mahadevan, N. R., Rodvold, J., Almanza, G., Perez, A. F., Wheeler, M. C. and Zanetti, M. (2011) 'ER stress drives Lipocalin 2 upregulation in prostate cancer cells in an NF-kappaB-dependent manner', *BMC cancer,* 11, pp. 229.

Majewski, P. M., Thurston, R. D., Ramalingam, R., Kiela, P. R. and Ghishan, F. K. (2010) 'Cooperative role of NF-{kappa}B and poly(ADP-ribose) polymerase 1 (PARP-1) in the TNF-induced inhibition of PHEX expression in osteoblasts', *The Journal of biological chemistry,* 285, (45), pp. 34828-38.

Martin-Oliva, D., Aguilar-Quesada, R., O'Valle, F., Munoz-Gamez, J. A., Martinez-Romero, R., Garcia Del Moral, R., Ruiz de Almodovar, J. M., Villuendas, R., Piris, M. A. and Oliver, F. J. (2006) 'Inhibition of poly(ADP-ribose) polymerase modulates tumor-related gene expression, including hypoxia-inducible factor-1 activation, during skin carcinogenesis', *Cancer research,* 66, (11), pp. 5744-56.

Martin-Oliva, D., O'Valle, F., Munoz-Gamez, J. A., Valenzuela, M. T., Nunez, M. I., Aguilar, M., Ruiz de Almodovar, J. M., Garcia del Moral, R. and Oliver, F. J. (2004) 'Crosstalk between PARP-1 and NF-kappaB modulates the promotion of skin neoplasia', *Oncogene,* 23, (31), pp. 5275-83.

Marumoto, T., Honda, S., Hara, T., Nitta, M., Hirota, T., Kohmura, E. and Saya, H. (2003) 'Aurora-A kinase maintains the fidelity of early and late mitotic events in HeLa cells', *The Journal of biological chemistry,* 278, (51), pp. 51786-95.

Mascaux, C., Iannino, N., Martin, B., Paesmans, M., Berghmans, T., Dusart, M., Haller, A., Lothaire, P., Meert, A. P., Noel, S., Lafitte, J. J. and Sculier, J. P. (2005) 'The role of RAS oncogene in survival of patients with lung cancer: a systematic review of the literature with meta-analysis', *British journal of cancer,* 92, (1), pp. 131-9.

Masson, M., Niedergang, C., Schreiber, V., Muller, S., Menissier-de Murcia, J. and de Murcia, G. (1998) 'XRCC1 is specifically associated with poly(ADP-ribose) polymerase and negatively regulates its activity following DNA damage', *Molecular and cellular biology,* 18, (6), pp. 3563-71.

Masutani, M., Nakagama, H. and Sugimura, T. (2005) 'Poly(ADP-ribosyl)ation in relation to cancer and autoimmune disease', *Cellular and molecular life sciences : CMLS,* 62, (7-8), pp. 769-83.

Matsuda, A., Suzuki, Y., Honda, G., Muramatsu, S., Matsuzaki, O., Nagano, Y., Doi, T., Shimotohno, K., Harada, T., Nishida, E., Hayashi, H. and Sugano, S. (2003) 'Large-scale identification and characterization of human genes that activate NF-kappaB and MAPK signaling pathways', *Oncogene,* 22, (21), pp. 3307-18.

Matsui, K., Fine, A., Zhu, B., Marshak-Rothstein, A. and Ju, S. T. (1998) 'Identification of two NF-kappa B sites in mouse CD95 ligand (Fas ligand) promoter: functional analysis in T cell hybridoma', *Journal of immunology,* 161, (7), pp. 3469-73.

Matsumoto, Y., Kim, K., Hurwitz, J., Gary, R., Levin, D. S., Tomkinson, A. E. and Park, M. S. (1999) 'Reconstitution of proliferating cell nuclear antigen-dependent repair of apurinic/apyrimidinic sites with purified human proteins', *The Journal of biological chemistry*, 274, (47), pp. 33703-8.

May, M. J., D'Acquisto, F., Madge, L. A., Glockner, J., Pober, J. S. and Ghosh, S. (2000) 'Selective inhibition of NF-kappaB activation by a peptide that blocks the interaction of NEMO with the IkappaB kinase complex', *Science*, 289, (5484), pp. 1550-4.

Mazen, A., Menissier-de Murcia, J., Molinete, M., Simonin, F., Gradwohl, G., Poirier, G. and de Murcia, G. (1989) 'Poly(ADP-ribose)polymerase: a novel finger protein', *Nucleic acids research*, 17, (12), pp. 4689-98.

McCabe, N., Turner, N. C., Lord, C. J., Kluzek, K., Bialkowska, A., Swift, S., Giavara, S., O'Connor, M. J., Tutt, A. N., Zdzienicka, M. Z., Smith, G. C. and Ashworth, A. (2006) 'Deficiency in the repair of DNA damage by homologous recombination and sensitivity to poly(ADP-ribose) polymerase inhibition', *Cancer research*, 66, (16), pp. 8109-15.

Melvin, A., Mudie, S. and Rocha, S. (2011) 'Further insights into the mechanism of hypoxia-induced NFkappaB. [corrected]', *Cell cycle*, 10, (6), pp. 879-82.

Miagkov, A. V., Kovalenko, D. V., Brown, C. E., Didsbury, J. R., Cogswell, J. P., Stimpson, S. A., Baldwin, A. S. and Makarov, S. S. (1998) 'NF-kappaB activation provides the potential link between inflammation and hyperplasia in the arthritic joint', *Proceedings of the National Academy of Sciences of the United States of America*, 95, (23), pp. 13859-64.

Mineva, N. D., Wang, X., Yang, S., Ying, H., Xiao, Z. X., Holick, M. F. and Sonenshein, G. E. (2009) 'Inhibition of RelB by 1,25-dihydroxyvitamin D3 promotes sensitivity of breast cancer cells to radiation', *Journal of cellular physiology*, 220, (3), pp. 593-9.

Mitchell, J., Smith, G. C. and Curtin, N. J. (2009) 'Poly(ADP-Ribose) polymerase-1 and DNA-dependent protein kinase have equivalent roles in double strand break repair following ionizing radiation', *International journal of radiation oncology, biology, physics*, 75, (5), pp. 1520-7.

Monaco, L., Kolthur-Seetharam, U., Loury, R., Murcia, J. M., de Murcia, G. and Sassone-Corsi, P. (2005) 'Inhibition of Aurora-B kinase activity by poly(ADP-ribosyl)ation in response to DNA damage', *Proceedings of the National Academy of Sciences of the United States of America*, 102, (40), pp. 14244-8.

Mondal, G., Sengupta, S., Panda, C. K., Gollin, S. M., Saunders, W. S. and Roychoudhury, S. (2007) 'Overexpression of Cdc20 leads to impairment of the spindle assembly checkpoint and aneuploidization in oral cancer', *Carcinogenesis*, 28, (1), pp. 81-92.

Moon, M. R., Parikh, A. A., Pritts, T. A., Fischer, J. E., Cottongim, S., Szabo, C., Salzman, A. L. and Hasselgren, P. O. (1999) 'Complement component C3 production in IL-1beta-stimulated human intestinal epithelial cells is blocked by NF-kappaB inhibitors and by transfection with ser 32/36 mutant IkappaBalpha', *The Journal of surgical research*, 82, (1), pp. 48-55.

Moreno, V., Gemignani, F., Landi, S., Gioia-Patricola, L., Chabrier, A., Blanco, I., Gonzalez, S., Guino, E., Capella, G. and Canzian, F. (2006) 'Polymorphisms in genes of nucleotide and base excision repair: risk and prognosis of colorectal cancer', *Clinical cancer research : an official journal of the American Association for Cancer Research*, 12, (7 Pt 1), pp. 2101-8.

Mori, N., Yamada, Y., Ikeda, S., Yamasaki, Y., Tsukasaki, K., Tanaka, Y., Tomonaga, M., Yamamoto, N. and Fujii, M. (2002) 'Bay 11-7082 inhibits transcription factor NF-kappaB and induces apoptosis of HTLV-I-infected T-cell lines and primary adult T-cell leukemia cells', *Blood*, 100, (5), pp. 1828-34.

Moses, K., Willmore, E., Harris, A. L. and Durkacz, B. W. (1990) 'Correlation of enhanced 6-mercaptopurine cytotoxicity with increased phosphoribosylpyrophosphate levels in Chinese hamster ovary cells treated with 3-aminobenzamide', *Cancer research*, 50, (7), pp. 1992-6.

Mulligan EA, Hunter JE, Baird AEG, Elliott SL, Summerfield GP, Hamlen K, Veuger, S. J., Durkacz, B. W. and Willmore, E. (2010) 'Relationships between aberrant activity of the NF-kB subunits and outcome in chronic lymphocytic leukaemia:the dual role of DNA damage sensor kinases.', *Blood*, 116, pp. 1477.

Munoz-Gamez, J. A., Martin-Oliva, D., Aguilar-Quesada, R., Canuelo, A., Nunez, M. I., Valenzuela, M. T., Ruiz de Almodovar, J. M., De Murcia, G. and Oliver, F. J. (2005) 'PARP inhibition sensitizes p53-deficient breast cancer cells to doxorubicin-induced apoptosis', *The Biochemical journal*, 386, (Pt 1), pp. 119-25.

Musacchio, A. and Salmon, E. D. (2007) 'The spindle-assembly checkpoint in space and time', *Nature reviews. Molecular cell biology*, 8, (5), pp. 379-93.

Nakajima, H., Nagaso, H., Kakui, N., Ishikawa, M., Hiranuma, T. and Hoshiko, S. (2004) 'Critical role of the automodification of poly(ADP-ribose) polymerase-1 in nuclear factor-kappaB-dependent gene expression in primary cultured mouse glial cells', *The Journal of biological chemistry*, 279, (41), pp. 42774-86.

Nakshatri, H., Bhat-Nakshatri, P., Martin, D. A., Goulet, R. J., Jr. and Sledge, G. W., Jr. (1997) 'Constitutive activation of NF-kappaB during progression of breast cancer to hormone-independent growth', *Molecular and cellular biology*, 17, (7), pp. 3629-39.

Nelson, D. E., Ihekwaba, A. E., Elliott, M., Johnson, J. R., Gibney, C. A., Foreman, B. E., Nelson, G., See, V., Horton, C. A., Spiller, D. G., Edwards, S. W., McDowell, H. P., Unitt, J. F., Sullivan, E., Grimley, R., Benson, N., Broomhead, D., Kell, D. B. and White, M. R. (2004) 'Oscillations in NF-kappaB signaling control the dynamics of gene expression', *Science*, 306, (5696), pp. 704-8.

Neri, A., Chang, C. C., Lombardi, L., Salina, M., Corradini, P., Maiolo, A. T., Chaganti, R. S. and Dalla-Favera, R. (1991) 'B cell lymphoma-associated chromosomal translocation involves candidate oncogene lyt-10, homologous to NF-kappa B p50', *Cell*, 67, (6), pp. 1075-87.

Newlands, E. S., Stevens, M. F., Wedge, S. R., Wheelhouse, R. T. and Brock, C. (1997) 'Temozolomide: a review of its discovery, chemical properties, pre-clinical development and clinical trials', *Cancer treatment reviews*, 23, (1), pp. 35-61.

Nicholson, D. W. and Thornberry, N. A. (1997) 'Caspases: killer proteases', *Trends in biochemical sciences*, 22, (8), pp. 299-306.

Niculescu, A. B., 3rd, Chen, X., Smeets, M., Hengst, L., Prives, C. and Reed, S. I. (1998) 'Effects of p21(Cip1/Waf1) at both the G1/S and the G2/M cell cycle transitions: pRb is a critical determinant in blocking DNA replication and in preventing endoreduplication', *Molecular and cellular biology*, 18, (1), pp. 629-43.

Nie, J., Sakamoto, S., Song, D., Qu, Z., Ota, K. and Taniguchi, T. (1998) 'Interaction of Oct-1 and automodification domain of poly(ADP-ribose) synthetase', *FEBS letters*, 424, (1-2), pp. 27-32.

Ning, Y., Riggins, R. B., Mulla, J. E., Chung, H., Zwart, A. and Clarke, R. (2010) 'IFNgamma restores breast cancer sensitivity to fulvestrant by regulating STAT1, IFN regulatory factor 1, NF-kappaB, BCL2 family members, and signaling to caspase-dependent apoptosis', *Molecular cancer therapeutics*, 9, (5), pp. 1274-85.

Nishizuka, Y., Ueda, K., Nakazawa, K. and Hayaishi, O. (1967) 'Studies on the polymer of adenosine diphosphate ribose. I. Enzymic formation from nicotinamide adenine dinuclotide in mammalian nuclei', *The Journal of biological chemistry*, 242, (13), pp. 3164-71.

Nomura, N., Takahashi, M., Matsui, M., Ishii, S., Date, T., Sasamoto, S. and Ishizaki, R. (1988) 'Isolation of human cDNA clones of myb-related genes, A-myb and B-myb', *Nucleic acids research*, 16, (23), pp. 11075-89.

Nosho, K., Yamamoto, H., Mikami, M., Taniguchi, H., Takahashi, T., Adachi, Y., Imamura, A., Imai, K. and Shinomura, Y. (2006) 'Overexpression of poly(ADP-ribose) polymerase-1 (PARP-1) in the early stage of colorectal carcinogenesis', *European journal of cancer*, 42, (14), pp. 2374-81.

O'Shea, J. M. and Perkins, N. D. (2010) 'Thr435 phosphorylation regulates RelA (p65) NF-kappaB subunit transactivation', *The Biochemical journal*, 426, (3), pp. 345-54.

Ogorek, B. and Bryant, P. E. (1985a) 'Repair of DNA single-strand breaks in X-irradiated yeast. I. Use of the DNA-unwinding method to measure DNA strand breaks', *Mutation research*, 146, (1), pp. 55-61.

Ogorek, B. and Bryant, P. E. (1985b) 'Repair of DNA single-strand breaks in X-irradiated yeast. II. Kinetics of repair as measured by the DNA-unwinding method', *Mutation research*, 146, (1), pp. 63-70.

Oh, U., McCormick, M. J., Datta, D., Turner, R. V., Bobb, K., Monie, D. D., Sliskovic, D. R., Tanaka, Y., Zhang, J., Meshulam, J. and Jacobson, S. (2011) 'Inhibition of immune activation by a novel nuclear factor-kappa B inhibitor in HTLV-I-associated neurologic disease', *Blood*, 117, (12), pp. 3363-9.

Ohanna, M., Giuliano, S., Bonet, C., Imbert, V., Hofman, V., Zangari, J., Bille, K., Robert, C., Bressac-de Paillerets, B., Hofman, P., Rocchi, S., Peyron, J. F., Lacour, J. P., Ballotti, R. and Bertolotto, C. (2011) 'Senescent cells develop a PARP-1 and nuclear factor-{kappa}B-associated secretome (PNAS)', *Genes & development*, 25, (12), pp. 1245-61.

Okano, S., Lan, L., Caldecott, K. W., Mori, T. and Yasui, A. (2003) 'Spatial and temporal cellular responses to single-strand breaks in human cells', *Molecular and cellular biology*, 23, (11), pp. 3974-81.

Olabisi, O. A., Soto-Nieves, N., Nieves, E., Yang, T. T., Yang, X., Yu, R. Y., Suk, H. Y., Macian, F. and Chow, C. W. (2008) 'Regulation of transcription factor NFAT by ADP-ribosylation', *Molecular and cellular biology*, 28, (9), pp. 2860-71.

Oliver, F. J., Menissier-de Murcia, J. and de Murcia, G. (1999a) 'Poly(ADP-ribose) polymerase in the cellular response to DNA damage, apoptosis, and disease', *American journal of human genetics*, 64, (5), pp. 1282-8.

Oliver, F. J., Menissier-de Murcia, J., Nacci, C., Decker, P., Andriantsitohaina, R., Muller, S., de la Rubia, G., Stoclet, J. C. and de Murcia, G. (1999b) 'Resistance to endotoxic shock as a

consequence of defective NF-kappaB activation in poly (ADP-ribose) polymerase-1 deficient mice', *The EMBO journal*, 18, (16), pp. 4446-54.

Osborn, L., Kunkel, S. and Nabel, G. J. (1989) 'Tumor necrosis factor alpha and interleukin 1 stimulate the human immunodeficiency virus enhancer by activation of the nuclear factor kappa B', *Proceedings of the National Academy of Sciences of the United States of America*, 86, (7), pp. 2336-40.

Ota, T., Suto, S., Katayama, H., Han, Z. B., Suzuki, F., Maeda, M., Tanino, M., Terada, Y. and Tatsuka, M. (2002) 'Increased mitotic phosphorylation of histone H3 attributable to AIM-1/Aurora-B overexpression contributes to chromosome number instability', *Cancer research*, 62, (18), pp. 5168-77.

Oumouna-Benachour, K., Hans, C. P., Suzuki, Y., Naura, A., Datta, R., Belmadani, S., Fallon, K., Woods, C. and Boulares, A. H. (2007) 'Poly(ADP-ribose) polymerase inhibition reduces atherosclerotic plaque size and promotes factors of plaque stability in apolipoprotein E-deficient mice: effects on macrophage recruitment, nuclear factor-kappaB nuclear translocation, and foam cell death', *Circulation*, 115, (18), pp. 2442-50.

Ozaki, T. and Nakagawara, A. (2011) 'p53: the attractive tumor suppressor in the cancer research field', *Journal of biomedicine & biotechnology*, 2011, pp. 603925.

Pacifico, F., Paolillo, M., Chiappetta, G., Crescenzi, E., Arena, S., Scaloni, A., Monaco, M., Vascotto, C., Tell, G., Formisano, S. and Leonardi, A. (2007) 'RbAp48 is a target of nuclear factor-kappaB activity in thyroid cancer', *The Journal of clinical endocrinology and metabolism*, 92, (4), pp. 1458-66.

Pahl, H. L. (1999) 'Activators and target genes of Rel/NF-kappaB transcription factors', *Oncogene*, 18, (49), pp. 6853-66.

Panta, G. R., Kaur, S., Cavin, L. G., Cortes, M. L., Mercurio, F., Lothstein, L., Sweatman, T. W., Israel, M. and Arsura, M. (2004) 'ATM and the catalytic subunit of DNA-dependent protein kinase activate NF-kappaB through a common MEK/extracellular signal-regulated kinase/p90(rsk) signaling pathway in response to distinct forms of DNA damage', *Molecular and cellular biology*, 24, (5), pp. 1823-35.

Pasparakis, M., Luedde, T. and Schmidt-Supprian, M. (2006) 'Dissection of the NF-kappaB signalling cascade in transgenic and knockout mice', *Cell death and differentiation*, 13, (5), pp. 861-72.

Pavri, R., Lewis, B., Kim, T. K., Dilworth, F. J., Erdjument-Bromage, H., Tempst, P., de Murcia, G., Evans, R., Chambon, P. and Reinberg, D. (2005) 'PARP-1 determines specificity in a retinoid signaling pathway via direct modulation of mediator', *Molecular cell*, 18, (1), pp. 83-96.

Perissi, V., Aggarwal, A., Glass, C. K., Rose, D. W. and Rosenfeld, M. G. (2004) 'A corepressor/coactivator exchange complex required for transcriptional activation by nuclear receptors and other regulated transcription factors', *Cell*, 116, (4), pp. 511-26.

Perkins, N. D. (2003) 'Oncogenes, tumor suppressors and p52 NF-kappaB', *Oncogene*, 22, (48), pp. 7553-6.

Perkins, N. D. (2006) 'Post-translational modifications regulating the activity and function of the nuclear factor kappa B pathway', *Oncogene*, 25, (51), pp. 6717-30.

Perkins, N. D. (2007) 'Integrating cell-signalling pathways with NF-kappaB and IKK function', *Nature reviews. Molecular cell biology*, 8, (1), pp. 49-62.

Perkins, N. D. and Gilmore, T. D. (2006) 'Good cop, bad cop: the different faces of NF-kappaB', *Cell death and differentiation*, 13, (5), pp. 759-72.

Pierani, A., Heguy, A., Fujii, H. and Roeder, R. G. (1990) 'Activation of octamer-containing promoters by either octamer-binding transcription factor 1 (OTF-1) or OTF-2 and requirement of an additional B-cell-specific component for optimal transcription of immunoglobulin promoters', *Molecular and cellular biology*, 10, (12), pp. 6204-15.

Pizzoferrato, E., Liu, Y., Gambotto, A., Armstrong, M. J., Stang, M. T., Gooding, W. E., Alber, S. M., Shand, S. H., Watkins, S. C., Storkus, W. J. and Yim, J. H. (2004) 'Ectopic expression of interferon regulatory factor-1 promotes human breast cancer cell death and results in reduced expression of survivin', *Cancer research*, 64, (22), pp. 8381-8.

Plasterk, R. H. (2002) 'RNA silencing: the genome's immune system', *Science*, 296, (5571), pp. 1263-5.

Plummer, E. R., Middleton, M. R., Jones, C., Olsen, A., Hickson, I., McHugh, P., Margison, G. P., McGown, G., Thorncroft, M., Watson, A. J., Boddy, A. V., Calvert, A. H., Harris, A. L., Newell, D. R. and Curtin, N. J. (2005) 'Temozolomide pharmacodynamics in patients with metastatic melanoma: dna damage and activity of repair enzymes O6-alkylguanine alkyltransferase and poly(ADP-ribose) polymerase-1', *Clinical cancer research : an official journal of the American Association for Cancer Research*, 11, (9), pp. 3402-9.

Plummer, R. (2010) 'Perspective on the pipeline of drugs being developed with modulation of DNA damage as a target', *Clinical cancer research : an official journal of the American Association for Cancer Research*, 16, (18), pp. 4527-31.

Plummer, R., Jones, C., Middleton, M., Wilson, R., Evans, J., Olsen, A., Curtin, N., Boddy, A., McHugh, P., Newell, D., Harris, A., Johnson, P., Steinfeldt, H., Dewji, R., Wang, D., Robson, L. and Calvert, H. (2008) 'Phase I study of the poly(ADP-ribose) polymerase inhibitor, AG014699, in combination with temozolomide in patients with advanced solid tumors', *Clinical cancer research : an official journal of the American Association for Cancer Research,* 14, (23), pp. 7917-23.

Porter, A. G. and Janicke, R. U. (1999) 'Emerging roles of caspase-3 in apoptosis', *Cell death and differentiation,* 6, (2), pp. 99-104.

Prasad, R., Lavrik, O. I., Kim, S. J., Kedar, P., Yang, X. P., Vande Berg, B. J. and Wilson, S. H. (2001) 'DNA polymerase beta -mediated long patch base excision repair. Poly(ADP-ribose)polymerase-1 stimulates strand displacement DNA synthesis', *The Journal of biological chemistry,* 276, (35), pp. 32411-4.

Prasad, S., Ravindran, J. and Aggarwal, B. B. (2010) 'NF-kappaB and cancer: how intimate is this relationship', *Molecular and cellular biochemistry,* 336, (1-2), pp. 25-37.

Purnell, M. R. and Whish, W. J. (1980) 'Novel inhibitors of poly(ADP-ribose) synthetase', *The Biochemical journal,* 185, (3), pp. 775-7.

Quemener, V., Moulinoux, J. P., Khan, N. A. and Seiler, N. (1990) 'Effects of a series of homologous alpha,omega-dimethylaminoalkanes on cell proliferation: binding and uptake of putrescine by a human glioblastoma cell line (U251) in culture', *Biology of the cell / under the auspices of the European Cell Biology Organization,* 70, (3), pp. 133-7.

Ramadoss, S., Li, J., Ding, X., Al Hezaimi, K. and Wang, C. Y. (2011) 'Transducin beta-like protein 1 recruits nuclear factor kappaB to the target gene promoter for transcriptional activation', *Molecular and cellular biology,* 31, (5), pp. 924-34.

Raschella, G., Cesi, V., Amendola, R., Negroni, A., Tanno, B., Altavista, P., Tonini, G. P., De Bernardi, B. and Calabretta, B. (1999) 'Expression of B-myb in neuroblastoma tumors is a poor prognostic factor independent from MYCN amplification', *Cancer research,* 59, (14), pp. 3365-8.

Ravi, R., Mookerjee, B., van Hensbergen, Y., Bedi, G. C., Giordano, A., El-Deiry, W. S., Fuchs, E. J. and Bedi, A. (1998) 'p53-mediated repression of nuclear factor-kappaB RelA via the transcriptional integrator p300', *Cancer research,* 58, (20), pp. 4531-6.

Rayet, B. and Gelinas, C. (1999) 'Aberrant rel/nfkb genes and activity in human cancer', *Oncogene,* 18, (49), pp. 6938-47.

Realini, C. A. and Althaus, F. R. (1992) 'Histone shuttling by poly(ADP-ribosylation)', *The Journal of biological chemistry,* 267, (26), pp. 18858-65.

Reeder, R. H., Ueda, K., Honjo, T., Nishizuka, Y. and Hayaishi, O. (1967) 'Studies on the polymer of adenosine diphosphate ribose. II. Characterization of the polymer', *The Journal of biological chemistry,* 242, (13), pp. 3172-9.

Renner, F., Moreno, R. and Schmitz, M. L. (2010) 'SUMOylation-dependent localization of IKKepsilon in PML nuclear bodies is essential for protection against DNA-damage-triggered cell death', *Molecular cell,* 37, (4), pp. 503-15.

Ricca, A., Biroccio, A., Del Bufalo, D., Mackay, A. R., Santoni, A. and Cippitelli, M. (2000) 'bcl-2 over-expression enhances NF-kappaB activity and induces mmp-9 transcription in human MCF7(ADR) breast-cancer cells', *International journal of cancer. Journal international du cancer,* 86, (2), pp. 188-96.

Rius, J., Guma, M., Schachtrup, C., Akassoglou, K., Zinkernagel, A. S., Nizet, V., Johnson, R. S., Haddad, G. G. and Karin, M. (2008) 'NF-kappaB links innate immunity to the hypoxic response through transcriptional regulation of HIF-1alpha', *Nature,* 453, (7196), pp. 807-11.

Robinson, C. M., Hale, P. T. and Carlin, J. M. (2006) 'NF-kappa B activation contributes to indoleamine dioxygenase transcriptional synergy induced by IFN-gamma and tumor necrosis factor-alpha', *Cytokine,* 35, (1-2), pp. 53-61.

Robson, C. N. and Hickson, I. D. (1991) 'Isolation of cDNA clones encoding a human apurinic/apyrimidinic endonuclease that corrects DNA repair and mutagenesis defects in E. coli xth (exonuclease III) mutants', *Nucleic acids research,* 19, (20), pp. 5519-23.

Rocha, S., Garrett, M. D., Campbell, K. J., Schumm, K. and Perkins, N. D. (2005) 'Regulation of NF-kappaB and p53 through activation of ATR and Chk1 by the ARF tumour suppressor', *The EMBO journal,* 24, (6), pp. 1157-69.

Rocha, S., Martin, A. M., Meek, D. W. and Perkins, N. D. (2003) 'p53 represses cyclin D1 transcription through down regulation of Bcl-3 and inducing increased association of the p52 NF-kappaB subunit with histone deacetylase 1', *Molecular and cellular biology,* 23, (13), pp. 4713-27.

Roitt, I. M. (1956) 'The inhibition of carbohydrate metabolism in ascites-tumour cells by ethyleneimines', *The Biochemical journal,* 63, (2), pp. 300-7.

Rosenwald, A., Wright, G., Chan, W. C., Connors, J. M., Campo, E., Fisher, R. I., Gascoyne, R. D., Muller-Hermelink, H. K., Smeland, E. B., Giltnane, J. M., Hurt, E. M., Zhao, H., Averett, L.,

Yang, L., Wilson, W. H., Jaffe, E. S., Simon, R., Klausner, R. D., Powell, J., Duffey, P. L., Longo, D. L., Greiner, T. C., Weisenburger, D. D., Sanger, W. G., Dave, B. J., Lynch, J. C., Vose, J., Armitage, J. O., Montserrat, E., Lopez-Guillermo, A., Grogan, T. M., Miller, T. P., LeBlanc, M., Ott, G., Kvaloy, S., Delabie, J., Holte, H., Krajci, P., Stokke, T. and Staudt, L. M. (2002) 'The use of molecular profiling to predict survival after chemotherapy for diffuse large-B-cell lymphoma', *The New England journal of medicine*, 346, (25), pp. 1937-47.

Rosenwald, A., Wright, G., Leroy, K., Yu, X., Gaulard, P., Gascoyne, R. D., Chan, W. C., Zhao, T., Haioun, C., Greiner, T. C., Weisenburger, D. D., Lynch, J. C., Vose, J., Armitage, J. O., Smeland, E. B., Kvaloy, S., Holte, H., Delabie, J., Campo, E., Montserrat, E., Lopez-Guillermo, A., Ott, G., Muller-Hermelink, H. K., Connors, J. M., Braziel, R., Grogan, T. M., Fisher, R. I., Miller, T. P., LeBlanc, M., Chiorazzi, M., Zhao, H., Yang, L., Powell, J., Wilson, W. H., Jaffe, E. S., Simon, R., Klausner, R. D. and Staudt, L. M. (2003) 'Molecular diagnosis of primary mediastinal B cell lymphoma identifies a clinically favorable subgroup of diffuse large B cell lymphoma related to Hodgkin lymphoma', *The Journal of experimental medicine*, 198, (6), pp. 851-62.

Rosenzweig, K. E., Youmell, M. B., Palayoor, S. T. and Price, B. D. (1997) 'Radiosensitization of human tumor cells by the phosphatidylinositol3-kinase inhibitors wortmannin and LY294002 correlates with inhibition of DNA-dependent protein kinase and prolonged G2-M delay', *Clinical cancer research : an official journal of the American Association for Cancer Research*, 3, (7), pp. 1149-56.

Rudolph, D., Yeh, W. C., Wakeham, A., Rudolph, B., Nallainathan, D., Potter, J., Elia, A. J. and Mak, T. W. (2000) 'Severe liver degeneration and lack of NF-kappaB activation in NEMO/IKKgamma-deficient mice', *Genes & development*, 14, (7), pp. 854-62.

Russo, S. M., Tepper, J. E., Baldwin, A. S., Jr., Liu, R., Adams, J., Elliott, P. and Cusack, J. C., Jr. (2001) 'Enhancement of radiosensitivity by proteasome inhibition: implications for a role of NF-kappaB', *International journal of radiation oncology, biology, physics*, 50, (1), pp. 183-93.

Ryan, K. M., Ernst, M. K., Rice, N. R. and Vousden, K. H. (2000) 'Role of NF-kappaB in p53-mediated programmed cell death', *Nature*, 404, (6780), pp. 892-7.

Ryseck, R. P., Weih, F., Carrasco, D. and Bravo, R. (1996) 'RelB, a member of the Rel/NF-kappa B family of transcription factors', *Brazilian journal of medical and biological research = Revista brasileira de pesquisas medicas e biologicas / Sociedade Brasileira de Biofisica ... [et al.]*, 29, (7), pp. 895-903.

Saccani, S., Marazzi, I., Beg, A. A. and Natoli, G. (2004) 'Degradation of promoter-bound p65/RelA is essential for the prompt termination of the nuclear factor kappaB response', *The Journal of experimental medicine*, 200, (1), pp. 107-13.

Sahijdak, W. M., Yang, C. R., Zuckerman, J. S., Meyers, M. and Boothman, D. A. (1994) 'Alterations in transcription factor binding in radioresistant human melanoma cells after ionizing radiation', *Radiation research*, 138, (1 Suppl), pp. S47-51.

Saiki, R. K., Walsh, P. S., Levenson, C. H. and Erlich, H. A. (1989) 'Genetic analysis of amplified DNA with immobilized sequence-specific oligonucleotide probes', *Proceedings of the National Academy of Sciences of the United States of America*, 86, (16), pp. 6230-4.

Sak, S. C., Harnden, P., Johnston, C. F., Paul, A. B. and Kiltie, A. E. (2005) 'APE1 and XRCC1 protein expression levels predict cancer-specific survival following radical radiotherapy in bladder cancer', *Clinical cancer research : an official journal of the American Association for Cancer Research*, 11, (17), pp. 6205-11.

Sakakura, C., Hagiwara, A., Yasuoka, R., Fujita, Y., Nakanishi, M., Masuda, K., Shimomura, K., Nakamura, Y., Inazawa, J., Abe, T. and Yamagishi, H. (2001) 'Tumour-amplified kinase BTAK is amplified and overexpressed in gastric cancers with possible involvement in aneuploid formation', *British journal of cancer*, 84, (6), pp. 824-31.

Sancar, A., Lindsey-Boltz, L. A., Unsal-Kacmaz, K. and Linn, S. (2004) 'Molecular mechanisms of mammalian DNA repair and the DNA damage checkpoints', *Annual review of biochemistry*, 73, pp. 39-85.

Sanceau, J., Hiscott, J., Delattre, O. and Wietzerbin, J. (2000) 'IFN-beta induces serine phosphorylation of Stat-1 in Ewing's sarcoma cells and mediates apoptosis via induction of IRF-1 and activation of caspase-7', *Oncogene*, 19, (30), pp. 3372-83.

Sanceau, J., Kaisho, T., Hirano, T. and Wietzerbin, J. (1995) 'Triggering of the human interleukin-6 gene by interferon-gamma and tumor necrosis factor-alpha in monocytic cells involves cooperation between interferon regulatory factor-1, NF kappa B, and Sp1 transcription factors', *The Journal of biological chemistry*, 270, (46), pp. 27920-31.

Satoh, M. S., Poirier, G. G. and Lindahl, T. (1994) 'Dual function for poly(ADP-ribose) synthesis in response to DNA strand breakage', *Biochemistry*, 33, (23), pp. 7099-106.

Saxena, A., Saffery, R., Wong, L. H., Kalitsis, P. and Choo, K. H. (2002a) 'Centromere proteins Cenpa, Cenpb, and Bub3 interact with poly(ADP-ribose) polymerase-1 protein and are poly(ADP-ribosyl)ated', *The Journal of biological chemistry*, 277, (30), pp. 26921-6.

Saxena, A., Wong, L. H., Kalitsis, P., Earle, E., Shaffer, L. G. and Choo, K. H. (2002b) 'Poly(ADP-ribose) polymerase 2 localizes to mammalian active centromeres and interacts with PARP-1, Cenpa, Cenpb and Bub3, but not Cenpc', *Human molecular genetics*, 11, (19), pp. 2319-29.

Schauvliege, R., Vanrobaeys, J., Schotte, P. and Beyaert, R. (2002) 'Caspase-11 gene expression in response to lipopolysaccharide and interferon-gamma requires nuclear factor-kappa B and signal transducer and activator of transcription (STAT) 1', *The Journal of biological chemistry*, 277, (44), pp. 41624-30.

Scheidereit, C. (2006) 'IkappaB kinase complexes: gateways to NF-kappaB activation and transcription', *Oncogene*, 25, (51), pp. 6685-705.

Schreiber, J., Jenner, R. G., Murray, H. L., Gerber, G. K., Gifford, D. K. and Young, R. A. (2006a) 'Coordinated binding of NF-kappaB family members in the response of human cells to lipopolysaccharide', *Proceedings of the National Academy of Sciences of the United States of America*, 103, (15), pp. 5899-904.

Schreiber, V., Ame, J. C., Dolle, P., Schultz, I., Rinaldi, B., Fraulob, V., Menissier-de Murcia, J. and de Murcia, G. (2002) 'Poly(ADP-ribose) polymerase-2 (PARP-2) is required for efficient base excision DNA repair in association with PARP-1 and XRCC1', *The Journal of biological chemistry*, 277, (25), pp. 23028-36.

Schreiber, V., Dantzer, F., Ame, J. C. and de Murcia, G. (2006b) 'Poly(ADP-ribose): novel functions for an old molecule', *Nature reviews. Molecular cell biology*, 7, (7), pp. 517-28.

Schreiber, V., Molinete, M., Boeuf, H., de Murcia, G. and Menissier-de Murcia, J. (1992) 'The human poly(ADP-ribose) polymerase nuclear localization signal is a bipartite element functionally separate from DNA binding and catalytic activity', *The EMBO journal*, 11, (9), pp. 3263-9.

Schwenzer, R., Siemienski, K., Liptay, S., Schubert, G., Peters, N., Scheurich, P., Schmid, R. M. and Wajant, H. (1999) 'The human tumor necrosis factor (TNF) receptor-associated factor 1 gene (TRAF1) is up-regulated by cytokines of the TNF ligand family and modulates TNF-induced activation of NF-kappaB and c-Jun N-terminal kinase', *The Journal of biological chemistry*, 274, (27), pp. 19368-74.

Sen, R. and Baltimore, D. (1986) 'Multiple nuclear factors interact with the immunoglobulin enhancer sequences', *Cell*, 46, (5), pp. 705-16.

Sha, W. C., Liou, H. C., Tuomanen, E. I. and Baltimore, D. (1995) 'Targeted disruption of the p50 subunit of NF-kappa B leads to multifocal defects in immune responses', *Cell*, 80, (2), pp. 321-30.

Shakhov, A. N., Collart, M. A., Vassalli, P., Nedospasov, S. A. and Jongeneel, C. V. (1990) 'Kappa B-type enhancers are involved in lipopolysaccharide-mediated transcriptional activation of the tumor necrosis factor alpha gene in primary macrophages', *The Journal of experimental medicine*, 171, (1), pp. 35-47.

Shall, S. (1975) 'Proceedings: Experimental manipulation of the specific activity of poly(ADP-ribose) polymerase', *Journal of biochemistry*, 77, (1?), pp. 2p.

Shang, Z. F., Huang, B., Xu, Q. Z., Zhang, S. M., Fan, R., Liu, X. D., Wang, Y. and Zhou, P. K. (2010) 'Inactivation of DNA-dependent protein kinase leads to spindle disruption and mitotic catastrophe with attenuated checkpoint protein 2 Phosphorylation in response to DNA damage', *Cancer research*, 70, (9), pp. 3657-66.

Shiloh, Y. (2003) 'ATM and related protein kinases: safeguarding genome integrity', *Nature reviews. Cancer*, 3, (3), pp. 155-68.

Shimizu, H., Mitomo, K., Watanabe, T., Okamoto, S. and Yamamoto, K. (1990) 'Involvement of a NF-kappa B-like transcription factor in the activation of the interleukin-6 gene by inflammatory lymphokines', *Molecular and cellular biology*, 10, (2), pp. 561-8.

Shu, H. B., Agranoff, A. B., Nabel, E. G., Leung, K., Duckett, C. S., Neish, A. S., Collins, T. and Nabel, G. J. (1993) 'Differential regulation of vascular cell adhesion molecule 1 gene expression by specific NF-kappa B subunits in endothelial and epithelial cells', *Molecular and cellular biology*, 13, (10), pp. 6283-9.

Sipley, J. D., Menninger, J. C., Hartley, K. O., Ward, D. C., Jackson, S. P. and Anderson, C. W. (1995) 'Gene for the catalytic subunit of the human DNA-activated protein kinase maps to the site of the XRCC7 gene on chromosome 8', *Proceedings of the National Academy of Sciences of the United States of America*, 92, (16), pp. 7515-9.

Slama, J. T., Aboul-Ela, N., Goli, D. M., Cheesman, B. V., Simmons, A. M. and Jacobson, M. K. (1995) 'Specific inhibition of poly(ADP-ribose) glycohydrolase by adenosine diphosphate (hydroxymethyl)pyrrolidinediol', *Journal of medicinal chemistry*, 38, (2), pp. 389-93.

Smith, B. T. (1977) 'Cell line A549: a model system for the study of alveolar type II cell function', *The American review of respiratory disease*, 115, (2), pp. 285-93.

Smith, G. C. and Jackson, S. P. (1999) 'The DNA-dependent protein kinase', *Genes & development*, 13, (8), pp. 916-34.

Smith, L. M., Willmore, E., Austin, C. A. and Curtin, N. J. (2005) 'The novel poly(ADP-Ribose) polymerase inhibitor, AG14361, sensitizes cells to topoisomerase I poisons by increasing the persistence of DNA strand breaks', *Clinical cancer research : an official journal of the American Association for Cancer Research*, 11, (23), pp. 8449-57.

Sourisseau, T., Maniotis, D., McCarthy, A., Tang, C., Lord, C. J., Ashworth, A. and Linardopoulos, S. (2010) 'Aurora-A expressing tumour cells are deficient for homology-directed DNA double strand-break repair and sensitive to PARP inhibition', *EMBO molecular medicine*, 2, (4), pp. 130-42.

Southern, E. M. (1975) 'Detection of specific sequences among DNA fragments separated by gel electrophoresis', *Journal of molecular biology*, 98, (3), pp. 503-17.

Sovak, M. A., Bellas, R. E., Kim, D. W., Zanieski, G. J., Rogers, A. E., Traish, A. M. and Sonenshein, G. E. (1997) 'Aberrant nuclear factor-kappaB/Rel expression and the pathogenesis of breast cancer', *The Journal of clinical investigation*, 100, (12), pp. 2952-60.

Starczynowski, D. T., Reynolds, J. G. and Gilmore, T. D. (2003) 'Deletion of either C-terminal transactivation subdomain enhances the in vitro transforming activity of human transcription factor REL in chicken spleen cells', *Oncogene*, 22, (44), pp. 6928-36.

Stehlik, C., de Martin, R., Kumabashiri, I., Schmid, J. A., Binder, B. R. and Lipp, J. (1998) 'Nuclear factor (NF)-kappaB-regulated X-chromosome-linked iap gene expression protects endothelial cells from tumor necrosis factor alpha-induced apoptosis', *The Journal of experimental medicine*, 188, (1), pp. 211-6.

Stilmann, M., Hinz, M., Arslan, S. C., Zimmer, A., Schreiber, V. and Scheidereit, C. (2009) 'A nuclear poly(ADP-ribose)-dependent signalosome confers DNA damage-induced IkappaB kinase activation', *Molecular cell*, 36, (3), pp. 365-78.

Strnad, J. and Burke, J. R. (2007) 'IkappaB kinase inhibitors for treating autoimmune and inflammatory disorders: potential and challenges', *Trends in pharmacological sciences*, 28, (3), pp. 142-8.

Strozyk, E., Poppelmann, B., Schwarz, T. and Kulms, D. (2006) 'Differential effects of NF-kappaB on apoptosis induced by DNA-damaging agents: the type of DNA damage determines the final outcome', *Oncogene*, 25, (47), pp. 6239-51.

Suh, J. and Rabson, A. B. (2004) 'NF-kappaB activation in human prostate cancer: important mediator or epiphenomenon?', *Journal of cellular biochemistry*, 91, (1), pp. 100-17.

Sun, C., Chan, F., Briassouli, P. and Linardopoulos, S. (2007) 'Aurora kinase inhibition downregulates NF-kappaB and sensitises tumour cells to chemotherapeutic agents', *Biochemical and biophysical research communications*, 352, (1), pp. 220-5.

Susse, S., Scholz, C. J., Burkle, A. and Wiesmuller, L. (2004) 'Poly(ADP-ribose) polymerase (PARP-1) and p53 independently function in regulating double-strand break repair in primate cells', *Nucleic acids research*, 32, (2), pp. 669-80.

Suto, M. J., Stier, M. A., Winters, R. T., Turner, W. R., Pinter, C. D., Elliott, W. E. and Sebolt-Leopold, J. S. (1991) 'Synthesis and evaluation of a series of 3,5-disubstituted benzisoxazole-4,7-diones. Potent radiosensitizers in vitro', *Journal of medicinal chemistry*, 34, (11), pp. 3290-4.

Tak, P. P. and Firestein, G. S. (2001) 'NF-kappaB: a key role in inflammatory diseases', *The Journal of clinical investigation*, 107, (1), pp. 7-11.

Takahashi, T., Sano, B., Nagata, T., Kato, H., Sugiyama, Y., Kunieda, K., Kimura, M., Okano, Y. and Saji, S. (2003) 'Polo-like kinase 1 (PLK1) is overexpressed in primary colorectal cancers', *Cancer science*, 94, (2), pp. 148-52.

Tamatani, M., Che, Y. H., Matsuzaki, H., Ogawa, S., Okado, H., Miyake, S., Mizuno, T. and Tohyama, M. (1999) 'Tumor necrosis factor induces Bcl-2 and Bcl-x expression through NFkappaB activation in primary hippocampal neurons', *The Journal of biological chemistry*, 274, (13), pp. 8531-8.

Tamura, T., Ishihara, M., Lamphier, M. S., Tanaka, N., Oishi, I., Aizawa, S., Matsuyama, T., Mak, T. W., Taki, S. and Taniguchi, T. (1995) 'An IRF-1-dependent pathway of DNA damage-induced apoptosis in mitogen-activated T lymphocytes', *Nature*, 376, (6541), pp. 596-9.

Tanaka, M., Fuentes, M. E., Yamaguchi, K., Durnin, M. H., Dalrymple, S. A., Hardy, K. L. and Goeddel, D. V. (1999a) 'Embryonic lethality, liver degeneration, and impaired NF-kappa B activation in IKK-beta-deficient mice', *Immunity*, 10, (4), pp. 421-9.

Tanaka, T., Kimura, M., Matsunaga, K., Fukada, D., Mori, H. and Okano, Y. (1999b) 'Centrosomal kinase AIK1 is overexpressed in invasive ductal carcinoma of the breast', *Cancer research*, 59, (9), pp. 2041-4.

Tang, X., Liu, D., Shishodia, S., Ozburn, N., Behrens, C., Lee, J. J., Hong, W. K., Aggarwal, B. B. and Wistuba, II. (2006) 'Nuclear factor-kappaB (NF-kappaB) is frequently expressed in lung cancer and preneoplastic lesions', *Cancer*, 107, (11), pp. 2637-46.

Taub, R., Kirsch, I., Morton, C., Lenoir, G., Swan, D., Tronick, S., Aaronson, S. and Leder, P. (1982) 'Translocation of the c-myc gene into the immunoglobulin heavy chain locus in human Burkitt lymphoma and murine plasmacytoma cells', *Proceedings of the National Academy of Sciences of the United States of America*, 79, (24), pp. 7837-41.

Tentori, L., Portarena, I., Vernole, P., De Fabritiis, P., Madaio, R., Balduzzi, A., Roy, R., Bonmassar, E. and Graziani, G. (2001) 'Effects of single or split exposure of leukemic cells to temozolomide, combined with poly(ADP-ribose) polymerase inhibitors on cell growth, chromosomal aberrations and base excision repair components', *Cancer chemotherapy and pharmacology*, 47, (4), pp. 361-9.

Tergaonkar, V., Pando, M., Vafa, O., Wahl, G. and Verma, I. (2002) 'p53 stabilization is decreased upon NFkappaB activation: a role for NFkappaB in acquisition of resistance to chemotherapy', *Cancer cell*, 1, (5), pp. 493-503.

Tergaonkar, V. and Perkins, N. D. (2007) 'p53 and NF-kappaB crosstalk: IKKalpha tips the balance', *Molecular cell*, 26, (2), pp. 158-9.

Thomas, H. D., Calabrese, C. R., Batey, M. A., Canan, S., Hostomsky, Z., Kyle, S., Maegley, K. A., Newell, D. R., Skalitzky, D., Wang, L. Z., Webber, S. E. and Curtin, N. J. (2007) 'Preclinical selection of a novel poly(ADP-ribose) polymerase inhibitor for clinical trial', *Molecular cancer therapeutics*, 6, (3), pp. 945-56.

Tian, B., Nowak, D. E., Jamaluddin, M., Wang, S. and Brasier, A. R. (2005) 'Identification of direct genomic targets downstream of the nuclear factor-kappaB transcription factor mediating tumor necrosis factor signaling', *The Journal of biological chemistry*, 280, (17), pp. 17435-48.

Tong, W. M., Cortes, U., Hande, M. P., Ohgaki, H., Cavalli, L. R., Lansdorp, P. M., Haddad, B. R. and Wang, Z. Q. (2002) 'Synergistic role of Ku80 and poly(ADP-ribose) polymerase in suppressing chromosomal aberrations and liver cancer formation', *Cancer research*, 62, (23), pp. 6990-6.

Tong, W. M., Hande, M. P., Lansdorp, P. M. and Wang, Z. Q. (2001) 'DNA strand break-sensing molecule poly(ADP-Ribose) polymerase cooperates with p53 in telomere function, chromosome stability, and tumor suppression', *Molecular and cellular biology*, 21, (12), pp. 4046-54.

Trucco, C., Oliver, F. J., de Murcia, G. and Menissier-de Murcia, J. (1998) 'DNA repair defect in poly(ADP-ribose) polymerase-deficient cell lines', *Nucleic acids research*, 26, (11), pp. 2644-9.

Tsao, B. P., Cantor, R. M., Grossman, J. M., Shen, N., Teophilov, N. T., Wallace, D. J., Arnett, F. C., Hartung, K., Goldstein, R., Kalunian, K. C., Hahn, B. H. and Rotter, J. I. (1999) 'PARP alleles within the linked chromosomal region are associated with systemic lupus erythematosus', *The Journal of clinical investigation*, 103, (8), pp. 1135-40.

Tschaharganeh, D., Ehemann, V., Nussbaum, T., Schirmacher, P. and Breuhahn, K. (2007) 'Non-specific effects of siRNAs on tumor cells with implications on therapeutic applicability using RNA interference', *Pathology oncology research : POR*, 13, (2), pp. 84-90.

Tu, Z., Prajapati, S., Park, K. J., Kelly, N. J., Yamamoto, Y. and Gaynor, R. B. (2006) 'IKK alpha regulates estrogen-induced cell cycle progression by modulating E2F1 expression', *The Journal of biological chemistry*, 281, (10), pp. 6699-706.

Tulin, A. and Spradling, A. (2003) 'Chromatin loosening by poly(ADP)-ribose polymerase (PARP) at Drosophila puff loci', *Science*, 299, (5606), pp. 560-2.

Tulin, A., Stewart, D. and Spradling, A. C. (2002) 'The Drosophila heterochromatic gene encoding poly(ADP-ribose) polymerase (PARP) is required to modulate chromatin structure during development', *Genes & development*, 16, (16), pp. 2108-19.

Turco, M. C., Romano, M. F., Petrella, A., Bisogni, R., Tassone, P. and Venuta, S. (2004) 'NF-kappaB/Rel-mediated regulation of apoptosis in hematologic malignancies and normal hematopoietic progenitors', *Leukemia : official journal of the Leukemia Society of America, Leukemia Research Fund, U.K*, 18, (1), pp. 11-7.

Turner, D. J., Alaish, S. M., Zou, T., Rao, J. N., Wang, J. Y. and Strauch, E. D. (2007) 'Bile salts induce resistance to apoptosis through NF-kappaB-mediated XIAP expression', *Annals of surgery*, 245, (3), pp. 415-25.

Uchida, K., Hanai, S., Ishikawa, K., Ozawa, Y., Uchida, M., Sugimura, T. and Miwa, M. (1993) 'Cloning of cDNA encoding Drosophila poly(ADP-ribose) polymerase: leucine zipper in the auto-modification domain', *Proceedings of the National Academy of Sciences of the United States of America*, 90, (8), pp. 3481-5.

Ueda, K. and Hayaishi, O. (1985) 'ADP-ribosylation', *Annual review of biochemistry*, 54, pp. 73-100.

Ulich, T. R., Guo, K. Z., Remick, D., del Castillo, J. and Yin, S. M. (1991) 'Endotoxin-induced cytokine gene expression in vivo. III. IL-6 mRNA and serum protein expression and the in vivo hematologic effects of IL-6', *Journal of immunology*, 146, (7), pp. 2316-23.

van Den Brink, G. R., ten Kate, F. J., Ponsioen, C. Y., Rive, M. M., Tytgat, G. N., van Deventer, S. J. and Peppelenbosch, M. P. (2000) 'Expression and activation of NF-kappa B in the antrum of the human stomach', *Journal of immunology*, 164, (6), pp. 3353-9.

van Uden, P., Kenneth, N. S. and Rocha, S. (2008) 'Regulation of hypoxia-inducible factor-1alpha by NF-kappaB', *The Biochemical journal,* 412, (3), pp. 477-84.

Vaupel, P. (2004) 'The role of hypoxia-induced factors in tumor progression', *The oncologist,* 9 Suppl 5, pp. 10-7.

Veuger, S. J., Curtin, N. J., Richardson, C. J., Smith, G. C. and Durkacz, B. W. (2003) 'Radiosensitization and DNA repair inhibition by the combined use of novel inhibitors of DNA-dependent protein kinase and poly(ADP-ribose) polymerase-1', *Cancer research,* 63, (18), pp. 6008-15.

Veuger, S. J., Curtin, N. J., Smith, G. C. and Durkacz, B. W. (2004) 'Effects of novel inhibitors of poly(ADP-ribose) polymerase-1 and the DNA-dependent protein kinase on enzyme activities and DNA repair', *Oncogene,* 23, (44), pp. 7322-9.

Veuger, S. J. and Durkacz, B. W. (2011) 'Persistence of unrepaired DNA double strand breaks caused by inhibition of ATM does not lead to radio-sensitisation in the absence of NF-kappaB activation', *DNA repair,* 10, (2), pp. 235-44.

Veuger, S. J., Hunter, J. E. and Durkacz, B. W. (2009) 'Ionizing radiation-induced NF-kappaB activation requires PARP-1 function to confer radioresistance', *Oncogene,* 28, (6), pp. 832-42.

Walker-Nasir, E., Codington, J. F., Jahnke, M. R., Fuller, T. C. and Jeanloz, R. W. (1982) 'Isolation and partial characterization of surface components of cell line MDA-MB-231 derived from a human metastatic breast carcinoma', *Journal of the National Cancer Institute,* 69, (2), pp. 371-80.

Walsby, E. J., Pratt, G., Hewamana, S., Crooks, P. A., Burnett, A. K., Fegan, C. and Pepper, C. (2010) 'The NF-kappaB inhibitor LC-1 has single agent activity in multiple myeloma cells and synergizes with bortezomib', *Molecular cancer therapeutics,* 9, (6), pp. 1574-82.

Wang, C. Y., Mayo, M. W., Korneluk, R. G., Goeddel, D. V. and Baldwin, A. S., Jr. (1998) 'NF-kappaB antiapoptosis: induction of TRAF1 and TRAF2 and c-IAP1 and c-IAP2 to suppress caspase-8 activation', *Science,* 281, (5383), pp. 1680-3.

Wang, H., Zhang, W., Huang, H. J., Liao, W. S. and Fuller, G. N. (2004) 'Analysis of the activation status of Akt, NFkappaB, and Stat3 in human diffuse gliomas', *Laboratory investigation; a journal of technical methods and pathology,* 84, (8), pp. 941-51.

Wang, M., Wu, W., Rosidi, B., Zhang, L., Wang, H. and Iliakis, G. (2006) 'PARP-1 and Ku compete for repair of DNA double strand breaks by distinct NHEJ pathways', *Nucleic acids research,* 34, (21), pp. 6170-82.

Wang, T., Hu, Y. C., Dong, S., Fan, M., Tamae, D., Ozeki, M., Gao, Q., Gius, D. and Li, J. J. (2005) 'Co-activation of ERK, NF-kappaB, and GADD45beta in response to ionizing radiation', *The Journal of biological chemistry,* 280, (13), pp. 12593-601.

Wang, Z. Q., Stingl, L., Morrison, C., Jantsch, M., Los, M., Schulze-Osthoff, K. and Wagner, E. F. (1997) 'PARP is important for genomic stability but dispensable in apoptosis', *Genes & development,* 11, (18), pp. 2347-58.

Waterfield, M., Jin, W., Reiley, W., Zhang, M. and Sun, S. C. (2004) 'IkappaB kinase is an essential component of the Tpl2 signaling pathway', *Molecular and cellular biology,* 24, (13), pp. 6040-8.

Webster, G. A. and Perkins, N. D. (1999) 'Transcriptional cross talk between NF-kappaB and p53', *Molecular and cellular biology,* 19, (5), pp. 3485-95.

Weih, F., Carrasco, D., Durham, S. K., Barton, D. S., Rizzo, C. A., Ryseck, R. P., Lira, S. A. and Bravo, R. (1995) 'Multiorgan inflammation and hematopoietic abnormalities in mice with a targeted disruption of RelB, a member of the NF-kappa B/Rel family', *Cell,* 80, (2), pp. 331-40.

Westley, B. and Rochefort, H. (1979) 'Estradiol induced proteins in the MCF7 human breast cancer cell line', *Biochemical and biophysical research communications,* 90, (2), pp. 410-6.

Weston, V. J., Oldreive, C. E., Skowronska, A., Oscier, D. G., Pratt, G., Dyer, M. J., Smith, G., Powell, J. E., Rudzki, Z., Kearns, P., Moss, P. A., Taylor, A. M. and Stankovic, T. (2010) 'The PARP inhibitor olaparib induces significant killing of ATM-deficient lymphoid tumor cells in vitro and in vivo', *Blood,* 116, (22), pp. 4578-87.

White, A. W., Almassy, R., Calvert, A. H., Curtin, N. J., Griffin, R. J., Hostomsky, Z., Maegley, K., Newell, D. R., Srinivasan, S. and Golding, B. T. (2000) 'Resistance-modifying agents. 9. Synthesis and biological properties of benzimidazole inhibitors of the DNA repair enzyme poly(ADP-ribose) polymerase', *Journal of medicinal chemistry,* 43, (22), pp. 4084-97.

Wickremasinghe, M. I., Thomas, L. H., O'Kane, C. M., Uddin, J. and Friedland, J. S. (2004) 'Transcriptional mechanisms regulating alveolar epithelial cell-specific CCL5 secretion in pulmonary tuberculosis', *The Journal of biological chemistry,* 279, (26), pp. 27199-210.

Wietek, C., Miggin, S. M., Jefferies, C. A. and O'Neill, L. A. (2003) 'Interferon regulatory factor-3-mediated activation of the interferon-sensitive response element by Toll-like receptor (TLR) 4 but not TLR3 requires the p65 subunit of NF-kappa', *The Journal of biological chemistry,* 278, (51), pp. 50923-31.

Wooster, R., Bignell, G., Lancaster, J., Swift, S., Seal, S., Mangion, J., Collins, N., Gregory, S., Gumbs, C. and Micklem, G. (1995) 'Identification of the breast cancer susceptibility gene BRCA2', *Nature*, 378, (6559), pp. 789-92.

Wu, J. T. and Kral, J. G. (2005) 'The NF-kappaB/IkappaB signaling system: a molecular target in breast cancer therapy', *The Journal of surgical research*, 123, (1), pp. 158-69.

Wu, K., Jiang, S. W., Thangaraju, M., Wu, G. and Couch, F. J. (2000) 'Induction of the BRCA2 promoter by nuclear factor-kappa B', *The Journal of biological chemistry*, 275, (45), pp. 35548-56.

Wu, M. X., Ao, Z., Prasad, K. V., Wu, R. and Schlossman, S. F. (1998) 'IEX-1L, an apoptosis inhibitor involved in NF-kappaB-mediated cell survival', *Science*, 281, (5379), pp. 998-1001.

Wu, Z. H., Shi, Y., Tibbetts, R. S. and Miyamoto, S. (2006) 'Molecular linkage between the kinase ATM and NF-kappaB signaling in response to genotoxic stimuli', *Science*, 311, (5764), pp. 1141-6.

Wuerzberger-Davis, S. M., Nakamura, Y., Seufzer, B. J. and Miyamoto, S. (2007) 'NF-kappaB activation by combinations of NEMO SUMOylation and ATM activation stresses in the absence of DNA damage', *Oncogene*, 26, (5), pp. 641-51.

Yamamoto, Y., Matsuyama, H., Kawauchi, S., Matsumoto, H., Nagao, K., Ohmi, C., Sakano, S., Furuya, T., Oga, A., Naito, K. and Sasaki, K. (2006) 'Overexpression of polo-like kinase 1 (PLK1) and chromosomal instability in bladder cancer', *Oncology*, 70, (3), pp. 231-7.

Yip, K. H., Zheng, M. H., Feng, H. T., Steer, J. H., Joyce, D. A. and Xu, J. (2004) 'Sesquiterpene lactone parthenolide blocks lipopolysaccharide-induced osteolysis through the suppression of NF-kappaB activity', *Journal of bone and mineral research : the official journal of the American Society for Bone and Mineral Research*, 19, (11), pp. 1905-16.

You, L. R., Chen, C. M. and Lee, Y. H. (1999) 'Hepatitis C virus core protein enhances NF-kappaB signal pathway triggering by lymphotoxin-beta receptor ligand and tumor necrosis factor alpha', *Journal of virology*, 73, (2), pp. 1672-81.

Zaniolo, K., Desnoyers, S., Leclerc, S. and Guerin, S. L. (2007) 'Regulation of poly(ADP-ribose) polymerase-1 (PARP-1) gene expression through the post-translational modification of Sp1: a nuclear target protein of PARP-1', *BMC molecular biology*, 8, pp. 96.

Zaremba, T. and Curtin, N. J. (2007) 'PARP inhibitor development for systemic cancer targeting', *Anti-cancer agents in medicinal chemistry*, 7, (5), pp. 515-23.

Zaremba, T., Ketzer, P., Cole, M., Coulthard, S., Plummer, E. R. and Curtin, N. J. (2009) 'Poly(ADP-ribose) polymerase-1 polymorphisms, expression and activity in selected human tumour cell lines', *British journal of cancer*, 101, (2), pp. 256-62.

Zaremba, T., Thomas, H. D., Cole, M., Coulthard, S. A., Plummer, E. R. and Curtin, N. J. (2011) 'Poly(ADP-ribose) polymerase-1 (PARP-1) pharmacogenetics, activity and expression analysis in cancer patients and healthy volunteers', *The Biochemical journal*, 436, (3), pp. 671-9.

Zerfaoui, M., Suzuki, Y., Naura, A. S., Hans, C. P., Nichols, C. and Boulares, A. H. (2008) 'Nuclear translocation of p65 NF-kappaB is sufficient for VCAM-1, but not ICAM-1, expression in TNF-stimulated smooth muscle cells: Differential requirement for PARP-1 expression and interaction', *Cellular signalling*, 20, (1), pp. 186-94.

Zhang, H. and Rudkevich, D. M. (2007) 'A FRET approach to phosgene detection', *Chemical communications*, (12), pp. 1238-9.

Zhang, X., Miao, X., Liang, G., Hao, B., Wang, Y., Tan, W., Li, Y., Guo, Y., He, F., Wei, Q. and Lin, D. (2005a) 'Polymorphisms in DNA base excision repair genes ADPRT and XRCC1 and risk of lung cancer', *Cancer research*, 65, (3), pp. 722-6.

Zhang, Y. W., Luo, W. J., Wang, H., Lin, P., Vetrivel, K. S., Liao, F., Li, F., Wong, P. C., Farquhar, M. G., Thinakaran, G. and Xu, H. (2005b) 'Nicastrin is critical for stability and trafficking but not association of other presenilin/gamma-secretase components', *The Journal of biological chemistry*, 280, (17), pp. 17020-6.

Zhou, B. B. and Elledge, S. J. (2000) 'The DNA damage response: putting checkpoints in perspective', *Nature*, 408, (6811), pp. 433-9.

Zhou, H., Kuang, J., Zhong, L., Kuo, W. L., Gray, J. W., Sahin, A., Brinkley, B. R. and Sen, S. (1998) 'Tumour amplified kinase STK15/BTAK induces centrosome amplification, aneuploidy and transformation', *Nature genetics*, 20, (2), pp. 189-93.

Zhou, H., Monack, D. M., Kayagaki, N., Wertz, I., Yin, J., Wolf, B. and Dixit, V. M. (2005) 'Yersinia virulence factor YopJ acts as a deubiquitinase to inhibit NF-kappa B activation', *The Journal of experimental medicine*, 202, (10), pp. 1327-32.

Zhou, J., Zhang, H., Gu, P., Bai, J., Margolick, J. B. and Zhang, Y. (2008) 'NF-kappaB pathway inhibitors preferentially inhibit breast cancer stem-like cells', *Breast cancer research and treatment*, 111, (3), pp. 419-27.

Zingarelli, B., Hake, P. W., O'Connor, M., Denenberg, A., Kong, S. and Aronow, B. J. (2003a) 'Absence of poly(ADP-ribose)polymerase-1 alters nuclear factor-kappa B activation and gene expression of apoptosis regulators after reperfusion injury', *Molecular medicine*, 9, (5-8), pp. 143-53.

Zingarelli, B., O'Connor, M. and Hake, P. W. (2003b) 'Inhibitors of poly (ADP-ribose) polymerase modulate signal transduction pathways in colitis', *European journal of pharmacology,* 469, (1-3), pp. 183-94.

Zingarelli, B., Salzman, A. L. and Szabo, C. (1998) 'Genetic disruption of poly (ADP-ribose) synthetase inhibits the expression of P-selectin and intercellular adhesion molecule-1 in myocardial ischemia/reperfusion injury', *Circulation research,* 83, (1), pp. 85-94.

Zong, W. X., Edelstein, L. C., Chen, C., Bash, J. and Gelinas, C. (1999) 'The prosurvival Bcl-2 homolog Bfl-1/A1 is a direct transcriptional target of NF-kappaB that blocks TNFalpha-induced apoptosis', *Genes & development,* 13, (4), pp. 382-7.

Appendix I

I.I Differentially expressed genes 8 hours following treatment with TNF-α

Table A.I, below contains list of genes of over 400 genes differentially expressed following 8 hours after treatment with TNF-α, compared with untreated controls, as well as the accession/identification number and the fold change.

Gene	Symbol	ID	Fold change
ATP-binding cassette, sub family A (ABC1), member 3	ABCA3	NM_013855.2	-1.320
ATP-binding cassette, sub family A (ABC1), member 7	ABCA7	NM_013850.1	-1.290
ATP-binding cassette, family B (MDR/TAP) member 1B	Abcb1b	NM_011075.1	1.501
Acyl-coA dehydrogenase, C-4 to C-12 straight chain	ACADM	NM_007382.1	-1.415
Acyl-coA binding domain containing 4	ACBD4	NM_025988.2	-1.230
Amiloride-sensitive cation channel 2, neuronal	ACCN2	NM_009597.1	-1.567
Acyl-coA synthetase thioesterase 7	ACOT7	NM_133348.1	1.211
Acid phosphatase-like 2	ACPL2	NM_153420.2	1.301
Acyl-coA synthetase long-chain family member 3	ACSL3	NM_028817.2	-1.285
Actinin, alpha 4	ACTN4	NM_021895.2	-1.285
ADAMTS-like 4	ADAMTSL4	NM_144899.2	-1.385
Adenylate kinase 2	AK2	NM_016895.3	1.331
Aldehyde dehydrogenase 3 family, member A1	ALDH3A1	NM_007436.1	-1.594
Aldehyde dehydrogenase 6 family, member A1	ALDH6A1	NM_134042.2	-1.345
Angiopoietin-like 2	ANGPTL2	NM_0119234	-1.310
Annexin A8	ANXA8	NM_013473.3.	-1.288
Amyloid beta (A4) precursor protein-binding, family B member 1 (Fe65)	APBB1	NM_009685.2	-1.349
Aquaporin 1	AQP1	NM_007472.2	-1.412
Aquaporin 5	AQP5	NM_009701.4	-2.065
Rho GTPase activating protein 18	ARGGAP18	NM_176837.2	-1.399
Rho GTPase activating protein 22	ARGGAP22	NM_153800.3	-1.909
Rho GTPase activating protein 24	ARGGAP24	NM_29270.1	-1.305
Rho guanine nucleotide exchange factor 15	ARGGEF15	AK052570	-1.219
Rho guanine nucleotide exchange factor 18	ARGGEF18	NM_133962.3	-1.218
Armadillo repeat containing, X-linked 2	ARMCX2	NM_026139.3	-1.264
ARV1 homolog	ARV1	NM_026855.1	1.205
Argininosuccinate sythetase 1	ASS1	NM_007494.3	1.509
ATPase, H^+ transporting, lysosomal VO subunit a1	ATP6VOA1	NM_016920.1	-1.439
Arginine vasopressin-induced 1	AVPI1	NM_027106.3	-1.328
UDP-GlcNac: betaGal beta-1,3-N-acetyl glucosaminyltransferase-like 1	B3GTNL1	NM_178664.3	-1.274
Bcl-2 binding component 3	BBC3	NM_133234.1	1.358
BCL-2 associated athanogene 6	BAG6	NM_057171.1	-1.266
BCL-2-like 11 (apoptosis facilitator)	BCL2L11	NM_009754.2	1.374
BMP binding endothetial regulator	BMPER	NM_028472.1	-1.356
BCL2/adenovirus E1B 19kDa interacting protein-3-like	BNIP3L	NM_009761.2	-1.213
C1q and TNF related protein 1	C1QTNF1	NM_019959.2	-1.222
Chromosome 21 open reading frame 63	C21orf63	NM_027627.1	-1.282
Chromosome 3 open reading frame 17	C3orf17	NM_145972.1	1.229
Chromosome 5 open reading frame 13	C5orf13	NM_053078.3	-1.688
Chromosome 7 open reading frame 43	C7orf43	NM_153161.1	1.211
Complement component 3	C3	NM_009778.1	1.332
Caspase recruitment domain family member 10	CARD10	NM_130859.2	1.750
Caspase 4	CASP4	NM_007609.1	1.386
Caveolin 1	CAV1	NM_007616.3	-1.399
Coiled coil domain containing 137	CCDC137	NM_152807.3	1.306
Coiled coil domain containing 85B	CCDC85B	NM_198616.2	1.576
Chemokine (C-C motif) ligand 13	CCL13	NM_011333.3	3.293
Chemokine (C-C motif) ligand 17	CCL17	NM_011332.2	1.606
Chemokine (C-C motif) ligand 5	CCL5	NM_013653.2	6.558

Chemokine (C-C motif) ligand 7	CCL7	NM_013654	3.427
Chemokine (C-C motif) ligand 9	CCL9	NM_011338	6.106
CD109 molecule	CD109	NM_153098.2	-1.298
CD151 molecule	CD151	NM_00942.1	1.281
CD75 molecule	CD75	NM_010545.3	1.229
CD82 molecule	CD82	NM_007656.4	1.783
CDC42 effector protein 2	CDC42EP2	NM_026772.1	1.246
CDC42 effector protein 5	CDC42EP5	NM_021454.3	1.343
Cyclin-dependent kinase 19	CDK19	NM-198164.2	-1.319
Cyclin-dependent kinase inhibitor 1A (p21)	CDKN1A	NM_007669.2	1.937
Cdon homolog	CDON	AK040711	-1.293
C-type lectin domain family 2, member d	Cled2	NM_053109.2	1.806
Collagen, type IV, alpha 5	COL4A5	NM_007736.2	-1.480
Collagen, type V, alpha 1	COL5A1	NM_0157734.1	-1.394
Collagen, type VII, alpha 1	COL7A1	NM_007738.8	-1.277
Cellular retinoic acid binding protein 2	CRABP2	NM_007759.2	-1.674
Cysteine and glycine ricj protein 2	CSRP2	NM_007792.3	1.409
CTD small phosphatase like cyastathionase	CTH	NM_145953.3	1.329
Catenin, alpha-like 1	CTNNAL1	NM_018761.2	1.609
Catenin, beta interacting protein 1	CTNNBIP1	NM_023465.3	1.532
Cystinosis, nephropathic	CTNS	NM_031251.4	-1.271
Coxscakie virus and adenovirus receptor	CXADR	NM_001025192.2	-1.338
Chemokine (C-XC motif) ligand 10	CXCL10	NM_021274.1	5.986
Diasabled homolog 2, mitogen response protein	DAB2	NM_23118.1	1.557
D site of albumin promoter binding protein	DBP	NM_016974.1	-1.680
Decorin	DCN	NM_007833.4	1.818
Density-regulated protein	DENR	NM_026603.1	1.759
Deafness-autosomal dominant 5	DFNA5	NM_08769.3	-1.280
Dickkoff homolog 3	DKK3	NM_015814.2	-1.796
Discs, large homolog 5	DLG5	XM_981375.2	-1.309
DPH1 homolog	DPH1	NM_144491	1.229
DTW domain containing 1	DTWD1	NM_026981.1	1.243
Dual specificity phosphatase 4	DUSP4	NM_176933	-1.493
Dual specificity phosphatase 6	DUSP6	NM_026268.1	-1.315
Dual specificity tyrosine phosphorylation regulating kinase 1B	DYRK1B	NM_001037957.1	-1.249
Enoyl coA hydratase, short chain 1	ECHS1	NM_050119.1	-1.246
Eukaryotic translation initiation factor 6	EIF6	NM_010579.2	1.389
Ectonucleotide pyrophosphatase/phosphodiesterase 2	ENPP2	NM_015744.1	1.499
Epoxide hydrolase 1	EPHX1	NM_010145.2	1.320
Epidermal growth factor receptor pathway substrate 8	EPS8	NM_007945.2	1.628
Ecotrophic viral integration site 2A	EVI2A	NM_010161.1	1.813
Ecotrophic viral integration site 5 like	EVI5L	NM_001039578.2	-1.221
Coagulation factor II receptor	F2R	NM_010169.3	-1.540
Family with sequence similarity 114 member A1	FAM114A1	NM_026667.2	-1.362
Family with sequence similarity 195 member A	FAM195A	NM_26633.3	1.350
Family with sequence similarity 20 member A	FAM20A	NM_153782.1	-1.313
Fas	FAS	NM_007987.1	3.635
Fibroblast growth factor 7	FGF7	NM_008008.3	1.343
Four jointed box 1	FJX1	NM_010218.2	1.244
Flotillin 2	FLOT2	NM_001040403.1	-1.202
Formin-like 3	FMNL3	NM_011711.1	-1.254
FBI murine osteosarcoma viral oncogene homolog	FOS	NM_010234.2	-1.375
Forkhead box Q1	FOXQ1	NM_008239.3	-1.839
Growth arrest and DNA damage inducible beta	GADD45B	NM_008655.1	1.322
UDP-N-acetyl-alpha-galactosamine:polypeptide N-acetylgalactosaminyltranferase 10	GALNT10	NM_134189.2	-1.219
UDP-N-acetyl-alpha-galactosamine:polypeptide N-acetylgalactosaminyltranferase 2	GALNT2	NM_139272.2	-1.314
UDP-N-acetyl-alpha-galactosamine:polypeptide N-acetylgalactosaminyltranferase like 2	GALNTL2	NM_030166.1	-1.377
Guanylate binding protein 2	GBP2	NM_010260.1	1.424

Guanylate binding protein 4	GBP4	NM_018734.4	1.266
Glucosaminyl (N-acetyl) transferase 2	GCNT2	NM_133219.1	-1.398
Glucosaminyl (N-acetyl) transferase 3	GCNT3	NM_028087.2	-1.242
Gamma-glutamyl cyclotransferase	GGCT	NM_026637.3	1.373
Golgi glycoprotein 1	CLC1	NM_009149	-1.300
GLI pathogenesis related 2	GLIPR2	NM_027450	1.551
Glutaredoxin	GLRX	NM_053108.2	-1.268
G-protein coupled estrogen receptor 1	GPER	NM_029771.2	-1.266
G-protein coupled receptor 176	GPR176	NM_201367.2	1.691
Growth factor receptor protein 10	GRB10	NM_010345	-1.263
Glutamate receptor, ionotrophic AMDA10	GRIA1	NM_008165.2	-1.287
Granulin	GRN	NM_008175.3	-1.242
Gasdermin D	GSDMD	NM_026960.1	1.572
Glutathione S-transferase, alpha 4	Gsta4	NM+0103571.1	-1.465
Histocompatibility 2, Q region locus 5	H2-Q5	NM_010393.1	1.767
HECT domain and ankyrin repeat containing E3 ubiquitin protein ligase 1	HACE1	NM_172432.2	1.224
HMG box transcription factor 1	HBP1	NM_135198.1	-1.488
Histone deaccetylase 5	HDAC5	NM_001077696.1	-1.455
High density lipoprotein binding protein	HDLBP	NM_133808.2	-1.238
Major histocompatibility complex, class 1B	HLA-B	NM_001081032.1	1.941
Major histocompatibility complex, class C	HLA-C	NM_019909.1	1.26
Major histocompatibility complex, class E	HLA-E	NM_010398.1	1.976
Major histocompatibility complex, class G	HLA-G	NM_013819.2	1.461
Homeobox A2	HOXA2	NM_010451.1	-1.770
Homeobox A5	HOXA5	NM_010453.2	-2.574
Homeobox C6	HOXC^	NM_010465.2	1.245
HtrA serine peptidase 2	HTRA2	NM_019752.2	1.270
Inhibitor of DNA binding 1	ID1	NM_010495.2	-1.553
Inhibitor of DNA binding 3	ID3	NM_008321.1	-1.531
Interferon activated gene 20B	Ifi202b	NM_008327.1	-1.446
Immediate early response 3	IER3	NM_133662.2	1.683
Interferon induced protein 35	IFI35	NM_027320.4	1.359
Interferon gamma receptor 2	IFNGR2	NM_008338.3	1.579
Insulin-like growth factor binding protein 6	IGFBP6	NM_008344.2	-1.349
Interleukin 1 receptor like 1	IL1RL1	NM_010743.1	3.318
Interleukin 1 receptor associated kinase 1 binding protein	ILAK1BP1	AK014712	1.228
Interferon regulatory factor 1	IRF1	NM_008390.1	1.628
Interferon regulatory factor 2 binding protein 2	IRF2BP2	NM_001002523.2	-1.346
Insulin receptor substrate 2	TRS2	NNM_001081212.1	-1.502
Integrin beta 5	ITGB2	NM_010580.1	-1.339
Integrin beta-like 1	ITGBL1	NM_145467.1	-1.484
Inositol-1,4,5-triphophate receptor interacting protein like 2	ITPRIPL2	NM_001033380.3	1.700
Isovaleryl-coA-dehydrogenase	IVD	NM_019826.3	-1.367
Potassium gated channel shaker related subfamily beta member1	KCNAB1	NM_010597.2	-1.455
Potassium gated channel subfamily F, member 1	KCNF1	NM_0201531.2	-1.258
Kin of IRRE like 3	KIRREL3	NM_026324.2	-1.730
Keratin 13	KRT13	NM_010662.1	-1.388
Kinesin light chain 4	KLC4	NM_029091.2	-1.341
LIM and SH3 protein 1	LASP1	NM_010688.2	-1.320
Limb bud and heart development homolog	LBH	NM_029999.3	-1.609
Leprecan-like 4	LEPREL4	NM_176830.2	-1.279
Neuralized homolog 3	LINCR	NM_153408.2	1.312
Lysophosphatidic acid receptor 6	LPAR6	NM_175116.2	-1.277
Leucine rich repeats and immune globulin domains 1	LRIG1	NM_008377.2	1.251
Leucine rich repeats and immune globulin domains 3	LRIG3	NM_172152.4	-1.329
Leucine rich repeats kinase 1	LRRK1	NM_146191.3	-1.344
Latent transforming growth factor beta binding protein 3	LTBP3	NM_008520.2	-1.552

Leucine zipper protein 1	LUZP1	NM_024452.2	1.370
Melanoma antigen family D1	MAGED1	NM_019791.2	-1.276
Melanoma antigen family E1	MAGEE1	NM_053201.2	-1.400
MAK16 homolog	MAK16	NM_026453.1	1.245
Mitogen activated kinase 11	MAPK11	NM_011161.4	1.343
Myristoylated alanine rich protein kinase C substrate	MARCKS	NM_008538.2	1.406
Muscleblind like 2	MBNL2	NM_175341.3	-1.277
Membrane bound O-acyltransferase domain containing 1	MBOAT1	NM_153546.3	-1.201
Mediator complex substrate 11	MED11	NM_025397.2	1.301
Mediator complex substrate 24	MED24	NM_011869.2	1.331
Meis homobox 1	MEIS1	NM_010789.2	-1.773
Meis homobox 2	MEIS2	NM_010825.3	-2.124
Major facilitator superfamily domain containing 2A	MFSD2A	NM_029662.1	-1.362
Matrix Gla protein	MGP	NM_008597.3	-2.698
Makoglinin, ring finger 1	MRGN1	NM_029657.2	-1.223
Microsomal glutathione S-transferase 2	MGST2	NM_174995.2	-1.419
Mindbomb homolog 2	MIB2	NM_145124.2	-1.390
MK167 interacting nucleolar phosphoprotein	MK167IP	NM_026178.3	1.315
Monocyte to macrophage differentiation associated	MMD	NM_026178.2	1.419
Matrix metallopeptidase 9	MMP9	NM_013599.2	2.013
Myosin phosphatase Rho interacting protein	MPRIP	NM-201245.2	-1.248
Mannose receptor C, type I	MRC1	NM_008625.1	1.538
Mitochondrial ribsosomal protein S18B	MRPS18B	NM_025878.1	1.226
Mitochondrial ribsosomal protein S2	MRPS2	NM_080452.2	1.208
mRNA turnover 4 homolog	MRTO4	NM_023536.2	1.236
Myotubularin related protein 11	MTMR11	NM_181409.2	-1.546
Muscle related coiled-col protein	MURC	NM_026509.1	-1.386
Major vault protein	MVP	NM_080638.1	1.549
Matrix remodelling associated 8	MXRA8	NM_024263.3	-1.434
v-myc myelocytomatosis viral oncogene homolog 1	MYCL1	NM_008506.2	1.736
NACC2 family member 2	NACC2	NM_001037098.1	-1.44
Neuronal calcium sensor 1	NCS1	NM_019681.3	1.218
Nuclear factor of activated T-cells, calcineurin-dependent 4	NFATC4	NM_023699.3	-1.418
Nuclear factor I/x	NFIX	NM_010906.2	-1.302
Nuclear factor of kappa light polypeptide gene enhancer in B cells (p49/p100)	NFKB2	NM_019408.1	1.669
Nuclear factor of kappa light polypeptide gene enhancer inhibitor epsilon	NFKBIE	NM_008690.2	2.484
Nuclear factor of kappa light polypeptide gene enhancer inhibitor alpha	NFKBIA	NM_010907.1	3.562
NIPA-like domain containing 1	NIPAL1	NM_001081205.1	1.605
Nucleolar protein 10	NOL10	NM_001008421.1	1.257
Nucleolar protein 3	NOL3	NM_030152.4	1.255
Notchless homolog 1	NLE1	NM_145431.1	1.310
Natriuretic peptide receptor B	NRP2	NM_173788.3	-1.204
Neuritin 1	NRN1	NM_153529.1	-1.882
Neuropilin 1	NRP1	NM_008737.1	-1.522
Nuclear protein transcriptional regulator 1	NUPR1	NM_019738.1	-1.448
Oligosaccharide-binding fold containing 2A	OBFC2A	NM_028696.2	1.423
Oculocerebrorenal syndrome of lowe	OCRL	NM_177215.2	-1.204
Oestogylcin	OGN	NM_008760.4	-1.941
Olfactomedin-like 2B	OLFML2B	NM_177068.3	-1.381
Phosphofurin acid cluster sorting protein 2	PACS2	NM_001081170.1	-1.283
Polyamine oxidase	PAOX	NM_153783.2	-1.441
PreB-cell leukemia homeobox 1	PBX1	NM_008783.1	-1.357
PreB-cell leukemia homeobox 4	PBX4	NM_001024954.1	1.315
Photocadherin 7	PCDH7	NM_018764.1	1.305
Phosphate cytidylyltranscferase 1, choline beta	PCYTIB	NM_177546.2	-1.447
Programmed cell death 4	PDCD4	NM_011050.3	-1.422
Platelet derived growth factor receptor alpha	PDGFRA	NM-011058.2	-1.617

polypeptide			
Podoplanin	PDPN	NM_010329.1	1.259
PDZ domain containing ring finger 3	PDZRN3	NM_018884.1	-1.235
Pelota homolog	PELO	NM_134058.1	1.233
Period homolog 2	PER2	NM_011066.1	-1.499
6-Phosphofructo-2-kinase	PFKFB4	NM_173019.5	-1.213
Phospofructokinase, muscle	PFKM	NM_021514.3	-1.277
Pyroglutyml 1-peptidase 1	PGPEP1	NM_023217.2	-1.283
Paired like homodomain 2	PITX2	NM_011098.3	-1.738
Praja ring finger 2	PJA2	NM_144859.2	-1.404
Pleckstrin homology domain containing family G, member 2	PLEKHG2	NM_138752.1	-1.214
Polo-like kinase 2	PLK2	NM_152804.1	1.527
Phospholipid scramblase 1	PLSCR1	NM_011636.1	1.737
Phospholipid scramblase 2	PLSCR2	NM_008880.2	1.488
Promyelocytic leukemia	`PML	NM_008884.4	-1.237
Peripheral myelin protein22	PMP22	NM_008885.2	-1.301
Paroxysmal nonkinesigenic dyskinesia	PNKD	NM_019999.1	1.670
P450 oxidoreductase	POR	NM_008898.1	-1.243
Phosphatidic acid phosphate type 2A	PPAP2A	NM_008247.2	-1.261
Peroxisome proliferator-activated receptor delta	PPARD	NM_011145.3	1.265
Pro-platelet basic protein	PPBP	NM-023785.2	1.827
PQ loop repeat containing 3	PQLC3	NM_172574.1	-1.273
Protein kinase C, delta binding protein	PRKCDBP	NM_028444.1	-1.512
PRKR interacting protein 1	PRKRIP1	NM_025774.1	1.212
Prolactin family 2, subfamily c, member 2	Prl2c1	NM_011118.1	1.878
Prolactin family 2, subfamily c, member 4	Prl2c4	NM_011954.2	1.746
Proline dehydrogenase (oxidase) 1	PSMDH	NM_011172.1	1.256
Proteasome subunit, beta type 10	PSMB10	NM_013640.1	1.624
Proteasome subunit, beta type 8	PSMB8	NM_010724	1.386
Proteasome 26S subunit, non ATPase 10	PSMD10	NM_016883.3	1.427
Proteasome activator subunit 1	PSME1	NM_011189.1	1.286
Parathymosin	PTMS	NM_026988.1	-1.234
Protein tyrosine phosphatase, non-receptor type 22	PTPN22	NM_008979.1	1.661
RAB11 family interacting protein 5	RAB11FIP5	NM_001003955.2	-1.241
RAB31, member RAS oncogene family	RAB31	NM_133685.1	-1.243
RAB1B, member RAS oncogene family	RAB1B	NM_024457.2	1.317
RAP1 GTPase activating protein	RAP1GAP	NM_001081155.1	-1.335
Retinoic acid receptor gamma	RARG	NM_011244.3	-1.542
Regulator of calcineurin 2	RCAN2	NM_207649.1	-1.294
RNA terminal phosphate cyclase-like 1	RCL-1	NM_021525.2	1.206
v-rel reticuloendotheliosis viral oncogene homolog A	RELA	NM_009045.4	-1.264
v-rel reticuloendotheliosis viral oncogene homolog B	RELB	NM_009046.2	2.074
Raftlin family member 2	RFTN2	NM_028713.1	-1.388
Regulatory factor X, 2	FRX2	NM_009056.1	-1.375
Ral guanine nucleotide dissociation stimulation like 1	RGL1	NM_016846.3	-1.379
Ribosome production factor 1 homolog	REF1	NM_027371.2	1.202
Ras-related associated with diabetes	RRAD	NM_019662.1	1.374
Ribosomal processing 15 homolog	RRP15	NM_026041.2	1.225
Ribosomal processing 9 homolog	RRP9	NM_145620.4	1.296
Ribosomal L1 domain containing 1	RSL1D1	NM)025546.1	1.226
Sphingosine-1-phosphate receptor 2	S1PR2	NM_010333	1.27
Scavenger receptor class A, member 3	SCARA3	NM_172604.3	-1.526
Scleraxis homolog A	SCXA	NM_198885.2	-1.423
Syndecan 2	SDC2	NM_008304.2	-1.213
Syndecan binding protein 2	SDCBP2	NM_145535.1	1.338
Sema domain 3A	SEMA3A	NM_009152.2	-1.439
Serpin peptidase inhibitor, clade B, member2	SERPINB2	NM_011111.3	1.396
Sestrin 1	SENS1	NM_001013370.1	-1.202
SH3 and PX domains 2B	SH£PXD2B	NM+177364.3	-1.418
Shroom family member 2	SHROOM2	NM_172441.2	-1.772
Single minded homolog 2	SIM2	NM_011377.2	-1.567

SIX homolog 1	SIX1	NM_009189.1	-1.753
Solute carrier family 11, member 1	SLC11A1	NM_013612.1	1.578
Solute carrier family 11, member 2	SLC11A2	AK083478.	1.316
Solute carrier family 16, member 13	SLC16A13	NM_172371.3	-1.408
Solute carrier family 19, member 1	SLC19A1	NM_031196.2	1.293
Solute carrier family 1, member 3	SLC1A3	NM_148938.2	-1.965
Solute carrier family 1, member 4	SLC1A4	NM_018861.2	-1.362
Solute carrier family 25, member 33	SLC23A33	NM_027460.2	1.284
Solute carrier family 2, member 6	SLC2A6	NM_172659.2	2.584
Solute carrier family 44, member 2	SLC44A2	NM_152808.2	-1.268
Solute carrier family 6, member 6	SLC6A6	NM_009320.3	-1.423
SWI/SNF related matrix assocated, actin dependent regulator of chromatin, subfamily a, member 2	SMARCA	NM_011416.2	-1.233
Snail homolog 2	SNAI3	NM_013914.2	-1.285
Sorting nexin 16	SNX16	NM_029068.2	-1.292
Suppressor of cytokine signalling 2	SOCS2	NM_007706.3	-1.377
Sphingosine kinase 1	SPHK1	NM_011451.2	-1.662
Spondin 2	SPON2	NM_133903.2	-1.736
Secreted phosphoprotein 1	SPP1	NM_009263.1	-1.401
Single stranded DNA binding protein 2	SSBP2	NM_024186.1	-1.334
Single stranded DNA binding protein 3	SSBP3	NM_023672.2	-1.339
Sacrospan	SSPN	NM_010656.2	-1.367
Stabilin 1	STAB1	AK087634	-1.437
Serine/threonine kinase 36	STK36	AK047284	-1.210
Suppressor of ty3 homolog	SUPT3H	NM_178652.2	-1.230
Surfiet 2	SURF2	NM_013678.2	1.216
Synaptic vesicle glycoprotein 2A	SV2A	NM_022030.3	-1.248
Synapsin 1	SYN1	NM_013680.3	-1.260
TRAF family member-associated NFKB activator	TANK	NM_011529.1	1.370
TAP binding protein	TAPBP	NM_009318.1	-1.811
TBC1 domain containing family member 5	TBCIC5	NM_028162.2	-1.241
Transcription factor 4	TCF4	NM_013685.2	1.531
Transcription factor like 7	TCF7L2	NM_009333.2	-1.485
TGF beta-induced 68 kDA	TGFB1	NM_009369.1	1.543
Translocase of inner mitochondrial membrane 44 homolog	TIMM44	NM_011592.1	1.237
TIMP metalloprotease inhibitor 3	TIMP3	NM_015595.2	-1.356
Transducin-like enhance of split 1	TLE1	NM_011599.3	-1.376
Toll like receptor 4	TLR4	NM_021297.1	-1.272
Transmembrane protein 130	TMEM130	NM_177735.4	1.305
Transmembrane protein 176B	TMEM176B	NM_023056.3	1.732
Transmembrane protein 199	TMEM199	NM_199199.2	1.211
Transmembrane protein 200B	TMEM200B	NM_887671.3	-1.279
Transmembrane protein 53	TMEM53	NM_026837.1	-1.96
Transmembrane protein 86A	TMEM86A	NM_026436.3	-1.322
Tenasin C	TNC	NM_011607.2	1.609
TNFAIP3 interacting protein 1	TNIP1	NM_021327.1	2.211
TNF-alpha-induced protein 3	TNFAIP3	NM_009397.2	1.931
TNR receptor superfamily member 11B	TNFRSF11B	NM_008764.3	-1.603
TNR receptor superfamily member 9	TNFRSF9	NM_011612.2	1.546
TNF receptor associated factor 1	TRAF1	AK089281	3.162
Tribbles homolog 3	TRIB3	NM_175093.2	-1.708
tRNA methyltransferase 6 homolog A	TRMT61A	NM_177374.2	1.277
Trichorhinophalangeal syndrome 1	TRPS1	NM_032000.1	-1.376
Tetraspanin 17	TSPAN17	NM-028841.1	-1.212
Tetratrocopeptide repeat domain 28	TTC28	XM_001476544.1	-1.644
Tetratrocopeptide repeat domain 3	TTC3	NM_009441.2	-1.266
Tetratrocopeptide repeat domain 39C	TTC39C	NM_028341.2	1.500
Tubulin tyrosine ligase-like family member 5	TTLL5	NM_001081423.1	-1.389
U2 small nuclear RNA auxiliary factor 1	U2AF1	NM_024187	1.246
Unc-5 homolog C	UNC5C	NM_009472.2	-1.309
Uridine phophorylase 1	UPP1	NM_009477.1	2.466

UV radiation resistance associated gene	UVRAG	NM_178635.2	-1.222
Vasorin	VASN	NM_139307.2	-1.352
WAS protein family member 1	WASF1	NM_031877.2	-1.278
WD repeat domain 43	WDR43	XM_917905.3	1.223
WD repeat domain 55	WDR55	NM_026464.2	1.281
WD repeat domain 77	WDR77	NM_027432.3	1.221
WAS/WASL interacting protein family member 1	WIPF1	NM_153138.3	-1.290
Wntless homolog	WLS	NM_026582-	-1.396
Wingless type MMTV integration site family member 10B	WNT10B	NM_011718.1	-1.464
Werner syndrome, RecQ helicase like	WRN	NM-011721.3	-1.237
WW domain containing E3 ubiquitin protein ligase 2	WWP2	NM_025830.1	-1.291
Exportin 4	XPO4	NM_20506.1	1.206
Zinc finger, CCHC domain containing 24	ZCCHCZ4	XM_908180.3	-1.275
Zinc finger DHHC (8)	ZDNNC8	NM_172151.3	-1.268
Zer-1 homolog	ZER1	NM_178694.3	-1.362
Zinc finger homeobox 3	ZFHX3	NM_007496.2	-1.341
Zinc finger protein 365	ZNF365	XM_980150.1	-1.309

Table A.1: Differentially expressed genes 8 hours following treatment with TNF-α in $p65^{+/+}$ MEFs, compared with untreated controls

I.II qRT-PCR validation

Aurora kinase A

Microarray data (section 5.4.1) showed that the gene, AURKA, encoding aurora kinase A was up-regulated 2.2-fold in $p65^{+/+}$ MEFs harvested 2 hours after treatment with 10 Gy IR, and interestingly that this effect was abrogated in the presence of AG-014699 at this timepoint. This gene did not appeared to be differentially expressed following TNF-α at either of the timepoints assessed, suggesting that *AURKA* may be a novel NF-κB regulated gene following DNA-damage, and thus requiring further investigation using qRT-PCR, as described in section 5.4.10.

Figure A.1A shows that the mRNA expression of AURKA is increased approximately 2-fold 2 hours after treatment with 10 Gy IR. This was shown to be statistically significant using an unpaired Student's t-test (p=0.0006). Although knockdown of NF-κB p65 did not decrease IR-induced *AURKA* expression (p=0.8075, unpaired Student's test), co-incubation with the pan-IKK inhibitor, BAY11-7082 significantly decrease this IR-induced AURKA expression (p=0.030, unpaired Student's t-test). IR in combination with either AG-014699, PARP-1 siRNA or NS siRNA had no effect on the IR-induced AURKA expression, compared with IR alone (p=0.8047, p=0.4873 and p=9425, respectively, unpaired Student's t-test). Figure A.1B shows that *AURKA* is not induced by TNF-α alone, and that is also unaffected by TNF-α in combination with p65 siRNA, BAY11-7082, AG-014699, PARP-1 siRNA or NS siRNA. These data suggest that *AURKA* expression is induced following IR and that this may be regulated by NF-κB, since the lack of the p65 subunit, had no effect, it is possible that one of the other subunits, was inhibited by BAY11-7082.

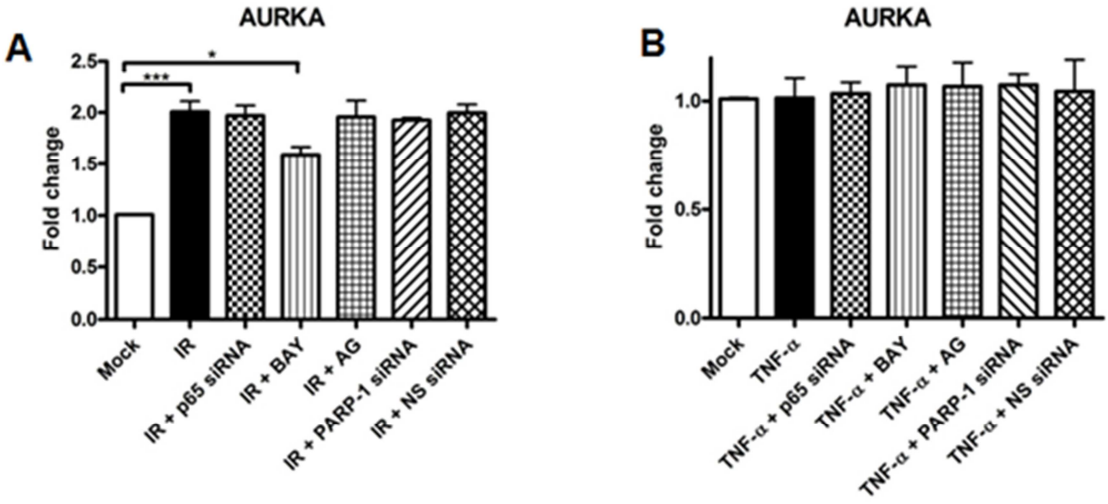

Figure A.1: Expression of AURKA following either IR or TNF-α
Bar chart showing the effect of IR or TNF-α ± p65 siRNA ± BAY11-7082 (BAY) ± AG-014699 (AG) ± PARP-1 siRNA ± Non-specific (NS) siRNA control on the transcription of AURKA 2 h following treatment with IR (**A**) or TNF-α (**B**) All results are the mean of three independent experiments with SEM. *** Significance relative to mock treated control p<0.001 **Significance relative to mock treated control was p<0.01 using unpaired Student's t-test. *Significance relative to mock treated control was p<0.05 using

Baculoviral IAP repeat containing 6

Microarray data (section 5.4.1) showed that the gene, *BIRC6*, encoding Baculoviral IAP repeat containing 6 was up-regulated 1.2-fold in $p65^{+/+}$ MEFs harvested 2 hours after treatment with 10 Gy IR, and interestingly that this affect was attenuated in the presence of AG-014699 at this timepoint. Other groups have showed that the inhibitor of apoptosis proteins (IAPs), of which *BIRC6* is an associated gene, are regulated by NF-κB following DNA damage (Stehlik et al., 1998, You et al., 1999). Therefore the microarray data and existing literature suggested that BIRC6 required further investigation using qRT-PCR described in section 5.4.10.

Figure A.2A shows that there is a small, 1.2-fold, increase in the expression of *BIRC6* 2 hours after treatment with IR, and that using an unpaired Student's t-test, this is statistically significant (p=0.027). It also illustrates that either p65 siRNA, BAY11-7082, AG-014699 or PARP-1 siRNA all inhibit this IR-induced *BIRC6* expression. However, although the results shown are the mean of three independent experiments, the trend observed with these treatments are not statistically significant when compared with IR alone (p65 siRNA: p=0.134; BAY11-7082: p=0.110; AG-014699: p=0.062; PARP-1 siRNA: p=0.091, unpaired Student's t-test). Importantly, however NS siRNA has no effect on IR-induced *BIRC6* expression, compared with IR alone (p=0.8330, unpaired Student's t-test). Figure A.2B shows that BIRC6 is not induced by TNF-α alone, and that is also unaffected by TNF-α in combination with p65 siRNA, BAY11-7082, AG-014699, PARP-1 siRNA or NS siRNA. Taken together these data suggest that expression of *BIRC6* is likely to be regulated by NF-κB following DNA damage, not TNF-α.

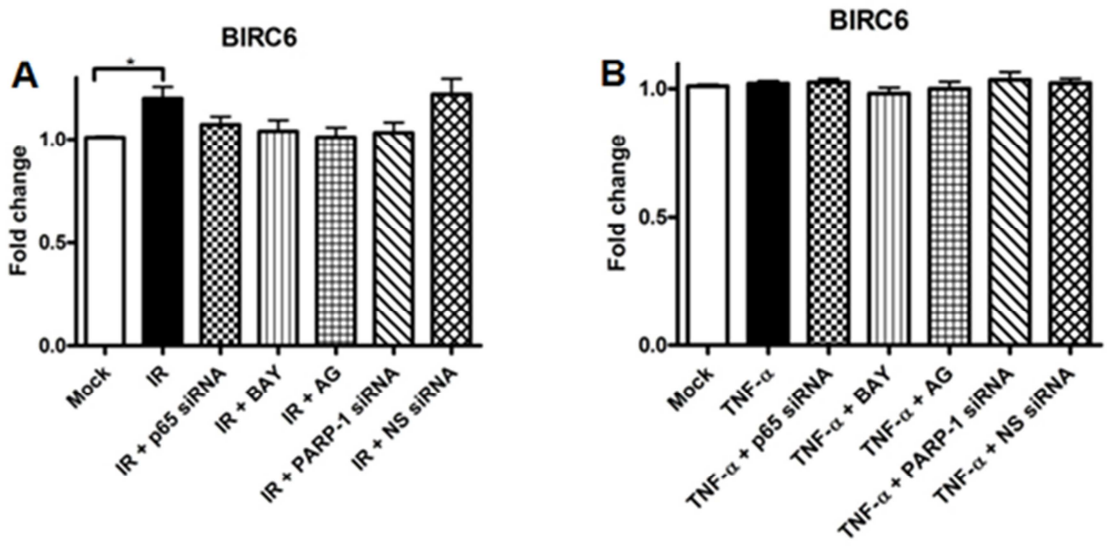

Figure A.2B: Expression of BIRC6 following either IR or TNF-α
Bar chart showing the effect of IR or TNF-α ± p65 siRNA ± BAY11-7082 (BAY) ± AG-014699 (AG) ± PARP-1 siRNA ± Non-specific (NS) siRNA control on the transcription of BIRC6 2 h following treatment with IR (**A**) or TNF-α (**B**) All results are the mean of three independent experiments with SEM *Significance relative to mock treated control was $p<0.05$ using unpaired Student's t-test.

Chemokines; CCL5 and CXCL10
Microarray data (sections 5.4.3 and 5.4.7) showed that, *CCL5*, encoding the chemokine ligand 5 was up-regulated 3-fold and 6.5-fold in $p65^{+/+}$ MEFs harvested 2 and 8 hours after treatment with 10 ng/ml TNF-α, respectively. The expression of *CCL5* appeared to remain unaffected by treatment with AG-014699 in combination with TNF-α. Furthermore, this gene did not appear to be differentially expressed following IR at either of the timepoints assessed. Interestingly this gene is known to be regulated by NF-κB following inflammatory stimuli (Wickremasinghe et al., 2004), therefore these studies allowed further testing of the hypothesis that NF-κB-dependent gene transcription following TNF-α requires PARP-1 protein alone, and is unaffected by PARP-1 enzymatic inhibition by directly comparing the PARP inhibitor, AG-014699 and PARP-1 siRNA in qRT-PCR analyses, described in section 5.4.10.

Figures A.3A and A.3B show the regulation of *CCL5* gene expression in $p65^{+/+}$ MEFs harvested 2 hours (Figure 5.13A) and 8 hours (Figure 5.13B) after IR treatment. In both cases there was no significant change in CCL5 expression following treatment with IR alone or in combination with p65 siRNA, BAY11-7082, AG-014699, PARP-1 siRNA or NS siRNA, consistent with the microarray findings. Figure 5.13C illustrates that the mRNA expression of *CCL5* was increased approximately 5-fold 2 hours after treatment with 10 ng/ml TNF-α. This was shown to be statistically significant using an unpaired Student's t-test ($p<0.0001$). Furthermore, knockdown of NF-κB p65 significantly decreased this TNF-α-induced *CCL5* expression ($p=0.0013$, unpaired Student's test), as did co-incubation with BAY11-7082 ($p=0.0032$, unpaired Student's t-test). Importantly, TNF-α in combination with knockdown of PARP-1 protein significantly decreased TNF-α-induced *CCL5* expression ($p=0.0161$, unpaired Student's t-test), whereas this was unaffected by co-incubation with AG-014699 ($p=0.8118$), thus supporting the data in Chapter 4 which suggests that PARP-1 protein alone is essential for NF-κB-dependent gene transcription following TNF-α. NS siRNA had no effect on TNF-α-induced *CCL5* expression, compared with TNF-α alone ($p=0.3129$, unpaired Student's t-test). Similar results were also observed in the $p65^{+/+}$ MEFs harvested 8 hours after treatment with TNF-α (Figure 5.13D). In this case the mRNA expression of *CCL5* was increased approximately 5.5-fold ($p=0.0001$, unpaired Student's t-test). Furthermore, knockdown of NF-κB p65 significantly decreased this TNF-α-induced *CCL5* expression ($p=0.0014$, unpaired Student's test), as did co-incubation with BAY11-7082 ($p=0.0141$, unpaired Student's t-test). Importantly, TNF-α in combination with knockdown of PARP-1 protein significantly decreased TNF-α-induced *CCL5* expression ($p=0.0066$, unpaired Student's t-test), whereas this was unaffected by co-incubation with AG-014699 ($p=0.6959$). NS siRNA had no effect on TNF-α-induced CCL5 expression, compared with TNF-α alone ($p=0.8197$, unpaired Student's t-test). These data also support the hypothesis which stated that AG-014699 would not affect the expression of key inflammatory response genes regulated by NF-κB following inflammatory stimuli.

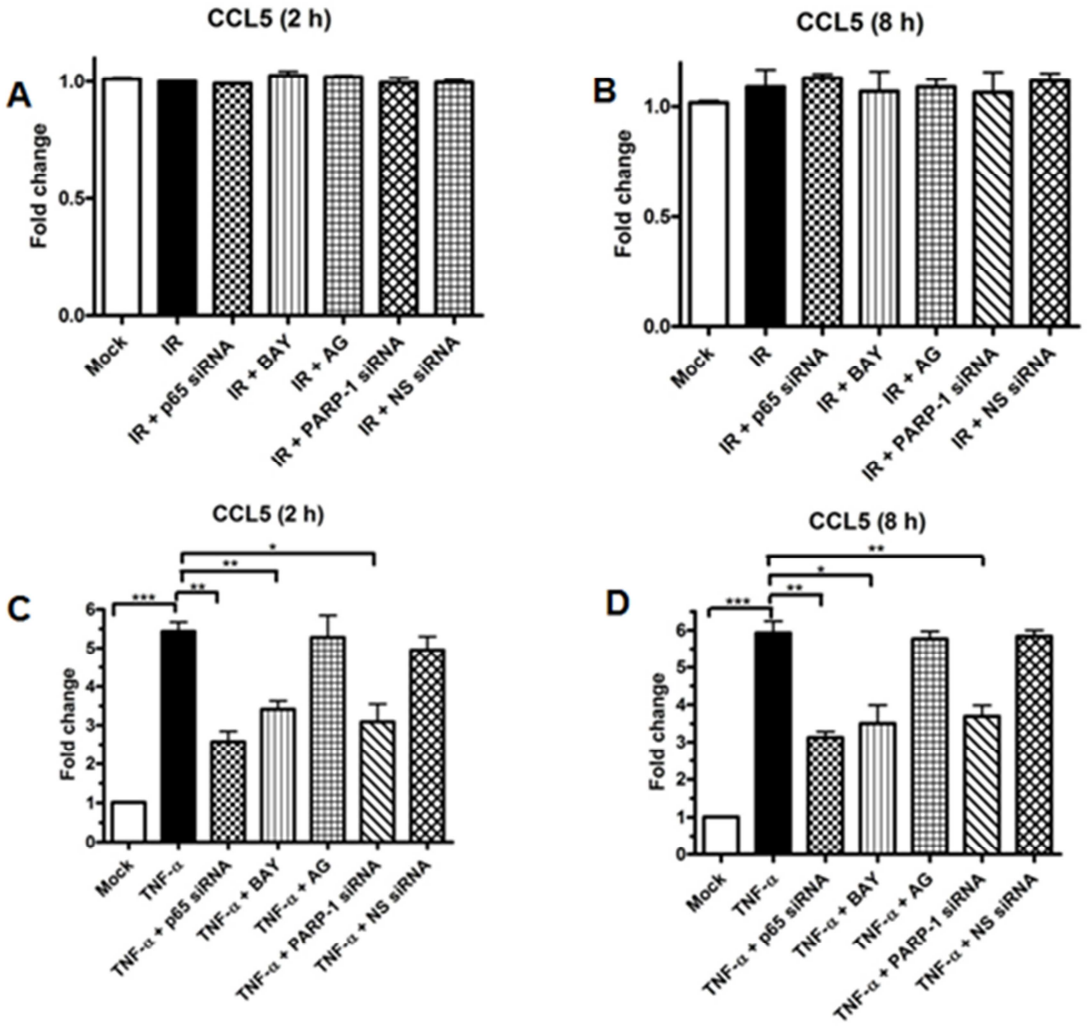

<u>Figure A.3</u>: Expression of CCL5 following either IR or TNF-α
Bar chart showing the effect of IR or TNF-α ± p65 siRNA ± BAY11-7082 (BAY) ± AG-014699 (AG) ± PARP-1 siRNA ± Non-specific (NS) siRNA control on the transcription of CCL5 following IR at 2 h (**A**) or 8 h (**B**) or following TNF-α at 2 h (**C**) or 8 h (**D**) All results are the mean of three independent experiments with SEM. *** Significance relative to mock treated control $p<0.001$ **Significance relative to mock treated control was $p<0.01$ using unpaired Student's t-test. *Significance relative to mock treated control was $p<0.05$ using unpaired Student's t-test.

Microarray data (sections 5.4.3 and 5.4.7) showed that the gene, *CXCL10*, encoding the chemokine (C-XC motif) ligand 10, was up-regulated 3.7-fold and 6-fold in $p65^{+/+}$ MEFs harvested 2 and 8 hours after treatment with 10 ng/ml TNF-α, respectively. The expression of *CXCL10* appeared to remain unaffected by treatment with AG-014699 in combination with TNF-α. Furthermore, this gene did not appear to be differentially expressed following IR at either of the timepoints assessed. Interestingly this gene is known to be regulated by NF-κB following inflammatory stimuli (Hein et al., 1997), therefore allowing further testing of the hypothesis that NF-κB-dependent gene transcription following TNF-α requires PARP-1 protein alone, and is unaffected by PARP-1 enzymatic inhibition by directly comparing the PARP inhibitor, AG-014699 and PARP-1 siRNA in qRT-PCR analyses, described in section 5.4.10.

Figures A.4A and A.4B show the regulation of CXCL10 gene expression in $p65^{+/+}$ MEFs harvested 2 hours (Figure 5.14A) and 8 hours (Figure 5.14B) after IR treatment. In both cases there was no significant change in *CXCL10* expression following treatment with IR alone or in combination with p65 siRNA, BAY11-7082, AG-014699, PARP-1 siRNA or NS siRNA, consistent with the microarray away findings. Figure A.4C illustrates that the mRNA expression of *CXCL10* was increased approximately 6.5-fold 2 hours after treatment with 10 ng/ml TNF-α ($p=0.0005$, unpaired Student's t-test). Markedly, knockdown of NF-κB p65 significantly decreased this TNF-α-induced *CXCL10* expression ($p=0.0250$, unpaired Student's test), as did co-incubation with BAY11-7082 ($p=0.0118$, unpaired Student's t-test). Importantly, TNF-α in combination with knockdown of PARP-1 protein significantly decreased TNF-α-

induced *CXCL10* expression (p=0.0288, unpaired Student's t-test), whereas this was unaffected by co-incubation with AG-014699 (p=0.9702), thus supporting the data in Chapter 4 which suggests that PARP-1 protein alone is essential for NF-κB-dependent gene transcription following TNF-α. NS siRNA had no effect on TNF-α-induced *CXCL10* expression, compared with TNF-α alone (p=0.7830, unpaired Student's t-test).

Similar results were also observed in the $p65^{+/+}$ MEFs harvested 8 hours after treatment with TNF-α (Figure A.4D). In this case the mRNA expression of *CXCL10* was increased approximately 5.5-fold (p=0.0002, unpaired Student's t-test). Moreover, knockdown of NF-κB p65 significantly decreased this TNF-α-induced CXCL10 expression (p=0.0022, unpaired Student's test), as did co-incubation with BAY11-7082 (p=0.0046, unpaired Student's t-test). Importantly, TNF-α in combination with knockdown of PARP-1 protein significantly decreased TNF-α-induced *CXCL10* expression (p=0.0136, unpaired Student's t-test), whereas this was unaffected by co-incubation with AG-014699 (p=0.6135). NS siRNA had no effect on TNF-α-induced *CXCL10* expression, compared with TNF-α alone (p=0.7886, unpaired Student's t-test). These data also support the results observed when investigating the regulation of *CCL5* (Figure A.4) and also the hypothesis which stated that AG-014699 would affect the expression of key inflammatory response genes regulated by NF-κB following inflammatory stimuli.

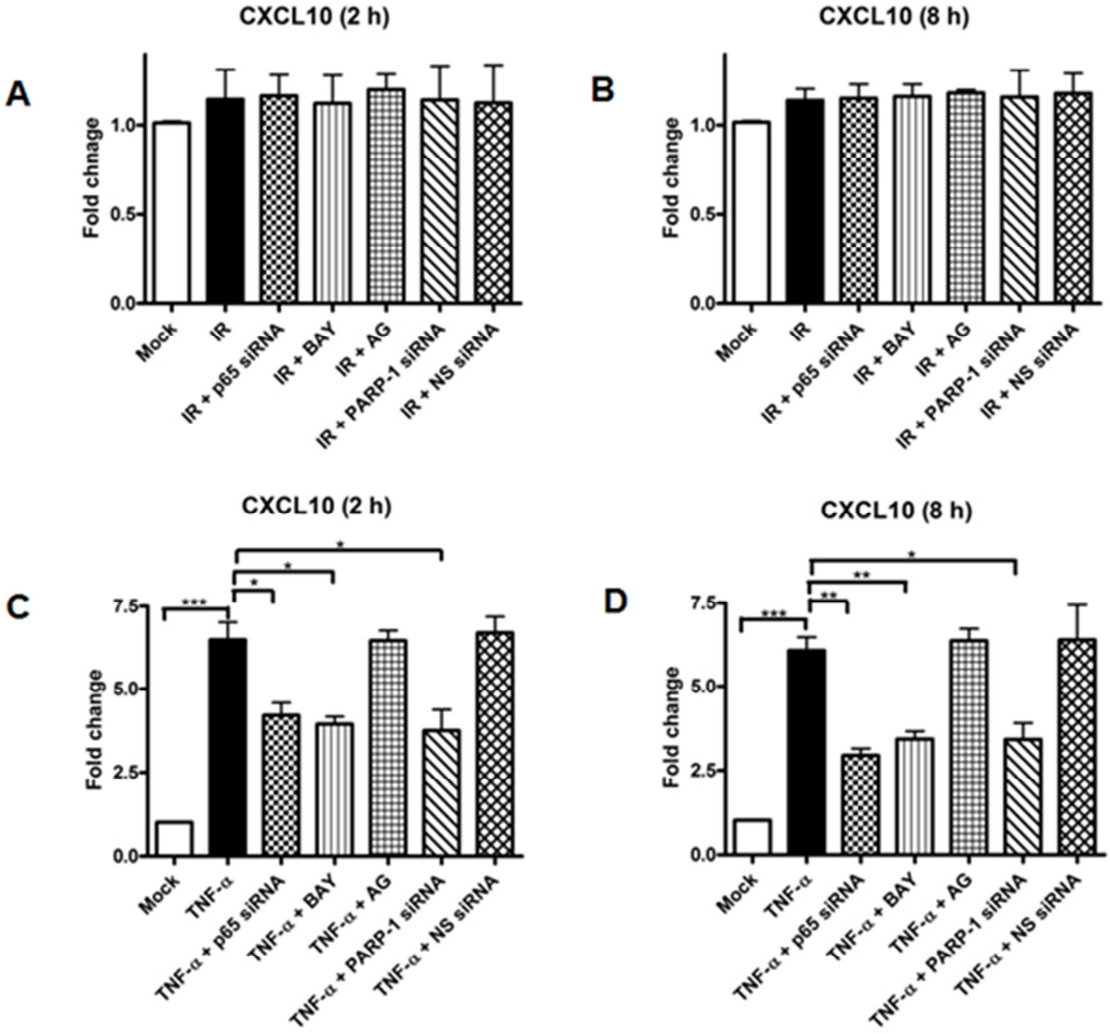

<u>Figure A.4:</u> Expression of CXCL10 following either IR or TNF-α
Bar chart showing the effect of IR or TNF-α ± p65 siRNA ± BAY11-7082 (BAY) ± AG-014699 (AG) ± PARP-1 siRNA ± Non-specific (NS) siRNA control on the transcription of CXCL10 following IR at 2 h (**A**) or 8 h (**B**) or following TNF-α at 2 h (**C**) or 8 h (**D**) All results are the mean of three independent experiments with SEM. *** Significance relative to mock treated control p<0.001 **Significance relative to mock treated control was p<0.01 using unpaired Student's t-test. *Significance relative to mock treated control was p<0.05 using unpaired Student's t-test.

Cell division cycle 20

Microarray data (sections 5.4.1 and 5.4.5) showed that the gene, *CDC20*, encoding the cell division cycle 20 protein was up-regulated 1.5-fold in $p65^{+/+}$ MEFs harvested 2 hours after treatment with 10 Gy IR, and 1.3-fold in $p65^{+/+}$ MEFs harvested 8 hours after treatment with 10 Gy IR. Interestingly, this affect was abrogated in the presence of AG-014699 at both timepoints. This gene did not appear to be differentially expressed following TNF-α at either of the timepoints assessed, suggesting that *CDC20* may be a novel NF-κB regulated gene following DNA-damage, and thus requiring further investigation using qRT-PCR, as described in section 5.4.10.

Figure A.5A shows that the mRNA expression of *CDC20* is increased approximately 1.4-fold 2 hours after treatment with 10 Gy IR (p=0.0016, unpaired Student's t-test). Knockdown of NF-κB p65 significantly decreased this IR-induced *CDC20* expression (p=0.0237, unpaired Student's test), as did co-incubation with BAY11-7082 (p=0.0472, unpaired Student's t-test). Importantly, IR in combination with either AG-014699 or PARP-1 siRNA also decreased IR-induced *CDC20* expression (AG-014699: p=0.0128; PARP-1 siRNA: p=0.0486, respectively, unpaired Student's t-test). NS siRNA had no effect on IR-induced *CDC20* expression, compared with IR alone (p=0.8354, unpaired Student's t-test). These data suggest that *CDC20* maybe a novel NF-κB regulated gene following DNA damage at this timepoint.

Although Figure A.5B shows that the mRNA expression of *CDC20* is significantly increased 8 hours following treatment with 10 Gy IR (p=0.0257, unpaired Student's t-test), it also shows that IR-induced *CDC20* expression is unaffected by co-incubation with p65 siRNA, BAY11-7082, AG-014699, PARP-1 siRNA or NS siRNA, at this timepoint (p65 siRNA: p=0.8157; BAY11-7082: p=0.9743, AG-014699: p=0.9021; PARP-1 siRNA; 0.8805; NS siRNA p=0.5883, unpaired Student's t-test). Figures A.5C and A.5D show the regulation of *CDC20* gene expression in $p65^{+/+}$ MEFs harvested 2 hours (Figure A.5C) and 8 hours (Figure A.5D) after TNF-α treatment. In both cases there was no significant change in *CDC20* expression following treatment with TNF-α alone or in combination with p65 siRNA, BAY11-7082, AG-014699, PARP-1 siRNA or NS siRNA, consistent with the microarray away findings.

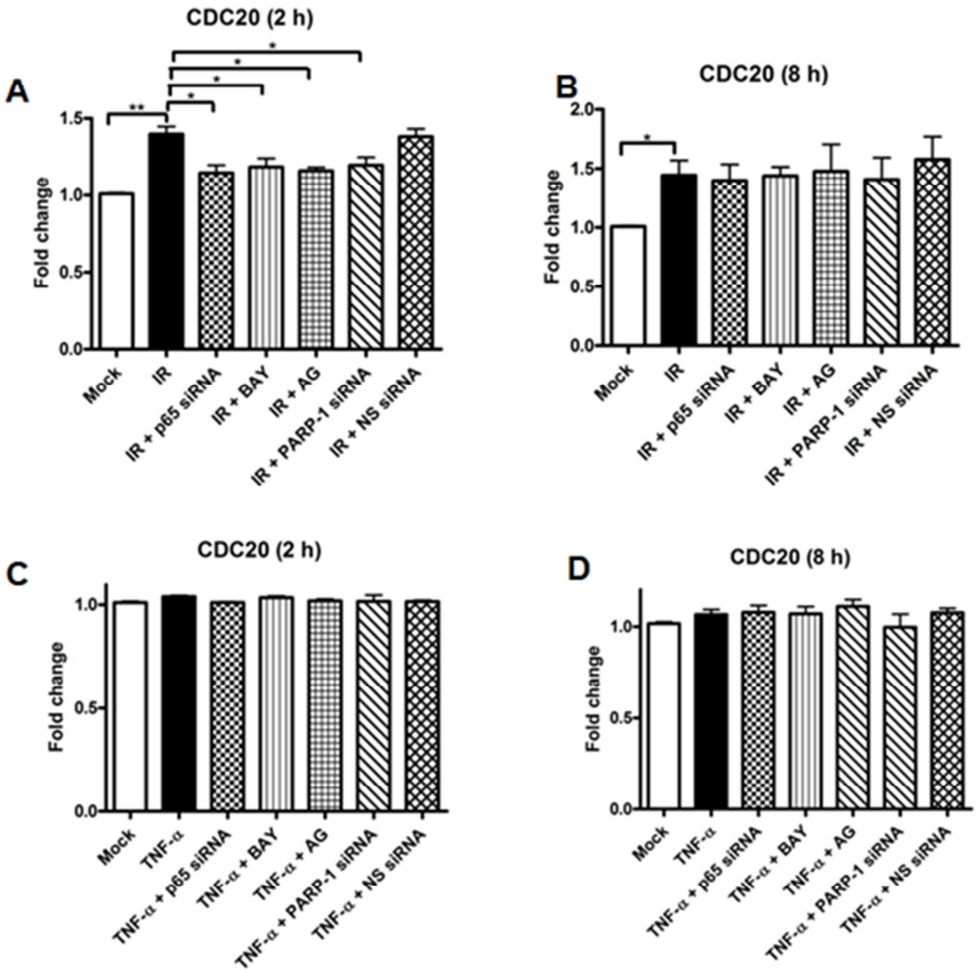

Figure A.5: Expression of CDC20 following either IR or TNF-α

Bar chart showing the effect of IR or TNF-α ± p65 siRNA ± BAY11-7082 (BAY) ± AG-014699 (AG) ± PARP-1 siRNA ± Non-specific (NS) siRNA control on the transcription of CDC20 following IR at 2 h (**A**) or 8 h (**B**) or following TNF-α at 2 h (**C**) or 8 h (**D**) All results are the mean of three independent experiments with SEM. *** Significance relative to mock treated control p<0.001 **Significance relative to mock treated control was p<0.01 using unpaired Student's t-test. *Significance relative to mock treated control was p<0.05 using unpaired Student's t-test.

FAS

Microarray data (section 5.4.7) showed that the gene, *FAS*, was up-regulated 3.6-fold in $p65^{+/+}$ MEFs harvested 8 hours after treatment with 10 ng/ml TNF-α. The expression of FAS appeared to remain unaffected by treatment with AG-014699 in combination with TNF-α. Furthermore, this gene did not appear to be differentially expressed following IR at either of the timepoints assessed. Interestingly this gene is known to be regulated by NF-κB following inflammatory stimuli (Chan et al., 1999), therefore it was of interest to further test the hypothesis that NF-κB-dependent gene transcription following TNF-α requires PARP-1 protein alone, and is unaffected by PARP-1 enzymatic inhibition by directly comparing the PARP inhibitor, AG-014699 and PARP-1 siRNA in qRT-PCR analyses, described in section 5.4.10.

Figures A.6A shows the regulation of the *FAS* gene expression in $p65^{+/+}$ MEFs harvested 8 hours after IR treatment. There was no significant change in *FAS* expression following treatment with IR alone or in combination with p65 siRNA, BAY11-7082, AG-014699, PARP-1 siRNA or NS siRNA, consistent with the microarray away findings. Figure A.6B shows that there is a 2.4-fold increase in the expression of FAS 8 hours after treatment with TNF-α, and that this was statistically significant (p=0.027, unpaired Student's t-test). It also illustrates that either p65 siRNA, BAY11-7082 or PARP-1 siRNA all inhibit this IR-induced *FAS* expression. However, although the results shown are the mean of three independent experiments, the trend observed with these treatments are not statistically significant when compared with TNF-α alone (p65 siRNA: p=0.066; BAY11-7082: p=0.070; PARP-1 siRNA: p=0.064, unpaired Student's t-test). Importantly, however co-incubation with AG-014699 had no effect on TNF-α induced *FAS* expression (p=0.8339, unpaired Student's t-test), once again suggesting that PARP inhibition does not affect TNF-α-induced NF-κB dependent gene transcription. NS siRNA also had no effect on TNF-α-induced *FAS* expression, compared with TNF-α alone (p=0.8368, unpaired Student's t-test).

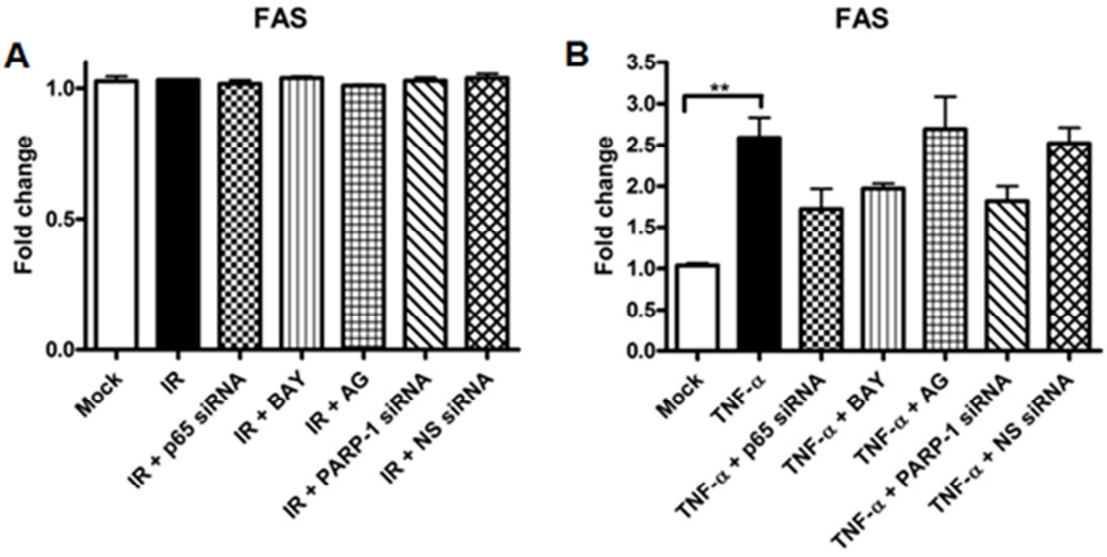

<u>Figure A.6:</u> Expression of FAS following either IR or TNF-α

Bar chart showing the effect of IR or TNF-α ± p65 siRNA ± BAY11-7082 (BAY) ± AG-014699 (AG) ± PARP-1 siRNA ± Non-specific (NS) siRNA control on the transcription of FAS 8 h following treatment with IR (**A**) or TNF-α (**B**) All results are the mean of three independent experiments with SEM. *** Significance relative to mock treated control p<0.001 **Significance relative to mock treated control was p<0.01 using unpaired Student's t-test. *Significance relative to mock treated control was p<0.05 using unpaired Student's t-test.

Interferon regulatory factor-1

Microarray data (section 5.4.1) showed that the gene, *IRF1*, encoding the interferon regulatory factor-1 protein was down-regulated 1.5-fold in $p65^{+/+}$ MEFs harvested 2 hours after treatment with 10 Gy IR and interestingly that this gene was up-regulated in the presence of AG-014699 at this timepoint. Microarray data (sections 5.4.3) also showed that *IRF1* was up-regulated 2.8-fold in these cells 2 hours after treatment with 10 ng/ml TNF-α. The expression of *IRF1* appeared to remain unaffected by treatment with AG-014699 in combination with TNF-α. IRF1 is known to be regulated by NF-κB following inflammatory stimuli (Harada et al., 1994), but not following DNA damage, hence the requirement for further investigation here using qRT-PCR analyses, as described in section 5.4.10.

Figure A.7A shows that the mRNA expression of *IRF1* is significantly decreased approximately 2 hours after treatment with 10 Gy IR compared with mock treated controls, (p=0.0004, unpaired Student's t-test).

This reduction in mRNA was also seen after co-incubation with either p65 siRNA or BAY11-7082. Interestingly, IR in combination with either AG-014699 or PARP-1 siRNA increased IR-induced IRF1 expression back to levels comparable with mock treated controls (AG-014699: p=0.0032; PARP-1 siRNA: p=0.0064, respectively, compared with IR alone, unpaired Student's t-test). NS siRNA in combination with IR was not significantly different from either IR alone (p=0.1840, unpaired Student's t-test) or mock treated controls (p=0.2371, unpaired Student's t-test).

Figure A.7B illustrates that the mRNA expression of *IRF1* was increased approximately 2-fold 2 hours after treatment with 10 ng/ml TNF-α(p=0.0003, unpaired Student's t-test). Furthermore, knockdown of NF-κB p65 significantly decreased this TNF-α-induced *IRF1* expression (p=0.0317, unpaired Student's test). Although the trend was very similar with TNF-α in conjunction with either BAY11-7082 or PARP-1 siRNA, this was not statistically significant compared with TNF-α alone (BAY11-7082: p=0.0625; PARP-1 siRNA: p=0.1756, unpaired Student's t-test). The expression of *IRF1* was not affected by co-incubation with AG-014699 (p=0.5591, compared with TNF-α alone, unpaired Student's t-test). NS siRNA had no effect on TNF-α-induced *IRF1* expression, compared with TNF-α alone (p=0.3700, unpaired Student's t-test).

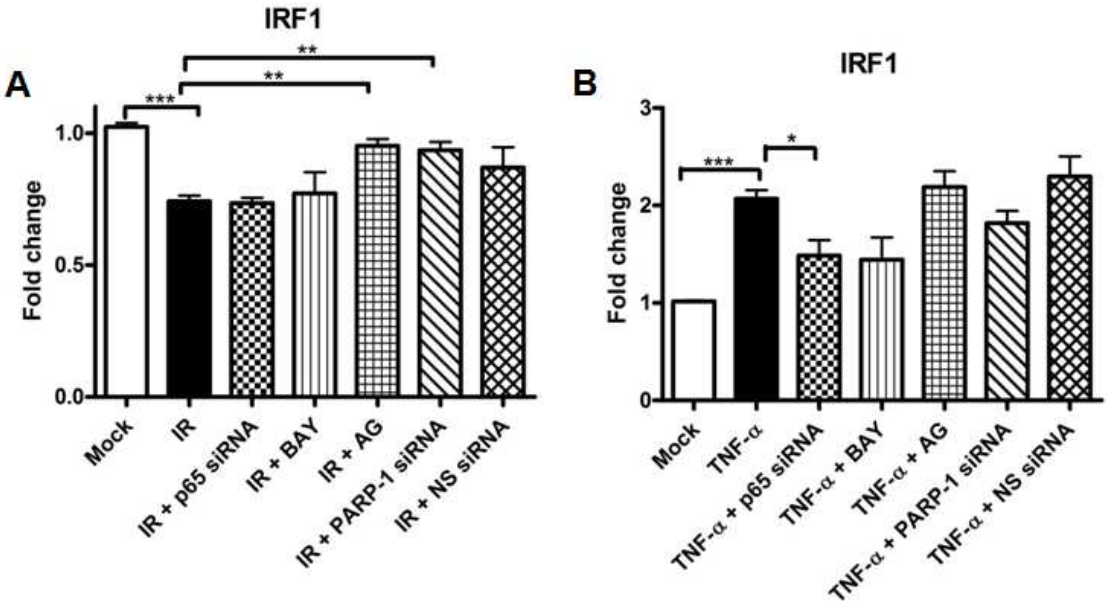

Figure A.7: Expression of IRF1 following either IR or TNF-α
Bar chart showing the effect of IR or TNF-α ± p65 siRNA ± BAY11-7082 (BAY) ± AG-014699 (AG) ± PARP-1 siRNA ± Non-specific (NS) siRNA control on the transcription of IRF1 2 h following treatment with IR (**A**) or TNF-α (**B**) All results are the mean of three independent experiments with SEM. *** Significance relative to mock treated control p<0.001 **Significance relative to mock treated control was p<0.01 using unpaired Student's t-test. *Significance relative to mock treated control was p<0.05 using unpaired Student's t-test.

JUNB proto-oncogene
Microarray data (section 5.4.1) showed that the gene, *JUNB*, encoding the Jun proto-oncogene was up-regulated 1.6-fold in $p65^{+/+}$ MEFs harvested 2 hours after treatment with 10 Gy IR and interestingly this affect was attenuated in the presence of AG-014699 at this timepoint. Microarray data (sections 5.4.3) also showed that *JUNB* was up-regulated 1.9-fold in these cells 2 hours after treatment with 10 ng/ml TNF-α. The expression of *JUNB* appeared to remain unaffected by treatment with AG-014699 in combination with TNF-α. Interestingly this gene is known to be regulated by NF-κB following inflammatory stimuli (Brown et al., 1995), but not following DNA damage, therefore the microarray data warrant validation by qRT-PCR as described in section 5.4.10.

Figure A.8A shows that there are is a very small increase in the expression of *JUNB* 2 hours after treatment with 10 Gy IR in the $p65^{+/+}$ MEFs, however this was not significant when compared with mock treated controls (p=0.7249). Furthermore, IR in combination with either p65 siRNA, BAY11-7082, AG-014699, PARP-1 siRNA or NS siRNA had no effect on JUNB expression when compared with IR alone (p65 siRNA: p=0.5899; BAY11-7082: p=0.7442; AG-014699: p=0.5395; PARP-1 siRNA: p=0.8402; NS siRNA: p=0.6641). These data suggest that JUNB is not regulated by NF-κB following DNA damage.

Figure A.8B illustrates that *JUNB* mRNA expression is increased 1.6-fold 2 hours after treatment with 10ng/ml TNF-α (p=0.041, unpaired Student's t-test), consistent with other reports (Brown et al., 1995). However, although TNF-α in combination with either p65 siRNA or BAY11-7082 appeared to decrease this TNF-α induced *JUNB* expression, this was not found to be statistically significant when compared with TNF-α alone (p=0.4540 and p=0.3685, respectively, unpaired Student's t-test). The expression of *JUNB* was not affected by co-incubation with either PARP-1 siRNA, AG-014699 or NS siRNA (p=0.8990, p=0.9140 and p=0.9743 compared with TNF-α alone, unpaired Student's t-test).

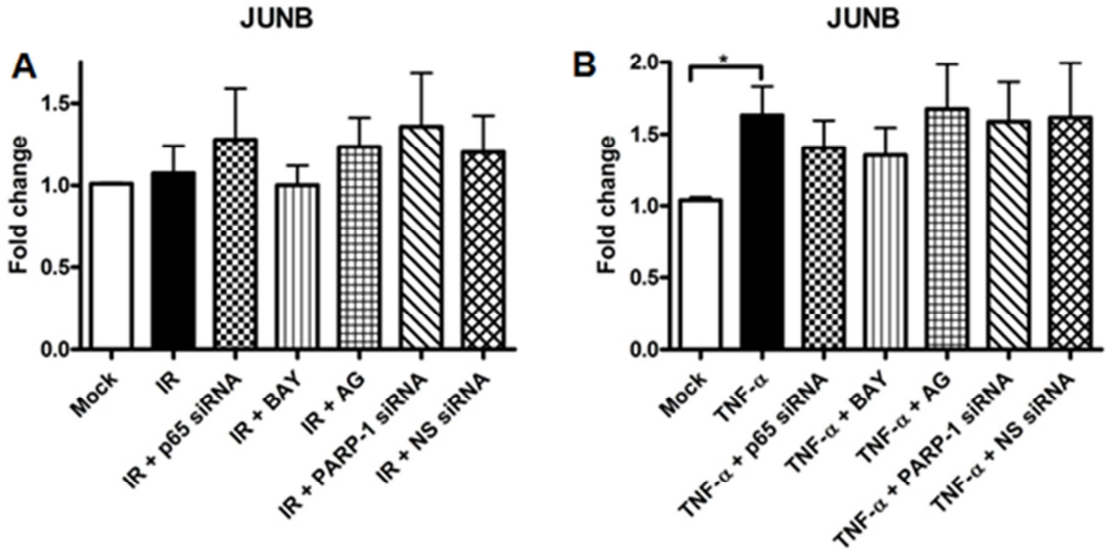

Figure A.8: Expression of JUNB following either IR or TNF-α
Bar chart showing the effect of IR or TNF-α ± p65 siRNA ± BAY11-7082 (BAY) ± AG-014699 (AG) ± PARP-1 siRNA ± Non-specific (NS) siRNA control on the transcription of JUNB 2 h following treatment with IR (**A**) or TNF-α (**B**) All results are the mean of three independent experiments with SEM. *** Significance relative to mock treated control p<0.001 **Significance relative to mock treated control was p<0.01 using unpaired Student's t-test. *Significance relative to mock treated control was p<0.05 using unpaired Student's t-test.

Polo-like kinases 1

Microarray data (section 5.4.1) showed that the gene, *PLK1*, encoding polo-like kinase 1 was up-regulated 1.6-fold in $p65^{+/+}$ MEFs harvested 2 hours after treatment with 10 Gy IR, and interestingly that this affect was abrogated in the presence of AG-014699 at this timepoint. This gene did not appeared to be differentially expressed following TNF-α at either of the timepoints assessed, suggesting that *PLK1* may be a novel NF-κB regulated gene following DNA-damage, and thus requiring further investigation using qRT-PCR, as described in section 5.4.10.

Figure A.9A show that the mRNA expression of *PLK1* is significantly increased approximately 1.5-fold 2 hours after treatment with 10 Gy IR in the $p65^{+/+}$ MEFs (p=0.0001, unpaired Student's t-test). Furthermore, knockdown of NF-κB p65 was shown to significantly decrease IR-induced expression, when compared with IR alone (p=0.0011, unpaired Student's test). A similar decrease in *PLK1* expression was also observed following co-incubation with BAY11-7082, AG-014699 or PARP-1 siRNA (p=0.0134, p=0.0259 and p=0.0108, respectively, compared with IR alone, unpaired Student's t-test). Importantly, NS siRNA had no effect on the IR-induced *PLK1* expression, compared with IR alone (p=0.7916, unpaired Student's t-test). Figure A.9B shows that *PLK1* is not induced by TNF-α alone, and that the expression is also unaffected by TNF-α in combination with p65 siRNA, BAY11-7082, AG-014699, PARP-1 siRNA or NS siRNA. These data suggest that *PLK1* expression is induced following IR and that this may be regulated by NF-κB, therefore warranting further investigation (discussed section 5.6).

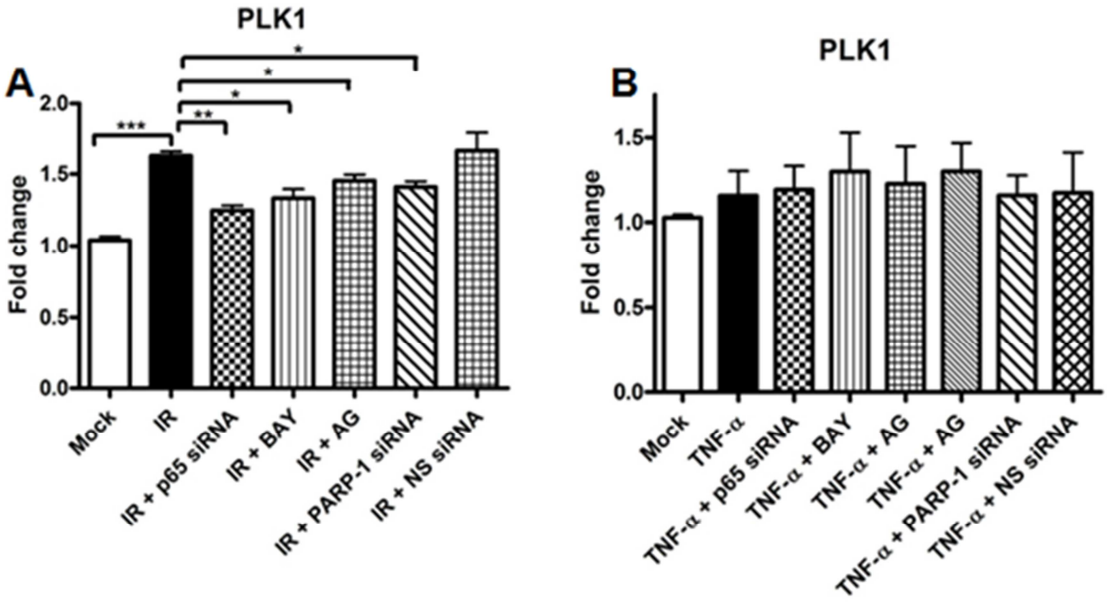

Figure A.9: Expression of PLK1 following either IR or TNF-α
Bar chart showing the effect of IR or TNF-α ± p65 siRNA ± BAY11-7082 (BAY) ± AG-014699 (AG) ± PARP-1 siRNA ± Non-specific (NS) siRNA control on the transcription of PLK1 2 h following treatment with IR (**A**) or TNF-α (**B**) All results are the mean of three independent experiments with SEM. *** Significance relative to mock treated control $p<0.001$ **Significance relative to mock treated control was $p<0.01$ using unpaired Student's t-test. *Significance relative to mock treated control was $p<0.05$ using unpaired Student's t-test.

TNFAIP3 interacting protein 1 (TNIP1)
Microarray data (section 5.4.1) showed that the gene, *TNIP1* was up-regulated 1.6-fold in $p65^{+/+}$ MEFs harvested 2 hours after treatment with 10 Gy IR and interestingly that this gene was up-regulated in the presence of AG-014699 at this timepoint. Microarray data (sections 5.4.3) also showed that TNIP1 was up-regulated 2.8-fold in these cells 2 hours after treatment with 10 ng/ml TNF-α. The expression of *TNIP1* appeared to remain unaffected by treatment with AG-014699 in combination with TNF-α. Interestingly this gene is known to be regulated by NF-κB following inflammatory stimuli (Heyninck et al., 1999, Tian et al., 2005), therefore allowing further testing of the hypothesis that NF-κB-dependent gene transcription following TNF-α requires PARP-1 protein alone, and is unaffected by PARP-1 enzymatic inhibition by directly comparing the PARP inhibitor, AG-014699 and PARP-1 siRNA in qRT-PCR analyses, described in section 5.4.10.

Figure A.10A shows that there is no significant change in the expression of *TNIP1* 2 hours after treatment with 10 Gy IR in the $p65^{+/+}$ MEFs, compared with mock treated controls ($p=0.6142$, unpaired Student's unpaired t-test) Furthermore, IR in combination with either p65 siRNA, BAY11-7082, AG-014699, PARP-1 siRNA or NS siRNA had no effect on TNIP1 expression when compared with IR alone (p65 siRNA: p0.6547; BAY11-7082: $p=0.9882$; AG-014699: $p=0.8427$; PARP-1 siRNA: $p=0.6817$; NS siRNA: $p=0.6450$). These data suggest that TNIP1 is not regulated by NF-κB following DNA damage.

Figure A.10B illustrates that *TNIP1* mRNA expression is increased 2-fold 2 hours after treatment with 10ng/ml TNF-α ($p=0.0046$, unpaired Student's t-test). PARP-1 siRNA in combination with TNF-α appeared to also decrease TNF-α-induced *TNIP1* expression slightly, compared with TNF-α alone although this was not statistically significant ($p=0.3286$, unpaired Student's t-test). However, although TNF-α in combination with either p65 siRNA or BAY11-7082 appeared to decrease this TNF-α induced *TNIP1* expression, this trend was not found to be statistically significant when compared with TNF-α alone ($p=0.0860$ and $p=0.0601$, respectively, unpaired Student's t-test), consistent with reports that *TNIP1* is regulated by NF-κB following TNF-α stimulation (Heyninck et al., 1999, Tian et al., 2005). The expression of TNIP1 was not affected by co-incubation with either AG-014699 or NS siRNA ($p=0.6171$ and $p=0.8548$ compared with TNF-α alone, unpaired Student's t-test).

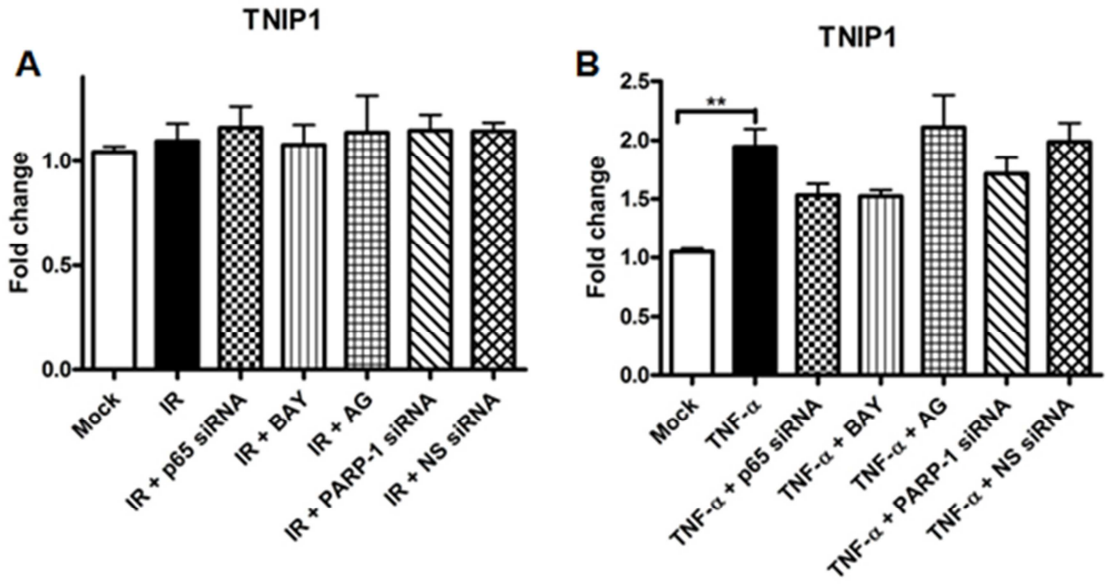

Figure A.10: Expression of TNIP1 following either IR or TNF-α
Bar chart showing the effect of IR or TNF-α ± p65 siRNA ± BAY11-7082 (BAY) ± AG-014699 (AG) ± PARP-1 siRNA ± Non-specific (NS) siRNA control on the transcription of TNIP1 2 h following treatment with IR (**A**) or TNF-α (**B**) All results are the mean of three independent experiments with SEM. *** Significance relative to mock treated control $p<0.001$ **Significance relative to mock treated control was $p<0.01$ using unpaired Student's t-test. *Significance relative to mock treated control was $p<0.05$ using unpaired Student's t-test.

Aurora kinase B
Microarray data showed that AURKB, which encodes the related family protein kinase, aurora kinase B, was up-regulated 1.2-fold in $p65^{+/+}$ MEFs harvested 8 hours after treatment with 10 Gy IR (section 5.4.5) but that the expression of this gene was unaffected following treatment with TNF-α, suggesting that AURKB may be novel NF-κB regulated genes following DNA-damage, and thus requiring further investigation using qRT-PCR, as described in section 5.4.10.

Figure A.11A illustrates that, using qRT-PCR analysis, AURKB is not induced by 10 Gy IR, 8 hours following treatment, as had been observed in the microarray analysis (5.4.5). It also shows that the expression of AURKB is unaffected by IR in combination with p65 siRNA, BAY11-7082, AG-014699, PARP-1 siRNA or NS siRNA. Furthermore, Figure xB indicates that shows that AURKB is not induced by TNF-α alone, and that is also unaffected by TNF-α in combination with p65 siRNA, BAY11-7082, AG-014699, PARP-1 siRNA or NS siRNA. These data suggest that AURKB is not regulated by NF-κB in response to either stimuli.

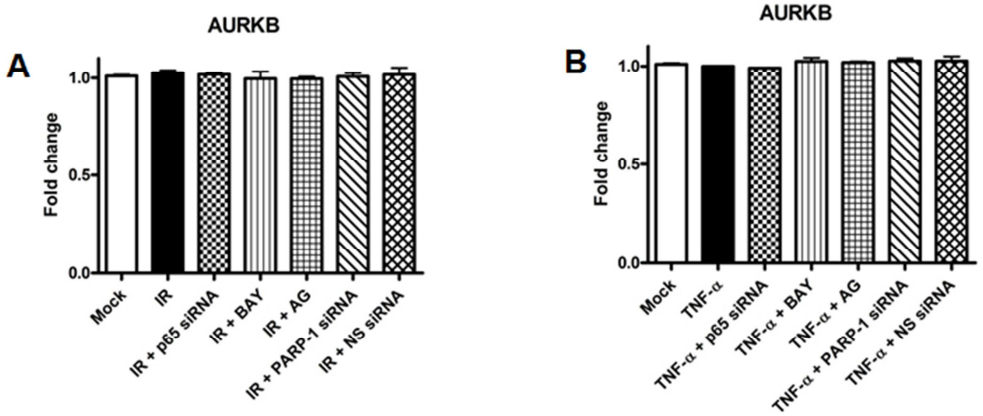

Figure A11: Expression of AURKB following either IR or TNF-α
Bar chart showing the effect of IR or TNF-α ± p65 siRNA ± BAY11-7082 (BAY) ± AG-014699 (AG) ± PARP-1 siRNA ± Non-specific (NS) siRNA control on the transcription of AURKB 8 h following treatment with IR (**A**) or TNF-α (**B**) All results are the mean of three independent experiments with SEM.

Polo-like kinase 2

Microarray data showed that PLK2, which encodes the protein kinase, polo-like kinase 2, was up-regulated 1.5-fold in $p65^{+/+}$ MEFs harvested 8 hours after treatment with 10 Gy IR (section 5.4.5). This gene did not appeared to be differentially expressed following TNF-α at either of the timepoints assessed, suggesting that PLK2 may be a novel NF-κB regulated gene following DNA-damage, and thus requiring further investigation using qRT-PCR, as described in section 5.4.10.

Figure A.12A illustrates that, using qRT-PCR analysis, PLK2 is not induced by 10 Gy IR, 8 hours following treatment, in contrast to the results from the microarray analysis (5.4.5). It also shows that the expression of PLK2 is unaffected by IR in combination with p65 siRNA, BAY11-7082, AG-014699, PARP-1 siRNA or NS siRNA. Furthermore, Figure A.11B indicates that shows that PLK2 is not induced by TNF-α alone, and that is also unaffected by TNF-α in combination with p65 siRNA, BAY11-7082, AG-014699, PARP-1 siRNA or NS siRNA. These data suggest that PLK2 is not regulated by NF-κB in response to either stimuli.

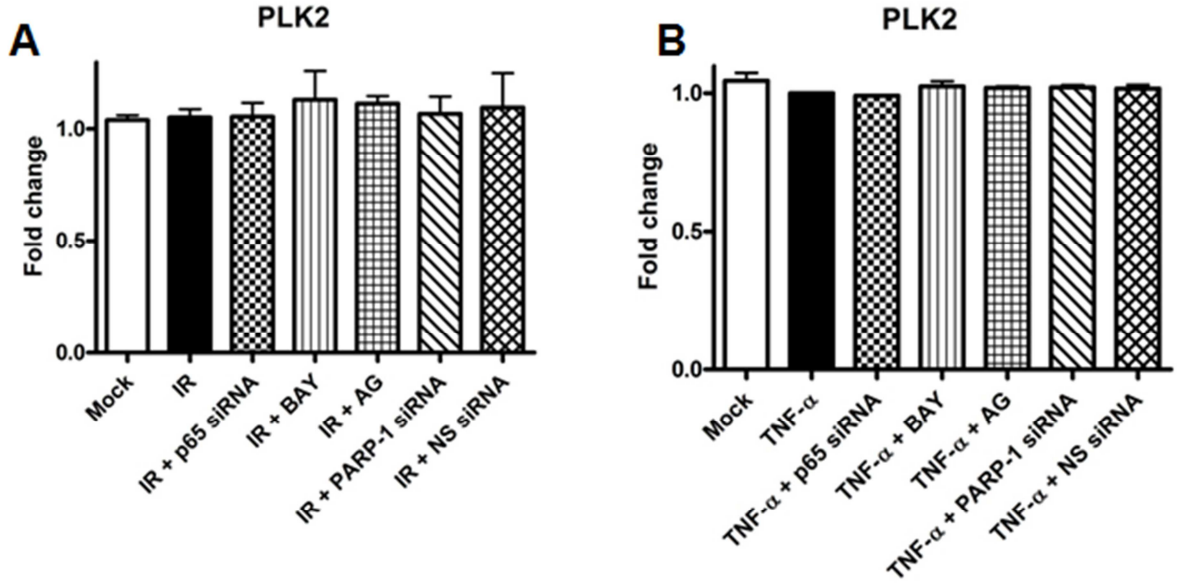

Figure A.11B: Expression of PLK2 following either IR or TNF-α

Bar chart showing the effect of IR or TNF-α ± p65 siRNA ± BAY11-7082 (BAY) ± AG-014699 (AG) ± PARP-1 siRNA ± Non-specific (NS) siRNA control on the transcription of PLK2 8 h following treatment with IR (**A**) or TNF-α (**B**) All results are the mean of three independent experiments with SEM.

Topoisomerase (DNA) II alpha

Microarray data (section 5.4.1) showed that the gene, TOP2A, encoding DNA topoisomerase II alpha was up-regulated 1.6-fold in $p65^{+/+}$ MEFs harvested 2 hours after treatment with 10 Gy IR, and interestingly that this affect was abrogated in the presence of AG-014699 at this timepoint. This gene did not appeared to be differentially expressed following TNF-α at either of the timepoints assessed, suggesting that TOP2A may be a novel NF-κB regulated genes following DNA-damage, and thus requiring further investigation using qRT-PCR, as described in section 5.4.10.

Figure A.13A shows that there is no significant change in the expression of TOP2A 2 hours after treatment with 10 Gy IR in the $p65^{+/+}$ MEFs, compared with mock treated controls (p=0.1209, unpaired Student's unpaired t-test) Furthermore, IR in combination with either p65 siRNA, BAY11-7082, AG-014699, PARP-1 siRNA or NS siRNA had no effect on TOP2A expression when compared with IR alone (p65 siRNA: p0.9611; BAY11-7082: p=0.4093; AG-014699: p=0.7587; PARP-1 siRNA: p=0.8732; NS siRNA: p=0.9218). These data suggest that TOP2A is not regulated by NF-κB following DNA damage. Figure xB shows that TOP2A is not induced by TNF-α alone, and that is also unaffected by TNF-α in combination with p65 siRNA, BAY11-7082, AG-014699, PARP-1 siRNA or NS siRNA. Taken together these data suggest that expression of TOP2A is not likely to be regulated by NF-κB following TNF-α.

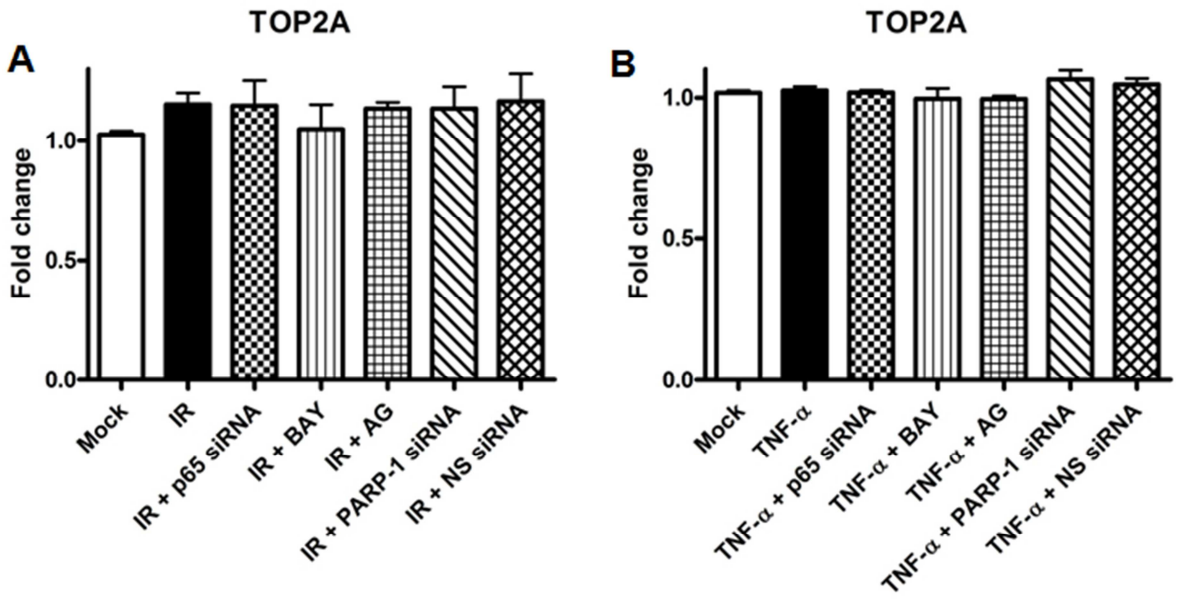

Figure A.13: Expression of TOP2A following either IR or TNF-α
Bar chart showing the effect of IR or TNF-α ± p65 siRNA ± BAY11-7082 (BAY) ± AG-014699 (AG) ± PARP-1 siRNA ± Non-specific (NS) siRNA control on the transcription of TOP2A 2 h following treatment with IR (**A**) or TNF-α (**B**) All results are the mean of three independent experiments with SEM.

Appendix II